



# Membrane action in fire design of composite slab with solid and cellular steel beams — valorisation (MACS+)

**EUROPEAN COMMISSION**

Directorate-General for Research and Innovation  
Directorate D — Key Enabling Technologies  
Unit D.4 — Coal and Steel

E-mail: [rtd-steel-coal@ec.europa.eu](mailto:rtd-steel-coal@ec.europa.eu)  
[RTD-PUBLICATIONS@ec.europa.eu](mailto:RTD-PUBLICATIONS@ec.europa.eu)

Contact: RFCS Publications

European Commission  
B-1049 Brussels

# Research Fund for Coal and Steel

## **Membrane action in fire design of composite slab with solid and cellular steel beams — valorisation (MACS+)**

O. Vassart<sup>1</sup>, B. Zhao<sup>2</sup>, R. Hamerlink<sup>3</sup>, B. Hauke<sup>4</sup>, J. de la Quintana<sup>5</sup>, I. Talvik<sup>6</sup>, Z. Sokol<sup>7</sup>,  
S. Pustorino<sup>8</sup>, P. Vila Real<sup>9</sup>, M. Hawes<sup>10</sup>, A. Nadjai<sup>11</sup>, B. Åstedt<sup>12</sup>, K. Jarmai<sup>13</sup>,  
R. D. Zaharia<sup>14</sup>, A. K. Kvedaras<sup>15</sup>, C. Baniotopoulos<sup>16</sup>, D. Beg<sup>17</sup>, J. M. Franssen<sup>18</sup>, G. Wozniak<sup>19</sup>

- 1. ArcelorMittal Belval & Differdange S.A., LUXEMBOURG**
- 2. Centre Technique Industriel de la Construction Metallique, FRANCE**
- 3. Bouwen met Staal, THE NETHERLANDS**
- 4. Bauforumstahl, GERMANY**
- 5. Fundacion Labein, SPAIN**
- 6. Tallinn Technical University, ESTONIA**
- 7. Ceske vysoke uceni technicke v Praze, CZECH REPUBLIC**
- 8. Structura Engineering srl, ITALY**
- 9. Universidade de Aveiro, PORTUGAL**
- 10. ASD Westok, UNITED KINGDOM**
- 11. University of Ulster, UNITED KINGDOM**
- 12. Stiftelsen Svensk Stalbyggnadsforskning, SWEDEN**
- 13. University of Miskolc, HUNGARY**
- 14. Politehnica University Timisoara, ROMANIA**
- 15. Vilnius Gediminas Technical University, LITHUANIA**
- 16. Aristotle University of Thessaloniki, GREECE**
- 17. University of Ljubljana, SLOVENIA**
- 18. University of Liège, BELGIUM**
- 19. Instytut Techniki Budowlanej, POLAND**

Grant Agreement RFS2-CT-2011-00025  
1 July 2011 to 31 December 2012

### **Final report**

Directorate-General for Research and Innovation

## **LEGAL NOTICE**

Neither the European Commission nor any person acting on behalf of the Commission is responsible for the use which might be made of the following information.

The views expressed in this publication are the sole responsibility of the authors and do not necessarily reflect the views of the European Commission.

***Europe Direct is a service to help you find answers  
to your questions about the European Union***

**Freephone number (\*):  
00 800 6 7 8 9 10 11**

(\* ) Certain mobile telephone operators do not allow access to 00 800 numbers or these calls may be billed.

More information on the European Union is available on the Internet (<http://europa.eu>).

Luxembourg: Publications Office of the European Union, 2014

ISBN 978-92-79-38540-7  
doi:10.2777/76136

© European Union, 2014  
Reproduction is authorised provided the source is acknowledged.

*Printed in Luxembourg*

PRINTED ON WHITE CHLORINE-FREE PAPER

# TABLE OF CONTENT

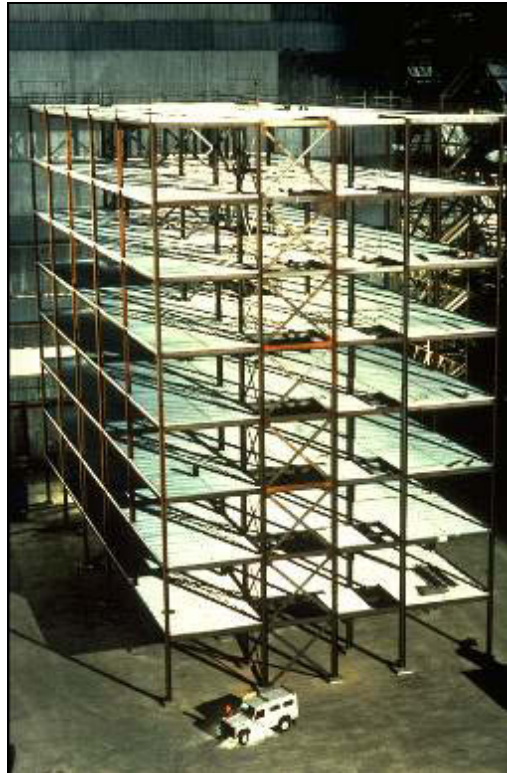
Final summary	5
Scientific and technical description of the results	11
1. WP1 : Realisation of documentation in English and software about design of composite floor system with unprotected secondary beams	11
1.1. Preparation of the design guide	11
1.2. Preparation of the background documentation	12
1.3. Preparation of PowerPoint presentations	12
1.4. Adaptation of the software	13
2. WP2 : Translation of the documentation and software interface	14
3. WP3 : Training of the new partners that are organising the seminars	14
4. WP4 : Post dissemination activities	15
5. WP4 : Organisation of seminars	16
5.1. France Seminar	17
5.2. Netherlands Seminar	19
5.3. German Seminar	20
5.4. Spain Seminar	20
5.5. Estonia Seminar	22
5.6. Czech Seminar	23
5.7. Italy Seminar	26
5.8. Portugal Seminar	28
5.9. UK Seminar	31
5.10. UK Northern Ireland Seminar	31
5.11. Sweden Seminar	35
5.12. Hungary Seminar	37
5.13. Romania Seminar	38
5.14. Lithuania Seminar	41
5.15. Greece Seminar	43
5.16. Slovenia Seminar	45
5.17. Belgium Seminar	46
5.18. Poland Seminar	49
6. Conclusion and Outlook	51
7. List of Figures and Tables	54
8. Appendices	56
8.1. PowerPoint presentations	56
8.2. Design guide	56
8.3. Engineering Background	56



# FINAL SUMMARY

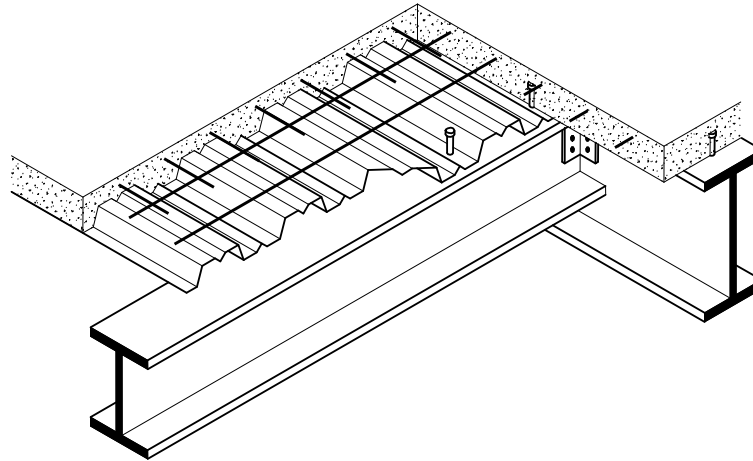
## Background

Large scale fire tests conducted in a number of countries and observations of actual building fires have shown that the fire performance of composite steel framed buildings is much better than indicated by standard fire resistance tests on isolated structural elements. It is clear that there are large reserves of fire resistance in modern steel framed buildings and that standard fire resistance tests on single unrestrained members do not provide a satisfactory indicator of the performance of such structures.



**Figure I : Cardington test building prior to the concreting of the floors**

Results of natural fire tests on the eight storey building at Cardington (see Figure I) performed in 1987 indicated that the stability of composite steel framed buildings, where some of the beams are unprotected, can be maintained by the beam/slab interaction even when the temperature of the unprotected beams exceeds 1000°C. The analyses made thereafter show that this excellent fire behaviour is due to membrane effects in the reinforced composite slab. The membrane action is activated in the slab when the steel beams reach temperatures at which they are no longer capable of supporting the applied load.



**Figure II : Cut away view of a typical composite floor construction**

In the UK a design method has been developed based on observation and analysis of the results of the extensive programme of full scale tests carried out at BRE Cardington during 1995 and 1996. The methodology has been incorporated into a specific design guide published by SCI. This design method is in fact conservative when compared to results of fire tests and it is limited to structures that are constructed in a similar manner to the tested structure, that is non-sway steel framed buildings with composite floors. The design method is utilised in the design of modern multi storey steel framed buildings using composite construction, i.e. the floors are constructed using shallow composite slabs with profiled steel decking attached by shear connectors to downstand beams (see Figure II).

When using this method, designers can benefit from the behaviour of the whole building instead of single members only. This enables them to determine which steel members of the structure can remain unprotected and yet maintaining the same safety level that would be provided by fully protected structure. Moreover, this design method allows fire resistance assessment of partially protected composite floors not only under natural fire condition but also in a standard ISO fire situation. The later is of particular interest because it means that the design method may be commonly applied by any design engineers in their fire resistance assessment of composite floors. Also, it may happen that authorities are more comfortable when an ISO fire is being used. They may accept more easily the utilisation of a new structural concept (a matter in which they trust the designers) then the utilisation of a new type of fire.

A second edition of this design guide is available now which allows the application of the design method to standard fire ratings up to 120 minutes. In parallel to this SCI design guide, a practical design tool based on Excel calculation sheets is also provided to assist designers in using this concept for the fire design of a composite floor. However, several features concerning the application of this design guide have to be taken into account, which are:

- Firstly, at this moment the design guide provided by SCI is only recognised in the UK and its application in other European countries requires an approval of the country national regulatory authority;
- Secondly, the design method is only based on Cardington fire tests under natural fire conditions. There is no evidence that the design method is also valid in a standard fire situation, in particular for fire rating up to 120 minutes. It was extremely important to perform a fire test under standard fire conditions in order to confirm on one hand the simple design method and on the other hand convince the authorities about validity of the design concept;



- Thirdly, some application conditions of the design method given in the SCI design guide need to be investigated in more details according to national requirements;
- Finally, because the design guide and corresponding Excel calculation sheets are all in English, there is a need to translate these tools into official languages of different European countries and to modify them in order to extend the application to these countries

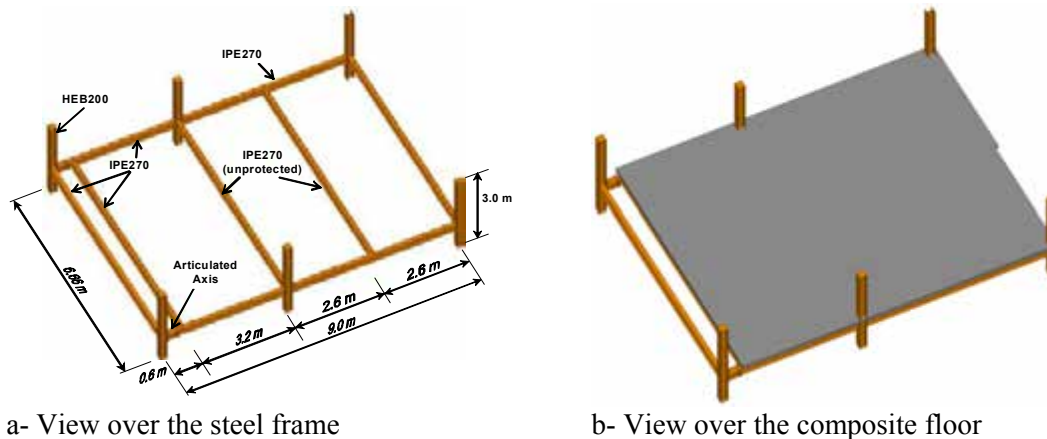
Some enquiries have been made in France by CTICM with the French ministry of interior about the possible extension of this fire design concept in France. The results of the first contacts are very encouraging. The French Ministry of Interior is willing to establish a special French fire safety committee to review the design method, once all the necessary information is available. The outcome could be a national agreement regarding the application of this design method in France.

## Objectives

This project proposal is a response to the demand for dissemination of the methodology coming from the European market. This request emerged after some new experimental work performed in different RFCS projects (FICEB+ and COSSFIRE).

### COSSFIRE

In the scope of COSSFIRE project, a composite floor was fire tested (see Figure III).



**Figure III : View of the composite floor**

In compliance with the existing simple engineering design method of such a type of floor under membrane action, the two intermediate secondary beams and the composite slab are unprotected. However, all the boundary beams of the floor are fire protected for a fire rating of 120 minutes. The steel columns were also protected except the protection around the joints which was intentionally reduced so that the heating of the joint components was important enough during heating phase in order to investigate the impact of such heating on their behaviour during cooling phase.

From measured global deflection of the floor, it was found that it increased to more than 500 mm after 120 minutes. However, the floor behaved still very well and there was no sign of failure in the central part of the floor. Local buckling of the unprotected secondary beam connected to central steel beams near joints is observed in its lower flange and web.

However, the most remarkable feature from this test regarding the steel joints is that they all performed very well during both heating and cooling phases. Also, for unprotected secondary beams connected to steel main beams near joint, no local buckling can be found. In addition, no failure of the edge connections between concrete slab and steel members is observed.

### **FICEB+**

In the scope of this project a full scale fire test was performed on a composite floor for analysing the possibility of tensile membrane action to develop when the unprotected steel beams in the central part of the floor are made of cellular beams (see Figure IV).

The natural fire was created by a wood crib fire load of 700 MJ/m<sup>2</sup> and the 9 x 15 m floor survived the fire that peaked at 1000°C and lasted for 90 minutes.



**Figure IV : Fire test and structural elements after the fire**

All chosen partners are well known structural and/or fire engineering experts in their countries. Nevertheless, some of the partners may not be fully familiar with this design approach. It was therefore necessary to provide training to the new partners in a form of internal workshop before they were in position to organise the national seminars on their own.

The next step was the translation of all data and documents produced in the project into the languages of the partners' countries. Experience shows that, due large number of technical expressions used in this field of application, a local language is always better received on larger scale by designers and engineers than English in most of European countries.

The organisation of the seminars in each country was one of the main activities in the project. One seminar was organised in each of the partner countries. With this aim, suitable and centralised locations were found, in order to attract as many people as possible. Due to the fact that this project deals with larger number of partners than usual and in order to keep the global research budget reasonable, a registration fee was sometimes charged to the participants of the seminar allowing the organisers to limit their own contribution. The fact of asking a limited fee is generally attracting more attention as the perception is often that "what costs nothing is worth nothing". Beside this, the number of people who register but don't show up at the seminar is usually smaller.

As the project duration was only 18 months and required coordination of number of partners, all steps have been well prepared and synchronised and the invitations for the seminars have been sent out well in advance. All the seminars were held in second semester of 2012, which was the best period for attracting maximum number of people. During the seminars printed and electronic version of the data were distributed to the participants. The data consists of all the presentations, documents and freely available software.

In order to ensure a larger dissemination and easy access to the materials produced in the project, an Internet webpage ([www.macsfire.eu](http://www.macsfire.eu)) was opened for the project and is available to the public.

The dissemination, informative and promotional actions has contributed to improvement of the situation of steel structures fire design in Europe and will allow increasing structural steel market share all over Europe.



## SCIENTIFIC AND TECHNICAL DESCRIPTION OF THE RESULTS

### 1. WP1 : REALISATION OF DOCUMENTATION IN ENGLISH AND SOFTWARE ABOUT DESIGN OF COMPOSITE FLOOR SYSTEM WITH UNPROTECTED SECONDARY BEAMS

*WP Leader: CTICM (Other partners: AM, UU, PUT, ULj and ULG)*

#### 1.1. Preparation of the design guide

The design guide has been created and contains examples of calculation for solid beam and will be updated for Cellular beam with the new version of the Software. The English version can be found in Annex and the Figure 1-1 hereafter shows the cover page of the document.

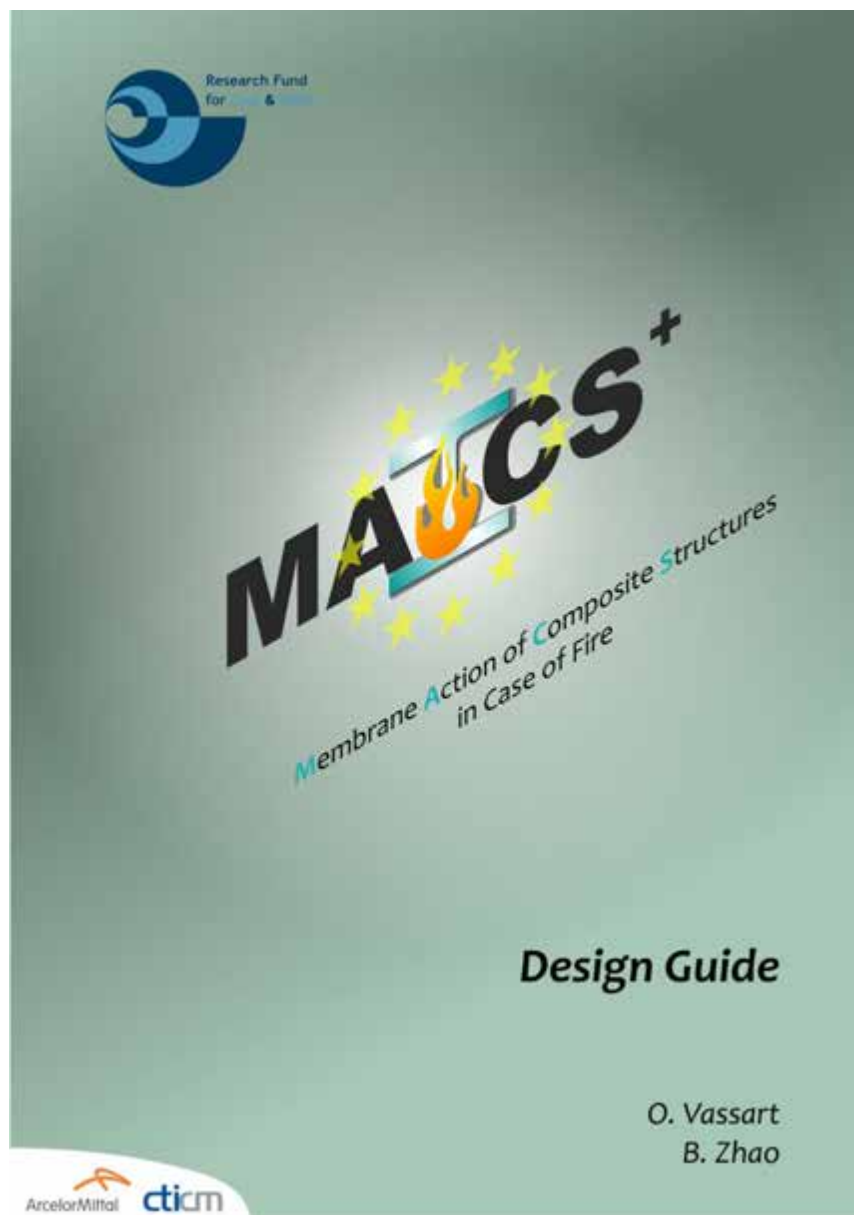


Figure 1-1 : Cover page of the Design Guide

## 1.2. Preparation of the background documentation

The Background has been created and contains the different fire tests and the validation of FEM ANSYS and SAFIR and the description of the simplified approach. The English version can be found in Annex and the Figure 1-2 hereafter shows the cover page of the document.”

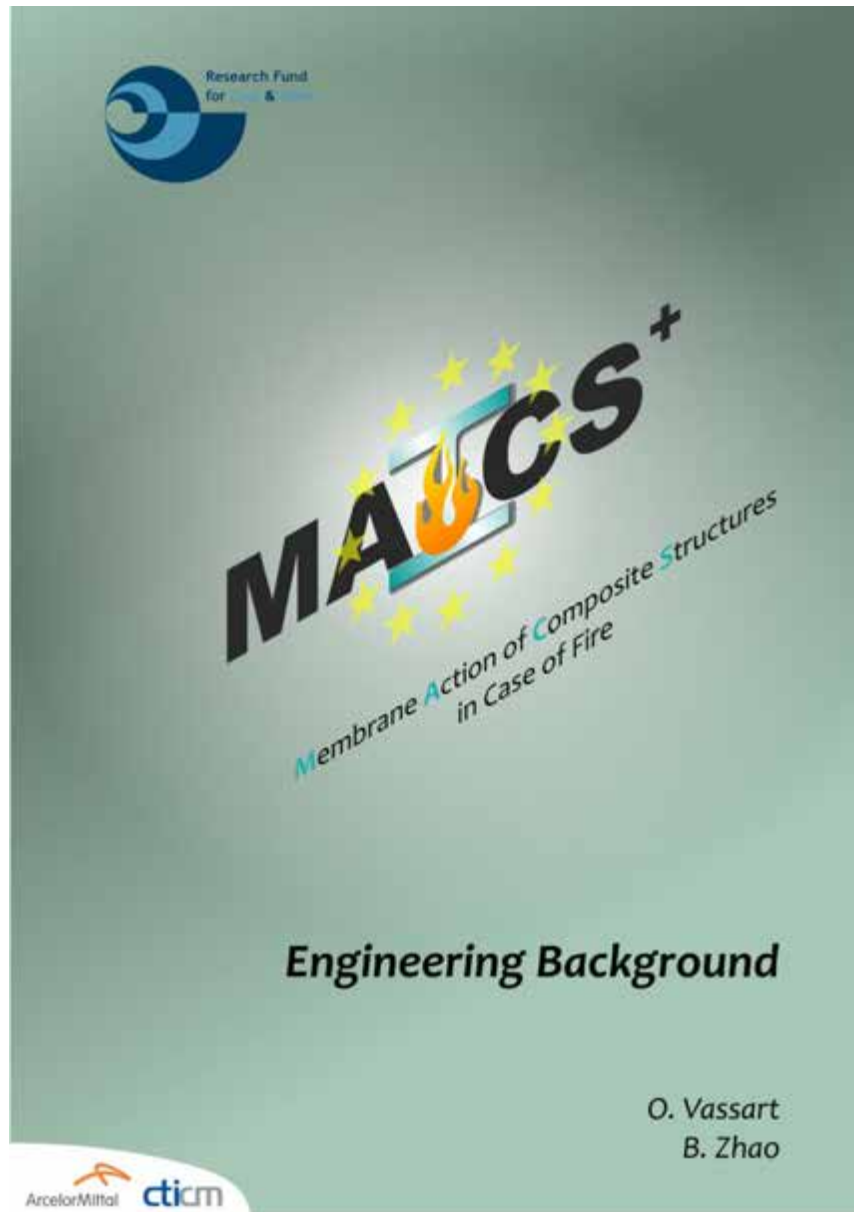


Figure 1-2 : Cover page of the Engineering Background

## 1.3. Preparation of PowerPoint presentations

A layout has been chosen for the different PowerPoint presentations in order to have uniformity in all the languages. A full set of presentation in English has been put in annex.

## 1.4. Adaptation of the software

The Software has been adapted in order to take into account the specificities of cellular beams. The Figure 1-3 and Figure 1-4 here after shows the adapted interface for cellular beams. The Software is available on the website of the project [www.macsfire.eu](http://www.macsfire.eu) and on the ArcelorMittal website [www.arcelormittal.com/scetions](http://www.arcelormittal.com/scetions)



Figure 1-3 : Software interface (About MACS+ Software)

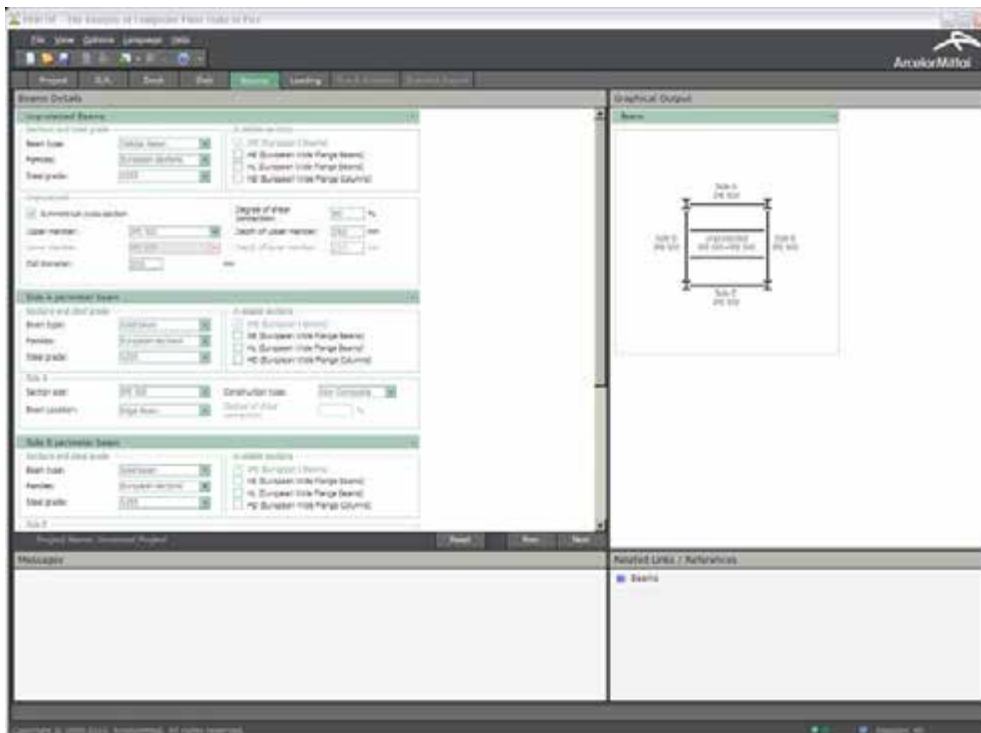


Figure 1-4 : Software interface (DATA)

## **2. WP2 : TRANSLATION OF THE DOCUMENTATION AND SOFTWARE INTERFACE**

*WP Leader: CTU Prague(Other partners: All)*

All the documents and PowerPoint presentations and Software developed in WP1 were translated in the different languages of the partners, in order to be able to present them in the mother tongue to all seminar participants. This action is not required for the United Kingdom and Belgium as they will use the English & Dutch versions. So the documents were translated in :

- ⇒ French
- ⇒ Czech
- ⇒ Dutch
- ⇒ German
- ⇒ Spanish
- ⇒ Italian
- ⇒ Portuguese
- ⇒ Polish
- ⇒ Swedish
- ⇒ Hungarian
- ⇒ Romanian
- ⇒ Lithuanian
- ⇒ Greek
- ⇒ Estonian
- ⇒ Slovenian

All these translated documents will not be put in annex of this report due to the lack of place. But all these documents can be downloadable for free on the website of the project [www.macsfire.eu](http://www.macsfire.eu) in pdf version. Original version can be sent on request contacting each national partner.

## **3. WP3 : TRAINING OF THE NEW PARTNERS THAT ARE ORGANISING THE SEMINARS**

*WP Leader: ArcelorMittal (Other partners: All)*

The partners of the former projects (ArcelorMittal, CTICM, ULG, Ulster) have attended the fire tests and have created the different documents and software. The other partners of this project have all been chosen as experts in their countries as far as structural steel and fire engineering is concerned. However, their level of understanding of the membrane action concept might differ. Therefore, in order to provide high quality, professional and consistent seminars across Europe a special training for the project's partners has been organised.

During the Workshop, the FICEB+ and COSSFIRE partners have presented and explained the global approach as well as the Software based on the WP1 data. In this way, it was ensured that all the 18 seminars have provided the same harmonised information.

In order to avoid additional travel cost, the second coordination meeting was extended to two days and the second day was used to perform the training.



#### 4. WP4 : POST DISSEMINATION ACTIVITIES

*WP Leader: University of Hannover (Other partners: ArcelorMittal)*

After the seminars, all data were prepared for a further dissemination. USB stick were created with a HTML based menu that guide users through all Presentations, Documents and free available software that are included in all languages on it. As it will be based on HTML, the content can easily be put on internet.

A homepage [www.macsfire.eu](http://www.macsfire.eu) was created by BFS and will be maintained for duration of minimum 5 years after the completion of the project (see Figure 4-1).

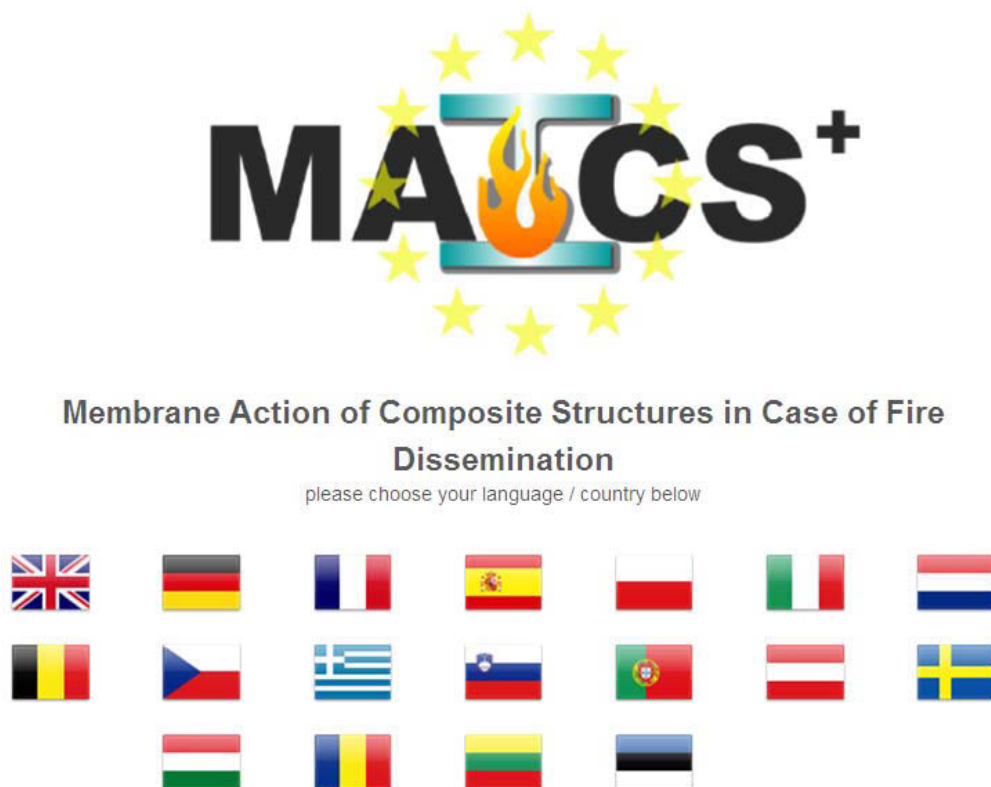


Figure 4-1 : Homepage [www.macsfire.eu](http://www.macsfire.eu)

Each flag correspond to one langue, when the visitor click on a given flag, he will have access to the different documents and presentation in direct download (see Figure 4-2).



## Membrane Action of Composite Structures in Case of Fire Dissemination

The following documents are available for download:  
Please note: document descriptions will follow soon.

Title	Description	Downloads
General introduction		PDF (0.2 MB)
Observation of real fires		PDF (1.6 MB)
New fire tests		PDF (6.4 MB)
Simple design method		PDF (1.4 MB)
MACS+ Numerical simulation		PDF (2.5 MB)
Worked example		PDF (2.6 MB)
Design guide		PDF (2.5 MB)
Background Document		PDF (10.1 MB)
Software		EXE (4.1 MB)



[Home](#) | [Contact](#)

Figure 4-2 : Document page [www.macsfire.eu](http://www.macsfire.eu)

The third part of this WP is the organisation of a workshop with each local authority. This part will be reported with the organisation of the seminar in the next paragraph.

### 5. WP4 : ORGANISATION OF SEMINARS

*WP Leader: Tecnalía (Other partners: All)*

The main task of this project was the organisation of seminars in each of the participating countries (see Table 5-1). Each partner was responsible for the organisation of the seminar in his country. This was organised on University campus as well as in conference centres. In front of the event, invitations were prepared and distributed to the target people. Those were steel customers with designers, architects, building owners, but also future customers with students, and professors as well as last but not least decision makers with authorities, insurance companies and firemen. The full day seminar was organised in a central place in order to target a high attendance. During the seminar, printed

documents as well as USB keys were distributed that contains all data. As no Belgian partner is available and no seminar has yet been organised in Belgium, AM has taken in charge the Belgian seminars.. There will be no additional seminar in Luxembourg. Due to the huge size and importance of Germany, France and Spain a second seminar was organised in those three countries whereas the geographical location was totally different from those from the initial DIFISEK project.

**Table 5-1 : Organisation of the seminars**

<i>Country</i>	<i>Partner</i>	<i>Date and location</i>	<i>number of participant</i>
<i>France</i>	<i>CTICM</i>	<i>8th of November 2012 in Paris</i>	<i>55</i>
<i>Netherlands</i>	<i>BMS</i>	<i>6<sup>th</sup> of December 2012 in Breda</i>	<i>48</i>
<i>Germany</i>	<i>BFS</i>	<i>28<sup>th</sup> of November 2012 Ostfildern</i>	<i>28</i>
<i>Spain</i>	<i>Tecnalía</i>	<i>18<sup>th</sup> of December 2012 Bilbao</i>	<i>74</i>
<i>Estonia</i>	<i>TTU</i>	<i>3<sup>rd</sup> of December 2012 Tallinn</i>	<i>55</i>
<i>Czech Rep.</i>	<i>CTU</i>	<i>11<sup>th</sup> of September 2012 Prague</i>	<i>164</i>
<i>Italy</i>	<i>StrEng</i>	<i>29<sup>th</sup> of November 2012 Rome</i>	<i>76</i>
<i>Portugal</i>	<i>UniAv</i>	<i>10<sup>th</sup> of December 2012 Lisbon</i>	<i>90</i>
<i>UK</i>	<i>ASD West.</i>	<i>12<sup>th</sup> of December 2012</i>	<i>74</i>
<i>UK (Northern Ireland)</i>	<i>UU</i>	<i>15<sup>th</sup> of November Ulster</i>	<i>96</i>
<i>Sweden</i>	<i>SBI</i>	<i>11<sup>th</sup> of December Stockholm</i>	<i>39</i>
<i>Hungary</i>	<i>Uni Misk</i>	<i>16<sup>th</sup> of November 2012 Budapest</i>	<i>70</i>
<i>Romania</i>	<i>UniTi</i>	<i>7<sup>th</sup> of December 2012 Timisoara</i>	<i>50</i>
<i>Lithuania</i>	<i>VGTU</i>	<i>18<sup>th</sup> of December 2012 Vilnius</i>	<i>71</i>
<i>Greece</i>	<i>AUTH</i>	<i>18<sup>th</sup> of November 2012 Thessaloniki</i>	<i>20</i>
<i>Slovenia</i>	<i>UniLj</i>	<i>27<sup>th</sup> of November 2012 Ljubljana</i>	<i>60</i>
<i>Belgium</i>	<i>ULG</i>	<i>13<sup>th</sup> of December 201, Liège</i>	<i>68</i>
<i>Poland</i>	<i>ITB</i>	<i>8<sup>th</sup> of November 2012</i>	<i>93</i>
<b><i>Total</i></b>			<b><i>1231</i></b>

### **5.1. France Seminar**

The MACS<sup>+</sup> seminar was held by CTICM on the 8<sup>th</sup> of November 2012 in Paris. More than 50 persons have taken part in the seminar, where they could discuss with seminar speakers not only the new possibilities of calculation with the membrane action but also on all the possibilities given by the EN versions of the Fire parts of Eurocodes and also their application conditions in the context of the French fire regulation. The participants were from different building branches, such as steel

construction companies, building control offices, building design offices, building owners, architects, fire brigades and regulators.

Programme of the seminar is given in Figure 5-1.

An USB key including all technical documents and presentations of MACS<sup>+</sup> project as well as the software, was distributed to the participants. Furthermore participants received a folder with printed PowerPoint presentations to lead them through the seminar.

At the end of the day, the feedback of the participants and attendants was very positive.




**Innovations et maîtrise du risque incendie**

Depuis plusieurs décennies, la profession de la construction met tout son savoir-faire pour améliorer la performance des ouvrages en ce qui concerne le risque d'incendie. Les efforts scientifiques et techniques mis en œuvre ont permis de développer une large gamme de solutions innovantes, aboutissant à la réalisation d'ouvrages métalliques non seulement plus sûrs mais aussi plus économiques. Un exemple récent est la mise au point d'un nouveau concept de réalisation pour les bâtiments à ossature métallique, consistant à ne protéger que partiellement les poteaux métalliques de plancher mixte et ainsi la robustesse a été mise en évidence par de nombreux essais aussi bien à échelle réduite qu'à échelle réelle.

Cette journée a pour objet d'illustrer en premier lieu les solutions constructives actuellement disponibles pour assurer la résistance au feu des ouvrages en acier, et les moyens de justification adaptés en matière. Par ailleurs, un bureau d'études et un laboratoire agréés témoignent respectivement de leurs expériences sur la procédure de vérification de la résistance au feu à travers des exemples concrets de constructions métalliques dont la tenue au feu est basée sur des conceptions spécifiques et innovantes. La deuxième partie de cette journée sera consacrée en détail aux divers aspects techniques de la méthode de calcul simplifiée relative au comportement en situation d'incendie des planchers mixtes partiellement protégés, ainsi qu'à son outil d'application concret permettant à tout concepteur de déterminer de façon efficace les solutions adaptées.

Cet événement est parfaitement intégré dans le cadre du projet RECS Macs+ de démonstration de la technique Eurocode et RECS Eurocode et Fibec. Nous remercions vivement tous les intervenants pour leur contribution précieuse.

**Informations et inscription**  
8 novembre 2012 - Théâtre Adyar, Paris 7<sup>e</sup>

**Organisateurs:**  
CTICM et Aciac  
en partenariat avec Animateur

**Lieu:**  
Théâtre Adyar - 4 Square Rapp - 75007 Paris



**Associations:**  
CTICM - Service Formation  
Généraliste Paris  
Tél : +33 (0) 1 47 23 23 01  
www.cticm.com

**Correspondance:**  
CTICM - Service Formation  
Espace Technologique  
7 Avenue des Minimes  
Bâtiment Agulle  
91191 Saclay Cedex  
Tél : +33 (0) 1 12 12 00 - Fax : +33 (0) 1 12 12 01  
formation@cticm.com

**Innovations et maîtrise du risque incendie**  
Journée technique - Paris

**8 novembre 2012**





**Innovations et maîtrise du risque incendie**

**Matinée : généralités**

9h30 Accueil

10h00 Ouverture de la journée et introduction

10h15 Réglementation incendie relative à la justification de la résistance au feu des ouvrages Ministère de l'Intérieur.

10h45 Résistance au feu des structures métalliques - solutions constructives (CTICM), - justifications (Iffecy France).

11h45 Etudes de cas: - parking en superstructure à l'aéroport de Toulouse-Magnac (E2C Atlantique), - centre commercial à Thionville (CSTB).

12h15 Déjeuner

**Après-midi : méthodologie Fraçof**  
(présentation CTICM - AnimateurMétal)

14h00 Introduction du projet RECS Macs+ : Calcul au feu des planchers mixtes acier-béton avec poutres métalliques pleines et ajourées sous l'effet de membranes

14h10 Observation du comportement du plancher mixte acier-béton sous feu réel

14h40 Nouvelles évidences expérimentales du comportement au feu du plancher mixte acier-béton

15h10 Pause

15h30 Méthode de calcul simplifiée relative à la résistance au feu du plancher mixte acier-béton partiellement protégé

16h00 Exemples de conception et logiciel d'application

16h30 Clôture

**INSCRIPTION**  
8 novembre 2012 - Théâtre Adyar, Paris 7<sup>e</sup>

Nom et patronyme \_\_\_\_\_

Raison sociale \_\_\_\_\_

Adresse \_\_\_\_\_

Code postal \_\_\_\_\_

Ville \_\_\_\_\_

Pays \_\_\_\_\_

Tel. \_\_\_\_\_

Fax \_\_\_\_\_

E-mail \_\_\_\_\_

■ Retour à  
CTICM - Service Formation  
Espace Technologique  
7 Avenue des Minimes  
Bâtiment Agulle  
91191 Saclay Cedex  
Tél : +33 (0) 1 12 12 00 - Fax : +33 (0) 1 12 12 01  
formation@cticm.com






Figure 5-1 : Flyer and program of the French seminar



**Figure 5-2 : Some pictures of the French seminar**

## **5.2. Netherlands Seminar**

The Seminar was organised by BMS the 6<sup>th</sup> of December in Breda near the Belgian border. The seminar was highly appreciated by the participants, as shown by an inquiry filled in by the participants.

55 persons subscribed to the seminar of which 48 attended. From the persons participating were 24 structural engineer (50 %), 3 fire engineer (6 %), 5 steel contractor (10 %), 3 general contractor (6 %), 11 (steel) supplier (23 %) and 2 others (principal, education) (4 %). 42 participants were Dutch; 6 Belgian (Flemish).

The pictures show the first speaker, ing. Rob Stark (introduction), and the last speaker, ir. Pascal Steenbakkers (practical cases). In between dr. Ralph Hamerlinck gave 5 presentations about the backgrounds of MACS+, the simple design method and the software.



**Figure 5-3 : Two of the speakers during the seminar in Breda.**

### 5.3. German Seminar

Date: 28.11.2012 (12.00 - 16.00)  
Venue: Akademie der Ingenieure  
Hellmuth-Hirth-Str. 7  
73760 Ostfildern



Figure 5-4 : Speaker during the German seminar

### 5.4. Spain Seminar

The MACS+ conference was held in Bilbao in the “BIZKAIA ARETOA”, which is a new modern auditorium of the Basque Public University, on Tuesday 18th of December 2012.

74 people attended the conference.



Figure 5-5 : “BIZKAIA ARETOA” building in Bilbao

#### Building Description

The building donated by BBK, to Basque Public University, is a building designed by the Portuguese architect in 1992 awarded the Pritzker Prize Álvaro Siza and stands as a new architectural landmark in Bilbao. This university infrastructure in the heart of Bilbao will host all sorts of events academic, cultural and scientific.

The auditorium has more than 9,000 m<sup>2</sup> and has parking, a large 2,300 m<sup>2</sup> ground floor and four upper floors as 'L'. It has a mixed structure of steel and concrete slab. The exterior walls are clad in white marble material also present in the interior stairs, while the two that make the L are covered with gray tiles are colored craft with light.



Figure 5-6 : Fernando Morente from Tecnalía was one of the speaker

**Spaces and building applications**

BIZKAIA ARETOA has three auditoriums, Mitxelena, Baroja and Arriaga; a room with capacity for 69 people, and four exhibition spaces, Chillida, Oteiza, Axular and Etxepare. It has meeting rooms and computer, a garden terrace, and various ancillary spaces. It hosts also, various university departments, as the store of the UPV / EHU, Uniberts, located at street level, a meeting room that will host various university bodies, including the Governing Council, and the headquarters of the Department of Scientific Culture and the Institute of Euskara, Basque Language.

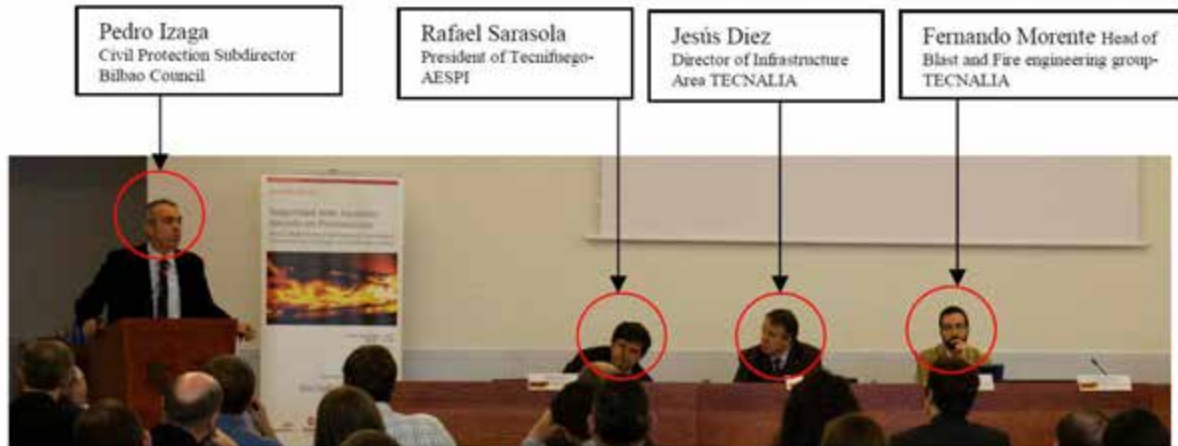
During the conference, the different documents were distributed to the participants.



Figure 5-7 : View during the conference

## Local Authority Meeting

The meeting was held during the café break of the Conference. The attendees to this meeting were:



**Figure 5-8 : View of the attendees**

All the attendees were agreeing to encourage the performance based fire safety design among the designers and architects, in order to promote the usage of alternative solutions without reducing the required safety levels described in the normative building codes.

Moreover, the attendees were so impressive about the all presented European harmonized research works related to Membrane action in fire design of composite slabs with solid and cellular steel beams, in the different European Research projects, and especially with the verification and validation of the tests with numerical studies and simplifying them to useful analytical design method implemented in an user-friendly software.

### 5.5. Estonia Seminar

The seminar took place on the 3<sup>rd</sup> of December, 2012 in Tallinn, Tallinn University of Technology. Target group for the seminar was chosen according to the analysis of the needs of different specialist groups and previous long time experience in training specialists in the field of construction and design.

The number of participants was 55, which is considered good in the country with total population of 1,4 million.

The audience consisted of engineers from design offices and construction companies, academic persons. Officials and trainers of rescue field were also represented. People came from different locations, not only from Tallinn (the capital).

The presentations of the main part of the seminar were based on the MACS+ project materials (Engineering Background, Design Guide and software) and presented by representatives of TUT (partner in the Project), who had experience in structural fire design before the Project and were specially trained in the course of the Project.





The only guest lecturer was the Head of the Supervisory Division, Estonian Rescue Board. The Supervisory Division represents the authorities and is responsible for the monitoring of fire safety in buildings in the country. The presentation gave basis to the topic of the day and created a logical link between the requirements and the new methods of design to fulfill the requirements. The presentation convinced, that the authorities are very positively minded towards the advanced methods of fire safety design, if only they are handled by experts and professionals.

Copies of slides and CD with design software were delivered. Project material in the form of books, was also distributed to the participants.

### **Meeting with authorities**

In the course of the project, representatives of Tallinn University of Technology (partner in MACS+) had a meeting with Mr Rait Pukk, the chief of the fire safety department at Estonian Rescue Service. The fire safety department is responsible for monitoring and supervision of fire safety of buildings in the country. The meeting took place during the preparing phase of the project seminar on October 24, 2012 in the office of the Rescue Services.

We agreed about the presentation of Mr Pukk at the seminar, organised in the project. The presentation would provide the audience the general principles and approach of the fire safety department to fire safety issues, regarding the target group and the general objective of the seminar. We introduced the project, its objectives and workpackages. In general the fire safety department is very positively minded towards the advanced methods of fire safety design, if only they are handled by experts and professionals. Tallinn University of Technology has long lasting and good cooperation with the Rescue Service and it is recognised as an independent expert institution in the construction field. As Mr Pukk will take part in the seminar, he will have a more thorough presentation of the membrane action method. He also received all the background and supporting documentation.

The general conclusion is that new methods can be introduced, if they are sufficiently validated. Application of the new methods is handled case by case by the authorities. The same is valid for the membrane action method.

### **5.6. Czech Seminar**

Date: 11. 09. 2012 (9.30 - 13.00)  
Venue: CTU in Prague, Faculty of Civil Engineering  
Thakurova 7  
Prague 6  
Czech Republic

This seminar was oriented to new developments in fire design of structures and focussed to fire behaviour of steel and composite floor systems. Particularly relevant theme was application of simple design method, which considers the behaviour of an assembly of structural members acting together. Large-scale fire tests carried out in a number of countries have shown that the fire performance of composite steel framed buildings with composite floors (concrete slabs connected to steel beams by means of headed studs) is much better than indicated by standard fire resistance tests on isolated composite slabs or isolated composite beams. Analysis reveals that this excellent fire performance is due to the development of tensile membrane action in the reinforced concrete slab and the catenary action of steel beams. Therefore the simple design method on the basis of membrane action of steel and concrete composite floor has been developed which allows designers to take advantage of the inherent fire resistance of a composite floor plate without the need to resort to complex finite element analysis of whole building behaviour. Simple design method and fire behaviour of steel and composite floor systems were head parts of the seminar.

The seminar was held at The Czech Technical University in Prague. It was jointly organised by The Professional Chamber of Fire Protection and The Ministry of The Interior, General Directorate of Fire Rescue Service of the Czech Republic. The seminar was total attended by 164 participants (109 preregistered), mainly fire authorities, design engineers and fire engineers (see list of participants in attachment). Photos from the seminar and the programme of the seminar are followed.



**Figure 5-9 : Seminar entry in Praha**



**Figure 5-10 : Seminar in Praha (view 1)**



**Figure 5-11 : Seminar in Praha (view 2)**

**Meeting with authority**

Date: 21. 02. 2012, 9:00-11:00

Venue: Ministry of Interior, General Directorate of Fire Rescue Service of the Czech Republic, Kloknerova 26, 148 01 Praha 414, Czech Republic

Present:

- Ministry of Interior: plk. Ing. Drahoslav Ryba,
- Director General of FRS CR, plk. Ing. Rudolf Kaiser,
- Director for Department of Prevention, pplk. Ing. Květa Skalská,
- Department of Prevention Czech Technical University In Prague: prof. František Wald, Ing. Eva Dvořáková, Ing. Jan Bednář

The meeting was held at Ministry of Interior, General Directorate of Fire Rescue Service of the Czech Republic. On the agenda was the education in structural fire engineering, cooperation of partners and new knowledge in structural fire engineering. The opportunity of European design standards were discussed in contents of Czech Republic and application of new knowledge. The history and current stage of fire safety of composite floors was stresses.

**5.7. Italy Seminar**

**Le costruzioni in acciaio – La progettazione in caso di incendio dei solai composti acciaio-calcestruzzo** (Istituto Superiore Antincendio, Roma - 29 Novembre 2012).

The seminar was held at the Istituto Superiore Antincendio of the Corpo Nazionale dei Vigili del Fuoco in Rome. This hall is one of the most widely in national auditors in order to present technical seminars concerning the issue of fire safety. This is because this is a place easily accessible by the designers, by the researcher and also allows the participation of the national firemen.

Informazioni per la partecipazione

Roma, 29 novembre 2012  
**MACCS**  
 Istituto Superiore Antincendi  
 del Corpo Nazionale Vigili del Fuoco  
 Via dei Colonnati, 12 - Roma

L'Istituto Superiore Antincendi è raggiungibile con metropolitana (linea D) e autobus urbano. Della linea 400 metri dalla stazione F.lli. Celentano, collegata con l'Anagnino internazionale di Fiumicino.

Per informazioni:  
 @STRUCTURIA Engineering  
 Via Biana 10, 57100 Livorno  
 Tel. (+39) 0586 814030, Fax (+39)0586 814010  
 E-mail: info@structuria.it

**LE COSTRUZIONI IN ACCIAIO**  
 la progettazione in caso di incendio dei solai composti acciaio-calcestruzzo

Con la recente evoluzione della normativa tecnica sono stati aggiornati i criteri di valutazione della sicurezza strutturale in caso di incendio. In questo nuovo progetto si è studiato la costruzione in acciaio ha emerso alcuni aspetti cruciali per assicurare elementi di innovazione nel processo della progettazione strutturale con l'obiettivo di migliorare le prestazioni delle strutture di acciaio e gli standard di controllo del rischio di incendio.

I risultati di questo impegno hanno consentito di sviluppare i criteri progettuali di una serie di soluzioni costruttive. Un recente esempio è lo sviluppo di un nuovo criterio di progettazione per la realizzazione di solai a letto in acciaio, che impiegano travi e solai composti acciaio-calcestruzzo e che richiama la protezione parziale delle travi. L'efficacia di questo criterio progettuale è stata dimostrata mediante simulazioni sperimentali, sia in piccoli solai che in solai reali.

La giornata tecnica di approfondimento è dedicata alla presentazione di questo innovativo criterio di progettazione degli edifici realizzati con strutture di acciaio. Essa si svolge con l'illustrazione del comportamento generale dei solai composti acciaio-calcestruzzo, dei nuovi criteri di calcolo e degli strumenti applicativi a disposizione del progettista per dimensionare situazioni tecniche sottoposte alle diverse esigenze del progetto.

L'evento è organizzato nell'ambito del progetto RECS MACCS in un parco europeo. In aggiunta tutte le parti interessate per i suoi contenuti scientifici.

**Documentazione tecnica del seminario**

Ai partecipanti, regolarmente iscritti, sarà distribuita una copia della documentazione tecnica del progetto RECS, consistente in:

- il volume "Stati scientifici"
- il volume "Criteri alla progettazione"
- i software e i manuali di software applicativi MACCS

**MACCS** in collaborazione con

**GIORNATA TECNICA DI APPROFONDIMENTO**  
 Innovazione nella progettazione per il controllo del rischio di incendio

Roma, 29 novembre 2012

**LE COSTRUZIONI IN ACCIAIO**  
 la progettazione in caso di incendio dei solai composti acciaio-calcestruzzo

**Il progetto MACS+**

Le prove di resistenza al fuoco su grande scala condotte in diversi paesi e le analisi degli incendi che si sono recentemente verificati in edifici reali hanno mostrato che la protezione degli edifici a forte uso strutturale in acciaio e cemento armato-calcestruzzo possono essere migliorati in questo modo: creare tralicci provati di resistenza al fuoco su elementi locali.

Finalità dei risultati del programma di prove di resistenza al fuoco in grande scala condotte sul sito presso Garbagnate Milanese: gli anni 1995 e 1996, è stato sviluppato un modello di calcolo semplificato basato sull'effetto membranario del sistema composito acciaio-calcestruzzo. Questo metodo consente di progettare il lavoro contro dell'effetto membranario e di valutare la resistenza al fuoco del sistema piano composto senza necessità di ricorrere alla complessa analisi agli elementi finiti del comportamento di una porzione significativa dell'intero edificio.

Questo lavoro consente di progettare molto più facilmente alla maggior parte dei progetti e delle autorità proposte al sistema. Pertanto è stata elaborata una documentazione tecnica finalizzata a fornire le informazioni necessarie per consentire la comprensione di questa metodologia e gli strumenti per la sua corretta applicazione.

La documentazione tecnica è presentata attraverso seminari che si svolgono in 10 paesi europei e sarà distribuita i partecipanti regolarmente tutti.



**LE COSTRUZIONI IN ACCIAIO**  
La progettazione in caso di incendio  
dei solai composti acciaio-calcestruzzo

13:30 Ascolto del lavoro  
Piero CUBIO - CNVVF - Direttore Centrale DCPST  
Claudio MASTROGIANNI - CNVVF - Dirigente Area V DCPST  
Evoluzione della Norma Tecnica per la Protezione  
Estrinseca (Fire) - Servizio Tecnico Centrale del Consiglio  
Superiore dei Lavori Pubblici

14:00 Il comportamento in caso di incendio del sistema di  
edilizia composita acciaio-calcestruzzo  
Sandro PASTORIS - Structure Engineering

14:30 La base teorica del metodo  
Erika FAGGI - Università degli Studi "Gabriele D'Annunzio"  
di Pescara

15:00 Le prove di carico e sperimentale  
Sandro PASTORIS - Structure Engineering

15:30 Lo stato parametrico  
Claudio CROCI - Università degli Studi "La Sapienza" di Roma

16:00 L'applicazione nell'ambito della normativa nazionale  
Luca FANTUCCI - CNVVF - Area V DCPST

16:30 Esempi di applicazione  
Paolo FERRI - Structure Engineering

17:00 Discussioni

**SCHEDA ISCRIZIONE**  
Roma, Istituto Superiore Antincendi  
29 novembre 2012

**LE COSTRUZIONI IN ACCIAIO**  
la progettazione in caso di incendio  
dei solai composti acciaio-calcestruzzo

Nome e cognome \_\_\_\_\_  
Ragione sociale \_\_\_\_\_  
Indirizzo \_\_\_\_\_  
Codice postale \_\_\_\_\_  
Città \_\_\_\_\_  
Paese \_\_\_\_\_  
Tel. \_\_\_\_\_  
Fax \_\_\_\_\_  
E-mail \_\_\_\_\_

Regole per la partecipazione:

- La partecipazione è gratuita. Per ricevere e ricevere inviare la scheda di iscrizione compilata all'indirizzo e-mail: info@strueng.it
- Saranno accettate iscrizioni fino ad un numero massimo di 80 partecipanti
- Termine di iscrizione: entro il 27 novembre 2012
- Per informazioni contattare: STRUCTURA Engineering Via Botta 35, 57100 Livorno Tel. (+39) 0586 834333 Fax (+39)0586 834610 E-mail: info@strueng.it



Figure 5-12 : Invitation flyer for the seminar in Italy

The seminar was held according to the schedule reported in the Invitation, with the participation of the national working group of protection who participated in the European project, of some national authorities and some expert researchers in the national contest for the subject treated.

The final discussion was centered mainly on the applicability of the method proposed by the European project in the context of the national legislation in force.

In this regard is to report that the day of the seminar there was a national strike train. This has been mainly due to the difference that can be noted between number of subscribers and number of participants in the seminar.



Figure 5-13 : Seminar MACS+, Istituto Superiore Antincendio, Roma - 29 Novembre 2012

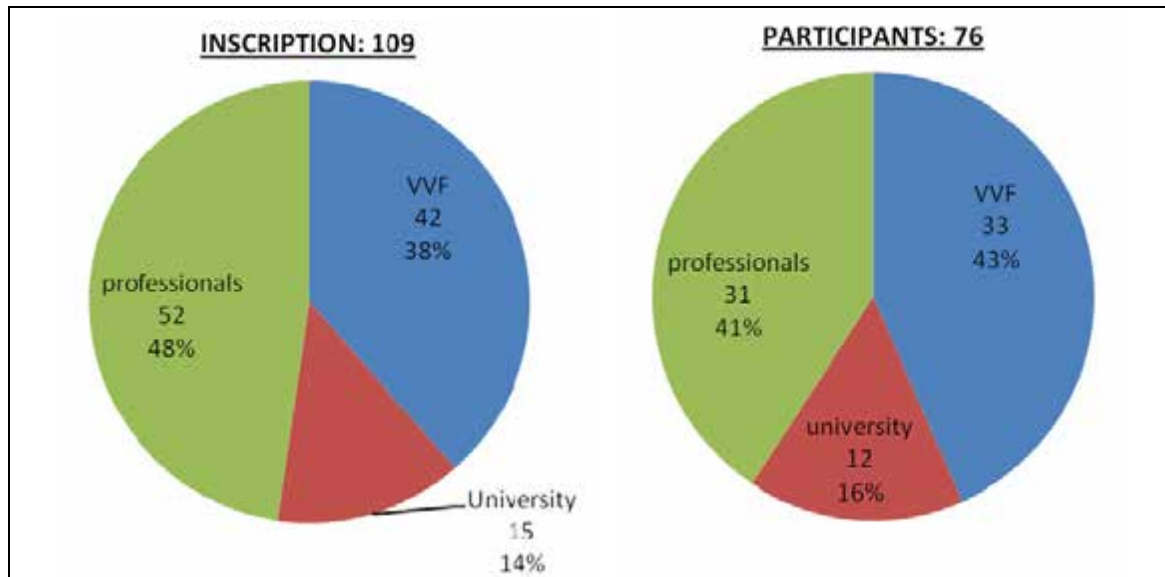


Figure 5-14 : Participation rate to the seminar in Roma

### 5.8. Portugal Seminar

The seminar was held at the Order of Engineers, the Professional Associations of Engineers, in Lisbon, on December 10 of 2012. More than 90 participants attended the seminar and the feed back was very positive. The opening session had the presence of Dr. Henrique Vicêncio representing the National Authority for Civil Protection of the Ministry of Home Affairs who was one of the invited speakers, Dr. Carlos Matias Ramos President of the Order of Engineers, Eng. Cristina Machado President of the Civil Engineers Association as well as the President of LNEC, Dr. Carlos Pina, which proves the interest of the Portuguese authorities to the problematic of fire safety. These three personalities have spoken in the open session.

The invited speakers were Dr. Carlos Pina who has spoken on the status of implementation of the Eurocodes in Portugal and Dr. Henrique Vicêncio who has given an over view of the process of implementation of the new Portuguese regulation on fire safety of buildings, introduced in Portugal in the beginning of 2008.

The other speakers were Prof. Paulo Vila Real who gives the welcome to the participants, an overview of the project MACS+ as well as talked about the behaviour of composite slabs under fire conditions and the advantage of taking in to account the development of membrane actions; Dr. Nuno Lopes has presented experimental tests and numerical simulations and Eng. Ricardo Correia has presented a case study. All the presentations and the software MACS+ are available on the following web page of the Department of Civil Engineering of the University of Aveiro:

<http://www.ua.pt/decivil/PageText.aspx?id=16315>

Prof. Paulo Vila Real took the opportunity of the presence of Dr. Henrique Vicêncio from ANPC at the Seminar, to explain the benefits of taking in to account the effect of membrane actions on the fire resistance of composite slabs. ANPC is the authority that approves the fire safety projects in Portugal.

Concluding:

Date: December 10, 2012

Nº of participants: 90

Invited Speakers: Dr. Henrique Vicêncio, ANPC - National Authority for Civil Protection of the Ministry of Home Affairs  
Dr. Carlos Pina, President of LNEC - Nacional Laboratoty of Civil Engineering

Other Speakers: Prof. Paulo Vila Real, University of Aveiro

Dr. Nuno Lopes, University of Aveiro  
Eng. Ricardo Correia



**Figure 5-15 :** Opening Session table. From left: Eng. Cristina Machado (President of the Civil Engineers Association), Dr. Carlos Pina (President of LNEC), Dr. Carlos Matias Ramos (President of the Order of Engineers), Dr. Henrique Vicêncio (Director of the Unit Risk Prediction and Alert, ANPC) and Prof. Paulo Vila Real (President of the Organizing Committee of MACS+ Seminar)

## Seminário

# COMPORTAMENTO AO FOGO DE ESTRUTURAS MISTAS AÇO-BETÃO: NOVA METODOLOGIA DE CÁLCULO

Auditório da Sede da Ordem dos Engenheiros em Lisboa  
10 de Dezembro



Incêndios reais e ensaios à escala real têm demonstrado que as lajes mistas aço-betão apresentam uma resistência ao fogo superior àquela que resulta do cálculo baseado na avaliação do seu comportamento como elemento estrutural isolado trabalhando essencialmente à flexão. As grandes deformações provocadas pela perda de resistência devido ao aumento da temperatura favorecem o desenvolvimento de esforços de membrana nas lajes, responsáveis pelo aumento da sua resistência ao fogo.

A Universidade de Aveiro e a Ordem dos Engenheiros, no âmbito do projecto Europeu MACS+, envolvendo 19 Países, organizam este seminário que se destina a divulgar uma nova metodologia de cálculo de lajes mistas aço-betão em situação de incêndio que tem em conta os esforços de membrana referidos. Os participantes no seminário receberão documentação e software de cálculo que será objeto de demonstração através da sua utilização a um caso de estudo real. Será também feito o balanço da implementação dos Eurocódigos Estruturais em Portugal, bem como da nova regulamentação de segurança contra incêndios em edifícios.

### Programa

14h00 – Recepção dos Participantes

14h15 – *Sessão de Abertura*

14h45 – *Os Eurocódigos Estruturais: Estado da sua implementação em Portugal*

- Eng. Carlos Pina, Presidente do LNEC

15h10 – *Balanço da implementação da regulamentação de segurança contra Incêndios em edifícios*

- Dr. Henrique Viçêncio, Autoridade Nacional de Protecção Civil

15h35 – *O comportamento de lajes mistas aço-betão em situação de incêndio: Observação de casos reais*

- Prof. Paulo Vila Real, Universidade de Aveiro

16h00 - Intervalo / Coffee-Break

16h25 – *Fundamentos do método de cálculo*

- Prof. Paulo Vila Real, Universidade de Aveiro

16h50 – *Ensaio experimentais e simulações numéricas*

- Prof. Nuno Lopes, Universidade de Aveiro

17h15 – *Caso de estudo e apresentação de Software*

- Eng. Ricardo Correia

17h40 – *Debate e Conclusões*

18h15 – *Encerramento*

### Organização:



### Apoios:



Para inscrição consultar site da Ordem dos Engenheiros:  
<http://www.ordemengeheiros.pt/ot/agenda/2012/12/>  
Morada: Av. António Augusto de Aguiar n.º3D, 1069-030 - Lisboa  
Telefone: 213 132 600  
Fax: 213 524 632  
E-mail: [secretariogeral@ordemengeheiros.pt](mailto:secretariogeral@ordemengeheiros.pt)

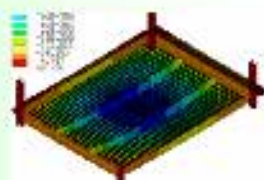
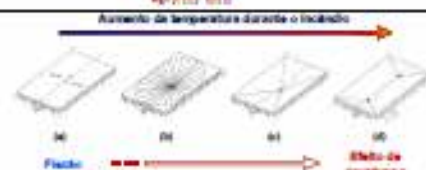


Figure 5-16 : Program of the Portuguese seminar



**5.9. UK Seminar**

For the workshop dissemination event to be held in England, to conclude the MACS+ research project, the city of London was chosen as the most suitable location to host the event. The Welcome Collection conference centre was chosen as the most appropriate venue, due to its central location and vicinity to London Kings Cross, with the aim of attracting the largest target audience possible.

In order to attract a suitable audience, the format of London event comprised a free to attend, half day conference with a variety of speakers, splitting presentations in to discrete blocks. The presentations included discussed the background, theory and practical application of the MACS+ design methodology, in conjunction with some general background information on structural fire engineering.

In total (including speakers) the event attracted 74 delegates on the day, from a variety of backgrounds, with feedback that the overall format and content of the conference was very informative and useful. Each delegate was provided with an A5 printed copy of the design guide and background document, in conjunction with a USB memory stick containing the design software.

Due to the nature of the building design process and regulations in England, numerous building control checking consultants, fire authorities, local authorities and specialist fire design consultants were invited to attend the conference, in addition to the main target audience of consultant structural engineers. Through this we allowed for a transparent process to discuss the MACS+ methodology to both design engineers and checking authorities at the same time, with unbiased comments from a range of speakers and allowing for an open dialogue of questions on the subject. Following which, no adverse comments or reservations against using the methodology in appropriate circumstances were raised.



**Figure 5-17 : Photographs of speakers from ASD Westok and Arup during the conference**

**5.10. UK Northern Ireland Seminar**

The Seminar was organised by the university of Ulster the 15<sup>th</sup> of November 2012 unUlster. 96 persons coming from different profiles (Engineering offices, firemen, authorithies, academics, steel fabricators, fire consultant,..) attended the seminar.

The programme and invitation can be found herafter.

**Fire Safety Training Workshop: New European  
Fire Design Guidance Including Cellular Steel Beams**

# Innovative Construction Design for Fire Safety Engineering

**Venue: Ulster University, Jordanstown  
Loughview conference room  
15 November 2012,  
Belfast, UK**



**During the workshop printed and electronic version of the data will be distributed to the participants. The data consists of all the presentations, documents and freely available software.**



**Further Information Contact workshop chairman:**  
Prof Ali Nadjai, Head of Fire Structures Division  
BEng(H), MSc, PhD, CEng, MStructE, MIFireE  
Tel +44(0)28 90368294  
email: [a.nadjai@ulster.ac.uk](mailto:a.nadjai@ulster.ac.uk)



Main Sponsor: Coal and Steel European Commission



Figure 5-18 : Invitation for the UK Northern Ireland Seminar

## Innovative Construction Design for Fire Safety Engineering: European Training Course

Morning Session	Afternoon Session
08:00 - 08:50 Workshop Registration	
09:00 Official Opening: Professor Stanley McGreal BERE Director	
Chair – Prof Colin Bailey/ Prof Ali Nadjai	Chair – Prof Faris Ali/ Prof Michal Delichatsios
09:15 – 09:45 Large scale fire testing: focusing on the lessons learnt  <b>Tom Lennon</b>  Structural Fire Engineering, BRE Global, Bucknalls Lane, Garston, Watford,	14:00 – 14:30 Fire safety engineering: the industrial challenge  <b>Ahmed Allam /Paul Bryant</b>  12th Floor Capital Tower, 91 Waterloo Road London SE1 8RT
09:45 - 10:15 New European Design software for composite floor with longer span cellular beams  <b>Ali Nadjai</b>  School Built Environment, FireSERT, Block 27, University of Ulster	14.30 - 15:00 Heat Fluxes and Toxic Gases in Enclosure Fires  <b>Michael Delichatsios</b>  School Built Environment, FireSERT, Block 27, University of Ulster
10:15 - 10:45 Break for coffee	15:00- 15:30 Break for coffee
10:45 – 11:15 Fire Behaviour of Steel and Composite Floor Systems: Simple Design Method  <b>Colin Bailey</b>  The University of Manchester, Manchester, M13 9PL, UK	15:30- 16:00 Performance of EHS Columns Subjected to severe Fire  <b>Faris Ali</b>  School Built Environment, FireSERT, Block 27, University of Ulster
11:15 – 11:45 Structural design for fire overview and Cellular Beam Recent Design Developments  <b>Peter Dixon</b>  ASD Westock, Valley Farm Way, Stourton, Leeds LS10 1SE	16:00- 16:30 Lessons from the Rosepark Care Home Tragedy  <b>Janathan Hayes</b>  Building Control, Armagh City and District Council The Palace Demesne Armagh BT60 4EL
11:45 - 12:00 Roundtable Discussion	16:30 - 16:45 Roundtable Discussion
12:00 - 14:00 Break for lunch	16:45 End of the workshop
16:45- 17:00 Official closing: Professor Ian Montgomery- Dean of the Faculty	



**Figure 5-19 : Programme for the UK Northern Ireland Seminar**

## Innovative Construction Design for Fire Safety Engineering: European Training Course

Having in hands the new knowledge acquired in the Cardington fire test, in FICEB+ and COSSFIRE and the tools such as the design guide and software developed in the Leonardo Da Vinci project, it is time to inform design offices and authorities in number of European countries and to educate them to utilise in their design all the mechanisms activated in this type of structure in fire conditions.

The added value is in the fact that the results of research currently accessible mainly by researchers will be presented to practicing engineers throughout Europe. By translating the design guides and software to local languages, the partners will access even broader audience.

### Booking form/No Fees

Name (s) \_\_\_\_\_

Company/Institution \_\_\_\_\_

Position \_\_\_\_\_

Address \_\_\_\_\_

Telephone \_\_\_\_\_ Fax \_\_\_\_\_

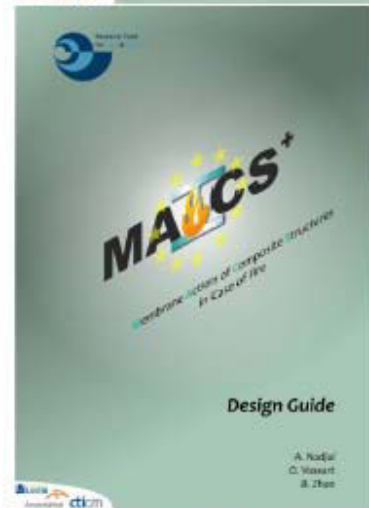
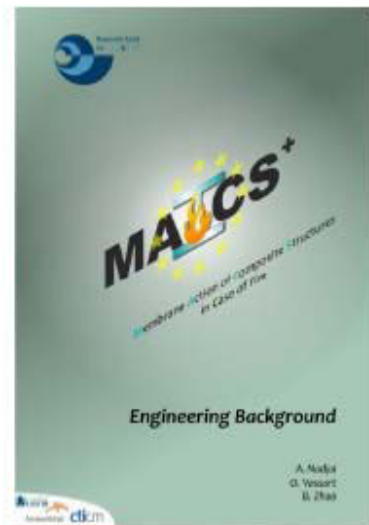
E-mail \_\_\_\_\_

**Please contact Miss Louise Sabolocka**  
Course Administrator, to book your place.  
Tel: 02890 366603 Fax: 02890 366523  
E-mail: [l.sabolocka@ulster.ac.uk](mailto:l.sabolocka@ulster.ac.uk) or [a.nadai@ulster.ac.uk](mailto:a.nadai@ulster.ac.uk)

**Please note that places are limited, so early booking is recommended to avoid disappointment.**

**Venue:** Ulster University, Loughview conference room  
Jordanstown Campus, Shore Road, Newtownabbey,  
Co-Antrim, BT37 0QB  
**Date:** Thursday 15<sup>th</sup> November 2012

**Maps and directions for the Jordanstown campus:**  
<http://www.ulster.ac.uk/information/location/jordanstownsigns.html>  
<http://www.ulster.ac.uk/information/location/jordanstowncampus.html>



Free Copies of the new EU Design Guidance and Software will be provided



Figure 5-20 : Booking form for the UK Northern Ireland Seminar

## 5.11. Sweden Seminar

All documents have been adapted to Swedish National Annex and translated to Swedish. The method and underlying principles was presented to Boverket (National Board of Housing, Building and Planning) at a meeting november 7. Participants were Björn Mattson (Boverket) and Björn Uppfeldt (SBI). The conclusion was that in Sweden it is allowed to use other methods than the Eurocodes as long as they can be verified. The method presented in the project Macs+ is no exception.

The seminar was held from 13-17 on 11<sup>th</sup> December in Stockholm. The seminar was held in connection with a seminar on composite structures at normal temperatures. Invited speakers were Rob Stark and Ralph Hammerlinck from Bouwen met Staal in the Netherlands. Structural engineers and Fire design engineers in a total of over 1000 people were personally invited by e-mail. An invitation was also sent together with the magazine Nyheter om Stålbyggnad to over 9000 people and an advert was published on the SBI website. The seminar was free of charge and the presentation material as well as the Macs+ documents (in Swedish) were handed out at the seminar as well as made available at the SBI website for download. In total 39 people attended the seminar, see the list of attendees on the following page.

Pictures from the seminar and the invitation with the full program are shown here after:



**Figure 5-21 : A part of the interested audience**

Kurser om samverkanskonstruktioner  
11 december på Westmanska Palatset, Holländargatan 17 i Stockholm

# KURSER

## Kurs i samverkanskonstruktioner

Kursen riktar sig till konstruktörer och behandlar samverkansbalkar, -bjälklag och -pelare, den innehåller också teori blandat med praktiska exempel.

Föreläsare: Professor Rob Stark, Holland (OBS föreläsningarna är på engelska)

### KURSPROGRAM

- 09:00-09:30 Samverkanskonstruktioner i Eurokod 4
- 09:30-10:00 Samverkansbalkar
- 10:00-10:30 Kaffe
- 10:30-11:15 Samverkansbjälklag
- 11:15-11:45 Samverkanspelare
- 11:45-13:00 Lunch

### Kostnad

1750:- för medlemsföretag och 2500:- för övriga.  
SBI:s nya läromedel Publikation 193 Samverkanskonstruktioner - stål och betong ingår i deltagaravgiften.

## Kurs i brandutsatta samverkanskonstruktioner

Denna kurs i brandutsatta samverkanskonstruktioner är en del i projektet MACS+ och genomförs med stöd av Research Fund for Coal and Steel (RFCS).

Föreläsare: Ralph Hammerinck, Bouwen met Staal, Holland (OBS föreläsningarna är på engelska)

### KURSPROGRAM

- 13:00-14:30 Samverkanskonstruktioner i brand enligt Euro kod 4 del 1-2
- 14:30-15:00 Kaffe
- 15:00-17:00 Membranverkan i brandutsatta samverkansbjälklag. Genomgång av ny beräkningsmodell, beräkningsexempel och kostnadsfri programvara

### Kostnadsfritt

anmälan skickas senast 3 december till maria@sbi.se eller 08-661 02 80



**SBI** Stålbyggnadsinstitutet  
The Swedish Institute of Steel Construction

Figure 5-22 : Swedish invitation to the MACS+ seminar

## 5.12. Hungary Seminar

The Symposium was held in Budapest, in the lecture hall of the Iron and Steel Industry Association.

The event had about 70 participants. The lecturers represented very diverse areas: from the National Directorate General for Disaster Management Sándor Roland major spoke about the new OTSZ 5 (National Fire Safety Regulations). Károly Jármái spoke about the details of MACS+ project. Described the Engineering background and the Design guide and showed the MACS+ software for calculation. From the EMI Office representative Mónika Hajpál spoke about the fire tests, from the Danube Fire Protection Inc. Tibor Sebestyén spoke about concrete structures in fire. János Butcher from TÜV Rheinland colors discussed practical aspects of fire protection. What are the problems faced by the fire protection professionals in the design and execution of context? We heard a lecture on the scientific dimension of composite slab design from Viktória Vass and László Horváth from TU Budapest, as well as from the industry István Kotormán from Lindab Ltd.

In the MACS+ project each participant received two books: Engineering background and the Design guide, which are 154 and 79 pages describing the membrane effect calculation and applicability. They got the MACS+ software for calculation on a CD-ROM on which the presentations, the MACS + calculation program can be found.

The conference participants argued that they appreciated the symposium, because it combined the theoretical calculations, design aspects and went through the qualification of the technical issues connected with the subject of fire protection. They got a lot of useful information.



Sándor Roland from the National Directorate General for Disaster Management



Participants



Figure 5-23 : Hungary seminar (view 1)



Participants



Karoly Jarmai lecture about MACS+



Karoly Jarmai lecture about MACS+



Janos Zellei, president of Danube Fire Protection Ltd.

**Figure 5-24 : Hungary seminar (view 1)**

### 5.13. Romania Seminar

The Seminar was organised at the “Politehnica” University of Timisoara, Faculty of Civil Engineering, in 7 December 2012, in the “Constantin Avram” Amphitheatre.

The Seminar was free of charge, no fees were asked to the participants. A coffee break and a buffet lunch at the end of the event were offered to the participants.

More than 50 persons attended the event, representing authorities, experts and design checkers, academic staff and engineering offices. It is emphasised the participation of the Romanian authority for fire safety, from 6 different regions of Romania (Inspectorates for Emergency Situations – I.S.U.).



**Figure 5-25 : Romania Seminar (view 1)**





**Figure 5-26 : Romania Seminar (view 2)**

The seminar was opened by the Dean of the Faculty of Civil Engineering, Prof. Gheorghe LUCACI and by Assoc. Prof. Raul ZAHARIA, coordinator of the MACS+ project for the “Politehnica” University of Timisoara. Before the lectures of the MACS+ Seminar, Prof. Dan DUBINA, Corresponding member of the Romanian Academy, had a contribution concerning the harmonisation of Romanian national standards for fire safety in the European context and the importance of collaboration between the fire authorities and designers.



**Figure 5-27 : Romania Seminar (view 3)**

The lectures on MACS+ Seminar were presented by Assoc. Prof. Raul ZAHARIA, responsible of MACS+ project for the “Politehnica” University of Timisoara.

In the first part of the Seminar, two theoretical lectures were included: the first one about the principles of fire calculation and the second one about the theoretical basis of the fire design method for composite slabs, including the experimental programmes. These presentations were followed by a coffee break of 30 minutes.



**Figure 5-28 : Romania Seminar (view 4)**

After the coffee break, in the second part of the Seminar, the formulation of the fire design method for partially protected composite floors with solid and cellular steel beams was presented in detail, followed by the design examples.

The participants showed a great interest on the topic of the Seminar. At the end of the Seminar, the free discussions lasted for more than one hour (the lunch scheduled initially at 13:30, started around 14:00).



**Figure 5-29 : Romania Seminar (view 5)**

After the lunch, the meeting with the relevant authorities started in the same location. At the meeting participated relevant Romanian authorities for fire security, together with experts and project checkers (in Romania there are no check offices, this activity is sustained by experienced individual engineers, attested by the Ministry of Public Works). All these persons participated to the Seminar. All the participants had a positive reaction regarding the implementation of the fire design method for composite slabs in practice.

The use of the fire parts of the Eurocodes in the design practice will be enforced in Romania, by the new National Normative for Fire Security (which will be officially issued in 2013) in which it is clearly stated that for the evaluation of the fire resistance of the structural elements, the calculation methods of the Eurocodes should be used. In the previous normative, only the fire tests were mentioned in the evaluation of the fire resistance of the structural elements. In this context, taking also into account that, in fact, the design method for the evaluation of the fire resistance of composite slabs using the membrane effect is based on the acknowledged engineering principles and calculation methods provided in the Eurocodes, the participants to the meeting agreed that the design method may be used for real projects in Romania.

### 5.14. Lithuania Seminar

Vilnius Gediminas Technical University have organized 2 workshops in Vilnius:

First was organized at December 18, 2012, for designers and personal of construction companies, staff of universities and students.



**APIE MACS+ PROJEKTA**

Seminaras skirtas įgalinti žmonių su kompozitinių plieninis-betoninių perdangomis išlaidų tyrimų apžvalga ir atsparumo ugniai skaičiavimo, taikant naują paprastesnį skaičiavimo metodą, pristatymu. Pristatomi paprastesnio skaičiavimo metodo pagrindai, parodoma, kad šiuo metodu galima pagrįsti gaisro veikiamos perdangos garantuojamą konstrukcinę saugą atsilveigus į jos membraninę elgseną, o per aptariamus praktinių skaičiavimų pavyzdžius parodomos galimybės pritaikyti jį gaisro inžinerijoje. Paprastesnio metodo rezultatai palyginami su daugelyje pasaulio šalių atliktų natūralaus dydžio pastatų gaisrinių bandymų ir šiluminių stebėjimų metu bei sudėtingesniais skaičiavimo metodais gautais rezultatais. Apžvelgiama kompiuterinė programa, skirta skaičiuoti kompozitinių plieninis-betoninių perdangų su naujo gaisro poveikio apsaugotomis ir neapsaugotomis vientisomis ir skykliuotomis plieninėmis sijomis atsparumą ugniai.

Šis seminaras pirmiausia turėtų sudominti:

- gaisrinės saugos specialistus;
- architektus ir inžinierius, rengiančius projektuojamų pastatų ir konstrukcijų gaisrinės saugos priemonės arba išduodančius statybos leidimus;
- universitetų ir aukštųjų mokyklų studentus.

Dalyviams bus perskaityti pranešimai (pagal programą) pristatantys MACS+ projekto rezultatus. Visiems bus įteiktas USB atmintinė su projekto MACS+ medžiaga, du leidiniai – „Projektavimo vadovas“ ir „Inžineriniai pagrindai“, bei kompiuterinė skaičiavimo programa, skirta praktiškai taikyti naują paprastesnį konstrukcijų elgsenos ugnyje skaičiavimo metodą. Dalyviams bus įteiktas pažymėjimas apie išlaikytas paskaitas.

Dalyvavimas seminare yra nemokamas iš anksto patvirtinus dalyvavimą ir užsiregistravus (tel. 852745228; faksu 852370569 arba el. paštu [steel@vgtu.lt](mailto:steel@vgtu.lt)).

**SEMINARO PROGRAMA**

Data: 2012 m. gruodžio 21 d.  
Vieta: VGTU Saulėtekio al. 11,  
Auditorinio korpuso Senato posėdžių salė

Programa:

10<sup>00</sup> seminaro dalyvių registracija  
10<sup>30</sup> seminaro atidarymas  
Sveikinimo žodis - VGTU kancleris  
doc. dr. Arūnas Komka  
Sveikinimo žodis - EK Anglijos ir plieno tyrimų fondo projekto „MACS+“ VGTU dalies vadovas prof. habil. dr. Audronis Kazimieras Kvedaras

11<sup>00</sup>, 12<sup>00</sup> **1-oji dalis**  
1-oji dalis – Tikrųjų gaisrų apžvalga (pranešėjas asist. Žygmantas Blaževičius)  
2-oji dalis – Nauji eksperimentų duomenys (pranešėjas doc. dr. Gintas Saučiūnas)

12<sup>30</sup>, 13<sup>00</sup> **Kavos pertraukėlė**

13<sup>00</sup>, 14<sup>00</sup> **2-oji dalis**  
3-oji dalis – Paprastesnis skaičiavimo būdas (pranešėjas prof. habil. dr. Audronis Kazimieras Kvedaras)  
4-oji dalis – Paprastesnio skaičiavimo būdo skaitinė parametrinė analizė (pranešėjas prof. dr. Arūnas Sapalas)

14<sup>00</sup>, 15<sup>00</sup> Seminaro uždarymas  
Prof. habil. dr. Audronio Kazimiero Kvedaro pasisakymas  
Seminaro medžiagos padalinimas



Europos komisijos Generalinio tyrimų departamento Anglijos ir plieno tyrimų fondo MACS+ projekto „Membraninis poveikis skaičiuojant kompozitinius plieninių su vientisomis ir perforuotomis plieninėmis sijomis elgsenų ugnyje – norminimas“.

**PARTNERIAI**

ARCELOMITAL BELVAL & DIFFERDANGE S.A., „ARCELOPROFE“, Luxemburg	CENTRE TECHNIQUE INDUSTRIEL DE LA CONSTRUCTION METALLIQUE „CTICM“, France
BOUWEN MET STAAL „BOUWMI“, Netherlands	BAUFORMSTAHL BV BFL „BFLV“, Germany
FUNDACION TECNICA RESEARCH & INNOVATION „TECHALLA“, Spain	TALLENBA TENSILBLOEK TECHNICAL UNIVERSITY OF TALLEN „TUTAL“, Estonia
CEHEŢ VYSOKÉ UČENÉ TECHNICKÉ V PRAHE „CTU“, Czech Republic	STRUKTURA INŽENIERING „STRUKO“, Belg
UNIVERSITATE DE AVERIG „IAVE“, Portugal	ASB WESTOX LIMITED „WESTOXLED“, United Kingdom
UNIVERSITY OF ULSTER „ULUP“, United Kingdom	STALBYGOS NAUDODUODUOTIŲ ISTITUTAS „STALBYG“, Sweden
METALLOI BOVTEEM UNIVERSITY OF MEGHOLE „UMR“, Hungary	UNIVERSITATEA POLITEHNICA DEI TRAIANIA „TUTP“, Romania
VILNIAUS GEDIMINO TECHNINIO UNIVERSITETAS Lithuania	BIBLOS LOGARISMASIOS KONSTRUKCIJŲ AEROSTATILIS PASIRYTIKOSIOS TRIS SALONIS ARISTOTELE UNIVERSITY OF TRIGALONIS „AUTH“, Greece
UNIVERSITA V LAWLJANA „ULJL“, Greece	UNIVERSITY TECHNICAL BODOWLANE „UBB“, Poland
UNIVERSITE DE LIEGE „ULOG“, Belgium	

Figure 5-30 : MACS+ Lithuanian seminar invitation (Part 1)

**Informacija dalyviams**

**Registracija:**  
 Telefonu 8 5 2745228  
 Faksu 8 5 2370569 arba  
 El. paštu [steel@vgtu.lt](mailto:steel@vgtu.lt) (nurodant temą-  
 MACS+ seminaras)

**Rengėjai:**

VILNIAUS GEDIMINO  
TECHNIKOS UNIVERSITETAS

OF. Mėšalinių ir medinių  
konstrukcijų katedra  
MŠ "Kongresas"

**Organizatoriai:**  
 prof. habil. dr. Audronis Kazimieras Kvedaras  
 doc. dr. Gintas Šaučiūvenas  
 prof. dr. Artanas Šapatas  
 asist. Žygmantas Blaževičius  
 Nijolė Dzikatė  
 Rimantė Mikulųytė  
 Nikolajus Vaškevičius

Iš Geležinkelio (Autobusų) stoties į VGTU, Saulėtekio al. 11 (žemėlapyje žymima 1) važiuoti troleibusu nr.2 iki stotelės „Gedimino technikos universitetas“  
 Iš įvairių miesto vietų iki „Gedimino technikos universitetas“ stotelės taip pat važiuoja troleibusai nr.10, nr.14, nr.19 ir nr.21, bei autobusai nr.5, nr.18, nr.30 ir nr.45.



1 - Vilniaus Gedimino Technikos  
Universitetas  
Saulėtekio al. 11 (Senato posėdžių salė).  
Vilnius LT- 10223  
Lietuva

**KVIETIMAS !**  
 Gaisrinės saugos inžinerinių žinių  
 sklaidimo  
**SEMINARĄ**



Plieninių ir kompozitinių perdangų  
konstrukcijų elgsena gaisro metu

2012 m. gruodžio 21 d., Vilniuje



VILNIAUS GEDIMINO  
TECHNIKOS UNIVERSITETAS

**Figure 5-31 : MACS+ Lithuanian seminar invitation (Part 2)**

Total number of participants was 59 (23 participants from industry, 22 participants from staff of universities and 5 participants – students).

Here also take part 9 participants representing the local authorities, such as Department of Fire Safety and Rescue of Home Office (3 participants), Centre of Certification of Building Products and Centre of Project Expertize of the Ministry of the Environment (6 participants), in spite that these representatives were invited for next workshop specially for local authorities.



**Figure 5-32 : Prof. A. K. Kvedaras presenting his lecture in workshop**

All participants were supplied with 2 Editions in Lithuanian (Design Guide and Engineering Background), flashes with all workshop material including Software, and with the Certificate about heart out a course of lectures. Invitation for this workshop is attached. For participants café break was organized. Some discussion about presented during the workshop material was carried out during the café breaks as well as after the seminar. Participants were happy with participation in workshop and knowledge gained in it, which will be very useful in their practice.



**Figure 5-33 : Prof. A. Šapalas presenting his lecture in workshop**

Second was organized at December 21, 2012, for representatives of local authority. Total number of participants was 12 representing the Ministry of Education and Science, Lithuanian Department of Standards, Technical Committees No. 22 (Fire Safety) and No. 38 (Building Structures) of Standardization, Inspecta, LTD, and leadership of Vilnius Gediminas Technical University.

All participants were supplied with 2 Editions in Lithuanian (Design Guide and Engineering Background), flashes with all workshop material including Software, and with the Certificate about heart out a course of lectures. Invitation for this workshop is attached. For participants café break was organized. Some discussion about presented during the workshop material was carried out during the café breaks as well as after the seminar. Participants were happy with participation in workshop and knowledge gained in it, which will be very useful in their practice.

They paid an attention on large and important material of workshop which will be useful preparing or improving the Lithuanian normative documentation in the field of fire resistance of steel and composite steel and concrete structures. It was said that material received during the workshop will be distributed also between the members of above mentioned Technical Committees of Lithuanian Department of Standards and the leadership of the Department of Fire Safety and Rescue of Home Office.

### **5.15. Greece Seminar**

The Seminar in Greek language took place at the Institute of Steel Structures at the premises of the Department of Civil Engineering, Faculty of Engineering, Aristotle University of Thessaloniki, Greece on Sunday, November 18th, 2012. There were 20 participants and the lectures were delivered by Prof. Dr.-Ing. C.Baniotopoulos and Dr. Christos Tsalikis. During the Seminar, the MACS+ material that has

been recently translated into Greek, has been presented in details, thoroughly discussed and distributed to the participants in the form of hardcopies.

In addition, the Greek research group presented the MACS+ material to the Northern Greece Firefighting Service and in particular, the produced MACS+ material has been given to the contact person who was Vice-Major Dr. Dimitrios Tsatsoulas. Interesting discussions on the MACS+ proposed procedures took place between the research group members and the Firefighting Service staff.

The invitation is a multi-column document. On the left is the MACS+ logo with the text 'International Journal of Construction Management in Case of Fire'. The main body contains a detailed Greek text paragraph about the seminar's purpose. To the right, there are logos for 'ArcelorMittal' and 'cticm'. At the bottom right is the 'ARISTOTLE UNIVERSITY OF THESSALONIKI' logo. The text includes dates and times for various sessions: 10:00-10:30 (Registration), 10:30 (Start), 12:15-12:30 (Lunch), and 17:00 (End).

Figure 5-34 : MACS+ Greek seminar invitation (Part 1)

This part of the invitation includes contact information, a map, and event details. The 'Επικοινωνία' (Contact) section provides an email address (info@macs+.gr) and a website (www.macs+.gr). The 'Τοποθεσία Ημερίδας' (Event Location) section features a map of Thessaloniki with a red circle and arrow pointing to the event location, and a small photograph of the building. The 'Ημερίδα-παραδείση Ευρωπαϊκού προγράμματος' (European program demonstration day) section states the event is on 'Κυριακή 18 Νοεμβρίου 2012' at the 'Εργαστήριο Μεταλλικών Κατασκευών Θεσσαλονίκη'. The MACS+ logo and the Aristotle University of Thessaloniki logo are also present.

Figure 5-35 : MACS+ Greek seminar invitation (Part 2)

### 5.16. Slovenia Seminar

The seminar in Slovenia was organized by the University of Ljubljana and the Faculty of civil and geodetic engineering (<http://www3.fgg.uni-lj.si/en>). The seminar, held at the Faculty of civil and geodetic engineering lasted one day and it took place on the 27th of November 2011 in the afternoon from 1500 to 1900. All documents and Power Point presentations were translated in the Slovenian language. Each participant received the paper copy of MACS+ publication in the Slovenian language as well as the DVD media with the MACS+ software and the electronic version of the publication. All seminar documents are freely accessible on the web page <http://www.macsfire.eu>.

The lectures were given by Prof. Darko Beg and Dr. Franc Sinur from the University of Ljubljana. The subject of the seminar was the technical background of the simple design method of fire resistance of composite floors and the application of this method. Prof. Darko Beg presented the technical background of the simple design method, the full scale fire tests (CARDINGTON, COSSFIRE, FRACOF, FICEB), the numerical model verification and numerical parametric study and finally the evidence of real fires. The participants were very enthusiastic about the seminar topic and the seminar was concluded by a very productive discussion. Dr. Franc Sinur presented the design software to the participants, who actively built numerical model in the MACS+ software and solved two given problems.

In the audience there were 40 experts from design offices and also 10 students of the University of Ljubljana. The seminar was free of charge for all participants.



**Figure 5-36 : Prof. Darko Beg giving a lecture on behaviour of structures in cas of fire**



**Figure 5-37 : Introduction of design software by Dr. Franc Sinur**



**Figure 5-38 : The participants**

### **5.17. Belgium Seminar**

The University of Liege was responsible for the organisation of the seminar in the French speaking part of Belgium for Belgium and Luxembourg in order to present the findings from several previous research projects (RFCS project FRACOF,...) and the accompanying measures project MACS+ to practitioners and Authorities.

The organization of the workshop started right after the first project meeting. The invitation distributed to the targeted people can be found hereafter.





## Action membranaire dans les structures mixtes soumises au feu

Alors qu'il était traditionnel de protéger contre l'incendie toutes les poutres métalliques des planchers mixtes acier-béton lors de la réalisation de bâtiments à ossature métallique, un nouveau concept de réalisation consistant à ne protéger que partiellement les poutres du plancher mixte a été développé, dont la robustesse a été mise en évidence par de nombreux essais aussi bien à échelle réduite qu'à échelle réelle.

Cette solution innovante permet de tirer parti de l'action membranaire qui se développe dans les dalles mixtes en condition d'incendie, conduisant à la réalisation d'ouvrages économiques et sécuritaires.

Cette manifestation sera consacrée aux principes de base de ce concept, aux aspects techniques de la méthode de calcul simplifiée relative au comportement en situation d'incendie des planchers mixtes partiellement protégés, ainsi qu'à son outil d'application convivial permettant à tout concepteur de dimensionner un plancher mixte selon cette méthode en accord avec les Eurocodes.

Cet événement est organisé dans le cadre du projet RFCS Macs+ de dissémination de la recherche Fraucof et RFCS Cossfire et Faceb. Nous remercions vivement tous les intervenants pour leur contribution volontaire.

### INSCRIPTION

13 Décembre 2012 - Université de Liège

Nom et Prénom

Raison sociale

Adresse

Code postal et Ville

Pays

Tél.

E-mail

- Séminaire gratuit
- Inscription avant le 30/11/2012  
Comprend les exposés, les documents d'information en version papier et électronique et la pause café
- Inscription après le 30/11/2012  
Comprend uniquement les exposés et la pause café
- Bulletin à renvoyer à :  
Sabine Houten  
Département ArGenCo - Université de Liège  
Tel : +32 4 3669357  
Sabine.Houten@ulg.ac.be

### Informations et inscriptions

Université de Liège  
13 décembre 2012

Organisateurs :  
Université de Liège  
en partenariat avec ArcelorMittal

Lieu et horaire :  
13h30 - 17h30  
Allée du 6 Août, 13  
Sart Tilman - 4000 Liège  
Bâtiment B6d - Salle R30



Inscription :  
Sabine Houten  
Département ArGenCo - Université de Liège  
Tel : +32 4 3669357  
Sabine.Houten@ulg.ac.be

## ACTION MEMBRANAIRE DANS LES STRUCTURES MIXTES SOUMISES AU FEU



### Action membranaire dans les structures mixtes soumises au feu



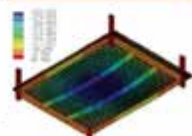

Programme :	17h00 Présentation du logiciel de calcul MACS+ relatif à la méthode de calcul simplifiée
13h30 Introduction du projet RFCS MACS+ : Action membranaire dans les structures mixtes soumises au feu	17h15 Questions-réponses
13h40 Présentation du laboratoire d'essais au feu de l'ULg et du logiciel SAFIR	17h30 Clôture
14h00 Observation du comportement de planchers mixtes acier-béton sous feux réels	Présentations :
14h30 Nouvelles preuves expérimentales du comportement au feu de planchers mixtes acier-béton	T. Fohn (Université de Liège)
15h00 Pause-café	J.M. Franssen (Université de Liège)
15h30 Physique du phénomène et principes de conception	O. Vassart (ArcelorMittal)
16h00 Méthode de calcul simplifiée relative à la résistance au feu du plancher mixte acier-béton partiellement protégée	
16h30 Vérification de la méthode de calcul simplifiée dans tout son domaine par des modèles de calcul avancé	
	
	

Figure 5-39 : Invitation of the Belgian workshop

The workshop took place on December 13<sup>rd</sup> 2012 at the University of Liege, from 13h30 to 17h30.

The workshop registration was organized by the University of Liege and was totally free of charge for the participants.

Finally 68 people from both Belgium and Luxembourg attended the seminar. The complete list of participants is added to this report. The participants were really interested and have asked a lot of question about the applicability of the method, the limitations of its field of application and the legislative aspect. After that all the presentations were done by the speakers, a large time was dedicated to answer to all the questions of the participants.

### **Deliverable**

During the seminar, printed documents (design guide and engineering background) as well as USB key have been distributed that contain all data about the simple design method.

### **Speakers**

<i>Name</i>	<i>Company</i>	<i>Email Adress</i>
Olivier Vassart	ArcelorMittal	olivier.vassart@arcelormittal.com
Jean-Marc Franssen	University of Liege	jm.franssen@ulg.ac.be
Thibaut Fohn	University of Liege	thibaut.fohn@ulg.ac.be

### ***Meeting with Belgian authorities***

### **Location**

SECO Office Brussels (Room Eugène François)

### **Date**

17<sup>th</sup> October (13h30 – 17h30)

### **Attendance**

<i>Name</i>	<i>Company</i>	<i>Email Address</i>
Pieter Poppe	ISIB	Pieter.poppe@isibfire.be
Jean-François Denoël	Febelcem	jf.denoel@febelcem.be
rik debruyckere	SECO	r.debruyckere@seco.be
Jean-Philippe Veriter	Infosteel	jp.veriter@infosteel.be
Stefaan Makkelberg	SPF Intérieur	Stefaan.Maekelberg@ibz.fgov.be
Frederic Ullens	SPF Intérieur	frederic.ulens@ibz.fgov.be

### **Speakers**

<i>Name</i>	<i>Company</i>	<i>Email Adress</i>
Olivier Vassart	ArcelorMittal	olivier.vassart@arcelormittal.com
Jean-Marc Franssen	University of Liege	jm.franssen@ulg.ac.be
Thibaut Fohn	University of Liege	Thibaut.fohn@ulg.ac.be

### **Feeling and outcome**

The simple design method and the physics of the phenomenon of the tensile membrane action acting in composite floor submitted to fire was presented in details.

The Authorities were really interested by this new concept.

It has been mentioned several times that the utilisation of the FRACOF method should be fully allowed without any restriction (i.e. without necessity to have a derogation) when it is applied with the standard ISO fire because this method is based Eurocode principle (material properties and calculation of the temperatures) and simple physical equilibrium. The authorities did not oppose to this statement. Because of the Belgian legislative environment, derogation will be required when the method is applied with a natural fire.

### **5.18. Poland Seminar**

The MACS+ seminar was organised in Warsaw the 8th of November 2012. 93 participants attended the meeting.



**Figure 5-40 : Grzegorz Wozniak presenting his lecture during the MACS+ seminar**



**Figure 5-41 : Andrzej Borowy presenting his lecture during the MACS+ seminar**

### **Meeting with local authorities**

The meeting was held on 6th of November 2012 during the VIIth International Conference Fire Safety of Construction Works.

The topics of the MACS+ project were discussed with:

Chief Commandant of the State Fire Service,

Director of the Office for Emergency Identification of the National Headquarters of the State Fire Service of Poland,

Deputy Director of Department of Spatial Development and Construction in Ministry of Transport, Construction and Maritime Economy,

Deputy General Inspector of Building Control,

Rector-Commandant and management of Main School of Fire Service, several fire experts associated in The Association of Fire Engineers and Technicians.

The results of MACS+ project were presented. The possible ways of implementation of this approach into daily practice was discussed. As the Polish regulations are still written in very prescriptive way at the moment the direct use of this approach in building design is not formally allowed – an administrative decision on each building design is required. The effect of the meeting was that participants became better informed on this modern tool of building fire design.

## 6. CONCLUSION AND OUTLOOK

This project has extended recent RFCS project FICEB+ and COSSFIRE. Results obtained within these two projects related to membrane action are the focus of this dissemination. The first one consisted of large scale natural fire test on a compartment made of composite cellular beams; the second one consisted, among other tests, of one large scale furnace test activating the membrane action with a prescriptive ISO Fire.

Both projects delivered a method, validated by a large scale fire test, which enables to avoid fire protection on most of the secondary beams. This is possible due to the fact that the bearing resistance offered by the beams at room temperature is transformed into a membrane resistance provided by the reinforced concrete slab at room temperature as shown by the following Figure 6-1.

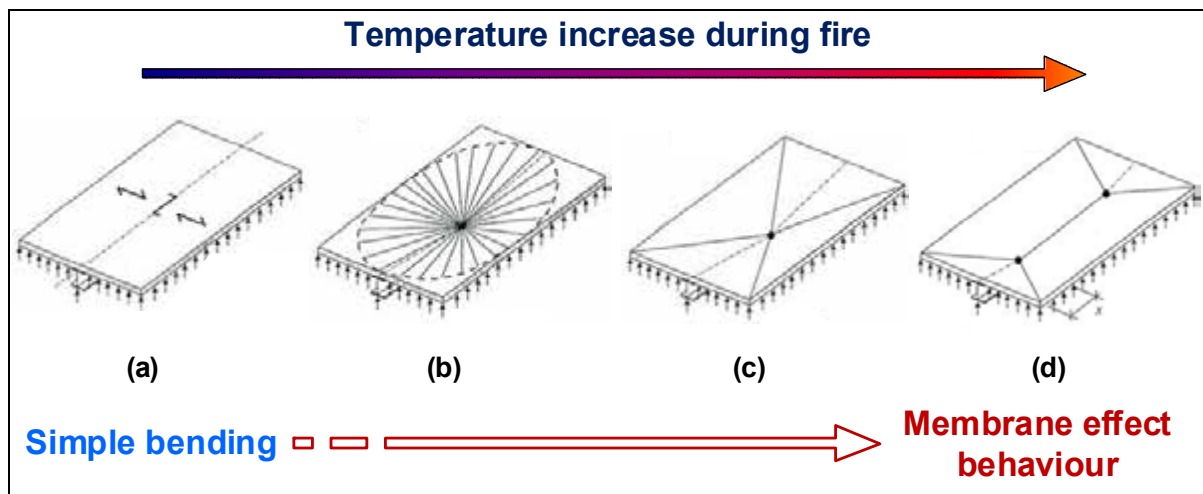


Figure 6-1 : Membrane resistance transformation scheme

The technical objective was to disseminate methodology for design of partially protected composite slabs for fire conditions with a focus on the connections and on Cellular Beams. Number of tests performed in various countries under natural and ISO fire enabled to gain good understanding of the behaviour of such structures. The project was addressed to practicing engineers in various countries and aimed to transfer knowledge about utilisation in their designs of membrane effect, which is created in the reinforced slab during fire.

The project was divided in 4 steps:

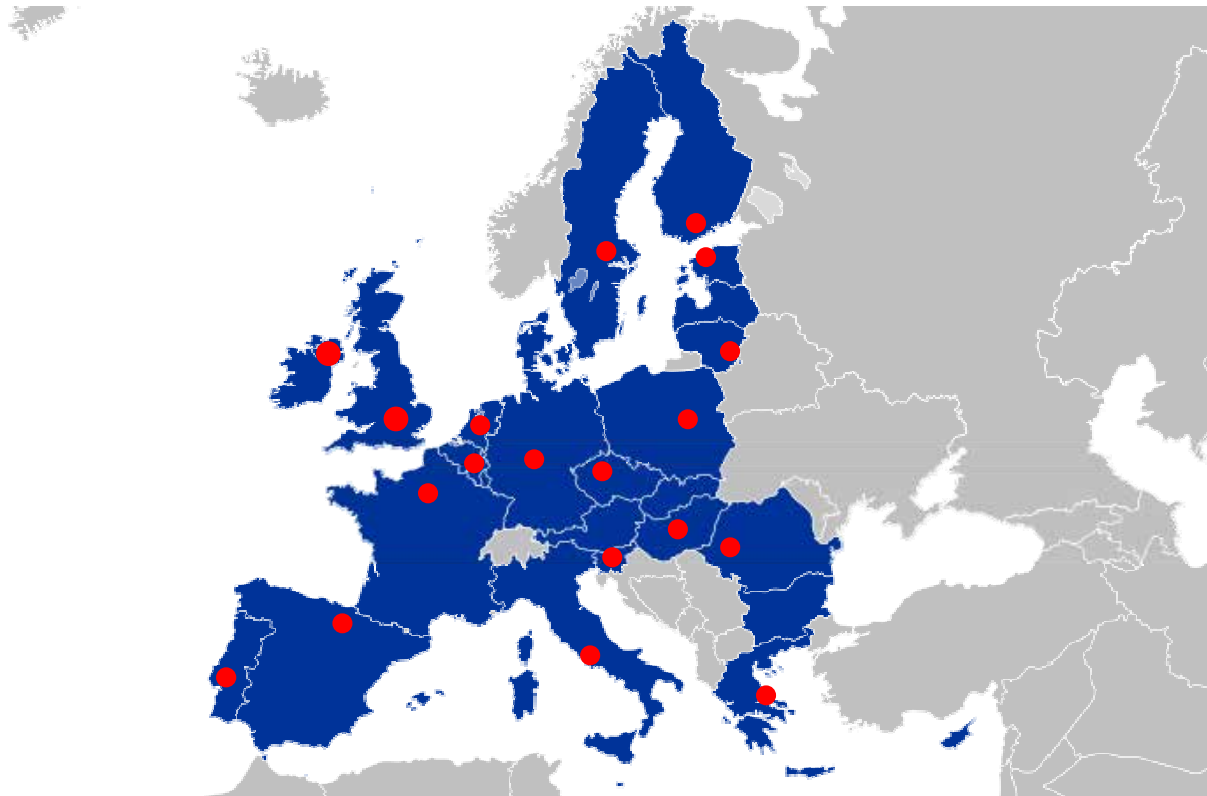
- Realisation of documentation and software about designing of composite floor system with unprotected secondary beams
- Translation of the documentation and software interface
- Training for partners involved in seminars
- Organisation of the Seminars in the different European countries.

The dissemination package consists in different documents and software which are available on the website <http://www.macsfire.eu>

- A design guide explaining how to apply the developed methodologies
- A background document explaining all the laboratory tests performed on membrane action in the last 20 years, summarising all the theoretical development made to define the calculation method.
- The Software MACS+, which is also available on [www.arcelormittal.com/sections](http://www.arcelormittal.com/sections).

- PowerPoint presentations has been realised to present the different documents and the design methodology.
- All the documents have been translated into nearly all the European languages, French, Czech, Dutch, German, Spanish, Italian, Portuguese, Polish, Swedish, Hungarian, Romanian, Lithuanian, Greek, Estonian and Slovenian, which sums up in a total of about **2256 sheets** and **3984 document pages**. In addition the documents have been adapted content to fit with local regulations and local good practice

Seminar were also organised by the different partners in 17 different countries in 16 languages:



**Figure 6-2 : Location of the different seminars that have been organised**

A paper version of the PowerPoint presentations in English is attached in Annex II of this document. Design guide and Background documents are quite long documents but they have been nevertheless attached to this report. All language versions of the documents as well as the free available software can be found on [www.macsfire.eu](http://www.macsfire.eu)

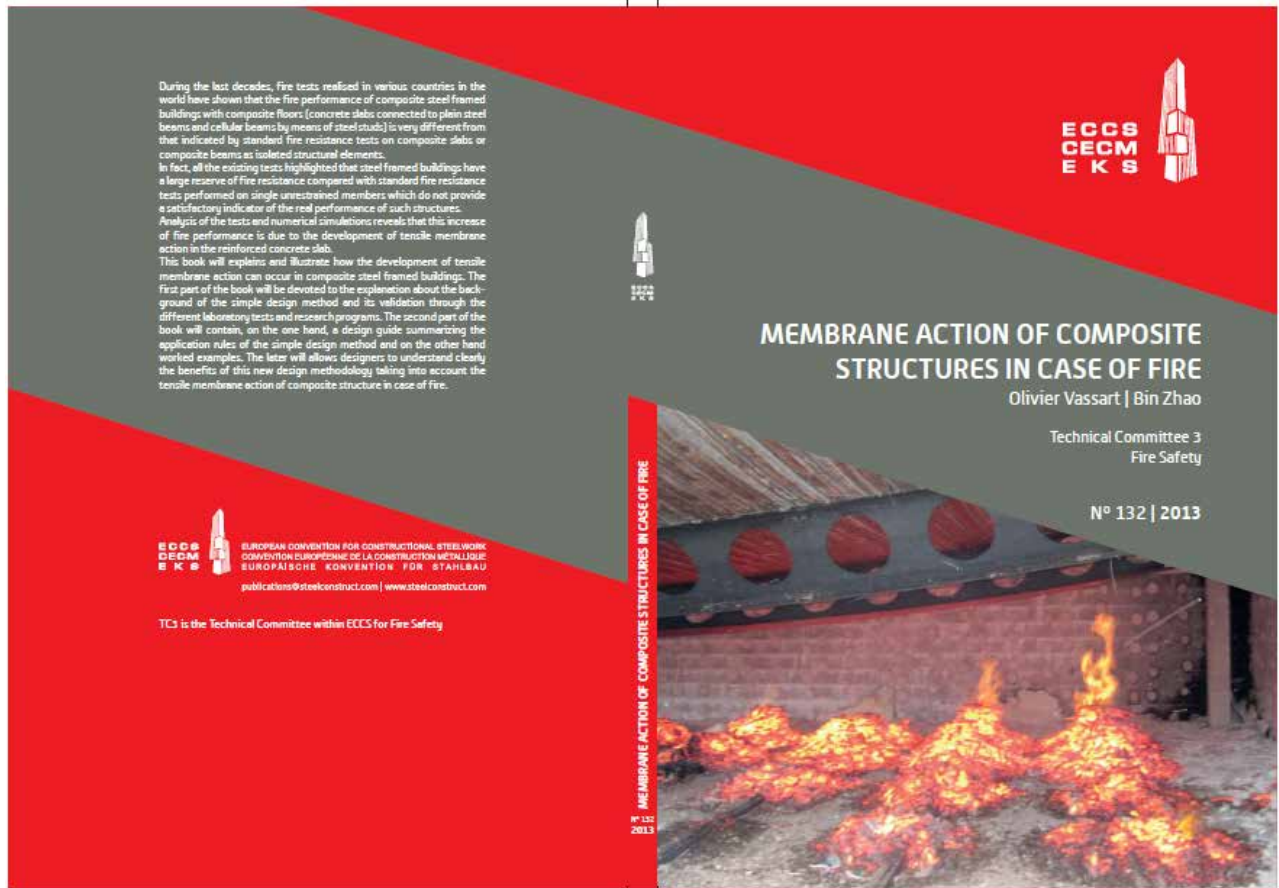
In total 1231 participants attended the different seminars.

***Actions consecutive to the project***

The fire resistance of several projects has been justified by using this innovative calculation technique MACS+:

- one office building in Liège (Belgium)
- Two office buildings in Lausanne (Switzerland)
- Two office building towers in Paris (France)
- One Commercial center in Thionville (France)

A book has been written for the ECCS in order to more largely spread the knowledge.



**Figure 6-3 : Cover sheets of the ECCS brochure**

This book will be published beginning of 2013 by ECCS.

After having done an ECCS design recommendation, the last step will be to introduce directly the membrane action methodology into the Eurocode 4 Fire part. This topic has been added into the agenda of the Evolution group of Eurocode 4 fire part and will be discussed for the next release of Eurocodes.

## 7. LIST OF FIGURES AND TABLES

### List of Figures

Figure I : Cardington test building prior to the concreting of the floors .....	5
Figure II : Cut away view of a typical composite floor construction .....	6
Figure III : View of the composite floor .....	7
Figure IV : Fire test and structural elements after the fire.....	8
Figure 1-1 : Cover page of the Design Guide.....	11
Figure 1-2 : Cover page of the Engineering Background.....	12
Figure 1-3 : Software interface (About MACS+ Software) .....	13
Figure 1-4 : Software interface (DATA) .....	13
Figure 4-1 : Homepage <i>www.macsfire.eu</i> .....	15
Figure 4-2 : Document page <i>www.macsfire.eu</i> .....	16
Figure 5-1 : Flyer and program of the French seminar.....	18
Figure 5-2 : Some pictures of the French seminar .....	19
Figure 5-3 : Two of the speakers during the seminar in Breda. ....	19
Figure 5-4 : Speaker during the German seminar .....	20
Figure 5-5 : “BIZKAIA ARETOA” building in Bilbao .....	20
Figure 5-6 : Fernando Morente from Tecnalia was one of the speaker.....	21
Figure 5-7 : View during the conference.....	21
Figure 5-8 : View of the attendees .....	22
Figure 5-9 : Seminar entry in Praha .....	24
Figure 5-10 : Seminar in Praha (view 1) .....	25
Figure 5-11 : Seminar in Praha (view 2) .....	26
Figure 5-12 : Invitation flyer for the seminar in Italy .....	27
Figure 5-13 : Seminar MACS+, Istituto Superiore Antincendio, Roma - 29 Novembre 2012 .....	27
Figure 5-14 : Participation rate to the seminar in Roma.....	28
Figure 5-15 : Opening Session table. From left: Eng. Cristina Machado (President of the Civil Engineers Association), Dr. Carlos Pina (President of LNEC), Dr. Carlos Matias Ramos (President of the Order of Engineers), Dr. Henrique Vicêncio (Director of the Unit Risk Prediction and Alert, ANPC) and Prof. Paulo Vila Real (President of the Organizing Committee of MACS+ Seminar) .....	29
Figure 5-16 : Program of the Portuguese seminar .....	30
Figure 5-17 : Photographs of speakers from ASD Westok and Arup during the conference.....	31
Figure 5-18 : Invitation for the UK Northern Ireland Seminar .....	32
Figure 5-19 : Programme for the UK Northern Ireland Seminar .....	33
Figure 5-20 : Booking form for the UK Northern Ireland Seminar .....	34
Figure 5-21 : A part of the interested audience .....	35
Figure 5-22 : Swedish invitation to the MACS+ seminar .....	36
Figure 5-23 : Hungary seminar (view 1) .....	37
Figure 5-24 : Hungary seminar (view 1) .....	38
Figure 5-25 : Romania Seminar (view 1).....	38
Figure 5-26 : Romania Seminar (view 2).....	39
Figure 5-27 : Romania Seminar (view 3).....	39
Figure 5-28 : Romania Seminar (view 4).....	40
Figure 5-29 : Romania Seminar (view 5).....	40
Figure 5-30 : MACS+ Lithuanian seminar invitation (Part 1) .....	41
Figure 5-31 : MACS+ Lithuanian seminar invitation (Part 2) .....	42
Figure 5-32 : Prof. A. K. Kvedaras presenting his lecture in workshop .....	42
Figure 5-33 : Prof. A. Šapalas presenting his lecture in workshop .....	43
Figure 5-34 : MACS+ Greek seminar invitation (Part 1).....	44
Figure 5-35 : MACS+ Greek seminar invitation (Part 2).....	44



Figure 5-36 : Prof. Darko Beg giving a lecture on behaviour of structures in cas of fire .....	45
Figure 5-37 : Introduction of design software by Dr. Franc Sinur .....	46
Figure 5-38 : The participants .....	46
Figure 5-39 : Invitation of the Belgian workshop .....	47
Figure 5-40 : Grzegorz Wozniak presenting his lecture during the MACS+ seminar .....	49
Figure 5-41 : Andrzej Borowy presenting his lecture during the MACS+ seminar .....	50
Figure 6-1 : Membrane resistance transformation scheme.....	51
Figure 6-2 : Location of the different seminars that have been organised .....	52
Figure 6-3 : Cover sheets of the ECCS brochure .....	53

### **List of Tables**

Table 5-1 : Organisation of the seminars .....	17
--	----

## **8. APPENDICES**

### **8.1. PowerPoint presentations**

The complete set of PowerPoint presentations in English.

### **8.2. Design guide**

Design guide in English.

### **8.3. Engineering Background**

Engineering Background in English.

## ANNEX I

### PowerPoint presentations







## General Introduction





### Content of presentation



- **Background of the project**
- **Partnership**
- **Acknowledgement**
- **Programme of the seminar**
  - Technical background of simple design method
  - Application of simple design method (design guide)
  - User-friendly design tools

<p>Background of the project</p> <p>Acknowledgment</p> <p>Programme of the seminar</p>	 <h2 style="text-align: center;">Background of the project</h2> 
	<ul style="list-style-type: none"> <li>• <b>New simple design method (1)</b> <ul style="list-style-type: none"> <li>– Full scale fire tests have revealed that the fire performance of global composite floor systems could be much higher than that obtained in standard fire tests with isolated structural members</li> <li>– <b>A new innovative simple design method was developed on the basis of large scale tests (Natural fire)</b></li> <li>– More experimental evidences have been obtained about such good behaviour in long duration ISO fire condition</li> <li>– <b>It provides economic and robust fire resistance solutions for various steel framed buildings</b></li> </ul> </li> </ul>
<p>General Introduction <span style="float: right;">3</span></p>	

<p>Background of the project</p> <p>Acknowledgment</p> <p>Programme of the seminar</p>	 <h2 style="text-align: center;">Acknowledgment</h2> 
	<ul style="list-style-type: none"> <li>• <b>Project sponsored by:</b> <ul style="list-style-type: none"> <li>– <b>European Commission through the programme:</b> <b>Research Fund for Coal and Steel</b></li> </ul> </li> </ul> <div style="text-align: center;">  <p><b>Research Fund for Coal &amp; Steel</b></p> </div>
<p>General Introduction <span style="float: right;">4</span></p>	



## Programme of the seminar



Background of the project

Acknowledgment

**Programme of the seminar**

- **Technical background of simple design method**
  - Fire performance of steel and concrete composite floor systems in real fires (full scale fire tests and accidental fires)
  - **Technical fundamentals of simple design method**
  - New experimental evidences derived from long duration standard fire furnace tests
  - Numerical investigation of simple design method
- **Application recommendations of the simple design method (Design Guide)**
- **User-friendly software and working examples**



## Fire Behaviour of Steel and Composite Floor Systems

*Review of Real Fires*



### Content of presentation



- **Evidence from accidental fire in real buildings**
  - Accidental fire
- **Cardington fire tests**
  - Beam test with burners
  - Frame test with burners
  - Corner tests with wood cribs
  - Demonstration tests with real office furniture





## Cardington fire tests



Cardington fire tests

Evidence from accidental fire

- **Eight storey steel framed building**



Beam to beam joint



Beam to column joint

Review of real fires

3



## Cardington fire tests



Cardington fire tests

Evidence from accidental fire

- **Main parameters of the building**

- Length: 42 m in 5 spans of 9 m
- Width: 21 m in 3 spans of 6 m, 9 m and 6 m
- Height of storey: 4.2 m
- Steel members: UB for beams and UC for columns
- Composite slab: lightweight concrete with a total depth of 130 mm and a trapezoidal steel deck
- Steel mesh: 142 mm<sup>2</sup>
- Steel joints: fin-plates for beam-beam joints and flexible end plates for beam-column joints
- Applied load: sand bags (the load will depend on the test)

Review of real fires

4



## Cardington fire tests



Cardington fire tests

Evidence from accidental fire

- **Video of Frantisek Wald**
  - Too long, must be shorten and then will be sent



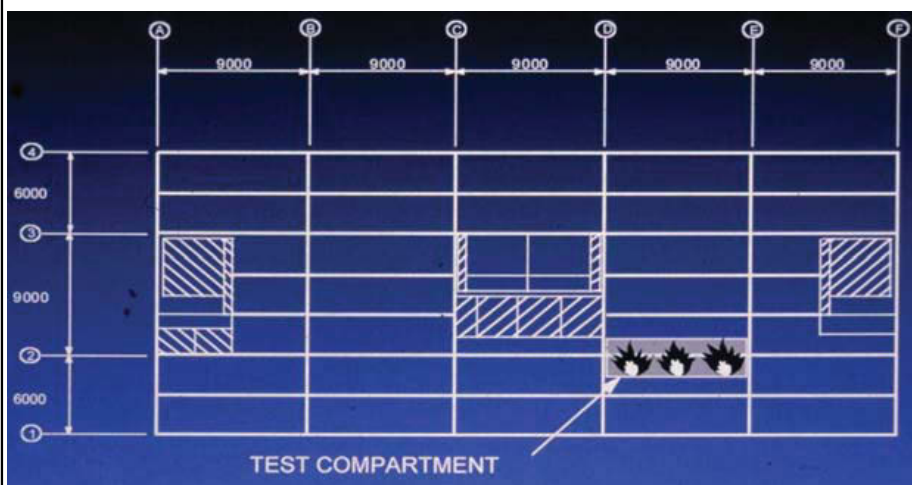
## Cardington fire tests



Cardington fire tests

Evidence from accidental fire

- **Restrained beam test : span = 9.0 m**





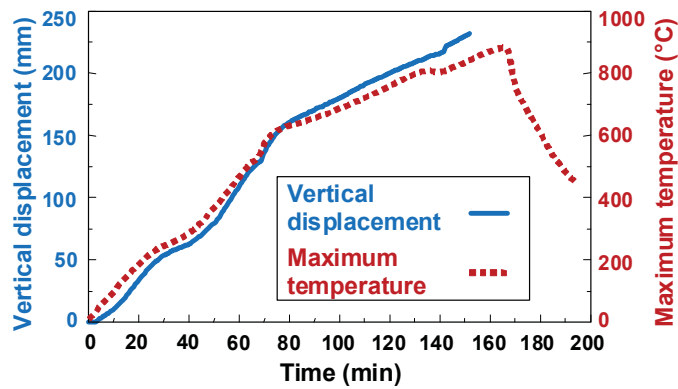
## Cardington fire tests



Cardington fire tests

Evidence from accidental fire

- **Restrained beam test : experimental results**



- **Observation**

- Maximum heating  $\approx 900$  °C
- Deflection of the beam:  $< 250$  mm



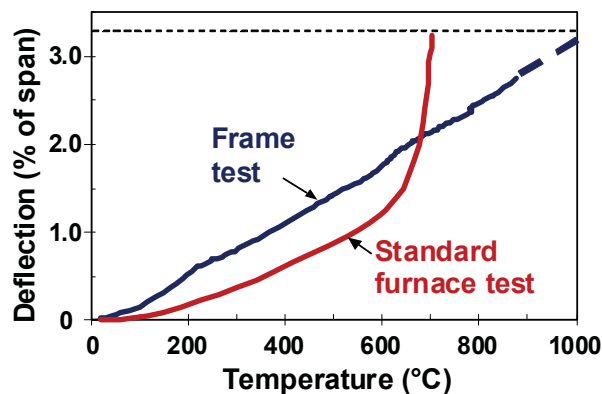
## Cardington fire tests



Cardington fire tests

Evidence from accidental fire

- **Comparison with standard furnace fire test**



- **Conclusion**

- No sign of failure in global composite floor system
- Collapse at  $\theta \approx 650$  °C if simply supported



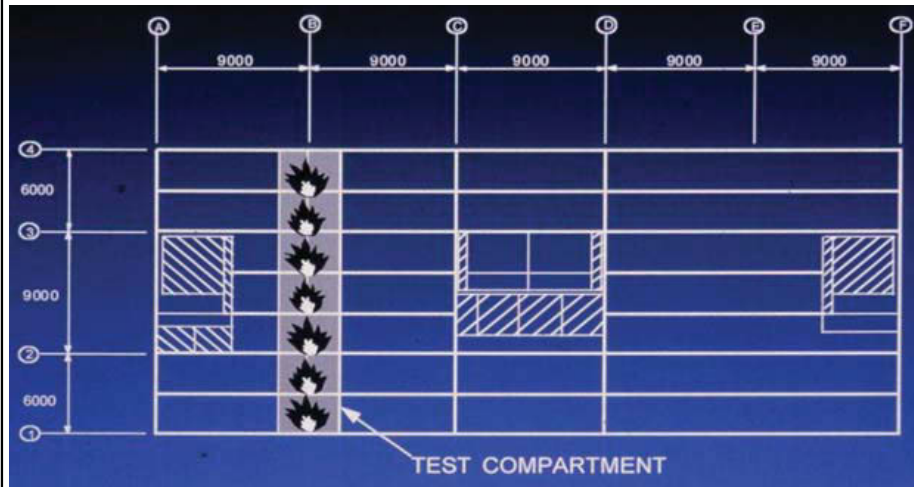
## Cardington fire tests



- Plane frame beam test

Cardington fire tests

Evidence from accidental fire



Review of real fires

9



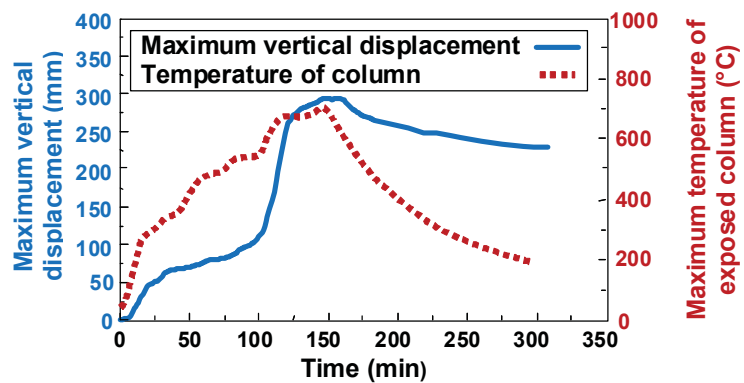
## Cardington fire tests



- Plane frame test : experimental results

Cardington fire tests

Evidence from accidental fire



- Observation

- Maximum heating  $\approx 750$  °C
- Deflection of the beam  $\approx 300$  mm

Review of real fires

10



## Cardington fire tests



Cardington fire tests

Evidence from accidental fire

- Deformed state of heated part of the floor



- Conclusion
  - Squashing of unprotected part of column
  - No further collapse despite above local failure



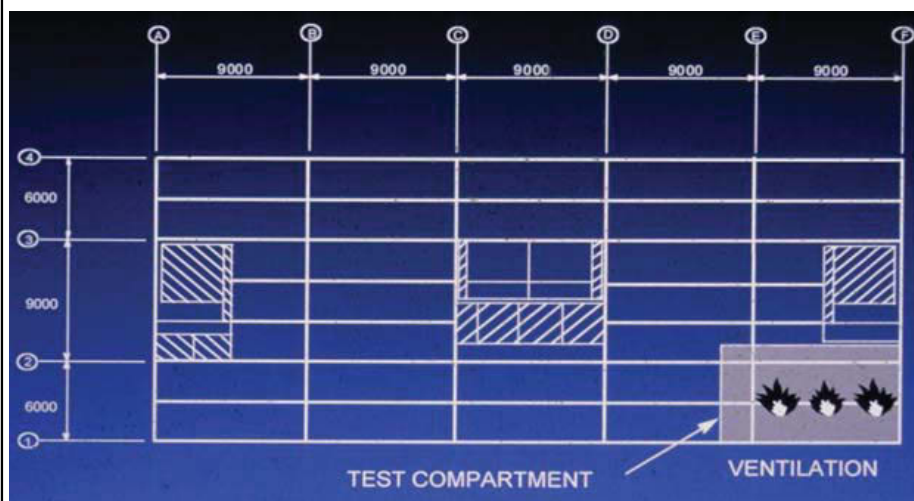
## Cardington fire tests



Cardington fire tests

Evidence from accidental fire

- Corner compartment test





## Cardington fire tests



Cardington fire tests

Evidence from accidental fire

- **Corner compartment test : set-up**



Walls of the compartment with hollow breeze-blocks

Fire load with wood cribs equals to  $45 \text{ kg/m}^2$



Review of real fires

13



## Cardington fire tests



Cardington fire tests

Evidence from accidental fire

- **Corner compartment test : experimental results**



Fire during the test

Deformed floor after the test



Review of real fires

14



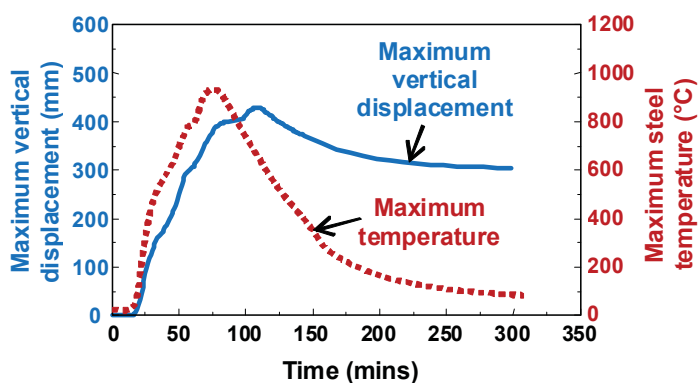
## Cardington fire tests



Cardington fire tests

Evidence from accidental fire

### • Corner compartment test : experimental results



### • Observation

- Maximum heating of steel  $\approx 1014$  °C
- Maximum deflection of the floor  $\approx 428$  mm

Review of real fires

15



## Cardington fire tests



Cardington fire tests

Evidence from accidental fire

### • Corner compartment test : structure after test



Deformed state of the heated part of the composite floor



Deformed state of steel members around protected steel column

### • Conclusion

- No sign of global failure of the floor as well as limited deflection of the floor despite important heating of steel

Review of real fires

16



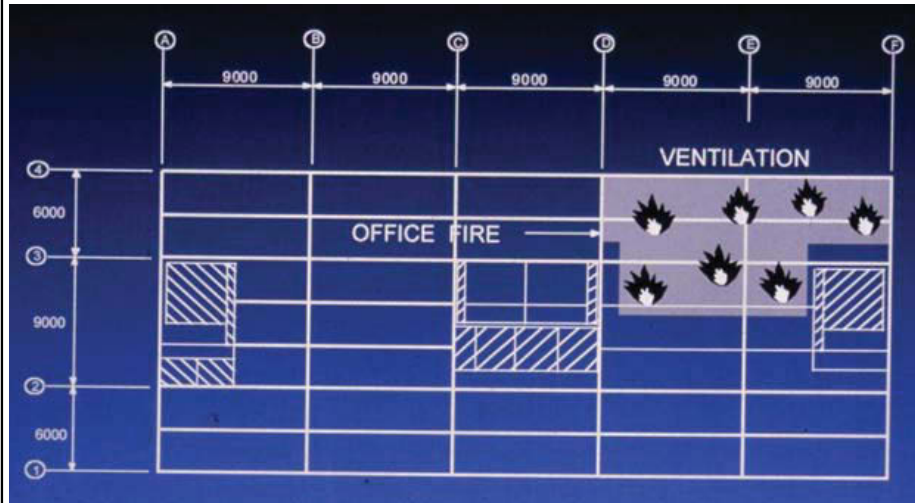
# Cardington fire tests



- **Demonstration test (an area of more than 130 m<sup>2</sup>)**

Cardington fire tests

Evidence from accidental fire



# Cardington fire tests



- **Demonstration test : set-up**

Cardington fire tests

Evidence from accidental fire



Fire load with real office furniture

Openings with normal glazed windows







## Cardington fire tests



Cardington fire tests

Evidence from accidental fire

- **Demonstration test : experimental results**



Early stage of fire

Fully developed fire



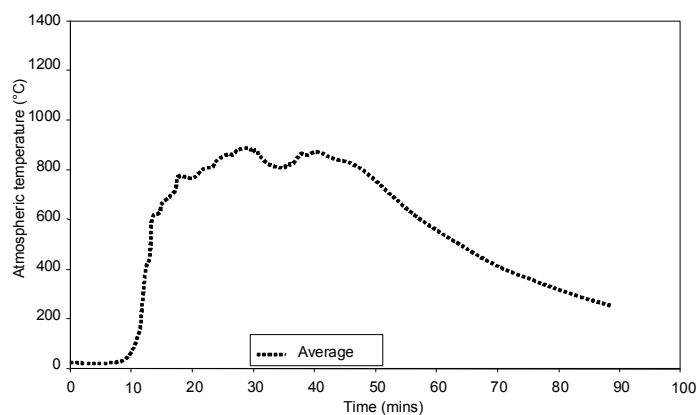
## Cardington fire tests



Cardington fire tests

Evidence from accidental fire

- **Demonstration test : experimental results**



- **Observation**
  - Maximum gas temperature  $\approx 1200\text{ }^{\circ}\text{C}$
  - Maximum heating of steel  $\approx 1150\text{ }^{\circ}\text{C}$



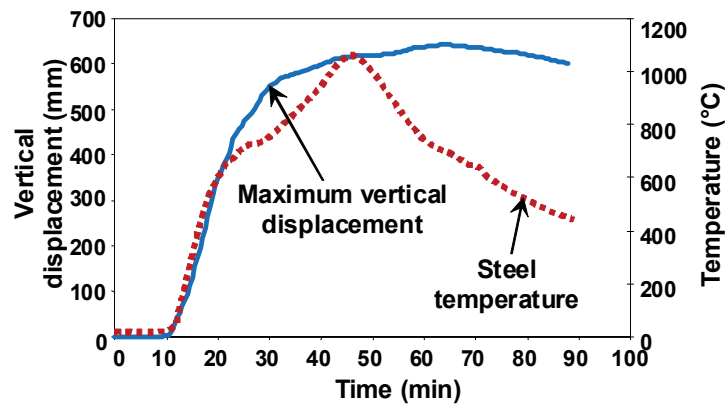
## Cardington fire tests



Cardington fire tests

Evidence from accidental fire

- **Demonstration test : experimental results**



- **Observation**

- Important deflection of the floor  $\approx 640$  mm
- No collapse of the floor

Review of real fires

21



## Cardington fire tests



Cardington fire tests

Evidence from accidental fire

- **Demonstration test : structure after test**



Deformed state of the heated part of the composite floor





Deformed state of steel members around protected steel column



- **Conclusion**

- No sign of global failure of the floor despite important heating of steel and deflection of the floor

Review of real fires

22

<p>Cardington fire tests</p> <p>Evidence from accidental fire</p>	 <h2 style="text-align: center;">Cardington fire tests</h2> 
	<ul style="list-style-type: none"> <li>• <b>Other fire tests</b> <ul style="list-style-type: none"> <li>– Second corner test</li> <li>– <b>Large compartment test</b></li> <li>– New corner test</li> </ul> </li> </ul>
<p>Review of real fires <span style="float: right;">23</span></p>	

<p>Cardington fire tests</p> <p>Evidence from accidental fire</p>	 <h2 style="text-align: center;">Cardington fire tests</h2> 
	<ul style="list-style-type: none"> <li>• <b>General remarks</b> <ul style="list-style-type: none"> <li>– Large number of severe fire tests performed in this steel framed building without collapse of the global structure</li> <li>– <b>Much better fire performance observed with respect to ordinary standard fire tests with isolated steel members</b></li> <li>– Excellent global behaviour of composite floor even if steel beams were heated up to more than 1000 °C</li> <li>– <b>Obvious enhancement of fire resistance of the composite floor owing to induced membrane effect under large deflection</b></li> <li>– Good structural robustness of the composite floor system in case of important concrete cracking</li> </ul> </li> </ul>
<p>Review of real fires <span style="float: right;">24</span></p>	



Cardington fire tests

Evidence from accidental fire

- **Broadgate fire**
  - 14 storey-office building with composite floor system
  - Fire temperature more than 1000 °C
  - Important deflection of the floor (more than 600 mm) but no collapse





## Fire Behaviour of Steel and Composite Floor Systems

*New Experimental Evidences*



### Content of presentation



- **Objectives of new fire tests**
- **Full scale fire tests within the projects of**
  - FRACOF (Test 1 ISO Fire)
  - COSSFIRE (Test 2 ISO Fire)
  - FICEB (Test 3 Natural fire & Cellular Beams)
- **Test set-up**
- **Experimental results**
  - Temperature
  - Displacement
- **Observation and analysis**
- **Comparison with simple design methods**
- **Conclusion**



## Why more fire tests?



Objectives

Test set-up

Experimental results & Observation

Comparison with simple design methods

Conclusion

- **Background**
  - Cardington fire tests
    - Excellent fire performance under natural fire condition
    - Max  $\theta$  of steel  $\approx 1150$  °C, fire duration  $\approx 60$  min ( $> 800$ °C)
    - UK construction details
- **Objectives**
  - To confirm same good performance under long fire duration (at least 90 minutes of ISO fire)
  - To investigate the impact of different construction details, such as reinforcing steel mesh and fire protection of edge beams
  - To validate different fire safety engineering tools



## Design of test specimens



Objectives

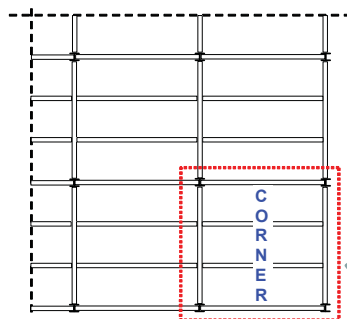
Test set-up

Experimental results & Observation

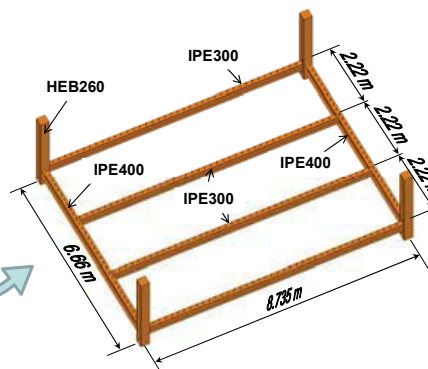
Comparison with simple design methods

Conclusion

- **Test 1 (FRACOF)**



Structure grid of a real building



Adopted steel frames for fire Test 1



## Design of test specimens



- **Test 2 (COSSFIRE)**

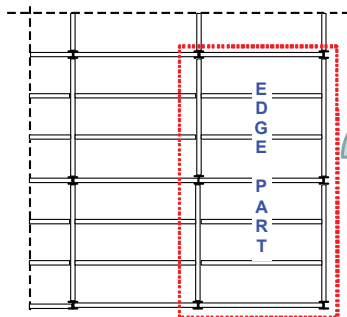
Objectives

Test set-up

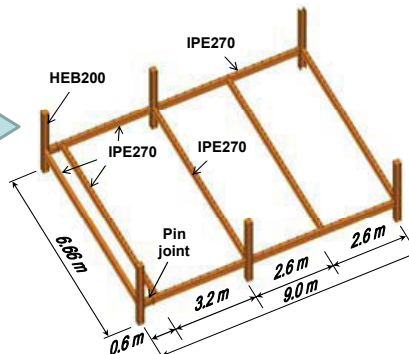
Experimental results & Observation

Comparison with simple design methods

Conclusion



Structure grid of a real building



Adopted steel frames for fire Test 2

New Experimental Evidences

5



## Design of test specimens



- **Final composite floor systems**

Objectives

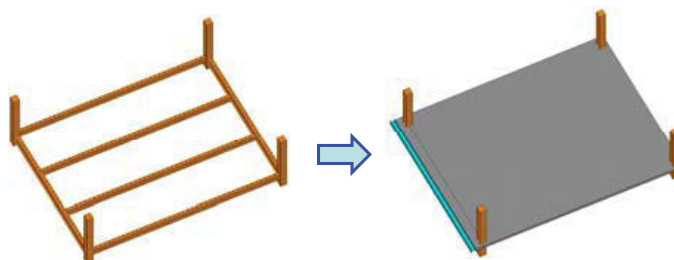
Test set-up

Experimental results & Observation

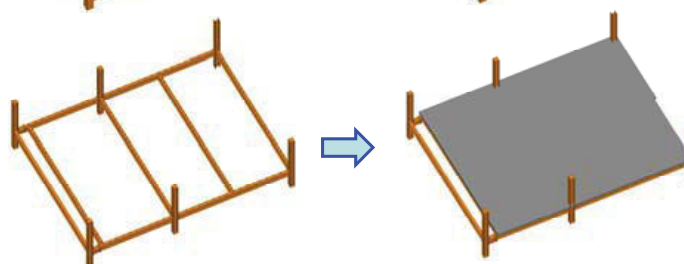
Comparison with simple design methods

Conclusion

Test 1







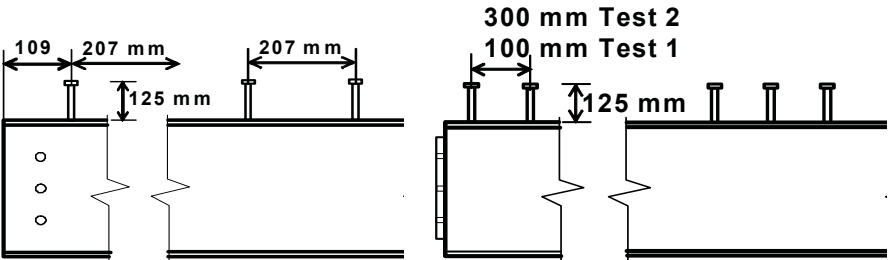
Test 2



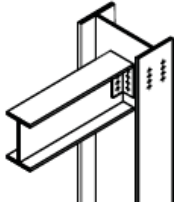
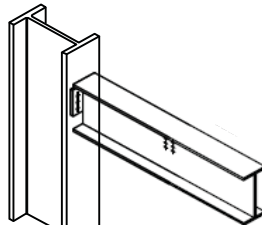
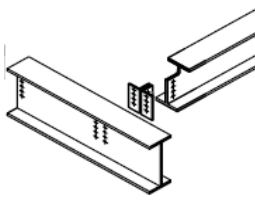
New Experimental Evidences

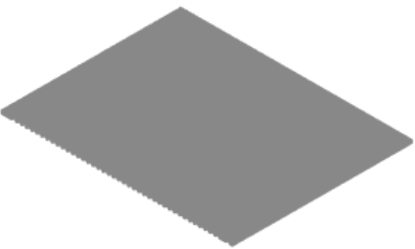
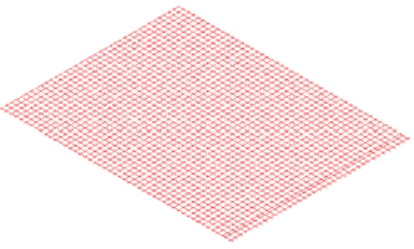
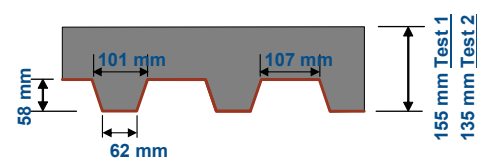
6

 <span style="margin-left: 100px;"><b>Design of structural members</b></span> 	
Objectives	<ul style="list-style-type: none"> <li>• <b>Steel frame</b> <ul style="list-style-type: none"> <li>– Steel and concrete composite beams               <ul style="list-style-type: none"> <li>• <b>According to Eurocode 4 part 1-1 (EN1994-1-1)</b></li> </ul> </li> <li>– Short steel columns</li> </ul> </li>   <li>• <b>Composite slab</b> <ul style="list-style-type: none"> <li>– Total depth               <ul style="list-style-type: none"> <li>• <b>According to Eurocode 4 part 1-2 (EN1994-1-2)</b></li> </ul> </li> <li>– Reinforcing steel mesh               <ul style="list-style-type: none"> <li>• <b>Based on simple design rules</b></li> </ul> </li> </ul> </li>   <li>• <b>Steel joints</b> <ul style="list-style-type: none"> <li>– Commonly used joints: double angle and end plate               <ul style="list-style-type: none"> <li>• <b>According to Eurocode 3 part 1.8 (EN1993-1-8)</b></li> </ul> </li> </ul> </li> </ul>
Test set-up	
Experimental results & Observation	
Comparison with simple design methods	
Conclusion	
New Experimental Evidences <span style="float: right;">7</span>	

 <span style="margin-left: 100px;"><b>Design of structural members</b></span> 	
Objectives	<ul style="list-style-type: none"> <li>• <b>Arrangement of headed studs over steel beams</b></li> </ul> <div style="text-align: center; margin: 20px 0;">  </div> <div style="display: flex; justify-content: space-around; margin: 10px 0;"> <div style="text-align: center;"><u>Secondary beams</u></div> <div style="text-align: center;"><u>Primary beams</u></div> </div> <ul style="list-style-type: none"> <li>• <b>Type of steel studs</b> <ul style="list-style-type: none"> <li>– TRW Nelson KB 3/4" – 125 (<math>\Phi = 19\text{mm}</math>; <math>h = 125\text{ mm}</math>; <math>f_y = 350\text{ N/mm}^2</math>; <math>f_u = 450\text{ N/mm}^2</math>)</li> </ul> </li> </ul>
Test set-up	
Experimental results & Observation	
Comparison with simple design methods	
Conclusion	
New Experimental Evidences <span style="float: right;">8</span>	



Steel joints			
Objectives	Beam to column		Beam to beam
	Secondary beam	Primary beam	
	Double angle web cleats		Double angle web cleats
			
Test set-up	Flexible end plate		
Experimental results & Observation			
Comparison with simple design methods			
Conclusion			
<p>Grade of steel bolts: 8.8 Diameter of steel bolt: 20 mm</p>			

Sizes of structural members		
Objectives		
	Test set-up	
	Experimental results & Observation	
	Comparison with simple design methods	
Conclusion	 <p>Steel deck: COFRAPLUS60 – 0.75 mm Concrete quality: C30/37</p> <p>Mesh size: 150x150 Diameter: 7 mm Steel grade: S500</p> <p>Axis distance from top of the slab:</p> <ul style="list-style-type: none"> <li>• 50 mm <u>Test 1</u></li> <li>• 35 mm <u>Test 2</u></li> </ul>	



## Mechanical loading condition



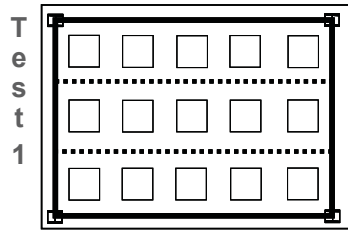
Objectives

Test set-up

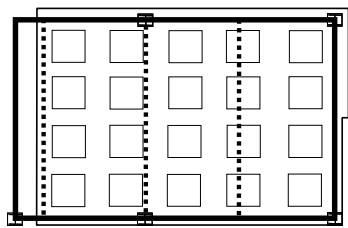
Experimental results & Observation

Comparison with simple design methods

Conclusion



15 sand bags  
of 1512 kg  
Equivalent  
uniform load:  
390 kg/m<sup>2</sup>



20 sand bags  
of 1098 kg  
Equivalent  
uniform load:  
393 kg/m<sup>2</sup>

Test 2



## Preparation of fire test 2



Objectives

Test set-up

Experimental results & Observation

Comparison with simple design methods

Conclusion

1



2



3



4



Behaviour of the floor during fire	
Objectives	
Test set-up	
Experimental results & Observation	
Comparison with simple design methods	
Conclusion	
New Experimental Evidences <span style="float: right;">13</span>	

Structure of the Test 3 (FICEB)	
Objectives	
Test set-up	
Experimental results & Observation	
Comparison with simple design methods	
Conclusion	
New Experimental Evidences <span style="float: right;">14</span>	



## Structure of the Test 3



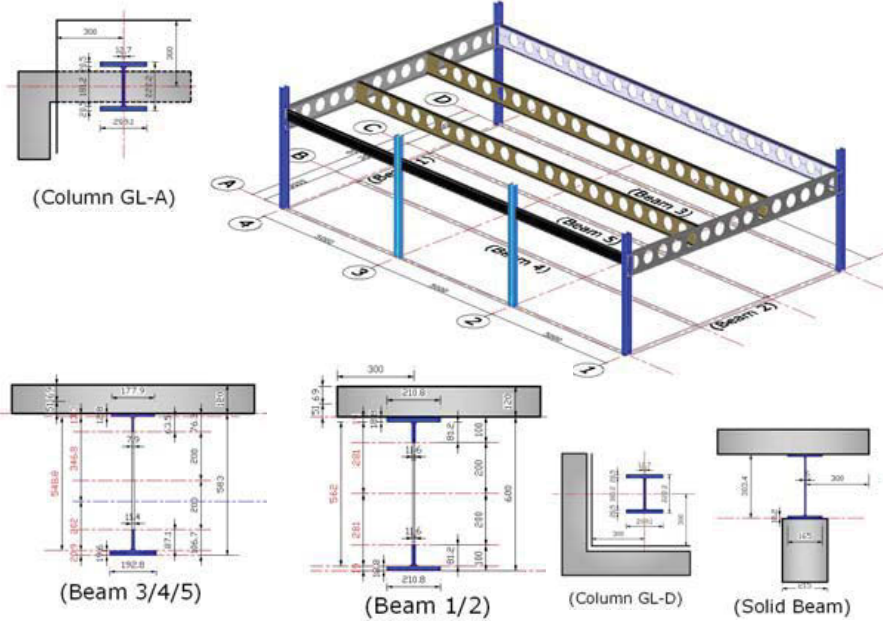
Objectives

Test set-up

Experimental results & Observation

Comparison with simple design methods

Conclusion



New Experimental Evidences

15



## Structure of the Test 3



### Beam - Beam Connections

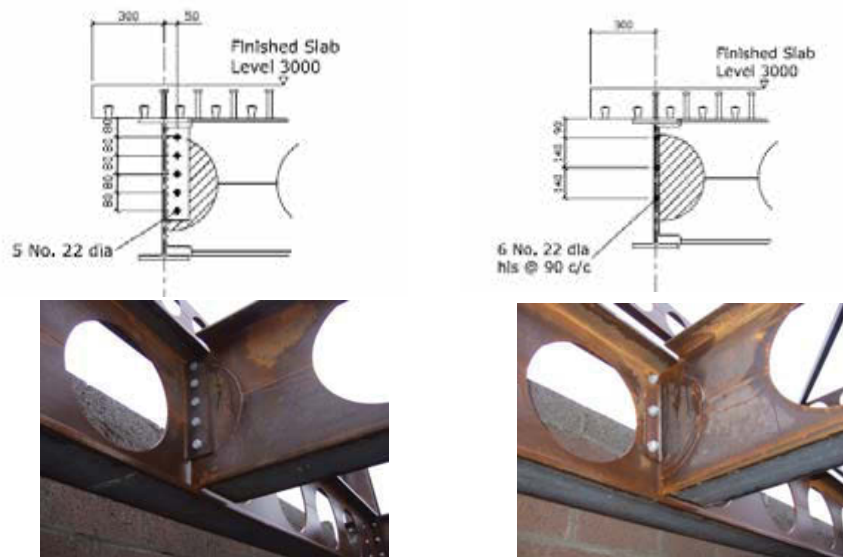
Objectives

Test set-up

Experimental results & Observation

Comparison with simple design methods

Conclusion



New Experimental Evidences

16



### Structure of the Test 3



Objectives

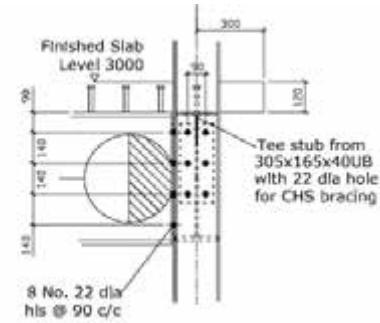
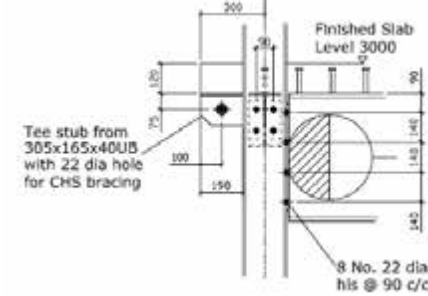
Test set-up

Experimental results & Observation

Comparison with simple design methods

Conclusion

#### Beam - Column Connections



### Structure of the Test 3



Objectives

Test set-up

Experimental results & Observation

Comparison with simple design methods

Conclusion

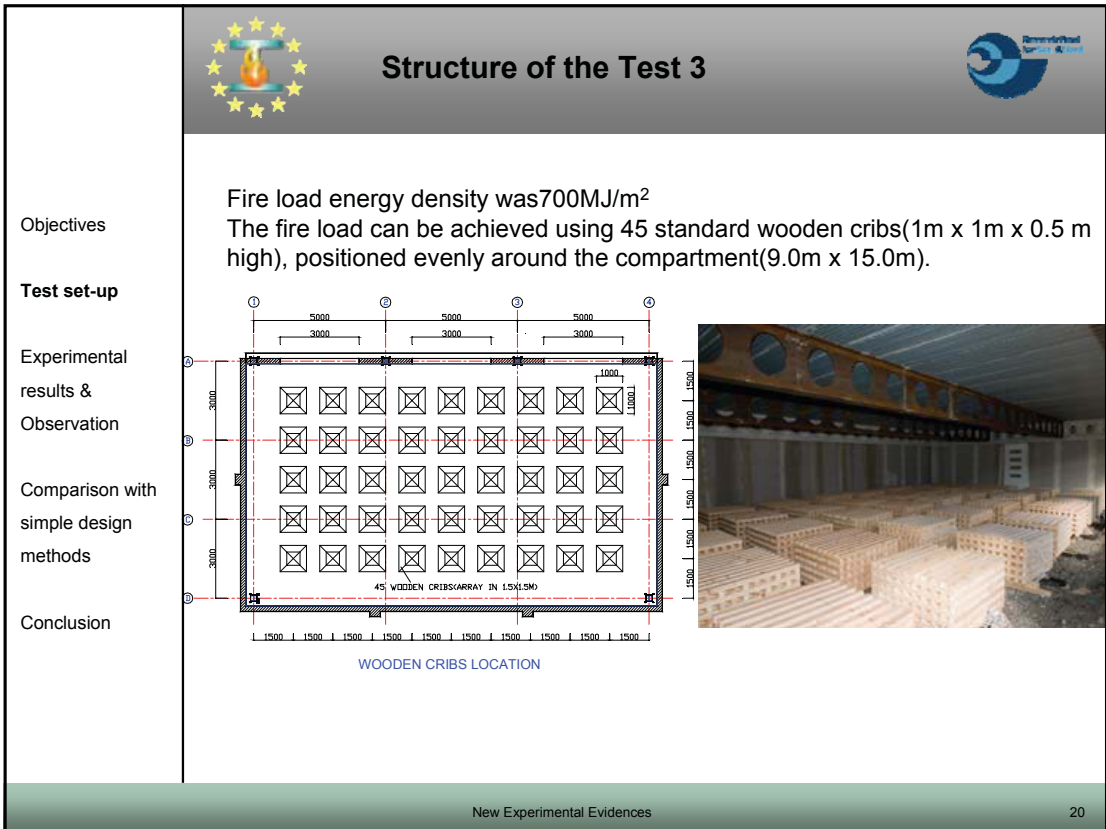
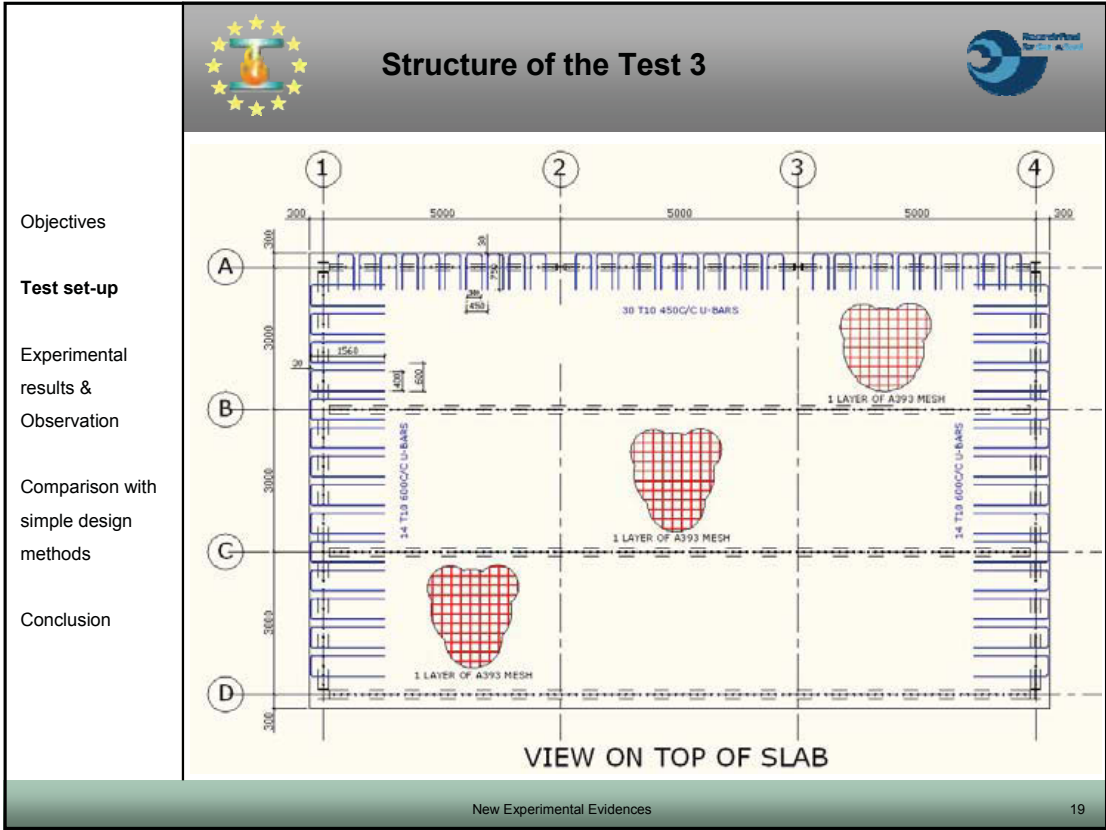




A393 Mesh Reinforcement, dia 10mm



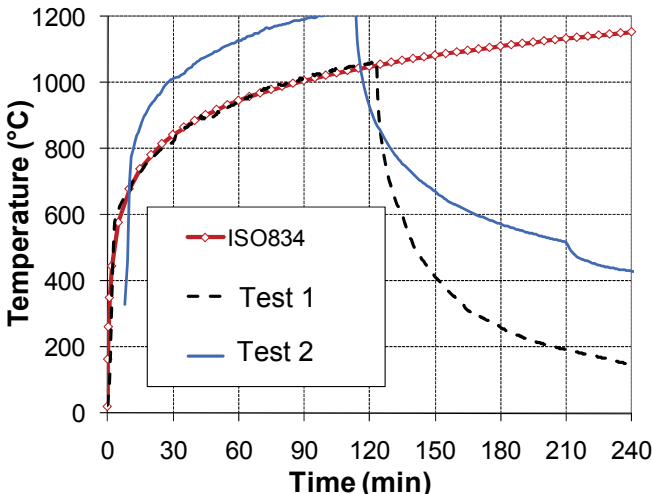


Full Interaction: between slab & beams, achieved by Shear connectors, dia 19, h=95mm

U-bars reinf. around the slab was added to ensure correct reinf. Detail requirement for Ambient Temp.



 <span style="margin-left: 100px;"><b>Experimental results</b></span> 	
Objectives	<ul style="list-style-type: none"> <li>• <b>Fire temperature</b></li> <li>• <b>Heating of unprotected steel beams</b></li> <li>• <b>Heating of protected steel members</b></li> <li>• <b>Heating of composite slab</b></li> <li>• <b>Deflection of the floor</b></li> <li>• <b>Observations over the behaviour of composite floor systems</b> <ul style="list-style-type: none"> <li>– <b>Concrete cracking and concrete crushing</b></li> <li>– <b>Failure of reinforcing steel mesh during the test</b></li> <li>– <b>Collapse of edge beams</b></li> </ul> </li> </ul>
Test set-up	
<b>Experimental results &amp; Observation</b>	
Comparison with simple design methods	
Conclusion	

 <span style="margin-left: 100px;"><b>Experimental results</b></span> 	
Objectives	<ul style="list-style-type: none"> <li>• <b>Fire temperature</b></li> </ul> <div style="text-align: center; margin-top: 20px;">  </div>
Test set-up	
<b>Experimental results &amp; Observation</b>	
Comparison with simple design methods	
Conclusion	



## Experimental results



Objectives

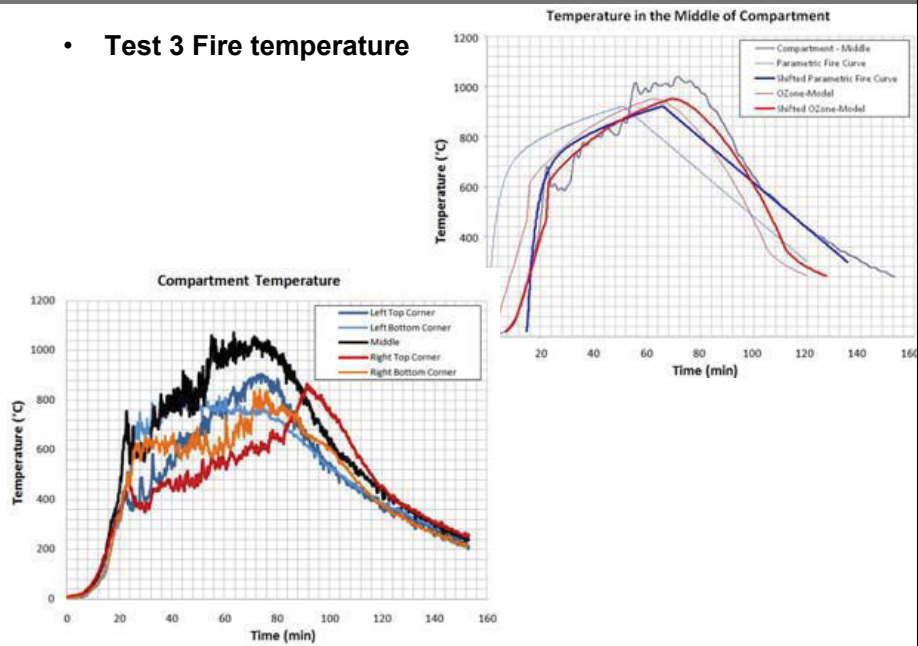
Test set-up

**Experimental results & Observation**

Comparison with simple design methods

Conclusion

### • Test 3 Fire temperature



New Experimental Evidences

23



## Experimental results



Objectives

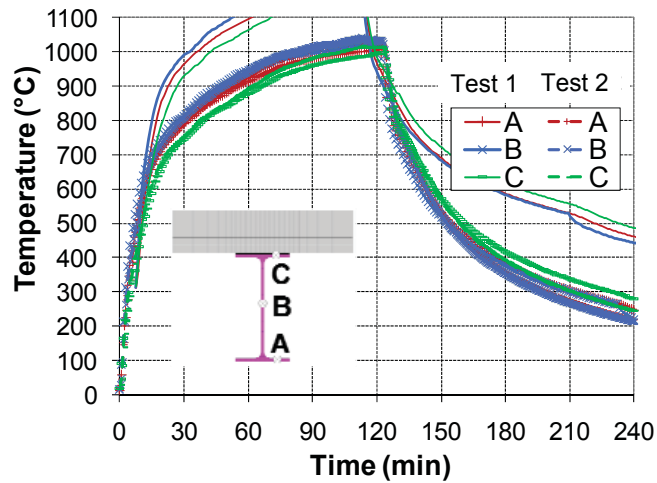
Test set-up

**Experimental results & Observation**

Comparison with simple design methods

Conclusion

### • Heating of unprotected steel beams



New Experimental Evidences

24





## Experimental results



Objectives

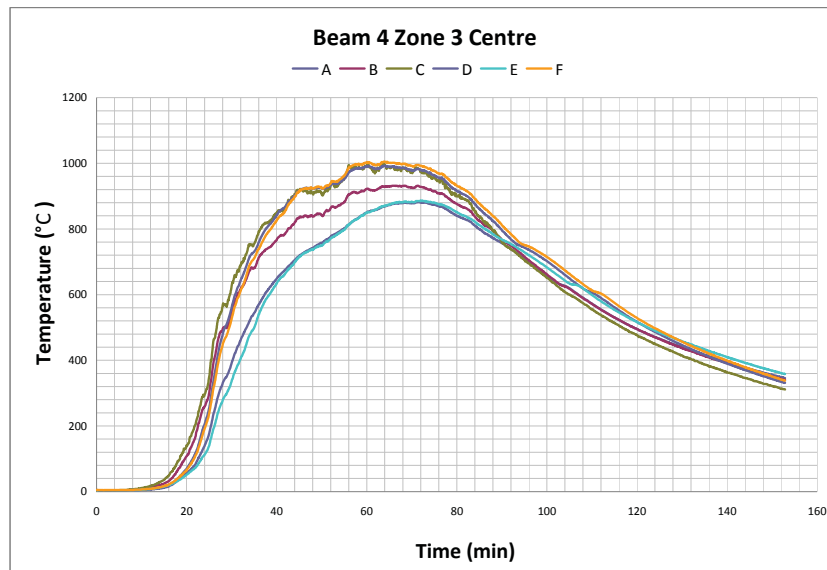
Test set-up

Experimental results & Observation

Comparison with simple design methods

Conclusion

### • Test 3 Heating of unprotected steel beams



New Experimental Evidences

25



## Experimental results



Objectives

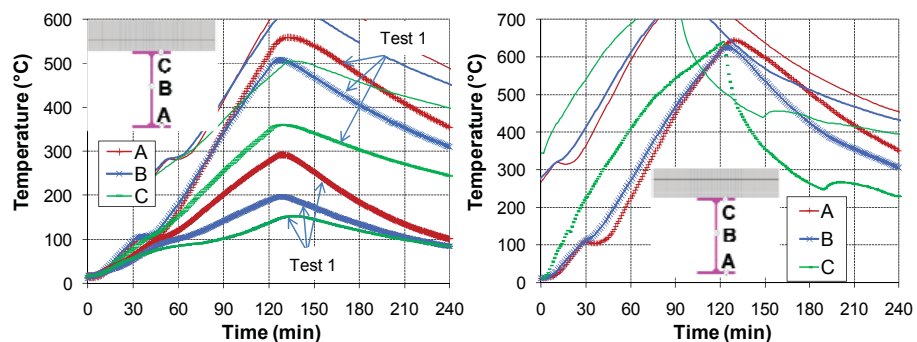
Test set-up

Experimental results & Observation

Comparison with simple design methods

Conclusion

### • Heating of protected steel beams

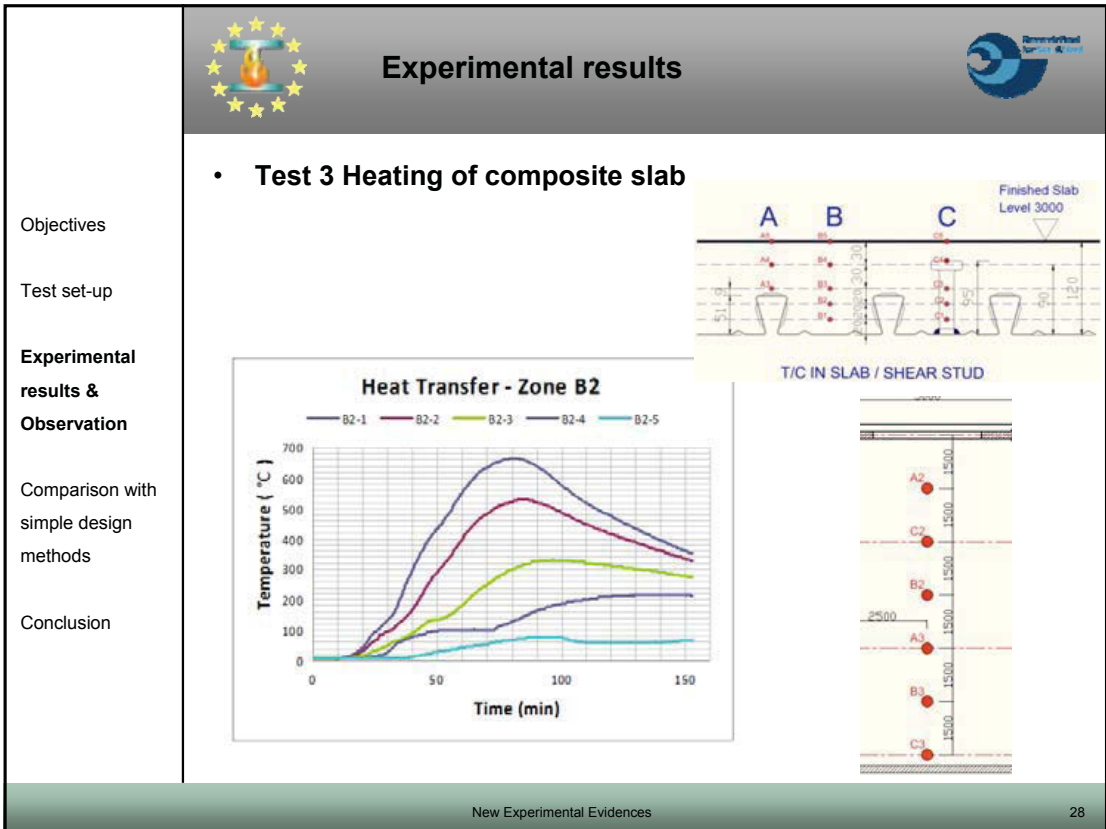
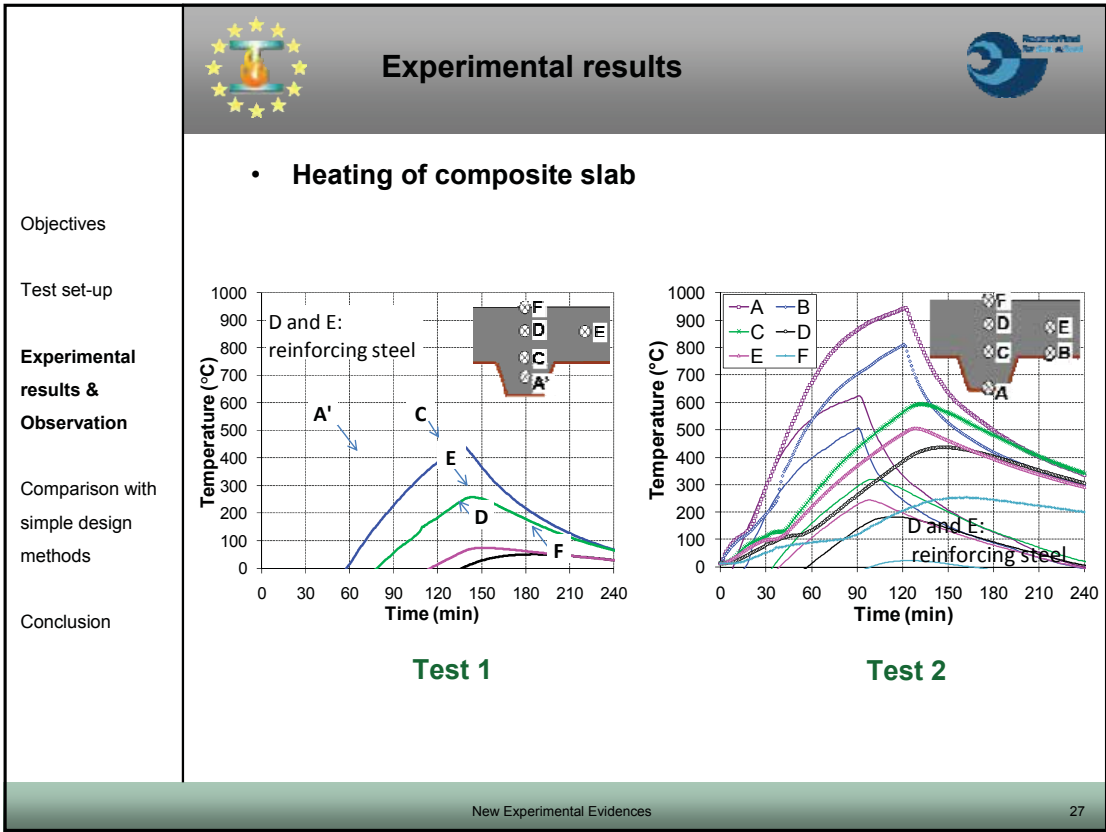


### • Observation

- Much hotter beams in Test 2  $\approx 550$  °C and one edge secondary beam heated up to  $> 600$  °C

New Experimental Evidences

26





## Experimental results



### Displacement transducers for deflection

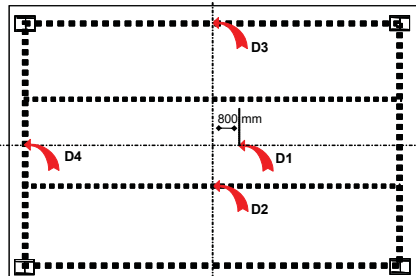
Objectives

Test set-up

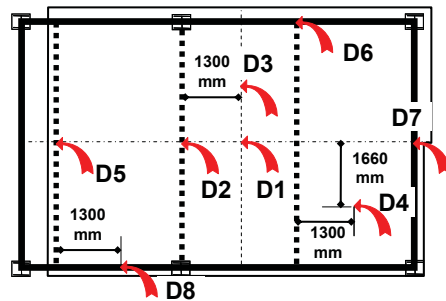
Experimental results & Observation

Comparison with simple design methods

Conclusion



Test 1



Test 2



## Experimental results



### Deflection of the floors

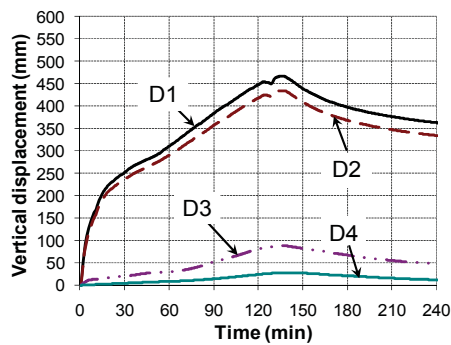
Objectives

Test set-up

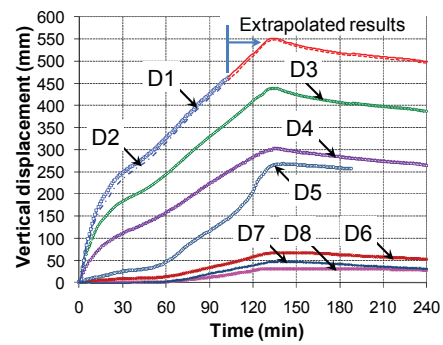
Experimental results & Observation

Comparison with simple design methods

Conclusion



Test 1



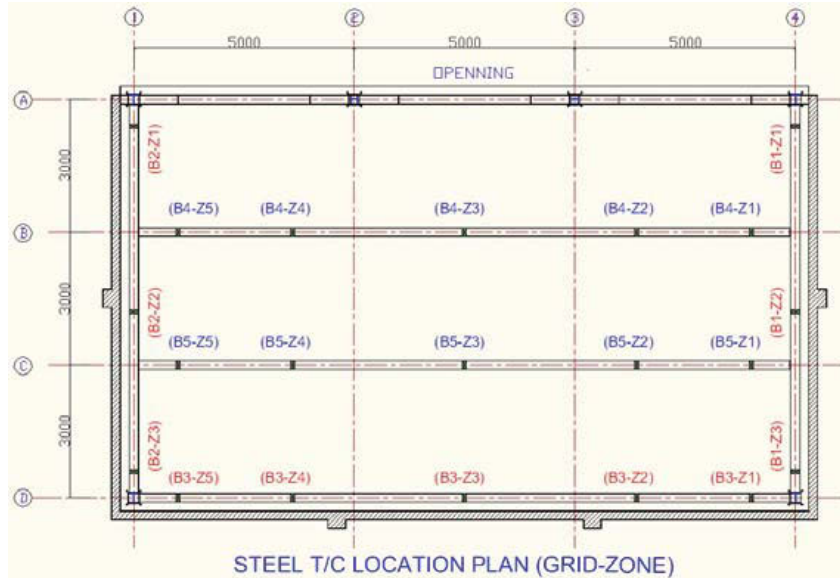
Test 2



## Experimental results



### • Test 3 Displacement transducers for deflection



Objectives

Test set-up

Experimental results & Observation

Comparison with simple design methods

Conclusion

New Experimental Evidences

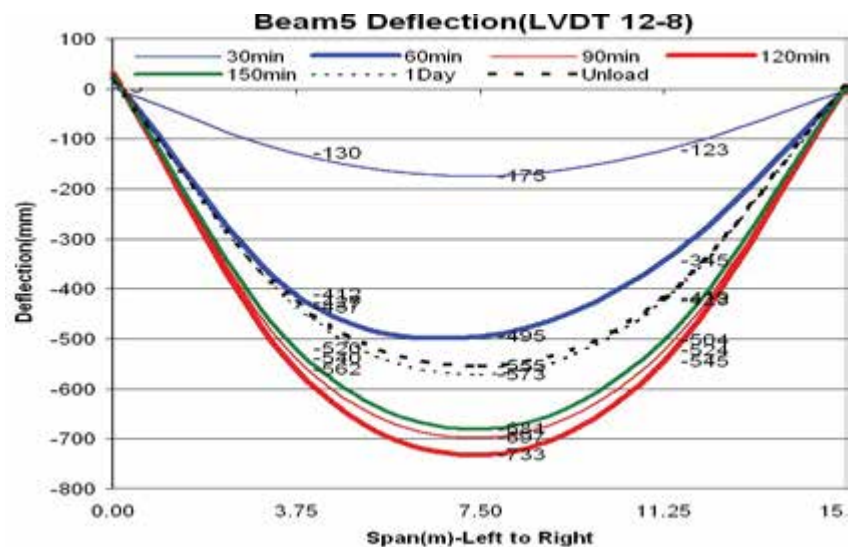
31



## Experimental results



### • Test 3 Deflection of the floors



Objectives

Test set-up



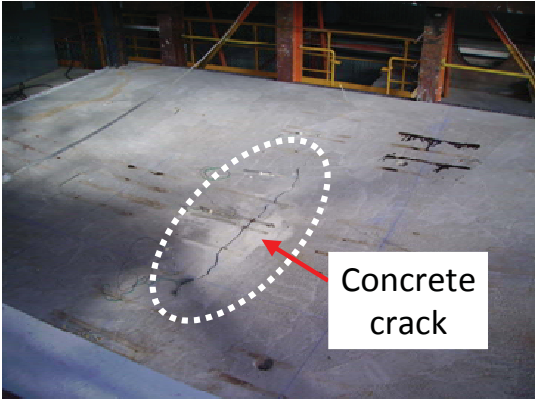

Experimental results & Observation




Comparison with simple design methods




Conclusion




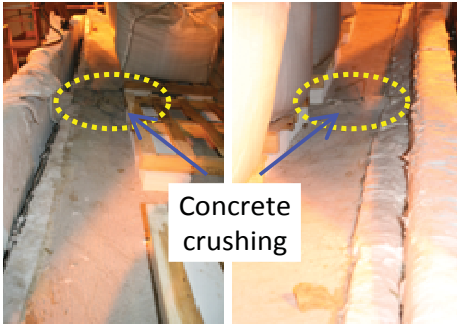
New Experimental Evidences


32

<p>Objectives</p> <p>Test set-up</p> <p><b>Experimental results &amp; Observation</b></p> <p>Comparison with simple design methods</p> <p>Conclusion</p>	<div style="text-align: right;">  <h2 style="margin: 0;">Experimental results</h2>  </div> <ul style="list-style-type: none"> <li>• <b>Cracking of concrete (Test 1)</b></li> </ul> <div style="display: flex; justify-content: space-around;">   </div> <ul style="list-style-type: none"> <li>• <b>Observation</b> <ul style="list-style-type: none"> <li>– Excellent global stability of the floor despite the failure of reinforcing steel mesh</li> </ul> </li> </ul>
<p>New Experimental Evidences <span style="float: right;">33</span></p>	


<p>Objectives</p> <p>Test set-up</p> <p><b>Experimental results &amp; Observation</b></p> <p>Comparison with simple design methods</p> <p>Conclusion</p>	<div style="text-align: right;">  <h2 style="margin: 0;">Experimental results</h2>  </div> <ul style="list-style-type: none"> <li>• <b>Cracking of concrete (Test 3)</b></li> </ul> <div style="display: flex; justify-content: space-around;">  </div> <ul style="list-style-type: none"> <li>• <b>Observation</b> <ul style="list-style-type: none"> <li>– Excellent global stability of the floor despite appearance of the crack</li> </ul> </li> </ul>
<p>New Experimental Evidences <span style="float: right;">34</span></p>	

<p>Objectives</p> <p>Test set-up</p> <p><b>Experimental results &amp; Observation</b></p> <p>Comparison with simple design methods</p> <p>Conclusion</p>	<div style="text-align: center;">  <h2 style="margin: 0;">Experimental results</h2>  </div> <ul style="list-style-type: none"> <li>• <b>Web instability of the beam (Test 3)</b></li> </ul>  <div style="text-align: center; margin-top: 10px;"> <p>New Experimental Evidences <span style="float: right;">35</span></p> </div>
--	---

<p>Objectives</p> <p>Test set-up</p> <p><b>Experimental results &amp; Observation</b></p> <p>Comparison with simple design methods</p> <p>Conclusion</p>	<div style="text-align: center;">  <h2 style="margin: 0;">Experimental results</h2>  </div> <ul style="list-style-type: none"> <li>• <b>Crushing of concrete (Test 2)</b></li> </ul> <div style="display: flex; justify-content: space-around; align-items: center;">   </div> <div style="text-align: center; margin-top: 10px;"> <p>Concrete crushing</p> </div> <ul style="list-style-type: none"> <li>• <b>Observation</b> <ul style="list-style-type: none"> <li>– Global stability of the floor maintained appropriately despite the failure of one edge beam</li> </ul> </li> </ul> <div style="text-align: center; margin-top: 10px;"> <p>New Experimental Evidences <span style="float: right;">36</span></p> </div>
--	--




## Comparison with simple design rules




	Test 1		Test 2	
	Test	Simple design methods	Test	Simple design methods
<b>Fire rating (min)</b>	<b>&gt; 120</b>	<b>120</b>	<b>&gt; 120</b>	<b>96</b>
<b>Deflection (mm)</b>	<b>450</b>	<b>366<sup>(*)</sup></b>	<b>510</b>	<b>376<sup>(*)</sup></b>

- **Observation**
  - Experimental results:
    - **Fire rating > 120 minutes**

New Experimental Evidences
37



## New experimental evidences



- **General conclusions relative to new fire tests**
  - **Excellent performance of the composite floor systems behaving under membrane action for long ISO fire exposure (>120 minutes)**
  - **High level of robustness of the composite floor system despite certain local failures**
  - **Specific attention to be paid to construction details with respect to reinforcing steel mesh in order to ensure a good performance of integrity criteria**
  - **Simple design method is on the safe side in comparison with test results**
  - **No sign of failure during cooling phase of the composite floor systems**

New Experimental Evidences
38



## Fire Behaviour of Steel and Composite Floor Systems

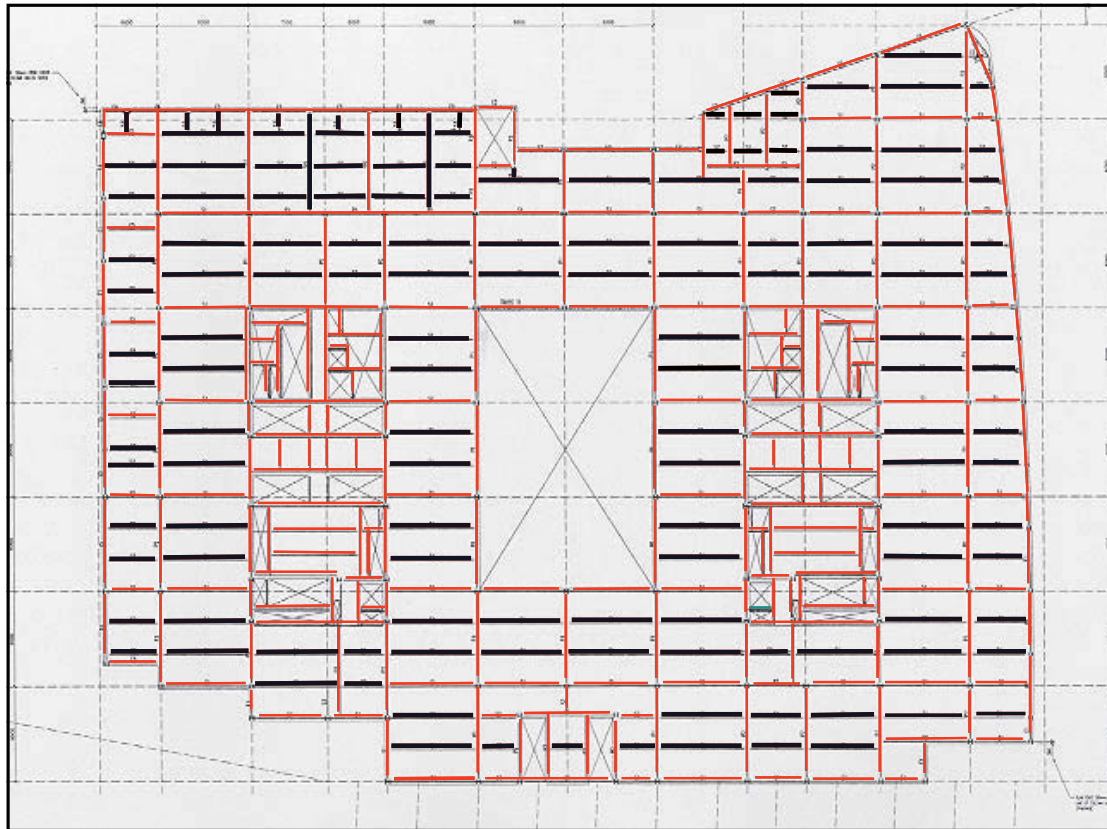
*Simple design method*



### Aim of the design method







## Content of presentation



- **Mechanical behaviour of composite floors in a fire situation**
- **Simple design method of reinforced concrete slabs at 20 °C**
  - Floor slab model
  - Failure modes
- **Simple design method of composite floors at elevated temperatures**
  - Extension to fire behaviour
  - Membrane effect at elevated temperatures
  - Contribution from unprotected beams
  - Design of protected beams

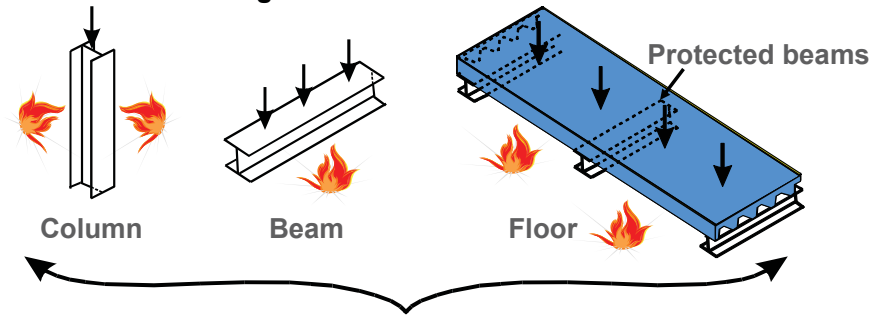


Mechanical behaviour of composite floors

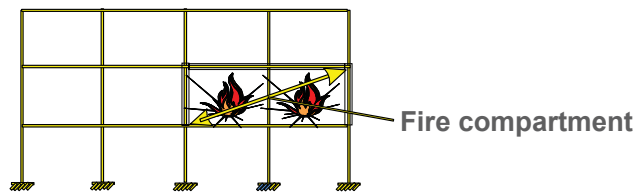
Simple design method of reinforced concrete slabs at 20°C

Simple design method of composite floors at elevated temperatures

## Traditional design method



Existing design methods assume isolated members will perform in a similar way in actual buildings

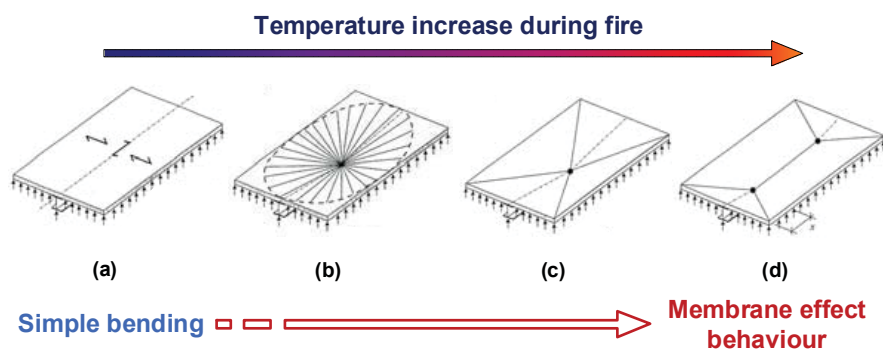


Mechanical behaviour of composite floors

Simple design method at 20°C

Simple design method at elevated temperatures

## Real behaviour of composite floor with reinforcing steel mesh in concrete slab





## Simple design method of reinforced concrete slabs at 20 °C



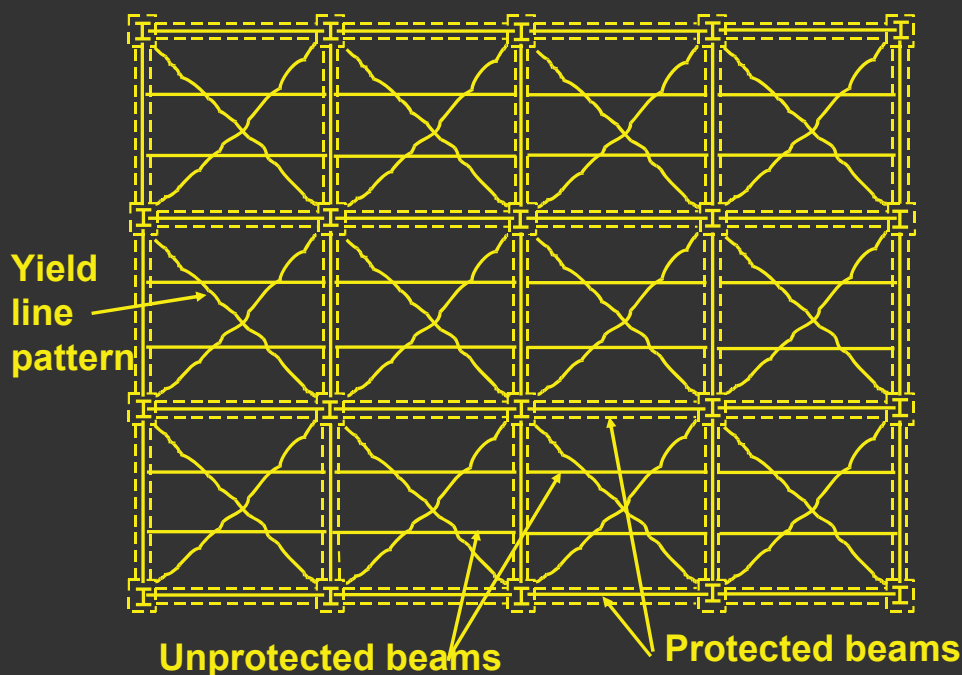
Mechanical behaviour of composite floors

Simple design method at 20 °C

Simple design method at elevated temperatures

- Method developed by Professor Colin Bailey  
University of Manchester  
formerly with Building Research Establishment (BRE)

## Designing for membrane action in fire





# Simple design method of reinforced concrete slabs at 20 °C

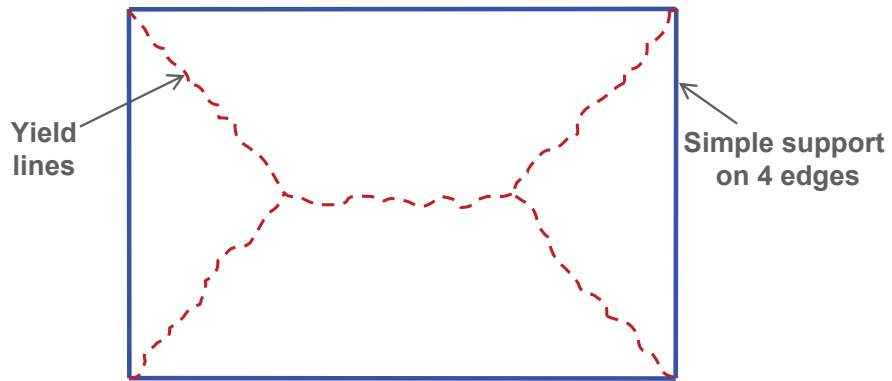


Mechanical behaviour of composite floors

Simple design method at 20°C

Simple design method at elevated temperatures

- **Floor slab model with 4 vertically restrained sides** (Plastic yield lines) – horizontally unrestrained – very conservative assumption



# Simple design method of reinforced concrete slabs at 20 °C

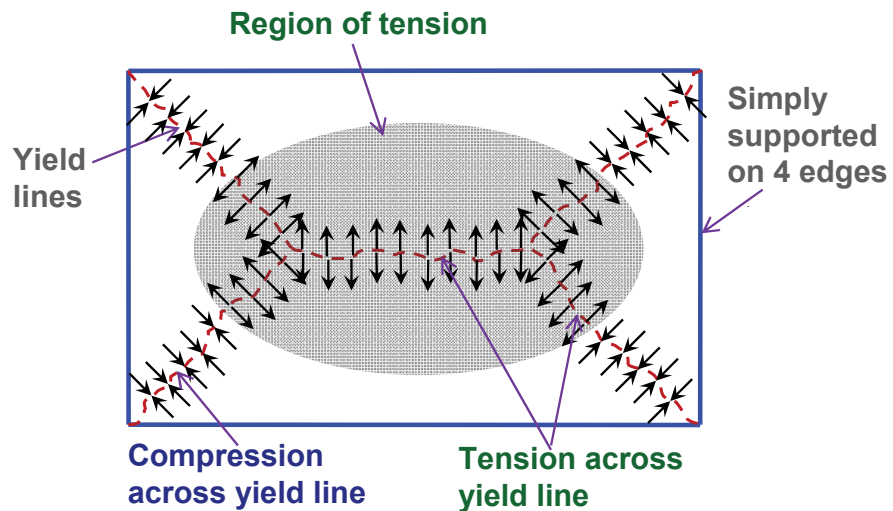


Mechanical behaviour of composite floors

Simple design method at 20°C

Simple design method at elevated temperatures

- **Floor slab model**
  - Membrane effect enhancing yield lines resistance



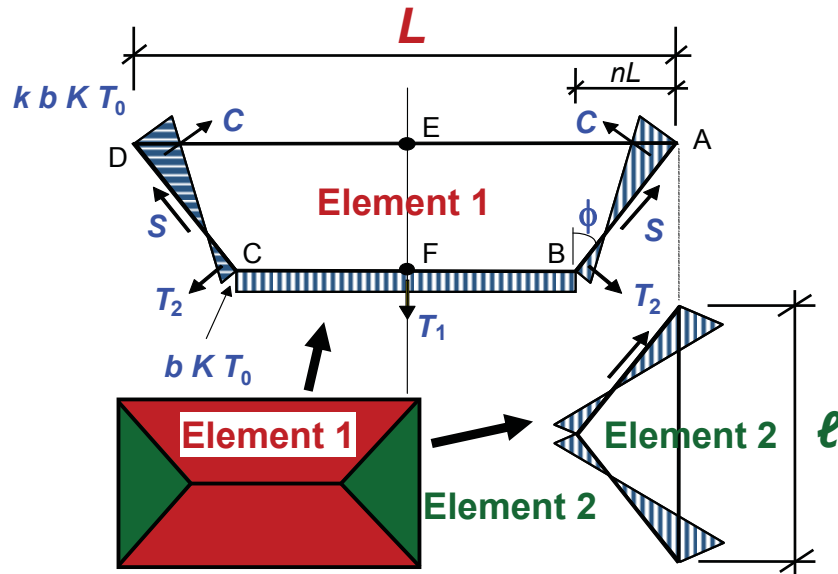


Mechanical behaviour of composite floors

Simple design method at 20°C

Simple design method at elevated temperatures

• Membrane forces along yield lines (1)



Mechanical behaviour of composite floors

Simple design method at 20°C

Simple design method at elevated temperatures

• Membrane forces along yield lines (2)

**$k, b$**  are parameters defining magnitude of membrane forces,

**$n$**  is a factor deduced from yield line theory,

**$K$**  is the ratio of the reinforcement in the shorter span to the reinforcement in the longer span,

**$KT_0$**  is the resistance of the steel reinforcing mesh per unit width,

**$T_1, T_2, C, S$**  are resulting membrane forces along yield lines.



## Simple design method of reinforced concrete slabs at 20 °C

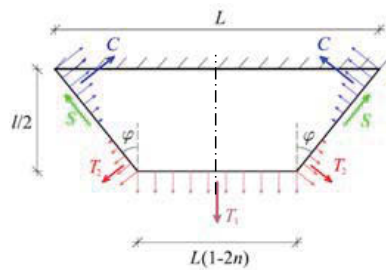


- Contribution of membrane action (1)
  - Element 1

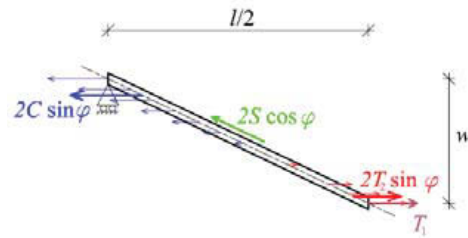
Mechanical behaviour of composite floors

Simple design method at 20°C

Simple design method at elevated temperatures



In-plane view of the resulting membrane forces



Side-view of the resulting membrane forces under a deflection equal to w

Background of simple design method

13



## Simple design method of reinforced concrete slabs at 20 °C

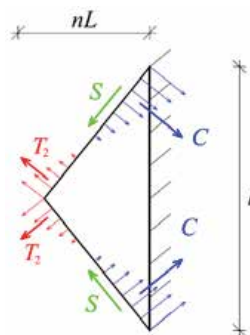


- Contribution of membrane action (2)
  - Element 2

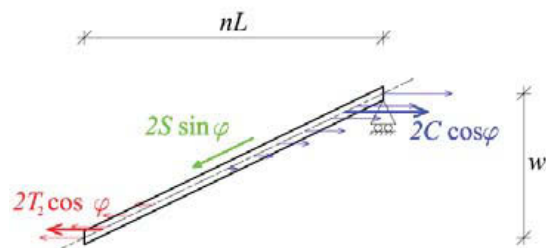
Mechanical behaviour of composite floors

Simple design method at 20°C

Simple design method at elevated temperatures



In-plane view of the resulting membrane forces



Side-view of the resulting membrane forces under a deflection equal to w

Background of simple design method

14

## Simple design method of reinforced concrete slabs at 20 °C

- **Contribution of membrane action (3)**

- **Enhancement factor for each element**

$$e_{i, i=1,2} = \begin{cases} e_{im} : \text{enhancement due to membrane forces on} \\ \text{element } i & + \\ e_{ib} : \text{Enhancement due to the effect of in-plane} \\ \text{forces on the bending capacity.} \end{cases}$$

- **Overall enhancement**

$$e = e_1 - \frac{e_1 - e_2}{1 + 2\mu a^2}$$

where:

$\mu$  is the coefficient of orthotropy of the reinforcement

$a$  is the aspect ratio of the slab =  $L/\ell$

Mechanical  
behaviour of  
composite floors

Simple design  
method at 20°C

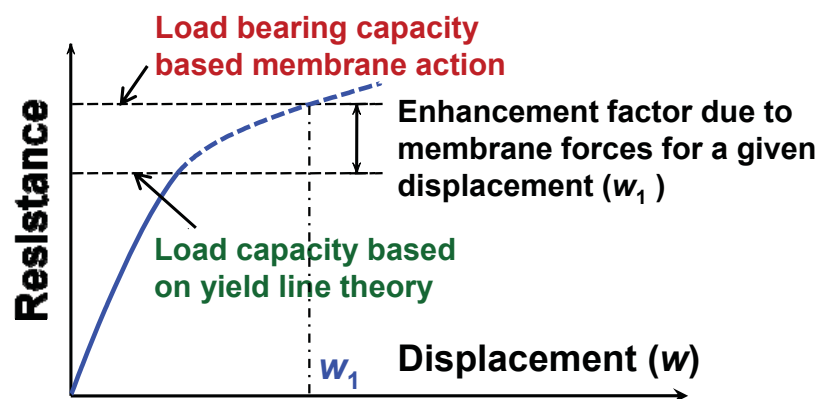
Simple design  
method at  
elevated  
temperatures



## Simple design method of reinforced concrete slabs at 20 °C



- **Contribution of membrane action (4)**



Mechanical  
behaviour of  
composite floors

Simple design  
method at 20°C

Simple design  
method at  
elevated  
temperatures



## Simple design method of reinforced concrete slabs at 20 °C

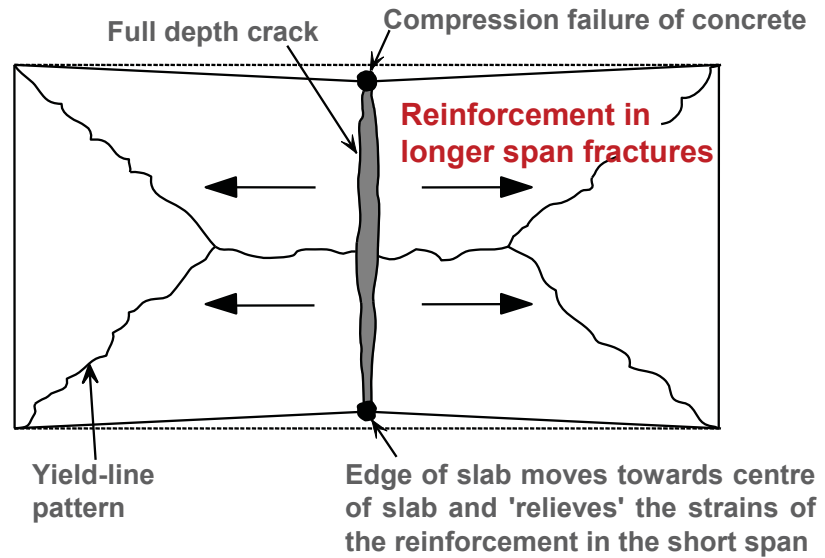


Mechanical behaviour of composite floors

Simple design method at 20°C

Simple design method at elevated temperatures

- **Failure modes** (tensile failure of reinforcement)



Background of simple design method

17



## Simple design method of reinforced concrete slabs at 20 °C

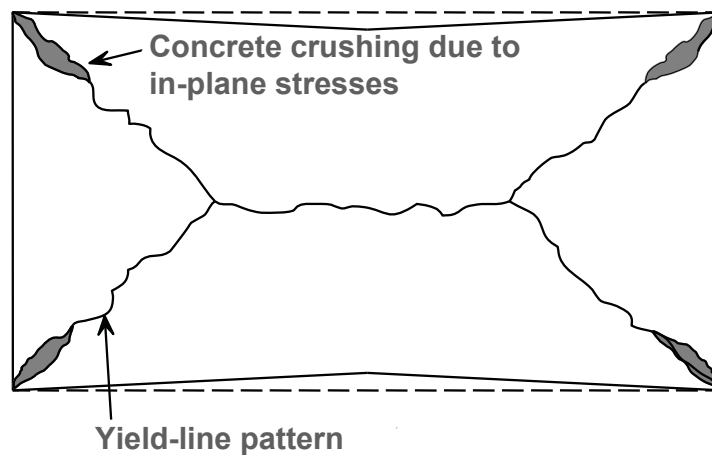


Mechanical behaviour of composite floors

Simple design method at 20°C

Simple design method at elevated temperatures

- **Failure modes** (compressive failure of concrete)
  - More likely to occur in case of strong reinforcement mesh



Background of simple design method

18





## Simple design method of reinforced concrete slabs at 20 °C



- **Failure modes** (experimental evidence)



**Tensile failure of reinforcement**

**Compressive failure of concrete**

Mechanical behaviour of composite floors

**Simple design method at 20°C**

Simple design method at elevated temperatures



## Simple design method at elevated temperatures



- **Floor slab model at elevated temperatures (1)**
  - On the basis of the same model at room temperature
  - Account taken of temperature effects on material properties.

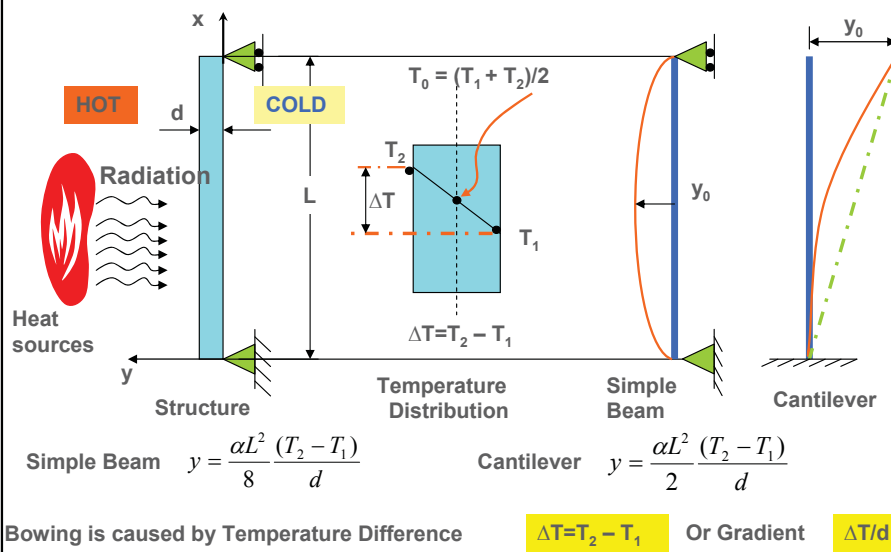
Mechanical behaviour of composite floors

Simple design method at 20°C

**Simple design method at elevated temperatures**



Free Bowing of a concrete slab



- Floor slab model at elevated temperatures (2)
  - Account for thermal bowing of the slab due to temperature gradient in depth which equals to:

$$w_{\theta} = \frac{\alpha (T_2 - T_1) \ell^2}{19.2 h}$$

where:

- h** is the effective depth of the slab
- ℓ** is the shorter span of the slab
- α** is the coefficient of thermal expansion for concrete
  - For LW concrete, EN 1994-1-2 value is taken  $\alpha_{LWC} = 0.8 \times 10^{-5} \text{ } ^\circ\text{K}^{-1}$
  - For NW concrete, a conservative value is taken  $\alpha_{NWC} = 1.2 \times 10^{-5} \text{ } ^\circ\text{K}^{-1} < 1.8 \times 10^{-5} \text{ } ^\circ\text{K}^{-1}$  (EN 1994-1-2 value)
- T<sub>2</sub>** is the temperature of the slab bottom side (fire-exposed side)
- T<sub>1</sub>** is the temperature of the slab top side (unexposed side)

Mechanical behaviour of composite floors

Simple design method at 20°C

Simple design method at elevated temperatures



Mechanical behaviour of composite floors

Simple design method at 20°C

Simple design method at elevated temperatures

• Floor slab model at elevated temperatures (3)

- Assuming mechanical average strain at a stress equal to half the yield stress at room temperature
- Deflection of slab on the basis of a parabolic deflected shape of the slab due to transverse loading:

$$w_{\epsilon} = \sqrt{\left(\frac{0.5f_{sy}}{E_s}\right) \frac{3L^2}{8}} \leq \frac{l}{30}$$

where:

- $E_s$  is the elastic modulus of the reinforcement at 20°C
- $f_{sy}$  is the yield strength of the reinforcement at 20°C
- $L$  is the longer span of the slab



Mechanical behaviour of composite floors

Simple design method at 20°C

Simple design method at elevated temperatures

• Floor slab model at elevated temperatures (4)



- Hence, the maximum deflection of the floor slab is:



$$w = \frac{\alpha(T_2 - T_1)l^2}{19.2h} + \sqrt{\left(\frac{0.5f_{sy}}{E_s}\right) \frac{3L^2}{8}}$$

- However, the maximum deflection of the floor slab is limited to:

$$w < \frac{\alpha(T_2 - T_1)l^2}{19.2h} + l/30$$

$$w \leq \frac{L + l}{30}$$

<p>Mechanical behaviour of composite floors</p> <p>Simple design method at 20°C</p> <p>Simple design method at elevated temperatures</p>	<div style="text-align: right;">  </div> <div style="text-align: center;">  <h2 style="margin: 0;">Simple design method at elevated temperatures</h2> </div> <ul style="list-style-type: none"> <li>• <b>Conservativeness of the floor slab model at elevated temperatures</b> <ul style="list-style-type: none"> <li>– Reinforcement over supports is assumed to fracture.</li> <li>– The estimated vertical displacements due to thermal curvature are underestimated compared to theoretical values</li> <li>– The thermal curvature is calculated based on the shorter span of the slab</li> <li>– Any additional vertical displacements induced by the restrained thermal expansion when the slab is in a post buckled state are ignored</li> <li>– Any contribution from the steel decking is ignored</li> <li>– The increase of the mesh ductility with the temperature increase is ignored</li> </ul> </li> </ul>
<p>Background of simple design method <span style="float: right;">25</span></p>	

<p>Mechanical behaviour of composite floors</p> <p>Simple design method at 20°C</p> <p>Simple design method at elevated temperatures</p>	<div style="text-align: right;">  </div> <div style="text-align: center;">  <h2 style="margin: 0;">Simple design method at elevated temperatures</h2> </div> <ul style="list-style-type: none"> <li>• <b>Load bearing capacity of the floor slab model enhanced in presence of unprotected steel beams (1)</b> <ul style="list-style-type: none"> <li>– Catenary action of unprotected beams is neglected</li> <li>– The bending moment resistance of unprotected beams is taken into account with following assumptions: <ul style="list-style-type: none"> <li>□ Simple support at both ends</li> <li>□ Heating of the steel cross-section calculated according to EN1994-1-2 4.3.4.2, considering shadow effect</li> <li>□ Thermal and mechanical properties for both steel and concrete given in EN 1994-1-2</li> </ul> </li> </ul> </li> </ul>
<p>Background of simple design method <span style="float: right;">26</span></p>	



## Simple design method at elevated temperatures



Mechanical behaviour of composite floors

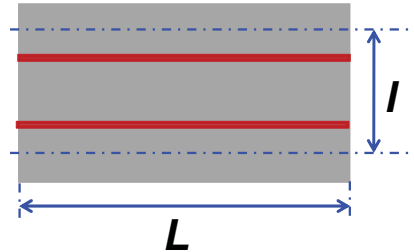
Simple design method at 20°C

Simple design method at elevated temperatures

### • Load bearing capacity of the floor slab model enhanced in presence of unprotected steel beams (2)

- Enhancement of load bearing capacity from unprotected beams is:

$$\frac{8M_{Rd,fi}}{L^2} \frac{1 + n_{ub}}{\ell}$$



where:

$n_{ub}$  is the number of unprotected beams

$M_{Rd,fi}$  is the moment resistance of each unprotected composite beam



## Simple design method at elevated temperatures



Mechanical behaviour of composite floors

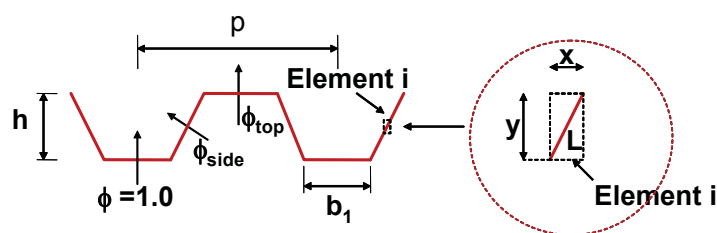
Simple design method at 20°C

Simple design method at elevated temperatures

### • Temperature calculation of composite slab

- On the basis of advanced calculation models

- 2D finite difference method
- Material thermal properties from Eurocode 4 part 1-2 for both steel and concrete
- Shadow effect is taken into account for composite slabs





Mechanical behaviour of composite floors

Simple design method at 20°C

Simple design method at elevated temperatures

- **Load bearing capacity of protected perimeter beams**
  - Overall floor plastic mechanism based on beam resistance
  - Load ratio in fire situation
    - Additional load on protected beams
  - Critical temperature simple calculation method (EN 1994-1-2)

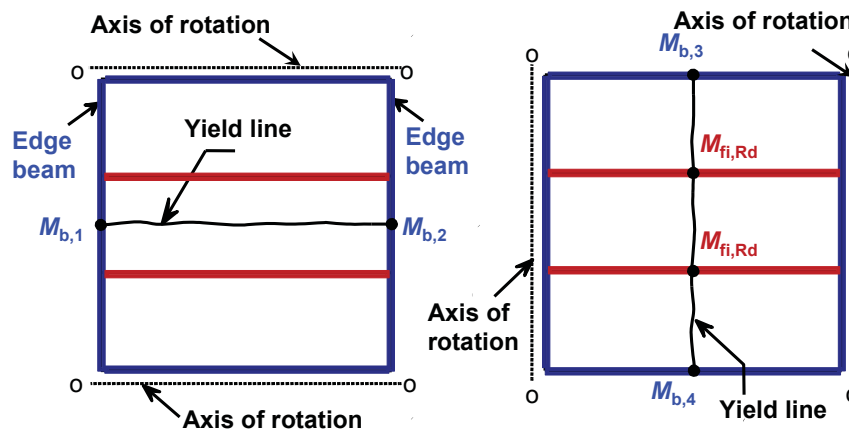


Mechanical behaviour of composite floors

Simple design method at 20°C

Simple design method at elevated temperatures

- **Load bearing capacity of protected perimeter beams on the basis of global plastic mechanism**





## Validation against test data



Mechanical  
behaviour of  
composite floors

Simple design  
method at 20°C

Simple design  
method at  
elevated  
temperatures

### 7 Full-scale Cardington Tests

1 large-scale BRE test (cold but simulated for fire)

10 Cold tests carried out in the 1960/1970s

15 small –scale tests conducted by Sheffield University in 2004

44 small-scale cold and fire tests carried out by the University of Manchester

FRACOF and COSSFIRE ISO Fire tests

Full-scale test carried out by Ulster University 2010.



## Small – Scale Experimental Behaviour and Design of Concrete Floor Slabs



Mechanical  
behaviour of  
composite floors

Simple design  
method at 20°C

Simple design  
method at  
elevated  
temperatures



22 Cold Tests and 22  
Identical Hot tests (Both MS  
and SS mesh reinforcement)





## Results obtained applying the methodology



Mechanical behaviour of composite floors

Simple design method at 20°C

Simple design method at elevated temperatures



*40 to 55% of beams can be left unprotected by placing protection where it is needed.*



Background of simple design method

33



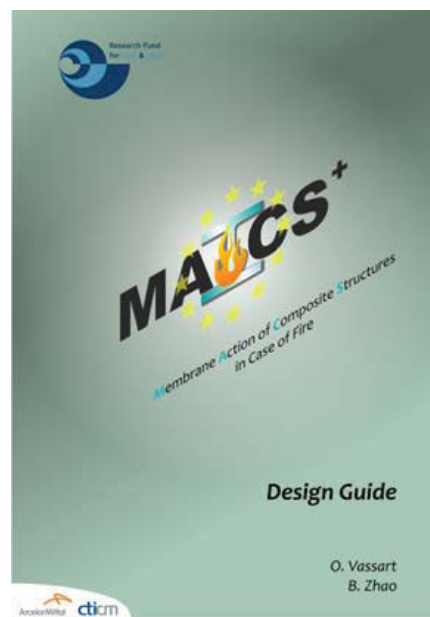
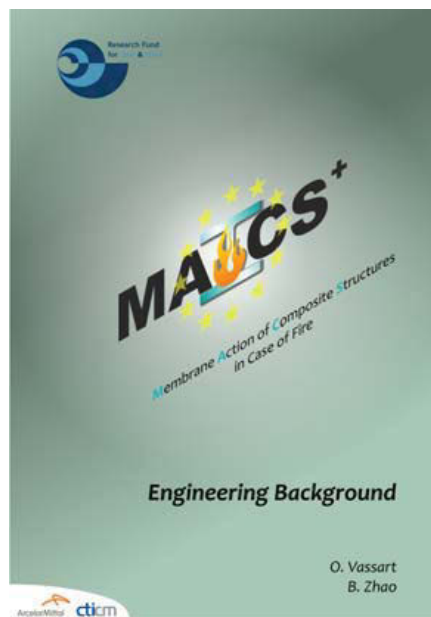
## Available documents



Mechanical behaviour of composite floors

Simple design method at 20°C

Simple design method at elevated temperatures



Background of simple design method

34





## Design Guide - Worked Example



### Table of Content



- ☞ Floor Layout
- ☞ Loading Details
  - ☐ In normal (cold) condition
  - ☐ In Fire (hot) condition
- ☞ Resistance of floor design
  - ☐ zone A
  - ☐ zone B
- ☞ Construction details



# Floor layout



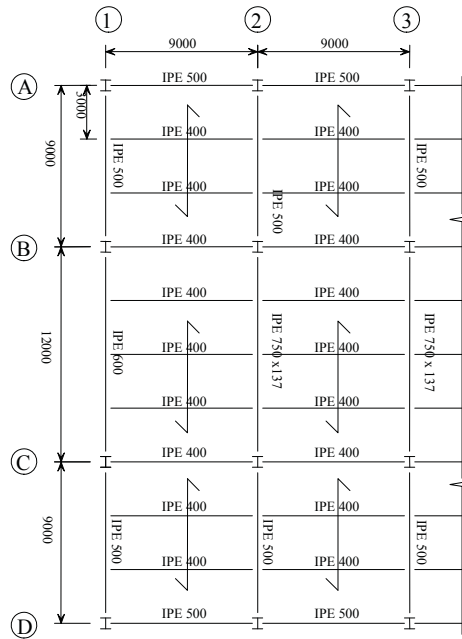
Floor Layout

Loading Details

Floor design zone A

Floor design zone B

Construction details



26<sup>th</sup> of May 2011

Worked Example

3



# Floor layout



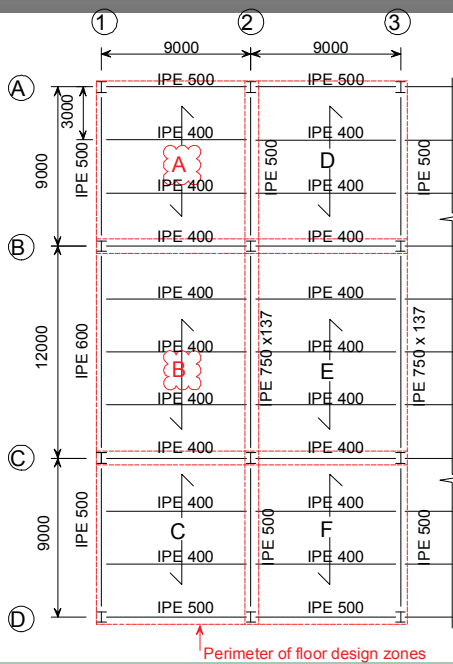
Floor Layout

Loading Details

Floor design zone A

Floor design zone B

Construction details



26<sup>th</sup> of May 2011

Worked Example

4



## Loading Details



Floor Layout

Loading Details

Floor design  
zone A

Floor design  
zone B

Construction  
details

- **Normal (Cold)**
  - Leading variable action:  $5 \text{ kN/m}^2$
  - Accompanying variable action:  $0 \text{ kN/m}^2$
  - Dead load including beam, excluding slab:  $1.2 \text{ kN/m}^2$
  - Calculated slab weight including mesh:  $2.65 \text{ kN/m}^2$
- **Fire (Hot)**
  - Combination Factor for permanent action: 1.0
  - Combination factor for leading variable action: 0.5
  - Combination factor for other variable action: 0.3

26<sup>th</sup> of May 2011

Worked Example

5



## Floor Design - Zone A



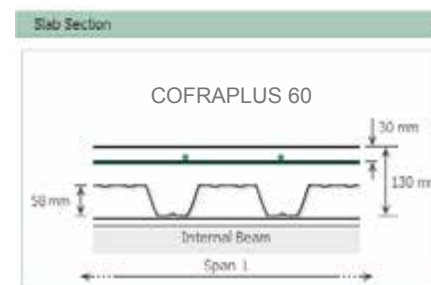
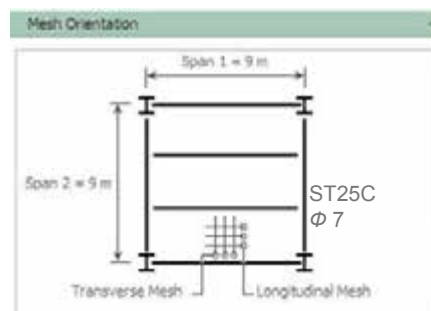
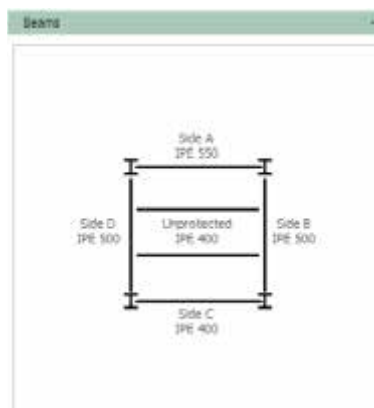
Floor Layout

Loading Details

Floor design  
zone A

Floor design  
zone B

Construction  
details



26<sup>th</sup> of May 2011

Worked Example

6



## Floor Design - Zone A



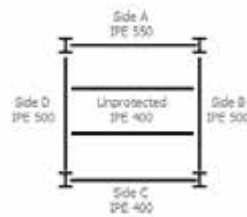
Floor Layout

Loading Details

Floor design zone A

Floor design zone B

Construction details



### BEAM check

**Unprotected Beams**

Sections and Steel Grade

Families:

Steel grade:

Available sections

IPE (European I Beams)

HE (European Wide Flange Beams)

HL (European Wide Flange Beams)

HD (European Wide Flange Columns)

Unprotected

Section size:

Degree of shear connection:  %

**Side A Perimeter Beam**

Sections and Steel Grade

Families:

Steel grade:

Available sections

IPE (European I Beams)

HE (European Wide Flange Beams)

HL (European Wide Flange Beams)

HD (European Wide Flange Columns)

Side A

Section size:

Construction type:

Beam Location:

Degree of shear connection:  %

**Side C Perimeter Beam**

Sections and Steel Grade

Families:

Steel grade:

Available sections

IPE (European I Beams)

HE (European Wide Flange Beams)

HL (European Wide Flange Beams)

HD (European Wide Flange Columns)

Side C

Section size:

Construction type:

Beam Location:

Degree of shear connection:  %

**Side B Perimeter Beam**

Sections and Steel Grade

Families:

Steel grade:

Available sections

IPE (European I Beams)

HE (European Wide Flange Beams)

HL (European Wide Flange Beams)

HD (European Wide Flange Columns)

Side B

Section size:

Construction type:

Beam Location:

Degree of shear connection:  %

**Side D Perimeter Beam**

Sections and Steel Grade

Families:

Steel grade:

Available sections

IPE (European I Beams)

HE (European Wide Flange Beams)

HL (European Wide Flange Beams)

HD (European Wide Flange Columns)

Side D

Section size:

Construction type:

Beam Location:

Degree of shear connection:  %

26<sup>th</sup> of May 2011

Worked Example

7



## Floor Design - Zone A



Floor Layout

Loading Details

Floor design zone A

Floor design zone B

Construction details

### Results for the resistance of floor

Longitudinal mesh area: 257 mm<sup>2</sup>/m Bar size: 7 mm  
 Transverse mesh area: 257 mm<sup>2</sup>/m Bar size: 7 mm  
 Factored load in fire: 6.35 kN/m<sup>2</sup>

#### • Tabular Results

Time	Beam	Mesh	Slab top	Slab bottom	Beam capacity	Maximum allowable deflection	Slab yield	Enhancement	Slab capacity	Total capacity	Unity factor
mins	°C	°C	°C	°C	kN/m <sup>2</sup>	mm	kN/m <sup>2</sup>		kN/m <sup>2</sup>	kN/m <sup>2</sup>	
0	20	20	20	20	24.12	190	1.03	2.39	2.46	26.57	0.24
5	150	24	20	148	24.12	259	1.03	2.91	2.99	27.11	0.23
10	378	37	22	365	24.10	373	1.03	3.79	3.89	27.98	0.23
15	578	53	28	505	15.61	445	1.03	4.33	4.45	30.06	0.32
20	708	71	36	600	8.70	491	1.03	4.69	4.81	31.51	0.55
25	779	94	47	668	4.13	522	1.03	4.92	5.05	33.18	0.69
30	821	118	59	719	3.08	543	1.03	5.07	5.21	34.37	0.77
35	850	123	69	759	2.62	559	1.03	5.20	5.34	34.96	0.80
40	873	140	76	792	2.27	572	1.03	5.30	5.44	34.71	0.82
45	893	170	86	820	1.97	582	1.03	5.37	5.52	34.48	0.85
50	910	193	90	843	1.79	592	1.03	5.46	5.60	34.40	0.86
55	925	212	98	864	1.70	599	1.03	5.51	5.65	34.35	0.86
60	929	232	110	882	1.61	600	1.03	5.51	5.66	34.28	0.87

Maximum unity factor: 0.87 **Floor slab adequate**

26<sup>th</sup> of May 2011

Worked Example

8

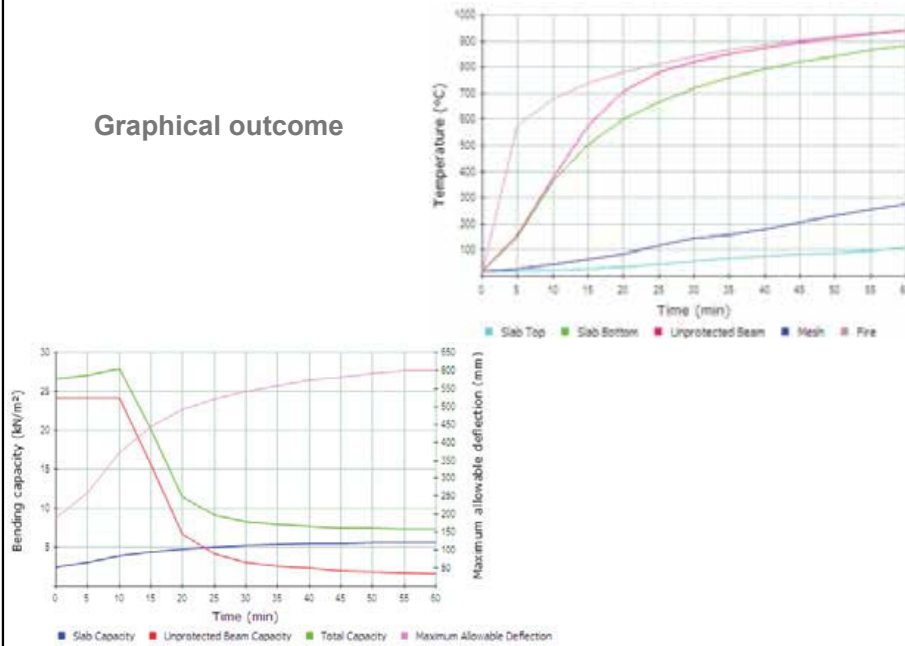


# Floor Design - Zone A



- Floor Layout
- Loading Details
- Floor design zone A**
- Floor design zone B
- Construction details

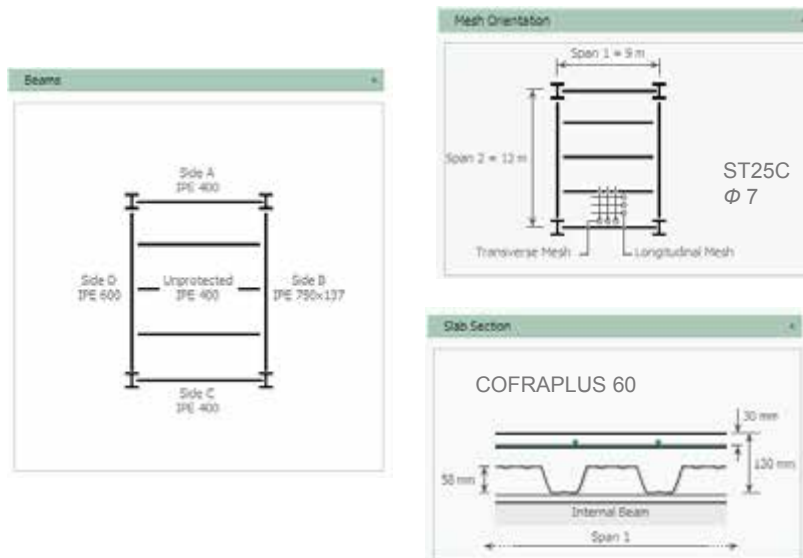
## Graphical outcome




# Floor Design - Zone B




- Floor Layout
- Loading Details
- Floor design zone A
- Floor design zone B**
- Construction details





## Floor Design - Zone B



Floor Layout

Loading Details

Floor design zone A

**Floor design zone B**

Construction details

### Beam check

**Unprotected Beams**

Sections and Steel Grade

Families: European sections

Steel grade: S355

Available sections

IPE (European I Beams)

HE (European Wide Flange Beams)

HL (European Wide Flange Beams)

HD (European Wide Flange Columns)

Unprotected

Section size: IPE 400 Degree of shear connection: 51 %

**Side A Perimeter Beam**

Sections and Steel Grade

Families: European sections

Steel grade: S355

Available sections

IPE (European I Beams)

HE (European Wide Flange Beams)

HL (European Wide Flange Beams)

HD (European Wide Flange Columns)

Side A

Section size: IPE 400 Construction type: Composite

Beam Location: Internal Beam Degree of shear connection: 51 %

**Side C Perimeter Beam**

Sections and Steel Grade

Families: European sections

Steel grade: S355

Available sections

IPE (European I Beams)

HE (European Wide Flange Beams)

HL (European Wide Flange Beams)

HD (European Wide Flange Columns)

Side C

Section size: IPE 400 Construction type: Composite

Beam Location: Internal Beam Degree of shear connection: 71 %

**Side B Perimeter Beam**

Sections and Steel Grade

Families: European sections

Steel grade: S355

Available sections

IPE (European I Beams)

HE (European Wide Flange Beams)

HL (European Wide Flange Beams)

HD (European Wide Flange Columns)

Side B

Section size: IPE 750x137 Construction type: Composite

Beam Location: Internal Beam Degree of shear connection: 71 %

**Side D Perimeter Beam**

Sections and Steel Grade

Families: European sections

Steel grade: S355

Available sections

IPE (European I Beams)

HE (European Wide Flange Beams)

HL (European Wide Flange Beams)


HD (European Wide Flange Columns)

Side D


Section size: IPE 600 Construction type: Non Composite

Beam Location: Edge Beam Degree of shear connection: 0 %

26<sup>th</sup> of May 2011
Worked Example
11



## Floor Design - Zone B



### Results for the resistance of floor

Longitudinal mesh area: 257 mm<sup>2</sup>/m    Bar size: 7 mm

Transverse mesh area: 257 mm<sup>2</sup>/m    Bar size: 7 mm

Factored load in fire: 6.35 kN/m<sup>2</sup>

• **Tabular Results**

Time	Beam	Mesh	Slab top	Slab bottom	Beam capacity	Maximum allowable deflection	Slab yield	Enhancement	Slab capacity	Total capacity	Unity factor
mins	°C	°C	°C	°C	kN/m <sup>2</sup>	mm	kN/m <sup>2</sup>		kN/m <sup>2</sup>	kN/m <sup>2</sup>	
0	20	20	20	20	24.12	254	0.79	2.94	2.34	26.45	0.24
5	158	24	20	148	24.12	322	0.79	3.48	2.76	26.88	0.24
10	378	37	22	365	24.10	437	0.79	4.38	3.48	27.88	0.23
15	578	53	28	505	15.61	588	0.79	4.95	3.93	19.54	0.32
20	708	71	36	600	6.70	855	0.79	5.31	4.22	10.92	0.88
25	779	94	47	668	4.13	985	0.79	5.55	4.41	8.54	0.74
30	821	118	59	719	3.06	906	0.79	5.71	4.54	7.60	0.84
35	890	123	89	759	2.63	822	0.79	5.84	4.64	7.28	0.88
40	873	140	76	792	2.27	636	0.79	5.95	4.72	6.99	0.91
45	893	170	86	820	1.97	665	0.79	6.02	4.78	6.75	0.94
50	910	192	90	843	1.79	656	0.79	6.11	4.85	6.64	0.96
55	925	212	98	864	1.70	663	0.79	6.16	4.90	6.59	0.96
60	939	232	110	883	1.61	566	0.79	6.19	4.91	6.53	0.97

Maximum unity factor: 0.97    **Floor slab adequate**

26<sup>th</sup> of May 2011
Worked Example
12

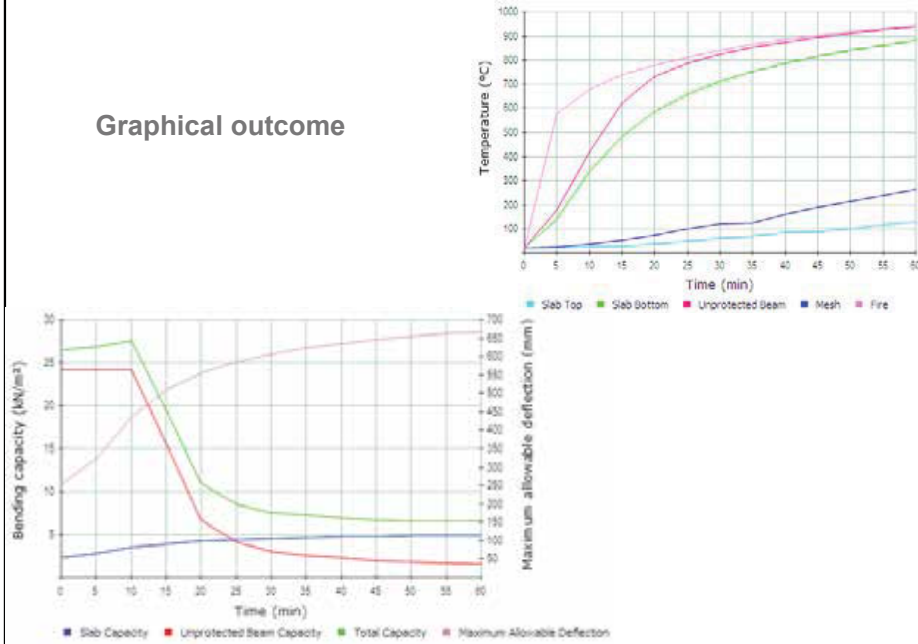


## Floor Design - Zone B



- Floor Layout
- Loading Details
- Floor design zone A
- Floor design zone B**
- Construction details

### Graphical outcome



26<sup>th</sup> of May 2011

Worked Example

13

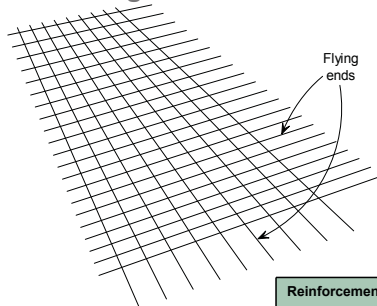


## Construction details



- Floor Layout
- Loading Details
- Floor design zone A
- Floor design zone B
- Construction details**

### Covering of the mesh in the slab to ensure continuity of the rebars



Reinforcement Type	Wire/Bar Type	Concrete Grade					
		LC 25/28	NC 25/30	LC 28/31	NC 28/35	LC 32/35	NC 32/40
Grade 500 Bar of diameter d	Ribbed	50d	40d	47d	38d	44d	35d
6 mm wires	Ribbed	300	250	300	250	275	250
7 mm wires	Ribbed	350	300	350	275	325	250
8 mm wires	Ribbed	400	325	400	325	350	300
10 mm wires	Ribbed	500	400	475	400	450	350

26<sup>th</sup> of May 2011

Worked Example

14



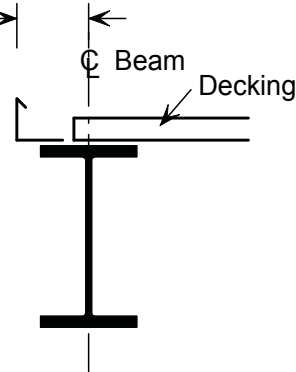
# Construction details



## requirements for the edge of a composite floor slab

- Floor Layout
- Loading Details
- Floor design zone A
- Floor design zone B
- Construction details**

Edge trim should be set out from centre line of beam (not grid) →

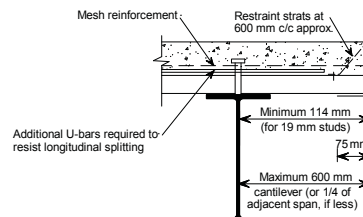


# Construction details

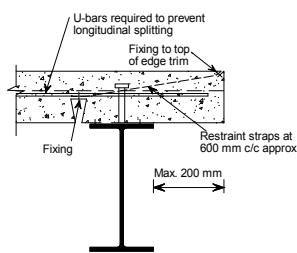


## Typical edge details

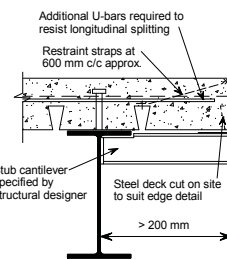
- Floor Layout
- Loading Details
- Floor design zone A
- Floor design zone B
- Construction details**



a) Typical end cantilever (decking ribs transverse to beam)



b) Typical edge detail (decking ribs parallel to beam)



c) Side cantilever with stub bracket (decking ribs parallel to beam)





Column protection

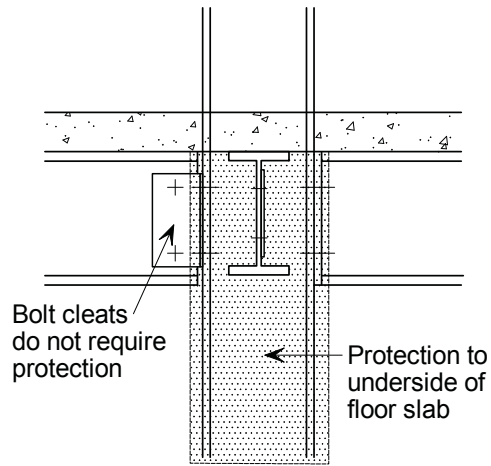
Floor Layout

Loading Details

Floor design  
zone A

Floor design  
zone B

**Construction  
details**





## ANNEX II

### Design Guide





Research Fund  
for Coal & Steel

# MAFCS<sup>+</sup>

Membrane Action of Composite Structures  
in Case of Fire

## Design Guide

O. Vassart  
B. Zhao



ArcelorMittal

ctim

# FOREWORD

## **Membrane Action in Fire design of Composite Slab with solid and cellular steel beams - Valorisation (MACS+)**

This project has been funded with support from the European Commission, Research Fund for Coal and Steel.

This publication reflects the views only of the author, and the Commission cannot be held responsible for any use which may be made of the information contained therein.

The publication has been produced as a result of different research projects:

- The RFCS Project FICEB+
- The RFCS Project COSSFIRE
- The project Leonardo Da Vinci ‘Fire Resistance Assessment of Partially Protected Composite Floors’ (FRACOF).
- A former project sponsored jointly by ArcelorMittal and CTICM and executed by a partnership of CTICM and SCI.

The simple design method was initially developed as the result of large scale fire testing conducted on a multi-storey steel framed building at the Building Research Establishment’s Cardington test facility in the UK. Much of the theoretical basis of the design method has been in existence since the late 1950’s, following studies of the structural behaviour of reinforcement concrete slabs at room temperature. The first version of the simple design method was available in the SCI Design Guide P288 ‘Fire Safe Design: A new approach to Multi-story Steel Framed Buildings’, 2 Ed.

Although the application of the method to fire resistance design is relatively new the engineering basis of the method is well established.

The simple design method was implemented in a software format by SCI in 2000 and an updated version was released in 2006, following improvements to the simple design method.

Valuable contributions were received from:

- Mary Brettle The Steel Construction Institute
- Ian Sims The Steel Construction Institute
- Louis Guy Cajot ArcelorMittal
- Renata Obiala ArcelorMittal
- Mohsen Roosefid CTICM
- Gisèle Bihina CTICM.

# Contents

	Page No
FOREWORD	i
SUMMARY	iii
1 INTRODUCTION	1
2 BASIS OF DESIGN	3
2.1 Fire safety	3
2.2 Type of structure	3
2.2.1 Simple joint models	3
2.2.2 Floor slabs and beams	5
2.3 Floor design zones	6
2.4 Combination of actions	7
2.5 Fire exposure	9
2.5.1 Fire resistance	9
2.5.2 Natural fire (parametric temperature-time curve)	10
3 RECOMMENDATIONS FOR STRUCTURAL ELEMENTS	12
3.1 Floor design zones	12
3.2 Floor slab and beams	13
3.2.1 Temperature calculation of floor slab	13
3.2.2 Temperature calculation of unprotected composite beams	15
3.2.3 Fire design of floor slab	16
3.2.4 Fire design of beams on the perimeter of the floor design zone	18
3.3 Reinforcement details	19
3.3.1 Detailing mesh reinforcement	19
3.3.2 Detailing requirements for the edge of a composite floor slab	20
3.4 Design of non composite edge beams	21
3.5 Columns	22
3.6 Joints	22
3.6.1 Joint classification	23
3.6.2 End plates	23
3.6.3 Fin plates	24
3.6.4 Web cleats	25
3.6.5 Fire protection	25
3.7 Overall building stability	25
4 COMPARTMENTATION	27
4.1 Beams above fire resistant walls	27
4.2 Stability	28
4.3 Integrity and insulation	28
5 WORKED EXAMPLE	29
5.1 Design of composite slab in fire conditions	35
5.1.1 Floor design: Zone B	35
5.1.2 Floor design: Zone A	51
5.1.3 Floor design: Zone E	56
5.1.4 Floor design: Zone D	68
5.2 Reinforcement details	76
5.3 Fire protection of columns	76
REFERENCES	78

## SUMMARY

Large-scale fire tests conducted in a number of countries and observations of actual building fires have shown that the fire performance of composite steel framed buildings is much better than is indicated by fire resistance tests on isolated elements. It is clear that there are large reserves of fire resistance in modern steel-framed buildings and that standard fire resistance tests on single unrestrained members do not provide a satisfactory indicator of the performance of such structures.

This publication presents guidance on the application of a simple design method, as implemented in MACS+ software. The recommendations are conservative and are limited to structures similar to that tested, i.e. non-sway steel-framed buildings with composite floors and composite floors with Cellular Beams. The guidance gives designers access to whole building behaviour and allows them to determine which members can remain unprotected while maintaining levels of safety equivalent to traditional methods.

In recognition that many fire safety engineers are now considering natural fires, a natural fire model is included alongside the use of the standard fire model, both expressed as temperature-time curves in Eurocode 1.

In addition to the design guidance provided by this publication, a separate Engineering Background document provides details of fire testing and finite element analysis conducted as part of the FRACOF, COSSFIRE and FICEB project and some details of the Cardington tests which were conducted on the eight-storey building at Cardington. The background document will assist the reader to understand the basis of the design recommendations in this publication.



# 1 INTRODUCTION

The design recommendations in this publication are based on the performance of composite floor plates, as interpreted from actual building fires and from full-scale fire tests<sup>(1,2,3)</sup>. These conservative recommendations for fire design may be considered as equivalent to advanced methods in the Eurocodes.

The elements of structure of multi-storey buildings are required by national building regulations to have fire resistance. The fire resistance may be established from performance in standard fire resistance tests or by calculations in accordance with recognised standards, notably EN 1991-1-2<sup>(4)</sup>, EN 1993-1-2<sup>(5)</sup> and EN 1994-1-2<sup>(6)</sup>. In a standard fire test, single, isolated and unprotected I or H section steel beams can only be expected to achieve 15 to 20 minutes fire resistance. It has thus been normal practice to protect steel beams and columns by use of fire resisting boards, sprays or intumescent coatings, or, in slim floor or shelf angle floor construction, by encasing the structural elements within floors.

Large-scale natural fire tests<sup>(7)</sup> carried out in a number of countries have shown consistently that the inherent fire performance of composite floor plates with unprotected steel elements is much better than the results of standard tests with isolated elements would suggest. Evidence from real fires indicates that the amount of protection being applied to steel elements may be excessive in some cases. In particular, the Cardington fire tests presented an opportunity to examine the behaviour of a real structure in fire and to assess the fire resistance of unprotected composite structures under realistic conditions.

As the design recommendations given in this publication are related to generalised compartment fire, they can be easily applied under standard fire condition such as it is demonstrated through the real scale floor test within the scope of FRACOF and COSSFIRE project. Obviously, this possibility provides a huge advantage to engineers in their fire safety design of multi-storey buildings with steel structures. Large scale fire test realised in Ulster in the scope of the FICEB project highlight that the membrane action theory can also be applied with Cellular Beams.

Where national building regulations permit performance-based design of buildings in fire, the design method provided by this guide may be applied to demonstrate the fire resistance of the structure without applied fire protection. In some countries acceptance of such demonstration may require special permission from the national building control authority.

The recommendations presented in this publication can be seen as extending the fire engineering approach in the area of structural performance and developing the concept of fire safe design. It is intended that designs carried out in accordance with these recommendations will achieve at least the level of safety required by national regulations while allowing some economies in construction costs.

In addition to fire resistance for the standard temperature-time curve, recommendations are presented for buildings designed to withstand a natural fire. Natural fires can be defined in the MACS+ software using the parametric temperature-time curve given in EN 1991-1-2. This takes account of the size of the compartment, the size of any

openings and the amount of combustibles. Alternatively, the MACS+ software permits temperature-time curves to be read from a text file, allowing output from other fire models to be used.

The recommendations apply to composite frames broadly similar to the eight-storey building tested at Cardington, as illustrated in Figure 1-1 and Figure 1-2.

The design recommendations are presented as guide to the application of the MACS+ software, which is available as a free download from [www.arcelormittal.com/sections](http://www.arcelormittal.com/sections).



**Figure 1-1** Cardington test building prior to the concreting of the floors



**Figure 1-2** View of unprotected steel structure

## 2 BASIS OF DESIGN

This Section gives an overview of the design principles and assumptions underlying the development of the simple design method; more detailed information is given in the accompanying background document<sup>(7)</sup>. The type of structure that the design guidance is applicable to is also outlined.

The design guidance has been developed from research based on the results from fire tests, ambient temperature tests and finite element analyses.

### 2.1 Fire safety

The design recommendations given in the simple design method have been prepared such that the following fundamental fire safety requirements are fulfilled:

- There should be no increased risk to life safety of occupants, fire fighters and others in the vicinity of the building, relative to current practice.
- On the floor exposed to fire, excessive deformation should not cause failure of compartmentation, in other words, the fire will be contained within its compartment of origin and should not spread horizontally or vertically.

### 2.2 Type of structure

The design guidance given in the simple design method applies only to steel-framed buildings with composite floor beams and slabs of the following general form:

- braced frames not sensitive to buckling in a sway mode,
- frames with connections designed using simple joint models,
- composite floor slabs comprising steel decking, a single layer of reinforcing mesh and normal or lightweight concrete, designed in accordance with EN 1994-1-1<sup>(9)</sup>,
- floor beams designed to act compositely with the floor slab and designed to EN 1994-1-1.
- beams with service openings.

The guidance does **not** apply to:

- floors constructed using pre fabricated concrete slabs,
- internal floor beams that have been designed to act non-compositely (beams at the edge of the floor slab may be non-composite).

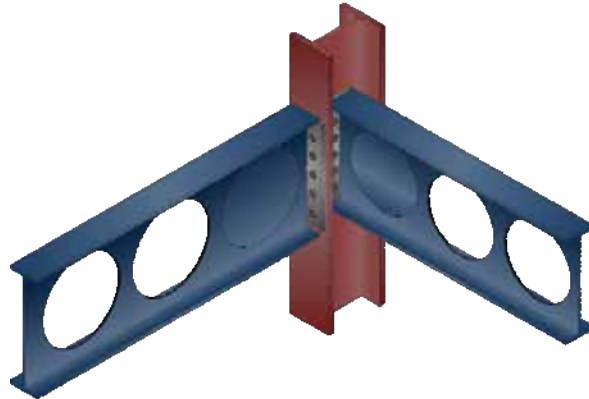
#### 2.2.1 Simple joint models

The joint models adopted during the development of the guidance given in this publication assume that bending moments are not transferred through the joint. The joints are known as ‘simple’.

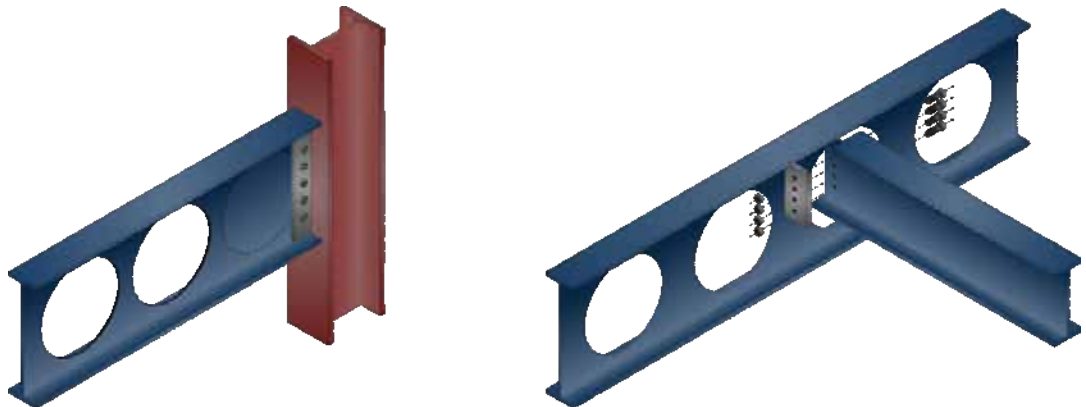
Beam-to-column joints that may be considered as ‘simple’ include joints with the following components:

- flexible end plates (Figure 2-1)
- fin plates (Figure 2-2)
- web cleats (Figure 2-3).

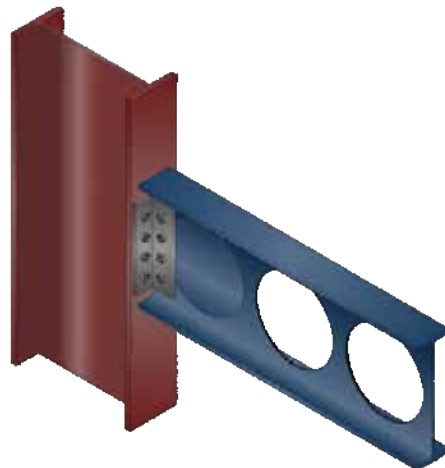
Further information on the design of the components of ‘simple’ joints is given in Section 3.6.



**Figure 2-1 Example of a joint with flexible end plate connections**



**Figure 2-2 Examples of joints with fin plate connections**



**Figure 2-3 Example of a joint with a web cleat connection**

## 2.2.2 Floor slabs and beams

The design recommendations given in this guide are applicable to profiled steel decking up to 80 mm deep with depths of concrete above the steel decking from 60 to 130 mm. The resistance of the steel decking is ignored in the fire design method but the presence of the steel decking prevents spalling of the concrete on the underside of the floor slab. This type of floor construction is illustrated in Figure 2-4.

The design method can be used with either isotropic or orthotropic reinforcing mesh, that is, meshes with either the same or different areas in orthogonal directions. The steel grade for the mesh reinforcement should be specified in accordance with EN 10080. The MACS+ software can only be used for welded mesh reinforcement and cannot consider more than one layer of reinforcement. Reinforcement bars in the ribs of the composite slab are **not** required.

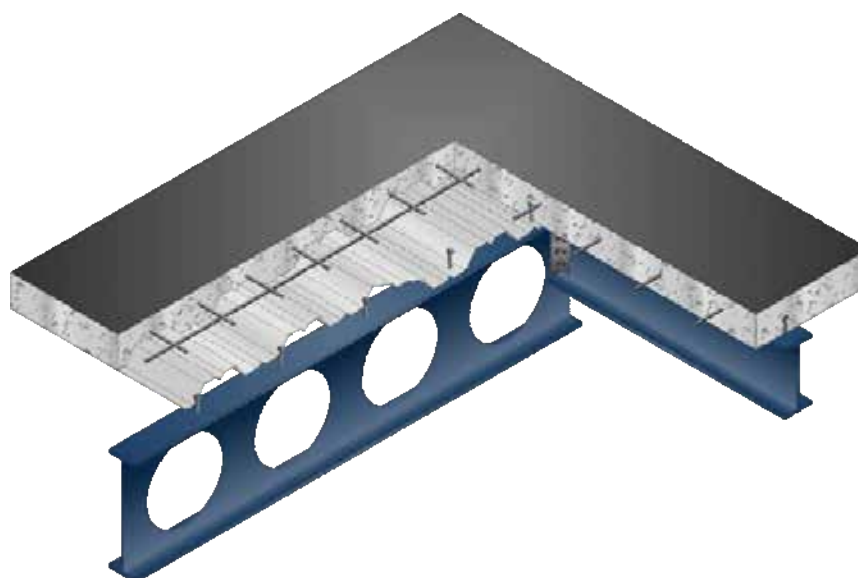
The software includes A and B series standard fabric meshes as defined by UK national standards<sup>(11,12)</sup> (Table 2-1) and a range of mesh sizes defined by French national standards<sup>(13,14)</sup> (Table 2-2), and commonly used in the French construction market. User defined sizes of welded mesh are also permitted in the MACS+ software.

**Table 2-1 Fabric mesh as defined by BS 4483<sup>(11)</sup>**

Mesh Reference	Size of mesh (mm)	Weight (kg/m <sup>2</sup> )	Longitudinal wires		Transverse wires	
			Size (mm)	Area (mm <sup>2</sup> /m)	Size (mm)	Area (mm <sup>2</sup> /m)
A142	200×200	2.22	6	142	6	142
A193	200×200	3.02	7	193	7	193
A252	200×200	3.95	8	252	8	252
A393	200×200	6.16	10	393	10	393
B196	100×200	3.05	5	196	7	193
B283	100×200	3.73	6	283	7	193
B385	100×200	4.53	7	385	7	193
B503	100×200	5.93	8	503	8	252

**Table 2-2 Fabric mesh commonly used in French market**

Mesh Reference	Size of mesh (mm)	Weight (kg/m <sup>2</sup> )	Longitudinal wires		Transverse wires	
			Size (mm)	Area (mm <sup>2</sup> /m)	Size (mm)	Area (mm <sup>2</sup> /m)
ST 20	150×300	2.487	6	189	7	128
ST 25	150×300	3.020	7	257	7	128
ST 30	100×300	3.226	6	283	7	128
ST 35	100×300	6.16	7	385	7	128
ST 50	100×300	3.05	8	503	8	168
ST 60	100×300	3.73	9	636	9	254
ST 15 C	200×200	2.22	6	142	6	142
ST 25 C	150×150	4.03	7	257	7	257
ST 40 C	100×100	6.04	7	385	7	385
ST 50 C	100×100	7.90	8	503	8	503
ST 60 C	100×100	9.98	9	636	9	636



**Figure 2-4 Cut away view of a typical composite floor construction**

It is important to define the beam sizes used in the construction of the floor plate as this will influence the fire performance of the floor plate. The designer will need to have details of the serial size, steel grade and degree of shear connection available for each beam in the floor plate. The MACS+ software interface allows the user to choose from a predefined list of serial sizes covering common British, European and American I and H sections.

### **2.3 Floor design zones**

The design method requires the designer to split the floor plate into a number of floor design zones as shown in Figure 2-5. The beams on the perimeter of these floor design zones must be designed to achieve the fire resistance required for the floor plate and will therefore normally be fire protected.

A floor design zone should meet the following criteria:

- Each zone should be rectangular.
- Each zone should be bounded on all sides by beams.
- The beams within a zone should only span in one direction.
- Columns should not be located within a floor design zone; they may be located on the perimeter of the floor design zone.
- For fire resistance periods in excess of 60 minutes, or when using the parametric temperature-time curve, all columns should be restrained by at least one fire protected beam in each orthogonal direction.

All internal beams within the zone may be left unprotected, provided that the fire resistance of the floor design zone is shown to be adequate using the MACS+ software. The size and spacing of these unprotected beams are not critical to the structural performance in fire conditions.

An example of a single floor design zone is given in Figure 2-5.

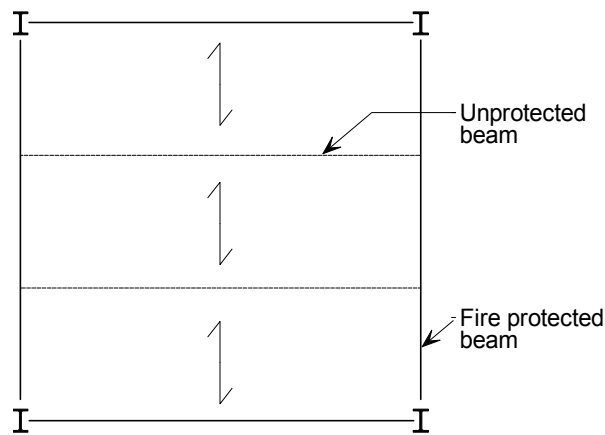


Figure 2-5 Example of a floor design zone

## 2.4 Combination of actions

The combination of actions for accidental design situations given in 6.4.3.3 and Table A1.3 of EN 1990<sup>(15)</sup> should be used for fire limit state verifications. With only unfavourable permanent actions and no prestressing actions present, the combination of actions to consider is:

$$\sum G_{k,j,\text{sup}} + A_d + (\psi_{1,1} \text{ or } \psi_{2,1}) Q_{k,1} + \sum \psi_{2,i} Q_{k,i}$$

with:

$G_{k,j,\text{sup}}$	unfavourable permanent action
$A_d$	leading accidental action
$Q_{k,1}$ and $Q_{k,i}$	accompanying variable actions, main and other respectively
$\psi_{1,1}$	factor for the frequent value of the leading variable action
$\psi_{2,i}$	factor for the quasi-permanent value of the $i^{\text{th}}$ variable action

The use of either  $\psi_{1,1}$  or  $\psi_{2,1}$  with  $Q_{k,1}$  should be specified in the relevant National Annex. The National Annex for the country where the building is to be constructed should be consulted to determine which factor to use.

The values used for the  $\psi$  factors relate to the category of the variable action they are applied to. The Eurocode recommended values for the  $\psi$  factors for buildings are given in Table A1.1 of EN 1990; those values are confirmed or modified by the relevant National Annex. The  $\psi$  factor values for buildings in the UK and France are summarised in Table 2-3. For floors that allow loads to be laterally distributed, the following uniformly distributed loads are given for moveable partitions in 6.3.1.2(8) of EN 1991-1-1<sup>(16)</sup>:

Movable partitions with a self-weight  $\leq 1.0$  kN/m wall length:  $q_k = 0.5$  kN/m<sup>2</sup>

Movable partitions with a self-weight  $\leq 2.0$  kN/m wall length:  $q_k = 0.8$  kN/m<sup>2</sup>

Movable partitions with a self-weight  $\leq 3.0$  kN/m wall length:  $q_k = 1.2$  kN/m<sup>2</sup>.

Movable partitions with self-weights greater than 3.0 kN/m length should be allowed for by considering their location.

The Eurocode recommended values for variable imposed loads on floors are given in Table 6.2 of EN 1991-1-1; those values may also be modified by the relevant National Annex. Table 2-4 presents the Eurocode recommended values and the values given in the UK and French National Annexes for the imposed load on an office floor.

**Table 2-3 Values of  $\psi$  factors**

Actions	Eurocode recommended values		UK National Annex values		French National Annex values	
	$\psi_1$	$\psi_2$	$\psi_1$	$\psi_2$	$\psi_1$	$\psi_2$
Domestic, office and traffic areas where: 30 kN < vehicle weight $\leq 160$ kN	0.5	0.3	0.5	0.3	0.5	0.3
Storage areas	0.9	0.8	0.9	0.8	0.9	0.8
Other*	0.7	0.6	0.7	0.6	0.7	0.6

\* Climatic actions are not included

**Table 2-4 Imposed load on an office floor**

Category of loaded area	Eurocode recommended values		UK National Annex values		French National Annex values	
	$q_k$ (kN/m <sup>2</sup> )	$Q_k$ (kN)	$q_k$ (kN/m <sup>2</sup> )	$Q_k$ (kN)	$q_k$ (kN/m <sup>2</sup> )	$Q_k$ (kN)
B – Office areas	3.0	4.5	2.5* or 3.0**	2.7	3.5 – 5.0	15.0

\* Above ground floor level

\*\*At or below ground floor level



## 2.5 Fire exposure

The recommendations given in the simple design method may be applied to buildings in which the structural elements are considered to be exposed to a standard temperature-time curve or parametric temperature-time curve, both as defined in EN 1991-1-2. Advanced model may also be used to define a temperature-time curve for a natural fire scenario. The resulting temperature-time curve may be input to the MACS+ software in the form of a text file.

In all cases, the normal provisions of national regulations regarding means of escape should be followed.

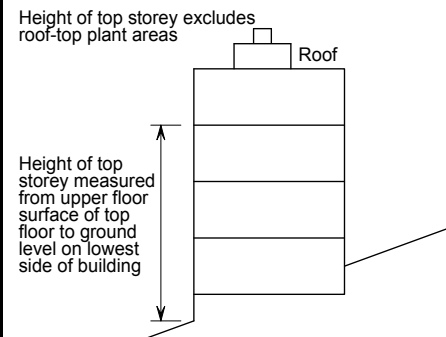
### 2.5.1 Fire resistance

The recommended periods of fire resistance for elements of construction in various types of building in national regulations are given in Table 2-5 and Table 2-6.

The following recommendations are for buildings in which the elements of structure are required to have up to 180 minutes fire resistance. Provided that they are followed, composite steel framed buildings will maintain their stability for this period of fire resistance, when any compartment is subject to the standard temperature-time curve<sup>(1)</sup>.

All composite steel framed buildings with composite floors may be considered to achieve 15 minutes fire resistance without fire protection, and so no specific recommendations are given in this case.

**Table 2-5 Summary of fire resistance requirements from Approved Document B for England and Wales**

	Fire resistance (mins) for height of top storey (m)				
	<5	≤18	≤30	>30	
Residential (non-domestic)	30	60	90	120	 <p>Height of top storey excludes roof-top plant areas</p> <p>Height of top storey measured from upper floor surface of top floor to ground level on lowest side of building</p>
Office	30	60	90	120*	
Shops, commercial, assembly and recreation	30	60	90	120*	
Closed car parks	30	60	90	120*	
Open-sided car parks	15	15	15	60	
Approved Document B allows the fire resistance periods to be reduced from 60 to 30 minutes or from 90 to 60 minutes, for most purpose groups.					
* Sprinklers are required, but the fire resistance of the floor may be 90 minutes only.					

**Table 2-6 Summary of fire resistance requirements from French Fire Regulations**

Residential (non-domestic)		< 2 levels	2 levels < ... ≤ 4 levels	4 levels < ... ≤ 28 m	28 m < H < 50 m	> 50 m
		R15	R30	R60	R90	R120
		Ground floor		Height of the top floor ≤ 8 m	Height of the top floor > 8 m	Height of the top floor > 28 m
Office <sup>1</sup>		0			R60	R 120
Shops, commercial, assembly and recreation	< 100 persons	0			R60	R120
	< 1500 persons	R30			R60	
	> 1500 persons	R30	R60	R90		
		Ground floor	> 2 levels	Height of the top floor > 28 m		
Closed car parks		R30	R60	R90		
Open-sided car parks						

Note: <sup>1</sup> Office which is not open to the public  
*H* is the height of the top floor

### 2.5.2 Natural fire (parametric temperature-time curve)

The MACS+ software allows the effect of natural fire on the floor plate to be considered using the parametric temperature-time curve as defined in EN 1991-1-2 Annex A<sup>(1)</sup>. It should be noted that this is an Informative Annex and its use may not be permitted in some European countries, such as France. Before final design is undertaken the designer should consult the relevant National Annex.

Using this parametric fire curve, the software defines the compartment temperature taking account of:

- the compartment size:
  - compartment length
  - compartment width
  - compartment height
- the height and area of windows:
  - window height
  - window length
  - percentage open window
- the amount of combustibles and their distribution in the compartment:
  - fire load
  - combustion factor
  - the rate of burning
- the thermal properties of the compartment linings.

The temperature of a parametric fire will often rise more quickly than the standard fire in the early stages but, as the combustibles are consumed, the temperature will decrease rapidly. The standard fire steadily increases in temperature indefinitely.

The standard temperature-time curve and a typical parametric temperature-time curve are shown in Figure 2-6.

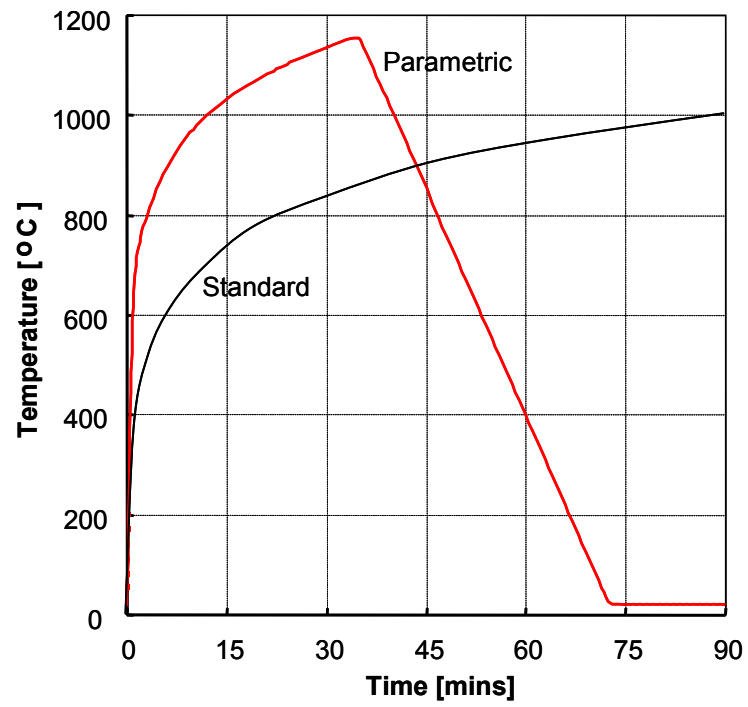


Figure 2-6 Comparison of typical parametric and standard temperature-time curve

## 3 RECOMMENDATIONS FOR STRUCTURAL ELEMENTS

### 3.1 Floor design zones

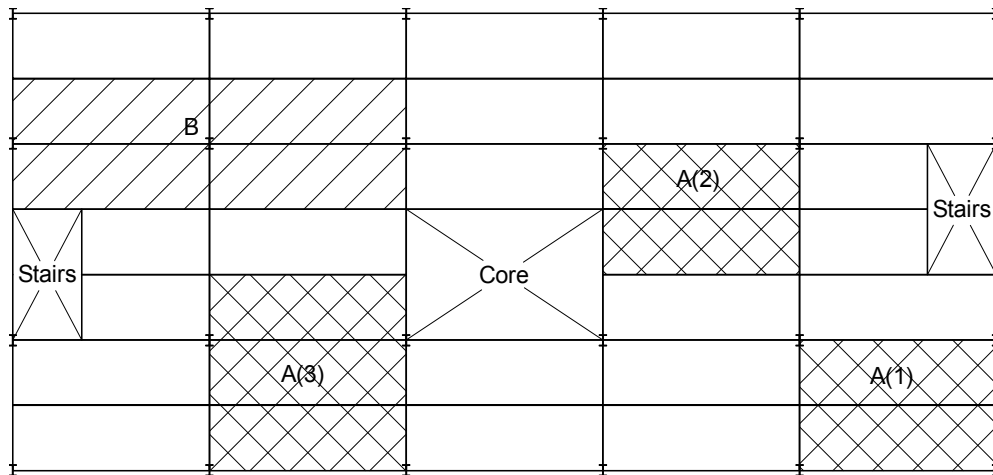
Each floor should be divided into design zones that meet the criteria given in Section 2.3.

The division of a floor into floor design zones is illustrated in Figure 3-1. Floor zones designated 'A' are within the scope of the MACS+ software and their load bearing performance in fire conditions may be determined using MACS+. The zone designated 'B' is outside the scope of the software because it contains a column and the beams within the zone do not all span in the same direction.

A single floor zone is illustrated in Figure 3-2 showing the beam span designations used in the MACS+ software. Normal design assumes that floor loads are supported by secondary beams which are themselves supported on primary beams.

The fire design method assumes that at the fire limit state, the resistance of the unprotected internal beams reduces significantly, leaving the composite slab as a two way spanning element simply supported around its perimeter. In order to ensure that the slab can develop membrane action, the MACS+ software computes the moment applied to each perimeter beam as a result of the actions on the floor design zone. To maintain the vertical support to the perimeter of the floor design zone in practice, the software calculates the degree of utilisation and hence the critical temperature of these perimeter beams. The fire protection for these beams should be designed on the basis of this critical temperature and the fire resistance period required for the floor plate in accordance with national regulations. The critical temperature and the degree of utilisation for each perimeter beam is reported for Side A to D of the floor design zone as shown by Figure 3-2.

As noted in Section 2.2.2, a restriction on the use of the MACS+ software is that for 60 minutes or more fire resistance, the zone boundaries should align with the column grid and the boundary beams should be fire protected. For 30 minutes fire resistance, this restriction does not apply and the zone boundaries do not have to align with the column grid. For example, in Table 3-3, zones A2 and A3 have columns at only two of their corners and could only be considered as design zones for a floor that requires no more than 30 minutes fire resistance.



**Key to figure**

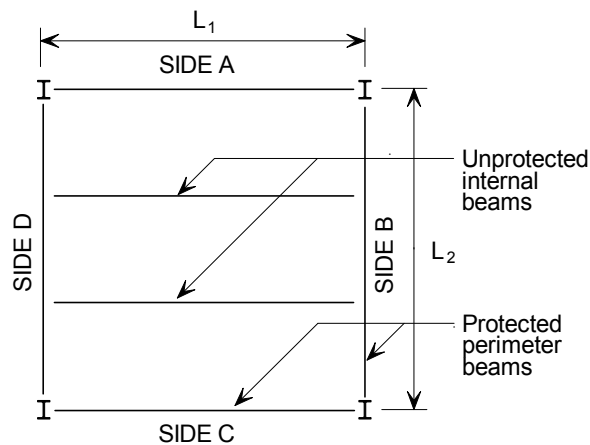
A: These zones may be designed using MACS+

B: Outside the scope of MACS+

A(1) Any period of fire resistance

A(2) & A(3) only 30 minutes fire resistance

**Figure 3-1 Possible floor design zones**



**Figure 3-2 Definition of span 1 ( $L_1$ ) and span 2 ( $L_2$ ) and the beam layout for a floor design zone in a building requiring fire resistance of 60 minutes or more.**

### 3.2 Floor slab and beams

The MACS+ software calculates the load bearing capacity of the floor slab and unprotected beams at the fire limit state. As the simple design method, implemented in the software, assumes that the slab will have adequate support on its perimeter the software also calculates the critical temperature for each perimeter beam based on the load bearing capacity of the floor design zone.

#### 3.2.1 Temperature calculation of floor slab

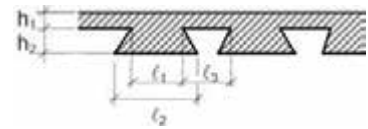
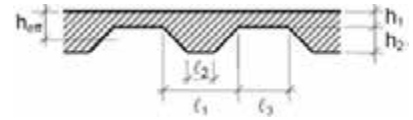
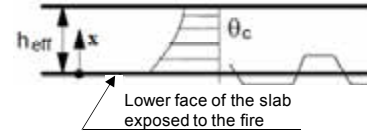
The temperature distribution in a composite slab can be determined using a calculation model by finite differences or finite elements taking into account the exact shape of the slab and respecting the principles and rules 4.4.2 of EN 1994-1-2 (6).

As an alternative, the temperature distribution in an unprotected composite slab subjected to standard fire can be determined from the values given in Table 3-1

established in accordance with EN 1992-1-2 (17) and its National Annex, depending on the effective thickness  $h_{\text{eff}}$  of the slab defined by D.4 of Annex D of EN1994-1-2 (6).

**Table 3-1 Temperature distribution in a slab ( $h_{\text{eff, max}} = 150\text{mm}$ ) for standard fire exposure of 30 to 180 min**

Distance $x$ [mm]	Temperature in the concrete slab $\theta_c$ [°C]				
	30 min	60 min	90 min	120 min	180 min
2.5	675	831	912	967	1 042
10	513	684	777	842	932
20	363	531	629	698	797
30	260	418	514	583	685
40	187	331	423	491	591
50	135	263	349	415	514
60	101	209	290	352	448
70	76	166	241	300	392
80	59	133	200	256	344
90	46	108	166	218	303
100	37	89	138	186	267
110	31	73	117	159	236
120	27	61	100	137	209
130	24	51	86	119	186
140	23	44	74	105	166
150	22	38	65	94	149



$$\Phi = \frac{2}{\pi} \tan^{-1} \frac{2h_2}{l_1 + l_3 - l_2}$$

From the above temperature distribution, the three following parameters can be determined:

- $\theta_2$  : temperature of the exposed face of the slab;
- $\theta_1$  : temperature of the non-exposed face of the slab;
- $\theta_s$  : temperature of the slab at the level of the reinforcing mesh.

Under standard fire, the following values of  $x$  should be used to determine the temperatures  $\theta_1$ ,  $\theta_2$ , and  $\theta_s$  from Table 3-1:

- For  $\theta_2$ ,  $x = 2.5$  mm;
- For  $\theta_1$ ,  $x = h_{\text{eff}}$ ;

- For  $\theta_s$ ,  $x = h_1 - d + 10 \Phi$  ( $d$ : distance between the reinforcing mesh axis and the non-exposed face of the concrete, see Figure 3-3, and  $\Phi$ : see Table 3-1).

### 3.2.2 Temperature calculation of unprotected composite beams

The temperatures of an unprotected steel beam under ISO fire can be determined in accordance with 4.3.4.2.2 of EN 1994-1-2. In order to facilitate the use of the calculation method, temperatures are given in Table 3-2 for unprotected steel cross-sections as a function of the resulting section factor (taken as the section factor multiplied by the correction factor for the shadow effect) and the fire exposure duration).

As an alternative, the temperature distribution in an unprotected composite slab subjected to standard fire can be determined from the values given in Table 3-1 established in accordance with EN 1992-1-2 (17) and its National Annex, depending on the effective thickness  $h_{\text{eff}}$  of the slab defined by D.4 of Annex D of EN1994-1-2 (6).

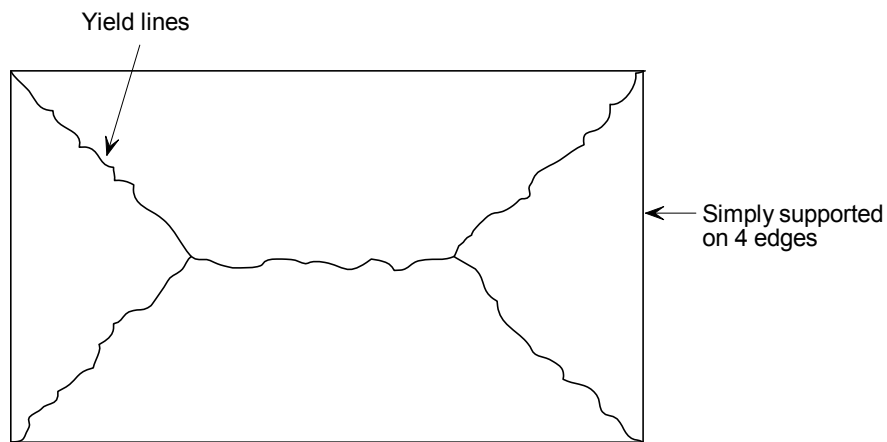
**Table 3-2 Temperature of an unprotected steel cross-section under ISO fire**

Resulting section factor $k_{sh} \left( \frac{A_s}{V_s} \right)$ [m <sup>-1</sup> ]	Temperature of the steel cross-section $\theta_a$ [°C]				
	30 min	60 min	90 min	120 min	180 min
20	432	736	942	1 030	1 101
30	555	835	987	1 039	1 104
40	637	901	995	1 042	1 106
50	691	923	997	1 043	1 106
60	722	931	999	1 044	1 107
70	734	934	1 000	1 045	1 107
80	742	936	1 001	1 046	1 108
90	754	937	1 001	1 046	1 108
100	768	938	1 002	1 046	1 108
110	782	939	1 002	1 047	1 108
120	793	939	1 003	1 047	1 108
130	802	940	1 003	1 047	1 109
140	810	940	1 003	1 047	1 109
150	815	941	1 003	1 047	1 109
200	829	942	1 004	1 048	1 109
500	838	944	1 005	1 048	1 109

### 3.2.3 Fire design of floor slab

#### Load bearing performance of the composite floor slab

When calculating the load bearing capacity of each floor design zone the resistance of the composite slab and the unprotected beams are calculated separately. The slab is assumed to have no continuity along the perimeter of the floor design zone. The load that can be supported by the flexural behaviour of the composite slab within the floor design zone is calculated based on a lower bound mechanism assuming a yield line pattern as shown in Figure 3-3.



**Figure 3-3 Assumed yield line pattern used to calculate slab resistance**

The value of the resistance calculated using the lower bound mechanism is enhanced by considering the beneficial effect of tensile membrane action at large displacements. This enhancement increases with increasing vertical deflection of the slab until failure occurs due to fracture of the reinforcement across the short slab span or compressive failure of the concrete in the corners of the slab, as shown by Figure 3-4. As the design method cannot predict the point of failure, the value of deflection considered when calculating the enhancement is based on a conservative estimate of slab deflection that includes allowance for the thermal curvature of the slab and the strain in the reinforcement, as shown below.

$$w = \frac{\alpha(T_2 - T_1)l^2}{19.2h_{eff}} + \sqrt{\left(\frac{0.5f_y}{E_a}\right)\frac{3L^2}{8}}$$

The deflection allowed due to elongation of the reinforcement is also limited by the following expression.

$$w \leq \frac{\alpha(T_2 - T_1)l^2}{19.2h_{eff}} + \frac{l}{30}$$

where:

- $(T_2 - T_1)$  is the temperature difference between the top and bottom surface of the slab
- $L$  is the longer dimension of the floor design zone
- $l$  is the shorter dimension of the floor design zone
- $f_y$  is the yield strength of the mesh reinforcement
- $E$  is the modulus of elasticity of the steel
- $h_{eff}$  is the effective depth of the composite slab

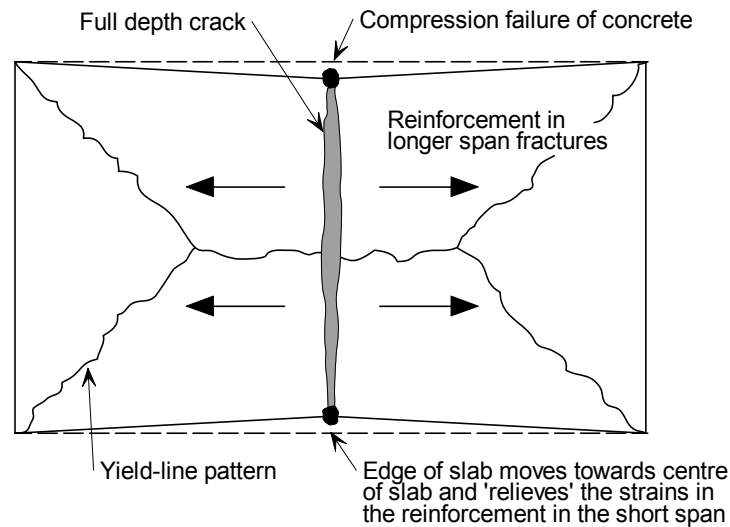


$\alpha$  is the coefficient of thermal expansion of concrete.

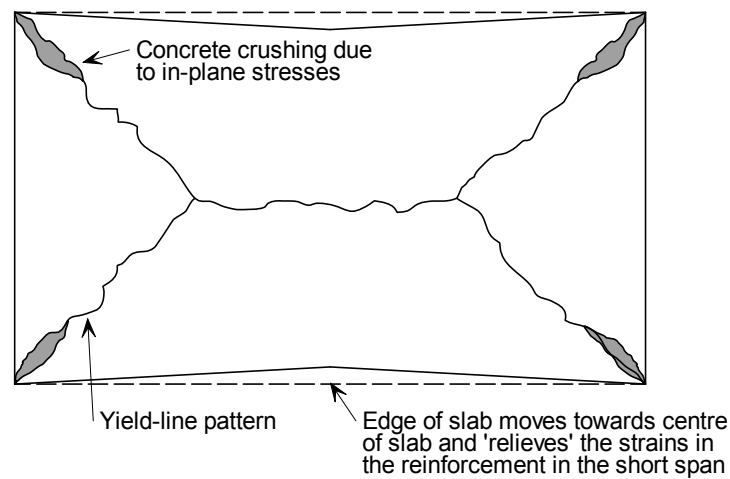
All of the available test evidence shows that this value of deflection will be exceeded before load bearing failure of the slab occurs. This implies that the resistance predicted using the design method will be conservative compared to its actual performance.

The overall deflection of the slab is also limited by the following expression:

$$w \leq \frac{L+l}{30}$$



(a) Tensile failure of the reinforcement



(b) Compressive failure of the concrete

**Figure 3-4 Failure mode due to fracture of the reinforcement**

The residual bending resistance of the unprotected composite beams is then added to the enhanced slab resistance to give the total resistance of the complete system.

### ***Integrity and insulation performance of the composite slab***

The MACS+ software does not explicitly check the insulation or integrity performance of the floor slab. The designer must therefore ensure that the slab thickness chosen is

sufficient to provide the necessary insulation performance in accordance with the recommendations given in EN1994-1-2.

To ensure that the composite slab maintains its integrity during the fire and that membrane action can develop, care must be taken to ensure that the reinforcing mesh is properly lapped. This is especially important in the region of unprotected beams and around columns. Further information on required lap lengths and placement of the reinforcing mesh is given in Section 3.3.

### 3.2.4 Fire design of beams on the perimeter of the floor design zone

The beams along the perimeter of the floor design zone, labelled A to D in Figure 3-2, should achieve the fire resistance required for the floor plate, in order to provide the required vertical support to the perimeter of the floor design zone. This usually results in these beams being fire protected.

The MACS+ software calculates the design effect of actions on these perimeter beams and the room temperature moment of resistance of the beam, in order to calculate the degree of utilisation for each perimeter beam, which is calculated using the guidance given in EN 1993-1-2 §4.2.4, as shown below.

$$\mu_0 = \frac{E_{fi,d}}{R_{fi,d,0}}$$

where:

$E_{fi,d}$  is the design effect of actions on the beam in fire

$R_{fi,d,0}$  is the design resistance of the beam at time  $t = 0$ .

Having calculated the degree of utilisation, the software can compute the critical temperature of the bottom flange of the perimeter beams. This critical temperature is reported in the MACS+ software output for use when specifying the fire protection required by each of the perimeter beams on the floor design zone. Full details of the calculation method can be obtained from the MACS+ Background document<sup>(7)</sup>.

For perimeter beams with floor design zones on both sides, the lower value of critical temperature given by the design of the adjacent floor design zones should be used to design the fire protection for that perimeter beam. The method of design for a perimeter beam that is shared by two floor design zones is illustrated in the work example, see Section 5.

When specifying fire protection for the perimeter beams, the fire protection supplier must be given the section factor for the member to be protected and the period of fire resistance required and the critical temperature of the member. Most reputable fire protection manufacturers will have a multi temperature assessment for their product which will have been assessed in accordance with EN 13381-4<sup>(17)</sup> for non-reactive materials or EN 13381-8<sup>(18)</sup> for reactive materials (intumescent). Design tables for fire protection which relate section factor to protection thickness are based on a single value of assessment temperature. This assessment temperature should be less than or equal to the critical temperature of the member.

### 3.3 Reinforcement details

The yield strength and ductility of the reinforcing steel material should be specified in accordance with the requirements of EN 10080. The characteristic yield strength of reinforcement to EN 10080 will be between 400 MPa and 600 MPa, depending on the national market.

In most countries, national standards for the specification of reinforcement may still exist as non-contradictory complimentary information (NCCI), as a common range of steel grades have not been agreed for EN 10080.

In composite slabs, the primary function of the mesh reinforcement is to control the cracking of the concrete. Therefore the mesh reinforcement tends to be located as close as possible to the surface of the concrete while maintaining the minimum depth of concrete cover required to provide adequate durability, in accordance with EN 1992-1-1<sup>(19)</sup>. In fire conditions, the position of the mesh will affect the mesh temperature and the lever arm when calculating the bending resistance. Typically, adequate fire performance is achieved with the mesh placed between 15 mm and 45 mm below the top surface of the concrete.

Section 3.3.1 gives general information regarding reinforcement details. Further guidance and information can be obtained from EN 1994-1-1<sup>(9)</sup> and EN 1994-1-2<sup>(6)</sup> or any national specifications such as those given in reference<sup>(20)</sup>.

#### 3.3.1 Detailing mesh reinforcement

Typically, sheets of mesh reinforcement are 4.8 m by 2.4 m and therefore must be lapped to achieve continuity of the reinforcement. Sufficient lap lengths must therefore be specified and adequate site control must be put in place to ensure that such details are implemented on site. Recommended lap lengths are given in section 8.7.5 of EN 1992-1-1<sup>(19)</sup> or can be in accordance with Table 3-3. The minimum lap length for mesh reinforcement should be 250 mm. Ideally, mesh should be specified with ‘flying ends’, as shown in Figure 3-5, to eliminate build up of bars at laps. It will often be economic to order ‘ready fit fabric’, to reduce wastage.

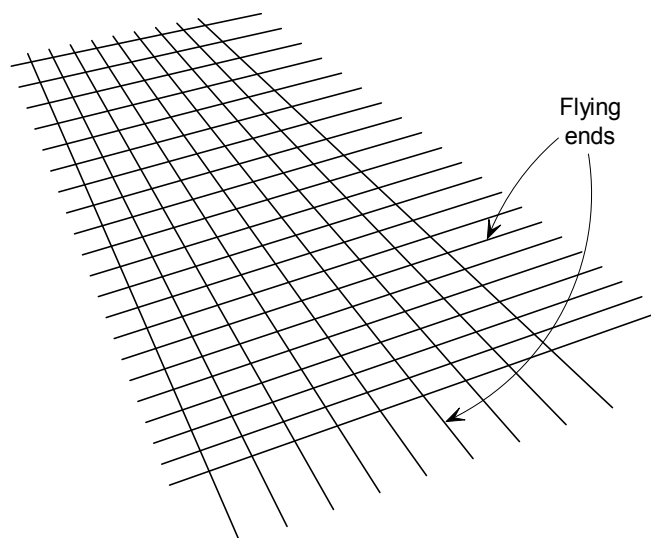


Figure 3-5 Mesh with flying ends

**Table 3-3 Recommended tension laps and anchorage lengths for welded mesh**

Reinforcement Type	Wire/Bar Type	Concrete class					
		LC 25/28	NC 25/30	LC 28/31	NC 28/35	LC 32/35	NC 32/40
Grade 500 Bar of diameter d	Ribbed	50d	40d	47d	38d	44d	35d
6 mm wires	Ribbed	300	250	300	250	275	250
7 mm wires	Ribbed	350	300	350	275	325	250
8 mm wires	Ribbed	400	325	400	325	350	300
10 mm wires	Ribbed	500	400	475	400	450	350

**Notes:**

These recommendations can be conservatively applied to design in accordance with EN 1992-1-1.

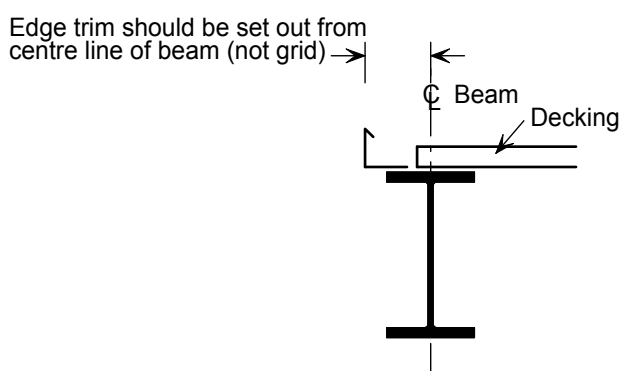
Where a lap occurs at the top of a section and the minimum cover is less than twice the size of the lapped reinforcement, the lap length should be increased by a factor of 1.4.

Ribbed Bars/Wires are defined in EN 10080.

The minimum Lap/Anchorage length for bars and fabric should be 300 mm and 250 mm respectively.

### 3.3.2 Detailing requirements for the edge of a composite floor slab

The detailing of reinforcement at the edge of the composite floor slab will have a significant effect on the performance of the edge beams and the floor slab in fire conditions. The following guidance is based on the best practice recommendations for the design and construction of composite floor slabs to meet the requirements for room temperature design. The fire design method and guidance presented in this document assumes that the composite floor is constructed in accordance with these recommendations.



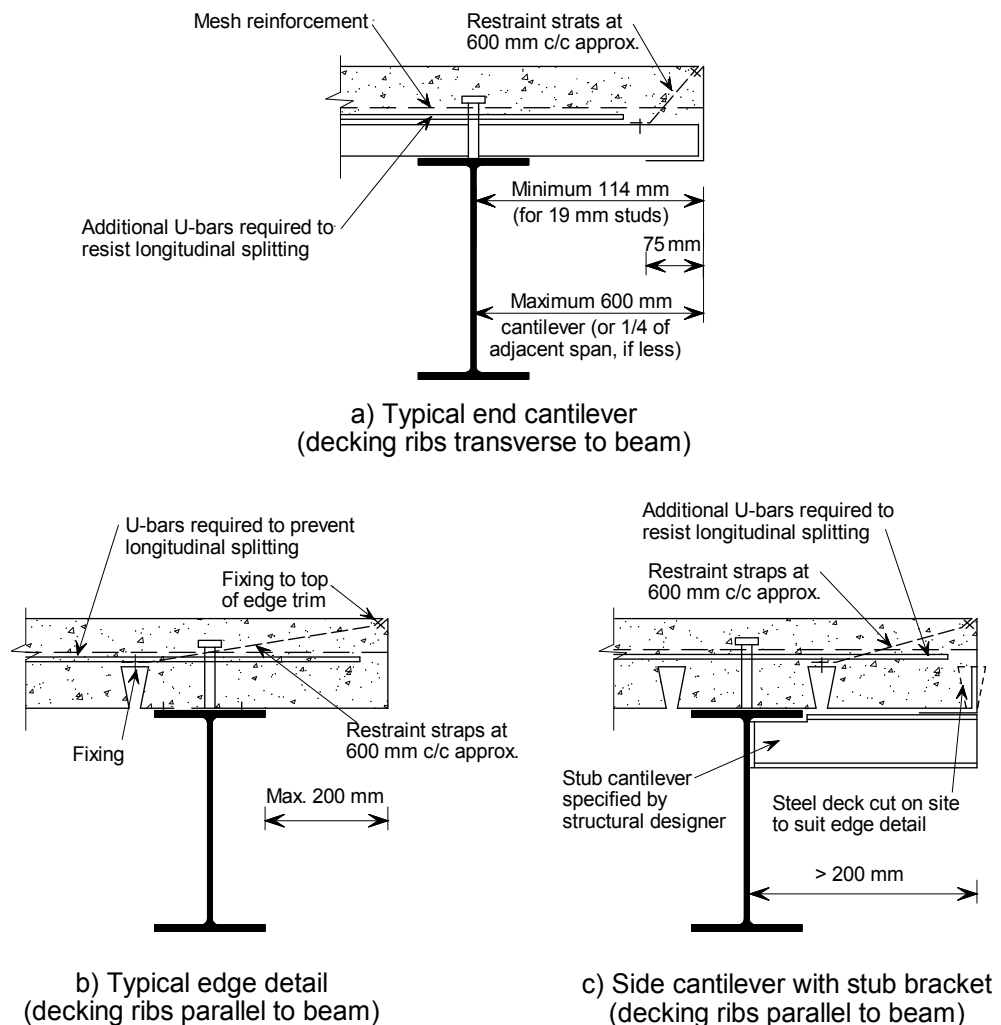
**Figure 3-6 Setting out of edge trim**

The edge of the composite slab is usually formed using 'edge trims' made from strips of light gauge galvanized steel fixed to the beam in the same way as the decking, as shown in Figure 3-6. In cases where the edge beam is designed to act compositely with the concrete slab, U shaped reinforcing bars are required to prevent longitudinal splitting of the concrete slab. These reinforcement bars also ensure that the edge beam is adequately anchored to the slab when using this simple design method.

Some typical slab edge details covering the two deck orientations are given in Figure 3-7. Where the decking ribs run transversely over the edge beam and cantilevers

out a short distance, the edge trim can be fastened in the manner suggested in Figure 3-7 (a). The cantilever projection should be no more than 600 mm, depending on the depth of the slab and deck type used.

The more difficult case is where the decking ribs run parallel to the edge beam, and the finished slab is required to project a short distance, so making the longitudinal edge of the sheet unsupported Figure 3-7 (b). When the slab projection is more than approximately 200 mm (depending on the specific details), the edge trim should span between stub beams attached to the edge beam, as shown in Figure 3-7 (c). These stub beams are usually less than 3 m apart, and should be designed and specified by the structural designer as part of the steelwork package.



**Figure 3-7 Typical edge details**

### 3.4 Design of non composite edge beams

It is common practice for beams at the edge of floor slabs to be designed as non composite beams. This is because the costs of meeting the requirements for transverse shear reinforcement are more than the costs of installing a slightly heavier non composite beam. For fire design, it is important that the floor slab is adequately anchored to the edge beams, as these beams will be at the edge of floor design zones. Although not usually required for room temperature design of non composite edge beams, this guide recommends that shear connectors are provided at not more than 300

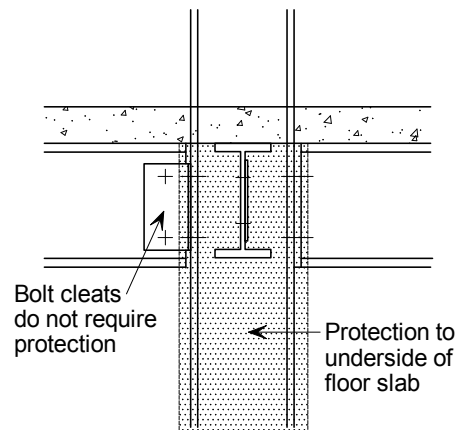
mm centres and U shaped reinforcing bars positioned around the shear connectors, as described in Section 3.3.2.

Edge beams often serve the dual function of supporting both the floors and the cladding. It is important that the deformation of edge beams should not affect the stability of cladding as it might increase the danger to fire fighters and others in the vicinity. This does not refer to the hazard from falling glass that results from thermal shock, which can only be addressed by use of special materials or sprinklers. Excessive deformation of the façade could increase the hazard, particularly when a building is tall and clad in masonry, by causing bricks to be dislodged.

### 3.5 Columns

The design guidance in this document is devised to confine structural damage and fire spread to the fire compartment itself. In order to achieve this, columns (other than those in the top storey) should be designed for the required period of fire resistance or designed to withstand the selected natural (parametric) fire.

In case of steel columns, any applied fire protection should extend over the full height of the column, including the connection zone (see Figure 3-8). This will ensure that no local squashing of the column occurs and that structural damage is confined to one floor.



**Figure 3-8 Extent of fire protection to columns**

If steel and concrete composite columns are used, the fire protection applied to steel beams connected to these columns have to cover the connection zone of each column over a height corresponding to the maximum height of all connected steel beams. The thickness of fire protection should be the maximum one applied to all connected steel beams.

### 3.6 Joints

As stated in Section 2.2.1 the values given by the design method relate to 'simple' joints such as those with flexible end plates, fin plates and web cleats.

The steel frame building tested at Cardington contained flexible end plate and fin plate connections. Partial and full failures of some of the joints were observed during the

cooling phase of the Cardington fire tests; however, no failure of the structure occurred as a result.

In the case where the plate was torn off the end of the beam, no collapse occurred because the floor slab transferred the shear to other load paths. This highlights the important role of the composite floor slab, which can be achieved with proper lapping of the reinforcement.

The resistances of the simple joints should be verified using the rules given in EN 1993-1-8<sup>(23)</sup>.

### 3.6.1 Joint classification

Joint details should be such that they fulfill the assumptions made in the design model. Three joint classifications are given in EN 1993-1-8:

- nominally pinned
  - joints that transfer internal shear forces without transferring significant moments
- semi-rigid
  - joints that do not satisfy the nominally pinned nor the rigid joint criteria
- rigid
  - joints that provide full continuity.

EN 1993-1-8 §5.2 gives principles for the classification of joints based on their stiffness and strength; the rotation capacity (ductility) of the joint should also be considered.

As stated in Section 2.2.1 the values given by the simple design method have been prepared assuming the use of nominally pinned (simple) joints. To ensure that a joint does not transfer significant bending moments and so that it is a 'simple' joint it must have sufficient ductility to allow a degree of rotation. This can be achieved by detailing the joint such that it meets geometrical limits. Guidance on geometrical limits and initial sizing to ensure sufficient ductility of the joint is given in Access-steel documents<sup>(25)</sup>.

### 3.6.2 End plates

There are two basic types of end plate connections; partial depth; and full depth. SN013 recommends the use of:

partial end plates when  $V_{Ed} \leq 0.75 V_{c,Rd}$

full depth end plates when  $0.75 V_{c,Rd} < V_{Ed} \leq V_{c,Rd}$

where:

$V_{Ed}$  is the design shear force applied to the joint

$V_{c,Rd}$  is the design shear resistance of the supported beam.

The resistance of the components of the joint should be verified against the requirements given in EN 1993-1-8. For persistent and transient design situations the following design resistances need to be verified at ambient temperatures:

- supporting member in bearing

- end plate in shear (gross section)
- end plate in shear (net section)
- end plate in shear (block shear)
- end plate in bending
- beam web in shear\*.

For completeness, all the design verifications given above should be carried out. However, in practice, for ‘normal’ joints, the verifications marked \* will usually be critical. Guidance on meeting the requirements of EN 1993-1-8 is given in Access-steel documents<sup>(26)</sup>.

EN 1993-1-8 does not give any guidance on design for tying resistance of end plates. Guidance is given in SN015<sup>(26)</sup> for the determination of the tying resistance of an end plate.

### 3.6.3 Fin plates

Single and double vertical lines of bolts may be used in fin plates. SN014<sup>(26)</sup> recommends the use of:

Single vertical lines of bolts when:  $V_{Ed} \leq 0.50 V_{c,Rd}$

Two vertical lines of bolts when:  $0.50 V_{c,Rd} < V_{Ed} \leq 0.75 V_{c,Rd}$

Use an end plate when:  $0.75 V_{c,Rd} < V_{Ed}$

where:

$V_{Ed}$  is the design shear force applied to the joint

$V_{c,Rd}$  is the design shear resistance of the supported beam.

For persistent and transient design situations, the following fin plate design resistances need to be verified at ambient temperature:

- bolts in shear\*
- fin plate in bearing\*
- fin plate in shear (gross section)
- fin plate in shear (net section)
- fin plate in shear (block shear)
- fin plate in bending
- fin plate in buckling (LTB)
- beam web in bearing\*
- beam web in shear (gross section)
- beam web in shear (net section)
- beam web in shear (block shear)



- supporting element (punching shear) (this mode is not appropriate for fin plates connected to column flanges).

For completeness, all the design verifications given above should be carried out. However, in practice, for ‘normal’ joints, the verifications marked \* will usually be critical. Guidance on meeting the requirements of EN 1993-1-8 is given in Access Steel documents<sup>(27)</sup>.

As for end plates EN1993-1-8 does not give any guidance on design for tying resistance of fin plates. Therefore, alternative guidance such as that given in SN018<sup>(27)</sup> may be used to determine the tying resistance of a fin plate.

### 3.6.4 Web cleats

Although there were no cleated joints used in the Cardington frame, SCI has conducted a number of tests on composite and non-composite cleated joints in fire<sup>(28)</sup>. These joints consisted of two steel angles bolted to either side of the beam web using two bolts in each angle leg, then attached to the flange of the column also using two bolts. The joints were found to be rotationally ductile under fire conditions and large rotations occurred. This ductility was due to plastic hinges that formed in the leg of the angle adjacent to the column face. No failure of bolts occurred during the fire test. The composite cleated joint had a better performance in fire than the non-composite joint.

For non-composite web cleat joints it is recommended that single vertical lines of bolts should only be used when:

$$V_{Ed} \leq 0.50 V_{c,Rd}$$

The design resistance of the cleated joint should be verified using the design rules given in Section 3 of EN 1993-1-8. Table 3.3 of EN 1993-1-8 gives the maximum and minimum values for the edge, end and spacing distances that should be met when detailing the position of bolts.

### 3.6.5 Fire protection

In cases where both structural elements to be connected are fire protected, the protection appropriate to each element should be applied to the parts of the plates or angles in contact with that element. If only one element requires fire protection, the plates or angles in contact with the unprotected elements may be left unprotected.

## 3.7 Overall building stability

In order to avoid sway collapse, the building should be braced by shear walls or other bracing systems. Masonry or reinforced concrete shear walls should be constructed with the appropriate fire resistance.

If bracing plays a major part in maintaining the overall stability of the building it should be protected to the appropriate standard.

In two-storey buildings, it may be possible to ensure overall stability without requiring fire resistance for all parts of the bracing system. In taller buildings, all parts of the bracing system should be appropriately fire protected.

One way in which fire resistance can be achieved without applied protection is to locate the bracing system in a protected shaft such as a stairwell, lift shaft or service core. It is important that the walls enclosing such shafts have adequate fire resistance to prevent the spread of any fire. Steel beams, columns and bracing totally contained within the shaft may be unprotected. Other steelwork supporting the walls of such shafts should have the appropriate fire resistance.

## 4 COMPARTMENTATION

National regulations require that compartment walls separating one fire compartment from another shall have stability, integrity and insulation for the required fire resistance period.

*Stability* is the ability of a wall not to collapse. For load bearing walls, the load bearing capacity must be maintained.

*Integrity* is the ability to resist the penetration of flames and hot gases.

*Insulation* is the ability to resist excessive transfer of heat from the side exposed to fire to the unexposed side.

### 4.1 Beams above fire resistant walls

When a beam is part of a fire resisting wall, the combined wall/beam separating element must have adequate insulation and integrity as well as stability. For optimum fire performance, compartment walls should, whenever possible, be located beneath and in line with beams.

#### *Beams in the wall plane*

The Cardington tests demonstrated that unprotected beams above and in the same plane as separating walls (see Figure 4-1), which are heated from one side only, do not deflect to a degree that would compromise compartment integrity, and normal movement allowances are sufficient. Insulation requirements must be fulfilled and protection for 30 or 60 minutes will be necessary; all voids and service penetrations must be fire stopped. Beams protected with intumescent coatings require additional insulation because the temperature on the non fire side is likely to exceed the limits required in the fire resistance testing standards<sup>(29,30)</sup>.

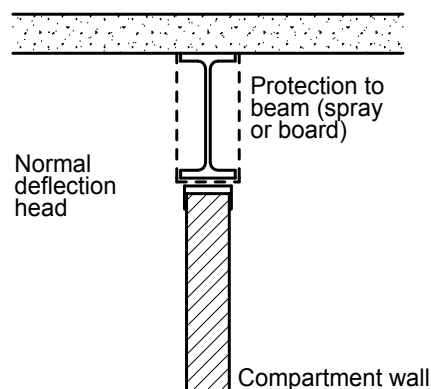
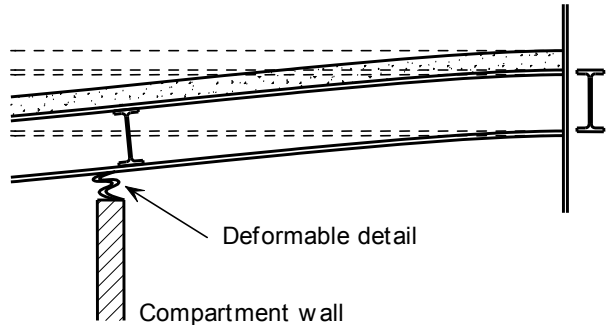


Figure 4-1 Beams above and in line with walls

#### *Beams through walls*

The Cardington tests showed that floor stability can be maintained even when unprotected beams suffer large deflections. However, when walls are located off the column grid, large deflections of unprotected beams can compromise integrity by displacing or cracking the walls through which they pass. In such cases, the beams

should either be protected or sufficient movement allowance provided. It is recommended that a deflection allowance of span/30 should be provided in walls crossing the middle half of an unprotected beam. For walls crossing the end quarters of the beam, this allowance may be reduced linearly to zero at end supports (see Figure 4-2). The compartment wall should extend to the underside of the floor.



**Figure 4-2 Deformation of beams crossing walls**

## 4.2 Stability

Walls that divide a storey into more than one fire compartment must be designed to accommodate expected structural movements without collapse (stability). Where beams span above and in the plane of the wall, movements, even of unprotected beams, may be small and the normal allowance for deflection should be adequate. If a wall is not located at a beam position, the floor deflection that the wall will be required to accommodate may be large. It is therefore recommended that fire compartment walls should be located at a beam positions whenever possible.

In some cases, the deflection allowance may be in the form of a sliding joint. In other cases, the potential deflection may be too large and some form of deformable blanket or curtain may be required, as illustrated in Figure 4-2.

National recommendations should be consulted for the structural deformations which should be considered when ensuring that compartmentation is maintained.

## 4.3 Integrity and insulation

Steel beams above fire compartment walls are part of the wall and are required to have the same separating characteristics as the wall. A steel beam without penetrations will have integrity. However, any service penetrations must be properly fire stopped and all voids above composite beams should also be fire stopped.

An unprotected beam in the plane of a compartment wall may not have the required insulation and will normally require applied fire protection. It is recommended that all beams at compartment boundaries should be fire protected, as shown in Figure 4-1.

## 5 WORKED EXAMPLE

In order to illustrate the application of the output from the MACS+ software, this Section contains a worked example based on a realistic composite floor plate and composite floor plate with cellular beams.

The building considered is a 4 storey steel framed office building. The building requires 60 minutes fire resistance for a given National Building Regulation.

The floor plate for each storey consists of a composite floor slab constructed using Cofraplus 60 trapezoidal metal decking, normal weight concrete and a single layer of mesh reinforcement. The slab spans between 9 m long secondary beams designed to act compositely with the floor slab. These secondary beams are also in turn supported on composite primary beams of 9 m and 12 m spans. The beams on the edge of the building are designed as non-composite in accordance with EN 1993-1-1. Some of the internal beams (part 1 to 2) are plain composite profiles and beams located in part 2 to 3 are composite cellular beams.

The construction of the floor plate is shown in Figure 5-3 to Figure 5-6.

Figure 5-3 shows the general arrangement of steelwork at floor level across the full width of the building and two bays along its length. It is assumed that this general arrangement is repeated in adjoining bays along the length of the building. The columns are HD320×158, designed as non-composite columns in accordance with EN 1993-1-1.

The floor loading considered was as follows:

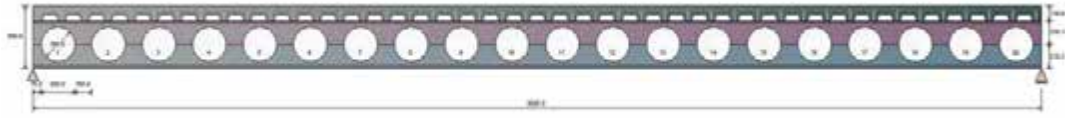
- variable action due to occupancy: 4 kN/m<sup>2</sup>
- variable action due to light weight partitions: 1 kN/m<sup>2</sup>
- permanent action due to ceilings and services: 0.7 kN/m<sup>2</sup>
- self weight of beam: 0.5 kN/m<sup>2</sup>

For the edge beams, an additional cladding load of 2 kN/m was considered in the design.

The beam sizes required to fulfil the normal stage checks for these values of actions are shown in Figure 5-3. The internal beams are composite and the degree of shear connection for each beam is shown in Table 5-1.

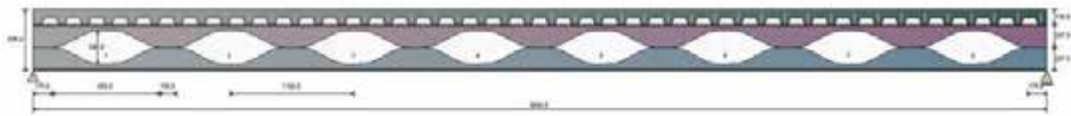
Figure 5-4 shows a cross section through the composite slab. The slab is C25/30 normal weight concrete with an overall thickness of 130 mm. The slab is reinforced with ST 15C mesh reinforcement with a yield strength of 500 MPa, this meets the requirements for normal temperature design but the mesh size may need to be increased in size if the performance in fire conditions is inadequate.

The floor Zone E has been designed using Composite Cellular beams with circular openings made from a hot rolled IPE 300 in S355 (see Figure 5-1 hereafter).

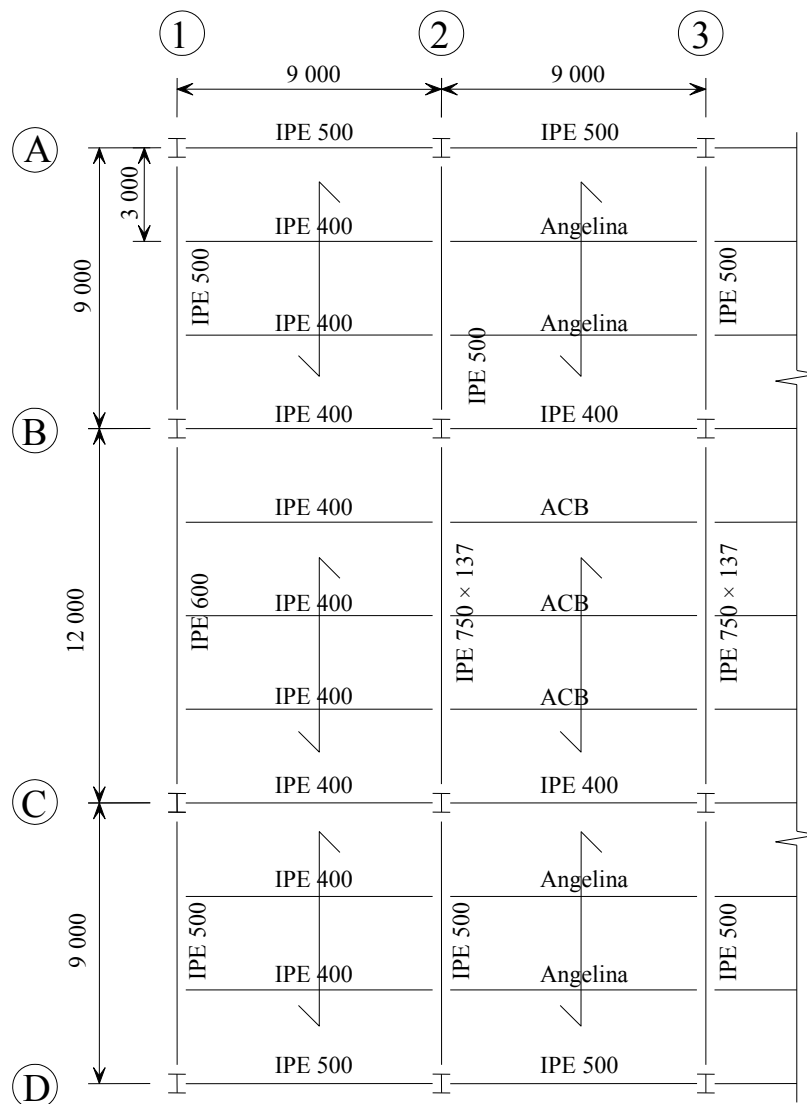


**Figure 5-1 Geometry of the Cellular Beam composite section**

The floor Zone D and F have been designed using Composite Angelina™ beams with sinusoidal openings made from a hot rolled IPE 270 in S355 (see Figure 5-2 hereafter).



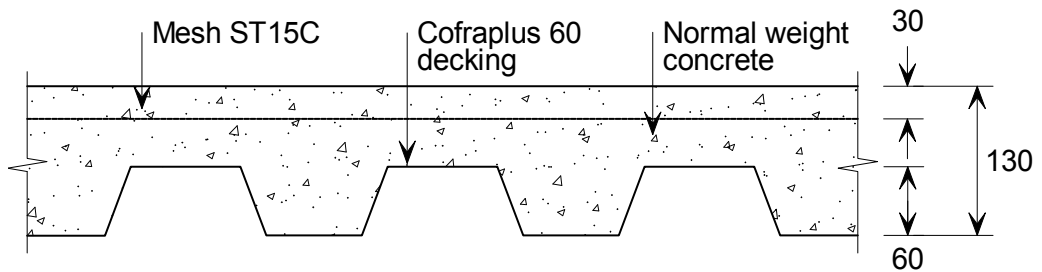
**Figure 5-2 Geometry of the ANGELINA™ beam composite section**



**Figure 5-3 General arrangement of steelwork at floor level**

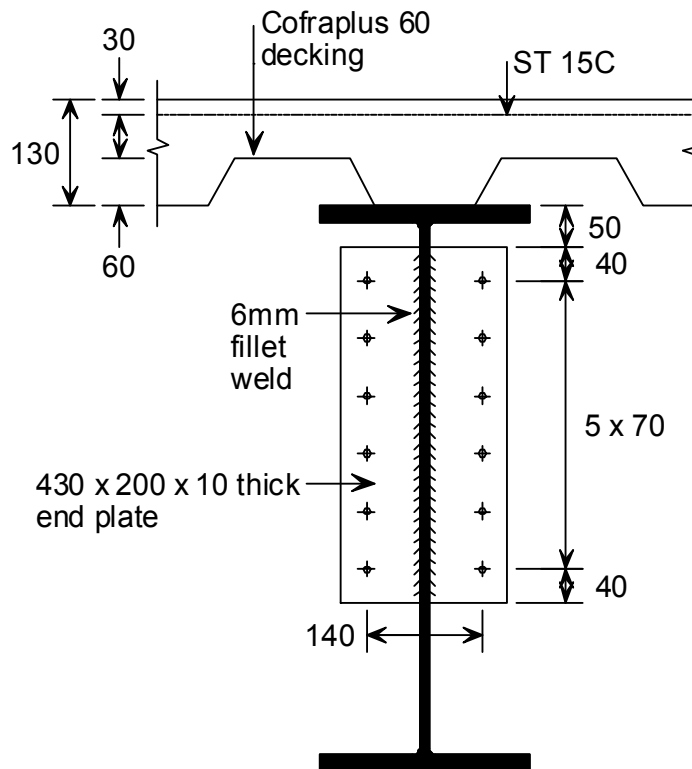
**Table 5-1 Beam details**

Beam Section (S355)	Location of beam	Construction Type	Degree of Shear Connection (%)	Number of shear studs per group and spacing
IPE 400	Secondary internal beam	Composite	51	1 @ 207mm
IPE 500	Secondary edge beam	Non composite	-	
IPE 500	Primary internal beam	Composite	72	2 @ 207mm
IPE 750 × 137	Primary internal beam	Composite	71	2 @ 207 mm
IPE 600	Primary edge beam	Non composite	-	
ACB IPE 300+IPE 300	Secondary internal beam	Composite	52	2 @ 207 mm
Angelina IPE270 + IPE 270	Secondary internal beam	Composite	52	2 @ 207 mm

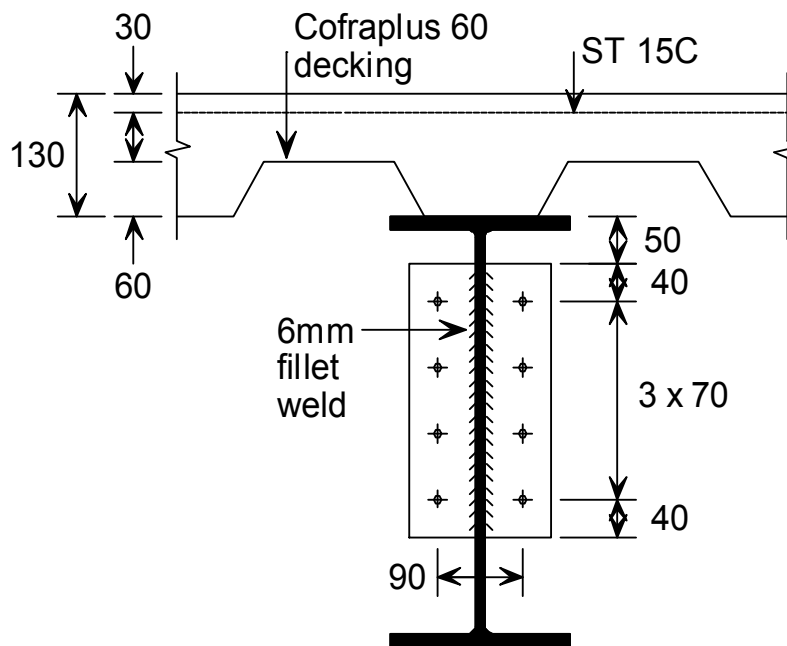


**Figure 5-4 Construction of floor slab**

All joints between the main steelwork elements use flexible end plate details and are designed as nominally pinned in accordance with EN 1993-1-8. Figure 5-5(a) shows the joint used between the primary beams and the columns. The beam-to-column joints for secondary beams are as shown in Figure 5-5(b). Figure 5-6 shows the endplate connection between the secondary beams and the primary beams.



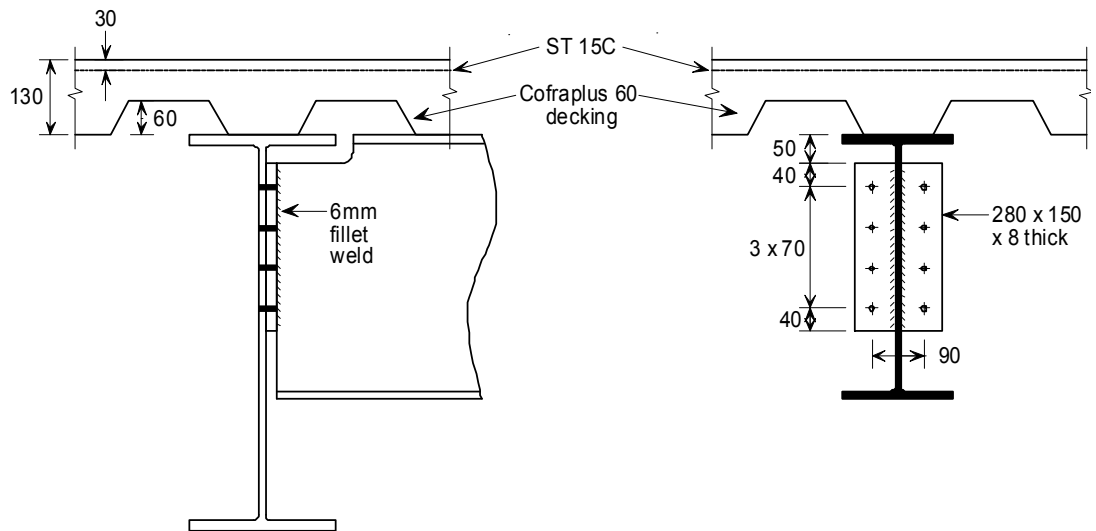
(a) Primary beam-to-column joint



(b) Secondary beam to column joint

Figure 5-5 Beam-to-column joints





**Figure 5-6 Secondary beam to primary beam connection**

Figure 5-7 shows the floor plate divided into floor design zones. It is likely that floor design zones A and B will give the most onerous design conditions. The design of both of these zones will be considered.

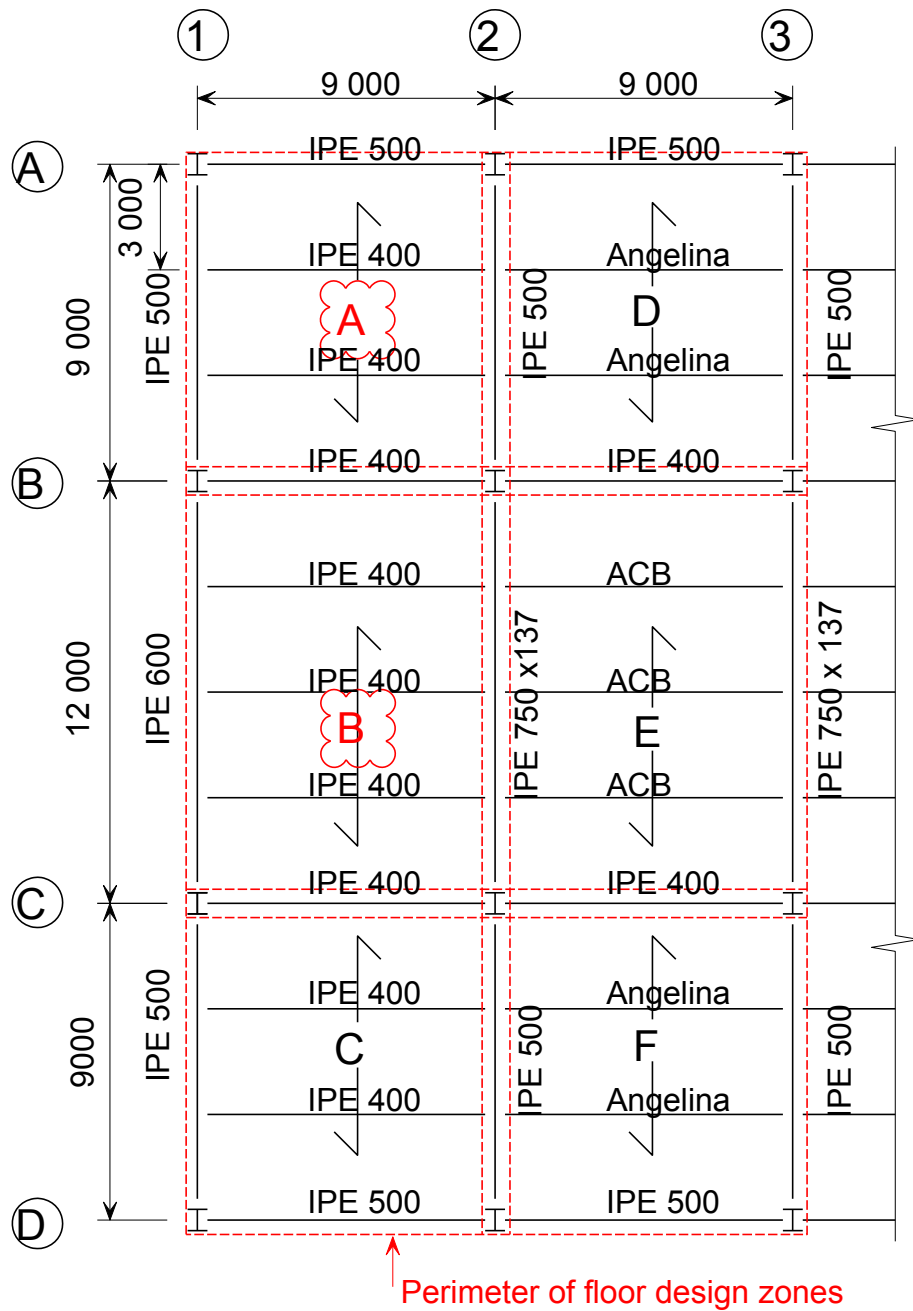


Figure 5-7 Floor design zones (A – F)

## 5.1 Design of composite slab in fire conditions

The following design checks carried out on the floor design zones are based on the floor construction required for room temperature design checks. If this construction proves to be inadequate for fire conditions then the mesh size and/or the floor depth will be increased to improve the performance in fire conditions. As the design Zone B seems more critical than design Zone A due to its larger span, we run the program with design Zone B first.

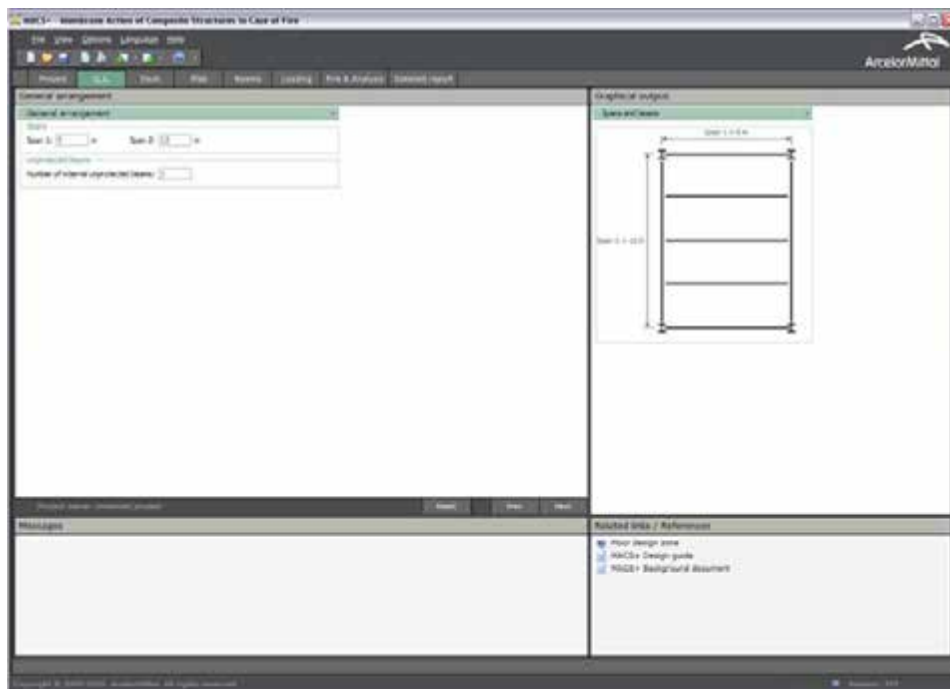
### 5.1.1 Floor design: Zone B

Table 5-2 shows the input data for floor design Zone B, which is 9 m by 12 m with the mesh size of ST 15C. Within this floor design zone, there are 3 unprotected composite beams.

**Table 5-2 Input data for floor design Zone B**

$L$ (mm)	$l$ (mm)	$f_c$ (MPa)	$A_s$ (mm <sup>2</sup> /m)	$f_{sy}$ (MPa)	Unprotected beams	Steel decking	Total thickness of the slab (mm)	$d$ : mesh axis distance (mm)
12 000	9 000	25	142	500	IPE400	Cofraplus60	130	30

Figure 5-8 to Figure 5-11 show the same information in the input windows of the MACS+ Software.



**Figure 5-8 Input data using the MACS+ software – General arrangement**

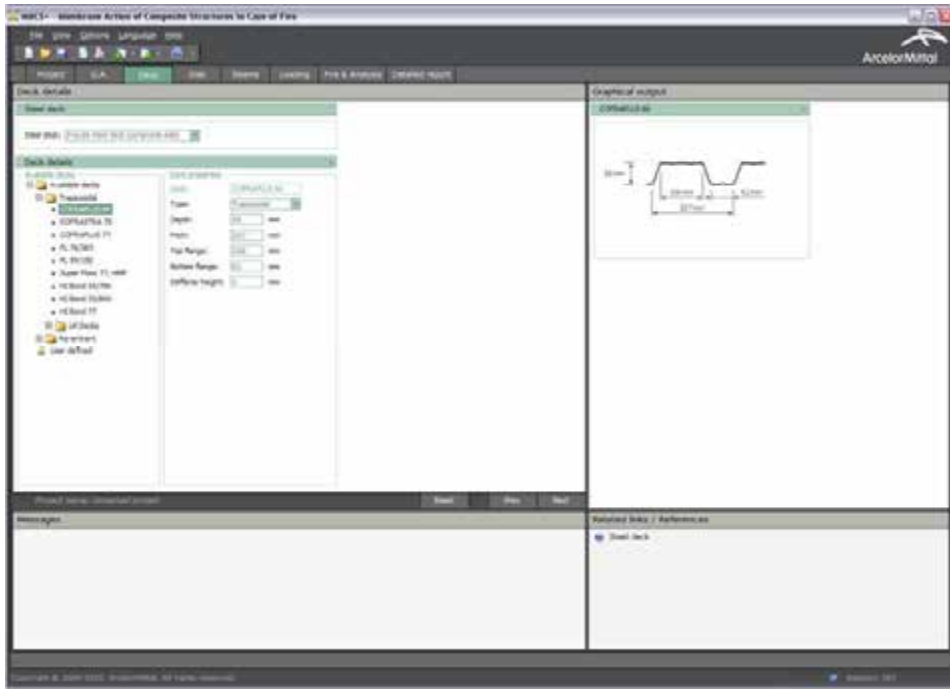


Figure 5-9 Input data using the MACS+ software - Deck

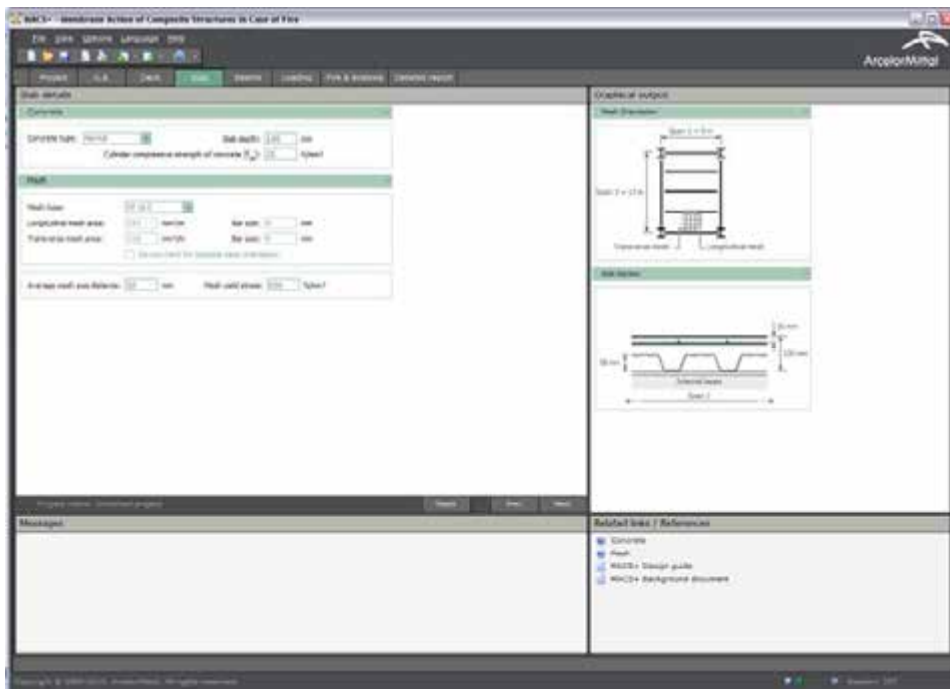


Figure 5-10 Input data using the MACS+ software - Slab

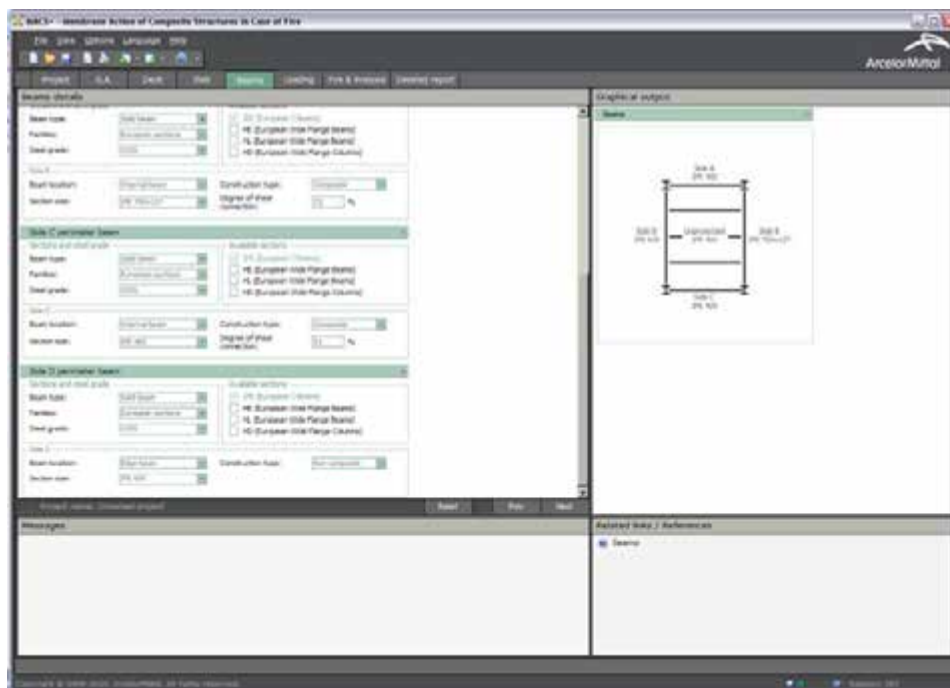
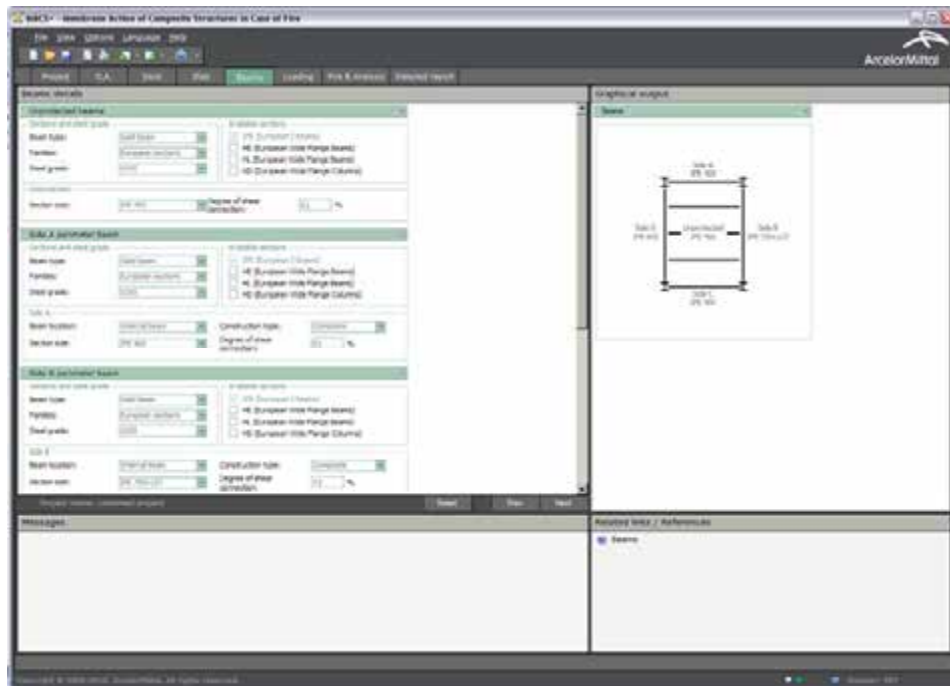


Figure 5-11 Input data using the MACS+ software – Beams in Zone B

The application of the simplified model is done in several steps as followed:

**Step 1: Calculation of the applied load on the slab in case of fire**

The applied load on the slab in case of fire with a self weight of 2.28 kN/m<sup>2</sup> for the slab can be determined by:

$$q_{fi,sl} = G + 0.5Q = (2.28 + 0.7 + 0.5) + 0.5 \times (4.0 + 1.0) = 5.98 \text{ kN/m}^2$$

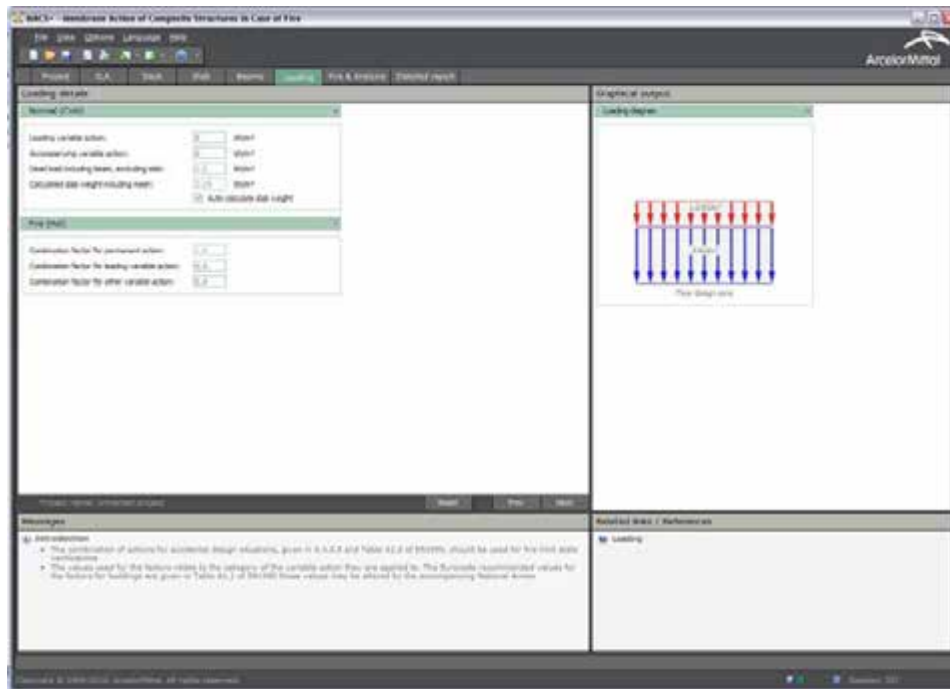


Figure 5-12 Input data using the MACS+ software - Loading

## Step 2: Calculation of the heat transfer into the composite slab Cofraplus 60

From the relation D.15a of the Annex D of the EN 1994-1-2<sup>(16)</sup>, the effective thickness of the slab can be expressed by:

$$h_{eff} = h_1 + 0.5 h_2 \left( \frac{\ell_1 + \ell_2}{\ell_1 + \ell_3} \right) = 72 + 0.5 \times 58 \times \left( \frac{101 + 62}{101 + 106} \right) \approx 95 \text{ mm}$$

This effective thickness allows to verify that the slab fulfill the criteria EI60 which request an effective thickness with creed of minimum 80 mm for the composite slab.

Moreover, this effective thickness leads to the following temperatures  $\theta_1$ ,  $\theta_2$  and  $\theta_s$  (see Table 3-1). For a time exposure of 60 minutes to normalized fire:

$$\theta_1 = 99 \text{ }^\circ\text{C}; \theta_2 = 831 \text{ }^\circ\text{C} \text{ and } \theta_s = 288 \text{ }^\circ\text{C}.$$

Following Table 3-4 of EN 1994-1-2, there is no reduction of the effective steel strength for the welded steel mesh:

$$f_{sy,\theta_s} = 500 \text{ MPa}$$

$$\gamma_{M,f_i,s} = 1.0$$

Moreover, there is also:

$$\gamma_{M,f_i,c} = 1.0$$

## Step 3: Calculation of the moment resistance of the slab section $M_{fi,0}$

For this calculation zone:

$$L_1 = 9 \text{ 000 mm (span of the secondary beams)}$$

$L_2 = 12\ 000\ \text{mm}$  (span of the primary beams)

So,  $L = \max \{L_1; L_2\} = 12\ 000\ \text{mm}$  and  $\ell = \min \{L_1; L_2\} = 9\ 000\ \text{mm}$ .

It can be obtained:

$$(g_0)_1 = 1 - \frac{2KA_s f_{sy,\theta_s} / \gamma_{M,fi,s}}{0.85 f_c / \gamma_{M,fi,c} d} = 1 - \frac{2 \times 1.0 \times \frac{142}{1000} \times 500 / 1.0}{0.85 \times 25 / 1.0 \times 30} = 0.777$$

$$(g_0)_2 = 1 - \frac{2A_s f_{sy,\theta_s} / \gamma_{M,fi,s}}{0.85 f_c / \gamma_{M,fi,c} d} = 1 - \frac{2 \times 1.0 \times \frac{142}{1000} \times 500 / 1.0}{0.85 \times 25 / 1.0 \times 30} = 0.777$$

It is to be noticed that the parameter  $K$  is equal to 1.0 because the reinforcing mesh has the same cross section in both dimensions.

So, the positive moment resistance of the slab section is:

$$M_{fi,0} = A_s f_{sy,\theta_s} / \gamma_{M,fi,s} d \frac{3 + (g_0)_2}{4} = \frac{142}{1000} \times 500 / 1.0 \times 30 \times \frac{3 + 0.777}{4} = 2\ 011.4\ \text{Nmm/mm}$$

In parallel, it is also possible to determine the other necessary parameters:

$$\mu = K \frac{3 + (g_0)_1}{3 + (g_0)_2} = 1.0 \times \frac{3 + 0.777}{3 + 0.777} = 1.0$$

$$a = \frac{L}{\ell} = \frac{12\ 000}{9\ 000} = 1.333$$

$$n = \frac{1}{2\mu a^2} (\sqrt{3\mu a^2 + 1} - 1) = \frac{1}{2 \times 1.0 \times 1.333^2} \times (\sqrt{3 \times 1.0 \times 1.333^2 + 1} - 1) = 0.427$$

#### Step 4: Determination of the reference bearing capacity of the slab

The reference bearing capacity of the slab can be determined from:

$$p_{fi} = 6 \frac{M_{fi,0}}{n^2 a^2 \ell^2} = 6 \times \frac{2\ 011.4}{0.427^2 \times 1.333^2 \times 9\ 000^2} = 0.461 \times 10^{-3}\ \text{N/mm}^2 = 0.461\ \text{kN/m}^2$$

#### Step 5: Determination of the deflection for the calculation of the membrane action

The deflection of the slab in fire situation to take into account membrane action can be obtained from:

$$\begin{aligned} w &= \min \left\{ \frac{\alpha(\theta_2 - \theta_1)\ell^2}{19.2h_{eff}} + \min \left[ \sqrt{\left( \frac{0.5f_{sy}}{E_d \gamma_{M,fi,s}} \right) \frac{3L^2}{8}}; \frac{\ell}{30} \right]; \frac{L + \ell}{30} \right\} \\ &= \min \left\{ \frac{1.2 \times 10^{-5} (831 - 99) \times 9\ 000^2}{19.2 \times 95} + \min \left[ \sqrt{\left( \frac{0.5 \times 500}{210\ 000 \times 1.0} \right) \frac{3 \times 12\ 000^2}{8}}; \frac{9\ 000}{30} \right]; \frac{12\ 000 + 9\ 000}{30} \right\} \\ &= \min \{391.0 + \min[253.5; 300]; 700\} = 644.6\ \text{mm} \end{aligned}$$

### **Step 6: Calculation of the parameters to determine the membrane action**

The determination of the different multiplication factors for the membrane action are based on the different parameters  $\alpha_1$ ,  $\alpha_2$ ,  $\beta_1$ ,  $\beta_2$ ,  $A$ ,  $B$ ,  $C$ ,  $D$ ,  $k$  and  $b$  that need to be determined. The values of these parameters are summarized in Table 5-3.



**Table 5-3 Parameters used for the assessment of the membrane action in Zone B**

Equation	Obtained value
$\alpha_1 = \frac{2(g_0)_1}{3+(g_0)_1}$	0.412
$\beta_1 = \frac{1-(g_0)_1}{3+(g_0)_1}$	0.059
$\alpha_2 = \frac{2(g_0)_2}{3+(g_0)_2}$	0.412
$\beta_2 = \frac{1-(g_0)_2}{3+(g_0)_2}$	0.059
$k = \frac{4na^2(1-2n)}{4n^2a^2 + 1} + 1$	1.194
$A = \frac{1}{2(1+k)} \left[ \frac{\ell^2}{8n} - \left( \frac{1-2n}{2n} + \frac{1}{3(1+k)} \right) \left( (nL)^2 + (\ell/2)^2 \right) \right]$	1 978 359 mm <sup>2</sup>
$B = \frac{k^2}{2(1+k)} \left[ \frac{nL^2}{2} - \frac{k}{3(1+k)} \left( (nL)^2 + (\ell/2)^2 \right) \right]$	7 242 376 mm <sup>2</sup>
$C = \frac{\ell^2}{16n} (k-1)$	2 305 602 mm <sup>2</sup>
$D = \frac{L^2}{8} (1-2n)^2$	388 465 mm <sup>2</sup>
$b = \min \left[ \frac{\ell^2}{8K(A+B+C-D)}, \frac{\gamma_{M,f,s}}{kK A_s \gamma_{s,y,\theta}} \left( 0.85 - \frac{f_c}{\gamma_{M,f,c}} \times 0.45d - A_s \frac{f_{s,y,\theta}}{\gamma_{M,f,s}} \frac{K+1}{2} \right) \right]$	0.909

### Step 7: Calculation of the enhancement factors for the membrane action

The multiplication factors  $e_{1b}$ ,  $e_{2b}$ ,  $e_{1m}$  and  $e_{2m}$  can be determined:

**Table 5-4 Enhancement factors the assessment of the membrane action in Zone B**

Equation	Obtained value
$e_{1b} = 2n \left( 1 + \alpha_1 b \frac{k-1}{2} - \frac{\beta_1 b^2}{3} (k^2 - k + 1) \right) + (1-2n)(1 - \alpha_1 b - \beta_1 b^2)$	0.952
$e_{1m} = \frac{4b}{3 + (g_0)_1} \frac{w}{d} \left( (1-2n) + n \frac{2+3k-k^3}{3(1+k)^2} \right)$	5.407
$e_1 = e_{1b} + e_{1m}$	6.360
$e_{2b} = 1 + \frac{\alpha_2 b K}{2} (k-1) - \frac{\beta_2 b^2 K}{3} (k^2 - k + 1)$	1.016
$e_{2m} = \frac{4bK}{3 + (g_0)_2} \frac{w}{d} \frac{2+3k-k^3}{6(1+k)^2}$	2.777
$e_2 = e_{2b} + e_{2m}$	3.794

Then, the global enhancement factor  $e$  is determined by:

$$e = e_1 - \frac{e_1 - e_2}{1 + 2\mu\alpha^2} = 6.360 - \frac{6.360 - 3.7948}{1 + 2 \times 1.0 \times 1.333^2} = 5.796$$

### Step 8: Total bearing capacity of the slab in fire condition

The total bearing capacity of the slab in fire condition taking into account the membrane action can be obtained from:

$$q_{fi,Rd,slab} = e \times p_{fi} = 5.796 \times 0.461 = 2.670 \text{ kN/m}^2$$

**Step 9: Bearing capacity of the slab taking into account the contribution of the unprotected composite beams**

From paragraph 4.3.4.2.2 of EN 1994-1-2, it is possible to determine the temperature of the unprotected composite beams. In a first step, it is necessary to calculate the section factor of the steel section IPE400. The calculated values are summarised in Table 5-5.

From Table 3-2, the temperatures of the steel part of the composite section are the following:

- temperature of the flanges: 938.6°C;
- temperature of the web: 941.5°C in Table 3-2 but taken as 938.6°C because the depth of the steel section is not greater than 500 mm;
- temperature of the studs (see 4.3.4.2.5 of EN 1994-1-2):  $938.6 \times 0.8 = 750.9^\circ\text{C}$

**Table 5-5 Section factor of the unprotected composite beam**

Steel section member	$k_{sh} = 0.9 \left( \frac{H + 0.5B}{H + 1.5B - t_w} \right)$	$\left( \frac{A_i}{V_i} \right) (\text{m}^{-1})$	$k_{sh} \left( \frac{A_i}{V_i} \right) (\text{m}^{-1})$
Lower flange	0.668	$\frac{2(B+t_f)}{Bt_f} = 159$	106
Web		$\frac{2}{t_w} = 233$	155
Upper flange		$\frac{2(B+t_f)}{Bt_f} = 159$	106
With: $H$ : depth of the steel section; $B$ : width of the steel section; $t_f$ : thickness of the flange; $t_w$ : thickness of the web.			

The temperatures of the steel section and of the steel studs allow determining the moment resistance of the internal non composite unprotected beams. The calculated values are given in Table 5-6.

**Table 5-6 Moment resistance for unprotected composite beams in Zone B**

Parameters	Calculated values
Effective width of the slab	$b_{eff} = \min\{9000/4; 3000\} = 2250 \text{ mm}$
Area of the steel section $A_i$	$A_i = 8446 \text{ mm}^2$
Reduction factor for the steel strength properties	$k_{y,\theta} = 0.0523$
Reduction factor for the stud strength properties	$k_{u,\theta} = 0.17$
Thickness of the slab in compression in fire situation	$h_u = \frac{\sum A_i f_y k_{y,\theta} / \gamma_{M,fi,a}}{b_{eff} f_c / \gamma_{M,fi,c}} = \frac{8446 \times 355 \times 0.0523 / 1.0}{2250 \times 25 / 1.0} = 2.787 \text{ mm}$
Connection degree of the beam at 20°C	$n_{c,20^\circ C} = 0.51$
Connection degree of the beam in fire situation	$n_{c,\theta} = \frac{n_{c,20^\circ C} k_{u,\theta} \gamma_{M,\nu}}{k_{y,\theta} \gamma_{M,fi,\nu}} = \frac{0.51 \times 0.17 \times 1.25}{0.0523 \times 1.0} = 2.09 > 1.0$ So full shear connection
Positive moment resistance	$M_{fi,Rd} = \frac{A_i f_y k_{y,\theta} \left( \frac{H}{2} + h_c - \frac{h_u}{2} \right)}{\gamma_{M,fi,a}} = \frac{8446 \times 355 \times 0.0523 \left( \frac{400}{2} + 130 - \frac{2.787}{2} \right)}{1.0} = 51.51 \times 10^6 \text{ Nmm} = 51.51 \text{ kNm}$
With: $h_c$ : total thickness of the slab; $\gamma_{M,fi,a}$ , $\gamma_{M,\nu}$ and $\gamma_{M,fi,\nu}$ partial safety factor for the steel profile, the steel stud in normal conditions and in fire conditions.	

Then, the bearing capacity of the slab thanks to the contribution of the unprotected composite beam can be obtained from:

$$q_{fi,Rd,ub} = \frac{8M_{fi,Rd}}{L_1^2} \frac{1+n_{ub}}{L_2} = \frac{8 \times 51.5}{9^2} \times \frac{(1+3)}{12} = 1.70 \text{ kN/m}^2$$

**Step 10: Total bearing capacity of the slab in fire conditions and verification of the fire resistance of the slab**

The total bearing capacity of the slab is:

$$q_{fi,Rd} = q_{fi,Rd,slab} + q_{fi,Rd,ub} = 2.67 + 1.70 = 4.37 \text{ kN/m}^2$$

With regards to the applied load on the slab in fire situation:

$$q_{fi,Sd} = 5.98 \text{ kN/m}^2 > q_{fi,Rd} = 4.37 \text{ kN/m}^2$$

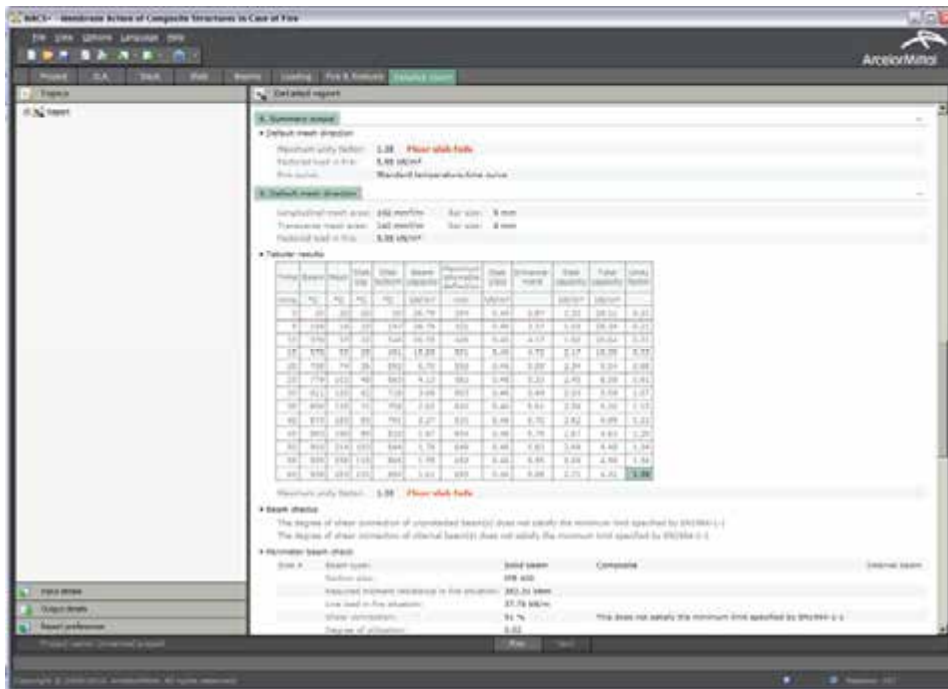


Figure 5-13 Output data using the MACS+ software - Detailed report

**Conclusion 1**

In conclusion, the stability of the slab system cannot be ensured for R60 with its actual dimensions in Zone B. So, it is necessary to modify the constructive parameters.

An adequate solution could be to increase the size of the reinforcing mesh to bring more resistance to the slab. So, the size of the welded mesh was increased from ST 15C (142 mm<sup>2</sup>/m) to ST 25C (257 mm<sup>2</sup>/m).

A new calculation needs to be performed with the new input data. But, it is only necessary to recalculate the bearing capacity of the slab because the unprotected composite beams remain unchanged.

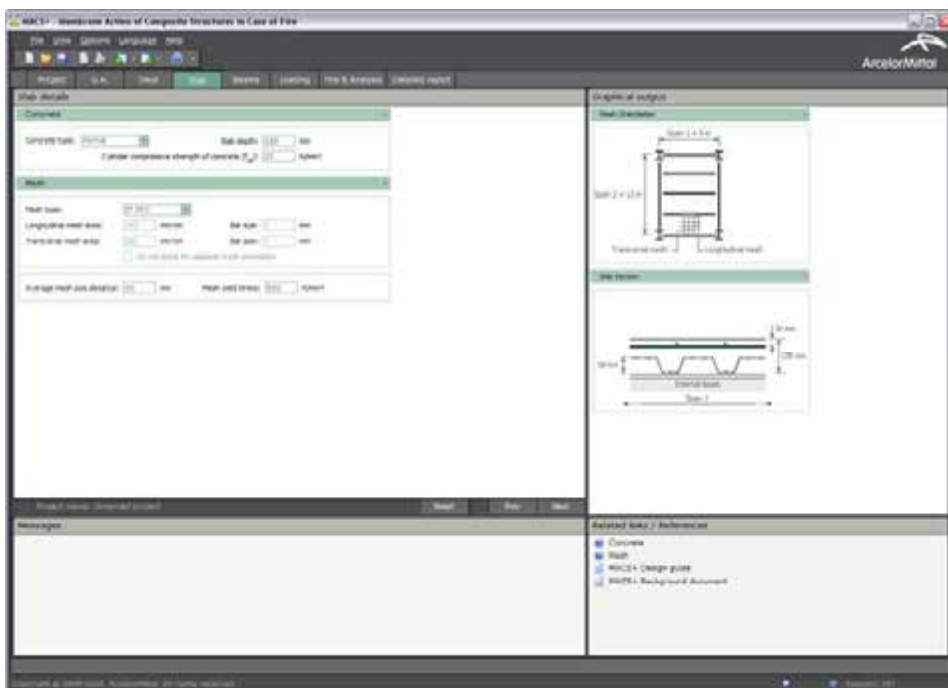


Figure 5-14 Input data using the MACS+ software - Slab

### Step 2a: Calculation of the heat transfer into the composite slab Cofraplus 60

The results are identical to the step 2 because the overall dimensions of the slab remain unchanged.

### Step 3a: Calculation of the resisting bending moment of the slab section $M_{fi,0}$

It can be obtained:

$$(g_0)_1 = 1 - \frac{2KA_s f_{sy,\theta_s} / \gamma_{M,fi,s}}{0.85 f_c / \gamma_{M,fi,c} d} = 1 - \frac{2 \times 1.0 \times \frac{257}{1000} \times 500 / 1.0}{0.85 \times 25 / 1.0 \times 30} = 0.597$$

$$(g_0)_2 = 1 - \frac{2A_s f_{sy,\theta_s} / \gamma_{M,fi,s}}{0.85 f_c / \gamma_{M,fi,c} d} = 1 - \frac{2 \times 1.0 \times \frac{257}{1000} \times 500 / 1.0}{0.85 \times 25 / 1.0 \times 30} = 0.597$$

It is to be noticed that the parameter  $K$  is equal to 1.0 because the reinforcing mesh has the same cross section in both dimensions.

So, the positive moment resistance of the slab section is:

$$M_{fi,0} = A_s f_{sy,\theta_s} / \gamma_{M,fi,s} d \frac{3 + (g_0)_2}{4} = \frac{257}{1000} \times 500 / 1.0 \times 30 \times \frac{3 + 0.597}{4} = 3466.5 \text{ Nmm/mm}$$

In parallel, it is also possible to determine the other necessary parameters:

$$\mu = K \frac{3 + (g_0)_1}{3 + (g_0)_2} = 1.0 \times \frac{3 + 0.597}{3 + 0.597} = 1.0$$

$$a = \frac{L}{\ell} = \frac{12000}{9000} = 1.333$$

$$n = \frac{1}{2\mu a^2} (\sqrt{3\mu a^2 + 1} - 1) = \frac{1}{2 \times 1.0 \times 1.333^2} \times (\sqrt{3 \times 1.0 \times 1.333^2 + 1} - 1) = 0.427$$

### Step 4a: Determination of the reference bearing capacity of the slab

The reference bearing capacity of the slab can be determined from:

$$p_{fi} = 6 \frac{M_{fi,0}}{n^2 a^2 \ell^2} = 6 \times \frac{3466.5}{0.427^2 \times 1.333^2 \times 9000^2} = 0.794 \times 10^{-3} \text{ N/mm}^2 = 0.794 \text{ kN/m}^2$$

### Step 5a: Determination of the deflection for the calculation of the membrane action

The deflection of the slab in fire situation to take into account membrane action can be obtained from:

$$\begin{aligned}
w &= \min \left\{ \frac{\alpha(\theta_2 - \theta_1)\ell^2}{19.2h_{eff}} + \min \left[ \sqrt{\left( \frac{0.5f_{sy}}{E_a\gamma_{M_s,fi,s}} \right) \frac{3L^2}{8}}; \frac{\ell}{30} \right]; \frac{L+\ell}{30} \right\} \\
&= \min \left\{ \frac{1.2 \times 10^{-5} (831 - 992) \times 9000^2}{19.2 \times 95} + \min \left[ \sqrt{\left( \frac{0.5 \times 500}{210000 \times 1.0} \right) \frac{3 \times 12000^2}{8}}; \frac{9000}{30} \right]; \frac{12000 + 9000}{30} \right\} \\
&= \min\{391.0 + \min[253.5; 300]; 700\} = 644.5 \text{ mm}
\end{aligned}$$

### Step 6a: Calculation of the parameters to determine the membrane action

The determination of the different multiplication factors for the membrane action are based on the different parameters  $\alpha_1$ ,  $\alpha_2$ ,  $\beta_1$ ,  $\beta_2$ ,  $A$ ,  $B$ ,  $C$ ,  $D$ ,  $k$  and  $b$  that need to be determined. The values of these parameters are summarized in Table 5-7.

**Table 5-7 Parameters used for the assessment of the membrane action in Zone B**

Equation	Obtained values
$\alpha_1 = \frac{2(g_0)_1}{3+(g_0)_1}$	0.332
$\beta_1 = \frac{1-(g_0)_1}{3+(g_0)_1}$	0.112
$\alpha_2 = \frac{2(g_0)_2}{3+(g_0)_2}$	0.332
$\beta_2 = \frac{1-(g_0)_2}{3+(g_0)_2}$	0.112
$k = \frac{4na^2(1-2n)}{4n^2a^2+1} + 1$	1.194
$A = \frac{1}{2(1+k)} \left[ \frac{\ell^2}{8n} - \left( \frac{1-2n}{2n} + \frac{1}{3(1+k)} \right) \left( (nL)^2 + (\ell/2)^2 \right) \right]$	1 978 359 mm <sup>2</sup>
$B = \frac{k^2}{2(1+k)} \left[ \frac{nL^2}{2} - \frac{k}{3(1+k)} \left( (nL)^2 + (\ell/2)^2 \right) \right]$	7 242 376 mm <sup>2</sup>
$C = \frac{\ell^2}{16n} (k-1)$	2 305 602 mm <sup>2</sup>
$D = \frac{L^2}{8} (1-2n)^2$	388 465 mm <sup>2</sup>
$b = \min \left[ \frac{\ell^2}{8K(A+B+C-D)}, \frac{\gamma_{M,fi,s}}{kK A_s f_{sy,fb}} \left( 0.85 \frac{f_c}{\gamma_{M,fi,c}} \times 0.45d - A_s \frac{f_{sy,fb}}{\gamma_{M,fi,s}} \frac{K+1}{2} \right) \right]$	0.909

**Step 7a: Calculation of the enhancement factors for the membrane action**

The multiplication factors  $e_{1b}$ ,  $e_{2b}$ ,  $e_{1m}$  and  $e_{2m}$  can be determined:



**Table 5-8 Enhancement factors the assessment of the membrane action in Zone B**

Equation	Obtained values
$e_{1b} = 2n \left( 1 + \alpha_1 b \frac{k-1}{2} - \frac{\beta_1 b^2}{3} (k^2 - k + 1) \right) + (1-2n)(1 - \alpha_1 b - \beta_1 b^2)$	0.935
$e_{1m} = \frac{4b}{3 + (g_0)_1} \frac{w}{d} \left( (1-2n) + n \frac{2+3k-k^3}{3(1+k)^2} \right)$	5.679
$e_1 = e_{1b} + e_{1m}$	6.614
$e_{2b} = 1 + \frac{\alpha_2 b K}{2} (k-1) - \frac{\beta_2 b^2 K}{3} (k^2 - k + 1)$	0.991
$e_{2m} = \frac{4bK}{3 + (g_0)_2} \frac{w}{d} \frac{2+3k-k^3}{6(1+k)^2}$	2.917
$e_2 = e_{2b} + e_{2m}$	3.908

Then, the global enhancement factor  $e$  is determined by:

$$e = e_1 - \frac{e_1 - e_2}{1 + 2\mu\alpha^2} = 6.614 - \frac{6.614 - 3.908}{1 + 2 \times 1.0 \times 1.333^2} = 6.020$$

#### Step 8a: Total bearing capacity of the slab in fire condition

The total bearing capacity of the slab in fire condition taking into account the membrane action can be obtained from:

$$q_{fi,Rd,slab} = e \times p_{fi} = 6.020 \times 0.794 = 4.78 \text{ kN/m}^2$$

#### Step 9a: Bearing capacity of the slab taking into account the contribution of the unprotected composite beams

Same as Step 9

#### Step 10a: Total bearing capacity of the slab in fire conditions and verification of the fire resistance of the slab

The total bearing capacity of the slab is:

$$q_{fi,Rd} = q_{fi,Rd,slab} + q_{fi,Rd,ub} = 4.78 + 1.70 = 6.48 \text{ kN/m}^2$$

With regards to the applied load on the slab in fire situation:

$$q_{fi,Sd} = 5.98 \text{ kN/m}^2 < q_{fi,Rd} = 6.48 \text{ kN/m}^2$$

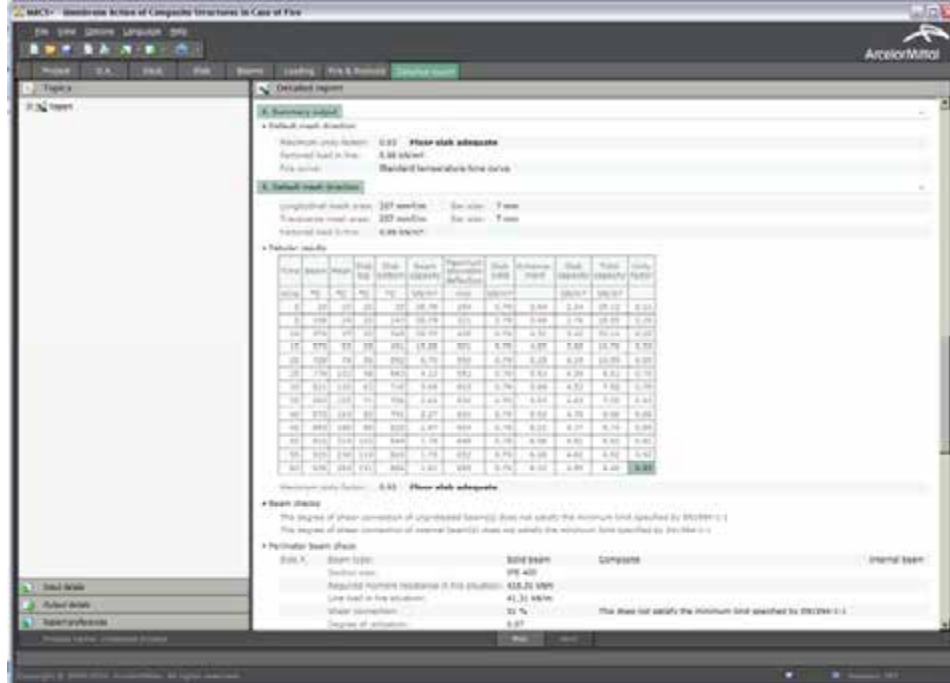


Figure 5-15 Output data using the MACS+ software – Detailed report

## Conclusion 2

In conclusion, the stability of the slab system is ensured for R60 with its actual dimensions in Zone B.

## Step 11: Applied load in fire situation for perimeter beams

The applied loads in fire situation on the secondary beams and perimeter beams of Zone B are calculated from relations 3.24 to 3.37:

- For the secondary perimeter beams

$$M_{fi,Sd,b,1} = \frac{q_{fi,Rd} L_1^2 L_2 - 8 \left( M_{fi,0} \left( L_2 - n_{ub} b_{eff,ub} - \sum_{i=1}^2 b_{eff,1,i} \right) + n_{ub} M_{fi,Rd} \right)}{c_M}$$

$$= \frac{6.48 \times 9^2 \times 12 - 8 \times \{ 3466.5 \times 10^{-3} \times [12 - 3 \times 2.25 - (0 + 2.25/2)] + 3 \times 51.5 \}}{12}$$

$$= 412.3 \text{ kNm}$$

$$V_{fi,Sd,b,1} = \frac{4M_{fi,Sd,b,1}}{L_1} = \frac{4 \times 412.3}{9} = 183.3 \text{ kN}$$

- For the primary perimeter beams

$$M_{f_i, Sd, b, 2} = \frac{q_{f_i, Rd} L_1 L_2^2 - 8 \mu M_{f_i, 0} \left( L_1 - \sum_{i=1}^2 b_{eff, 2, i} \right)}{c_M} = \frac{6.48 \times 9 \times 12^2 - 8 \times 1.0 \times 3466.5 \times 10^{-3} \times (9 - (12/8 + 12/8))}{12}$$

$$= 686.0 \text{ kNm}$$

$$V_{f_i, Sd, b, 2} = \frac{4M_{f_i, Sd, b, 2}}{L_2} = \frac{4 \times 686.0}{12} = 228.7 \text{ kN}$$

One of the primary beams of this zone is an edge beam at the façade level, it must support an additional load coming from the façade elements of 2.0 kN/m, which implies a modification of the applied load in fire condition following the next relations:

$$M_{f_i, Sd, b, 2} = 686.0 + \frac{2.0 \times 12^2}{8} = 722.0 \text{ kNm}$$

$$V_{f_i, Sd, b, 2} = 228.7 + \frac{2.0 \times 12}{2} = 234.8 \text{ kN}$$

So, the fire protection of this beam must be determined to ensure that the calculated bearing capacity in fire situation is not lower than the applied loads for the requested fire duration.

### 5.1.2 Floor design: Zone A

The applied calculation procedure is the same as the one applied for Zone B. Here, the dimensions are 9 m by 9 m. In order to simplify the construction, the mesh ST 25C will also be used in this area in order to have the same section for the entire slab surface. In consequence, Zone A will be also verified with this mesh section. This calculation zone is composed of 2 unprotected composite beams. The details of the calculation are given below:

#### Step 1: Calculation of the applied load on the slab in case of fire

Same as the calculation for Zone B

#### Step 2: Calculation of the heat transfer into the composite slab Cofraplus 60

Same as the calculation for Zone B

#### Step 3: Calculation of the moment resistance of the slab section $M_{f_i, 0}$

For this calculation zone:

$$L_1 = 9 \text{ 000 mm}$$

$$L_2 = 9 \text{ 000 mm}$$

So,  $L = \max \{L_1; L_2\} = 9 \text{ 000 mm}$  and  $\ell = \min \{L_1; L_2\} = 9 \text{ 000 mm}$ .

It can be obtained:

$$(g_0)_1 = 1 - \frac{2KA_s f_{sy,\theta_s} / \gamma_{M,fi,s}}{0.85 f_c / \gamma_{M,fi,c} d} = 1 - \frac{2 \times 1.0 \times \frac{257}{1000} \times 500 / 1.0}{0.85 \times 25 / 1.0 \times 30} = 0.597$$

$$(g_0)_2 = 1 - \frac{2A_s f_{sy,\theta_s} / \gamma_{M,fi,s}}{0.85 f_c / \gamma_{M,fi,c} d} = 1 - \frac{2 \times 1.0 \times \frac{257}{1000} \times 500 / 1.0}{0.85 \times 25 / 1.0 \times 30} = 0.597$$

It is to be noticed that the parameter  $K$  is equal to 1.0 because the reinforcing mesh has the same cross section in both dimensions.

So, the positive moment resistance of the slab section is:

$$M_{fi,0} = A_s f_{sy,\theta_s} / \gamma_{M,fi,s} d \frac{3 + (g_0)_2}{4} = \frac{257}{1000} \times 500 / 1.0 \times 30 \times \frac{3 + 0.597}{4} = 3466.5 \text{ Nmm/mm}$$

In parallel, it is also possible to determine the other necessary parameters:

$$\mu = K \frac{3 + (g_0)_1}{3 + (g_0)_2} = 1.0 \times \frac{3 + 0.597}{3 + 0.597} = 1.0$$

$$a = \frac{L}{\ell} = \frac{9000}{9000} = 1.0$$

$$n = \frac{1}{2\mu a^2} (\sqrt{3\mu a^2 + 1} - 1) = \frac{1}{2 \times 1.0 \times 1.0^2} \times (\sqrt{3 \times 1.0 \times 1.0^2 + 1} - 1) = 0.50$$

#### Step 4: Determination of the reference bearing capacity of the slab

The reference bearing capacity of the slab can be determined from:

$$p_{fi} = 6 \frac{M_{fi,0}}{n^2 a^2 \ell^2} = 6 \times \frac{3466.5}{0.5^2 \times 1.0^2 \times 9000^2} = 1.027 \times 10^{-3} \text{ N/mm}^2 = 1.027 \text{ kN/m}^2$$

#### Step 5: Determination of the deflection for the calculation of the membrane action

The deflection of the slab in fire situation to take into account membrane action can be obtained from:

$$\begin{aligned} w &= \min \left\{ \frac{\alpha(\theta_2 - \theta_1)\ell^2}{19.2h_{eff}} + \min \left[ \sqrt{\left( \frac{0.5f_{sy}}{E_a \gamma_{M,fi,s}} \right) \frac{3L^2}{8}}; \frac{\ell}{30} \right]; \frac{L + \ell}{30} \right\} \\ &= \min \left\{ \frac{1.2 \times 10^{-5} (831 - 99) \times 9000^2}{19.2 \times 95} + \min \left[ \sqrt{\left( \frac{0.5 \times 500}{210000 \times 1.0} \right) \frac{3 \times 9000^2}{8}}; \frac{9000}{30} \right]; \frac{9000 + 9000}{30} \right\} \\ &= \min \{ 391.0 + \min [190.2; 300]; 600 \} = 581.2 \text{ mm} \end{aligned}$$

#### Step 6: Calculation of the parameters to determine the membrane action

The determination of the different multiplication factors for the membrane action are based on the different parameters  $\alpha_1$ ,  $\alpha_2$ ,  $\beta_1$ ,  $\beta_2$ ,  $A$ ,  $B$ ,  $C$ ,  $D$ ,  $k$  and  $b$  that need to be determined. The values of these parameters are summarized in Table 5-9.

**Table 5-9 Parameters used for the assessment of the membrane action in Zone A**

Equation	Obtained value
$\alpha_1 = \frac{2(g_0)_1}{3+(g_0)_1}$	0.332
$\beta_1 = \frac{1-(g_0)_1}{3+(g_0)_1}$	0.112
$\alpha_2 = \frac{2(g_0)_2}{3+(g_0)_2}$	0.332
$\beta_2 = \frac{1-(g_0)_2}{3+(g_0)_2}$	0.112
$k = \frac{4na^2(1-2n)}{4n^2a^2+1} + 1$	1.0
$A = \frac{1}{2(1+k)} \left[ \frac{\ell^2}{8n} - \left( \frac{1-2n}{2n} + \frac{1}{3(1+k)} \right) \left( (nL)^2 + (\ell/2)^2 \right) \right]$	3 375 000 mm <sup>2</sup>
$B = \frac{k^2}{2(1+k)} \left[ \frac{nL^2}{2} - \frac{k}{3(1+k)} \left( (nL)^2 + (\ell/2)^2 \right) \right]$	3 375 000 mm <sup>2</sup>
$C = \frac{\ell^2}{16n} (k-1)$	0 mm <sup>2</sup>
$D = \frac{L^2}{8} (1-2n)^2$	0 mm <sup>2</sup>
$b = \min \left[ \frac{\ell^2}{8K(A+B+C-D)}, \frac{\gamma_{M,f1,s}}{kK_A f_{sy,th}} \left( 0.85 \frac{f_c}{\gamma_{M,f1,c}} \times 0.45d - A_s \frac{f_{sy,th}}{\gamma_{M,f1,s}} \frac{K+1}{2} \right) \right]$	1.232

**Step 7: Calculation of the enhancement factors for the membrane action**

The multiplication factors  $e_{1b}$ ,  $e_{2b}$ ,  $e_{1m}$  and  $e_{2m}$  can be determined:

**Table 5-10: Enhancement factors the assessment of the membrane action in Zone A**

Equation	Obtained Value
$e_{1b} = 2n \left( 1 + \alpha_1 b \frac{k-1}{2} - \frac{\beta_1 b^2}{3} (k^2 - k + 1) \right) + (1-2n)(1 - \alpha_1 b - \beta_1 b^2)$	0.943
$e_{1m} = \frac{4b}{3 + (g_0)_1} \frac{w}{d} \left( (1-2n) + n \frac{(2+3k-k^3)}{3(1+k)^2} \right)$	4.425
$e_1 = e_{1b} + e_{1m}$	5.368
$e_{2b} = 1 + \frac{\alpha_2 b K}{2} (k-1) - \frac{\beta_2 b^2 K}{3} (k^2 - k + 1)$	0.943
$e_{2m} = \frac{4bK}{3 + (g_0)_2} \frac{w}{d} \frac{(2+3k-k^3)}{6(1+k)^2}$	4.425
$e_2 = e_{2b} + e_{2m}$	5.368

Then, the global enhancement factor  $e$  is determined by:

$$e = e_1 - \frac{e_1 - e_2}{1 + 2\mu a^2} = 5.368 - \frac{5.368 - 5.368}{1 + 2 \times 1.0 \times 1.0^2} = 5.368$$

### Step 8: Total bearing capacity of the slab in fire condition

The total bearing capacity of the slab in fire condition taking into account the membrane action can be obtained from:

$$q_{fi,Rd,slab} = e \times p_{fi} = 5.368 \times 1.027 = 5.51 \text{ kN/m}^2$$

### Step 9: Bearing capacity of the slab taking into account the contribution of the unprotected composite beams

The moment resistance of the beams has the same value as in Zone A, but the calculation of their bearing capacity is modified due to a different number of internal unprotected beams, and a different span of the primary beams:

$$q_{fi,Rd,ub} = \frac{8M_{fi,Rd}}{L_1^2} \frac{1 + n_{ub}}{L_2} = \frac{8 \times 51.5}{9^2} \times \frac{(1+2)}{9} = 1.70 \text{ kN/m}^2$$

## Step 10: Total bearing capacity of the slab in fire conditions and verification of the fire resistance of the slab

The total bearing capacity of the slab is:

$$q_{fi,Rd} = q_{fi,Rd,slab} + q_{fi,Rd,ub} = 5.51 + 1.70 = 7.21 \text{ kN/m}^2$$

With regards to the applied load on the slab in fire situation

$$q_{fi,Sd} = 5.98 \text{ kN/m}^2 < q_{fi,Rd} = 7.21 \text{ kN/m}^2$$

The screenshot displays the MACS+ software interface with a detailed report for fire resistance verification. The report includes a table of results for various beams and slabs, with columns for beam ID, length, width, depth, and various resistance and capacity values. The table shows that the fire resistance is adequate for the specified conditions.

Beam ID	Length (m)	Width (m)	Depth (m)	Design fire resistance (min)	Design fire resistance (max)	Design fire resistance (avg)	Design fire resistance (std)	Design fire resistance (min)	Design fire resistance (max)	Design fire resistance (avg)	Design fire resistance (std)
1	9.00	2.25	0.225	1.70	1.70	1.70	0.00	1.70	1.70	1.70	0.00
2	9.00	2.25	0.225	1.70	1.70	1.70	0.00	1.70	1.70	1.70	0.00
3	9.00	2.25	0.225	1.70	1.70	1.70	0.00	1.70	1.70	1.70	0.00
4	9.00	2.25	0.225	1.70	1.70	1.70	0.00	1.70	1.70	1.70	0.00
5	9.00	2.25	0.225	1.70	1.70	1.70	0.00	1.70	1.70	1.70	0.00
6	9.00	2.25	0.225	1.70	1.70	1.70	0.00	1.70	1.70	1.70	0.00
7	9.00	2.25	0.225	1.70	1.70	1.70	0.00	1.70	1.70	1.70	0.00
8	9.00	2.25	0.225	1.70	1.70	1.70	0.00	1.70	1.70	1.70	0.00
9	9.00	2.25	0.225	1.70	1.70	1.70	0.00	1.70	1.70	1.70	0.00
10	9.00	2.25	0.225	1.70	1.70	1.70	0.00	1.70	1.70	1.70	0.00
11	9.00	2.25	0.225	1.70	1.70	1.70	0.00	1.70	1.70	1.70	0.00
12	9.00	2.25	0.225	1.70	1.70	1.70	0.00	1.70	1.70	1.70	0.00
13	9.00	2.25	0.225	1.70	1.70	1.70	0.00	1.70	1.70	1.70	0.00
14	9.00	2.25	0.225	1.70	1.70	1.70	0.00	1.70	1.70	1.70	0.00
15	9.00	2.25	0.225	1.70	1.70	1.70	0.00	1.70	1.70	1.70	0.00
16	9.00	2.25	0.225	1.70	1.70	1.70	0.00	1.70	1.70	1.70	0.00
17	9.00	2.25	0.225	1.70	1.70	1.70	0.00	1.70	1.70	1.70	0.00
18	9.00	2.25	0.225	1.70	1.70	1.70	0.00	1.70	1.70	1.70	0.00
19	9.00	2.25	0.225	1.70	1.70	1.70	0.00	1.70	1.70	1.70	0.00
20	9.00	2.25	0.225	1.70	1.70	1.70	0.00	1.70	1.70	1.70	0.00
21	9.00	2.25	0.225	1.70	1.70	1.70	0.00	1.70	1.70	1.70	0.00
22	9.00	2.25	0.225	1.70	1.70	1.70	0.00	1.70	1.70	1.70	0.00
23	9.00	2.25	0.225	1.70	1.70	1.70	0.00	1.70	1.70	1.70	0.00
24	9.00	2.25	0.225	1.70	1.70	1.70	0.00	1.70	1.70	1.70	0.00
25	9.00	2.25	0.225	1.70	1.70	1.70	0.00	1.70	1.70	1.70	0.00
26	9.00	2.25	0.225	1.70	1.70	1.70	0.00	1.70	1.70	1.70	0.00
27	9.00	2.25	0.225	1.70	1.70	1.70	0.00	1.70	1.70	1.70	0.00
28	9.00	2.25	0.225	1.70	1.70	1.70	0.00	1.70	1.70	1.70	0.00
29	9.00	2.25	0.225	1.70	1.70	1.70	0.00	1.70	1.70	1.70	0.00
30	9.00	2.25	0.225	1.70	1.70	1.70	0.00	1.70	1.70	1.70	0.00
31	9.00	2.25	0.225	1.70	1.70	1.70	0.00	1.70	1.70	1.70	0.00
32	9.00	2.25	0.225	1.70	1.70	1.70	0.00	1.70	1.70	1.70	0.00
33	9.00	2.25	0.225	1.70	1.70	1.70	0.00	1.70	1.70	1.70	0.00
34	9.00	2.25	0.225	1.70	1.70	1.70	0.00	1.70	1.70	1.70	0.00
35	9.00	2.25	0.225	1.70	1.70	1.70	0.00	1.70	1.70	1.70	0.00
36	9.00	2.25	0.225	1.70	1.70	1.70	0.00	1.70	1.70	1.70	0.00
37	9.00	2.25	0.225	1.70	1.70	1.70	0.00	1.70	1.70	1.70	0.00
38	9.00	2.25	0.225	1.70	1.70	1.70	0.00	1.70	1.70	1.70	0.00
39	9.00	2.25	0.225	1.70	1.70	1.70	0.00	1.70	1.70	1.70	0.00
40	9.00	2.25	0.225	1.70	1.70	1.70	0.00	1.70	1.70	1.70	0.00
41	9.00	2.25	0.225	1.70	1.70	1.70	0.00	1.70	1.70	1.70	0.00
42	9.00	2.25	0.225	1.70	1.70	1.70	0.00	1.70	1.70	1.70	0.00
43	9.00	2.25	0.225	1.70	1.70	1.70	0.00	1.70	1.70	1.70	0.00
44	9.00	2.25	0.225	1.70	1.70	1.70	0.00	1.70	1.70	1.70	0.00
45	9.00	2.25	0.225	1.70	1.70	1.70	0.00	1.70	1.70	1.70	0.00
46	9.00	2.25	0.225	1.70	1.70	1.70	0.00	1.70	1.70	1.70	0.00
47	9.00	2.25	0.225	1.70	1.70	1.70	0.00	1.70	1.70	1.70	0.00
48	9.00	2.25	0.225	1.70	1.70	1.70	0.00	1.70	1.70	1.70	0.00
49	9.00	2.25	0.225	1.70	1.70	1.70	0.00	1.70	1.70	1.70	0.00
50	9.00	2.25	0.225	1.70	1.70	1.70	0.00	1.70	1.70	1.70	0.00

Figure 5-16 Output data using the MACS+ software – Detailed report

In conclusion, the stability of the slab system is ensured for R60 with its actual dimensions in Zone A.

## Step 11: Applied load in fire situation for perimeter beams

The applied loads in fire situation on the secondary beams and perimeter beams of Zone A are calculated from relations 3.24 to 3.37:

- For the secondary perimeter beams

$$M_{fi,Sd,b,1} = \frac{q_{fi,Rd} L_1^2 L_2 - 8 \left( M_{fi,0} \left( L_2 - n_{ub} b_{eff,ub} - \sum_{i=1}^2 b_{eff,1,i} \right) + n_{ub} M_{fi,Rd} \right)}{c_M}$$

$$= \frac{7.21 \times 9^2 \times 9 - 8 \times \left[ 3466.5 \times 10^{-3} \times \left[ 9 - 2 \times 2.25 - (0 + 2.25/2) \right] + 2 \times 51.5 \right]}{12}$$

$$= 361.5 \text{ kNm}$$

$$V_{fi,Sd,b,1} = \frac{4M_{fi,Sd,b,1}}{L_1} = \frac{4 \times 361.5}{9} = 160.7 \text{ kN}$$

- For the primary perimeter beams

$$M_{fi,Sd,b,2} = \frac{q_{fi,Rd} L_1 L_2^2 - 8\mu M_{fi,0} \left( L_1 - \sum_{i=1}^2 b_{eff,2,i} \right)}{c_M} = \frac{7.21 \times 9 \times 9^2 - 8 \times 1.0 \times 3466.5 \times 10^{-3} \times (9 - (0 + 9/8))}{12}$$

$$= 419.8 \text{ kNm}$$

$$V_{fi,Sd,b,2} = \frac{4M_{fi,Sd,b,2}}{L_2} = \frac{4 \times 419.8}{9} = 186.6 \text{ kN}$$

Two of the perimeter beams of this zone are corner beams at the façade level, they must support an additional load coming from the façade elements of 2.0 kN/m, which implies a modification of the applied load in fire condition following the next relations:

- For the secondary perimeter edge beam

$$M_{fi,Sd,b,1} = 361.5 + \frac{2.0 \times 9^2}{8} = 381.7 \text{ kNm} \quad \text{and} \quad V_{fi,Sd,b,1} = 160.7 + \frac{2.0 \times 9}{2} = 169.7 \text{ kN}$$

- For the primary perimeter edge beam

$$M_{fi,Sd,b,2} = 419.8 + \frac{2.0 \times 9^2}{8} = 440.0 \text{ kNm} \quad \text{and} \quad V_{fi,Sd,b,2} = 186.6 + \frac{2.0 \times 9}{2} = 195.6 \text{ kN}$$

So, the fire protection of these beams must be determined to ensure that the calculated bearing capacity in fire situation is not lower than the applied loads for the requested fire duration.

### 5.1.3 Floor design: Zone E

In Zone E, the dimensions of the composite slab and the spans of the beams have the same values as in Zone B. However, solid beams are replaced by IPE 300+IPE 300 ACB beams (see cross-section in Figure 5-18).

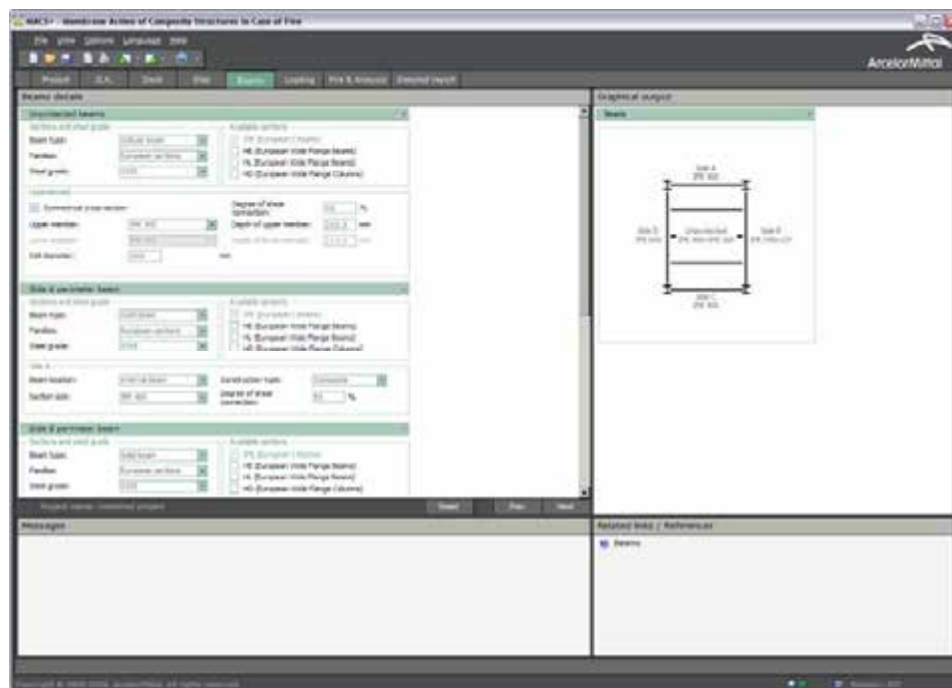


Figure 5-17 Input data using the MACS+ software – Beams in Zone E





Figure 5-18 Net cross-section of ACB beam in Zone E

In consequence, only the load-bearing capacity of the unprotected beams needs to be determined.

**Steps 1 to 8: same as Zone B**

**Step 9: Bearing capacity of the slab taking into account the contribution of the unprotected composite beams**

The values of the section factors of the steel section are summarized in Table 5-11.

From Table 3-2, the temperatures of the steel part of the composite section are the following:

- temperature of the flanges: 940.0°C;
- temperature of the lower web: 942.1°C in Table 3-2 but taken as 940.0°C because the depth of the steel section is not bigger than 500 mm;
- temperature of the upper web: 942.1°C;
- temperature of the studs (see 4.3.4.2.5 of EN 1994-1-2):  $940.0 \times 0.8 = 752.0^\circ\text{C}$

**Table 5-11 Section factor of the unprotected composite beam**

Steel section member	$k_{sh} = 0.9 \left( \frac{0.5B_1 + t_{f1} + t_{f2} + \sqrt{h_w^2 + (B_1 - B_2)^2/4}}{H + B_1 + B_2/2 - (t_{w1} + t_{w2})/2} \right)$	$\left( \frac{A_i}{V_i} \right) \text{ (m}^{-1}\text{)}$	$k_{sh} \left( \frac{A_i}{V_i} \right) \text{ (m}^{-1}\text{)}$
Lower flange	0.699	$\frac{2(B_1 + t_{f1})}{B_1 t_{f1}} = 200$	140
Lower web		$\frac{2h_{w1} + t_{w1}}{h_{w1} t_{w1}} = 302$	211
Upper web		$\frac{2h_{w2} + t_{w2}}{h_{w2} t_{w2}} = 302$	211
Upper flange		$\frac{2(B_2 + t_{f2})}{B_2 t_{f2}} = 200$	140
With:	$H$ : depth of the steel section; $h_w$ : overall depth of the web; $B_1$ : width of the lower flange; $t_{f1}$ : thickness of the lower flange; $t_{w1}$ : thickness of the lower web; $h_{w1}$ : depth of the lower web (net cross-section); $B_2$ : width of the upper flange; $t_{f2}$ : thickness of the upper flange; $t_{w2}$ : thickness of the upper web; $h_{w2}$ : depth of the upper web (net cross-section).		

The temperatures of the steel section and of the steel studs allow determining the moment resistance of the internal non composite unprotected beams. For Cellular Beams, the contribution of the lower member is neglected as its temperature exceeds 600°C. The calculated values are given in Table 5-12.

**Table 5-12 Moment resistance for unprotected composite beams in Zone E**

Parameters	Calculated values
Effective width of the slab	$b_{eff} = \min\{9000/4; 3000\} = 2250 \text{ mm}$
Area of the upper flange $A_{f2}$	$A_{f2} = 1605 \text{ mm}^2$
Area of the upper web $A_{w2}$	$A_{w2} = 352 \text{ mm}^2$
Reduction factor for the steel strength properties	$k_{y,\theta} = 0.052$
Reduction factor for the stud strength properties	$k_{u,\theta} = 0.17$
Tensile force $T^+ = \sum A_i f_y k_{y,\theta} / \gamma_{M,fi,a}$	$T^+ = (1605 + 352) \times 355 \times 0.052 / 1.0 = 36.08 \text{ kN}$
Thickness of the slab in compression in fire situation $h_u = \frac{T^+}{b_{eff} f_c / \gamma_{M,fi,c}}$	$h_u = \frac{36.08}{2250 \times 25 / 1.0} = 0.641 \text{ mm}$
Connection degree of the beam at 20°C	$n_{c,20^\circ C} = 0.52$
Connection degree of the beam in fire situation $n_{c,\theta} = \frac{n_{c,20^\circ C} k_{u,\theta} \gamma_{M,\nu}}{k_{y,\theta} \gamma_{M,fi,\nu}}$	$n_{c,\theta} = \frac{0.52 \times 0.17 \times 1.25}{0.052 \times 1.0} = 2.05 > 1.0$ So full shear connection
Tensile force application point $y_T = \frac{\sum A_i y_i f_y k_{y,\theta}}{T^+ \gamma_{M,fi,a}}$	$y_T = \frac{(352 \times 6.45 + 1605 \times 29.63) \times 355 \times 0.052}{36.08 \times 1.0} = 409.86 \text{ mm}$
Compressive force application point $y_F = H + h_c - h_u / 2$	$y_F = 420.6 + 130 - 0.641 / 2 = 550.28 \text{ mm}$
Positive moment resistance $M_{fi,Rd} = T^+ (y_F - y_T)$	$M_{fi,Rd} = 36.08 \times (550.28 - 409.86) = 5.07 \times 10^6 \text{ Nmm} = 5.07 \text{ kNm}$
With: $h_c$ : total thickness of the slab; $\gamma_{M,fi,a}$ , $\gamma_{M,\nu}$ and $\gamma_{M,fi,\nu}$ partial safety factor for the steel profile, the steel stud in normal conditions and in fire conditions.	

Then, the bearing capacity of the slab thanks to the contribution of the unprotected composite beam can be obtained from:

$$q_{fi,Rd,ub} = \frac{8M_{fi,Rd}}{L_1^2} \frac{1+n_{ub}}{L_2} = \frac{8 \times 5.07}{9^2} \times \frac{(1+3)}{12} = 0.17 \text{ kN/m}^2$$

### Step 10: Total bearing capacity of the slab in fire conditions and verification of the fire resistance of the slab

The total bearing capacity of the slab is:

$$q_{fi,Rd} = q_{fi,Rd,slab} + q_{fi,Rd,ub} = 4.78 + 0.17 = 4.95 \text{ kN/m}^2$$

With regards to the applied load on the slab in fire situation:

$$q_{fi, Sd} = 5.98 \text{ kN/m}^2 > q_{fi, Rd} = 4.95 \text{ kN/m}^2$$

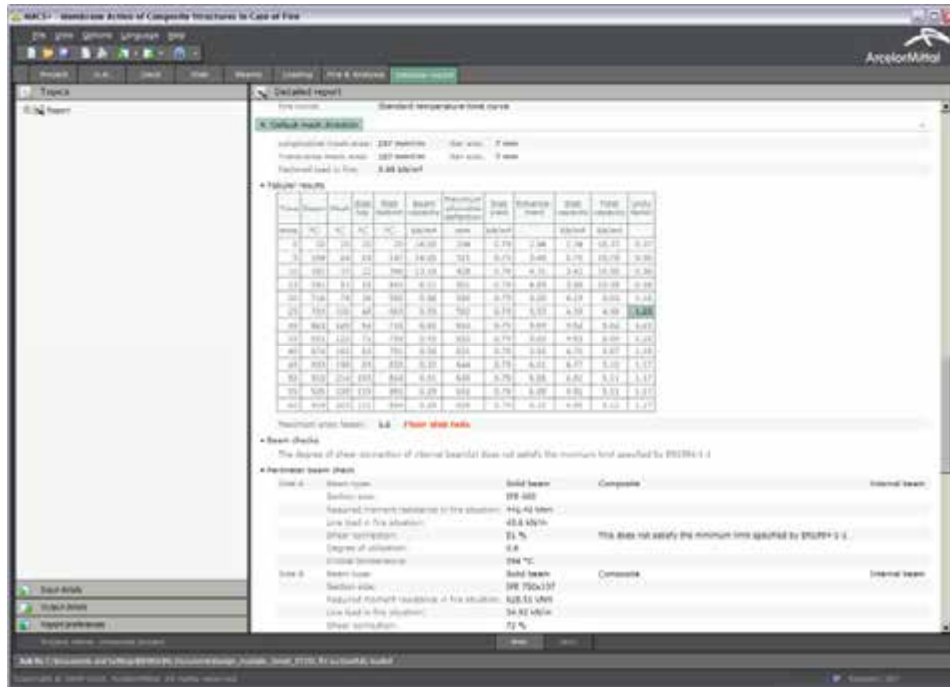


Figure 5-19 Output data using the MACS+ software – Detailed report

### Conclusion 1

In conclusion, the stability of the slab system cannot be ensured for R60 with its actual dimensions in Zone E. So, it is necessary to modify the constructive parameters.

An adequate solution could be to increase or the mesh axis distance or the mesh size.

The closest mesh area in the current mesh range is equal to 385 mm<sup>2</sup>/m, i.e. much greater than that of the current ST 25C mesh. So, the first option is to increase the mesh axis distance in such a way to as to keep its temperature below 400°C for a minimum yield strength reduction. The mesh axis distance was increased from 30 mm to 40 mm. In this case, the temperature of the reinforcement mesh increases from 288°C to 363°C. According to Table 3-4 of EN 1994-1-2, the effective yield strength of the reinforcement mesh is reduced to 96% of its value at room temperature.

For information purpose, using this increased mesh axis distance leads to the following load bearing capacities:

- Zone A:  $q_{fi, Rd} = q_{fi, Rd, slab} + q_{fi, Rd, ub} = 6.60 + 1.70 = 8.30 \text{ kN/m}^2 > 7.21 \text{ kN/m}^2$ ;
- Zone B:  $q_{fi, Rd} = q_{fi, Rd, slab} + q_{fi, Rd, ub} = 4.88 + 1.70 = 6.58 \text{ kN/m}^2 > 6.48 \text{ kN/m}^2$ .

In consequence, increasing this mesh axis distance does increase the overall load bearing capacity of Zone A and Zone B.

### Step 2a

Following Table 3-4 of EN 1994-1-2, the effective steel strength for the welded steel mesh is reduced as follows:

$$f_{sy, \theta_s} = 500 \times 0,962 = 481 \text{ MPa}$$

### Step 3a: Calculation of the moment resistance of the slab section $M_{fi,0}$

For this calculation zone:

$$L_1 = 9\,000 \text{ mm (span of the secondary beams)}$$

$$L_2 = 12\,000 \text{ mm (span of the primary beams)}$$

So,  $L = \max \{L_1; L_2\} = 12\,000 \text{ mm}$  and  $\ell = \min \{L_1; L_2\} = 9\,000 \text{ mm}$ .

It can be obtained:

$$(g_0)_1 = 1 - \frac{2KA_s f_{sy,\theta_s} / \gamma_{M,f_i,s}}{0.85 f_c / \gamma_{M,f_i,c} d} = 1 - \frac{2 \times 1.0 \times \frac{257}{1000} \times 4810 / 1.0}{0.85 \times 25 / 1.0 \times 40} = 0.709$$

$$(g_0)_2 = 1 - \frac{2A_s f_{sy,\theta_s} / \gamma_{M,f_i,s}}{0.85 f_c / \gamma_{M,f_i,c} d} = 1 - \frac{2 \times 1.0 \times \frac{257}{1000} \times 481 / 1.0}{0.85 \times 25 / 1.0 \times 40} = 0.709$$

So, the positive moment resistance of the slab section is:

$$M_{f_i,0} = A_s f_{sy,\theta_s} / \gamma_{M,f_i,s} d \frac{3 + (g_0)_2}{4} = \frac{257}{1000} \times 0.962 \times 500 / 1.0 \times 40 \times \frac{3 + 0.709}{4} = 4\,586.51 \text{ Nmm/mm}$$

In parallel, it is also possible to determine the other necessary parameters:

$$\mu = K \frac{3 + (g_0)_1}{3 + (g_0)_2} = 1.0 \times \frac{3 + 0.709}{3 + 0.709} = 1.0$$

$$a = \frac{L}{\ell} = \frac{12\,000}{9\,000} = 1.333$$

$$n = \frac{1}{2\mu a^2} (\sqrt{3\mu a^2 + 1} - 1) = \frac{1}{2 \times 1.0 \times 1.333^2} \times (\sqrt{3 \times 1.0 \times 1.333^2 + 1} - 1) = 0.427$$

#### Step 4a: Determination of the reference bearing capacity of the slab

The reference bearing capacity of the slab can be determined from:

$$p_{fi} = 6 \frac{M_{f_i,0}}{n^2 a^2 \ell^2} = 6 \times \frac{4\,586.51}{0.427^2 \times 1.333^2 \times 9\,000^2} = 1.050 \times 10^{-3} \text{ N/mm}^2 = 1.050 \text{ kN/m}^2$$

#### Step 5a: same as Step 5

#### Step 6a: Calculation of the parameters to determine the membrane action

The determination of the different multiplication factors for the membrane action are based on the different parameters  $\alpha_1$ ,  $\alpha_2$ ,  $\beta_1$ ,  $\beta_2$ ,  $A$ ,  $B$ ,  $C$ ,  $D$ ,  $k$  and  $b$  that need to be determined. The values of these parameters are summarized in Table 5-13.

**Table 5-13 Parameters used for the assessment of the membrane action in Zone E**

Equation	Obtained values
$\alpha_1 = \frac{2(g_0)_1}{3+(g_0)_1}$	0.382
$\beta_1 = \frac{1-(g_0)_1}{3+(g_0)_1}$	0.078
$\alpha_2 = \frac{2(g_0)_2}{3+(g_0)_2}$	0.382
$\beta_2 = \frac{1-(g_0)_2}{3+(g_0)_2}$	0.078
$k = \frac{4na^2(1-2n)}{4n^2a^2+1} + 1$	1.194
$A = \frac{1}{2(1+k)} \left[ \frac{\ell^2}{8n} - \left( \frac{1-2n}{2n} + \frac{1}{3(1+k)} \right) \left( (nL)^2 + (\ell/2)^2 \right) \right]$	1 978 359 mm <sup>2</sup>
$B = \frac{k^2}{2(1+k)} \left[ \frac{nL^2}{2} - \frac{k}{3(1+k)} \left( (nL)^2 + (\ell/2)^2 \right) \right]$	7 242 376 mm <sup>2</sup>
$C = \frac{\ell^2}{16n} (k-1)$	2 305 602 mm <sup>2</sup>
$D = \frac{L^2}{8} (1-2n)^2$	388 465 mm <sup>2</sup>
$b = \min \left[ \frac{\ell^2}{8K(A+B+C-D)}, \frac{\gamma_{M,f_i,s}}{kK A_s f_{sy,fb}} \left( 0.85 \frac{f_c}{\gamma_{M,f_i,c}} \times 0.45d - A_s \frac{f_{sy,fb}}{\gamma_{M,f_i,s}} \frac{K+1}{2} \right) \right]$	0.909

**Step 7a: Calculation of the enhancement factors for the membrane action**

The multiplication factors  $e_{1b}$ ,  $e_{2b}$ ,  $e_{1m}$  and  $e_{2m}$  can be determined:

**Table 5-14 Enhancement factors the assessment of the membrane action in Zone E**

Equation	Obtained values
$e_{1b} = 2n \left( 1 + \alpha_1 b \frac{k-1}{2} - \frac{\beta_1 b^2}{3} (k^2 - k + 1) \right) + (1-2n)(1 - \alpha_1 b - \beta_1 b^2)$	0.946
$e_{1m} = \frac{4b}{3 + (g_0)_1} \frac{w}{d} \left( (1-2n) + n \frac{2+3k-k^3}{3(1+k)^2} \right)$	4.130
$e_1 = e_{1b} + e_{1m}$	5.076
$e_{2b} = 1 + \frac{\alpha_2 b K}{2} (k-1) - \frac{\beta_2 b^2 K}{3} (k^2 - k + 1)$	1.007
$e_{2m} = \frac{4bK}{3 + (g_0)_2} \frac{w}{d} \frac{2+3k-k^3}{6(1+k)^2}$	2.121
$e_2 = e_{2b} + e_{2m}$	3.129

Then, the global enhancement factor  $e$  is determined by:

$$e = e_1 - \frac{e_1 - e_2}{1 + 2\mu\alpha^2} = 5.076 - \frac{5.076 - 3.129}{1 + 2 \times 1.0 \times 1.333^2} = 4.648$$

#### Step 8a: Total bearing capacity of the slab in fire condition

The total bearing capacity of the slab in fire condition taking into account the membrane action can be obtained from:

$$q_{fi,Rd,slab} = e \times p_{fi} = 4.648 \times 1.050 = 4.88 \text{ kN/m}^2$$

#### Step 9a: Bearing capacity of the slab taking into account the contribution of the unprotected composite beams

Same as Step 9

#### Step 10a: Total bearing capacity of the slab in fire conditions and verification of the fire resistance of the slab

The total bearing capacity of the slab is:

$$q_{fi,Rd} = q_{fi,Rd,slab} + q_{fi,Rd,ub} = 4.88 + 0.17 = 5.05 \text{ kN/m}^2$$

With regards to the applied load on the slab in fire situation:

$$q_{fi,Sd} = 5.98 \text{ kN/m}^2 > q_{fi,Rd} = 5.05 \text{ kN/m}^2$$

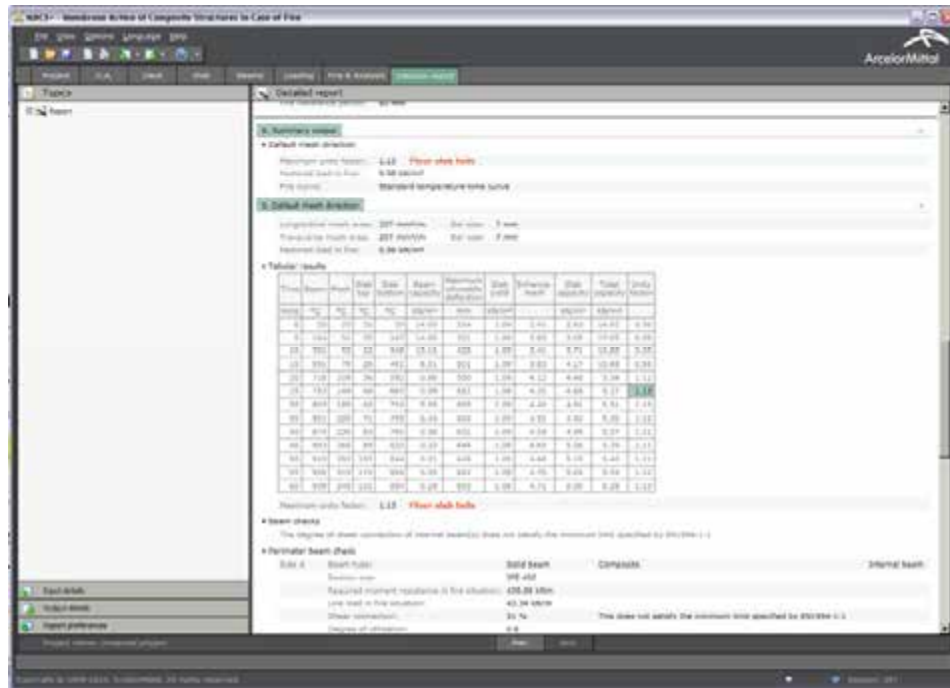


Figure 5-20 Output data using the MACS+ software – Detailed report

## Conclusion 2

In conclusion, the stability of the slab system cannot be ensured for R60 with its actual dimensions in Zone E. So, it is necessary to modify the constructive parameters, for instance by increasing the reinforcement mesh area.

The size of the welded mesh was increased from ST 25C (257 mm<sup>2</sup>/m) to ST 40C (385 mm<sup>2</sup>/m).

**Step 2b: same as Step 2a**

**Step 3b: Calculation of the moment resistance of the slab section  $M_{fi,0}$**

For this calculation zone:

$$L_1 = 9\,000 \text{ mm (span of the secondary beams)}$$

$$L_2 = 12\,000 \text{ mm (span of the primary beams)}$$

So,  $L = \max \{L_1; L_2\} = 12\,000 \text{ mm}$  and  $\ell = \min \{L_1; L_2\} = 9\,000 \text{ mm}$ .

It can be obtained:

$$(g_0)_1 = 1 - \frac{2KA_s f_{sy,\theta_s} / \gamma_{M_{fi,s}}}{0.85 f_c / \gamma_{M_{fi,c}} d} = 1 - \frac{2 \times 1.0 \times \frac{385}{1000} \times 481 / 1.0}{0.85 \times 25 / 1.0 \times 40} = 0.564$$

$$(g_0)_2 = 1 - \frac{2A_s f_{sy,\theta_s} / \gamma_{M,f_i,s}}{0.85 f_c / \gamma_{M,f_i,c} d} = 1 - \frac{2 \times 1.0 \times \frac{385}{1000} \times 481 / 1.0}{0.85 \times 25 / 1.0 \times 40} = 0.564$$

So, the positive moment resistance of the slab section is:

$$M_{f_i,0} = A_s f_{sy,\theta_s} / \gamma_{M,f_i,s} d \frac{3 + (g_0)_2}{4} = \frac{385}{1000} \times 0.962 \times 500 / 1.0 \times 40 \times \frac{3 + 0.564}{4} = 6\,602.40 \text{ Nmm/mm}$$

In parallel, it is also possible to determine the other necessary parameters:

$$\mu = K \frac{3 + (g_0)_1}{3 + (g_0)_2} = 1.0 \times \frac{3 + 0.564}{3 + 0.564} = 1.0$$

$$a = \frac{L}{\ell} = \frac{12\,000}{9\,000} = 1.333$$

$$n = \frac{1}{2\mu a^2} (\sqrt{3\mu a^2 + 1} - 1) = \frac{1}{2 \times 1.0 \times 1.333^2} \times (\sqrt{3 \times 1.0 \times 1.333^2 + 1} - 1) = 0.427$$

#### Step 4b: Determination of the reference bearing capacity of the slab

The reference bearing capacity of the slab can be determined:

$$p_{fi} = 6 \frac{M_{f_i,0}}{n^2 a^2 \ell^2} = 6 \times \frac{6\,602.40}{0.427^2 \times 1.333^2 \times 9\,000^2} = 1.512 \times 10^{-3} \text{ N/mm}^2 = 1.512 \text{ kN/m}^2$$

#### Step 5b: same as Step 5

#### Step 6b: Calculation of the parameters to determine the membrane action

The determination of the different multiplication factors for the membrane action are based on the different parameters  $\alpha_1$ ,  $\alpha_2$ ,  $\beta_1$ ,  $\beta_2$ ,  $A$ ,  $B$ ,  $C$ ,  $D$ ,  $k$  and  $b$  that need to be determined. The values of these parameters are summarized in Table 5-15.



**Table 5-15 Parameters used for the assessment of the membrane action in Zone E**

Equation	Obtained values
$\alpha_1 = \frac{2(g_0)_1}{3+(g_0)_1}$	0.317
$\beta_1 = \frac{1-(g_0)_1}{3+(g_0)_1}$	0.122
$\alpha_2 = \frac{2(g_0)_2}{3+(g_0)_2}$	0.317
$\beta_2 = \frac{1-(g_0)_2}{3+(g_0)_2}$	0.122
$k = \frac{4na^2(1-2n)}{4n^2a^2+1} + 1$	1.194
$A = \frac{1}{2(1+k)} \left[ \frac{\ell^2}{8n} - \left( \frac{1-2n}{2n} + \frac{1}{3(1+k)} \right) \left( (nL)^2 + (\ell/2)^2 \right) \right]$	1 978 359 mm <sup>2</sup>
$B = \frac{k^2}{2(1+k)} \left[ \frac{nL^2}{2} - \frac{k}{3(1+k)} \left( (nL)^2 + (\ell/2)^2 \right) \right]$	7 242 376 mm <sup>2</sup>
$C = \frac{\ell^2}{16n} (k-1)$	2 305 602 mm <sup>2</sup>
$D = \frac{L^2}{8} (1-2n)^2$	388 465 mm <sup>2</sup>
$b = \min \left[ \frac{\ell^2}{8K(A+B+C-D)}, \frac{\gamma_{M,fi,s}}{kK A_s f_{sy,fb}} \left( 0.85 \frac{f_c}{\gamma_{M,fi,c}} \times 0.45d - A_s \frac{f_{sy,fb}}{\gamma_{M,fi,s}} \frac{K+1}{2} \right) \right]$	0.892

**Step 7b: Calculation of the enhancement factors for the membrane action**

The multiplication factors  $e_{1b}$ ,  $e_{2b}$ ,  $e_{1m}$  and  $e_{2m}$  can be determined:

**Table 5-16 Enhancement factors the assessment of the membrane action in Zone E**

Equation	Obtained values
$e_{1b} = 2n \left( 1 + \alpha_1 b \frac{k-1}{2} - \frac{\beta_1 b^2}{3} (k^2 - k + 1) \right) + (1-2n)(1 - \alpha_1 b - \beta_1 b^2)$	0.934
$e_{1m} = \frac{4b}{3 + (g_0)_1} \frac{w}{d} \left( (1-2n) + n \frac{2+3k-k^3}{3(1+k)^2} \right)$	4.216
$e_1 = e_{1b} + e_{1m}$	5.150
$e_{2b} = 1 + \frac{\alpha_2 b K}{2} (k-1) - \frac{\beta_2 b^2 K}{3} (k^2 - k + 1)$	0.988
$e_{2m} = \frac{4bK}{3 + (g_0)_2} \frac{w}{d} \frac{2+3k-k^3}{6(1+k)^2}$	2.165
$e_2 = e_{2b} + e_{2m}$	3.153

Then, the global enhancement factor  $e$  is determined by:

$$e = e_1 - \frac{e_1 - e_2}{1 + 2\mu\alpha^2} = 5.150 - \frac{5.150 - 3.153}{1 + 2 \times 1.0 \times 1.333^2} = 4.711$$

### Step 8b: Total bearing capacity of the slab in fire condition

The total bearing capacity of the slab in fire condition taking into account the membrane action can be obtained from:

$$q_{fi,Rd,slab} = e \times p_{fi} = 4.711 \times 1.512 = 7.123 \text{ kN/m}^2$$

### Step 9b: Bearing capacity of the slab taking into account the contribution of the unprotected composite beams

Same as Step 9

### Step 10b: Total bearing capacity of the slab in fire conditions and verification of the fire resistance of the slab

The total bearing capacity of the slab is:

$$q_{fi,Rd} = q_{fi,Rd,slab} + q_{fi,Rd,ub} = 7.12 + 0.17 = 7.29 \text{ kN/m}^2$$

With regards to the applied load on the slab in fire situation:

$$q_{fi,Sd} = 5.98 \text{ kN/m}^2 < q_{fi,Rd} = 7.29 \text{ kN/m}^2$$

### Conclusion 3

In conclusion, the stability of the slab system is ensured for R60 with its actual dimensions in Zone E.

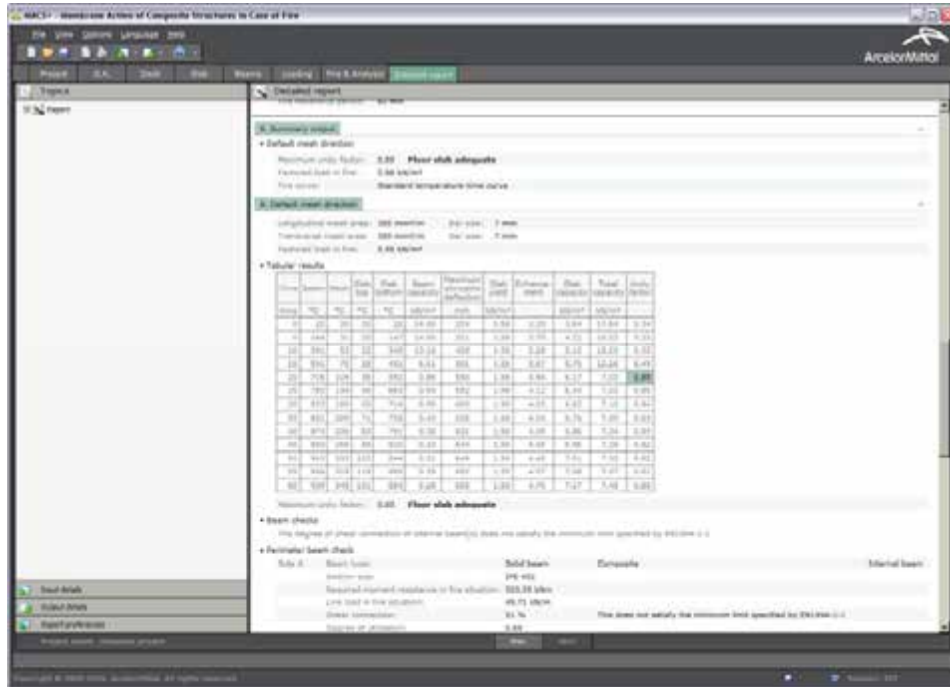


Figure 5-21 Output data using the MACS+ software – Detailed report

### Step 11: Applied load in fire situation for perimeter beams

The applied loads in fire situation on the secondary beams and perimeter beams of Zone E are calculated as follows:

- For the secondary perimeter beams

$$M_{fi,Sd,b,1} = \frac{q_{fi,Rd} L_1^2 L_2 - 8 \left( M_{fi,0} \left( L_2 - n_{ub} b_{eff,ub} - \sum_{i=1}^2 b_{eff,1,i} \right) + n_{ub} M_{fi,Rd} \right)}{c_M}$$

$$= \frac{7.29 \times 9^2 \times 12 - 8 \times \left\{ 6.602.40 \times 10^{-3} \times [12 - 3 \times 2.25 - (2.25/2 + 2.25/2)] + 3 \times 5.1 \right\}}{12}$$

$$= 567.08 \text{ kNm}$$

$$V_{fi,Sd,b,1} = \frac{4M_{fi,Sd,b,1}}{L_1} = \frac{4 \times 567.08}{9} = 252.04 \text{ kN}$$

- For the primary perimeter beams

$$M_{fi,Sd,b,2} = \frac{q_{fi,Rd} L_1 L_2^2 - 8\mu M_{fi,0} \left( L_1 - \sum_{i=1}^2 b_{eff,2,i} \right)}{c_M} = \frac{7.29 \times 9 \times 12^2 - 8 \times 1.0 \times 6602.40 \times 10^{-3} \times (9 - (12/8 + 12/8))}{12}$$

$$= 760.91 \text{ kNm}$$

$$V_{fi,Sd,b,2} = \frac{4M_{fi,Sd,b,2}}{L_2} = \frac{4 \times 760.91}{12} = 253.64 \text{ kN}$$

So, the fire protection of this beam must be determined to ensure that the calculated bearing capacity in fire situation is not lower than the applied loads for the requested fire duration.

### 5.1.4 Floor design: Zone D

In Zone D, the dimensions of the composite slab and the spans of the beams have the same values as in Zone A. However, solid beams are replaced by IPE 270+IPE 270 Angelina™ beams (see cross-section in Figure 5-23).

In consequence, only the load-bearing capacity of the unprotected beams needs to be determined.

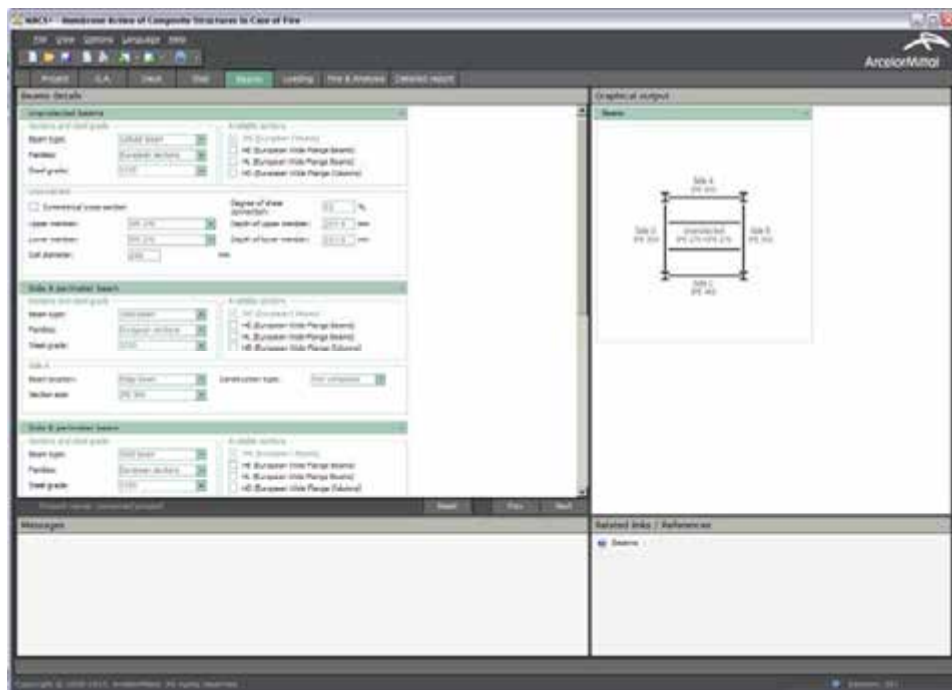


Figure 5-22 Input data using MACS+ software – Beams in Zone D



Figure 5-23 Net cross-section of Angelina beam in Zone D

Step 2: same as Zone E

Steps 3 to 8: same as Zone A

Step 9: Bearing capacity of the slab taking into account the contribution of the unprotected composite beams

The values of the section factors of the steel section are summarized in Table 5-17.

From Table 3-3, the temperatures of the steel part of the composite section are the following:

- temperature of the flanges: 941.0°C;
- temperature of the lower web: 942.2°C in Table 3-3 but taken as 941.0°C because the depth of the steel section is not greater than 500 mm;
- temperature of the upper web: 942.2°C;
- temperature of the studs (see 4.3.4.2.5 of EN 1994-1-2):  $941.0 \times 0.8 = 752.8^\circ\text{C}$ .

Table 5-17 Section factor of the unprotected composite beam in Zone D

Steel section member	$k_{sh} = 0.9 \left( \frac{0.5B_1 + t_{f1} + t_{f2} + \sqrt{h_w^2 + (B_1 - B_2)^2/4}}{H + B_1 + B_2/2 - (t_{w1} + t_{w2})/2} \right)$	$\left( \frac{A_i}{V_i} \right) (\text{m}^{-1})$	$k_{sh} \left( \frac{A_i}{V_i} \right) (\text{m}^{-1})$
Lower flange	0.711	$\frac{2(B_1 + t_{f1})}{B_1 t_{f1}} = 211$	150
Lower web		$\frac{2h_{w1} + t_{w1}}{h_{w1} t_{w1}} = 322$	229
Upper web		$\frac{2h_{w2} + t_{w2}}{h_{w2} t_{w2}} = 322$	229
Upper flange		$\frac{2(B_2 + t_{f2})}{B_2 t_{f2}} = 211$	150
With: $H$ : depth of the steel section; $h_w$ : overall depth of the web; $B_1$ : width of the lower flange; $t_{f1}$ : thickness of the lower flange; $t_{w1}$ : thickness of the lower web; $h_{w1}$ : depth of the lower web (net cross-section); $B_2$ : width of the upper flange; $t_{f2}$ : thickness of the upper flange; $t_{w2}$ : thickness of the upper web; $h_{w2}$ : depth of the upper web (net cross-section).			

The temperatures of the steel section and of the steel studs allow determining the moment resistance of the internal non composite unprotected beams. For Cellular

Beams, the contribution of the lower member is neglected as its temperature exceeds 600°C. The calculated values are given in Table 5-18.

**Table 5-18 Moment resistance for unprotected composite beams in Zone D**

Parameters	Calculated values
Effective width of the slab	$b_{eff} = \min\{9000/4; 3000\} = 2250 \text{ mm}$
Area of the upper flange $A_{f2}$	$A_{f2} = 1377 \text{ mm}^2$
Area of the upper web $A_{w2}$	$A_{w2} = 229.0 \text{ mm}^2$
Reduction factor for the steel strength properties	$k_{y,\theta} = 0.052$
Reduction factor for the stud strength properties	$k_{u,\theta} = 0.17$
Tensile force $T^+ = \sum A_i f_y k_{y,\theta} / \gamma_{M,fi,a}$	$T^+ = (1377 + 229) \times 355 \times 0.052 / 1.0 = 31.64 \text{ kN}$
Thickness of the slab in compression in fire situation $h_u = \frac{T^+}{b_{eff} f_c / \gamma_{M,fi,c}}$	$h_u = \frac{31.64}{2250 \times 25 / 1.0} = 0.562 \text{ mm}$
Connection degree of the beam at 20°C	$n_{c,20^\circ C} = 0.52$
Connection degree of the beam in fire situation $n_{c,\theta} = \frac{n_{c,20^\circ C} k_{u,\theta} \gamma_{M,\nu}}{k_{y,\theta} \gamma_{M,fi,\nu}}$	$n_{c,\theta} = \frac{0.52 \times 0.17 \times 1.25}{0.052 \times 1.0} = 2.04 > 1.0$ So full shear connection
Tensile force application point $y_T = \frac{\sum A_i y_i f_y k_{y,\theta}}{T^+ \gamma_{M,fi,a}}$	$y_T = \frac{(229 \times 6.32 + 1377 \times 25.32) \times 355 \times 0.052}{31.64 \times 1.0} = 403.66 \text{ mm}$
Compressive force application point $y_F = H + h_c - h_u / 2$	$y_F = 415 + 130 - 0.562 / 2 = 544.72 \text{ mm}$
Positive moment resistance $M_{fi,Rd} = T^+ (y_F - y_T)$	$M_{fi,Rd} = 31.64 \times (544.72 - 403.66) = 4.46 \times 10^6 \text{ Nmm} = 4.46 \text{ kNm}$
With: $h_c$ : total thickness of the slab; $\gamma_{M,fi,a}$ , $\gamma_{M,\nu}$ and $\gamma_{M,fi,\nu}$ partial safety factor for the steel profile, the steel stud in normal conditions and in fire conditions.	

Then, the bearing capacity of the slab thanks to the contribution of the unprotected composite beam can be obtained from:

$$q_{fi,Rd,ub} = \frac{8M_{fi,Rd}}{L_1^2} \frac{1+n_{ub}}{L_2} = \frac{8 \times 4.46}{9^2} \times \frac{(1+2)}{9} = 0.15 \text{ kN/m}^2$$

### Step 10: Total bearing capacity of the slab in fire conditions and verification of the fire resistance of the slab

The total bearing capacity of the slab is:

$$q_{fi,Rd} = q_{fi,Rd,slab} + q_{fi,Rd,ub} = 5.51 + 0.15 = 5.66 \text{ kN/m}^2$$

With regards to the applied load on the slab in fire situation:

$$q_{fi,Sd} = 5.98 \text{ kN/m}^2 > q_{fi,Rd} = 5.66 \text{ kN/m}^2$$

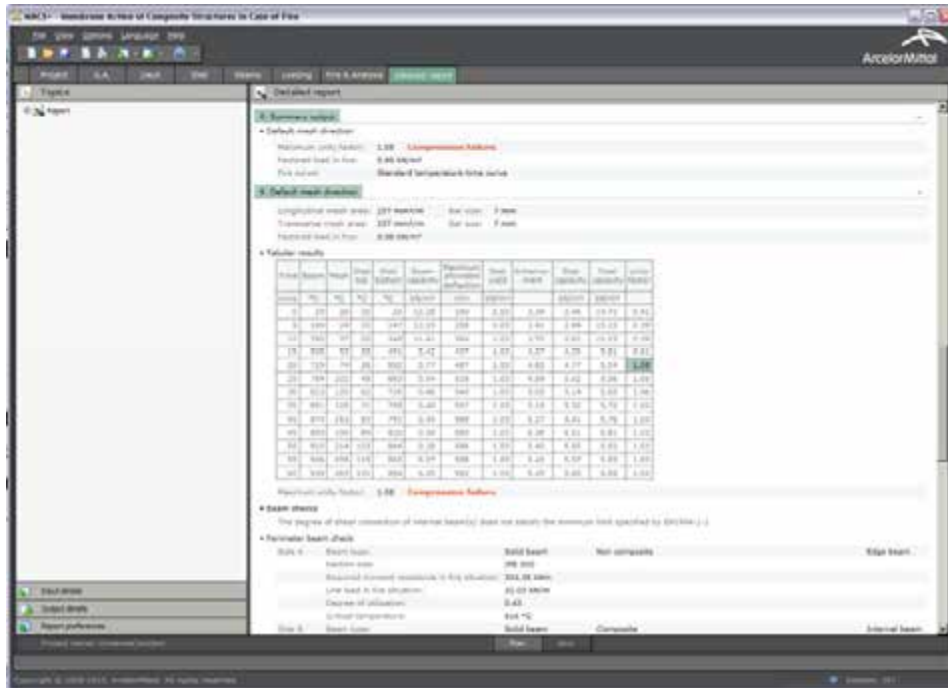


Figure 5-24 Output data using the MACS+ software – Detailed report

### Conclusion 1

In conclusion, the stability of the slab system cannot be ensured for R60 with its actual dimensions in Zone D. So, it is necessary to modify the constructive parameters.

An adequate solution could be to increase or the mesh axis distance or the mesh size.

So, the mesh axis distance was increased from 30 mm to 40 mm, modifying the welded mesh temperature from 288 °C to 362 °C.

### Step 2a

Following Table 3-4 of EN 1994-1-2, the effective steel strength for the welded steel mesh is reduced as follows:

$$f_{sy,\theta_s} = 500 \times 0,962 = 481 \text{ MPa}$$

### Step 3a: Calculation of the moment resistance of the slab section $M_{fi,0}$

For this calculation zone:

$$L_1 = 9\,000 \text{ mm (span of the secondary beams)}$$

$$L_2 = 9\,000 \text{ mm (span of the primary beams)}$$

So,  $L = \max \{L_1; L_2\} = 9\,000 \text{ mm}$  and  $\ell = \min \{L_1; L_2\} = 9\,000 \text{ mm}$ .

It can be obtained:

$$(g_0)_1 = 1 - \frac{2KA_s f_{sy,\theta_s} / \gamma_{M,fi,s}}{0.85 f_c / \gamma_{M,fi,c} d} = 1 - \frac{2 \times 1.0 \times \frac{257}{1000} \times 481 / 1.0}{0.85 \times 25 / 1.0 \times 40} = 0.709$$

$$(g_0)_2 = 1 - \frac{2A_s f_{sy,\theta_s} / \gamma_{M,f_i,s}}{0.85 f_c / \gamma_{M,f_i,c} d} = 1 - \frac{2 \times 1.0 \times \frac{257}{1000} \times 481 / 1.0}{0.85 \times 25 / 1.0 \times 40} = 0.709$$

So, the positive moment resistance of the slab section is:

$$M_{f_i,0} = A_s f_{sy,\theta_s} / \gamma_{M,f_i,s} d \frac{3 + (g_0)_2}{4} = \frac{257}{1000} \times 481 / 1.0 \times 40 \times \frac{3 + 0.709}{4} = 4\,586.51 \text{ Nmm/mm}$$

In parallel, it is also possible to determine the other necessary parameters:

$$\mu = K \frac{3 + (g_0)_1}{3 + (g_0)_2} = 1.0 \times \frac{3 + 0.709}{3 + 0.709} = 1.0$$

$$a = \frac{L}{\ell} = \frac{9\,000}{9\,000} = 1.0$$

$$n = \frac{1}{2\mu a^2} (\sqrt{3\mu a^2 + 1} - 1) = \frac{1}{2 \times 1.0 \times 1.0^2} \times (\sqrt{3 \times 1.0 \times 1.0^2 + 1} - 1) = 0.5$$

#### Step 4a: Determination of the reference bearing capacity of the slab

The reference bearing capacity of the slab can be determined from:

$$p_{f_i} = 6 \frac{M_{f_i,0}}{n^2 a^2 \ell^2} = 6 \times \frac{4\,586.51}{0.427^2 \times 1.0^2 \times 9\,000^2} = 1.359 \times 10^{-3} \text{ N/mm}^2 = 1.359 \text{ kN/m}^2$$

#### Step 5a: same as Step 5

#### Step 6a: Calculation of the parameters to determine the membrane action

The determination of the different multiplication factors for the membrane action are based on the different parameters  $\alpha_1$ ,  $\alpha_2$ ,  $\beta_1$ ,  $\beta_2$ ,  $A$ ,  $B$ ,  $C$ ,  $D$ ,  $k$  and  $b$  that need to be determined from. The values of these parameters are summarized in Table 5-19.



**Table 5-19 Parameters used for the assessment of the membrane action in Zone D**

Equation	Obtained values
$\alpha_1 = \frac{2(g_0)_1}{3+(g_0)_1}$	0.382
$\beta_1 = \frac{1-(g_0)_1}{3+(g_0)_1}$	0.078
$\alpha_2 = \frac{2(g_0)_2}{3+(g_0)_2}$	0.382
$\beta_2 = \frac{1-(g_0)_2}{3+(g_0)_2}$	0.078
$k = \frac{4na^2(1-2n)}{4n^2a^2+1} + 1$	1.0
$A = \frac{1}{2(1+k)} \left[ \frac{\ell^2}{8n} - \left( \frac{1-2n}{2n} + \frac{1}{3(1+k)} \right) \left( (nL)^2 + (\ell/2)^2 \right) \right]$	3 375 000 mm <sup>2</sup>
$B = \frac{k^2}{2(1+k)} \left[ \frac{nL^2}{2} - \frac{k}{3(1+k)} \left( (nL)^2 + (\ell/2)^2 \right) \right]$	3 375 000 mm <sup>2</sup>
$C = \frac{\ell^2}{16n} (k-1)$	0 mm <sup>2</sup>
$D = \frac{L^2}{8} (1-2n)^2$	0 mm <sup>2</sup>
$b = \min \left[ \frac{\ell^2}{8K(A+B+C-D)}, \frac{\gamma_{M,f1,s}}{kK A_s f_{sy,fb}} \left( 0.85 \frac{f_c}{\gamma_{M,f1,c}} \times 0.45d - A_s \frac{f_{sy,fb}}{\gamma_{M,f1,s}} \frac{K+1}{2} \right) \right]$	1.5

**Step 7a: Calculation of the enhancement factors for the membrane action**

The multiplication factors  $e_{1b}$ ,  $e_{2b}$ ,  $e_{1m}$  and  $e_{2m}$  can be determined:

**Table 5-20 Enhancement factors the assessment of the membrane action in Zone D**

Equation	Obtained values
$e_{1b} = 2n \left( 1 + \alpha_1 b \frac{k-1}{2} - \frac{\beta_1 b^2}{3} (k^2 - k + 1) \right) + (1-2n)(1 - \alpha_1 b - \beta_1 b^2)$	0.941
$e_{1m} = \frac{4b}{3 + (g_0)_1} \frac{w}{d} \left( (1-2n) + n \frac{2+3k-k^3}{3(1+k)^2} \right)$	3.917
$e_1 = e_{1b} + e_{1m}$	4.858
$e_{2b} = 1 + \frac{\alpha_2 b K}{2} (k-1) - \frac{\beta_2 b^2 K}{3} (k^2 - k + 1)$	0.941
$e_{2m} = \frac{4bK}{3 + (g_0)_2} \frac{w}{d} \frac{2+3k-k^3}{6(1+k)^2}$	3.917
$e_2 = e_{2b} + e_{2m}$	4.858

Then, the global enhancement factor  $e$  is determined by:

$$e = e_1 - \frac{e_1 - e_2}{1 + 2\mu\alpha^2} = 4.858 - \frac{4.858 - 4.858}{1 + 2 \times 1.0 \times 1.0^2} = 4.858$$

#### Step 8a: Total bearing capacity of the slab in fire condition

The total bearing capacity of the slab in fire condition taking into account the membrane action can be obtained from:

$$q_{fi,Rd,slab} = e \times p_{fi} = 4.858 \times 1.359 = 6.60 \text{ kN/m}^2$$

#### Step 9a: Bearing capacity of the slab taking into account the contribution of the unprotected composite beams

Same as Step 9

#### Step 10a: Total bearing capacity of the slab in fire conditions and verification of the fire resistance of the slab

The total bearing capacity of the slab is:

$$q_{fi,Rd} = q_{fi,Rd,slab} + q_{fi,Rd,ub} = 6.60 + 0.15 = 6.75 \text{ kN/m}^2$$

With regards to the applied load on the slab in fire situation:

$$q_{fi,Sd} = 5.98 \text{ kN/m}^2 < q_{fi,Rd} = 6.75 \text{ kN/m}^2$$

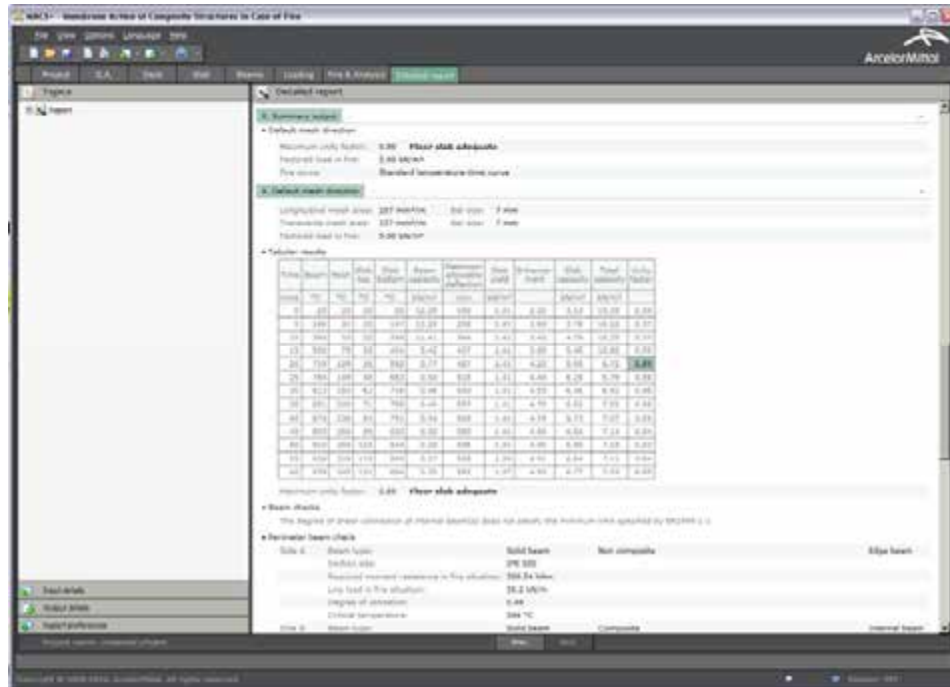


Figure 5-25 Output data using the MACS+ software – Detailed report

## Conclusion 2

In conclusion, the stability of the slab system is ensured for R60 with its actual dimensions in Zone D.

## Step 11: Applied load in fire situation for perimeter beams

The applied loads in fire situation on the secondary beams and perimeter beams of Zone D are calculated as follows:

- For the secondary perimeter beams

$$M_{fi,Sd,b,1} = \frac{q_{fi,Rd} L_1^2 L_2 - 8 \left( M_{fi,0} \left( L_2 - n_{ub} b_{eff,ub} - \sum_{i=1}^2 b_{eff,1,i} \right) + n_{ub} M_{fi,Rd} \right)}{c_M}$$

$$= \frac{6.75 \times 9^2 \times 9 - 8 \times \left[ 4.58651 \times 10^{-3} \times \left( 9 - 2 \times 2.25 - (0 + 2.25/2) \right) + 2 \times 4.5 \right]}{12}$$

$$= 393.74 \text{ kNm}$$

$$V_{fi,Sd,b,1} = \frac{4M_{fi,Sd,b,1}}{L_1} = \frac{4 \times 393.74}{9} = 175.00 \text{ kN}$$

- For the primary perimeter beams

$$M_{fi,Sd,b,2} = \frac{q_{fi,Rd} L_1 L_2^2 - 8\mu M_{fi,0} \left( L_1 - \sum_{i=1}^2 b_{eff,2,i} \right)}{c_M} = \frac{6.75 \times 9 \times 9^2 - 8 \times 1.0 \times 4586.51 \times 10^{-3} \times (9 - (9/8 + 9/8))}{12}$$

$$= 389.42 \text{ kNm}$$

$$V_{fi,Sd,b,2} = \frac{4M_{fi,Sd,b,2}}{L_2} = \frac{4 \times 389.42}{9} = 173.08 \text{ kN}$$

One of the perimeter beams of this zone is an edge beam at the façade level, it must support an additional load coming from the façade elements of 2.0 kN/m, which implies a modification of the applied load in fire condition following the next relations:

$$M_{fi,Sd,b,1} = 393.74 + \frac{2.0 \times 9^2}{8} = 414.00 \text{ kNm}$$

$$V_{fi,Sd,b,1} = 175.00 + \frac{2.0 \times 9}{2} = 184.00 \text{ kN}$$

So, the fire protection of this beam must be determined to ensure that the calculated bearing capacity in fire situation is not lower than the applied loads for the requested fire duration.

## 5.2 Reinforcement details

Since the output confirms that the load bearing capacity of zones A and B are both adequate, the ST 25C mesh provided is adequate for fire design.

This mesh has an area of 257 mm<sup>2</sup>/m in both directions and has 7 mm wires spaced at 150 mm centres in both directions.

The mesh in this example has a yield strength of 500 N/mm<sup>2</sup>. For fire design the Class of reinforcement should be specified as Class A in accordance with EN 10080.

At joints between sheets the mesh must be adequately lapped in order to ensure that its full tensile resistance can be developed in the event of a fire in the building. For the 7 mm diameter bars of the ST 25C mesh the minimum lap length required would be 300 mm, as shown in Table 3-3. In order to avoid the build up of bars at lapped joints, sheets of mesh with flying ends should be specified as shown in Figure 3-5.

Additional reinforcement in the form of U-shaped bars should be provided at the edge beams to ensure adequate tying between these beams and the composite slab.

## 5.3 Fire protection of columns

Fire protection should also be specified for all of the columns in this example. The following information should be provided when specifying the fire protection.

Fire resistance period 60 minutes

Section size HD320×158

Section Factor 63 m<sup>-1</sup> box protection heated on 4 sides

89 m<sup>-1</sup> profiled protection heated on 4 sides

Critical temperature 500°C or 80°C less than the critical temperature calculated on the basis of the EN 1993-1-2 design rules, whichever is the lower.

The applied fire protection should extend over the full height of the column, up to the underside of the composite floor slab.

## REFERENCES

1. BAILEY, C. G. and MOORE, D. B.  
The structural behaviour of steel frames with composite floor slabs subject to fire,  
Part 1: Theory  
The Structural Engineer, June 2000
2. BAILEY, C. G. and MOORE, D. B.  
The structural behaviour of steel frames with composite floor slabs subject to fire,  
Part 2: Design  
The Structural Engineer, June 2000
3. BAILEY, C. G.  
Membrane action of slab/beam composite floor systems in fire  
Engineering Structures 26
4. EN 1991-1-2:2002 Eurocode 1: Actions on structures – Part 1 2: General actions.  
Actions on structures exposed to fire  
CEN
5. EN 1993-1-2:2005 Eurocode 3. Design of steel structures. General rules. Structural  
fire design  
CEN
6. EN 1994-1-2:2005 Eurocode 4. Design of composite steel and concrete structures.  
Structural fire design  
CEN
7. VASSART O. and ZHAO B.  
Membrane action of Composite Slab in Case of Fire, Background document, Edition  
2012-1
8. The Building Regulations 2000, Approved Document B (Fire safety) 2006 Edition:  
Volume 2: Buildings other than dwelling houses, Department of Communities and  
Local Government, UK, 2006.
9. EN 1994-1-1:2004 Eurocode 4: Design of composite steel and concrete structures –  
Part 1 1: General rules and rules for buildings  
CEN
10. EN 10080:2005 Steel for the reinforcement of concrete - Weldable reinforcing steel  
– General, CEN.
11. BS 4483:2005 Steel fabric for the reinforcement of concrete. Specification. BSI
12. BS 4449:1:2005 Steel for the reinforcement of concrete. Weldable reinforcing steel.  
Bar, coil and decoiled product. Specification  
BSI
13. NF A 35-016-2 : Aciers pour béton armé – Aciers soudables à verrous – Partie 2 :  
Treillis soudés (novembre 2007) (AFNOR)
14. NF A 35-019-2 : Aciers pour béton armé – Aciers soudables à empreintes – Partie  
2 : Treillis soudés (novembre 2007) (AFNOR)
15. EN 1990:2002 Eurocode – Basis of structural design  
CEN

16. EN 1991-1-1:2003 Eurocode 1: Actions on structures – Part 1-1: General actions – Densities, self-weight, imposed loads for buildings  
CEN
17. EN13381-4 Test methods for determining the contribution to the fire resistance of structural members. Applied passive protection to steel members, CEN, (To be published 2009)
18. EN13381-8 Test methods for determining the contribution to the fire resistance of structural members. Applied reactive protection to steel members, CEN, (To be published 2009)
19. EN 1992-1-1 Design of concrete structures – Part 1-1: General rules and rule for buildings  
BSI
20. COUCHMAN, G. H , HICKS, S. J. and RACKHAM, J, W  
Composite Slabs and Beams Using Steel Decking: Best Practice for Design & Construction (2nd edition)  
SCI P300, The Steel Construction Institute, 2008
21. BS 8110-1 Structural use of concrete. Code of practice for design and construction,  
BSI, London, 1997.
22. BAILEY, C. G.  
The influence of thermal expansion of beams on the structural behaviour of columns in steel framed buildings during a fire  
Engineering Structures Vol. 22, July 2000, pp 755 768
23. EN 1993-1-8:2005 Eurocode 3: Design of steel structures – Design of joints  
BSI
24. Brown, D.G. Steel building design: Simple connections. SCI P358, The Steel Construction Institute, (To be published 2009)
25. Initial sizing of simple end plate connections  
Access-steel document SN013a  
Initial sizing of fin plate connections  
Access-steel document SN016a  
[www.access-steel.com](http://www.access-steel.com)
26. Shear resistance of a simple end plate connection  
Access-steel document SN014a and SN015a  
Tying resistance of a simple end plate connection  
Access-steel document SN015a  
[www.access-steel.com](http://www.access-steel.com)
27. Shear resistance of a fin plate connection  
Access-steel document SN017a  
Tying resistance of a fin plate connection  
Access-steel document SN018a  
[www.access-steel.com](http://www.access-steel.com)
28. LAWSON, R. M.  
Enhancement of fire resistance of beams by beam to column connections  
The Steel Construction Institute, 1990
29. EN 1363-1:1999 Fire resistance tests. General requirements  
CEN

- 30. EN 1365 Fire resistance tests for load-bearing elements.
    - EN 1365-1:1999 Walls
    - EN 1365-2:2000 Floors and roofs
    - EN 1365-3:2000 Beams
    - EN 1365-4:1999 Columns
- CEN



**MACS\***  
**Membrane Action of Composite Structures**  
**in Case of Fire**

*Design Guide*

Version 2012-1



## ANNEX III

### Engineering Background





Research Fund  
for Coal & Steel

# MAFCS<sup>+</sup>

Membrane Action of Composite Structures  
in Case of Fire

## Engineering Background

O. Vassart  
B. Zhao



ArcelorMittal

ctim

# FOREWORD

This project has been funded with support from the European Commission, Research Fund for Coal and Steel.

This publication reflects the views only of the author, and the Commission cannot be held responsible for any use which may be made of the information contained therein.

The publication has been produced as a result of different research projects:

- The RFCS Project FICEB+
- The RFCS Project COSSFIRE
- The project Leonardo Da Vinci ‘Fire Resistance Assessment of Partially Protected Composite Floors’ (FRACOF).
- A former project sponsored jointly by ArcelorMittal and CTICM and executed by a partnership of CTICM and SCI.

The simple design method was initially developed as the result of large scale fire testing conducted on a multi-storey steel framed building at the Building Research Establishment’s Cardington test facility in the UK. Much of the theoretical basis of the design method has been in existence since the late 1950’s, following studies of the structural behaviour of reinforcement concrete slabs at room temperature. The first version of the simple design method was available in the SCI Design Guide P288 ‘Fire Safe Design: A new approach to Multi-story Steel Framed Buildings’, 2 Ed.

Although the application of the method to fire resistance design is relatively new the engineering basis of the method is well established.

The simple design method was implemented in a software format by SCI in 2000 and an updated version was released in 2006, following improvements to the simple design method.

Valuable contributions were received from:

- Mary Brettle The Steel Construction Institute
- Ian Sims The Steel Construction Institute
- Louis Guy Cajot ArcelorMittal
- Renata Obiala ArcelorMittal
- Mohsen Roosefid CTICM
- Gisèle Bihina CTICM.



# Contents

	<b>Page No.</b>
1 INTRODUCTION	1
2 CARDINGTON FIRE TEST PROGRAM	2
2.1 Research programme	2
2.2 Test 1: Restrained beam	3
2.3 Test 2: Plane frame	5
2.4 Test 3: Corner	7
2.5 Test 4: Corner	9
2.6 Test 5: Large compartment	10
2.7 Test 6: The office demonstration test	11
2.8 Test 7: Central compartment	15
2.9 General comments on observed behaviour	18
3 CAR PARK FIRE TESTS, FRANCE	19
4 EVIDENCE FROM ACCIDENTAL FIRES AND OTHER COUNTRIES	25
4.1 Broadgate	25
4.2 Churchill Plaza building, Basingstoke	27
4.3 Australian fire tests	28
4.3.1 William Street fire tests and design approach	28
4.3.2 Collins Street fire tests	30
4.3.3 Conclusions from Australian research	31
4.4 German fire test	31
4.5 Experimental work at room temperature	32
4.6 Experimental work at elevated temperature	33
5 SIMPLE DESIGN METHOD	34
5.1 Introduction to yield line theory and membrane action	34
5.1.1 Slab with full in-plane restraint	35
5.1.2 Slab with no in-plane restraint	36
5.1.3 Effect of membrane stresses on yield lines	37
5.2 Calculation of resistance of composite floors in accordance with the simple design method	39
5.2.1 Calculation of resistance	39
5.2.2 Derivation of an expression for parameter k	42
5.2.3 Derivation of an expression for parameter b	44
5.2.4 Membrane forces	46
5.3 Compressive failure of concrete	52
6 DEVELOPMENT OF DESIGN GUIDANCE	54
6.1 Design assumptions	54
6.2 Failure criterion	55
6.2.1 Slab deflection	56
6.2.1.1 Thermal effects	56
6.2.1.2 Mechanical strains in the reinforcement	57
6.2.1.3 Calculation of slab deflection to allow the calculation of membrane forces	58
6.2.2 Calibration against Cardington fire tests	58
6.3 Design methodology	60
6.3.1 Calculation of load bearing capacity for the slab	61
6.3.2 Calculation of load bearing capacity for unprotected beams	61
6.4 Design of fire resisting perimeter beams	62
6.4.1 Unprotected beams with edge beams on both sides	64
6.4.1.1 Yield line parallel to unprotected beams	64
6.4.1.2 Yield line perpendicular to unprotected beams	65



6.4.2	Unprotected beams with an edge beam on one side	66
6.4.2.1	Yield line parallel to unprotected beams	66
6.4.2.2	Yield line perpendicular to unprotected beams	68
6.4.3	Floor zone without edge beams	69
6.4.4	Design of edge beams	69
6.5	Thermal Analysis	69
6.5.1	Configuration Factors	71
6.5.2	Material Properties	72
6.5.3	Internal heat transfer by conduction	73
6.5.4	Design temperatures for unprotected steel beams	74
7	FIRE RESISTANCE TEST OF A FULL SCALE COMPOSITE FLOOR SYSTEM	76
7.1	Scope	76
7.2	FRACOF Test	76
7.2.1	Test specimen	76
7.2.2	Test methodology	80
7.2.3	Results	83
7.2.3.1	Temperature variation in structure	83
7.2.3.2	Displacement variation of the structural members	86
7.2.3.3	Behaviour of composite slab observed during the test	88
7.2.4	Comments on the test results	90
7.3	COSSFIRE Fire test programme	91
7.3.1	Test specimen	91
7.3.2	Measurement of test results	93
7.3.3	Principal experimental results	95
7.3.4	Observation of the fire tests	98
7.4	Full -scale fire test on a composite floor slab incorporating long span cellular steel beams.	102
7.4.1	Test specimen	102
7.4.2	Design Loads	105
7.4.3	Design of the Fire	105
7.4.4	Instrumentation	106
7.4.5	Beam/Slab Deflection	107
7.4.6	Membrane Action in Floor Slabs	114
7.4.7	Conclusions	114
8	PARAMETRIC NUMERICAL STUDIES	116
8.1	Scope	116
8.2	Verification of ANSYS numerical model against FRACOF test	116
8.2.1	General	116
8.2.2	Structural Analysis	116
8.2.3	Heat transfer analysis	117
8.2.4	Mechanical behaviour of structural members	119
8.3	Verification of SAFIR numerical model against fire tests	121
8.3.1	General	121
8.3.2	SAFIR Vs FRACOF test	121
8.3.2.1	Fire load	121
8.3.2.2	Thermal analyses : Numerical models and main results	121
8.3.2.3	Structural analysis	124
8.3.3	SAFIR Vs COSSFIRE test	126
8.3.3.1	Fire load	126
8.3.3.2	Thermal analyses : Numerical models and main results	126
8.3.3.3	Structural analysis	129
8.3.4	SAFIR Vs FICEB test	131
8.3.4.1	Fire load	131
8.3.4.2	Thermal analyses : Numerical models and main results	132
8.3.4.3	Structural analysis	135

8.4	Parametric numerical study using standard temperature-time curve	136
8.4.1	Input data for parametric study	136
8.4.2	Input data for parametric study	143
8.4.2.1	Maximum deflection of floor	143
8.4.2.2	Elongation of the steel reinforcing mesh	147
8.5	Conclusion	153
9	REFERENCES	154

# SUMMARY

Large-scale fire tests conducted in a number of countries and observations of actual building fires have shown that the fire performance of composite steel framed buildings is much better than is indicated by fire resistance tests on isolated elements. It is clear that there are large reserves of fire resistance in modern steel-framed buildings and that standard fire resistance tests on single unrestrained members do not provide a satisfactory indicator of the performance of such structures.

As a result of observation and analysis of the BRE Cardington large-scale building fire test programme carried out during 1995 and 1996, a simple design model on the basis of membrane action of steel and concrete composite floor has been developed which allows designers to take advantage of the inherent fire resistance of a composite floor plate without the need to resort to complex finite element analysis of whole building behaviour. However, because of its specific feature, this innovative design concept remains still unfamiliar to most of engineers and authorities. In consequence, this technical document is established to provide all necessary background information in order to assist the reader to understand easily the basis of the design recommendations of above simple design model.

In this technical document, the theoretical basis of the simple design method and its development for application to fire engineering is described. An important review of existing relevant fire tests carried out in full scale buildings around the world is described and the corresponding test data are summarized as well in this document. Information is also included on observations of the behaviour of multi-storey buildings in accidental fires. On the other hand, the document gives detailed explanation of the new large-scale fire tests of composite floor systems conducted under long duration ISO fire which provides more evidences about the validity of the simple design model. The conservativeness of the simple design model is also clearly illustrated through the comparison with the parametric numerical study conducted with help of advanced calculation models.

# 1 INTRODUCTION

Large-scale fire tests conducted in a number of countries and observations of actual building fires have shown that the fire performance of composite steel framed buildings with composite floors (concrete slabs connected to steel beams by means of headed studs) is much better than indicated by standard fire resistance tests on composite slabs or composite beams as isolated structural elements. It is clear that there are large reserves of fire resistance in modern steel-framed buildings and that standard fire resistance tests on single unrestrained members do not provide a satisfactory indicator of the real performance of such structures.

Analysis reveals that this excellent fire performance is due to the development of tensile membrane action in the reinforced concrete slab and the catenary action of steel beams.

As a result of the above observation and analysis, a new fire design concept for modern multi-storey steel-framed buildings was developed in the UK. Design guidance and software design tools for composite floor plates based on this method were first published in 2000. Many buildings in the UK have since benefited from the application of the simple design method, resulting in reduced fire protection costs<sup>(1)</sup>.

The design concept allows designers to take advantage of whole building behaviour, allowing some members to remain unprotected while maintaining the safety levels expected from fully fire-protected structures. The design method allows the fire resistance of partially protected composite floors to be assessed for natural fire or standard fire exposure. The latter is of particular interest because it means that the design concept may be applied by design engineers without the need for specialist fire engineering knowledge.

Although widely used in the UK, the enhancement of fire resistance provided by membrane and catenary actions is still a very new concept for the majority of engineers and regulatory authorities within Europe. To inform these potential user groups, this document aims to provide a solid technical support package for this design concept, comprising:

- a review of the evidence available about the performance of composite structures in large-scale fire tests and accidental building fires;
- a detailed explanation of the theoretical basis of the simple design model for composite floor systems supported by plain profiles and by cellular beams;
- a description of the fundamental assumptions adopted in the simple design model for fire resistance assessment of steel and concrete composite floor systems;
- details of a demonstration fire test on a full scale steel and concrete composite floor system using the standard time-temperature curve in accordance with EN 1365-2, for a duration of more than 120 minutes
- a detailed numerical parametric investigation to verify the output from the simple design model.

## 2 CARDINGTON FIRE TEST PROGRAM

### 2.1 Research programme

In September 1996, a programme of fire tests was completed in the UK at the Building Research Establishment's Cardington Laboratory. The tests were carried out on an eight-storey composite steel-framed building that had been designed and constructed as a typical multi-storey office building. The purpose of the tests was to investigate the behaviour of a real structure under real fire conditions and to collect data that would allow computer programs for the analysis of structures in fire to be verified.

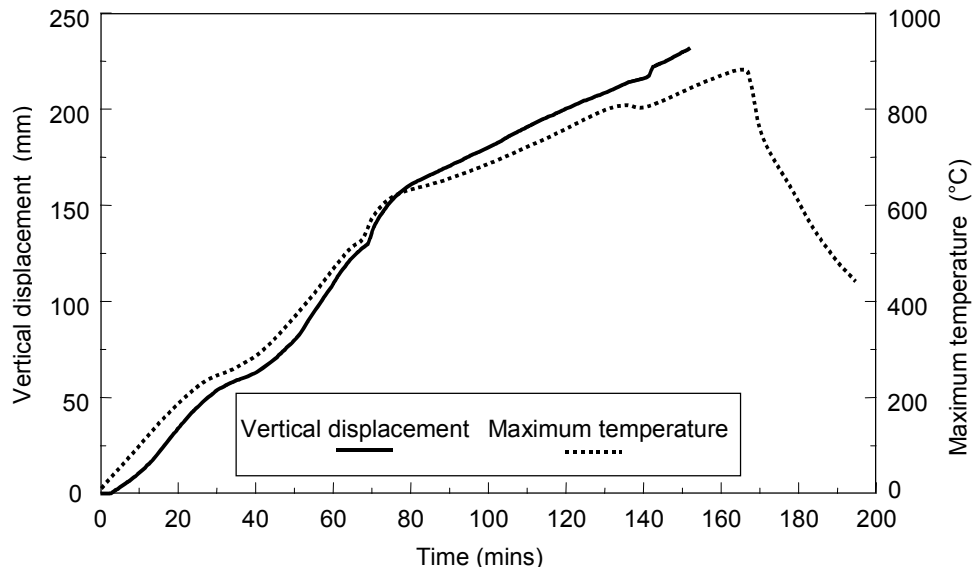


**Figure 2.1** *Cardington test building prior to concreting of the floors*

The test building (see Figure 2.1.) was designed to be a typical example of both the type of braced structure and the load levels that are commonly found in the UK. In plan, the building covered an area of 21 m × 45 m and had an overall height of 33 m. The beams were designed as simply supported, acting compositely with a 130 mm floor slab. Normally, a building of this type would be required to have 90 minutes fire resistance. Fin-plates were used for the beam-to-beam connections and flexible end plates for the beam-to-column connections. The structure was loaded using sandbags distributed over each floor to simulate typical office loading.

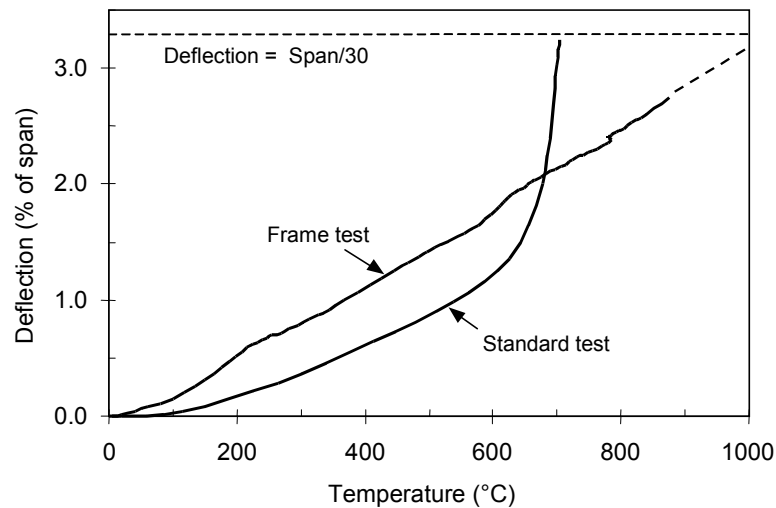
There were two projects in the research programme. One project was funded by Corus (formerly British Steel) and the European Coal and Steel Community (ECSC); the other was funded by the UK Government via the Building Research Establishment (BRE). Other organisations involved in the research programme included Sheffield University, TNO (The Netherlands), CTICM (France) and The Steel Construction Institute. Fire tests took place between January 1995 and July





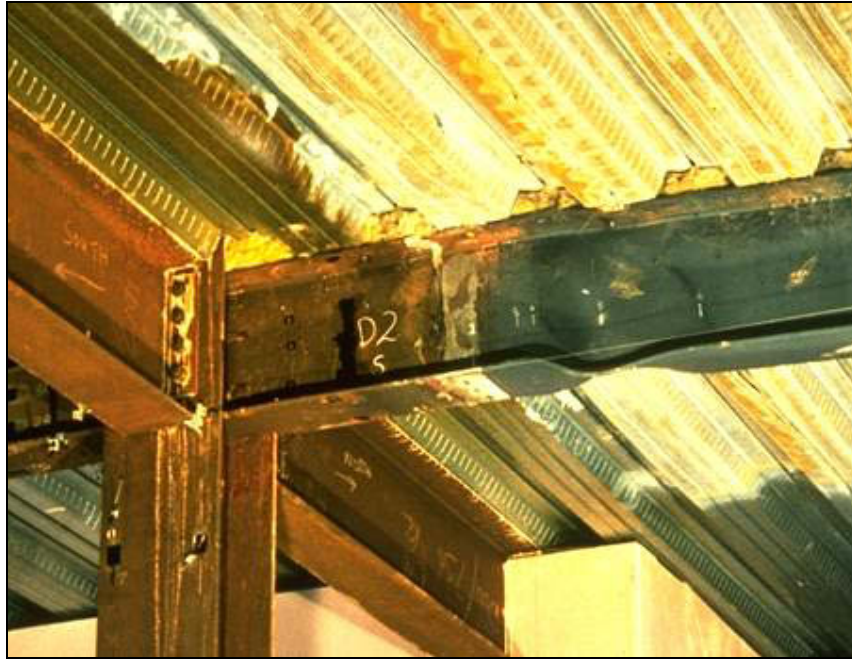
**Figure 2.3** *Central displacement and maximum temperature in restrained beam test*

The contrast between the behaviour of this beam and a similar unprotected beam tested in a standard fire test under a similar load<sup>(5)</sup> is shown in Figure 2.4. The ‘runaway’ displacement typical of simply supported beams in the standard test did not occur to the beam in the building frame even though, at a temperature of about 900°C, structural steel retains only about 6% of its yield strength at ambient temperature.



**Figure 2.4** *Central displacement and maximum temperature in standard fire test and restrained beam test*

During the test, local buckling occurred at both ends of the test beam, just inside the furnace wall (see Figure 2.5).



**Figure 2.5** *Flange buckling in restrained beam*

Visual inspection of the beam after the test showed that the end-plate connection at both ends of the beam had fractured near, but outside, the heat-affected zone of the weld on one side of the beam. This was caused by thermal contraction of the beam during cooling, which generated very high tensile forces. Although the plate sheared down one side, this mechanism relieved the induced tensile strains, with the plate on the other side of the beam retaining its integrity and thus providing shear capacity to the beam. The fracture of the plate can be identified from the strain gauge readings, which indicate that, during cooling, the crack progressed over a period of time rather than by a sudden fracture.

### **2.3 Test 2: Plane frame**

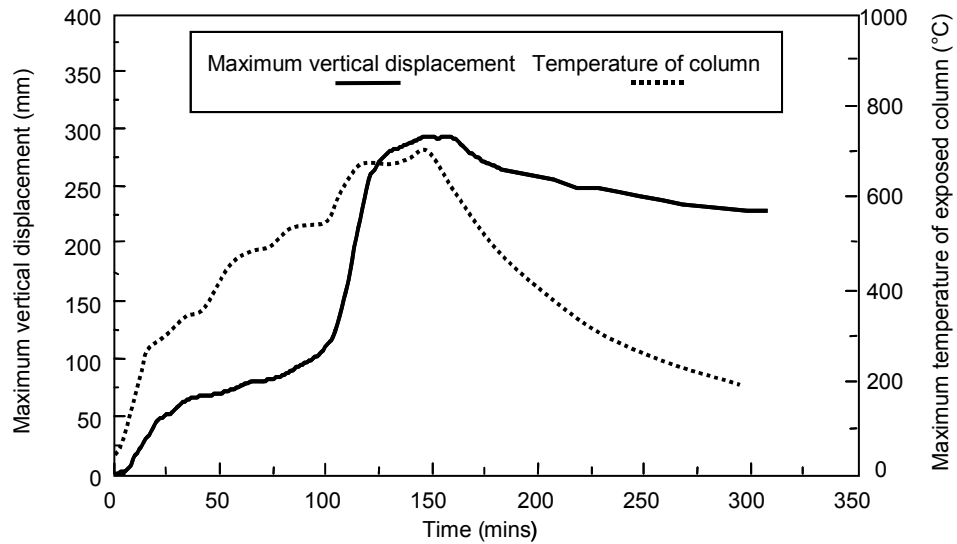
This test was carried out on a plane frame consisting of four columns and three primary beams spanning across the width of the building on gridline B, as shown in Figure 2.2.

A gas-fired furnace 21 m long  $\times$  2.5 m wide  $\times$  4.0 m high was constructed using blockwork across the full width of the building.

The primary and secondary beams, together with the underside of the composite floor, were left unprotected. The columns were fire protected to a height at which a suspended ceiling might be installed (although no such ceiling was present). This resulted in the top 800 mm of the columns, which incorporated the connections, being unprotected.

The rate of vertical displacement at midspan of the 9 m span steel beam increased rapidly between approximately 110 and 125 minutes (see Figure 2.6). This was caused by vertical displacements of its supporting columns. The exposed areas of the internal columns squashed by approximately 180 mm (see Figure 2.7). The temperature of the exposed part of the column was approximately 670°C when local buckling occurred.





**Figure 2.6** Maximum vertical displacement of central 9 m beam and temperature of exposed top section of internal column

The reduction in column height which resulted from this local buckling caused a permanent deformation of approximately 180 mm in all the floors above the fire compartment. To avoid this behaviour, columns in later tests were protected over their full height.



**Figure 2.7** Squashed column head following the test

On both sides of the primary beams, the secondary beams were each heated over a length of approximately 1.0 m. After the test, investigation showed that many of the bolts in the fin-plate connections had sheared (see Figure 2.8). The bolts had only sheared on one side of the primary beam. In a similar manner to the fracturing of the plate in Test 1, the bolts sheared due to thermal contraction of the beam during cooling. The thermal contraction generated very high tensile forces, which were relieved once the bolts sheared in the fin-plate on one side of the primary beam.



**Figure 2.8** *Fin-plate connection following test*

## **2.4 Test 3: Corner**

The objective of this test was to investigate the behaviour of a complete floor system and, in particular, the role of ‘bridging’ or membrane action of the floor in providing alternative load paths as the supporting beams lose strength. Using concrete blockwork, a compartment 10 m wide  $\times$  7.6 m deep was constructed in one corner of the first floor of the building (E2/F1).

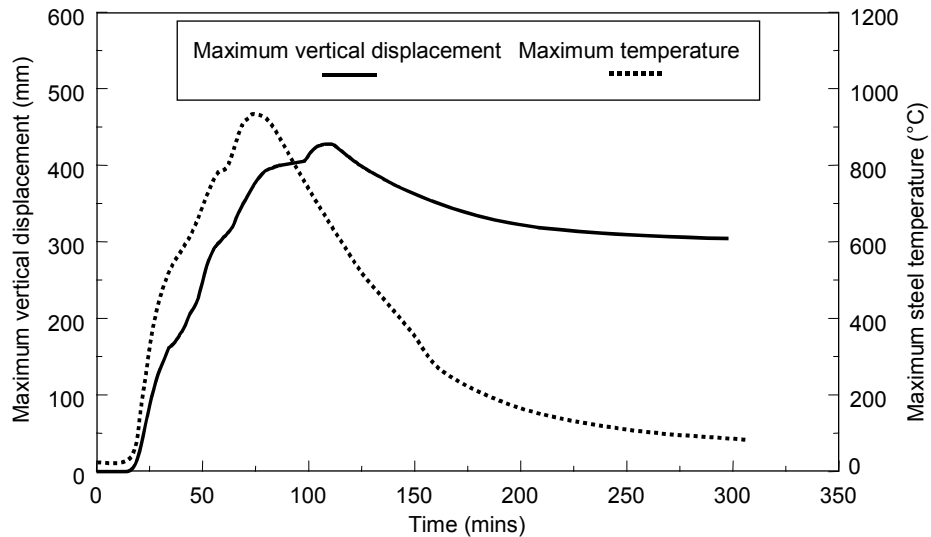
To ensure that the compartment walls did not contribute to supporting the applied loads, all the restraints and ties in the gable wall and the top layer of blockwork were removed. The mineral fibre board in the expansion joints was replaced with a ceramic blanket.

Similarly, the wind posts on the external wall were detached from the edge beam above the compartment opening, to ensure that this edge beam did not have additional support.

All columns, beam-to-column connections and edge beams were fire protected.

The fire load was 45 kg/m<sup>2</sup>, in the form of timber cribs. This fire load is quite high and is equivalent to the 95% fractile loading for office buildings. Fire safety engineering calculations are normally based on the 80% fractile loading. Ventilation was provided by a single 6.6 m wide  $\times$  1.8 m high opening. The peak atmospheric temperature recorded in the compartment was 1071°C.

The maximum steel temperature was 1014°C, recorded on the inner beam on gridline 2 (E2/F2). The maximum vertical displacement of 428 mm (just less than span/20) occurred at the centre of the secondary beam, which had a peak temperature of 954°C. On cooling, this beam recovered to a permanent displacement of 296 mm. The variations of deflection and temperature with time are shown in Figure 2.9.



**Figure 2.9** *Maximum vertical displacement and temperature of secondary beam*

All the combustible material within the compartment was consumed by the fire. The structure behaved extremely well, with no signs of collapse (see Figure 2.10).

Buckling occurred in the proximity of some of the beam-to-column connections but, unlike Test 2, bolts in the connections did not suffer shear failure. This might indicate either that the high tensile forces did not develop or that the connection had adequate ductility to cope with the tensile displacements.



**Figure 2.10** *View of structure following test*

## 2.5 Test 4: Corner

This test was carried out on the second floor, in a corner bay (E4/F3) with an area of 54 m<sup>2</sup>. The internal boundaries of the compartment on gridlines E and 3 were constructed using steel stud partitions with fire resistant board. The stud partition was specified to have 120 minutes fire resistance, with a deflection head of 15 mm. An existing full-height blockwork wall formed the boundary on the gable wall on gridline F; the outer wall, gridline 4, was glazed above 1 metre of blockwork. The compartment was totally enclosed, with all windows and doors closed. The columns were fire protected up to the underside of the floor slab, including the connections but, unlike Test 3, the lintel beam (E4/F4) was unprotected and the wind posts above it remained connected. Twelve timber cribs were used to give a fire load of 40 kg/m<sup>2</sup>.

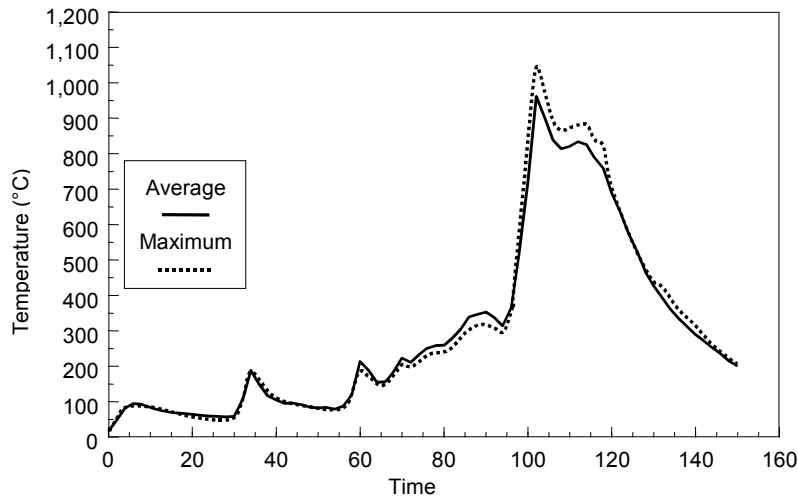
The development of the fire was largely influenced by the lack of oxygen within the compartment. After an initial rise in temperature, the fire died down and continued to smoulder until, after 55 minutes, the fire brigade intervened to vent the compartment by removal of a single pane of glazing. This resulted in a small increase in temperature followed by a decrease. A second pane, immediately above the first, was broken at 64 minutes and temperatures began to rise steadily; between 94 and 100 minutes the remaining panes shattered. This initiated a sharp increase in temperature that continued as the fire developed. The maximum recorded atmospheric temperature in the centre of the compartment was 1051°C after 102 minutes (see Figure 2.11). The maximum steel temperature of 903°C was recorded after 114 minutes in the bottom flange of the central secondary beam.

The maximum slab displacement was 269 mm and occurred in the centre of the compartment after 130 minutes. This recovered to 160 mm after the fire.

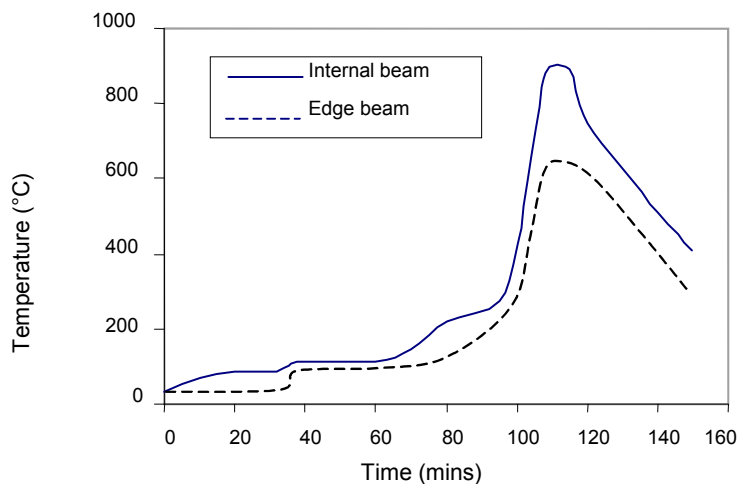
The unprotected edge beam on gridline 4 was observed during the test to be completely engulfed in fire. However, the maximum temperature of this beam was 680°C, which is relatively low compared to that of the internal beams, as shown by Figure 2.12. The corresponding maximum displacement of the edge beam was 52 mm, recorded after 114 minutes. This small displacement was attributed to the additional support provided by wind posts above the compartment, which acted in tension during the test.

The internal compartment walls were constructed directly under unprotected beams and performed well. Their integrity was maintained for the duration of the test. On removal of the wall, it could be seen that one of the beams had distortionally buckled over most of its length. This was caused by the high thermal gradient through the cross section of the beam (caused by the positioning of the compartment wall), together with high restraint to thermal expansion.

No local buckling occurred in any of the beams, and the connections showed none of the characteristic signs of high tensile forces that were seen on cooling in the other tests.



**Figure 2.11** Furnace gas temperatures recorded in Test 4



**Figure 2.12** Maximum flange temperature of internal beam and edge beam

## 2.6 Test 5: Large compartment

This test was carried out between the second and third floor, with the fire compartment extending over the full width of the building, covering an area of 340 m<sup>2</sup>.

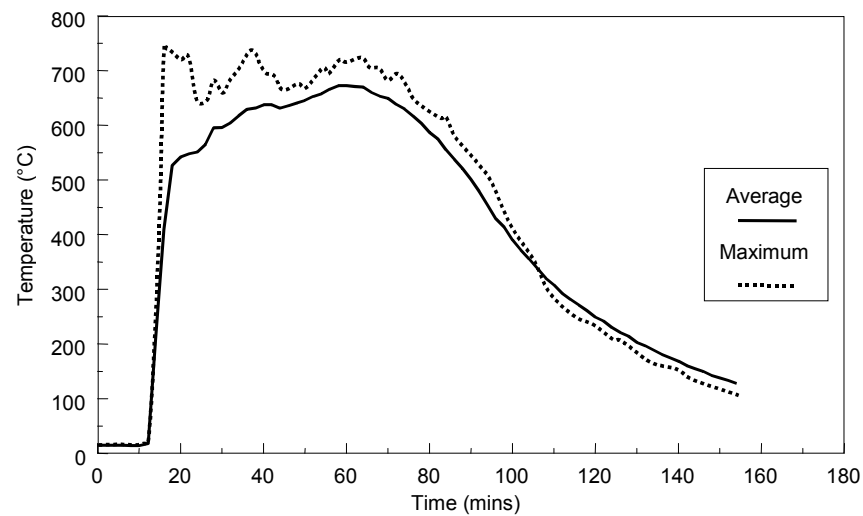
The fire load of 40 kg/m<sup>2</sup> was provided by timber cribs arranged uniformly over the floor area. The compartment was constructed by erecting a fire resistant stud and plasterboard wall across the full width of the building and by constructing additional protection to the lift shaft. Double glazing was installed on two sides of the building, but the middle third of the glazing on both sides of the building was left open. All the steel beams, including the edge beams, were left unprotected. The internal and external columns were protected up to and including the connections.

The ventilation condition governed the severity of the fire. There was an initial rapid rise in temperature as the glazing was destroyed, creating large openings on both sides of the building. The large ventilation area in two opposite sides of the compartment gave rise to a fire of long duration but lower than expected

temperatures. The maximum recorded atmosphere temperature was 746°C, with a maximum steel temperature of 691°C, recorded at the centre of the compartment. The recorded atmospheric temperatures in the compartment are shown by Figure 2.13. The structure towards the end of the fire is shown in Figure 2.14.

The maximum slab displacement reached a value of 557 mm. This recovered to 481 mm when the structure cooled.

Extensive local buckling occurred in the proximity of the beam-to-beam connections. On cooling, a number of the end-plate connections fractured down one side. In one instance the web detached itself from the end-plate such that the steel-to-steel connection had no shear capacity. This caused large cracks within the composite floor above this connection, but no collapse occurred, with the beam shear being carried by the composite floor slab.



**Figure 2.13** Maximum and average recorded atmosphere temperature



**Figure 2.14** Deformed structure during fire

## 2.7 Test 6: The office demonstration test

The aim of this test was to demonstrate structural behaviour in a realistic fire scenario.

A compartment 18 m wide and up to 10 m deep with a floor area of 135 m<sup>2</sup>, was constructed using concrete blockwork. The compartment represented an open plan office and contained a series of work-stations consisting of modern day furnishings, computers and filing systems (see Figure 2.15). The test conditions were set to create a very severe fire by incorporating additional wood/plastic cribs to create a total fire load of 46 kg/m<sup>2</sup> (less than 5% of offices would exceed this level) and by restricting the window area to the minimum allowed by regulations for office buildings. The fire load was made up of 69% wood, 20% plastic and 11% paper. The total area of windows was 25.6 m<sup>2</sup> (19% of the floor area) and the centre portion of each window, totalling 11.3 m<sup>2</sup>, was left unglazed to create the most pessimistic ventilation conditions at the start of the test.



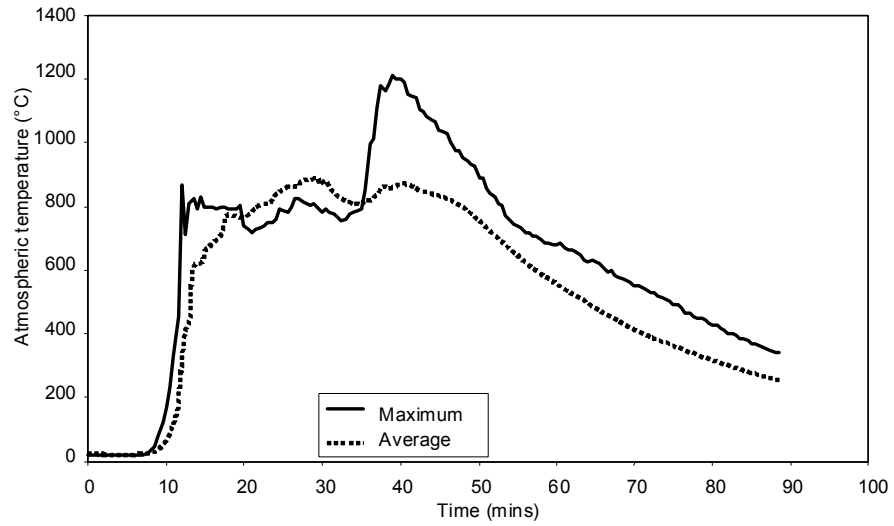
**Figure 2.15** Office before test

Within the compartment, the columns and the beam-to-column connections were fire protected. Both the primary and secondary beams, including all the beam-to-beam connections, remained totally exposed.

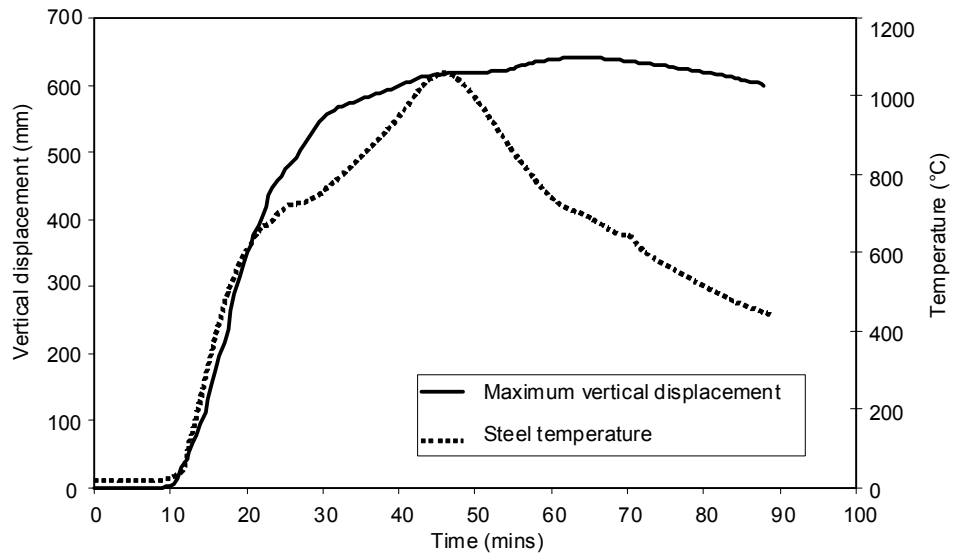
The wind posts were left connected to the edge beams, and thus gave some support during the fire.

The maximum atmospheric temperature was 1213°C and the maximum average temperature was approximately 900°C, as shown by Figure 2.16. The maximum temperature of the unprotected steel was 1150°C. The maximum vertical displacement was 640 mm, which recovered to a permanent deformation of 540 mm on cooling (see Figure 2.17). The peak temperature of the lintel beams, above the windows, was 813°C. All the combustible material in the compartment was completely burnt, including the contents of the filing cabinets. Towards the back of the compartment, the floor slab deflected and rested on the blockwork wall. The structure showed no signs of failure.

An external view of the fire near its peak is shown in Figure 2.18. The structure following the fire is shown in Figure 2.19 and Figure 2.20. Figure 2.19 shows a general view of the burned out compartment and Figure 2.20 shows the head of one of the columns. During the test, the floor slab cracked around one of the column heads, as shown in Figure 2.21. These cracks occurred during the cooling phase, possibly due to a partial failure of the steel beam to column connection in this location. Investigation of the slab after the test showed that the reinforcement had not been lapped correctly and that, in this area, adjacent sheets of mesh were simply butted together. This illustrates the importance of using full tension laps between adjacent sheets of mesh reinforcement.



**Figure 2.16** Measured atmosphere temperature



**Figure 2.17** Maximum steel temperature and vertical displacement





**Figure 2.18** *External view of fire*



**Figure 2.19** *Measured atmosphere temperature in the compartment*



**Figure 2.20** *Column head showing buckled beams*



**Figure 2.21** *Cracked floor slab in region of non-overlapped mesh*

## **2.8 Test 7: Central compartment**

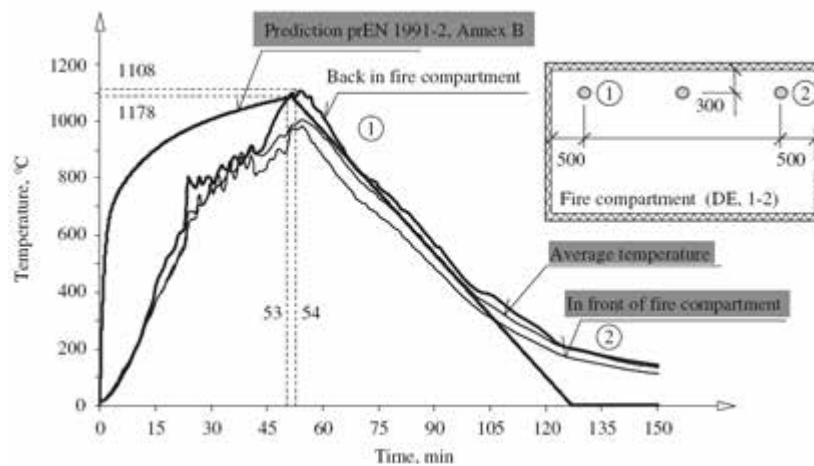
The test was carried out in a centrally located compartment on the fourth floor of the building, which is 11 m wide and 7 m deep. The steel structure exposed to fire consists of two primary beams in 356x171x51 UB, two columns in 305x305x198 UC and 305x305x137 UC, and three secondary beams in 305x165x40 UB, respectively.

The fire load was provided by wood cribs of 40 kg/m<sup>2</sup> covering whole compartment floor area. The ventilation was provided by a 1.27m high and 9m long opening on the façade.

About 130 thermocouples were disposed in the compartment and at various locations along the beams in both the steel profile and the composite slabs, as well as in the steel connections (fin plate and end plate). An additional 14 thermocouples were also disposed in the protected columns. In order to measure the distribution of internal forces, 2 different types of strain gauges were used: high

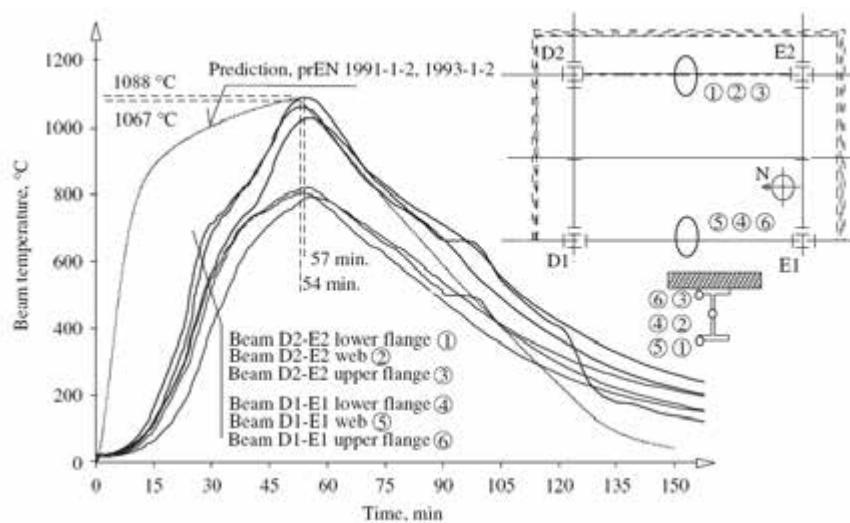
temperature ones in the connection and ambient temperature ones in the protected column and un-exposed elements. As for the instrumentation of the deflected shape of the floor and of the main structural members, a total of 37 displacement transducers were used to measure the deformation of the concrete slab and the horizontal movement of the columns. In addition, 10 video cameras and two thermo imaging cameras recorded the fire and smoke development, the structural deformations and the temperature distribution with time.

The recorded temperatures in different places of the compartment are compared with the parametric curve presented in prEN 1991-2, Annex B <sup>(37)</sup> (see figure 2.22). The maximum recorded compartment temperature was 1107.8 °C after 54 minutes of fire.



**Figure 2.22** *Compartment following fire*

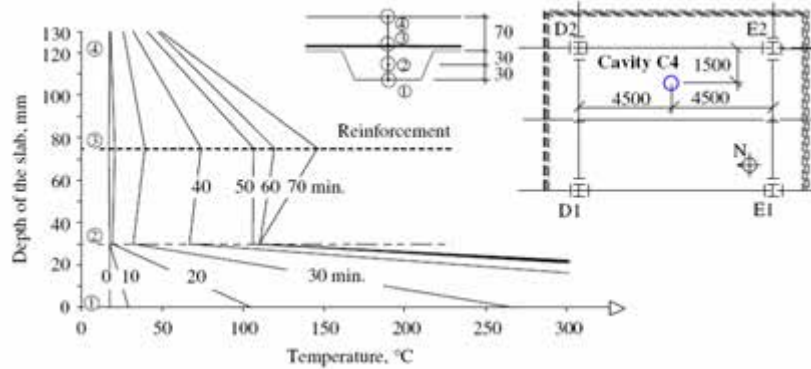
As far as the heating of steel beams is concerned, the unprotected steel beams were heated up to around 1087.5 °C which occurred after 57 min of fire on the bottom flange of the steel beam D2-E2 in the middle of the section (see figure 2.23). The maximum temperature recorded at the joints was around 200 °C.



**Figure 2.23** *Temperatures variations in steel beams*

A summary of the temperatures recorded in the composite slab is shown in 2.24 for temperatures in the reinforcement over the rib. It can be found that the maximum

heating measured at the unexposed side of the composite slab was less than 100 °C which was in accordance with the insulation criteria.



**Figure 2.24** Composite floor temperature variation

As far as the global deflection of the floor is concerned, the maximum deflections were about 1200 mm. Despite the occurrence of such an important deflection, the predicted collapse of the floor was not reached, as shown in Figure 2.25. During the cooling phase, the deflection recovery of the floor was about 925 mm.



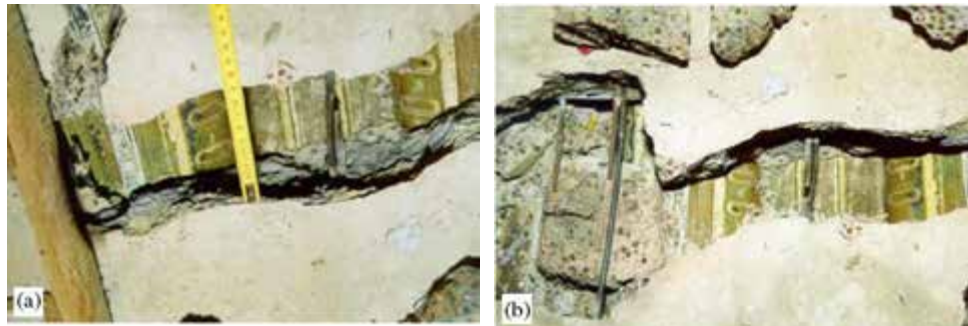
**Figure 2.25** View of the floor after the test

Buckling occurred in the lower beam flange and web adjacent to the joints during the heating phase after about 23 min of fire (see figure 2.26). This local buckling is caused by restraint to thermal expansion provided by the surrounding structure. In addition, the formation of a flexural plastic hinge was occurred in the beam's cross section adjacent to the protected zone due to the restraint to thermal elongation provided by the adjacent protected section.



**Figure 2.26** *Various deformed steel beams*

Figure 2.27 shows the open cracks in the concrete slab around one of the column heads. This crack developed along a line of mesh reinforcement overlap without adequate attachment.



**Figure 2.27** *Cracked floor slab around one of the column heads*

## **2.9 General comments on observed behaviour**

In all tests, the structure performed very well and overall structural stability was maintained.

The performance of the whole building in fire is manifestly very different from the behaviour of single unrestrained members in the standard fire test. It is clear that there are interactions and changes in load-carrying mechanisms in real structures that dominate the way they behave; it is entirely beyond the scope of the simple standard fire test to reproduce or assess such effects.

The Cardington tests demonstrated that modern steel frames acting compositely with steel deck floor slabs have a coherence that provides a resistance to fire far greater than that normally assumed. This confirms evidence from other sources.

### 3 CAR PARK FIRE TESTS, FRANCE

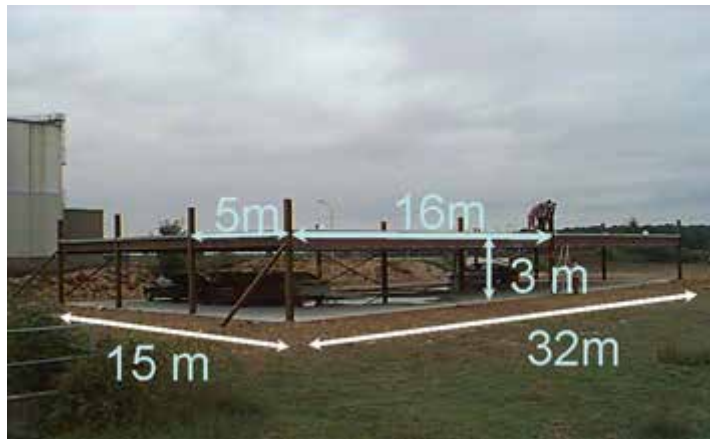
Between 1998 and 2001, as part of an ECSC funded project, fire tests were performed on an open car park with a composite steel and concrete structure.

A single storey composite steel-framed open car park was constructed specifically for full scale fire tests. The floor of the car park occupied an area of  $32 \times 16 \text{ m}^2$ , which is equivalent to a 48 space car park and the storey height was 3 m (see Figure 3.1).

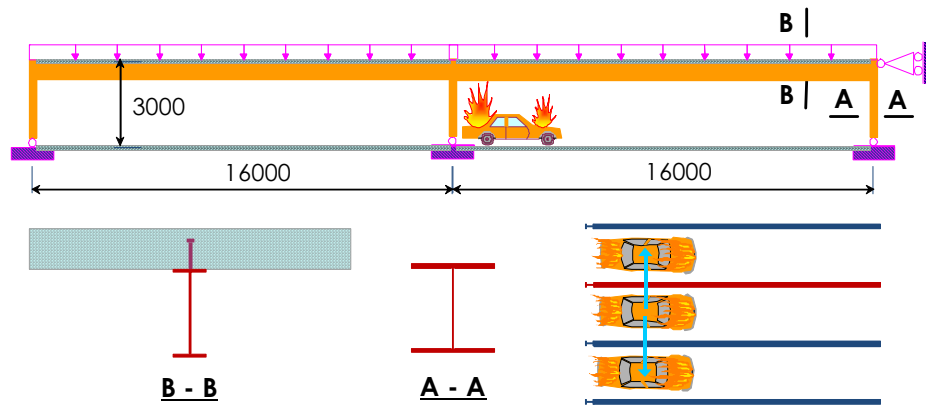
The structure was composed of:

- unprotected steel columns: HEA180 (edge columns) and HEB200 (central columns),
- composite beams: unprotected steel beams (IPE 550, IPE 400 and IPE 500) connected to the composite slab,
- composite slab with a total thickness of 120 mm (steel deck: COFRASTRA40).

The structural design of the open car park was based on a fire safety engineering method developed specifically for open car parks during an earlier European research project. For this method, a fire scenario was defined based on statistics of real car park fires. The structural resistance of the open car park was checked with an advanced model using 2D frame analysis that neglected the influence of membrane effects in the composite slab (see Figure 3.2).



**Figure 3.1** *Open car parks prior to fire tests*



**Figure 3.2** 2D modelling of tested open car park with planar composite frame

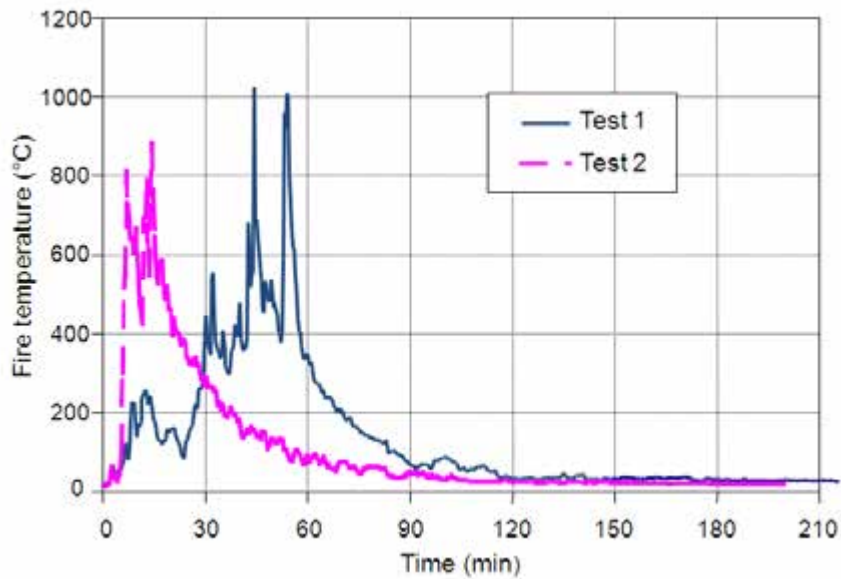
Three tests were performed on the open car park. The first two tests involved three cars; the third test was performed to assess the spread of fire between two cars placed facing each other. During each test the cars were allowed to burn themselves out.

The most severe fire was obtained in the second test, during which, under the affect of a strong wind, three cars burned together 10 minutes after the ignition of the first car (see Figure 3.3), which led to an significant area of the floor being exposed to the flames which reached a temperature of more than 800 °C (see Figure 3.4). The steel beams above the burned cars were heated up to at least 700 °C (see Figure 3.5).

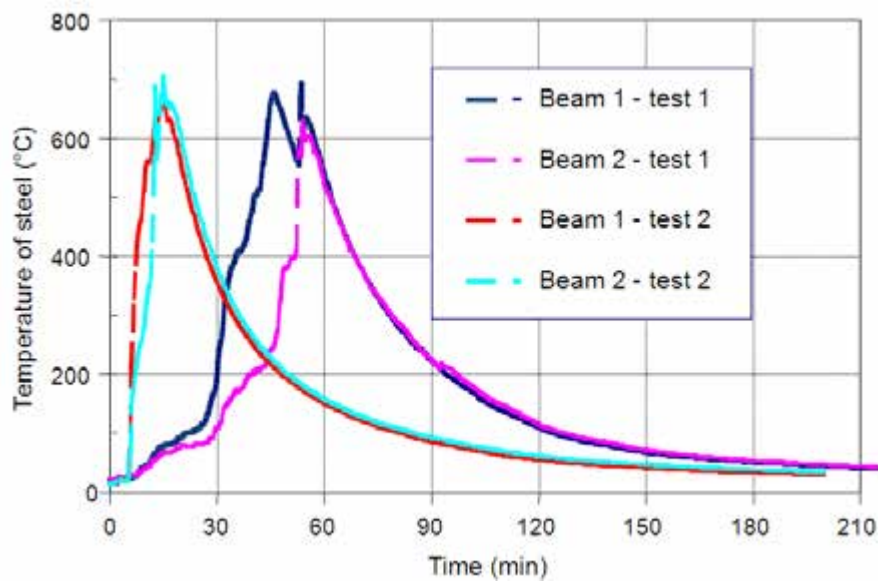


**Figure 3.3** Full fire development during one fire test

Although the heating of steel beams would result in a significant reduction of steel strength, no collapse of the unprotected steel structure occurred during these fire tests. Moreover, with respect to the structural behaviour, the measured maximum deflection of the composite floor was relatively low and did not exceed 150 mm.



**Figure 3.4** Measured temperature of hot gases (fire) above burned cars

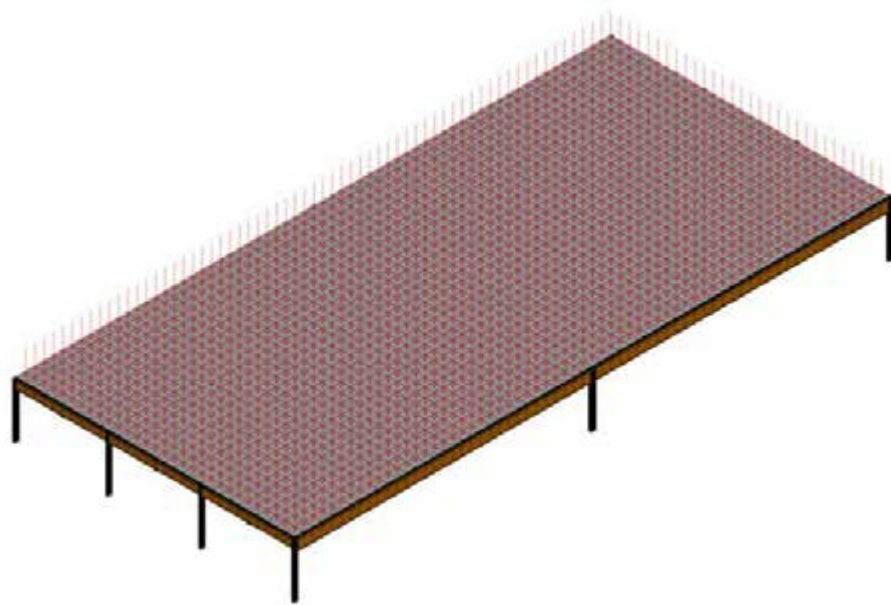


**Figure 3.5** Measured temperature of steel beams above burned cars

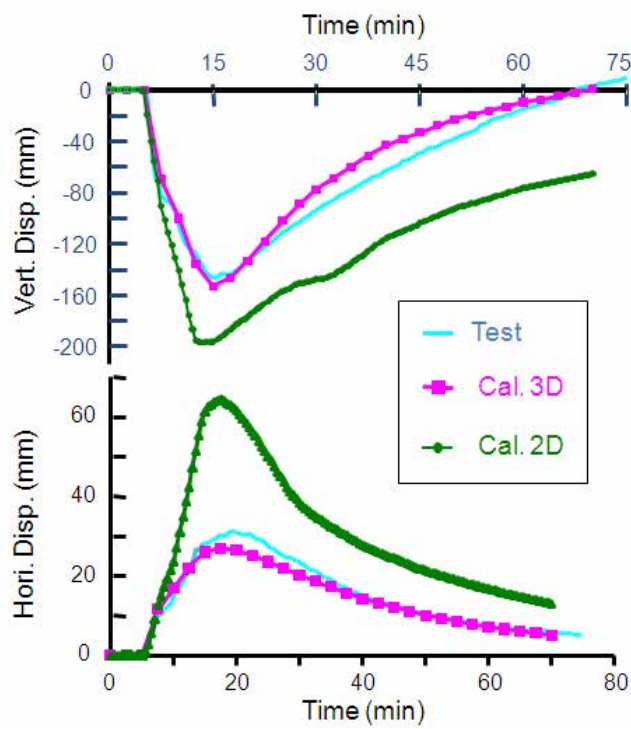
It was observed that the deflections predicted by a two-dimensional simulation were higher than the measured deflections recorded during the test. Therefore, a three-dimensional model was created to predict the structural behaviour of the car park (see Figure 3.6), using the modelling techniques that had been developed during the second phase of Cardington research project.

Figure 3.7 shows a comparison between measured deflections recorded in the test and those predicted by the two and three dimensional models, from which it can be seen that the predictions of the 3D modelling results in a closer correlation with the test results. It is clear that the membrane effect of the composite slab has already started to play a positive role even under relatively low deflection.



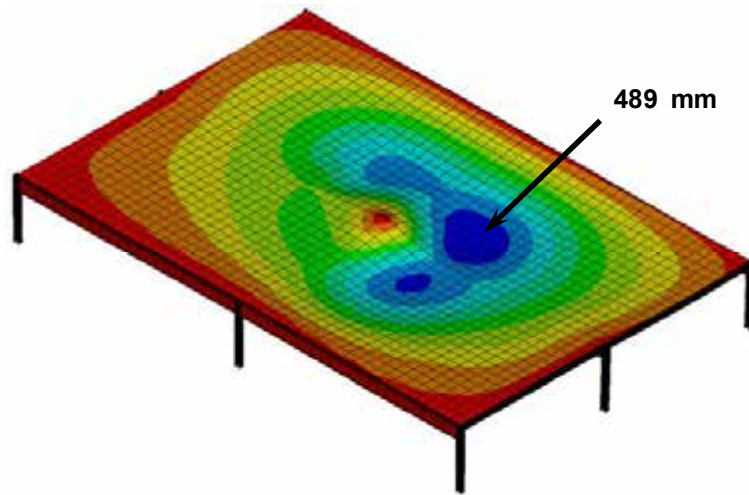


**Figure 3.6** 3D modelling of an open car park



**Figure 3.7** Comparison of vertical displacement between calculation and test

Nevertheless, according to the fire scenario adopted in fire safety engineering, the steel members of an open car park could be heated up to around 950°C. It is evident that under such heating, the deflection of the floor will be amplified and its structural resistance will rely strongly on the membrane effect (see Figure 3.8).



**Figure 3.8** *Example of the deflection of an open car park under fire scenario according to French regulation*

In consequence, the methodology based on 3D modelling of the composite floor of open car parks developed during this project was then used in various fire safety engineering projects in France to check the stability of unprotected composite steel-framed open car parks. It can be easily understood that the basis of this methodology is of course the membrane effect of the composite steel and concrete floor. In addition, in order to facilitate the application of this methodology, several design tables<sup>(38)</sup> were provided in which the standard sizes of steel members, the concrete slab as well as the necessary reinforcing steel mesh are recommended according to both applied load and structural frame system. One example of these design tables is given in Table 3.1.

**Table 3.2** Design table of open car parks related to fire resistance

	<p>Slab span: 2.5 m                  Secondary beam span: 7.5 m                  Main beam span: 7.5 m                  Spacing of columns: 7.5 m</p> <p>Applied load (except selfweight) :</p> <ul style="list-style-type: none"> <li>• Standard level:                         <ul style="list-style-type: none"> <li>- dead load : 0.20 kN/m<sup>2</sup></li> <li>- imposed load : 2.50 kN/m<sup>2</sup></li> </ul> </li> <li>• Last level:                         <ul style="list-style-type: none"> <li>- dead load : 1.45 kN/m<sup>2</sup></li> <li>- imposed load: 2.50 kN/m<sup>2</sup></li> </ul> </li> <li>• Selfweight of facade: 7.5 kN/m</li> </ul> <p>Orientation of parking place:</p> <ul style="list-style-type: none"> <li>• Perpendicular to secondary beam</li> </ul>	
Net height beneath steel beam: 2.1 m		
Minimum size of secondary beam cross section	Standard level	IPE240
	Last level	IPE270
Minimum size of main beam cross section	Standard level	IPE400
	Last level	IPE450
Design of column cross section	Available of section type	HEA, HEB et HEM
	Maximum load level (**)	0.35
Requirement to be applied to concrete slab	Total depth of slab	≥ 120 mm & ≤ 140 mm
	Maximum height of steel deck	62 mm
	Minimum compactness of rib of steel deck (*)	0.393
	Minimum thickness of steel sheet	0.75 mm
	Minimum mesh of reinforcing steel	φ7 150 mmx150 mm
	location of reinforcing steel mesh	30 mm from top of slab mesh
(*) compactness of rib of steel deck  $\frac{(l_1 + l_2)}{2(l_1 + l_3)}$		
(**) Load level: ratio of applied load under fire situation over ultimate load at room temperature design		

## 4 EVIDENCE FROM ACCIDENTAL FIRES AND OTHER COUNTRIES

Two building fires in England during the early 1990's (Broadgate and Churchill Plaza) provided the opportunity to observe how modern steel-framed buildings performed in fire. The experience from these fires was influential in stimulating thought about how buildings might be designed to resist fire and in bringing about the Cardington experiments.

Evidence of building behaviour is also available from large-scale fire tests in Australia and Germany. In both Australia and New Zealand, design approaches that allow the use of unprotected steel in multi-storey, steel-framed buildings have been developed.

### 4.1 Broadgate

In 1990, a fire occurred in a partly completed 14-storey office block on the Broadgate development in London<sup>(6)</sup>. The fire began inside a large site hut on the first level of the building. Fire temperatures were estimated to have reached over 1000°C.

The floor was constructed using composite long-span lattice trusses and composite beams supporting a composite floor slab. The floor slab was designed to have 90 minutes fire resistance. At the time of the fire, the building was under construction and the passive fire protection to the steelwork was incomplete. The sprinkler system and other active measures were not yet operational.

After the fire, a metallurgical investigation concluded that the temperature of the unprotected steelwork was unlikely to have exceeded 600°C. A similar investigation on the bolts used in the steel-to-steel connections concluded that the maximum temperature reached in the bolts, either during manufacture or as a consequence of the fire, was 540°C.

The distorted steel beams had permanent deflections of between 270 mm and 82 mm. Beams with permanent displacements at the higher end of that range showed evidence of local buckling of the bottom flange and web near their supports. From this evidence, it was concluded that the behaviour of the beams was influenced strongly by restraint to thermal expansion. This restraint was provided by the surrounding structure, which was at a substantially lower temperature than the fire-affected steel. Axial forces were induced into the heated beams resulting in an increase in vertical displacement due to the *P-delta* effect. The buckling of the lower flange and web of the beam near its supports was due to a combination of the induced axial force and the negative moment caused by the fixity of the connection.

Although the investigation showed the visually unfavourable effects of restraint on steel beams, the possible beneficial effects were not evident because only relatively low steel temperatures were reached during the fire. The beneficial effects that could have developed were catenary action of the beams and bridging or membrane action of the composite slab.

The fabricated steel trusses spanned 13.5 m and had a maximum permanent vertical displacement of 552 mm; some truss elements showed signs of buckling. It

was concluded that the restraint to thermal expansion provided by other elements of the truss, combined with non-uniform heating, caused additional compressive axial forces, which resulted in buckling.

At the time of the fire, not all the steel columns were fire protected. In cases where they were unprotected, the column had deformed and shortened by approximately 100 mm (see Figure 4.1). These columns were adjacent to much heavier columns that showed no signs of permanent deformation. It was thought that this shortening was a result of restrained thermal expansion. The restraint to thermal expansion was provided by a rigid transfer beam at an upper level of the building, together with the columns outside the fire affected area.



**Figure 4.1** *Buckled column and deformed beams at Broadgate*

Although some of the columns deformed, the structure showed no signs of collapse. It was thought that the less-affected parts of the structure were able to carry the additional loads that were redistributed away from the weakened areas.

Following the fire, the composite floor suffered gross deformations with a maximum permanent vertical displacement of 600 mm (see Figure 4.2). Some failure of the reinforcement was observed. In some areas, the steel profiled decking had debonded from the concrete. This was considered to be caused mainly by steam release from the concrete, together with the effects of thermal restraint and differential expansion.

A mixture of cleat and end-plate connections was used. Following the fire, none of the connections was observed to have failed, although deformation was evident. In cleated connections, there was some deformation of bolt holes. In one end-plate connection, two of the bolts had fractured; in another, the plate had fractured down one side of the beam but the connection was still able to transfer shear. The main cause of deformation was thought to be due to the tensile forces induced during cooling.

Following the fire, structural elements covering an area of approximately 40 m x 20 m were replaced, but it is important to note that no structural failure had occurred and the integrity of the floor slab was maintained during the fire. The direct fire loss was in excess of £25M, of which less than £2M was attributed to the repair of the structural frame and floor damage; the other costs resulted from smoke damage. Structural repairs were completed in 30 days.



**Figure 4.2** *View of deformed floor above the fire (the maximum deflection was about 600 mm)*

## **4.2 Churchill Plaza building, Basingstoke**

In 1991, a fire took place in the Mercantile Credit Insurance Building, Churchill Plaza, Basingstoke. The 12-storey building was constructed in 1988. The columns had board fire protection and the composite floor beams had spray-applied protection. The underside of the composite floor was not fire protected. The structure was designed to have 90 minutes fire resistance.

The fire started on the eighth floor and spread rapidly to the ninth and then the tenth floor as the glazing failed. During the fire, the fire protection performed well and there was no permanent deformation of the steel frame. The fire was believed to be comparatively ‘cool’ because the failed glazing allowed a cross wind to increase the ventilation. The protected connections showed no deformation.

In places, the dovetail steel decking showed some signs of debonding from the concrete floor slab. (as had also been observed in the Broadgate fire). A load test was conducted on the most badly affected area, with a load of 1.5 times the total design load being applied. The test showed that the slab had adequate load-carrying capacity and could be reused without repair.

The protected steelwork suffered no damage. The total cost of repair was in excess of £15M, most of which was due to smoke contamination, as in the Broadgate fire. Sprinklers were installed in the refurbished building.



**Figure 4.3** *Churchill Plaza, Basingstoke following the fire*

### **4.3 Australian fire tests**

BHP, Australia's biggest steel maker, has been researching and reporting<sup>(7, 8)</sup> fire-engineered solutions for steel-framed buildings for many years. A number of large-scale natural fire tests have been carried out in specially constructed facilities at Melbourne Laboratory, representing sports stadia, car parks and offices. The office test programme focussed on refurbishment projects that were to be carried out on major buildings in the commercial centre of Melbourne.

#### **4.3.1 William Street fire tests and design approach**

A 41-storey building in William Street in the centre of Melbourne was the tallest building in Australia when it was built in 1971. The building was square on plan, with a central square inner core. A light hazard sprinkler system was provided. The steelwork around the inner core and the perimeter steel columns were protected by concrete encasement. The beams and the soffit of the composite steel deck floors were protected with asbestos-based material. During a refurbishment programme in 1990, a decision was made to remove the hazardous asbestos.

The floor structure was designed to serviceability rather than strength requirements. This meant that there was a reserve of strength that would be very beneficial to the survival of the frame in fire, as higher temperatures could be sustained before the frame reached its limiting condition.

At the time of the refurbishment, the required fire resistance was 120 minutes. Normally this would have entailed the application of fire protection to the steel beams and to the soffit of the very lightly reinforced slab (Australian regulations have been revised and now allow the soffit of the slab to be left unprotected for 120 minutes fire resistance). In addition, the existing light hazard sprinkler system required upgrading to meet the prevailing regulations.

During 1990, the fire resistance of buildings was subject to national debate; the opportunity was therefore taken to conduct a risk assessment to assess whether fire protecting the steelwork and upgrading the sprinkler system was necessary for this building. Two assessments were made. The first was made on the basis that the building conformed to current regulations with no additional safety measures; the

second was made assuming no protection to the beams and soffit of the slab, together with the retention of the existing sprinkler system. The effect of detection systems and building management systems were also included in the second assessment. The authorities agreed that if the results from the second risk assessment were at least as favourable as those from the first assessment, the use of the existing sprinkler system and unprotected steel beams and composite slabs would be considered acceptable.

A series of four fire tests was carried out to obtain data for the second risk assessment. The tests were to study matters such as the probable nature of the fire, the performance of the existing sprinkler system, the behaviour of the unprotected composite slab and castellated beams subjected to real fires, and the probable generation of smoke and toxic products.

The tests were conducted on a purpose-built test building at the Melbourne Laboratories of BHP Research (see Figure 4.4). This simulated a typical storey height 12 m × 12 m corner bay of the building. The test building was furnished to resemble an office environment with a small, 4 m × 4 m, office constructed adjacent to the perimeter of the building. This office was enclosed by plasterboard, windows, a door, and the facade of the test building. Imposed loading was applied by water tanks.



**Figure 4.4** *BHP test building and fire test*

Four fire tests were conducted. The first two were concerned with testing the performance of the light hazard sprinkler system. In Test 1, a fire was started in the small office and the sprinklers were activated automatically. This office had a fire load of 52 kg/m<sup>2</sup>. The atmosphere temperatures reached 60°C before the sprinklers



controlled and extinguished the fire. In Test 2, a fire was started in the open-plan area midway between four sprinklers. This area had a fire load of 53.5 kg/m<sup>2</sup>. The atmosphere temperature reached 118°C before the sprinklers controlled and extinguished the fire. These two tests showed that the existing light hazard sprinkler system was adequate.

The structural and thermal performance of the composite slab was assessed in Test 3. The supporting beams were partially protected. The fire was started in the open plan area and allowed to develop with the sprinklers switched off. The maximum atmosphere temperature reached 1254°C. The fire was extinguished once it was considered that the atmosphere temperatures had peaked. The slab supported the imposed load. The maximum temperature recorded on the top surface of the floor slab was 72°C. The underside of the slab had been partially protected by the ceiling system, which remained substantially in place during the fire.

In Test 4, the steel beams were left unprotected and the fire was started in the small office. The fire did not spread to the open-plan area despite manual breaking of windows to increase the ventilation. Therefore fires were ignited from an external source in the open-plan area. The maximum recorded atmosphere temperature was 1228°C, with a maximum steel beam temperature of 632°C above the suspended ceiling. The fire was extinguished when it was considered that the atmosphere temperatures had peaked. Again, the steel beams and floor were partially shielded by the ceiling. The central displacement of the castellated beam was 120 mm and most of this deflection was recovered when the structure cooled to ambient temperature.

Three unloaded columns were placed in the fire compartment to test the effect of simple radiation shields. One column was shielded with galvanized steel sheet, one with aluminised steel sheet and one was an unprotected reference column. The maximum recorded column temperatures were 580°C, 427°C and 1064°C respectively, suggesting that simple radiation shields might provide sufficient protection to steel members in low fire load conditions.

It was concluded from the four fire tests that the existing light hazard sprinkler system was adequate and that no fire protection was required to the steel beams or soffit of the composite slab. Any fire in the William Street building should not deform the slab or steel beams excessively, provided that the steel temperatures do not exceed those recorded in the tests.

The temperature rise in the steel beams was affected by the suspended ceiling system, which remained largely intact during the tests.

The major city centre office building that was the subject of the technical investigation was owned by Australia's largest insurance company, which had initiated and funded the test programme. It was approved by the local authority without passive fire protection to the beams but with a light hazard sprinkler system of improved reliability and the suspended ceiling system that had proved to be successful during the test programme.

#### **4.3.2 Collins Street fire tests**

This test rig was constructed to simulate a section of a proposed steel-framed multi-storey building in Collins Street, Melbourne. The purpose of the test was to record temperature data in fire resulting from combustion of furniture in a typical office compartment.

The compartment was 8.4 m × 3.6 m and filled with typical office furniture, which gave a fire load between 44 and 49 kg/m<sup>2</sup>. A non-fire-rated suspended ceiling system was installed, with tiles consisting of plaster with a fibreglass backing blanket. An unloaded concrete slab formed the top of the compartment. During the test, temperatures were recorded in the steel beams between the concrete slab and the suspended ceiling. The temperatures of three internal free-standing columns were also recorded. Two of these columns were protected with aluminium foil and steel sheeting, acting simply as a radiation shield; the third remained unprotected. Three unloaded external columns were also constructed and placed 300 mm from the windows around the perimeter of the compartment.

The non-fire-rated ceiling system provided an effective fire barrier, causing the temperature of the steel beams to remain low. During the test the majority of the suspended ceiling remained in place. Atmosphere temperatures below the ceiling ranged from 831°C to 1163°C, with the lower value occurring near the broken windows. Above the ceiling, the air temperatures ranged from 344°C to 724°C, with higher temperatures occurring where the ceiling was breached. The maximum steel beam temperature was 470°C.

The unloaded indicative internal columns reached a peak temperature of 740°C for the unprotected case and below 403°C for the shielded cases. The bare external columns recorded a peak temperature of 490°C.

This fire test showed that the temperatures of the beams and external columns were sufficiently low to justify the use of unprotected steel and, as in the William Street tests, the protection afforded by a non-fire-rated suspended ceiling was beneficial.

### **4.3.3 Conclusions from Australian research**

The Australian tests and associated risk assessments concluded that, provided that high-rise office buildings incorporate a sprinkler system with a sufficient level of reliability, the use of unprotected beams would offer a higher level of life safety than similar buildings that satisfied the requirements of the Building Code of Australia by passive protection. Up to the beginning of 1999, six such buildings between 12 and 41 storeys were approved in Australia.

## **4.4 German fire test**

In 1985, a fire test was conducted on a four storey steel-framed demonstration building constructed at the Stuttgart-Vaihingen University in Germany<sup>(9)</sup>. Following the fire test, the building was used as an office and laboratory.

The building was constructed using many different forms of steel and concrete composite elements. These included water filled columns, partially encased columns, concrete filled columns, composite beams and various types of composite floor.

The main fire test was conducted on the third floor, in a compartment covering approximately one-third of the building. Wooden cribs provided the fire load and oil drums filled with water provided the gravity load. During the test, the atmosphere temperature exceeded 1000°C, with the floor beams reaching temperatures up to 650°C. Following the test, investigation of the beams showed that the concrete in-filled webs had spalled in some areas exposing the reinforcement. However, the beams behaved extremely well during the test with no significant permanent deformations following the fire. The external columns and those around the central core showed no signs of permanent deformation. The

composite floor reached a maximum displacement of 60 mm during the fire and retained its overall integrity.

Following the fire, the building was refurbished. The refurbishment work involved the complete replacement of the fire damaged external wall panels, the damaged portions of steel decking to the concrete floor slab, and the concrete infill to the beams. Overall, it was shown that refurbishment to the structure was economically possible.

## 4.5 Experimental work at room temperature

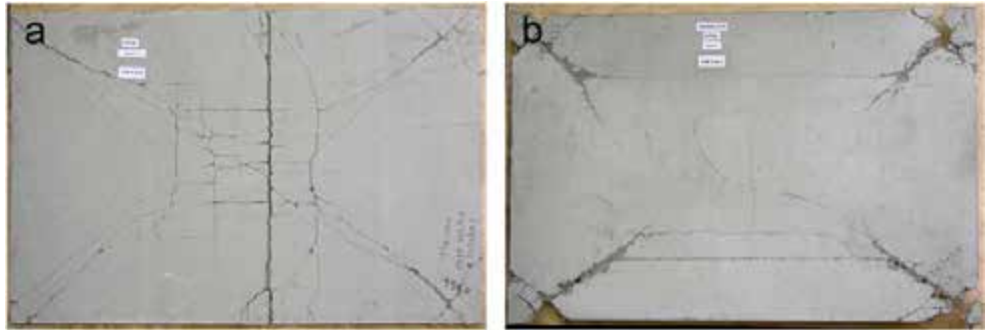
The simple design method presented in Section 5 has been based on theoretical models developed for room temperature design and verified with experimental investigations. Since 1961, a number of such experimental investigations have been conducted to investigate membrane action in concrete slabs (15,18,22,23,24) with no in-plane horizontal restraint. In all the tests, the specimen failed due to large cracks through the full depth of the slab across the shorter span and membrane action was clearly observed, as shown by Table 4.1

**Table 4.1** Comparison between the simple design method and previous room temperature tests<sup>(26)</sup>

Reference	Test No.	Slab Size (m)	Yield- line load (kN/m <sup>2</sup> )	Test load (kN/m <sup>2</sup> )	Enhancement observed from test	Calculated enhancement
Hayes & Taylor <sup>(22)</sup>	R11	0.914x0.914	15.43	31.97*	2.07	2.07
	R12	0.914x0.914	55.64	89.0*	1.60	2.11
	R13	0.914x0.914	29.05	60.8*	2.09	2.09
	R21	1.372x0.914	20.24	36.48*	1.80	1.80
	R31	1.828x0.914	16.37	25.08*	1.53	1.49
Taylor, Maher & Hayes <sup>(23)</sup>	S1	1.829x1.829	23.83	42.90*	1.80	1.48
	S7	1.829x1.829	23.83	39.03*	1.64	1.68
	S9	1.829x1.829	23.83	38.13*	1.60	1.31
Sawczuk & Winnicki <sup>(18)</sup>	Type 1 ( $\alpha = 2.0$ )	2.0x1.0	20.6	38.26*	1.86	1.71
	Type 2 ( $\alpha = 2.0$ )	2.0x1.0	10.99	17.18*	1.56	1.46
	Type 1 ( $\alpha = 1.45$ )	1.6x1.1	21.04	45.13*	2.14	2.15
Wood <sup>(15)</sup>		0.610 x0.610	10.45 (kN)	17.14* (kN)	1.64	1.36
BRE <sup>(20)</sup>		9.5 x 6.46	2.58	4.81	1.86	1.68

\* denotes that slab failure did not occur.

A series of 22 tests were recently conducted on horizontally unrestrained small-scale concrete slabs, with an aspect ratio of 1.0 or 1.55, by Bailey and Toh<sup>(27)</sup>. Two different modes of failure were generally witnessed in these ambient tests dependent to the reinforcement ratio, aspect ratio and the reinforcement ductility. Fracture of the reinforcement across the shorter span (Figure 4.5(a)) was the dominant failure mode in most of the lightly reinforced slabs whilst the heavily reinforced slabs and the ones with highly ductile reinforcement mostly failed due to the compressive failure at the corners of the slab (Figure 4.5(b)). These experimental data provided the necessary information to extend the method to orthotropic reinforcement and to include compressive failure in the concrete as an additional failure mode to be considered.



**Figure 4.5** *Two typical modes of failure for test slabs at ambient temperature*

## **4.6 Experimental work at elevated temperature**

In addition to the seven full-scale tests carried out on the full scale eight-storey steel framed building with composite floors at Cardington in 1996 and 2003<sup>(28,29)</sup> further small scale tests have also been conducted at elevated temperature by Bailey and Toh<sup>(27)</sup> in order to further investigate tensile membrane action in composite slabs. As a result of these tests the design method originally developed by Bailey and Moore has been modified, resulting in the formulation presented in Section 5.

Bailey and Toh<sup>(27)</sup> carried out a series of 15 small scale tests on horizontally unrestrained concrete slabs, with aspect ratios of 1.0 or 1.55. They concluded that unlike the slabs tested in ambient conditions, where the failure mode was influenced by compressive failure of the concrete, in all 15 slabs tested in fire conditions, the fracture of the reinforcement across the shorter span governed the failure, as shown in Figure 4.6.



**Figure 4.6** *Mode of failure for test slabs at elevated temperatures*

## 5 SIMPLE DESIGN METHOD

Since Johansen's pioneering work on yield line analysis<sup>(10)</sup> researchers have observed the beneficial effects of membrane forces in improving the load bearing capacity of concrete slabs, compared to estimates of capacity based only on flexural behaviour<sup>(11)</sup>.

A number of experimental and theoretical investigations have been carried out to investigate the beneficial effects of in-plane forces at room temperature, leading to a good theoretical understanding of the behaviour. Following the experimental work carried out at Cardington, this theory has been extended to fire design scenarios, as discussed below.

The experimental work at Cardington and evidence from other real fires in building structures had served to illustrate that there are significant reserves of strength in composite steel concrete buildings, which means that the performance of the structure in fire exceeds the expectations created by standard fire tests on individual structural elements. Cardington demonstrated that it was possible to leave the composite steel beams that supported the concrete floor slab unprotected; work commenced to investigate suitable design models to allow structural engineers to justify the fire design of a floor slab supported by unprotected steel beams.

Researchers at the Building Research Establishment (BRE), with funding from the Steel Construction Institute, developed a simple design method for composite steel concrete floor slabs following the experimental work at Cardington<sup>(12,13)</sup>. The BRE model has been validated against the Cardington large scale fire test results and previous experimental work conducted at room temperature. This method is presented and discussed in detail in Section 5.2.

The simple design method differs from the simple design procedures provided in design codes<sup>(32,33)</sup>, as it considers the behaviour of an assembly of structural members acting together, rather than individual elements. While it would also be technically possible to use non-linear finite elements to determine the load bearing capacity in fire, that is a more expensive solution requiring a significant amount of expertise and prior knowledge. The method presented in this document is more accessible to structural engineers with only a basic appreciation of fire engineering.

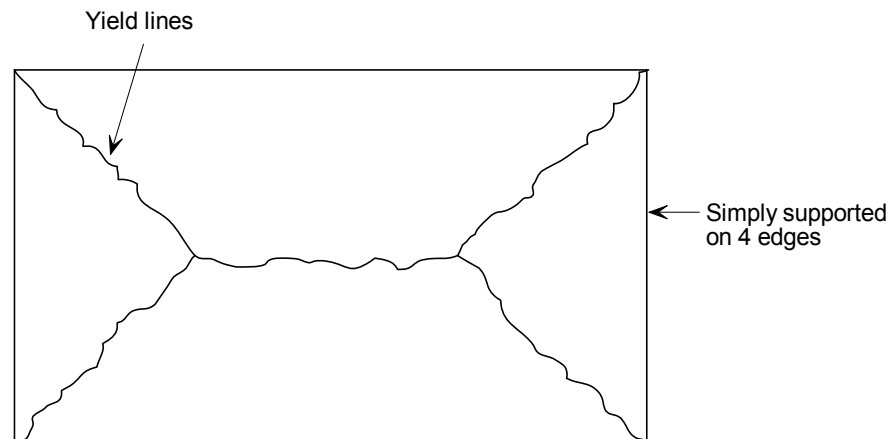
### 5.1 Introduction to yield line theory and membrane action

The yield line theory pioneered by Johansson is an ultimate load theory based on assumed collapse mechanisms and plastic properties of under-reinforced concrete slabs. The collapse mechanism is defined by a pattern of yield lines along which the reinforcement yields and the slab undergoes plastic deformations. The areas bounded by the yield lines are assumed to remain rigid with all rotation taking place at the yield line.

For yield line theory to be valid, shear failures, bond failures and compression failures must be prevented. The moment-curvature response of the slab must be sufficiently ductile to allow a mechanism to form; in practice this is not a problem as slabs are always under-reinforced, leading to ductile yielding of the

reinforcement before more brittle modes of failure such as compressive failure in the concrete.

For square and rectangular slabs that are simply supported along their free edges, the patterns of yield lines shown in Figure 5.1 are expected to occur. These are the yield line patterns which are assumed in the following theoretical development. In reality, for a steel framed building, the slab is supported on steel beams which will have a finite stiffness between column positions. This will be discussed in Section 6.



**Figure 5.1** *A typical yield line pattern for a rectangular slab simply supported on four sides*

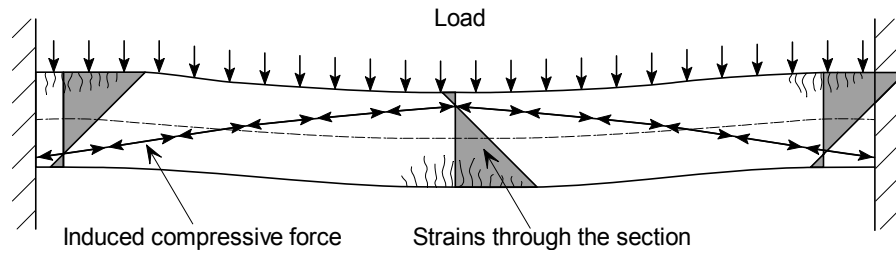
An upper bound solution may be obtained for an assumed yield line pattern. The solution is based on energy theory, with the external work done by the applied load due to a unit displacement of the rigid regions being equated to the internal work done by the rotation of the yield lines. The load which corresponds to any assumed failure mechanism will be greater than or equal to the true collapse load of the structure, thus giving an upper bound solution.

However, due to membrane action in the slab and strain hardening of the reinforcement after yielding, this theoretical upper bound solution from the yield line analysis tends to be significantly lower than the actual failure load of the slab observed during experiments.

Membrane action in slabs creates in-plane forces that are governed by the in-plane boundary conditions of the slab. Two extreme cases, of full restraint and no restraint, are considered below.

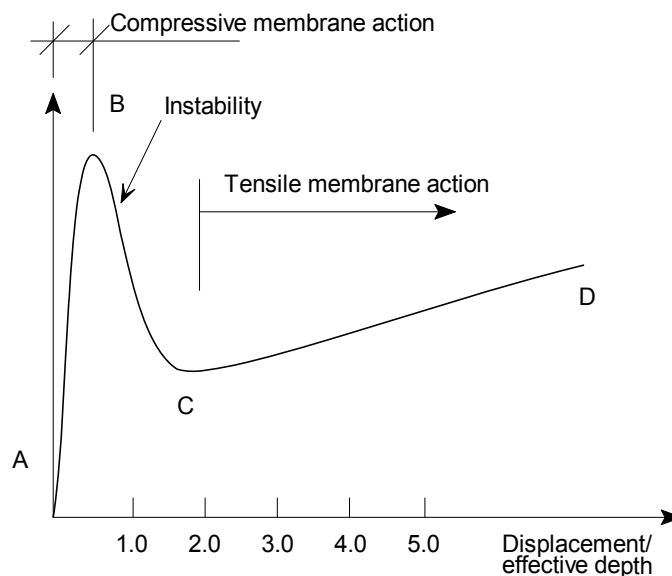
### **5.1.1 Slab with full in-plane restraint**

With full in-plane restraint to the slab boundaries, the initial small bending deflections of a slab result in compressive membrane action<sup>(14,15)</sup>. This mechanism is illustrated in Figure 5.2, for a one way spanning element. A compressive action along a path from the bottom surface at the boundary to the top surface at mid-span develops, inducing a compressive arching action in the slab, which results in an enhanced resistance as shown in Figure 5.3. However, this arching action becomes unstable once the magnitude of the vertical deflection exceeds a value equal to approximately half the slab thickness, resulting in the rapid decrease of resistance. The slab can then go on to develop tensile membrane action at larger displacements.



**Figure 5.2** *Compressive membrane action in a restrained slab*

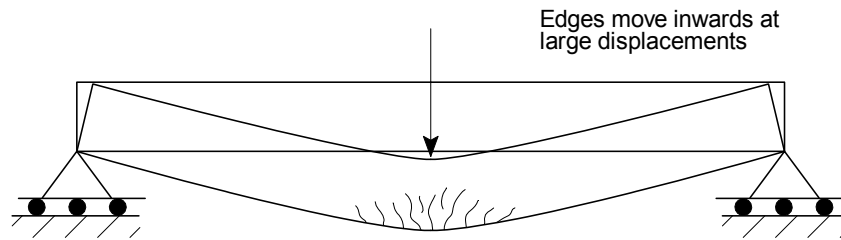
Park<sup>(14)</sup> illustrated the effect of compressive membrane action on a restrained slab using a figure similar to Figure 5.3. The initial peak load shown in this figure at displacements less than the slab thickness is due to compressive membrane action. When compression failure occurs in the concrete a sudden drop in capacity is observed, accompanied by an increase in displacement. The load capacity then increases with increasing deflection until fracture of the reinforcement occurs.



**Figure 5.3** *Membrane action in a slab with restrained in-plane boundaries<sup>(15)</sup>*

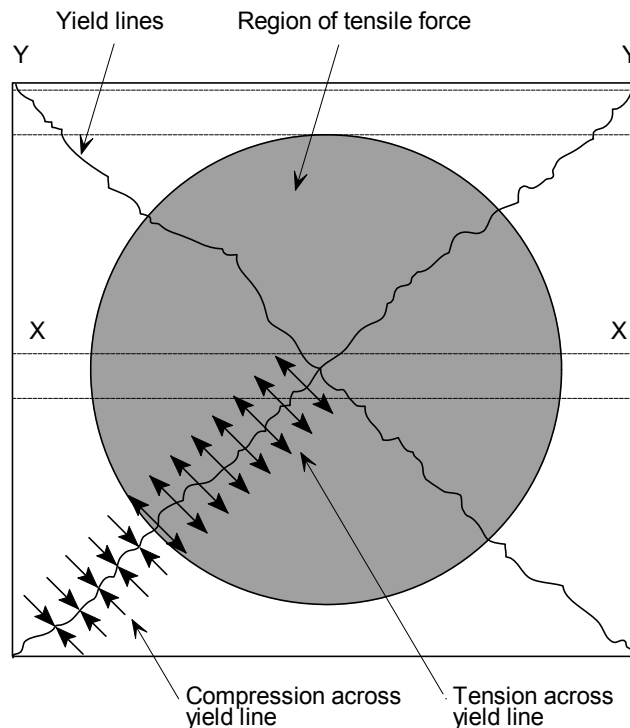
### 5.1.2 Slab with no in-plane restraint

Where the boundary of the slab is unrestrained, the slab behaviour is different. Compressive membrane action cannot occur and the post-yielding behaviour is characterised by tensile membrane action. For a one-way spanning element, large vertical displacements will cause end shortening of the member. If this end shortening is prevented then tensile forces will develop. For a one-way spanning member, these restraint forces would have to be developed externally at the supports. However, for a two way spanning slab, i.e. a slab with simple supports on four edges, external horizontal restraints are not required as the slab can develop an internal system of in-plane forces which has the same effect.



**Figure 5.4** *One way spanning structural members*

Considering the case of a two-way spanning slab, as shown in Figure 5.5. This slab has vertical supports around its perimeter but no in-plane horizontal restraints. The strip at the centre of the slab denoted X-X will tend to have end shortening behaviour similar to the one-way spanning element shown in Figure 5.4. However, the strips denoted Y-Y on a supported edge do not have the same vertical displacement and will therefore not have significant end shortening. In-plane forces will therefore occur at the interface of these strips of slab in order to maintain equilibrium, thus inducing tensile stresses in strips such as X-X and compressive stresses in strips such as Y-Y. As this behaviour occurs in two directions the result is an area of tensile stress in the centre of the slab denoted by the shaded area in Figure 5.5 and a compressive ring around the perimeter.



**Figure 5.5** *Development of in-plane membrane forces*

### 5.1.3 Effect of membrane stresses on yield lines

The development of tensile and compressive in-plane forces will influence the yield line moments developed in the slab, with reductions in bending resistance occurring in the tensile zone and enhancement of the bending resistance of the yield lines in the compression zone. In addition to this influence on bending resistance, there is also the additional load bearing capacity due to tensile membrane action.

Following the work of Johansson on yield line analysis, tests to destruction of a complete building were reported by Ockleston<sup>(11)</sup>. These test revealed that the loads that could be sustained by the floor slabs were considerably greater than those



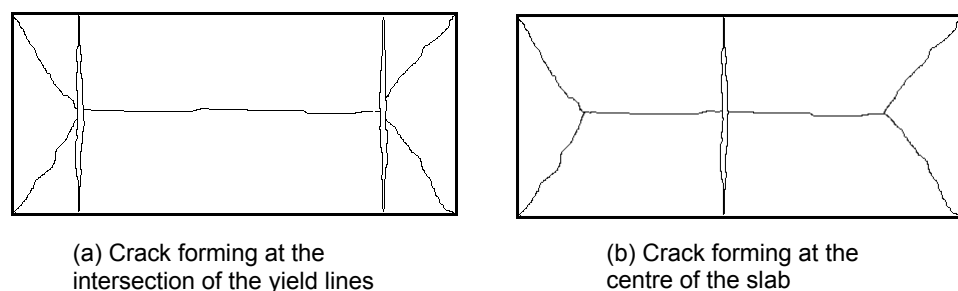
predicted by yield line theory. This generated considerable interest in research into membrane effects and a number of researchers investigated these effects both experimentally and analytically in subsequent years.

Observations from tests on unrestrained slabs show that the pattern of yield lines is unchanged at large displacements. The ultimate mode of failure has also been shown to be the development of large cracks across the shorter span of the slab and fracture of the reinforcement, as reported by Wood<sup>(15)</sup>

Methods of analysis taking account of membrane action have been developed for unrestrained slabs by Wood<sup>(15)</sup>, Kemp<sup>(17)</sup>, Taylor<sup>(16)</sup>, Sawczuk<sup>(18)</sup>, Hayes<sup>(19)</sup> and Bailey and Moore<sup>(12,13)</sup>

Wood developed a solution for a circular slab with simply supported boundaries subject to distributed loading. A similar solution was developed for square slabs by Kemp. Kemp's method involved a rigorous rigid-plastic solution, in which the load bearing capacity is determined from consideration of the equilibrium of the rigid regions of the slab. This enables the magnitude of the membrane forces and yield line moments to be determined as a function of the slab deflection. Kemp's theory demonstrates that the capacity of the slab is a function of the slab deflection. He notes that in practice a collapse load would be reached when fracture of the reinforcement occurs or when the concrete in the outer region crushes, although his model does not attempt to define this end point on the load deflection response.

In the approach used by Sawczuk, the formation of the crack across the short span was included. Sawczuk identified that the rigid triangular elements of the slab are subject to in-plane moments due to the variation of membrane forces along the yield lines. By estimating the bending resistance of the rigid regions, Sawczuk predicted the development of bending hinges along the centre line of the slab and cracking across the short span. This cracking is not allowed for by the methods developed by Taylor and Kemp. Sawczuk's energy based method, considered two possible crack formations, as shown in Figure 5.6. The conclusion was that the critical mode of failure was caused by cracks forming across the shorter span, at the intersection of the yield lines, as shown in Figure 5.6(a).



**Figure 5.6** Failure modes identified by Sawczuk

Hayes noted that the Sawczuk's analysis implied that boundary forces were present, when in reality these forces could not exist at an unrestrained simply supported edge. Hayes also observed that no increase in the load bearing capacity was apparent when moment equilibrium of the rigid regions was considered. Hayes went on to develop a solution for orthotropically reinforced rectangular slabs which addressed his criticisms of Sawczuk method and which was in good agreement with Kemp's solution for square slabs. In his method, Hayes also assumed that the cracks across the short span occur at the intersection of the yield lines. Comparing his method with Sawczuk's, Hayes concluded that the differences were not

significant. Importantly, Hayes also noted that the enhancement due to membrane effects decreases with increase in the aspect ratio of the slab or the orthotropy of the reinforcement.

Sawczuk's assumption, which was also adopted by Hayes, that the failure mode includes two cracks across the short span of the slab at the intersection of the yield lines contradicts a large portion of the test results, including a test conducted by Building Research Establishment in 2000<sup>(20)</sup>. Therefore, Bailey and Moore<sup>(12,13)</sup> modified the method developed by Hayes's approach and based their equilibrium method on the formation of a single crack in the centre of the slab, the mode of failure commonly observed in the tests conducted at ambient and elevated temperatures, Figure 5.7(b). The derivation used by Bailey and Moore is described in Section 5.2. Initially this was developed for isotropic reinforcement, but has been updated to include the effects of the orthotropic reinforcement and the catenary action of the steel beams<sup>(21)</sup>.

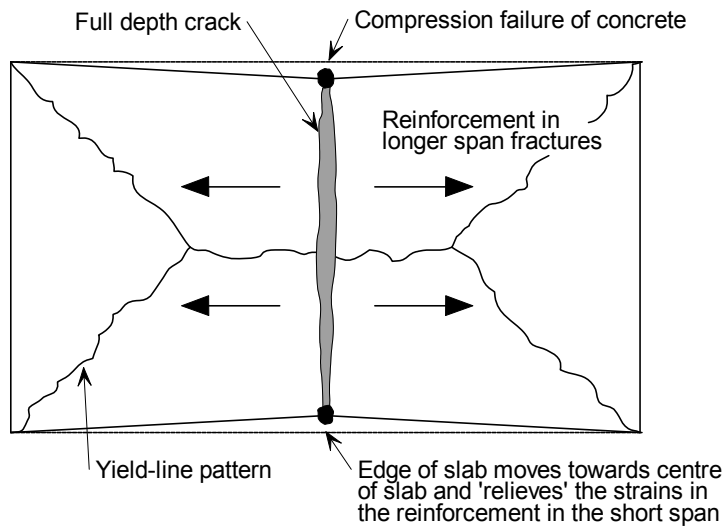
## **5.2 Calculation of resistance of composite floors in accordance with the simple design method**

This Section describes the development of a simple design method that can be used to calculate the resistance of rectangular composite floor plates. The method has developed over a number of years. The initial development<sup>(12,13)</sup> of the method for use with isotropic reinforcement only considered one failure mode, due to fracture of the mesh across the short span, as shown by Figure 5.7(a). Later developments<sup>(21,25)</sup> included a more general derivation allowing the use of orthotropic reinforcement, and also the inclusion of compression failure of the concrete at the slab corners (see Figure 5.7(b)).

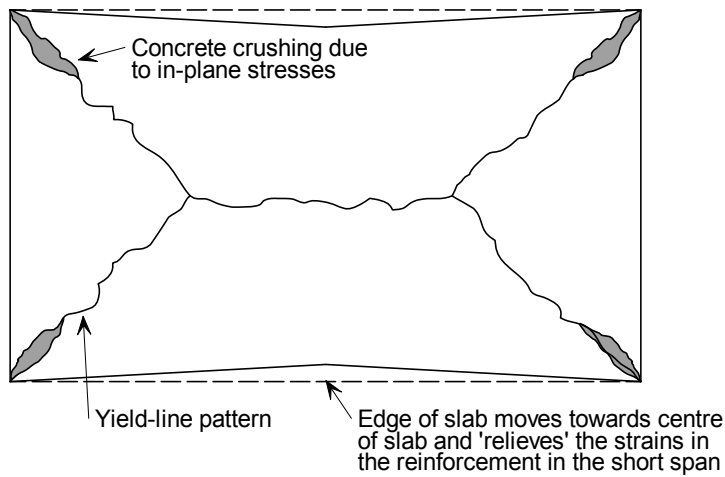
### **5.2.1 Calculation of resistance**

The load bearing capacity of a two-way spanning simply supported slab, with no in-plane horizontal restraint at its edges, is greater than that calculated using the normal yield line theory. The enhancement of the resistance is as a result of tensile membrane action developing in the slab at large displacement and also due to the increase of the yield moment in the outer regions of the slab, where compressive stresses occur across the yield lines (see Figure 5.8).

The enhancement of the resistance determined as a lower bound solution for yield line failure is based on the assumption that at ultimate conditions the yield line pattern will be as shown in Figure 5.7(a) and that failure will occur due to fracture of the mesh across the short span at the centre of the slab. A second mode of failure might, in some cases, occur due to crushing of the concrete in the corners of the slab where high compressive in-plane forces occur as shown by Figure 5.7(b). This mode of failure is discussed in Section 5.3.



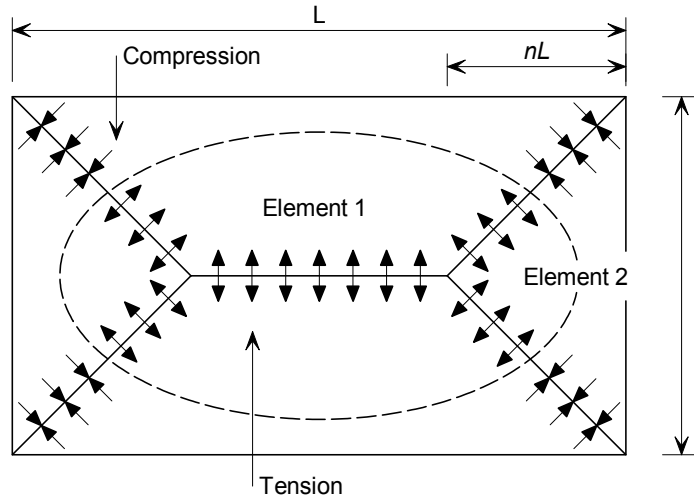
(a) Tensile failure of mesh reinforcement



(b) compressive failure of concrete

**Figure 5.7** Assumed failure mode for composite floor

The first failure mode will occur when the compressive strength of the concrete exceeds the ultimate strength of the mesh in tension, leading to fracture of the mesh. The second failure mode will occur in cases where the ultimate strength of the mesh exceeds the compressive strength of the concrete, resulting in compression failure of the concrete at the corners of the slab.



**Figure 5.8** Rectangular slab simply supported on four edges showing in-plane forces across the yield lines due to tensile membrane action.

Figure 5.8 shows a rectangular slab simply supported on its perimeter and the expected lower bound yield line pattern that would develop due to uniformly distributed loading. The intersection of the yield lines is defined by the parameter  $n$  calculated using the general yield line theory and given by:

$$n = \frac{1}{2\mu a^2} (\sqrt{3\mu a^2 + 1} - 1) \quad (5-1)$$

where

- $a$  is the aspect ratio of the slab ( $L/l$ )
- $\mu$  is the ratio of the yield moment capacity of the slab in orthogonal directions (should always be less than or equal to 1.0)

The shorter span should be defined by the span with the lower moment capacity resulting in coefficient of orthography ( $\mu$ ) being always less than, or equal to one. Therefore  $n$  would be limited to maximum of 0.5 resulting in a valid yield line pattern.

The resistance of the mechanism which occurs due to the formation of these yield lines is given by the following equation:

$$P = \frac{24\mu M}{l^2} \left[ \sqrt{3 + \frac{1}{(a')^2} - \frac{1}{a'}} \right]^{-2} \quad (5-2)$$

where

$$a' =$$

$$a' = \sqrt{\mu a}$$

Hayes<sup>(19)</sup> noted that assuming rigid-plastic behaviour, only rigid body translations and rotations are allowed. Further assumptions that the neutral axes along the yield lines are straight lines and that the concrete stress-block is rectangular, means that

the variations in membrane forces along the yield lines become linear, as shown in Figure 5.9. These assumptions and the resulting distribution of membrane forces were also adopted by Bailey<sup>(12,26)</sup>.

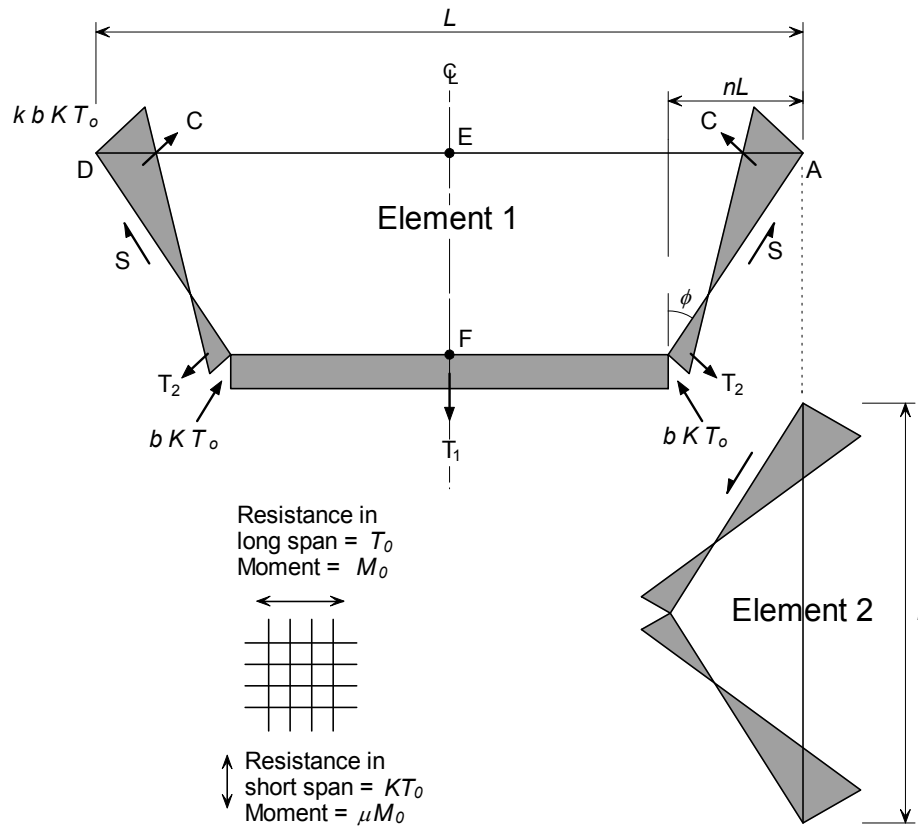


Figure 5.9 In-plane stress distribution for the elements 1 and 2

### 5.2.2 Derivation of an expression for parameter k

Considering the equilibrium of the in-plane forces  $T_1$ ,  $T_2$  and  $C$  acting on Element 1 allows the following relationships to be derived:

$$S \sin \phi = (C - T_2) \cos \phi$$

and

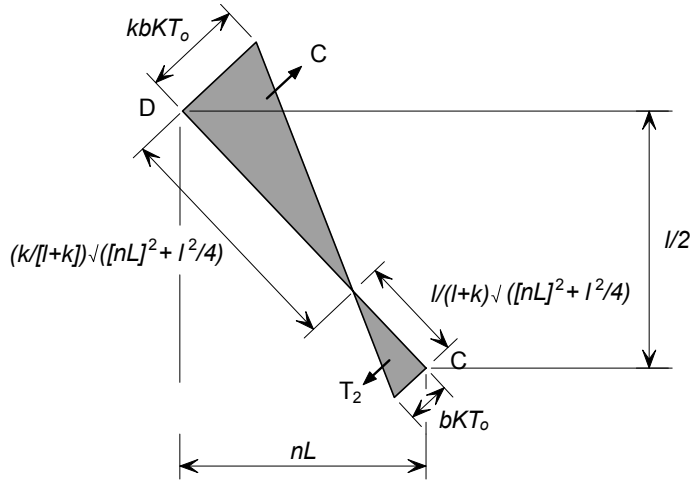
$$-S \cos \phi = (C - T_2) \sin \phi - \frac{T_1}{2}$$

Therefore,

$$\frac{T_1}{2} \sin \phi = (C - T_2) \quad (5-3)$$

where

$\phi$  is the angle defining the yield line pattern.



**Figure 5.10** In-plane stress distribution along yield line CD

Figure 5.10 shows the geometry of the stress distribution along yield line CD. Considering Figure 5.9 and Figure 5.10,

$$T_1 = bKT_0 (L - 2nL)$$

$$T_2 = \frac{bKT_0}{2} \left( \frac{1}{1+k} \right) \sqrt{(nL)^2 + \frac{l^2}{4}}$$

$$C = \frac{kbKT_0}{2} \left( \frac{k}{1+k} \right) \sqrt{(nL)^2 + \frac{l^2}{4}}$$

$$\sin \phi = \frac{nL}{\sqrt{(nL)^2 + \frac{l^2}{4}}}$$

where

- $b, k$  are parameters defining the magnitude of the membrane force,
- $KT_0$  is the resistance of the steel reinforcing mesh per unit width,
- $n$  is a parameter defining the yield line pattern

Substituting the above values into Equation (1) gives,

$$\frac{bKT_0(L - 2nL)}{2} \frac{nL}{\sqrt{(nL)^2 + \frac{l^2}{4}}} = \frac{kbKT_0}{2} \left( \frac{k}{1+k} \right) \sqrt{(nL)^2 + \frac{l^2}{4}} - \frac{bKT_0}{2} \left( \frac{1}{1+k} \right) \sqrt{(nL)^2 + \frac{l^2}{4}}$$

This expression can then be rearranged to give an expression for parameter  $k$ .

$$k = \frac{4na^2(1 - 2n)}{4n^2a^2 + 1} + 1 \quad (5-4)$$

### 5.2.3 Derivation of an expression for parameter b

Considering the fracture of the reinforcement across the short span of the slab, an expression for the parameter  $b$  can be developed. The line EF shown in Figure 5.11 represents the location of the mesh fracture, which will result in a full depth crack across the slab. An upper bound solution for the in-plane moment of resistance along the line EF can be obtained by assuming that all the reinforcement along the section is at ultimate stress ( $f_u$ ) and the centroid of the compressive stress block is at location E in Figure 5.11.

It is assumed that,

$$f_t = k_t f_{sy} \quad (5-5)$$

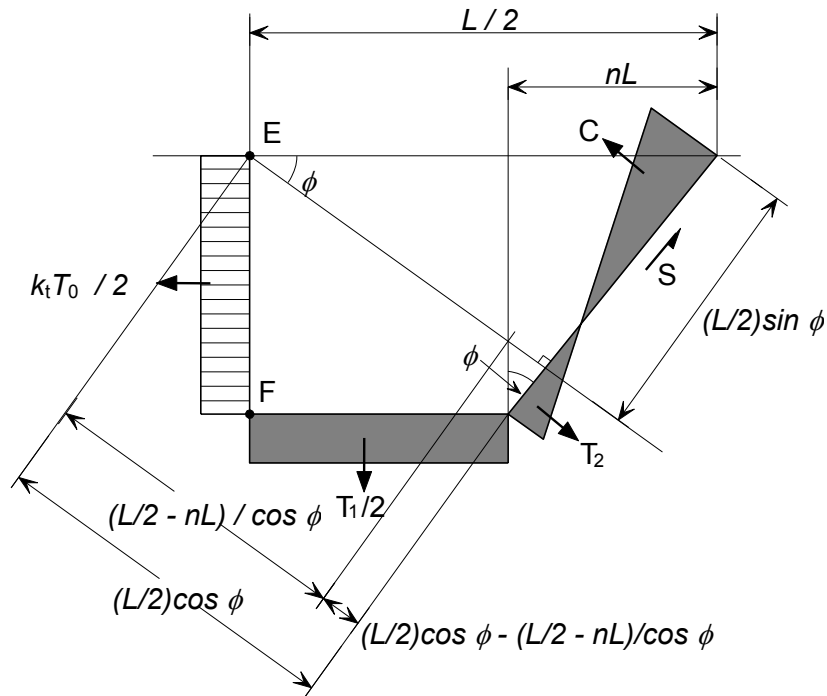
where

$f_y$  is the yield stress of the reinforcing steel.

$k_t$  is the ratio of tensile strength to the yield stress, ( $f_t/f_{sy}$ ).

According to Eurocode 2 part 1.1, the coefficient  $k_t$  varies between 1.05 and 1.35 for room temperature design. However, in fire situation, this coefficient shall be taken equal to 1.0.

Taking moment about E in Figure 5.11,



**Figure 5.11** In-plane stress distribution along fracture line EF

$$\begin{aligned}
& T_2 \left[ \left( \frac{L}{2} \cos \phi - \frac{\left(\frac{L}{2} - nL\right)}{\cos \phi} \right) \frac{1}{\tan \phi} - \frac{1}{3} \left( \frac{1}{1+k} \right) \sqrt{(nL)^2 + \frac{l^2}{4}} \right] \\
& + C \left[ \frac{L}{2} \sin \phi - \frac{l}{3} \left( \frac{k}{k+1} \right) \sqrt{(nL)^2 + \frac{l^2}{4}} \right] \\
& + S \frac{L}{2} \cos \phi - \frac{T_1}{2} \left[ \frac{1}{2} \left( \frac{L}{2} - nL \right) \right] = \frac{k_r T_o l^2}{8}
\end{aligned} \tag{5-6}$$

where

$$\begin{aligned}
\frac{T_1}{2} &= bKT_o \left( \frac{L}{2} - nL \right) \\
T_2 &= \frac{bKT_o}{2} \left( \frac{1}{1+k} \right) \sqrt{(nL)^2 + \frac{l^2}{4}} \\
C &= \frac{kbKT_o}{2} \left( \frac{k}{k+1} \right) \sqrt{(nL)^2 + \frac{l^2}{4}} \\
S &= \frac{bKT_o l}{4nL} (k-1) \sqrt{(nL)^2 + \frac{l^2}{4}} \\
\cos \phi &= \frac{(l/2)}{\sqrt{(nL)^2 + \frac{l^2}{4}}} \\
\sin \phi &= \frac{nL}{\sqrt{(nL)^2 + \frac{l^2}{4}}} \\
\tan \phi &= \frac{nL}{(l/2)}
\end{aligned}$$

Substituting these expressions into Equation (5-6) leads to,

$$\frac{bKT_o}{2} \left( \frac{1}{1+k} \right) \sqrt{(nL)^2 + \frac{l^2}{4}} \left[ \left( \frac{\left(\frac{l}{2}\right)}{\sqrt{(nL)^2 + \frac{l^2}{4}}} \frac{L}{2} - \frac{\left(\frac{L}{2} - nL\right)}{\left(\frac{l}{2}\right)} \sqrt{(nL)^2 + \frac{l^2}{4}} \right) \frac{\left(\frac{l}{2}\right)}{nL} \right. \\
\left. - \frac{1}{3} \left( \frac{1}{1+k} \right) \sqrt{(nL)^2 + \frac{l^2}{4}} \right]$$



$$\begin{aligned}
& + \frac{kbKT_o}{2} \left( \frac{k}{k+1} \right) \sqrt{(nL)^2 + \frac{l^2}{4}} \left[ \frac{nL}{\sqrt{(nL)^2 + \frac{l^2}{4}}} \frac{L}{2} - \frac{1}{3} \left( \frac{k}{1+k} \right) \sqrt{(nL)^2 + \frac{l^2}{4}} \right] \\
& + \frac{bKT_o l}{4nL} (k-1) \sqrt{(nL)^2 + \frac{l^2}{4}} \frac{\left( \frac{l}{2} \right)}{\sqrt{(nL)^2 + \frac{l^2}{4}}} \left( \frac{L}{2} \right) - bKT_o \left( \frac{L}{2} - nL \right) \left[ \frac{l}{2} \left( \frac{L}{2} - nL \right) \right] = \frac{k_t T_o l^2}{8}
\end{aligned}$$

which can be rearranged to give,

$$\begin{aligned}
& \frac{b}{2} \left( \frac{1}{1+k} \right) \left[ \left( \frac{l^2}{8n} - \frac{\left( \frac{L}{2} - nL \right)}{nL} \left( (nL)^2 + \frac{l^2}{4} \right) - \frac{1}{3} \left( \frac{1}{1+k} \right) \left( (nL)^2 + \frac{l^2}{4} \right) \right) \right] \\
& + \frac{b}{2} \left( \frac{k^2}{1+k} \right) \left[ \frac{nL^2}{2} - \frac{k}{3(1+k)} \left( (nL)^2 + \frac{l^2}{4} \right) \right] \\
& + \frac{bl^2}{16n} (k-1) - b \left( \frac{L}{2} - nL \right) \left( \frac{L}{4} - \frac{nL}{2} \right) = \frac{k_t l^2}{8K}
\end{aligned} \tag{5-7}$$

Equation (5-7) can be rewritten as,

$$Ab + Bb + Cb - Db = \frac{1 \cdot l^2}{8K}$$

Hence:

$$b = \frac{k_t l^2}{8K(A + B + C - D)} \tag{5-8}$$

where

$$A = \frac{1}{2} \left( \frac{1}{1+k} \right) \left[ \frac{l^2}{8n} - \frac{\left( \frac{L}{2} - nL \right)}{nL} \left( (nL)^2 + \frac{l^2}{4} \right) - \frac{1}{3} \left( \frac{1}{1+k} \right) \left( (nL)^2 + \frac{l^2}{4} \right) \right],$$

$$B = \frac{1}{2} \left( \frac{k^2}{1+k} \right) \left[ \frac{nL^2}{2} - \frac{k}{3(1+k)} \left( (nL)^2 + \frac{l^2}{4} \right) \right],$$

$$C = \frac{l^2}{16n} (k-1),$$

$$D = \left( \frac{L}{2} - nL \right) \left( \frac{L}{4} - \frac{nL}{2} \right).$$

The parameters  $k$  and  $b$ , which define the in-plane forces, can be calculated using equations (5-4) and (5-8) respectively.

#### 5.2.4 Membrane forces

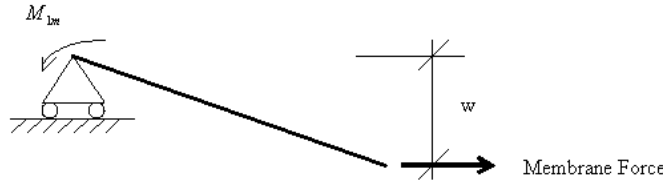
The load bearing capacity for Elements 1 and 2 of the slab can be determined by considering the contribution of the membrane forces to the resistance and the

increase in bending resistance across the yield lines separately as shown below. These effects are expressed in terms of an enhancement factor, to be applied to the lower bound yield line resistance. Initially, the effects of the in-plane shear  $S$  (Figure 5.9) or any vertical shear on the yield line was ignored, resulting in two unequal loads being calculated for Elements 1 and 2 respectively. An averaged value was then calculated, considering contribution of the shear forces.

**Contribution of membrane forces to load bearing capacity.**

**a) Element 1**

According to Figure 5.12, the moment about the support due to membrane force is given by:



**Figure 5.12** Calculating the moment caused by the membrane force

$$M_{1m} = bKT_0 (L - 2nL)w + bKT_0 nLw \left( \frac{3k + 2}{3(1 + k)^2} \right) - bKT_0 nLw \left( \frac{k^3}{3(1 + k)^2} \right)$$

where

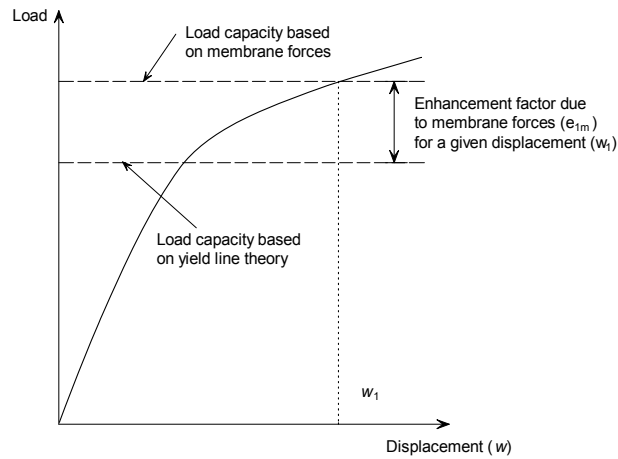
$M_{1m}$  is the moment about the support due to membrane forces for element 1.

The expression reduces to:

$$M_{1m} = KT_0 Lbw \left( (1 - 2n) + \frac{n(3k + 2) - nk^3}{3(1 + k)^2} \right).$$

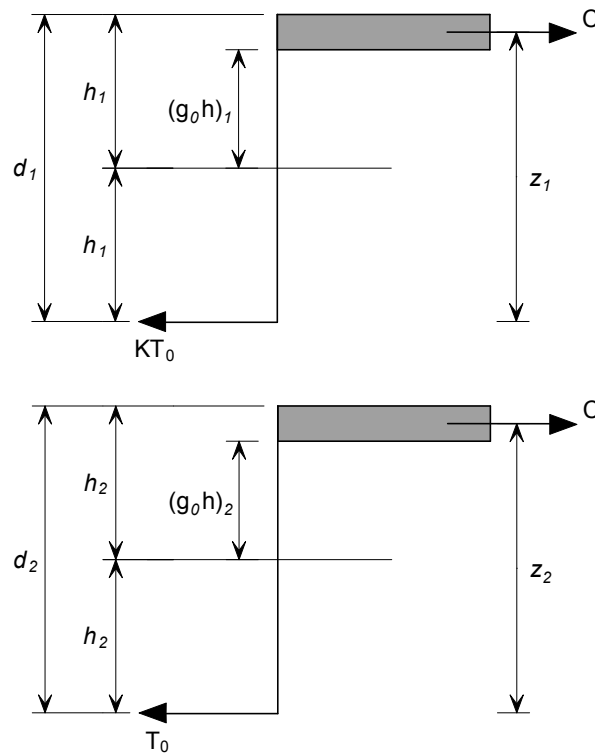
The above formulation defines the contribution from the membrane forces to the load bearing capacity that needs to be added to the contribution due to the enhanced bending capacity in the areas where the slab is experiencing compression forces. For simplicity, the contribution from the membrane forces and enhanced bending action is related to the normal yield line load. This allows an enhancement factor to be calculated for both the membrane force and also the enhanced bending moments. These enhancement factors can finally be added to give the overall enhancement of the slab due to membrane action.

Dividing  $M_{1m}$  by  $\mu M_o L$ , the moment of resistance of the slab, when no axial force is present, allows the effect of tensile membrane action to be expressed as an enhancement of yield line resistance (Figure 5.13).



**Figure 5.13** Enhancement factor due to membrane force

The value of  $\mu M_o$  is obtained by considering Figure 5.14.



**Figure 5.14** Calculation of the moment resistance

The bending moments  $\mu M_o$  and  $M_o$  per unit width of slab in each orthogonal direction are given by:

$$\mu M_o = KT_0 d_1 \left( \frac{3 + (g_0)_1}{4} \right)$$

$$M_o = T_0 d_2 \left( \frac{3 + (g_0)_2}{4} \right)$$

where

$(g_0)_1, (g_0)_2$  are parameters which define the flexural stress block in the two orthogonal directions (see Figure 5.14)

$d_1, d_2$  are the effective depths of the reinforcement in each direction.

The enhancement factor,  $e_{1m}$ , is given by:

$$e_{1m} = \frac{M_{1m}}{\mu M_0 L} = \frac{4b}{3 + (g_0)_1} \left( \frac{w}{d_1} \right) \left( (1 - 2n) + \frac{n(3k + 2) - nk^3}{3(1 + k)^2} \right) \quad (5-9)$$

### b) Element 2

The moment about the support due to the membrane forces is given by:

$$M_{2m} = KT_0 l b w \left( \frac{2 + 3k - k^3}{6(1 + k)^2} \right)$$

where

$M_{2m}$  is the moment about support due to membrane force for element 2.

The effect of tensile membrane action can be expressed as an enhancement of yield line resistance by dividing the moment about the support due to membrane action,  $M_{2m}$  by the moment resistance in the longitudinal direction, when no axial force is present,  $M_0 l$ , which results in,

$$e_{2m} = \frac{M_{2m}}{M_0 l} = \frac{4bK}{3 + (g_0)_2} \left( \frac{w}{d_2} \right) \left( \frac{2 + 3k - k^3}{6(1 + k)^2} \right) \quad (5-10)$$

The effect of the membrane forces on the bending resistance along the yield lines is evaluated by considering the yield criterion when axial load is also present, as given by Wood<sup>[6]</sup>. In the case of the short span the bending moment in the presence of an axial force is given by

$$\frac{M_N}{\mu M_0} = 1 + \alpha_1 \left( \frac{N}{KT_0} \right) - \beta_1 \left( \frac{N}{KT_0} \right)^2 \quad (5-11)$$

where

$$\alpha_1 = \frac{2(g_0)_1}{3 + (g_0)_1}$$

and

$$\beta_1 = \frac{1 - (g_0)_1}{3 + (g_0)_1}$$

Similarly for the long span,

$$\frac{M_N}{\mu M_0} = 1 + \alpha_2 \left( \frac{N}{T_0} \right) - \beta_2 \left( \frac{N}{T_0} \right)^2 \quad (5-12)$$

where

$$\alpha_2 = \frac{2(g_0)_2}{3 + (g_0)_2}$$

and

$$\beta_2 = \frac{1 - (g_0)_2}{3 + (g_0)_2}$$

**Effect of membrane forces on bending resistance**

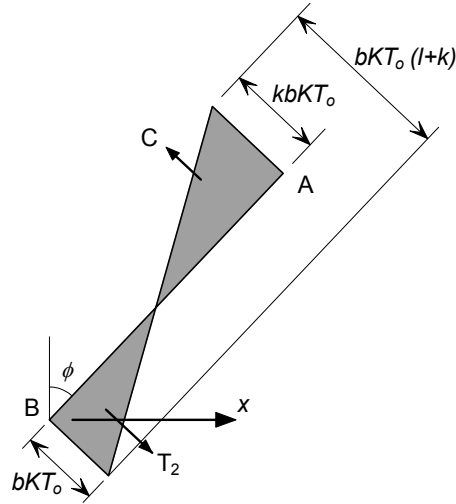
**a) Element 1**

The effect of the membrane forces on the bending resistance is considered separately for the each yield line,

For the yield line BC, the membrane force is constant and equals  $-bKT_0$  and therefore:

$$\left( \frac{M_N}{M_0} \right)_{BC} = 1 - \alpha_1 b - \beta_1 b^2$$

For the yield line AB (Figure 5.15),



**Figure 5.15** Forces applied to element 1, yield line CD

The membrane force across the yield line, at a distance of  $x$  from B is given by:

$$N_x = -bKT_0 + \frac{x}{nL} (K + 1)bKT_0$$

$$N_x = bKT_0 \left( \frac{x(k + 1)}{nL} - 1 \right)$$

Substitution into Equation (8a) gives, for yield lines AB and CD:

$$2 \int_0^{nL} \frac{M}{M_0} dx = 2 \int_0^{nL} \left[ 1 + \alpha_1 b \left( \frac{x(k + 1)}{nL} - 1 \right) - \beta_1 b^2 \left( \frac{x(k + 1)}{nL} - 1 \right)^2 \right] dx$$

This results in:

$$2 \int_0^{nL} \frac{M}{M_0} dx = 2nL \left[ 1 + \frac{\alpha_1 b}{2} (k-1) - \frac{\beta_1 b^2}{3} (k^2 - k + 1) \right]$$

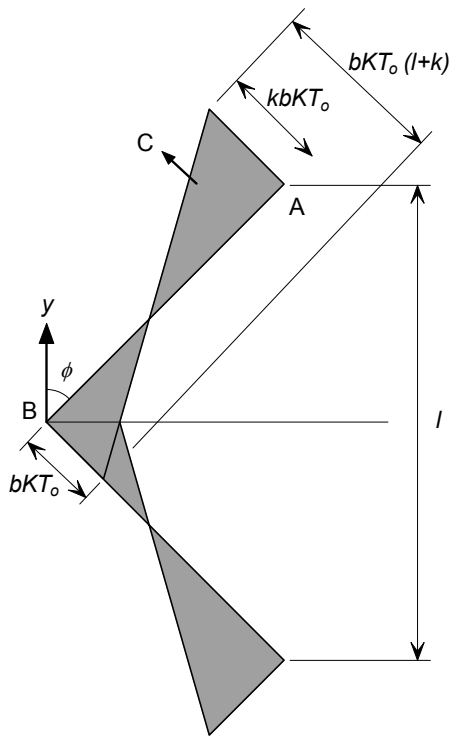
The enhancement of bending resistance due to membrane forces on Element 1 is given by:

$$e_{1b} = \frac{M}{\mu M_0 L} = 2n \left[ 1 + \frac{\alpha_1 b}{2} (k-1) - \frac{\beta_1 b^2}{3} (k^2 - k + 1) \right] + (1-2n)(1 - \alpha_1 b - \beta_1 b^2) \quad (5-13)$$

### b) Element 2

Referring to Figure 5.16 for element 2, the force at a distance  $y$  from B can be expressed as:

$$N_y = -bKT_0 + \frac{y}{l/2} (k+1)bKT_0$$



**Figure 5.16** Forces applied to element 2

By rearranging

$$N_y = bKT_0 \left( \frac{2y(k+1)}{l} - 1 \right)$$

Substitution into Equation (8b) gives:

$$\int_0^{1/2} \frac{M}{M_0} dy = 2 \int_0^{1/2} \left[ 1 + \alpha_2 bK \left( \frac{2y(k+1)}{l} - 1 \right) - \beta_2 b^2 K \left( \frac{2y(k+1)}{l} - 1 \right)^2 \right] dy$$

Resulting in,

$$2 \int_0^{1/2} \frac{M}{M_0} dx = l \left[ 1 + \frac{\alpha_2 b}{2} (k-1) - \frac{\beta_2 b^2}{3} (k^2 - k + 1) \right]$$

Which gives the enhancement factor due to the effect of the membrane forces on the bending resistance according to the following formulation,

$$e_{2b} = \frac{M}{M_0 l} = 1 + \frac{a_2 b K}{2} (k-1) - \frac{\beta_2 b^2 K}{3} (k^2 - k + 1) \quad (5-14)$$

Equations (5-9), (5-10), (5-13) and (5-14) provide the contribution to the load bearing capacity due to the membrane forces and the effect of the membrane forces on the bending resistance of the slab..

Consequently, the combined enhancement factor is obtained for each element as follows

$$e_1 = e_{1m} + e_{1b} \quad (5-15)$$

$$e_2 = e_{2m} + e_{2b} \quad (5-16)$$

As stated earlier, the values  $e_1$  and  $e_2$  calculated based on the equilibrium of elements 1 and 2 will not be the same and Hayes suggests that these differences can be explained by the effect of the vertical or in-plane shear and that the overall enhancement is given by.

$$e = e_1 - \frac{e_1 - e_2}{1 + 2\mu a^2} \quad (5-17)$$

### 5.3 Compressive failure of concrete

The enhancement factor in Section 5.2.1 was derived by considering tensile failure of the mesh reinforcement. However, compressive failure of the concrete in the proximity of the slab corners must also be considered as a possible mode of failure, which in some cases may precede mesh fracture. This was achieved by limiting the value of the parameter 'b', which represents the magnitude of the in-plane stresses.

According to Figure 5.9, the maximum in-plane compressive force at the corners of the slab is given by  $kbKT_0$ . The compressive force due to the bending should also be considered. By assuming that the maximum stress-block depth is limited to 0.45d, and adopting an average effective depth to the reinforcement in both orthogonal directions results in:

$$kbKT_0 + \left( \frac{KT_0 + T_0}{2} \right) = 0.85f_{ck} \times 0.45 \left( \frac{d_1 + d_2}{2} \right)$$

Where,  $f_{ck}$  is the concrete cylinder strength.

Solving for the constant  $b$  gives:

$$b = \frac{1}{kKT_0} \left( 0.85f_{ck} \times 0.45 \left( \frac{d_1 + d_2}{2} \right) - T_0 \left( \frac{K+1}{2} \right) \right) \quad (5-18)$$

The constant  $b$  is then taken as the minimum value given by the Equations (5) and (11).



## **6 DEVELOPMENT OF DESIGN GUIDANCE**

Previous tests at normal temperature, reviewed in Section 4.5, have shown that the load bearing capacity of concrete slabs will be enhanced by membrane forces provide that vertical support is maintained along the slab boundaries. Flat slabs, which only have vertical supports at their corners, do not develop significant tensile membrane forces and therefore benefit little from enhancement due to membrane action.

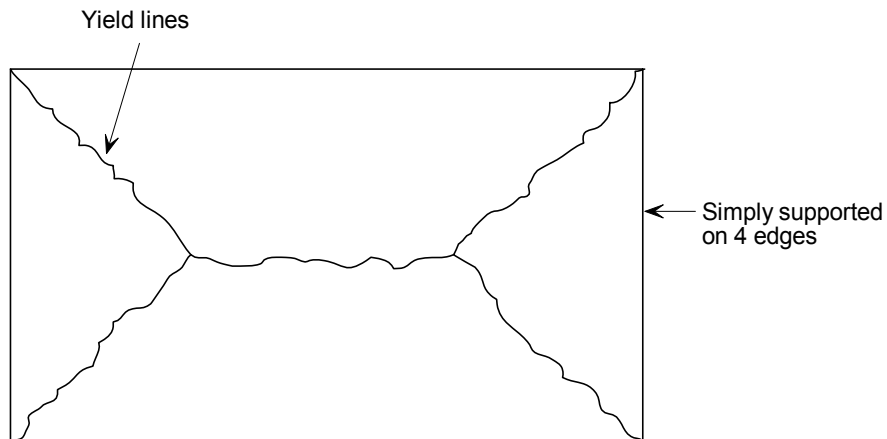
Therefore, for a composite slab supported on a grillage of steel beams in fire conditions, it is important to divide the slab into rectangular areas, referred to as floor design zones, where vertical support can be maintained on the perimeter of each area. These lines of vertical support are achieved by ensuring that the perimeter beams frame into column positions and are fire protected.

At ambient temperature, the floor is continuous over the boundary of each floor design zone. However, in fire conditions it is likely that cracks will form over the perimeter beams, due to the large thermal curvatures experienced by the slab. This may lead to fracture of the reinforcement, either due to the curvature or due to the combination of bending and membrane stresses. The fracture of the reinforcement in these hogging regions will occur before fracture of the reinforcement in the centre of the floor design zone. Therefore, the floor design zones are considered to have no rotational or transverse restraint along the boundary of the slab.

### **6.1 Design assumptions**

For a composite floor slab, the yield line pattern will depend on the behaviour of the unprotected composite beams, which are continually losing strength as the temperature increases. Unlike ambient conditions the load carrying mechanism of the floor changes with increasing temperature. Initially, the composite slab acts as a one-way spanning element supported on the secondary beams. As these beams lose strength with increasing temperature and the behaviour of the slab tends to the behaviour of a simple supported two-way spanning element, resulting in the formation of the yield line pattern shown in Figure 6.1. By assuming that this ultimate failure condition will occur when the beam strength is low relative to the slab, a conservative estimate of capacity can be obtained relatively simply.

The load bearing capacity of the slab is calculated on the assumption that the composite beams have no strength and is based on the yield line pattern which is compatible with the boundary conditions and which provides the lowest load bearing capacity. This resistance is then enhanced by taking account of the tensile membrane effects based on the estimated deflection of the slab and the modes of failure described in Section 5. The bending resistance of the composite beams are added to this enhanced slab resistance in order to give the total load bearing capacity of the system.

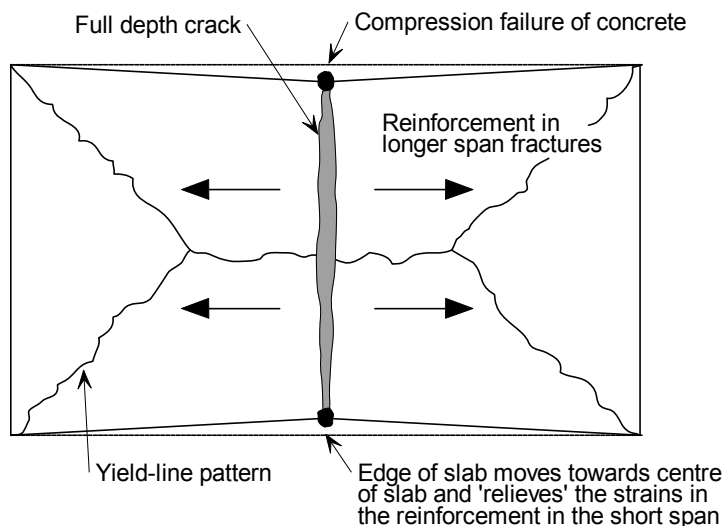


**Figure 6.1** Typical yield line pattern for a rectangular slab simply supported along four edges

## 6.2 Failure criterion

Two modes of failure have been witnessed in room temperature and elevated temperature tests, depending on the reinforcement ratio, slab aspect ratio and the reinforcement ductility. Fracture of the reinforcement across the shorter span dominates the failure mode in most of the lightly reinforced slabs, whilst the heavily reinforced slabs and slabs with highly ductile reinforcement may experience compressive failure at the corners of the slab. Both modes of failure are considered by the simple design method as described in Section 5.2

Most tests conducted at elevated temperatures on simply supported concrete slabs have failed due to full depth crack forming across the shorter span ( $l$ ), as shown in Figure 6.2. The design method presented in Section 5.2 predicts the load bearing capacity for a given deflection. Section 6.2.1 describes the development of an expression for estimating slab deflection just prior to slab failure which is required to calculate the effect of membrane action.



**Figure 6.2** Tensile failure of the slab due to fracture of the reinforcement

## 6.2.1 Slab deflection

As the simple design method is based on plastic theory, deflection cannot be calculated using the method. However, in order to calculate the membrane forces a value of deflection for the slab just prior to failure must be estimated. This estimate of slab deflection will include thermal strains due to the slabs temperature gradient as well as the mechanical strains in the reinforcement.

### 6.2.1.1 Thermal effects

Based on the previous investigations, when the maximum deflection of the slab is greater than almost 0.5 times its depth and tensile forces start to build up at the slab centre, any in-plane restraint to the thermal expansion would increase the vertical displacements (i.e. the slab is in the post-buckling phase) and therefore the tensile membrane action. Conservatively, and in order to allow this approach to be used also for the edge slabs, this beneficial effect is ignored and slab is assumed to be unrestrained.

The composite slab in the fire conditions would experience thermal curvature, which, for an unrestrained slab, increases the vertical displacement without inducing any mechanical strains into the mesh reinforcement. If the temperature distribution through the slab is assumed to be linear then the displacements caused by the thermal deflection is calculated as:

$$\frac{d^2w}{dx^2} = \frac{\alpha(T_2 - T_1)}{h}$$

where

- $w$  = Vertical displacement
- $\alpha$  = Coefficient of thermal expansion
- $T_2$  = Bottom temperature
- $T_1$  = Top temperature
- $h$  = Depth of slab

The vertical displacement of the slab due to thermal curvature can be obtained by integrating the above Equation, which gives:

$$w_\theta = \frac{\alpha(T_2 - T_1)l^2}{8h}$$

where

- $l$  is the length of the shorter span of the slab

This formulation is based on a constant atmospheric temperature throughout the fire compartment. To the estimated displacement, allowing for real fire conditions where uniform heating is less likely, a reduction factor of 2.0 is applied to the above expression. This results in the design value of vertical displacement due to the thermal curvature given by:

$$w_\theta = \frac{\alpha(T_2 - T_1)l^2}{16h}$$

### 6.2.1.2 Mechanical strains in the reinforcement

Assuming that the deflected shape of the slab due to transverse loading is parabolic, the length of the deflected slab is given by the following formulation in which the longer span is (L).

$$L_c = L \left( 1 + \frac{8w^2}{3L^2} - \frac{32w^4}{5L^4} + \dots \right)$$

where

$L_c$  is the length of the curve,

$L$  is the length of longer span of slab at zero displacement,

$w$  is the vertical displacement of the curve.

For flat curves,

$$L_c = L \left( 1 + \frac{8w^2}{3L^2} \right)$$

Hence, the strain in the mesh can be calculated by:

$$\varepsilon = \frac{8w^2}{3L^2}$$

This equation assumes the strain is the same value along the length of the slab. In reality, the slab will experience tension stiffening with strains being concentrated where cracks have occurred. The reinforcement across a crack will also experience a significant increase in the strain, resulting in the eventual fracture of the reinforcement. Therefore, to allow for tension stiffening the component of displacement due to strain in the reinforcement  $w_\varepsilon$  is based on a conservative value of average strain calculated at a stress equal to half the yield stress at room temperature. The displacement is then given by:

$$w_\varepsilon = \sqrt{\left( \frac{0.5 f_{sy}}{E_s} \right) \frac{3L^2}{8}} \quad (1)$$

where

$E_s$  is the room temperature elastic modulus of the reinforcement

$f_{sy}$  is the room temperature yield strength of the reinforcement

The displacements due to strain in the reinforcement calculated using Equation (1) have been compared to maximum deflections measured in tests at room temperature. In all the cases considered, the displacement predicted by equation 1 was lower than the maximum displacement recorded in the test, as shown in Table 6.1.

**Table 6.1** Comparison of allowable deflection from Equation (1) and maximum deflections measured in room temperature tests.

Test	Slab size (m)	Effective Depth (mm)	Reinforcement Diameter (mm)	Bar Spacing (mm)	Steel yield strength (N/mm <sup>2</sup> )	Max. test deflection (mm)	Allowable deflection Eqn. (1) (mm)
BRE	9.56x6.46	66.0	6.0	200	580	223	216
Sawczuk & Winnicki	1.6x1.1	26.0	3.0	30.0	263	127*	25
	2.0x1.0	26.0	3.0	60.0	263	76*	31
Hayes & Taylor	0.914x0.914	15.9	9.5	-†	505	50.8*	19.4
	0.914x1.372	15.9	9.5	-†	505	50.8*	29.1
	0.914x1.829	15.9	9.5	-†	505	50.8*	38.8
Taylor, Maher & Hayes	1.829x1.829	43.6	4.8	76.2	376	81	33.5
	1.829x1.829	37.3	4.8	63.5	376	98	33.5
	1.829x1.829	69.0	4.8	122	376	84	33.5
Brothie & Holley	0.381x0.381	14.2	2.3	-†	414	11.6	7.32
	0.381x0.381	31.0	3.4	-†	379	7.45	7.0

\*test terminated before fracture of the reinforcement

† Data not reported

### 6.2.1.3 Calculation of slab deflection to allow the calculation of membrane forces

The tensile membrane action of the slab is then calculated based on a slab displacement estimated by combining the components due to thermal curvature and strain in the reinforcement, resulting in:

$$w_m = \frac{\alpha(T_2 - T_1)l^2}{16h} + \sqrt{\left(\frac{0.5f_{sy}}{E_s}\right) \frac{3L^2}{8}} \quad (2)$$

This equation results in a conservative estimate of load bearing capacity since:

- the estimated vertical displacements due to thermal curvature are divided by two.
- the thermal curvature is calculated based on the shorter span of the slab
- any additional vertical displacements induced by the restrained thermal expansion when the slab is in a post buckled state are ignored
- any contribution from the steel decking is ignored
- the increase of the mesh ductility with the temperature increase is ignored.

### 6.2.2 Calibration against Cardington fire tests

Bailey & Moore<sup>(12)</sup> demonstrated that the design method in Section 5.2 provided a reasonable prediction of floor slab capacity when compared to the Cardington Fire Tests. As part on this project a further furnace based fire test has been conducted as described in Section 7.

The above expression for slab deflection was compared to the maximum deflections recorded during the Cardington fire tests. The object was to ensure that the deflections estimated would be conservative when compared to actual slab behaviour just prior to failure. The drawback in using these tests for this purpose was that failure was not reached by the slabs tested therefore the maximum measured deflections do not correspond to failure of the slab. However, it is known

that the results of the comparison will be conservative but the degree of conservatism can not be quantified.

Table 6.2 shows the comparison between the limiting deflection given by equation (2) and the maximum measured deflection from each of the Cardington tests. This comparison includes both thermal and mechanical strains, which are impossible to distinguish in test data.

In all cases, Equation (2) gives deflections which are greater than the measured deflections. In order to ensure that the deflection limit is conservative Bailey and Moore<sup>(12)</sup> limited the deflection to those recorded in the tests.

**Table 6.2** Comparison of the displacement given by equation (2) against the maximum displacements recorded in the six Cardington fire tests.

Test	L (m)	l (m)	Deflection due to thermal curvature (mm)	Deflection due to mechanical strain (mm)	Deflection limit Eqn. (2) (mm)	Maximum deflection recorded in test (mm)	Deflection Limit/test deflection
BRE Corner Test	9.0	6.0	135	208	343	269	1.28
British Steel Restrained Beam	9.0	6.0	135	208	343	232	1.50
British Steel 2-D test	14.0	9.0	0*	324	324	293	1.11
BS Corner Test	10.223	7.875	231	237	468	428	1.09
BRE Large Compartment Test	21.0	9.0	303	486	789	557	1.42
BS Office Demo Test	14.6	10.0	373	338	711	641	1.11

\*Due to the small area of slab heated in this test the displacement due to thermal curvature was taken as zero.

For mechanical strains, Bailey and Moore introduced an additional limit as shown below.

$$w_{\varepsilon} = \sqrt{\left(\frac{0.5f_y}{E}\right)_{reinf} \frac{3L^2}{8}} \text{ but } w_{\varepsilon} \leq \frac{l}{30}$$

For thermal deflection they also increased the ‘factor of safety’ from 2 to 2.4 giving the following conservative expressions for estimating slab deflections:

$$w_m = \frac{\alpha(T_2 - T_1)l^2}{19.2h} + \sqrt{\left(\frac{0.5f_{sy}}{E_s}\right) \frac{3L^2}{8}} \quad (3)$$

$$\text{but not more than } \frac{\alpha(T_2 - T_1)l^2}{19.2h} + \frac{l}{30}$$

Table 6.3 shows the comparison between the limiting deflection given by Equation (3). Given that failure did not occur in any of the tests it was felt that it would be overly conservative to reduce the deflection limit to a point where the

ratio of deflection limit to measured deflection was one for all tests. For the large compartment tests this limit appears to be reasonable.

**Table 6.3** *Comparison of the displacement given by equation (3) against the maximum displacements recorded in the six Cardington fire tests.*

Test	L	I	Deflection due to thermal curvature	Deflection due to mechanical strain	Deflection limit Eqn. (3)	Maximum deflection recorded in test	Deflection Limit/test deflection
	(m)	(m)	(mm)	(mm)	(mm)	(mm)	
BRE Corner Test	9.0	6.0	112	200	312	269	1.16
British Steel Restrained Beam	9.0	6.0	112	200	312	232	1.34
British Steel 2-D test	14.0	9.0	0*	300	300	293	1.02
BS Corner Test	10.223	7.875	193	237	430	428	1.00
BRE Large Compartment Test	21.0	9.0	252	300	552	557	0.99
BS Office Demo Test	14.6	10.0	311	333	644	641	1.00

\*Due to the small area of slab heated in this test the displacement due to thermal curvature was taken as zero.

### 6.3 Design methodology

The design methodology advocated in this document is based on two key principles.

- The risk to life safety of the building occupants, fire fighters and others in the vicinity of the building in the event of a fire should not increase relative to current practice as a result of using the method.
- The fire should be contained within its compartment of origin and the application of the design method should not lead to failure of the compartmentation of the building

The design method is intended to apply to composite steel-concrete floor plates supported on composite or non-composite columns. The structural frame should be braced (non-sway), the connections should be simple nominally pinned connections and the concrete floor slab should be constructed using steel decking not exceeding 80 mm in depth and supported on the top flange of the steel section. The steel beams should be designed to act compositely with the floor slab in accordance with the recommendations of EN 1994-1-1. Excluded from the scope of application are slabs with an exposed concrete soffit including precast concrete slabs.

In order to apply the simple design method described in Section 5 to a design scenario, the floor plate being considered must be divided into a number of 'floor design zones'. These floor design zones are bounded on their perimeters by beams (normally fire protected) which satisfy the fire resistance requirements specified for the floor plate. Each floor design zone may include a number of internal secondary beams without fire protection which have a much lower fire resistance. The provision of protected beams on the perimeter of the floor slab is intended to result

in slab behaviour in keeping with the assumption that the perimeter of the floor design zone is simply supported.

For periods of fire resistance of 60 minutes or above the perimeter of the floor design zones should correspond to the column gridlines and the perimeter beams should be connected to the columns at either end.

The composite slab may be designed in accordance with EN 1994-1-1 and should also satisfy the minimum insulation thickness recommended by EN 1994-1-2 in fire conditions. Reinforcement of the composite slab should be achieved using a steel mesh. Reinforcement in the ribs of the slab is not considered in the design method. The inclusion of such reinforcement can have a negative as well as a positive effect on the slab performance in fire conditions, as compressive failure in the concrete may result if the slab is over reinforced.

### 6.3.1 Calculation of load bearing capacity for the slab

The calculation of the yield line capacity of the composite slab and the associated enhancement of this resistance due to large slab deflections is described in detail in Section 5.

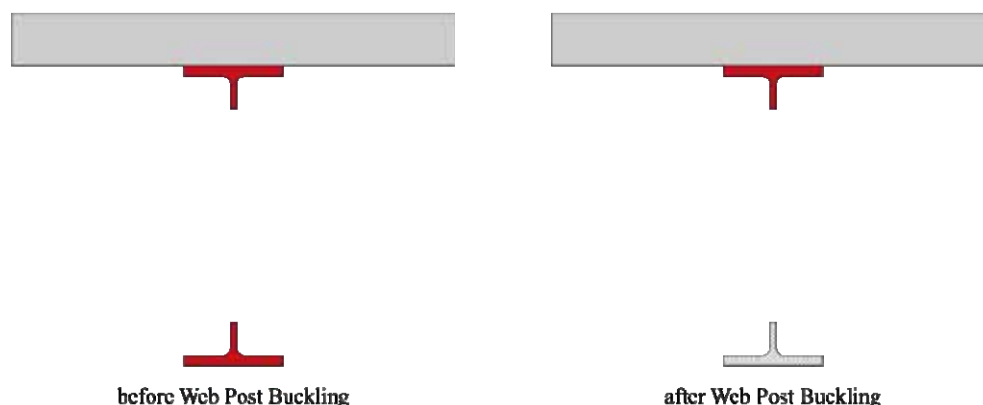
### 6.3.2 Calculation of load bearing capacity for unprotected beams

In fire conditions, the unprotected beams within each floor design zone will add to the tensile resistance of the slab via catenary action.

The temperature of the cross-section of the unprotected beams is calculated using the method given in EN 1994-1-2, 4.3.4.2.2. The bottom flange, the web and the top flange of the steel profile are assumed to be at have each a uniform temperature for the calculation of the moment resistance.

The calculation of the plastic moment resistance of the beams at elevated temperature follows the principles of EN 1994-1-2, 4.3 taking account of the degree of shear connection between the steel section and the concrete. The temperature of the slab is taken as 40 % of the temperature of the top flange

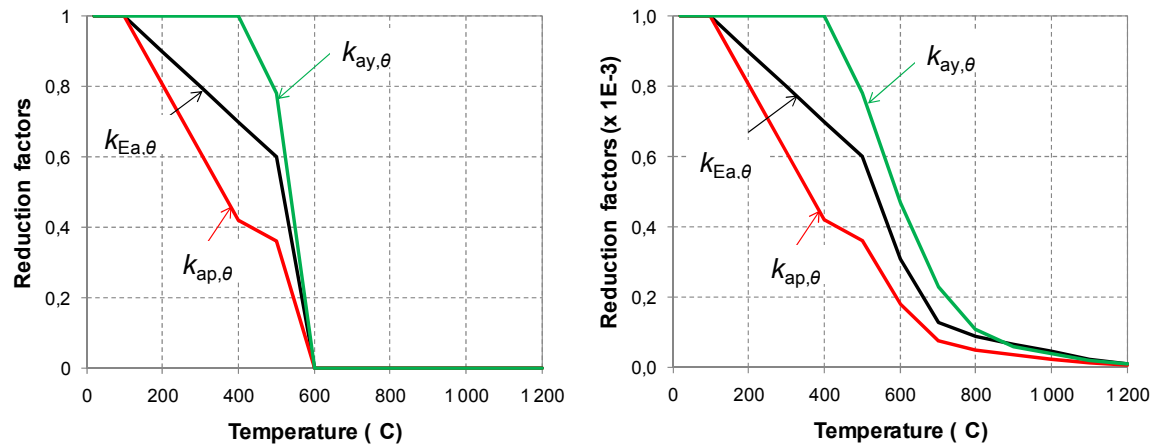
For the plain profiles, the complete steel profile is taken into account. For the Cellular beams, the test performed in Ulster (see paragraph 7.4) showed that after the web post buckling of the Cellular Beam, it is not relevant to take into account the plastic resistance of the complete beam. So after the Web post buckling of the Cellular Beam, in order to be safe sided, only the tension appearing in the upper tee of the section will be taken into account.



**Figure 6.3** : Steel section before and after Web Post Buckling



In order to implement that in the analytical method and to ensure the transition between the complete Cellular Beam profile and the Cellular Beam after the web post buckling, a new material law has been developed for the steel of the lower member:

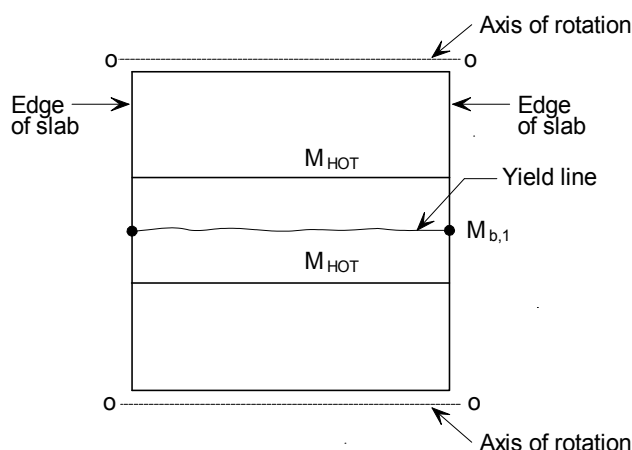


a)  $\theta < 600^\circ\text{C}$  b)  $\theta \geq 600^\circ\text{C}$  and cooling phase

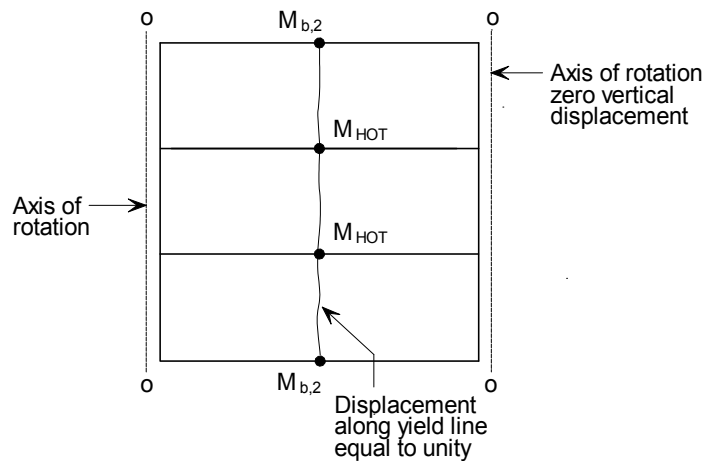
**Figure 6.4** : Reduction factors of structural steel in unprotected cell beam lower tee

## 6.4 Design of fire resisting perimeter beams

The perimeter beams which bound each floor design zone must be designed to achieve the period of fire resistance required by the floor slab. This will ensure that the pattern of yield lines and the associated enhancement due to tensile membrane action which are assumed to occur in the design methodology actually occur in practice. The required moment resistance of the edge beams is calculated by considering alternative yield line patterns that would allow the slab to fold along an axis of symmetry without developing tensile membrane action, as shown by Figure 6.5 and Figure 6.6.



**Figure 6.5** Alternative yield line patterns involving the formation of plastic hinges in the perimeter beams



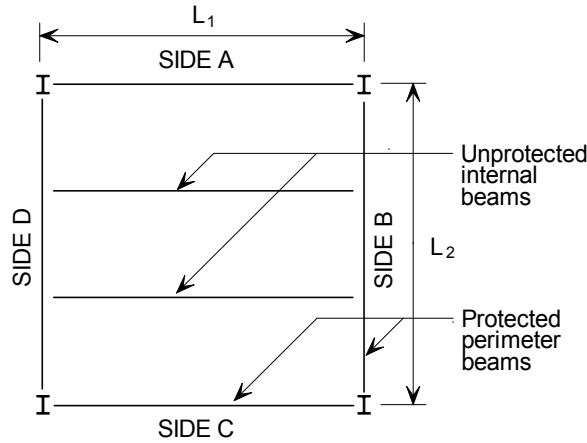
**Figure 6.6** *Alternative yield line patterns involving the formation of plastic hinges in the perimeter beams*

Having calculated the required moment capacity of these beams to ensure that they provide sufficient support to allow development of the tensile membrane enhancement of the slab load bearing resistance, a critical temperature for the beams can be calculated and appropriate levels of fire protection can be applied to ensure that this critical temperature is not exceeded during the required fire resistance period.

The design method described in Section 5 assumes that an envelope pattern of yield lines will form in the slab at the ultimate limit state. In order for this to occur, the beams on the perimeter of the floor design zone must have sufficient moment resistance to prevent a beam and slab mechanism occurring at a lower load level.

For a typical floor design zone, as shown in Figure 6.7, two yield line patterns have been considered which include the formation of a plastic hinge in the perimeter beams. The yield lines may occur across the centre of the slab, either parallel to the unprotected beams in the Span 1 direction with plastic hinges forming in the perimeter beams on Sides A and C or perpendicular to the unprotected beams in the Span 2 direction with plastic hinges forming in the perimeter beams on Side B and D and in the unprotected beams.

Using this pattern of yield lines and equating the internal and external work for the mechanism, the moment resistance of the perimeter beams required to achieve a load bearing capacity equal to that for the floor slab may be determined. The derivation of appropriate design equations is given below.

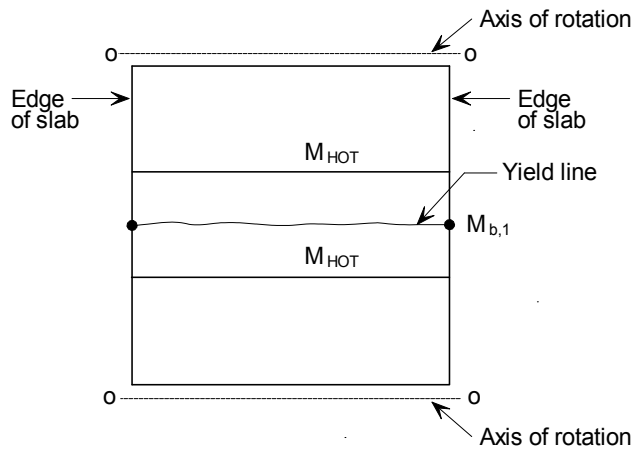


**Figure 6.7** Typical floor design zone

### 6.4.1 Unprotected beams with edge beams on both sides

#### 6.4.1.1 Yield line parallel to unprotected beams

This case considers the required moment resistance of the perimeter beams on Sides B and D of the floor design zone. These beams are also assumed to be at the edge of the slab. A single yield line is assumed to form across the centre of the floor design zone in the Span 1 direction, as shown in Figure 6.8. In keeping with the assumptions of the design method the perimeter of the floor design zone is assumed to be simply supported.



**Figure 6.8** Yield line in parallel to the unprotected beams edge condition on Sides B and D

Considering a unit displacement along the yield line, the rotation of the yield line can be calculated as follows:

$$\text{Yield line rotation} = 2 \frac{1}{L_2/2} = \frac{4}{L_2}$$

The internal work done due to the rotation of the yield line is given by:

$$\text{Internal Work} = (ML_{1,\text{eff}} + 2M_{b,1}) \frac{4}{L_2} = \frac{4ML_{1,\text{eff}}}{L_2} + \frac{8M_{b,1}}{L_2}$$

where

$L_{1,eff}$  is the effective length of the yield line discounting the effective width of slab assumed to act with the perimeter beams where these are design as composite members.

$M$  is the moment resistance of the slab per unit length of yield line

For a uniform load on the slab,  $p$ , the external work due to the displacement is given by:

$$\text{External Work} = \frac{1}{2}pL_1L_2$$

Equating internal and external work gives:

$$pL_1L_2 = \frac{8ML_{1,eff}}{L_2} + \frac{16M_{b,1}}{L_2}$$

If the load on the slab is the load bearing capacity determined in accordance with Section 5, the required minimum values of moment resistance for the perimeter beams on Side B and D is given by:

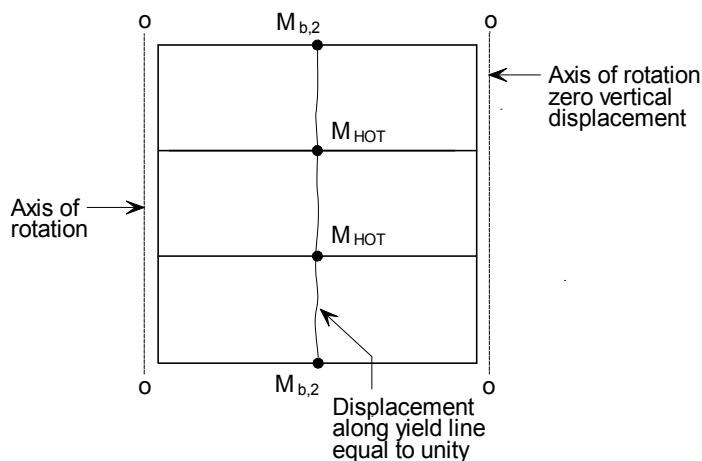
$$M_{b,1} = \frac{pL_1L_2^2 - 8ML_{1,eff}}{16}$$

where

$p$  is the uniformly distributed load to be supported by the floor design zone in fire conditions.

#### 6.4.1.2 Yield line perpendicular to unprotected beams

This case considers the required moment resistance of the perimeter beams on Sides A and C of the floor design zone. A single yield line is assumed to form across the centre of the floor design zone in the Span 2 direction, as shown in Figure 6.9. In keeping with the assumptions of the design method the perimeter of the floor design zone is assumed to be simply supported.



**Figure 6.9** Yield line perpendicular to the unprotected beams edge condition on Sides A and C

Considering a unity displacement along the yield line the rotation of the yield line can be calculated as follows:

$$\text{Yield line rotation} = 2 \frac{1}{L_1/2} = \frac{4}{L_1}$$

The internal work done due to the rotation of the yield line is given by:

$$\begin{aligned} \text{Internal Work} &= (ML_{2,\text{eff}} + 2M_{b,2} + nM_{\text{HOT}}) \frac{4}{L_1} \\ &= \frac{4ML_{2,\text{eff}}}{L_1} + \frac{8M_{b,2}}{L_1} + \frac{4nM_{\text{HOT}}}{L_1} \end{aligned}$$

where

$L_{2,\text{eff}}$  is the effective length of the yield line discounting the effective width of slab assumed to act with the perimeter beams where these are designed as composite members and the composite unprotected internal beams.

$M$  is the moment resistance of the slab per unit length of yield line

The external work due to the slab displacement is given by:

$$\text{External Work} = \frac{1}{2} pL_1L_2$$

Equating internal and external work gives:

$$pL_1L_2 = \frac{8ML_{2,\text{eff}}}{L_1} + \frac{16M_{b,2}}{L_1} + \frac{8nM_{\text{HOT}}}{L_1}$$

If the load on the slab is the load bearing capacity determined in accordance with Section 5, the required minimum values of moment resistance for the perimeter beams on Side A and C is given by:

$$M_{b,2} = \frac{pL_1^2 L_2 - 8ML_{2,\text{eff}} - 8nM_{\text{HOT}}}{16}$$

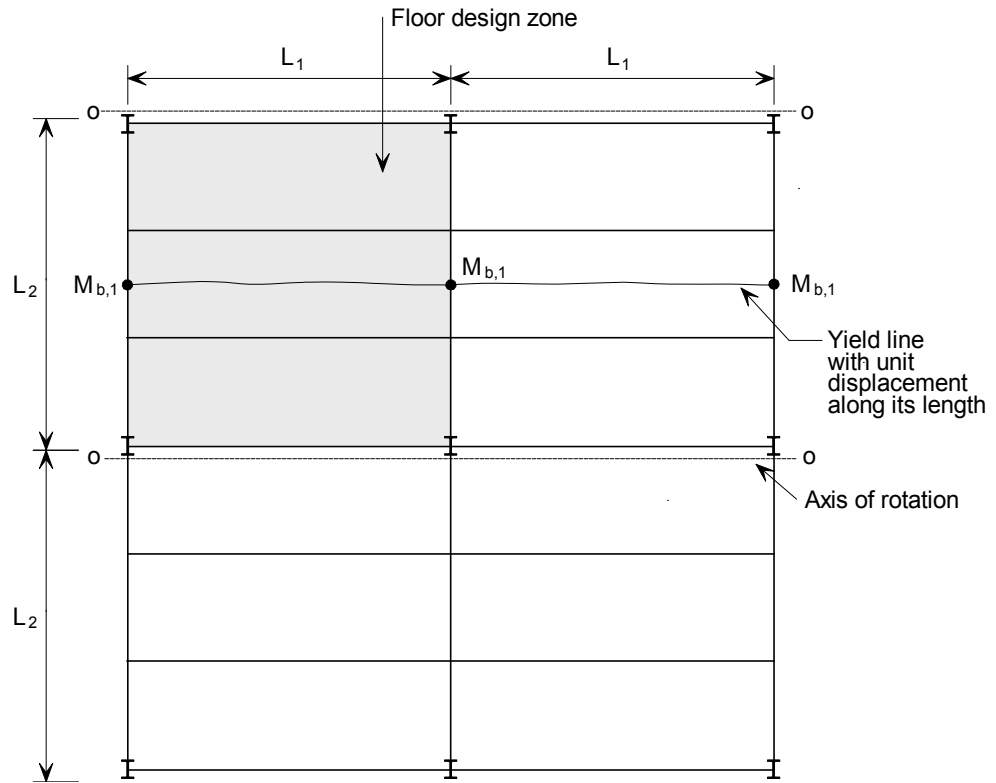
where

$p$  is the uniformly distributed load to be supported by the floor design zone in fire conditions.

## 6.4.2 Unprotected beams with an edge beam on one side

### 6.4.2.1 Yield line parallel to unprotected beams

This case considers the required moment resistance of the perimeter beams on Sides B and D of the floor design zone. In this case the beam on side B is an internal perimeter beam. As the software only deals with an isolated floor plate the calculation of resistance for an internal perimeter beam must assume that the floor design zone is adjacent to an identical area of slab sides where internal beams have been specified. A single yield line is assumed to form across the centre of the floor design zone in the Span 1 direction, as shown in Figure 6.8.



**Figure 6.10** Yield line parallel to the unprotected beams edge condition on Side D

Considering a unit displacement along the yield line the rotation of the yield line can be calculated as follows:

$$\text{Yield line rotation} = 2 \frac{1}{L_2/2} = \frac{4}{L_2}$$

The internal work done due to the rotation of the yield line is given by:

$$\text{Internal Work} = (2ML_{1,\text{eff}} + 3M_{b,1}) \frac{4}{L_2} = \frac{8ML_{1,\text{eff}}}{L_2} + \frac{12M_{b,1}}{L_2}$$

The external work due to the slab displacement is given by:

$$\text{External Work} = \frac{1}{2} p 2L_1 L_2$$

Equating internal and external work gives:

$$pL_1 L_2 = \frac{8ML_{1,\text{eff}}}{L_2} + \frac{12M_{b,1}}{L_2}$$

If the load on the slab is the load bearing capacity determined in accordance with Section 5, the required minimum values of moment resistance for the perimeter beams on Side B and D is given by:

$$M_{b,1} = \frac{pL_1 L_2^2 - 8ML_{1,\text{eff}}}{12}$$

where

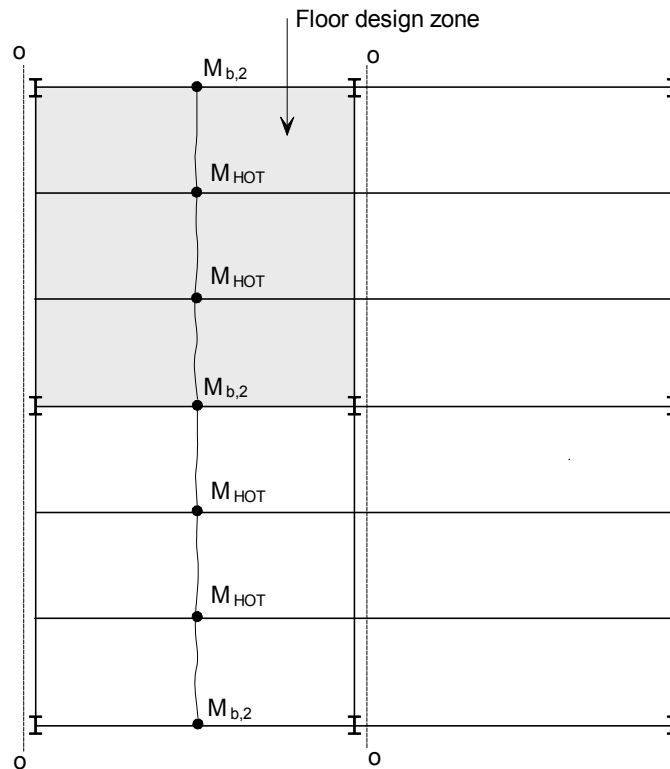
$L_{1,\text{eff}}$  is the effective length of the yield line discounting the effective width of slab assumed to act with the perimeter beams where these are design as composite members.

$M$  is the moment resistance of the slab per unit length of yield line

$p$  is the uniformly distributed load to be supported by the floor design zone in fire conditions.

#### 6.4.2.2 Yield line perpendicular to unprotected beams

A single yield line is assumed to form across the centre of the floor design zone in the Span 2 direction, as shown in Figure 6.11.



**Figure 6.11** Yield line perpendicular to the unprotected beams edge condition on Side A

Considering a unity displacement along the yield line the rotation of the yield line can be calculated as follows:

$$\text{Yield line rotation} = 2 \frac{1}{L_1/2} = \frac{4}{L_1}$$

The internal work done due to the rotation of the yield line is given by:

$$\begin{aligned} \text{Internal Work} &= (2ML_{2,\text{eff}} + 3M_{b,2} + 2nM_{\text{HOT}}) \frac{4}{L_1} \\ &= \frac{8ML_{2,\text{eff}}}{L_1} + \frac{12M_{b,2}}{L_1} + \frac{8nM_{\text{HOT}}}{L_1} \end{aligned}$$

The external work due to the slab displacement is given by:

$$\text{External Work} = \frac{1}{2} p L_1 2 L_2$$

Equating internal and external work gives:

$$p L_1 L_2 = \frac{8 M L_{2,\text{eff}}}{L_1} + \frac{12 M_{b,2}}{L_1} + \frac{8 n M_{\text{HOT}}}{L_1}$$

If the load on the slab is the load bearing capacity determined in accordance with Section 5, the required minimum values of moment resistance for the perimeter beams on Side A and C is given by:

$$M_{b,2} = \frac{p L_1^2 L_2 - 8 M L_{2,\text{eff}} - 8 n M_{\text{HOT}}}{12}$$

where

$L_{2,\text{eff}}$  is the effective length of the yield line discounting the effective width of slab assumed to act with the perimeter beams where these are design as composite members and the composite unprotected internal beams.

$M$  is the moment resistance of the slab per unit length of yield line

$p$  is the uniformly distributed load to be supported by the floor design zone in fire conditions.

### 6.4.3 Floor zone without edge beams

For zones where none of the perimeter beams are edge beams, it is conservative to use the values determined by the expressions in 6.4.2.

### 6.4.4 Design of edge beams

It is common practice for beams at the edge of floor slabs to be designed as non composite. This is because the costs of meeting the requirements for transverse shear reinforcement are more than the costs of installing a slightly heavier non composite beam. However, for fire design, it is important that the floor slab is adequately anchored to the edge beams, as these beams will be at the edge of floor design zones. For this purpose, if edge beams are designed as non composite, they must have shear connectors at not more than 300 mm centres and U-bars should be provided to tie the edge beam to the composite slab.

## 6.5 Thermal Analysis

The FRACOF software uses a 2D finite difference heat transfer method to predict the temperature distribution within the composite slab. This method has been used for many years by SCI to predict the temperature distributions in steel and steel-concrete composite cross sections and has been shown to be able to reasonably predict the behaviour of sections in fire resistance tests.

The object to be analysed must defined on a rectangular grid of cells. The method can also analyse the sloping sides of trapezoidal or re-entrant composite slabs by using configuration factors given below.

The thermal properties of steel and concrete used by the FRACOF software are based on the values given by EN1994-1-2.



The thermal actions are calculated on the basis of the net heat flux,  $\dot{h}_{\text{net}}$  to which the surface of the member is exposed. The net heat flux is determined considering the heat transfer by convection and radiation.

$$\dot{h}_{\text{net}} = \dot{h}_{\text{net,c}} + \dot{h}_{\text{net,r}} \quad (12)$$

The net convective heat flux component is determined as follows:

$$\dot{h}_{\text{net,c}} = \alpha_c (\theta_g - \theta_m) \quad (13)$$

Where

$\alpha_c$  is the coefficient of heat transfer by convection

$\theta_g$  is the gas temperature

$\theta_m$  is the surface temperature of the member

When carrying out a thermal analysis for a member exposed to the standard temperature –time curve the coefficient of heat transfer by convection on the exposed face is taken as  $\alpha_c = 25 \text{ W/m}^2\text{K}$ .

For natural fire models the coefficient of heat transfer by convection is increased to  $\alpha_c = 35 \text{ W/m}^2\text{K}$ .

On the unexposed side of the slab the net heat flux is based on heat transfer by convection, but the coefficient of heat transfer by convection is taken as  $\alpha_c = 9 \text{ W/m}^2\text{K}$ , to allow for the effects of heat transfer by radiation which are not considered explicitly in the model.

The net radiative heat flux is determined from the following formula

$$\dot{h}_{\text{net,r}} = \Phi \varepsilon_m \varepsilon_f \sigma \left[ (\theta_r + 273)^4 - (\theta_m + 273)^4 \right] \quad (14)$$

Where

$\Phi$  is the configuration factor

$\varepsilon_m$  is the surface emissivity of the member

$\varepsilon_f$  is the emissivity of the fire

$\sigma$  is the Stephan Boltzmann constant ( $5,67 \times 10^{-8} \text{ W/m}^2\text{K}^4$ )

$\theta_r$  is the effective radiation temperature of the fire

$\theta_m$  is the surface temperature of the member

The emissivity of the fire is taken as  $\varepsilon_f = 1.0$  in accordance with the recommended value in EN1994-1-2. The emissivity of the member may be determined from Table 6.4.

### 6.5.1 Configuration Factors

For steel decking profiles the following configuration factors are used to modify the net heat flux incident on each surface. The locations in which the following factors are applied are shown in Figure 6.12 for trapezoidal deck profiles and in Figure 6.13 for re-entrant deck profiles.

#### Trapezoidal Profiles

The bottom flange of the trapezoidal profile is assumed to have a configuration factor of 1.0. For the top flange the configuration factor,  $\Phi_{TOP}$ , is calculated as follows.

$$\Phi_{TOP} = \frac{2 \tan^{-1} \left( \frac{h}{2(p - b_1)} \right)}{3.14}$$

Similarly for the sloping web of the trapezoidal profile, the configuration factor,  $\Phi_{SIDE}$ , is calculated as follows,

$$\Phi_{SIDE} = 0.5 \frac{L}{x + y}$$

#### Re-entrant Deck

The bottom flange of re-entrant steel profiles is assumed to have a configuration factor of 1.0. The configuration factor for the surfaces of the re-entrant dovetail is calculated as follows,

$$\Phi_{INT} = 0.3 \frac{L}{x + y}$$

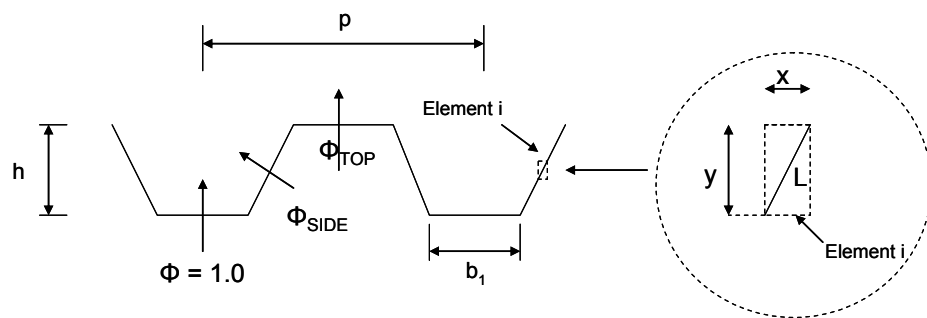
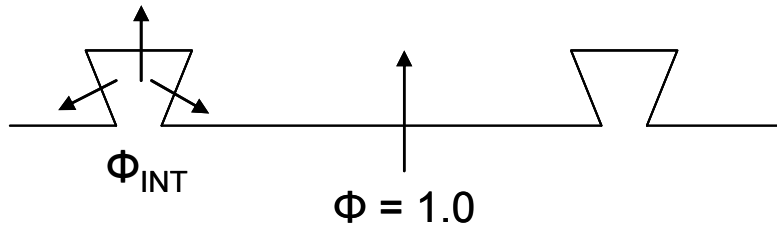


Figure 6.12 Configuration Factors for trapezoidal decks



**Figure 6.13** Configuration Factors for re-entrant decks

### 6.5.2 Material Properties

The following material properties are used for steel and concrete. These values are based on the recommendations of EN1994-1-2. Table 6.4 shows the values of surface emissivity, density and moisture content used for steel, normal weight concrete and light weight concrete.

**Table 6.4** Material properties for steel and concrete

	Steel	NWC	LWC
Emissivity, $\varepsilon_m$	0.7	0.7	0.7
Density, $\rho$	7850	2300	1850
% moisture by mass	0	4	4

The specific heat capacity of steel,  $C_a$ , for all structural and reinforcing steel is given by the following temperature dependant formulae:

$$C_a = 425 + 0.773\theta - 0.00169\theta^2 + 0.00000222\theta^3 \quad (\text{J/kg K}) \quad \text{for } 20^\circ\text{C} \leq \theta \leq 600^\circ\text{C}$$

$$C_a = 666 - \frac{13002}{(\theta - 738)} \quad (\text{J/kg K}) \quad \text{for } 600^\circ\text{C} \leq \theta \leq 735^\circ\text{C}$$

$$C_a = 545 - \frac{17820}{(\theta - 731)} \quad (\text{J/kg K}) \quad \text{for } 735^\circ\text{C} \leq \theta \leq 900^\circ\text{C}$$

$$C_a = 650 \quad (\text{J/kg K}) \quad \text{for } 900^\circ\text{C} \leq \theta \leq 1200^\circ\text{C}$$

The following temperature dependant values of specific heat capacity,  $C_c$ , are used for normal weight dry concrete with siliceous or calcareous aggregates.

$$C_c = 900 \quad (\text{J/kg K}) \quad \text{for } 20^\circ\text{C} \leq \theta \leq 100^\circ\text{C}$$

$$C_c = 900 + (\theta - 100) \quad (\text{J/kg K}) \quad \text{for } 100^\circ\text{C} \leq \theta \leq 200^\circ\text{C}$$

$$C_c = 1000 + (\theta - 200)/2 \quad (\text{J/kg K}) \quad \text{for } 200^\circ\text{C} \leq \theta \leq 400^\circ\text{C}$$

$$C_c = 1100 \quad (\text{J/kg K}) \quad \text{for } 400^\circ\text{C} \leq \theta \leq 1200^\circ\text{C}$$

As recommended by EN1994-1-2 the following temperature independent value of specific heat capacity is assumed for lightweight concrete.

$C_c = 840$  (J/kg K) for all temperatures

The thermal conductivity of steel is defined using the following temperature dependent relationship.

$$\lambda_a = 54 - 0.033(\theta - 20) \quad \text{but not less than } 27.3 \quad (\text{W/mK})$$

For normal weight concrete the upper limit of thermal conductivity as defined by EN1994-1-2 has been used. The thermal conductivity for normal weight concrete is determined from the following temperature dependent relationship.

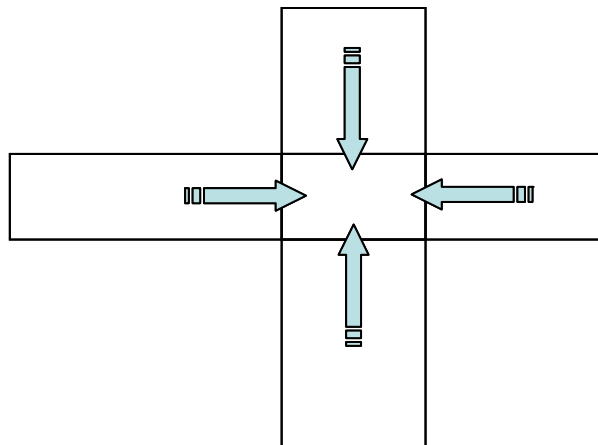
$$\lambda_c = 2 - 0.2451(\theta/100) + 0.0107(\theta/100)^2 \quad (\text{W/mK})$$

The thermal conductivity of lightweight concrete is also temperature dependent and is given by the following formula.

$$\lambda_c = 1 - (\theta/1600) \quad \text{but not less than } 0.5 \quad (\text{W/mK})$$

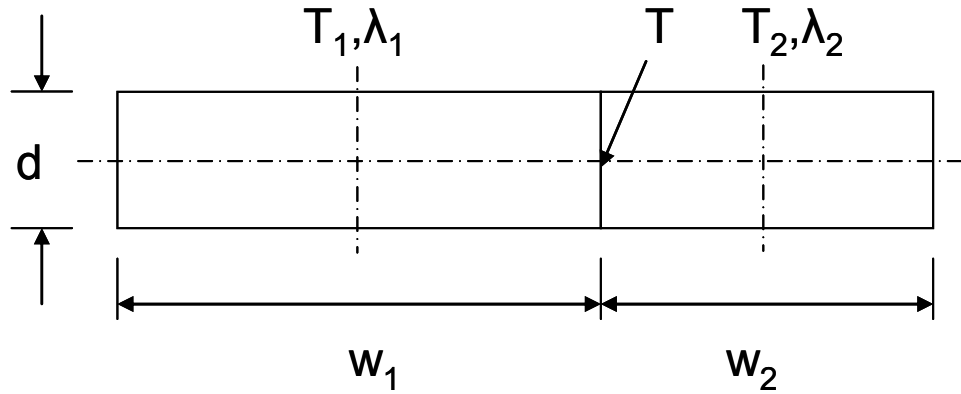
### 6.5.3 Internal heat transfer by conduction

The thermal analysis computes the conducted heat transfer between a cell and the four cells above, below and to the sides (Figure 6.14). No other cells are involved.



**Figure 6.14** Basis of conductive heat transfer

The heat transferred per unit time depends on the sizes of the cells, the temperature of each cells and the thermal conductivity of each cell. Each pair of cells are considered in turn and the net heat transferred into or out of a cell is computed. The basic conduction model is illustrated in Figure 6.15.



**Figure 6.15** Basic conduction model

The temperature of each cell is defined at its centre ( $T_1$ ,  $T_2$ ). The temperature of the interface between the cells is  $T$ . The heat transfer from cell 1 to the interface is the same as the heat transfer from the interface to cell 2. The thermal conductivities of each cell are  $\lambda_1$  and  $\lambda_2$ .

The heat transfer per unit time from the centre of cell 1 to the interface is:

$$h = \frac{2D\lambda_1}{w_1}(T - T_1)$$

This is equal to the heat transfer per unit time from the interface to the centre of cell 2:

$$h = \frac{2D\lambda_2}{w_2}(T_2 - T)$$

Thus, by eliminating the interface temperature,  $T$ :

$$h = \frac{(T_2 - T_1)}{\left(\frac{w_1}{2D\lambda_1} + \frac{w_2}{2D\lambda_2}\right)} \text{ per unit time}$$

This equation is used to compute the heat transfer between all cells. For each cell, the value of:

$$\frac{w}{2D}$$

is precalculated. The value of thermal conductivity will often vary with temperature and is calculated at preset intervals (normally 30 seconds) to speed up computation.

#### **6.5.4 Design temperatures for unprotected steel beams**

The design temperature of the unprotected steel beams are calculated based on the simple method given in EN1994-1-2 Section 4.3.4.2.2. The increase in steel temperature during a small time interval is calculated using the following equation.

$$\Delta\theta_{a,t} = k_{\text{shadow}} \left( \frac{1}{c_a \rho_a} \right) \left( \frac{A_i}{V_i} \right) \dot{h}_{\text{net}} \Delta t$$

Where

$k_{\text{shadow}}$  is the correction factor for shadow effect

$\rho_a$  is the density of the steel

$\Delta t$  is the time interval

$A_i/V_i$  is the section factor for part i of the cross section

The FRACOF software calculates the steel temperature for the bottom flange of the section for time increments of 2.5 seconds. The correction factor for the shadow effect is taken as 1.0.

The section factor for the bottom flange is expressed as a function of flange thickness,  $e_1$ , as follows

$$A_i/V_i = \frac{2000}{e_1}$$

The material properties are given in Section 6.5.2.

The net heat flux is calculated as shown in Equation 12, with the convective and radiative components calculated as shown by Equations 13 and 14 respectively. When calculating the radiative heat flux using Equation 14 the configuration factor should be taken as 1.0.

# 7 FIRE RESISTANCE TEST OF A FULL SCALE COMPOSITE FLOOR SYSTEM

## 7.1 Scope

As described in the Section 5, the simple design method was developed mainly on the basis of full scale natural fire tests in which floors were subjected to fully developed compartment fires. The design concept could also be applied in principle to fire design using the standard temperature-time curve. However, several questions require further investigation, such as the influence of:

- long duration fires (up to 120 minutes)
- different construction details
- the effect of higher values of design actions

These considerations resulted in a furnace fire test being undertaken as part of the FRACOF project. This latter was intended to provide experimental evidence about the behaviour of composite steel and concrete floors exposed to the standard temperature-time curve and to enlarge the application of the design concept based on membrane action. In addition, in order to investigate the fire resistance of connections between concrete slab and steel members at the edge parts of composite floor subjected to large deflection under membrane action, another furnace fire test was carried out in the framework of COSSFIRE project. The tests were conducted on two different full scales composite steel and concrete floor specimens in accordance with EN1365-2. The observed fire performance of these floor systems during the tests was extremely satisfactory and revealed a solid robustness of such type of structure systems in fire situation.

## 7.2 FRACOF Test

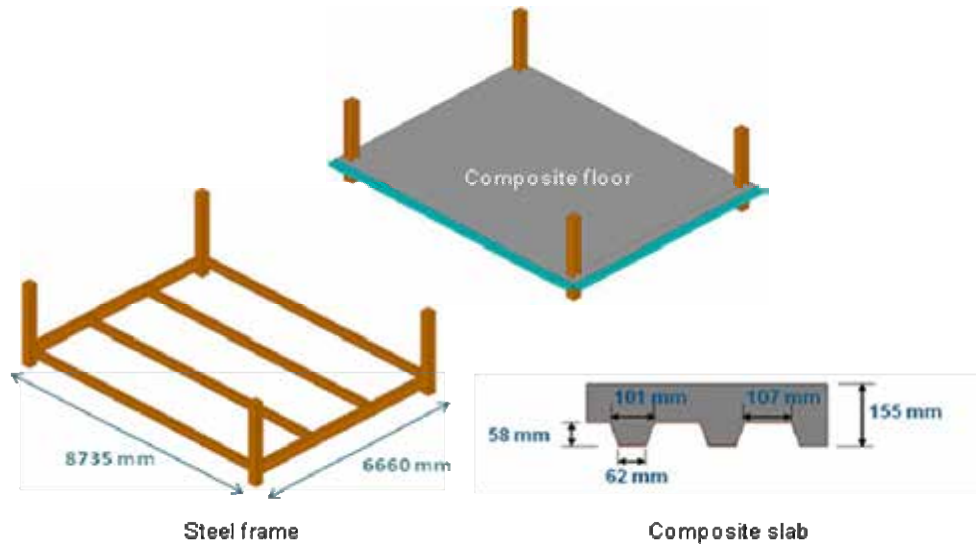
### 7.2.1 Test specimen

The arrangement of the test specimen is shown in Figure 7.1. The composite steel and concrete floor was composed of four secondary beams, two primary beams, four short columns and a 155 mm thick floor slab.

The test specimen was designed to achieve 120 minutes fire resistance. The beams framing into the column positions were fire protected and the secondary beams in the centre of the floor slab were left unprotected. The load bearing capacity of the test specimen was calculated in accordance with the simple design method, treating the test specimen as a floor design zone, see Section 6. This design showed that locating a steel reinforcing mesh with an area of  $256 \text{ mm}^2/\text{m}$  in both directions 50 mm below the top surface of the slab would provide adequate load bearing capacity. The simple design method predicted that the test specimen would have a load bearing capacity of  $7.58 \text{ kN/m}^2$ , following 120 minutes exposure to the standard temperature-time curve. The thickness of the slab was selected in order to fulfil the insulation requirements for 120 minutes fire resistance in accordance with the guidance given in EN 1994-1-2<sup>(33)</sup>.

The steel beams were connected to the concrete slab with headed studs. Beam to column joints were made using flexible endplates (to the flanges of the column) and double angle cleats (to the column web). Beam to beam joints were fabricated from double angle cleats (Figure 7.2). The composite steel and concrete slab was

constructed with 0.75mm thick COFRAPLUS60 steel decking which has a trapezoidal profile. This steel decking is commonly used in the French market. This deck has a small volume of concrete in the ribs and is therefore likely to heat up more quickly in a fire than other decks with a similar geometry.



**Figure 7.1** Fire test set-up

The dimensions of the test specimen were:

- span of secondary beam: 8.735 m
- span of primary beam: 6.66 m
- span of composite slab: 2.22 m
- total length of each steel column: 2.5 m, with 0.8 m below composite slab

The following characteristic values of actions were considered in the design of the structural members for this floor:

- Permanent action: self weight of the structure plus 1.25 kN/m<sup>2</sup> for non-structural elements.
- variable action: 5.0 kN/m<sup>2</sup>

For room temperature design, the following combination of actions was considered in accordance with EN1990.

$$\sum \gamma_{G,j,\text{sup}} G_{k,j,\text{sup}} + \gamma_{Q,1} Q_{k,1}$$

Where

$\gamma_{G,j,\text{sup}}$  is the partial factor for permanent action, j (taken as 1.35)

$G_{k,j,\text{sup}}$  is the permanent action, j

$\gamma_{Q,1}$  is the partial factor for the leading variable action (taken as 1.5)

$Q_{k,1}$  is the leading variable action.



On the basis of the above loading, the cross sections of all steel members and the shear connection of the composite beams was verified in accordance with the requirements of EN 1994-1-1<sup>(34)</sup> for room temperature design of composite structures. The steel joints were designed according to the requirements of EN 1993-1-8<sup>(35)</sup>. The following section sizes were selected for the main structural members:

- secondary beams: IPE300 with the steel grade of S235
- primary beams: IPE400 with the steel grade of S355
- columns: HEB260 with the steel grade of S235

Normal weight Grade C30/37 concrete was used for the floor slab.



(a) Beam to column joints with flexible end plates and double angle web cleats (b) Beam to beam joints with double angle web cleats

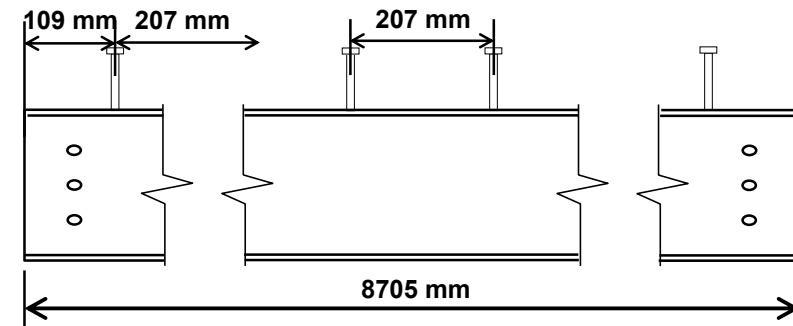
**Figure 7.2** Steel member joints

Actual material properties of the steel and concrete were measured at room temperature. Nominal and measured values are given in Table 7.1.

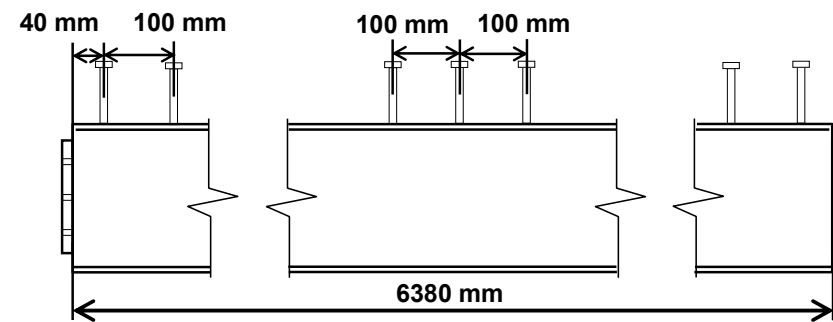
**Table 7.1** Material properties of tested elements

Type of material	Mechanical property items			
<b>Secondary Beams Grade S235</b>	Yield stress (MPa)		Ultimate tensile strength (MPa)	Measured maximum elongation
	Nominal	Measured	Measured	
	235	311	446	31.6 %
<b>Primary Beams Grade S355</b>	Yield stress (MPa)		Ultimate tensile strength (MPa)	Measured maximum elongation
	Nominal	Measured	Measured	
	355	423	549	29.9 %
<b>Steel Reinforcing mesh Grade B500A</b>	Yield stress (MPa)		Ultimate tensile strength (MPa)	Measured maximum elongation
	Nominal	Measured	631	
	500	594		15.5 %
<b>Concrete C30/37</b>	Compressive strength (MPa)			
	Characteristic value		Measured value	
	30		36.7	

The shear connectors were studs with a diameter of 19 mm and a height of 125 mm, the distribution of which is shown in Figure 7.3.



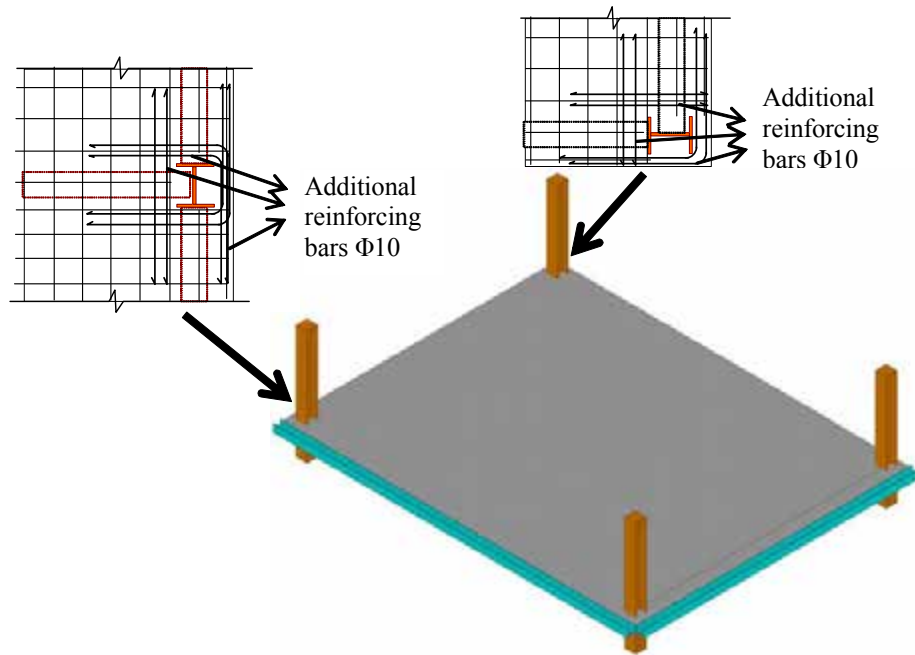
(a) Secondary Beams



(b) Primary Beam

**Figure 7.3** *Distribution of shear connectors for steel beams*

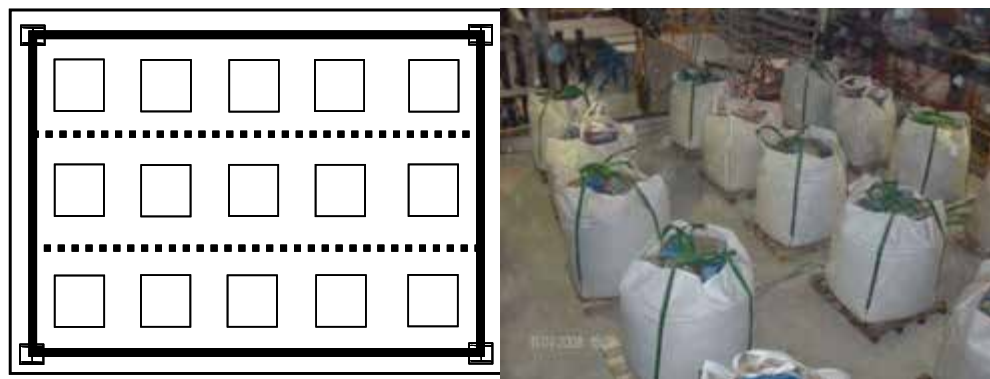
The reinforcing steel mesh was located at 50 mm from the top of the slab. The mesh was formed of 7 mm diameter bars, with a steel grade of S500, spaced at 150mm centres in both directions. Additional 10 mm diameter reinforcing bars were used for the edge steel and concrete composite connection (see Figure 7.4).



**Figure 7.4** Connection configurations investigated in the fire test

### 7.2.2 Test methodology

During the fire test, the mechanical loading on the floor was applied with fifteen sand bags uniformly distributed over the floor (see Figure 7.5). Each sand bag weighed exactly 15.0 kN, equivalent to a uniform load of 3.87 kN/m<sup>2</sup>. This value is slightly higher than a design value of 3.75 kN/m<sup>2</sup> for the Eurocode combination of actions for office buildings in a fire situation, using the recommended value of 0.5 for the combination factor,  $\psi_1$ .

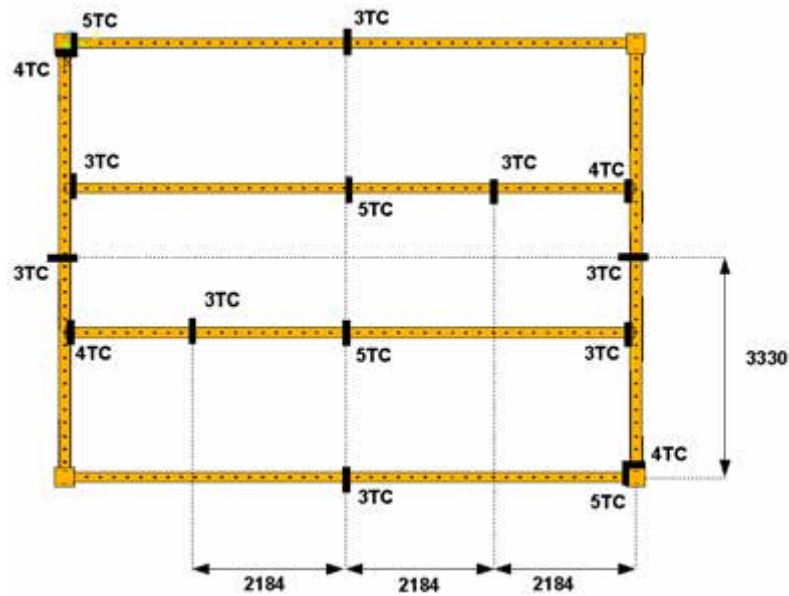


**Figure 7.5** Loading of the floor with sand bags

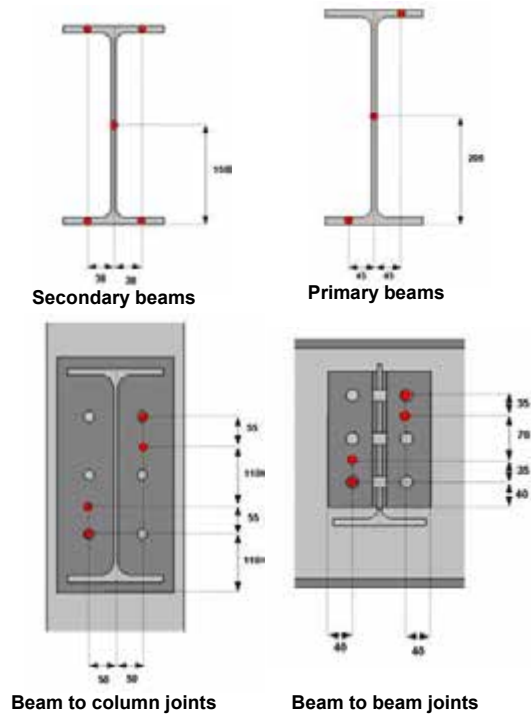
In conformance with the simple design method described in Section 5 for this type of floor, the two secondary beams and the composite slab were unprotected. However, all the boundary beams on the perimeter of the floor design zone (all beams connected directly to the columns) and all of the columns were fire protected to ensure that they maintained their structural stability in the fire situation. All the joints were also protected. The fire protection material used was two layers of mineral fibres blanket [25 mm-128 kg/m<sup>3</sup>]. The reinforcing steel mesh at two sides of the slab was welded to two steel beams placed along the edge

of the slab as shown in Figure 7.4. These beams were in turn fixed to the furnace structure in order to simulate the continuity condition of the composite floor.

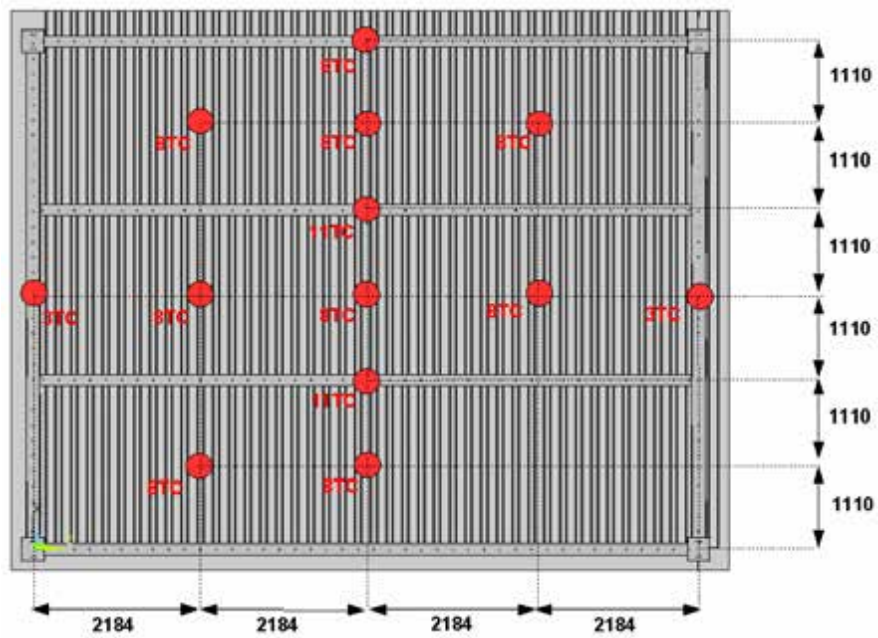
A total of 194 measurement locations were used to record the behaviour. The main measurements were the temperature and the deflected shape of the floor. Approximately 170 thermocouples were used to monitor the temperature of the steel frame (see Figure 7.6 and Figure 7.7 ) and the temperature distribution of the slab (see Figure 7.8 and Figure 7.9). Seven displacement transducers were installed to measure the vertical deflection of the floor (see Figure 7.10). Two other transducers were used to measure the horizontal movement of the floor. A special high temperature video camera was put inside the furnace to record visually the floor deformations with time.



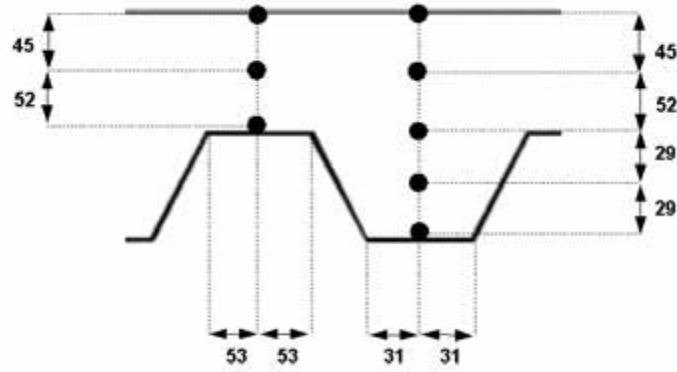
**Figure 7.6** Location of thermocouples on the steel frame



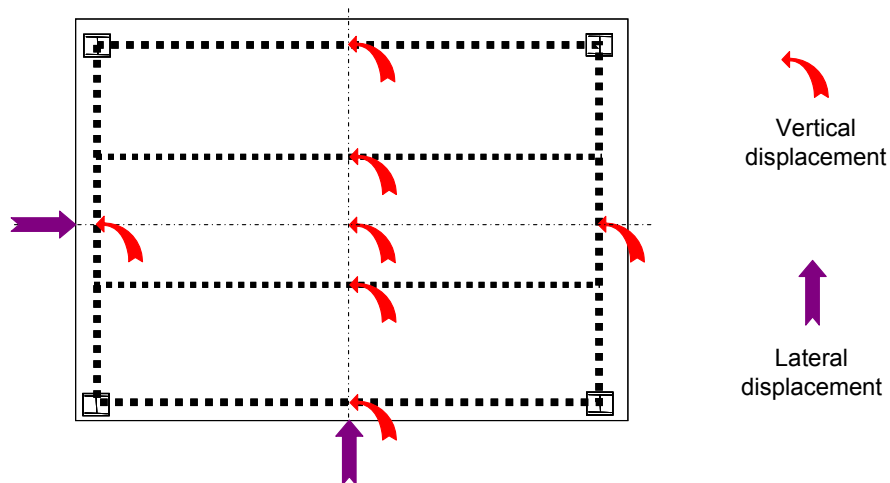
**Figure 7.7** Location of thermocouples on each instrumented steelwork cross section



**Figure 7.8** Locations and numbers of thermocouples in the composite slab



**Figure 7.9** Typical cross section through composite slab showing thermocouple locations



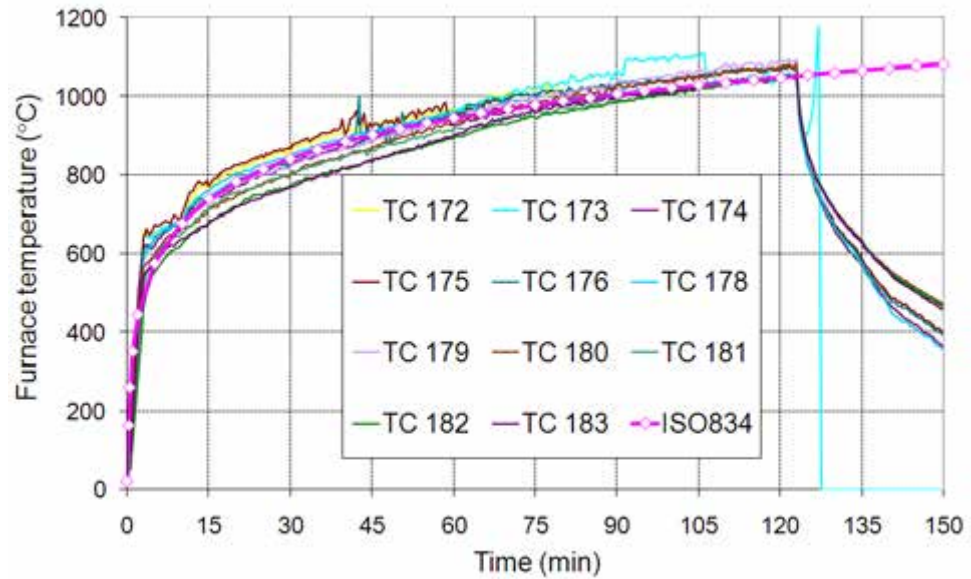
**Figure 7.10** Location of displacement transducers

## 7.2.3 Results

The test lasted for more than 120 minutes and the fire was stopped following integrity failure of the floor. However, the recording of specimen's behaviour continued until 900 minutes, allowing the performance of the floor during the cooling phase to be monitored.

### 7.2.3.1 Temperature variation in structure

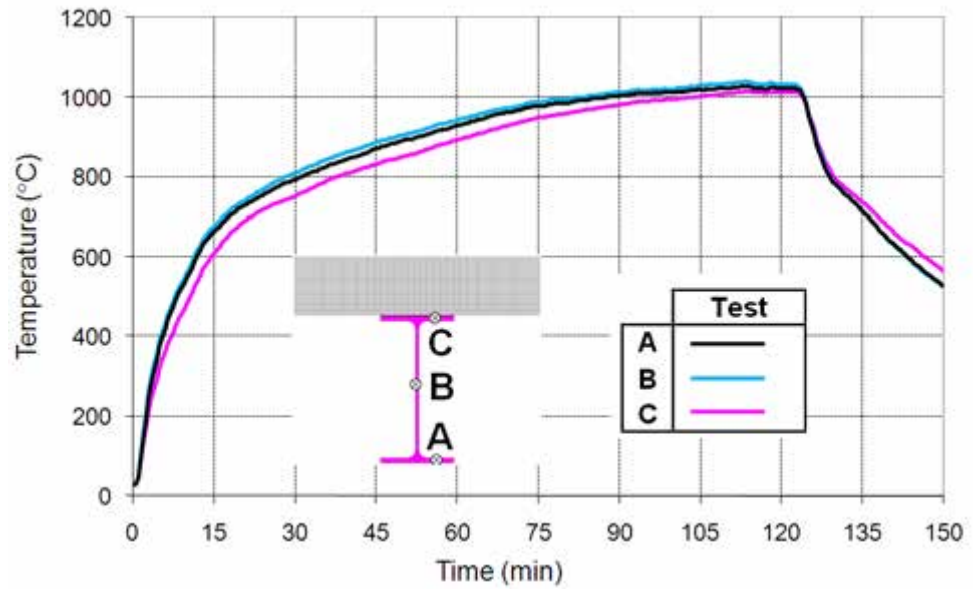
During the test, the furnace temperature was controlled with plate thermocouples in accordance with the recommendations of EN1363-1. These plate thermocouples were located just below the floor and the recorded temperatures from these instruments showed that the furnace temperature was controlled within the tolerances permitted by the fire testing standard EN1363-1 (see Figure 7.11).



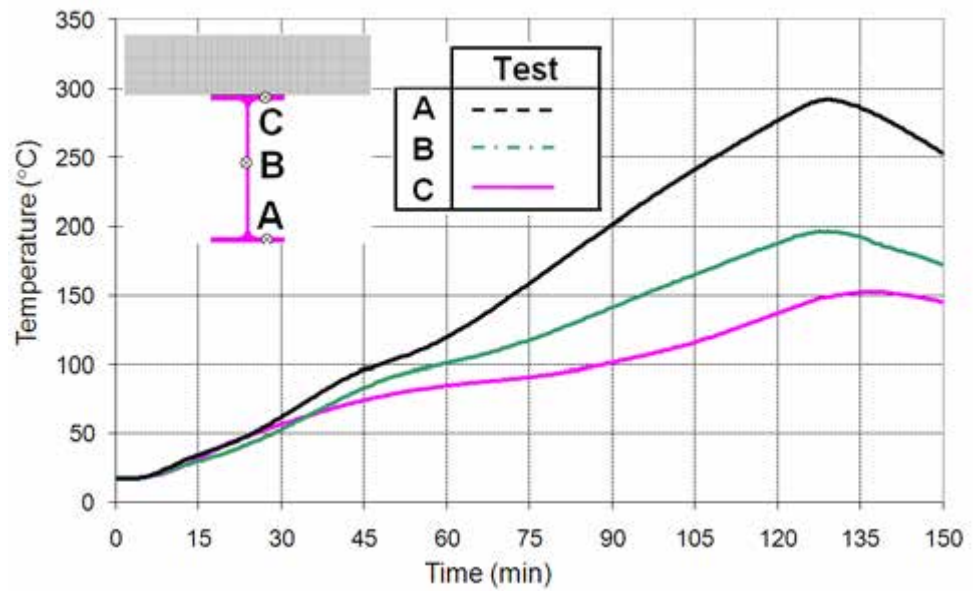
**Figure 7.11** *Furnace temperature versus standard temperature-time curve*

Measurements of the temperature at the mid-span of the composite beams were taken on the bottom flange, the web and upper flange of each section. A summary of the temperatures recorded in the beams is presented in Figure 7.12 and Figure 7.13. The unprotected steel beams reached a maximum temperature of 1040°C. In contrast, the protected steel beams reached a maximum temperature of 300°C; this temperature is lower than would be expected in practice, due to the reduced exposure of these members located at the edge parts of the furnace.

A summary of the temperatures recorded in the composite slab is presented in Figure 7.14. The temperatures of points A and B were not recorded because the thermocouples fixed to steel sheet failed early in the test, probably due to debonding between the steel sheet and the concrete once exposed to fire. Debonding of the steel sheet was observed over a large proportion of the soffit of the composite slab. The temperature recorded at the unexposed side of the composite slab is shown in Figure 7.15. The temperature rise at the unexposed face of the composite slab after 120 minutes of fire was slightly above 100°C, which is less than the upper limit of 140°C that defines the insulation criterion.

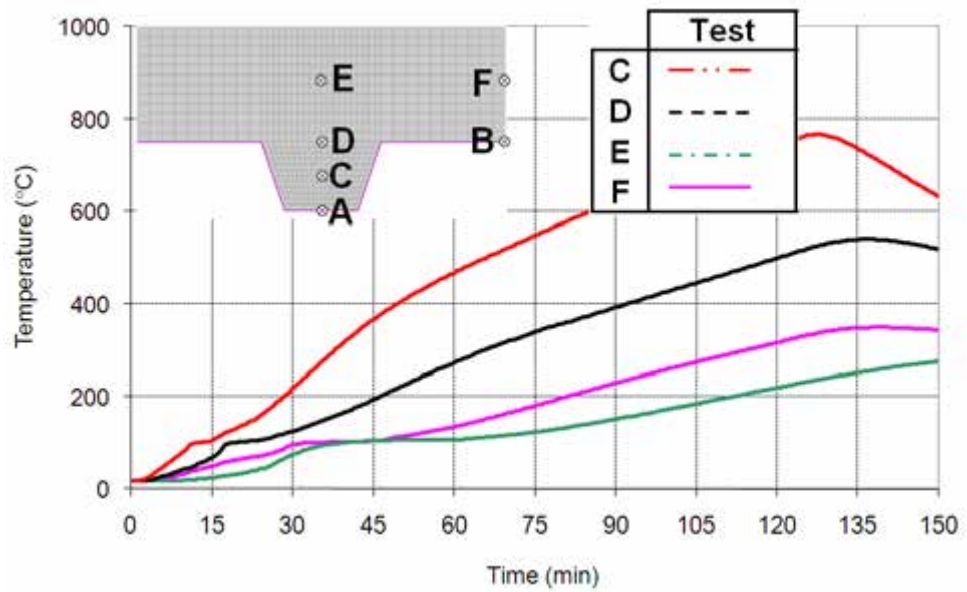


**Figure 7.12** Heating of unprotected steel beams

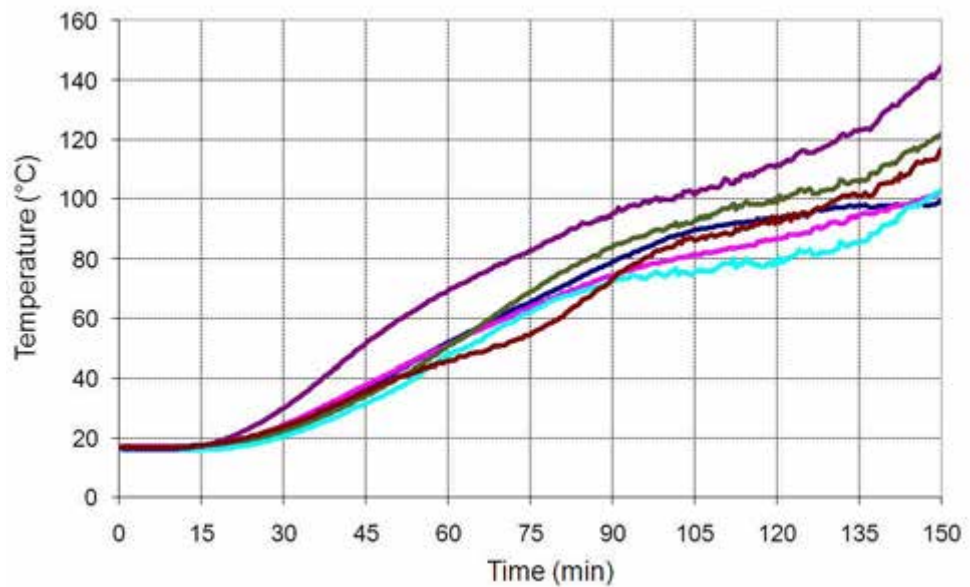


**Figure 7.13** Heating of protected steel beams





**Figure 7.14** Heating of composite slab



**Figure 7.15** Temperatures recorded at unexposed side of the composite slab

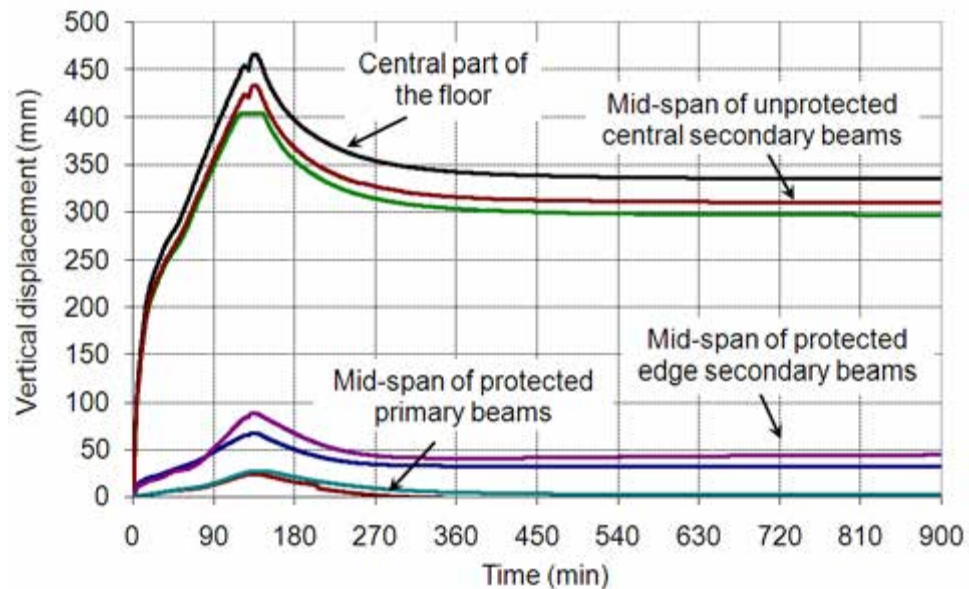
### 7.2.3.2 Displacement variation of the structural members

Figure 7.16 shows the vertical displacements of the floor over the whole period of test. The decrease of deflection after about 120 minutes corresponds to the time when the burners of the furnace were switched off. A more detailed illustration of these displacements, mainly during the heating phase of the test, is given in Figure 7.17. It can be observed that the maximum deflection of the floor is about 450 mm and the deflections measured at the two unprotected secondary beam positions were approximately 420 mm, less than one twentieth of their span. During the cooling phase, the deflection increased slightly and reached a maximum

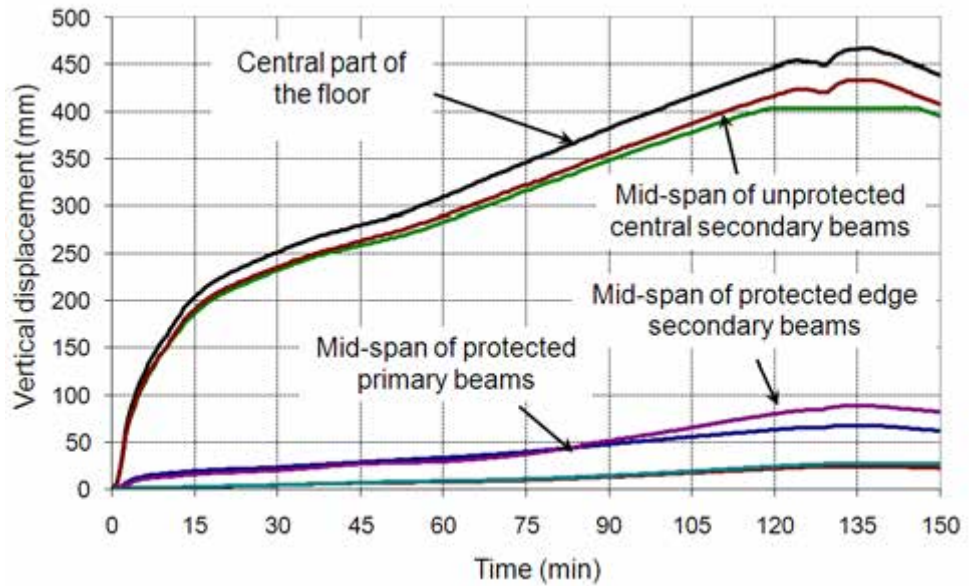
value at about 135 minutes. Although the furnace temperature had dropped from 1050°C to only 600°C (see Figure), heat was still being conducted through the thickness of the composite slab and at this time the maximum temperature of the mesh was reached (see Figure 7.14).

The fire protected beams located on the perimeter of the test specimen only reached a temperature of 300°C. As steel retains 100% of its room temperature yield stress at 300°C, the deflection of these beams is lower than expected, with a maximum of 100mm deflection measured at the mid span of secondary beams. In practice it would be reasonable to assume that the critical temperature for these beams would be between 500°C and 600°C with a deflection in excess of span/30.

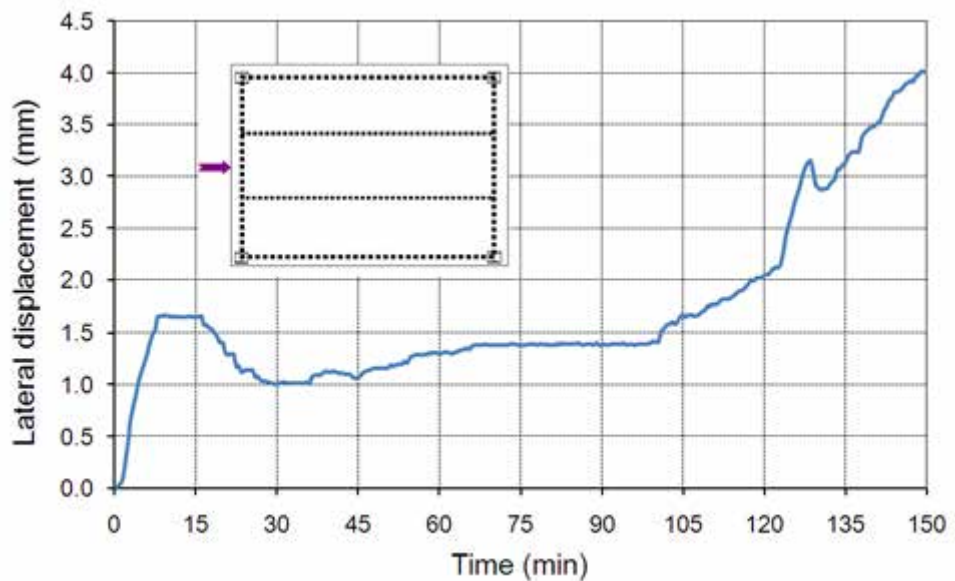
If more attention is paid to the evolution of the deflection of the floor, one can find that it increased very rapidly during the first 20 minutes of fire and then increased with nearly a constant speed. If this deflection is related to the heating of unprotected beams, it can be found also that these beams were heated gradually up to about 700 °C. Obviously their flexural load bearing capacity with this level of heating would no longer allow them to bear the applied load alone. In consequence, the membrane effect of the floor was progressively activated, to maintain the global stability of the floor. This tensile membrane effect was also clearly illustrated through the measurement of the lateral displacement at the edge of the floor, shown in Figure 7.18. Once again, one can find that following 15 minutes of fire, the edge part of the floor moved inwards due to the tensile membrane effect. The sudden increase of this displacement at around 105 minutes could be explained by the important failure of reinforcing steel mesh in the central part of the floor (for more details, see Section 7.4.3).



**Figure 7.16** Deflection of the floor recorded during the whole period of test



**Figure 7.17** Deflection of the floor recorded during the heating period of test



**Figure 7.18** Lateral displacement at the edge of the floor recorded during the heating period of test

### 7.2.3.3 Behaviour of composite slab observed during the test

The main observations regarding cracking of the concrete slab were:

- Small cracks occurred in the concrete, particularly around steel columns and continuous edges of the slab, at an early stage of the fire test, as shown in Figure 7.19(a).
- There was some enlargement of these cracks during the heating phase of the test, but this did not significantly influence the integrity performance of the floor (see Figure 7.19(b)).

- A more significant crack occurred in the central part of the floor after 105 minutes of fire exposure, as shown in Figure 7.20.

Investigation of the central crack after the test showed that the crack was caused by the failure of a welded joint between two steel reinforcing meshes, as shown in Figure 7.21. As the simple design method relies on being able to stress the reinforcement to its ultimate failure load across the centre of the slab, full tension laps must be provided at all joints between sheets of mesh reinforcement. This type of failure can be avoided if construction details in accordance with EN 1992-1-1<sup>(36)</sup> are adopted.

As the test specimen did not reach the point of collapse during the test, the occurrence of such an important crack and failure of steel reinforcing mesh in the longitudinal direction at the central part of the floor did not affect its load bearing capacity.



(a) At the beginning of fire test

(b) At the end of fire test

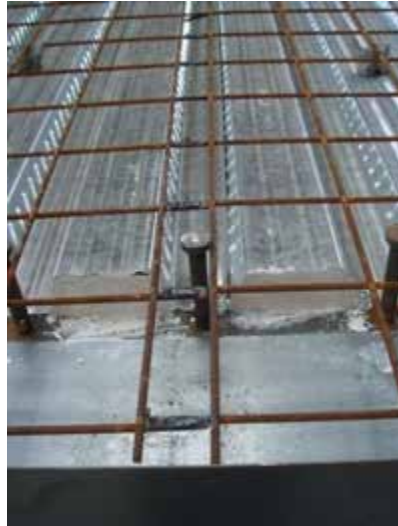
**Figure 7.19** *State of slab around steel column*



(a) State of the cracking at central part of the floor

(b) State of the cracking after cooling

**Figure 7.20** *State of slab at central part of the floor during and after the test*



(a) Welded reinforcement joint prior to the concrete casting



(b) State of the reinforcement joint at the location of the crack after cooling

**Figure 7.21** Joint of reinforcing steel meshes before and after test

#### 7.2.4 Comments on the test results

The test results have demonstrated the adequate performance of a composite floor slab designed in accordance with the simple design method. The remarks derived from test results regarding the fire performance of the floor are:

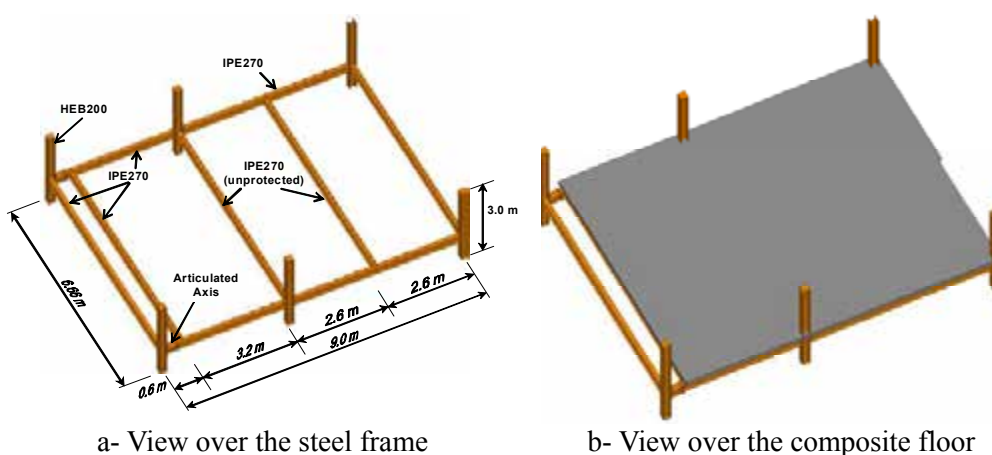
- even with unprotected secondary steel beams of a span of 8.735 m, the load bearing criterion (R) was fulfilled for a period of more than 120 minutes,
- the integrity criterion (E) and the insulation criteria (I) were fulfilled for a period of 105 minutes. Failure was due to the formation of a crack across the composite slab due to premature failure of reinforcing steel mesh, see Section 7.2.3.3.
- the whole floor remained structurally very robust under a long duration fire, despite the failure of steel mesh reinforcement in the concrete slab,
- it must be ensured that the reinforcing mesh is properly overlapped to activate the membrane action / to ensure continuity of load transfer, especially in the region of unprotected beams and around columns
- the concrete cracking at the edge of the floor was very limited and had no influence on the integrity and insulation performance of the floor,
- the floor behaved satisfactorily during the cooling phase of fire.
- the steel joints were all adequately protected and their maximum heating was limited to around 500°C. All joints between steel members performed very well during both heating and cooling phases.

## 7.3 COSSFIRE Fire test programme

### 7.3.1 Test specimen

In the scope of COSSFIRE project, another specific composite floor as shown in Figure 7.22 was fire tested. For this floor, the cross sections of steel beams and steel columns are respectively in IPE270 and HEB200. The nominal steel grade of all these structural members is S235. The design of this floor system was undertaken in accordance with the requirements of EN1994-1-1<sup>(34)</sup> for room temperature design of composite structures with a permanent load of 1.25 kN/m<sup>2</sup> in addition to self weight of the structure and a live load of 5.0 kN/m<sup>2</sup>. The fire test was conducted with a load of 3.93 kN/m<sup>2</sup> which corresponds approximately to 100% of various permanent actions and 50% of live actions according to Eurocode load combination in fire situation for office buildings. As far as steel joints are concerned, they are designed according to the requirements of EN1993-1-8<sup>(35)</sup>.

The composite slab was made of normal-weight in-situ concrete with a concrete quality of C30/37. The total depth of the slab was 135 mm and the profiled steel sheet is COFRAPLUS60 (trapezoidal). With respect to shear connectors, they were all in headed studs with a diameter of 19 mm and a height of 125 mm and their distributions over steel beams are respectively one stud every 207 mm for secondary beams and one stud every 300 mm for main beams. The reinforcing steel mesh located at 35 mm from the top of the slab is in grade S500 and has a diameter of 7 mm. Its grid size is 150 mm x 150 mm.



**Figure 7.22** Fire test set-up

The real mechanical properties of used materials in this test are summarised in Table C.1 given below.

**Table 7.2** Material properties of COSSFIRE tested elements

Item	Value
Steel grade of main beams	320 MPa
Steel grade of secondary beams	320 MPa
Steel grade of reinforcing steel	590 MPa
Compressive strength of concrete	38.0 MPa

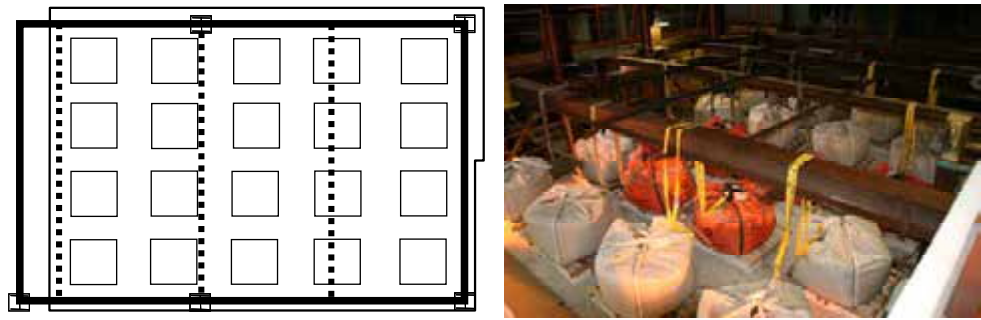
In compliance with the existing simple engineering design method of such a type of floor under membrane action, the two intermediate secondary beams and the composite slab are unprotected. However, all the boundary beams of the floor are fire protected for a fire rating of 120 minutes. The steel columns were also protected except the protection around the joints which was intentionally reduced so that the heating of the joint components was important enough during heating phase in order to investigate the impact of such heating on their behaviour during cooling phase.

In order to investigate the behaviour of connections between concrete slab and steel members at the edge parts of composite floor in fire, six edge connection configurations were adopted with this floor, as shown in Figure 7.23.

The mechanical load during fire was applied with help of twenty sand bags uniformly distributed over the floor. Each of these sand bags weighs exactly 11.0 kN, leading together with wood pallet and lightweight concrete blocks to an equivalent uniform load of 3.93 kN/m<sup>2</sup>. As far as thermal load is concerned, the ISO standard fire curve was imposed until the moment that the collapse of the floor begin to occur. However, the recording of test results was maintained during the cooling phase in order to know the behaviour of the floor during the whole period of fire.



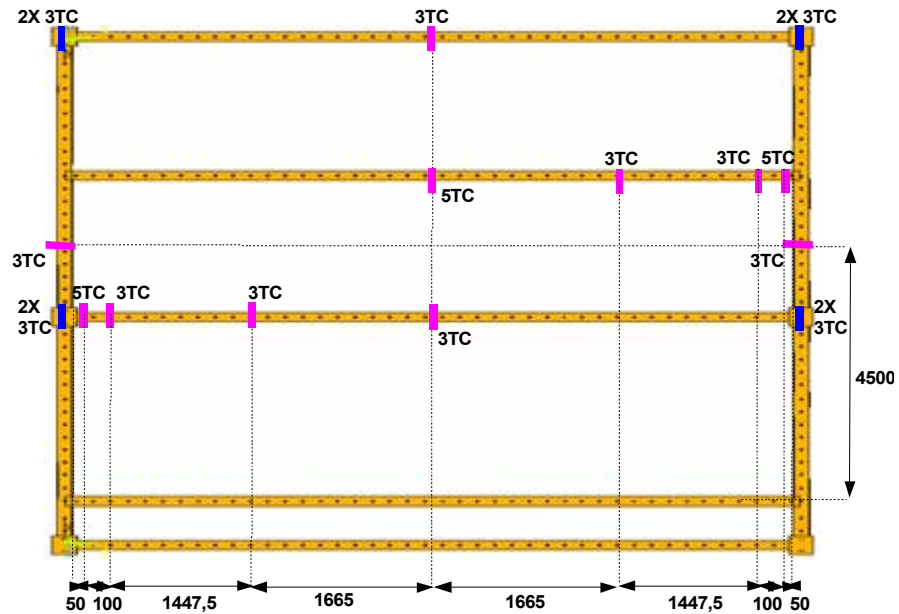
**Figure 7.23** *Different steel and concrete composite connection configurations*



**Figure 7.24** Loading conditions of steel and concrete composite floor exposed to fire

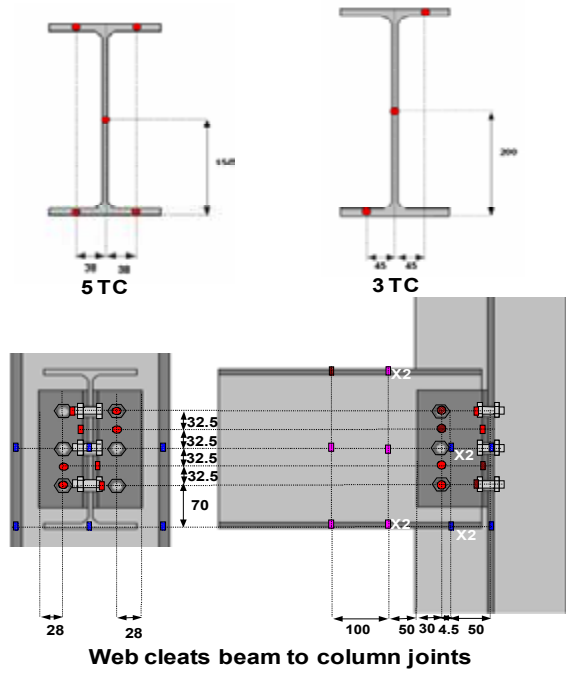
### 7.3.2 Measurement of test results

The main measurements of the test are related to temperature and the deflection of the floor. A total of 203 thermocouples of which 66 thermocouples on steel members (Figure 7.25), 80 thermocouples on connections (Figure 7.26) and 57 thermocouples in composite slab (see figures 7.27 & 7.28) were used to record both the gas and specimen's temperatures. In addition, 20 displacement transducers of which 16 vertical displacement transducers were installed to measure the deflection of the floor (Figure 7.29). The four remained transducers were used to measure the horizontal movement of the floor. In addition, a special video camera was put inside the furnace which has recorded visually the floor deflections versus time.

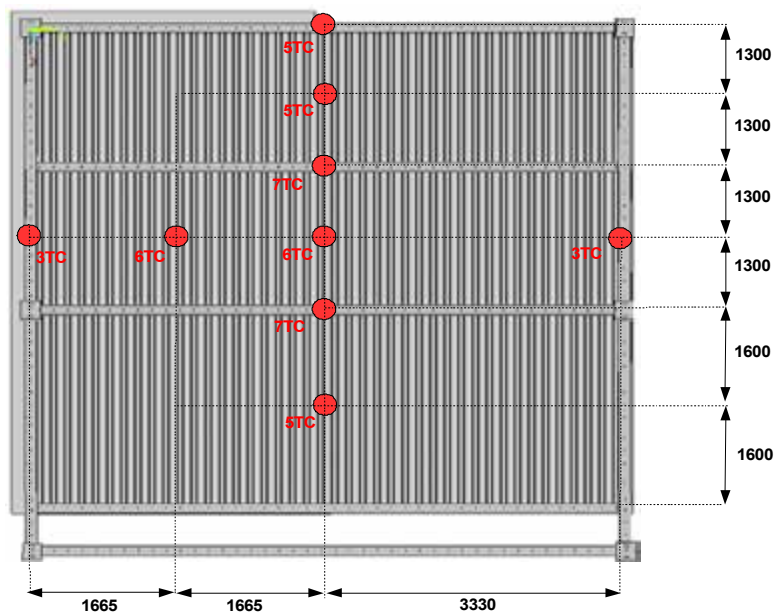


**Figure 7.25** Location of thermocouples on the steel frame





**Figure 7.26** Location of thermocouples on each instrumented steelwork cross section



**Figure 7.27** Locations and numbers of thermocouples in the composite slab

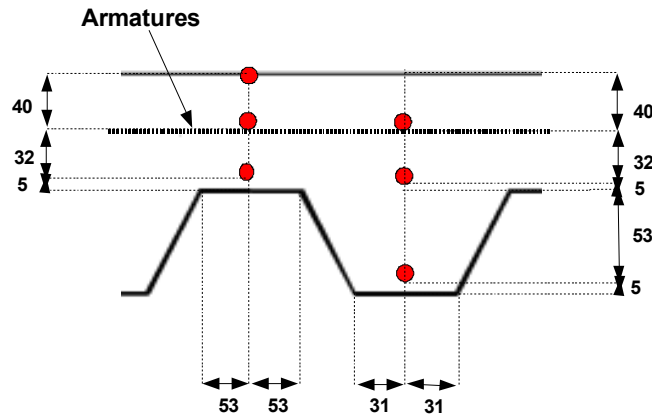


Figure 7.28 Typical cross section through composite slab showing thermocouple locations

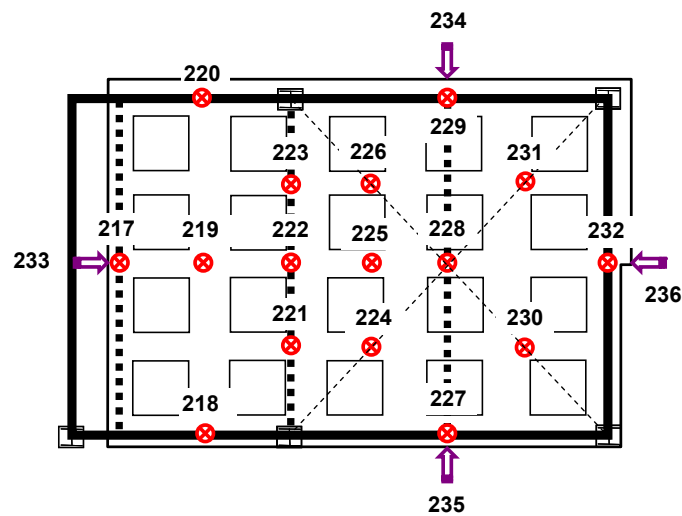
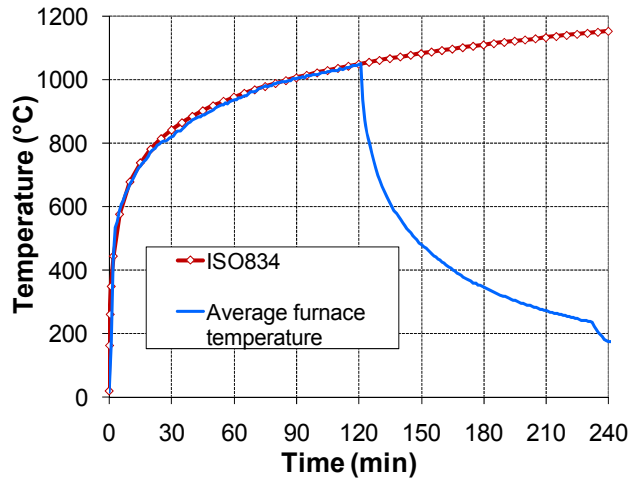


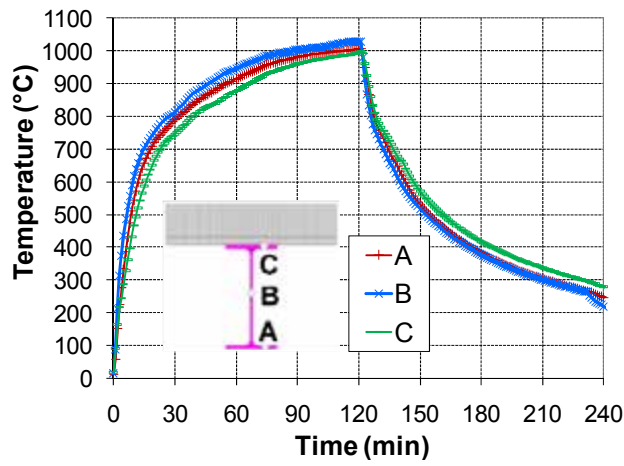
Figure 7.29 Location of displacement transducers

### 7.3.3 Principal experimental results

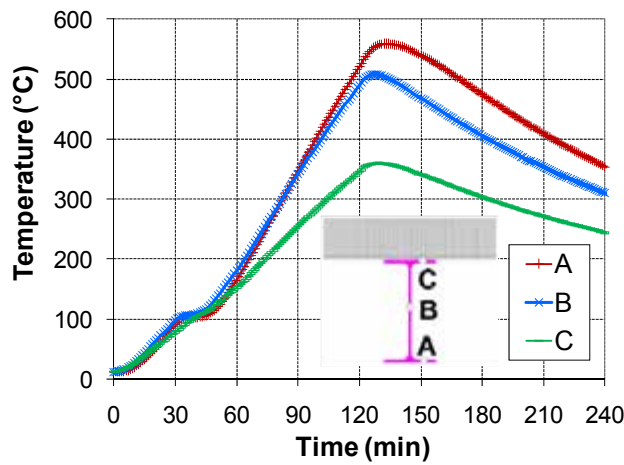
During the heating phase of this test, the ISO-834 fire curve was followed (Figure 7.30) which lasted for more than 120 minutes until the apparent collapse of one edge secondary beam linked to main beams (see D6 of Figure 7.36). After that, all burners were turned off and the furnace was cooled down naturally. As far as the heating of steel beams is concerned, it varied a lot according to the protection condition. In fact, the unprotected steel beams located at the middle of the floor were heated up to more than 1000 °C (Figure 7.31). On the contrary, the protected steel beams were heated up in general to around 550 °C (Figure 7.32) except one of the edge protected secondary beams which was significantly hotter than all other protected beams, certainly due to defective fire protection during test (Figure 7.33).



**Figure 7.30** *Furnace temperature versus ISO fire curve*



**Figure 7.31** *Heating of unprotected secondary beams*



**Figure 7.32** *Heating of one protected main beams*

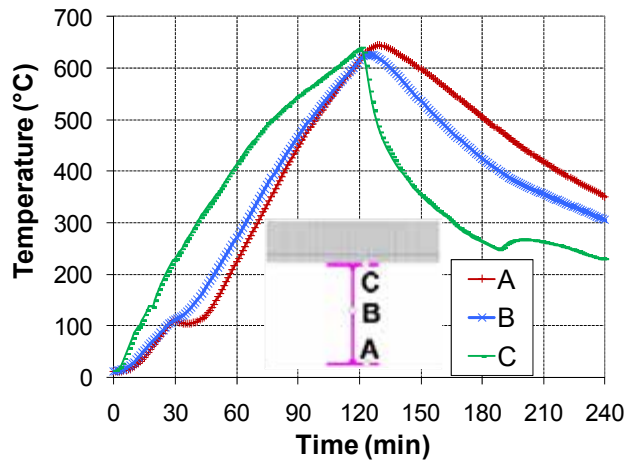


Figure 7.33 Heating of collapsed edge beam

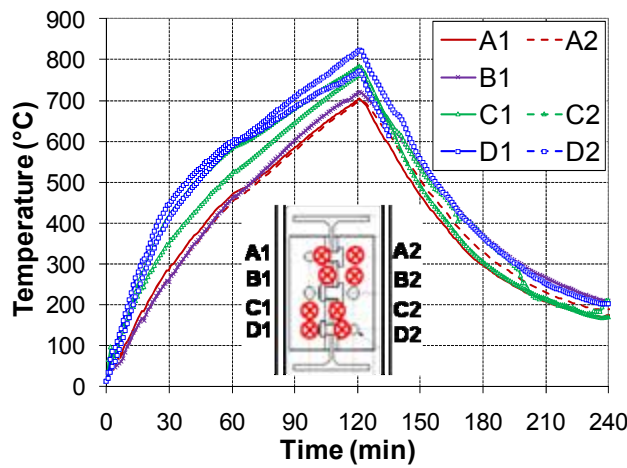


Figure 7.34 Heating of collapsed edge beam

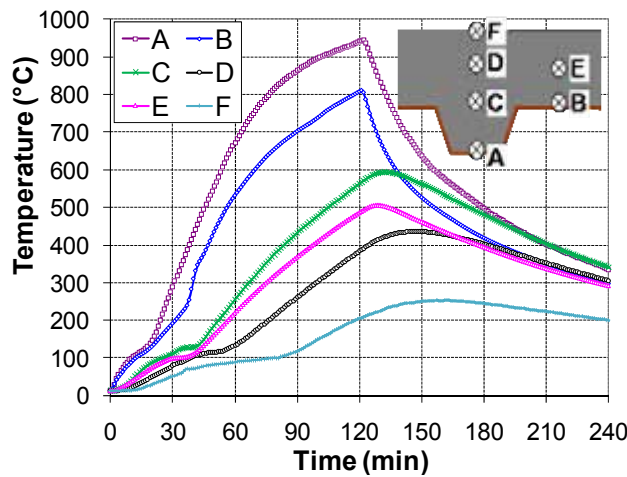
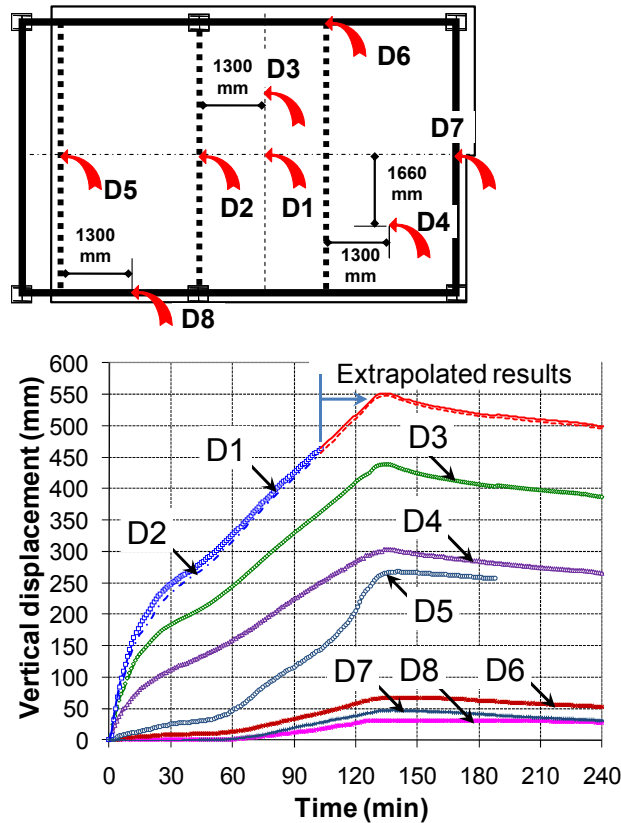


Figure 7.35 Heating of collapsed edge beam



**Figure 7.36** Measured vertical displacements of the floor during the test

As the steel joints in this test were not fully protected, some bolts of joints were heated up to more than 800 °C (Figure 7.34). From the temperature measurement in composite slab during the test, it can be found that the maximum temperatures at 5 mm from the exposed side of the composite slab were about 950 °C (Figure 7.35) and the reinforcing steel mesh was heated to about 500 °C. Moreover, the temperature measured at the unexposed side of the composite slab was more than 200 °C after more than 120 minutes of fire exposure which was beyond the insulation criteria.

During the test, the fire was stopped when it was observed that one edge beam was collapsing at around 120 minutes (see D6 in Figure 7.36). As far as the global deflection of the floor is concerned, it increased significantly at the beginning until 30 minutes of fire and slowed down since. At 120 minutes of ISO standard fire, the total deflection of the floor could be more than 500 mm. Once the heating was stopped, the deflection of the floor continued to increase for a while (about 15 minutes) before decreasing definitely and slowly. Finally, the deflection recovery of the floor was about 100 mm.

### 7.3.4 Observation of the fire tests

From measured global deflection of the floor, it is found that it increased very possibly to more than 500 mm after 120 minutes. However, the floor behaved still very well and there was no sign of failure in the central part of the floor. In fact, the fire was stopped due to an excessive deflection of the mostly heated secondary edge beam (Figure 7.37). A closer observation of this edge beam reveals that an important concrete crushing occurred at its mid-span, which means that this beam was really collapsing. Nevertheless, this failure did not lead to the collapse of the global floor owing apparently to load redistribution under membrane effect (see figure 7.38).

Local buckling of the unprotected secondary beam connected to central steel beams near joints is observed in its lower flange and web (see figure 7.39). However, the most remarkable feature from this test regarding the steel joints is that they all performed very well during both heating and cooling phases. Also, for unprotected secondary beams connected to steel main beams near joint, no local buckling can be found (Figure 7.40). In addition, no failure of the edge connections between concrete slab and steel members is observed.



**Figure 7.37** Collapse of edge beam



**Figure 7.38** Tested floor during and after the fire



**Figure 7.39** Local buckling of unprotected secondary beams

*connected to column*



**Figure 7.40** *No local buckling of unprotected secondary beams connected to main beams*



**Figure 7.41** *Cracking of concrete at corner parts of the floor*



**Figure 7.42** *Cracking of concrete around central columns*



**Figure 7.43** *Overlapping of reinforcing steel mesh in composite slab*

Another important feature to be mentioned here is the cracking of the composite floor around columns which could have a direct influence on fire performance of the floor. The main observed results in this respect are as follows:

- Concerning cracking of concrete at corner parts of the floor, it remained small and without any negative impact on integrity criteria (see figure 7.41).
- As for cracking of concrete around central columns, the important deflection of unprotected beam beneath created a large movement of slab toward inside and possible negative impact on integrity criteria can occur due to the opened crack in front of the column (see figure 7.42).
- There was no significant crack of concrete slab in the central part of the floor, which means that the reinforcing steel mesh behaved appropriately under membrane action even under a heating up to 500 °C. Such a good behaviour was without any doubt due to the appropriate overlapping of reinforcing steel meshes (see figure 7.43).
- The constructional details of putting reinforcing steel mesh behind the studs of edge beams are proved to be very efficient in case of membrane action of composite floor which could provide a beneficial lateral restraints to the floor slab.
- The residual loadbearing capacity of the floor remains adequate and is important enough despite significant deflection of the floor.



## 7.4 Full -scale fire test on a composite floor slab incorporating long span cellular steel beams

### 7.4.1 Test specimen

The tested floorplate was 9.6m by 15.6m supported on a steel frame spanning 9m by 15m between four corner columns (Figure 7.44). The cellular beams were positioned on gridlines 1, 4, B, C and D as primary and secondary beams of the structure (Figure 7.45). The dimensions of the beams are shown in Figure 7.45 and Figure 7.46. The unprotected secondary Beams 4 and 5 also had an elongated web opening at the centre of their span.



Figure 7.44 : Test compartment with long unprotected cellular beams

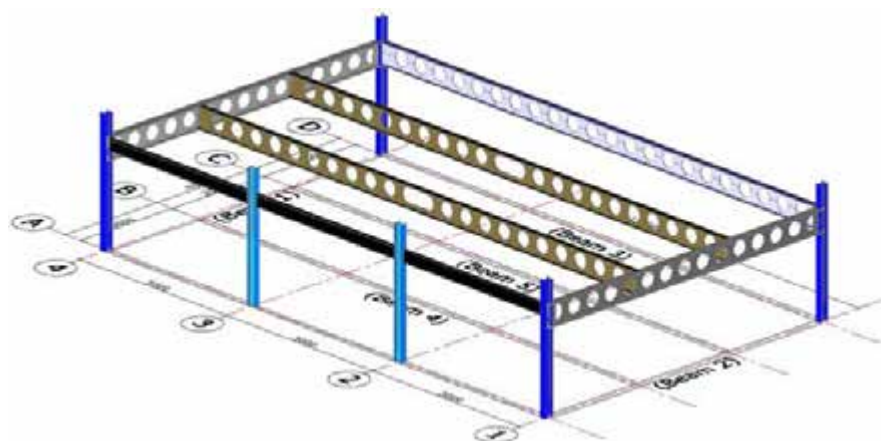
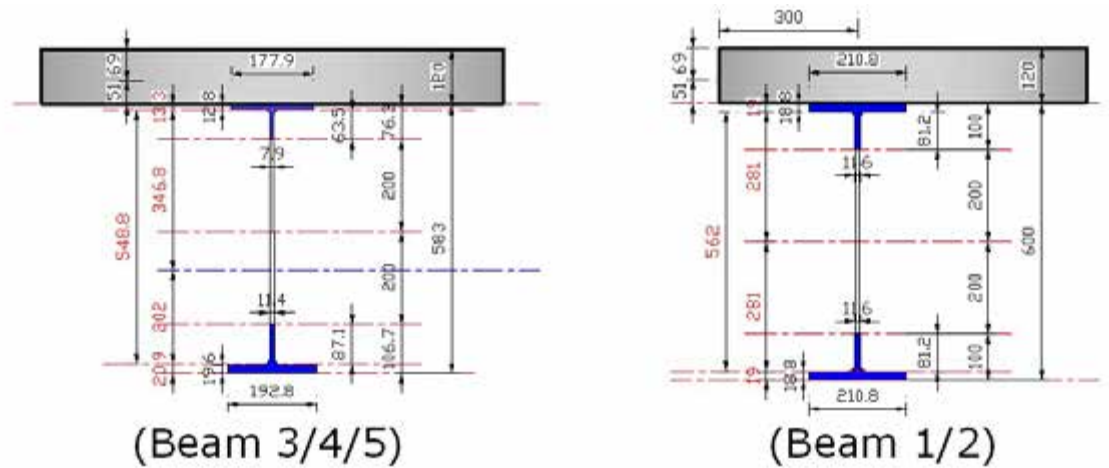


Figure 7.45 : Steel structural layout



**Figure 7.46** : Detail information of the steel sections.

The enclosed compartment was 9.2m by 15.6m, with an internal floor to soffit height of 2.88m. The surrounding walls were constructed using 7N/mm<sup>2</sup> blockwork, with three openings, each 1.5m by 3m. The surrounding compartment walls along gridlines 1, 4 and D were not fixed to the composite floor at the top which allowed free vertical movement of the floorplate along these boundaries. The front façade, with openings, was constructed such that the wall was extended up to the underside of the solid beam along gridline A, allowing no vertical deflection of the beam along this gridline. The frame was braced in the horizontal direction at the following locations; Column A1 was braced in both lateral directions, Column A4 was braced laterally parallel to gridline 4 and Column D1 was braced laterally parallel to gridline D. Bracing was provided using a diagonal CHS.

All the columns, and the solid beam along gridline A, were protected using commercially available 20mm thick fire board with a standard fire resistance period of 2 hours. The perimeter CBs on gridlines 1, 4, and D were protected using a ceramic fibre (see Figure 7.47), which also provided a standard fire resistance period of 2 hours. The fire protection was fitted using an approved contractor, following the manufacturer's specification. Plasterboard, 15mm thick, was also used to cover the inner face of the boundary walls to reduce heat loss through the blockwork (Figure 7.47).



**Figure 7.47 :** *Fibre and plasterboard protection used inside the compartment*

The concrete composite slab was 120mm thick and comprised a 51mm deep, 1mm thick, Holorib steel deck (HR51/150), normal-weight concrete and mesh steel reinforcement. The dovetail steel deck had a measured tensile strength of  $327\text{N/mm}^2$ . The welded wire A393 mesh reinforcement (Figure 7.48) comprised 10mm diameter ribbed bars at 200mm centres, with nominal yield strength of  $500\text{N/mm}^2$ , which was specified using the Bailey Method [3], based on the design parametric fire curve. The mesh reinforcement had a minimum lap length of 400mm and covered with 40mm thickness of concrete. The concrete mix design (for  $1\text{m}^3$ ) comprised: 320kg OPC, 918kg 10mm limestone, 691kg sharp sand, 380kg 6mm limestone, 30kg grey (recycled) water and 142kg cold (tap) water. No additives or air entraining agent was used in the concrete mixture. The measured average concrete compressive cube strength was  $50\text{N/mm}^2$  on the day of test.



**Figure 7.48 :** *Mesh reinforcement and steel decking before concrete casting*

Full interaction between the slab and beams was achieved using shear connectors, of 19mm diameter and 95mm height, placed at 200mm centres along the beams. The requirement for U-bar reinforcement around the slab's perimeter (as shown in Figure 7.48) is not a special requirement for fire design, but was needed to ensure correct reinforcement detailing for ambient design. The U-bars were 10mm diameter and placed with 30mm cover to the edge of the slab, as shown in Figure 7.48.

### 7.4.2 Design Loads

The design load was based on a characteristic live load of  $3.5\text{kN/m}^2$  together with a partition load of  $1.0\text{kN/m}^2$  and a services and finishes load of  $0.5\text{kN/m}^2$ . The partial load factors used for the Fire Limit State (FLS) correspond to the values given in the EN1990 for office buildings. The resulting applied load was  $3.25\text{kN/m}^2$ , as shown in Table 7.3.

**Table 7.3** : *Design Loads*

Description	Characteristic Load( $\text{kN/m}^2$ )	Load Factor at FLS	Design Load at FLS $\text{kN/m}^2$
Partition	1.0	1.0	1.0
Services & Finishes	0.5	1.0	0.5
Live Load	3.5	0.5	1.75
<b>Total</b>			<b>3.25</b>

The applied load was achieved using 44 sandbags (each weighting 1 tonne) evenly positioned over the floorplate, as shown in Figure 7.49a, providing a load of  $3.25\text{kN/m}^2$ . The self weight of the slab, which was 120mm thick, was calculated as  $2.90\text{kN/m}^2$ , creating a total load of  $6.15\text{kN/m}^2$ .



**Figure 7.49** : (a) *Vertical static load*, (b) *Wooden cribs used for the fire load*

### 7.4.3 Design of the Fire

The natural fire was designed using the parametric time-temperature curves in Annex A of EN1991-1-2 and OZone Software. The fire load comprised 45 standard ( $1\text{m} \times 1\text{m} \times 0.5\text{m}$  high) wooden cribs, built using  $50\text{mm} \times 50\text{mm} \times 1000\text{mm}$  wooden battens, positioned evenly around the compartment (Figure 7.49b). The fire load was equivalent to  $40\text{kg}$  of wood per square metre of floor area. Assuming a calorific value of  $17.5\text{MJ/kg}$  for wood, the fire load density for the tested compartment was  $700\text{MJ/m}^2$ . The fire load used was slightly higher than the office design fire load of  $511\text{MJ/m}^2$  (80% fractile) given in the EN1991-1-2. Each wooden crib was connected to its neighbour by a mild steel channel section, which

contained a porous fibre board. Approximately 30min before ignition, 20 litres of paraffin was poured into the channels, to ensure rapid fire development within the compartment.

### 7.4.4 Instrumentation

Extensive instrumentation devices were placed throughout the compartment to measure the atmosphere temperatures, temperature distribution through the composite floor, the temperature of the protected and unprotected cellular beams, and the vertical and horizontal displacements. The locations of the measurements taken are shown in Figure 7.50 and Figure 7.51. A free-standing steel structure was built around the compartment to create a reference outer frame, allowing the correct measurement of vertical and horizontal displacements. A total of 350 thermocouples were used to monitor the temperatures and a total of 17 transducers were used to measure the various displacements. The transducers were attached to a free-standing outer reference frame and were insulated, where required, to ensure that and heat effects to the transducers were eliminated.

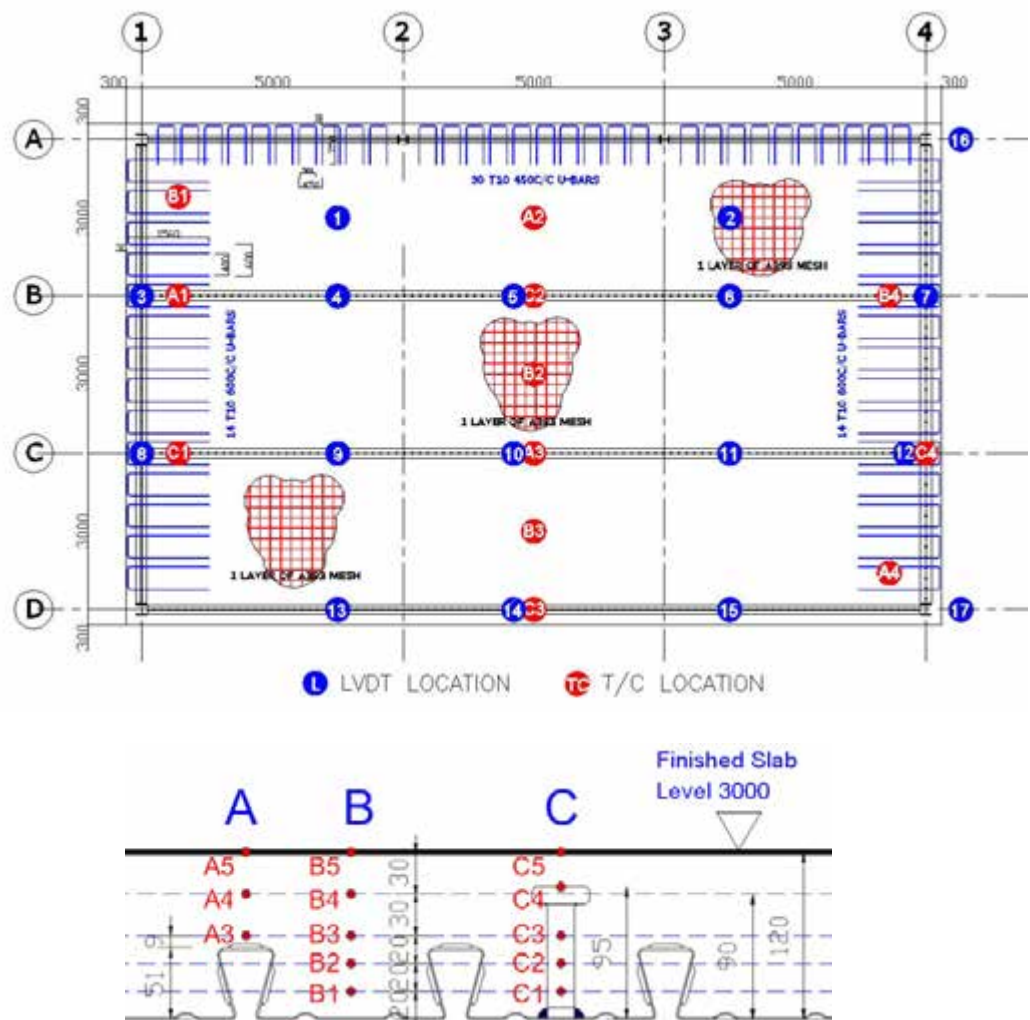
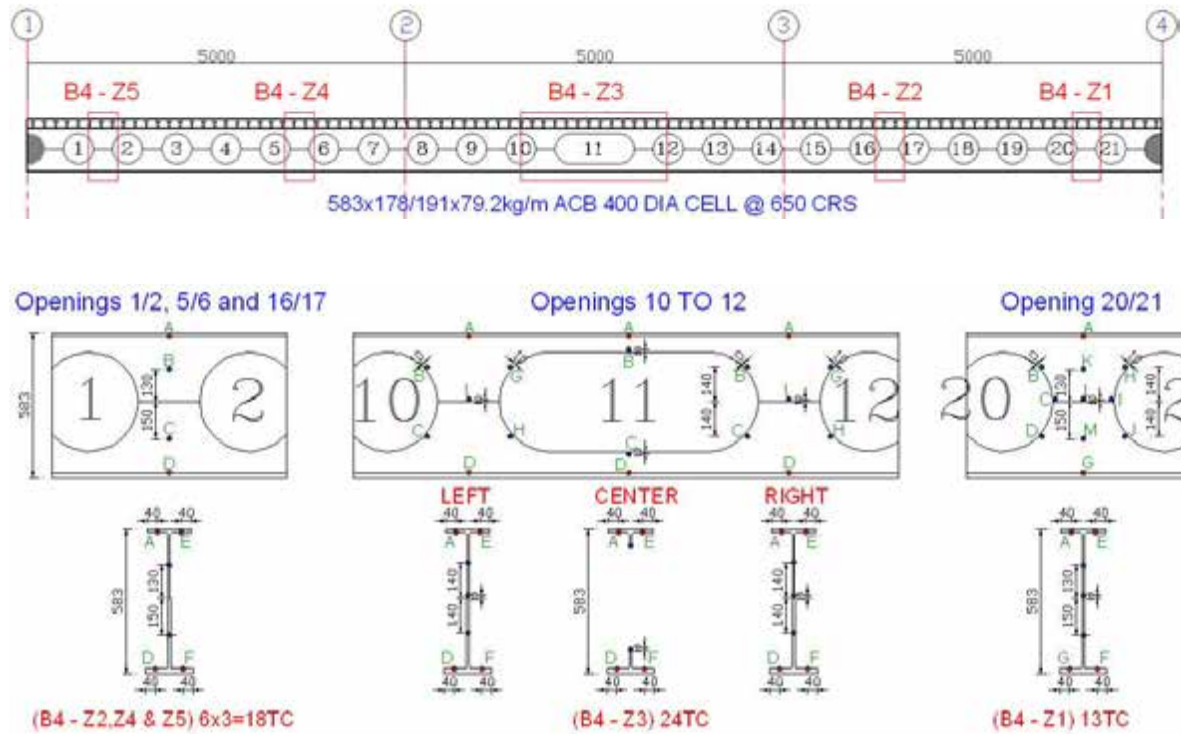


Figure 7.50 : Locations of measurement positions for deflections and temperatures throughout the slab.



**Figure 7.51** : Thermocouple locations on unprotected Beam 4 (Gridline B)

#### 7.4.5 Beam/Slab Deflection

Under fire conditions the deflection of the unprotected, axially unrestrained, composite steel beams (Figure 7.52) predominately comprises two parts; thermal bowing and mechanical deflection. Deflection due to thermal bowing is caused by the non-uniform temperature distribution through the steel beam and the connected composite slab. The mechanical deflection is due to the decrease in stiffness and strength of the structural material as the temperatures increase. At low temperatures (less than 400°C), the beam deflection is predominantly due to thermal bowing. At higher temperatures, mechanical deflection will dominate and the deflection increases at a faster rate.

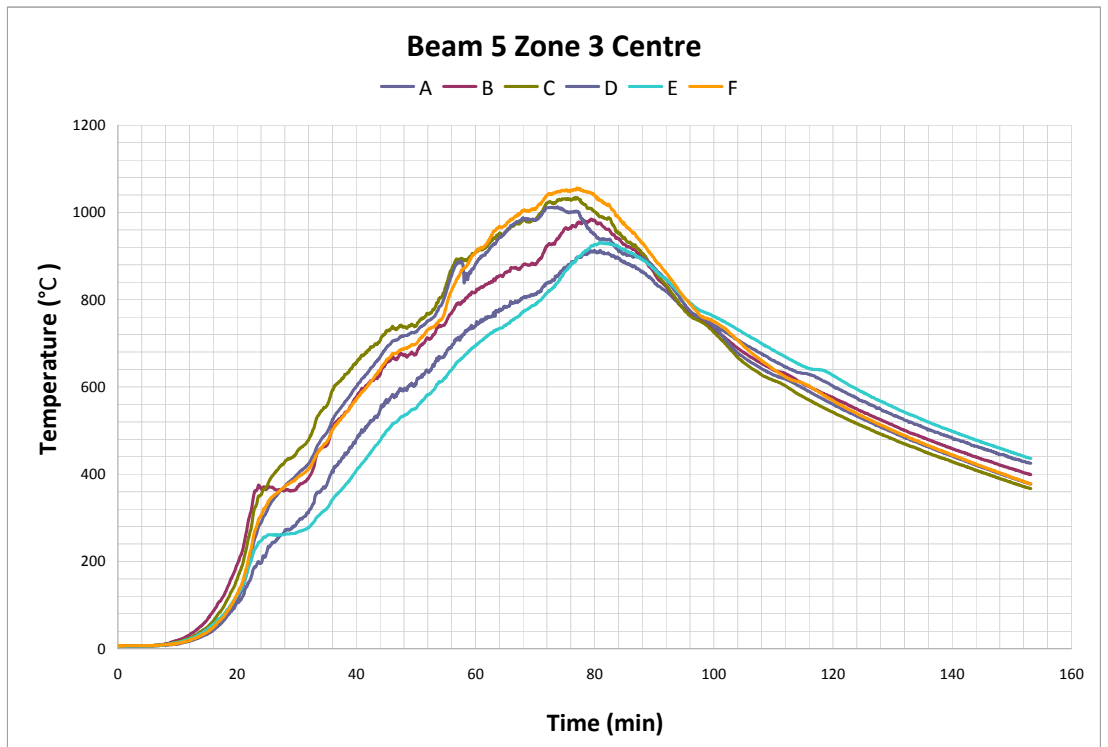
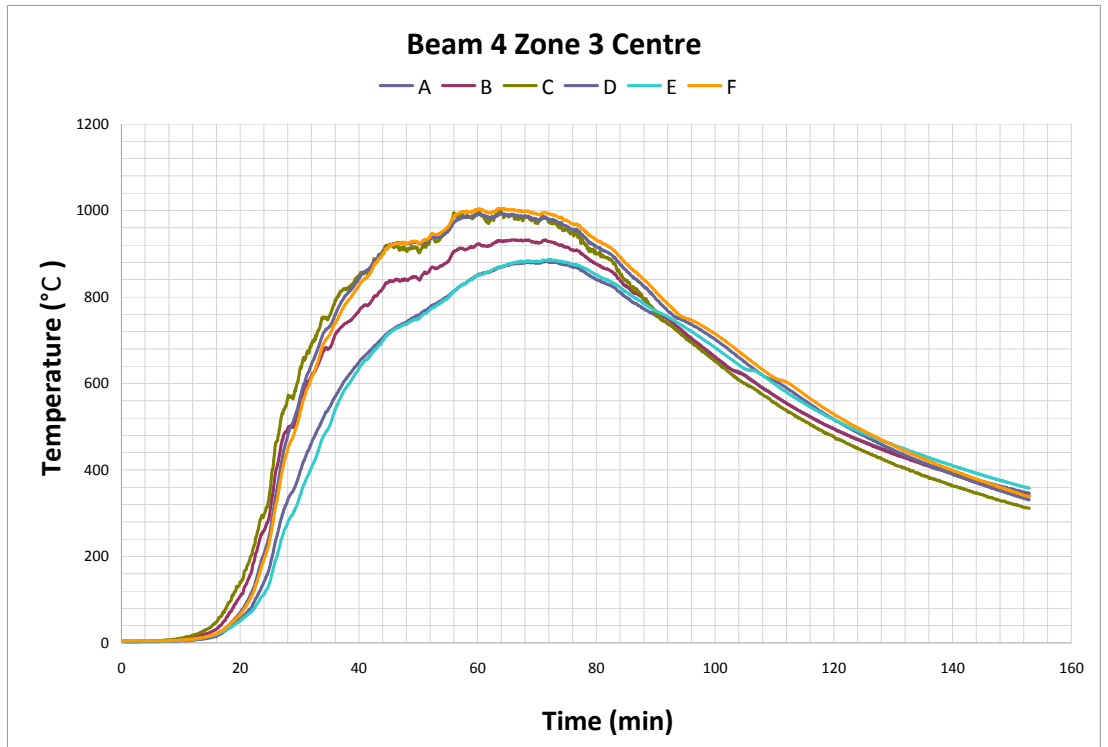


**Figure 7.52** : *Developed compartment fire*



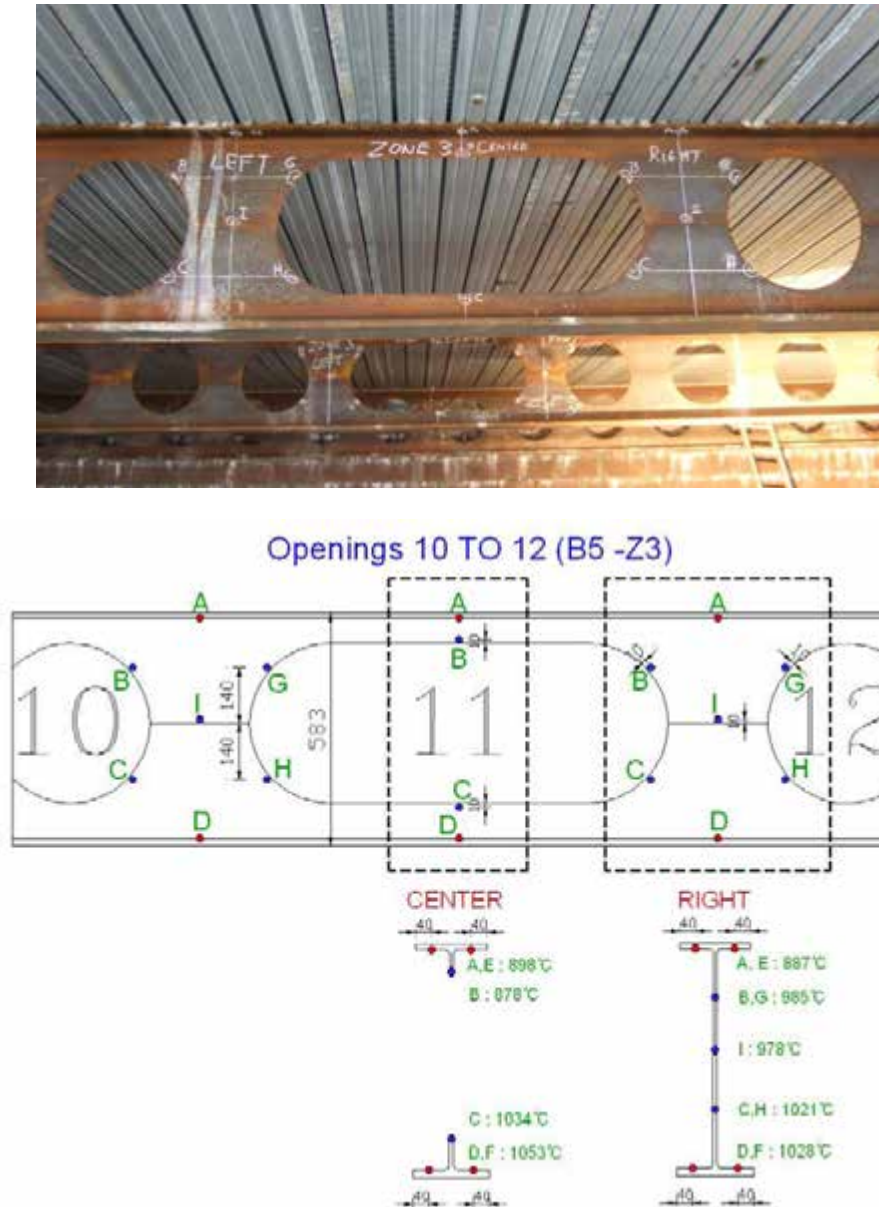
**Figure 7.53** : *Deflection of the slab/unprotected beam following the fire.*

The maximum recorded steel temperature of 1053°C occurred after 77 minutes at the centre span of Beams 4 and 5 (Figure 7.54). The maximum temperature occurred on the bottom flange below the elongated opening. Figure 7.55 shows the temperature distribution at the critical part of the unprotected CBs. It is worth noting that the temperatures are non-uniform across the web despite the beams being unprotected and the long duration of the fire. The temperature of the top flange of the beams is lower, as expected, due to the heat sink effect of the supporting concrete slab. At a maximum temperature of 1053°C the steel has lost 97% of its strength and stiffness and is contributing little to the load bearing capacity of the floor system.



**Figure 7.54** : Recorded temperatures at mid-span of the unprotected beams

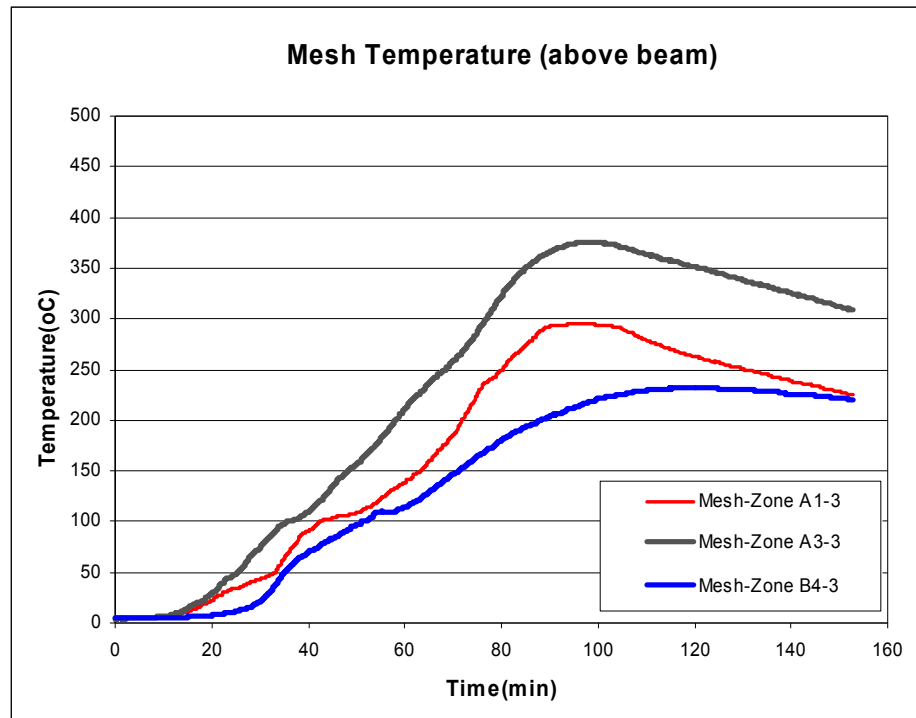




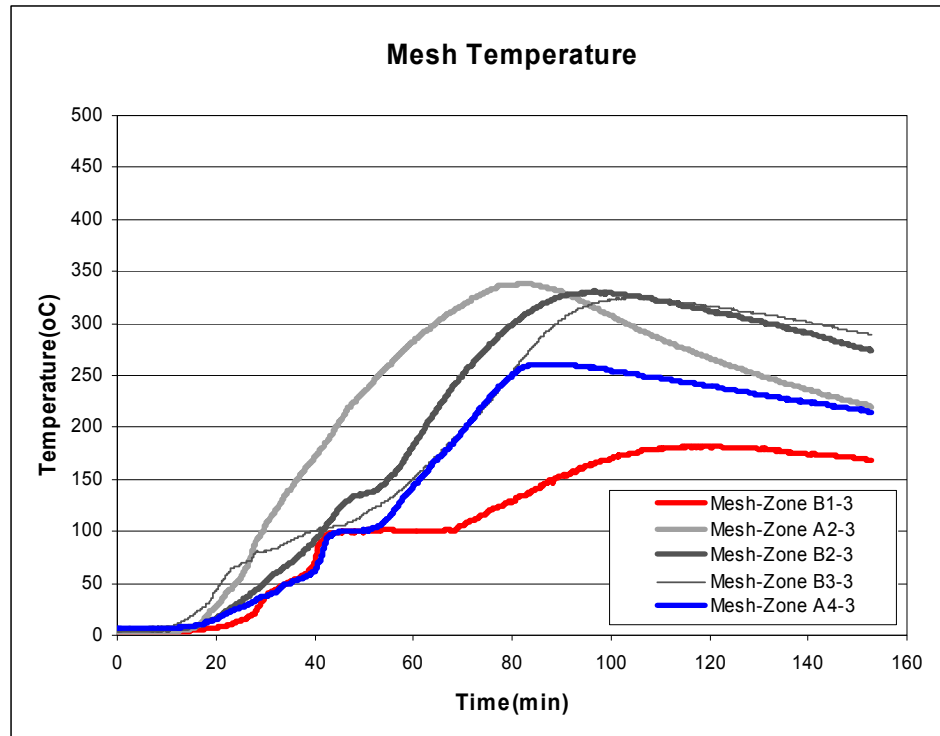
**Figure 7.55** : Recorded maximum temperatures in the unprotected beams.

With increasing temperatures on the unprotected CBs (Figure 7.53), it was observed that post web buckling occurred initially. The composite action between the CBs and slab prevented twisting of the beam as a whole. The tendency for the bottom flange to displace laterally caused bending of the beam's web leading to overall distortional buckling, as shown in Figure 7.53. At this stage the unprotected steel temperatures were approximately 800°C and only the top flange was considered to be providing support to the slab by acting as a catenary (Figure 7.53). The temperature of the mesh reinforcement, above the beams reached a maximum of 375°C at 95 minutes, as shown in Figure 7.56 which was well into the cooling stages of the fire. Figure 7.57 shows the maximum recorded temperature of the mesh reinforcement between the beams, where again the maximum temperature occurred during the cooling stages of the fire. The temperature in the concrete slab continues to rise after the maximum atmosphere temperature, which occurred at 75 mins. The recorded temperatures of the shear studs are shown in Figure 7.57, where the maximum temperature reached 585°C. Although the shear stud

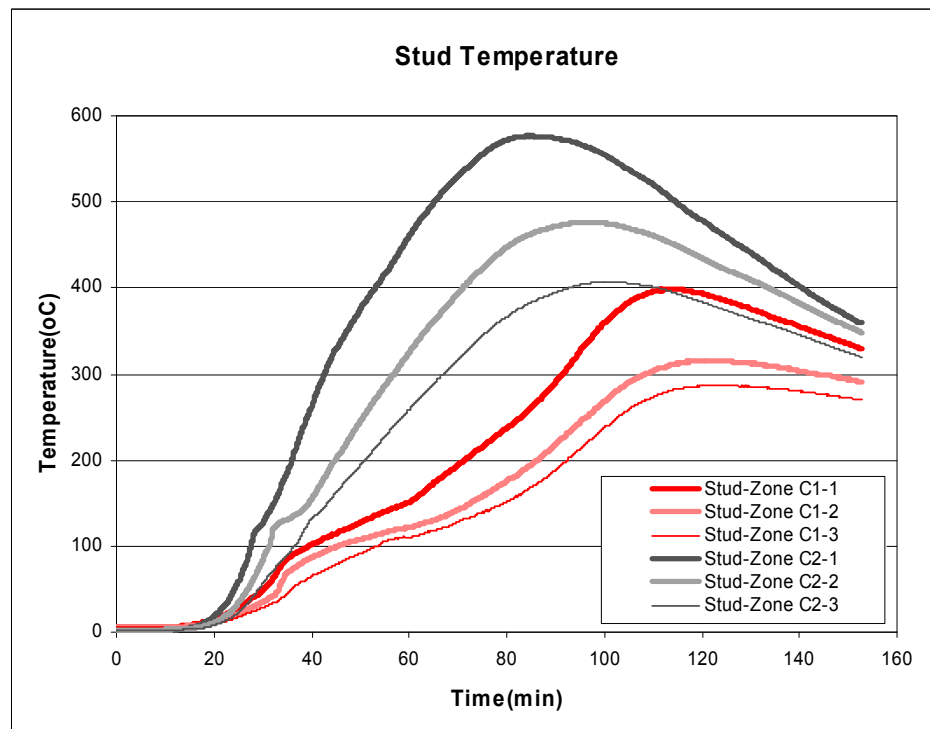
temperature is high the amount of horizontal shear required reduces as the unprotected beams increase in temperature and lose strength and stiffness. There was no sign of loss of composite action of the beams suggesting that the shear studs performed adequately and maintained composite action between the slab and beams during the full duration of the test.



**Figure 7.56** : Recorded temperatures of the mesh above the beams



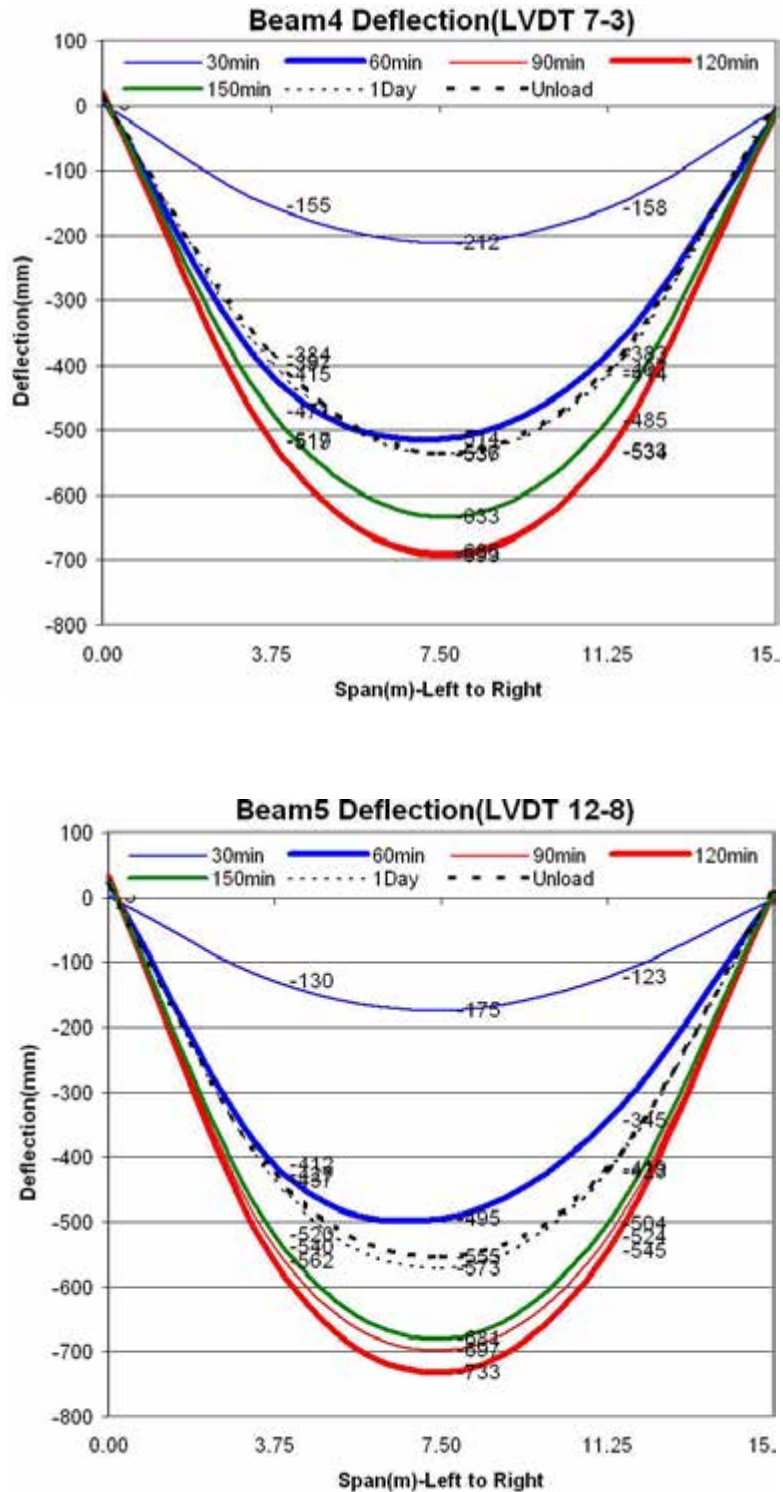
**Figure 7.57** : Recorded temperatures of the mesh between beams



**Figure 7.58** : Recorded temperatures of the shear studs

The maximum recorded deflection of the slab was 783mm, which occurred after 112 minutes (Figure 7.59), which is well into the cooling stage of the fire. Figure 7.59 shows the time/displacement curve for Beams 4 and 5, during the test

and after one day following the test. Figure 7.59 also shows the deflection after one month once the sandbags had been removed.



**Figure 7.59** : Deflection profile recorded on the slab/beam

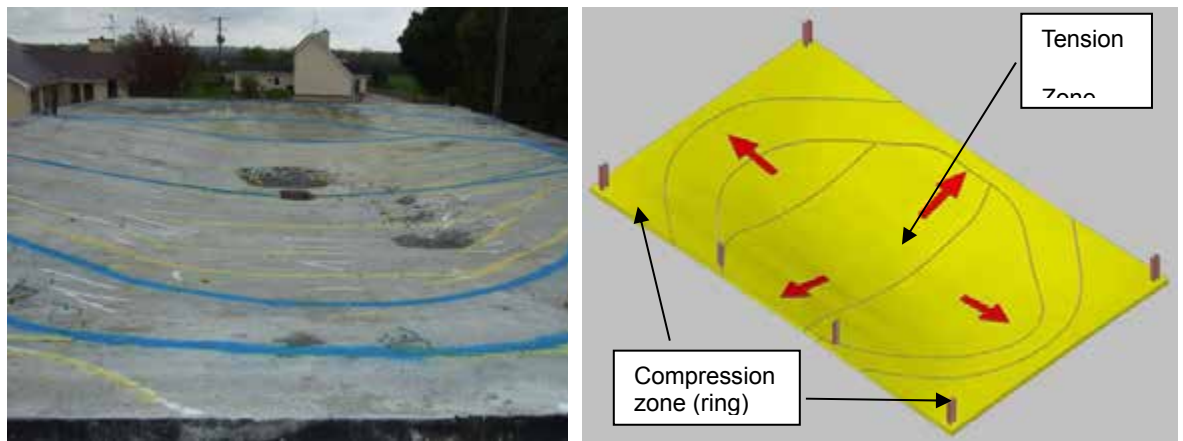
The deflection profile of the floor slab, coupled with the composite action between the beams and slab, caused rotation of the top flange of the steel beam. This induced a secondary moment into the beam section, together with vertical shear force, leading to distortional buckling of the CBs driving the lower tee laterally out

of its original plane. At this stage the load was predominately supported by membrane action of the floor slab, corresponding to fundamental principles outlined in the Bailey design method.

It can be seen that the unprotected cellular beams effectively went into catenary action, with only the top tee contributing to supporting the load. Web post buckling, which is commonly observed in isolated small-scale fire tests, occurred around the first opening in the beam where the overall displacements are restricted.

#### 7.4.6 Membrane Action in Floor Slabs

The steel deck reached temperatures in excess of 900°C and was observed to have de-bonded from the concrete in most areas. At a temperature of 900°C the steel deck had lost 94% of its strength and therefore, coupled with de-bonding, did not significantly contribute to the overall strength of the floorplate at the point of maximum fire severity. This corresponds to the design assumption by Bailey where the contribution from the steel deck is ignored in the calculation of the load capacity of the slab. However, it is worth noting that the steel deck does have the beneficial effect of reducing the consequence of any spalling since it ensures that any spalled/cracked concrete stays in place, provided that the deck does not significantly debond and creates a large gap between the deck and concrete. In the test a large crack occurred across the short span of the floor slab (Figure 7.60) corresponding to the previous test observations of membrane action.



**Figure 7.60** . Cracking pattern highlighting behaviour of the slab

The supported concrete slab was not horizontally restrained around its perimeter and the supporting protected perimeter beams maintained their load carrying capacity and were subjected to small vertical displacements. This allowed membrane action to develop with the in-plane forces in the central region of the slab going into tension and in-plane equilibrium compressive forces forming in the slab around its perimeter (Figure 7.60). This behaviour is analogous to a bicycle wheel; the spokes representing tensile membrane action, and the rim representing compressive membrane action.

#### 7.4.7 Conclusions

The floorplate performed extremely well supporting the applied load for the duration of the test and highlighted the inherent strength in the system due to membrane action of the floor plate. Based on the measured data it was shown that the reinforcement in the central region of the slab was under tensile force forming an elliptical parabolic tensile mesh anchored by a concrete compressive ring forming around the perimeter of the slab. Due to membrane action, the existence of secondary beams to support the slab is not necessary in the fire condition and these beams can be left unprotected.

In terms of the performance of the unprotected CBs the following conclusions can be drawn.

1. Due to the combined composite action of the supporting CBs and slab, distortional buckling of the CBs was the governing mode of structural failure rather than web post buckling or Vierendeel mechanism that was commonly observed in small-scale fire tests on CBs in fire.
2. From the time when distortional buckling occurred, only the top tee of the CB's contributed to the loading capacity of the floorplate through catenary action.
3. The CBs did not affect the membrane behaviour of the floorslab, which followed the classic behaviour as outlined in Bailey's design method and supported the load for the duration of the test.

The masonry wall forming the boundary of the compartment retained its integrity despite a significant thermal gradient across the wall and substantial lateral deformation. In addition, all the connections (although protected) performed very well and showed no signs of failure.

## **8 PARAMETRIC NUMERICAL STUDIES**

### **8.1 Scope**

The full scale standard fire resistance test has confirmed once again the excellent performance of the composite flooring system due to the presence of tensile membrane action in the slab as observed and described by Bailey & Moore<sup>(12,13)</sup>. Nevertheless, it is still necessary to extend the verification of the simple design method to its full application domain. With current knowledge in fire safety engineering, such verification can be achieved by means of a numerical parametric study on the basis of advanced calculation models, in which several specific features, such as deflection limit of the floor and elongation of reinforcing steel can be checked easily. However, before the parametric study in this project was carried out, the advanced numerical model had to be validated against the fire test.

### **8.2 Verification of ANSYS numerical model against FRACOF test**

#### **8.2.1 General**

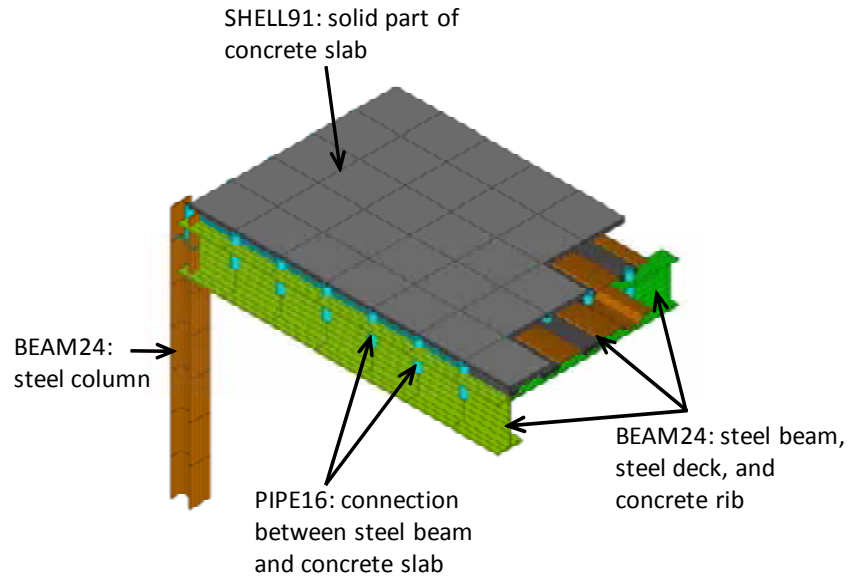
In order to provide a valid numerical model to simulate the fire behaviour of composite floors, numerical investigation of the full scale fire test described in Section 7 was performed using the computer software package ANSYS. The numerical model was composed of two different parts, one for heat transfer analysis and one for structural analysis.

#### **8.2.2 Structural Analysis**

The structural analysis was based on a hybrid structural model that took account of the steel beams; steel sheet; concrete rib and reinforcing steel mesh (see Figure 8.1). In this structural model, the following three types of finite elements were used:

- 3D non-linear line element - BEAM24,
- 3D non-linear multi-layer shell element - SHELL91
- 3D linear line element – PIPE16.

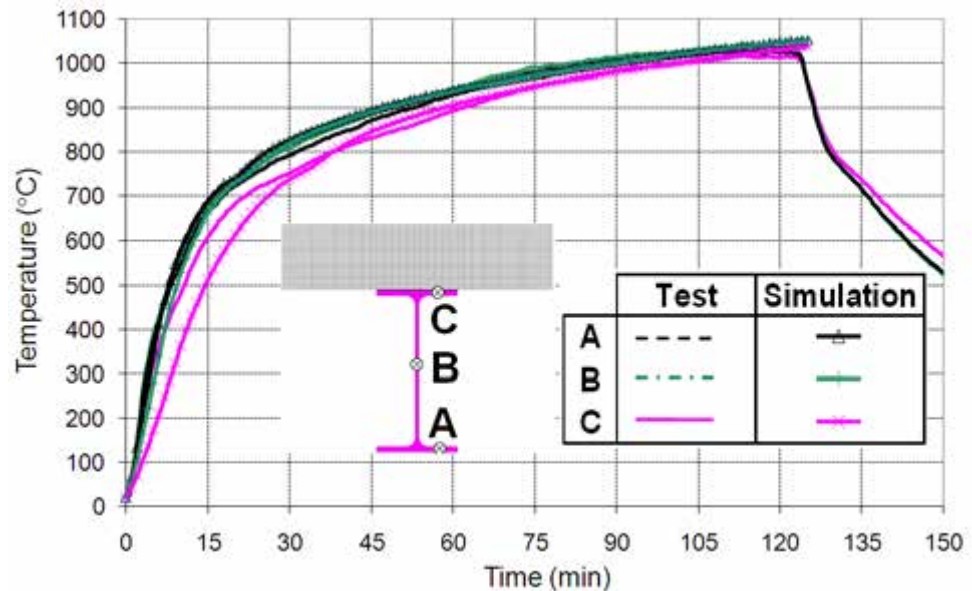
The composite floor was represented by shell elements for the solid part of the composite slab as well as reinforcing steel mesh. Beam-column elements were used for the steel members, the steel sheet and the ribs of the composite slab. Link elements were used for the shear connection between the steel beams and the composite slab.



**Figure 8.1** *Detail of the structural modelling*

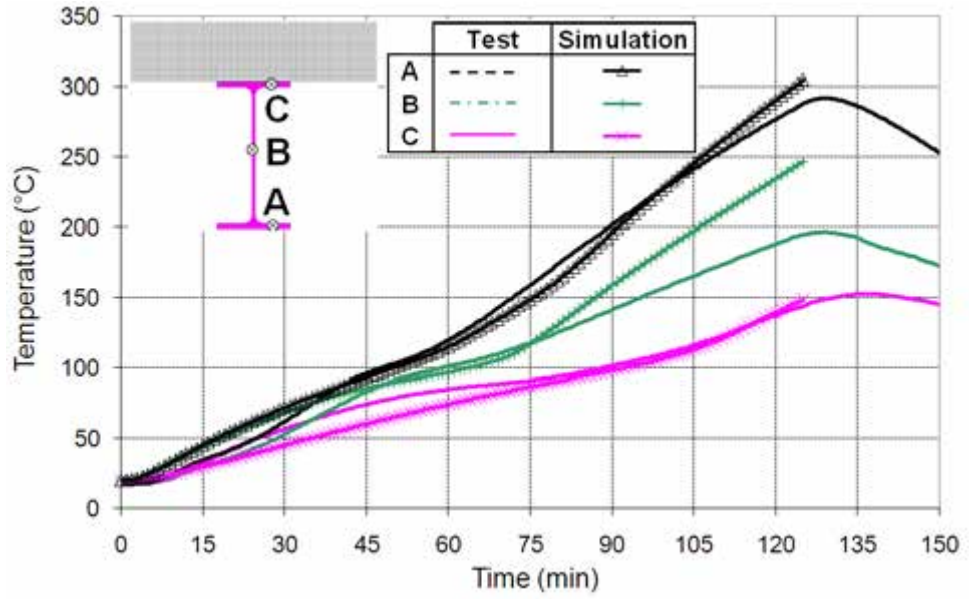
### 8.2.3 Heat transfer analysis

In the heat transfer analysis, the heating of all the structural members was predicted with help of 2D models using the typical cross section of each structural member. As the validation of the numerical model concerns mainly the structural behaviour, the thermal properties of insulation material were adjusted in order to simulate the heating of protected steel members recorded during the fire test. For the steel and concrete elements, their thermal properties are those given in EN1994-1-2<sup>(33)</sup>. A comparison of calculated temperatures with test temperatures for different structural members is illustrated by Figure 8.2 to Figure 8.5.

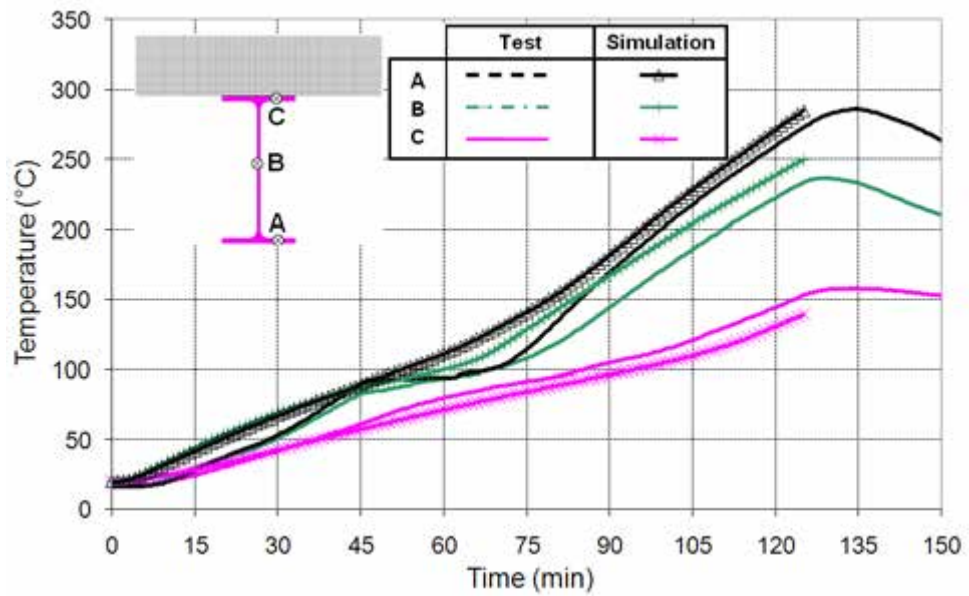


**Figure 8.2** *Temperature comparison between test and numerical calculation - unprotected steel beams*

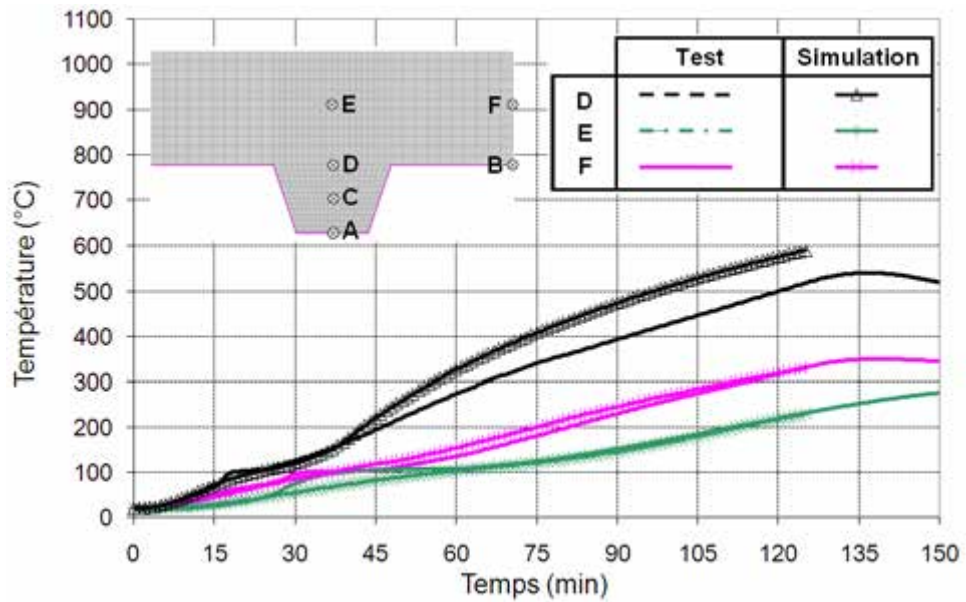




**Figure 8.3** *Temperature comparison between test and numerical calculation - Protected secondary beams*



**Figure 8.4** *Temperature comparison between test and numerical calculation - Protected main beams*

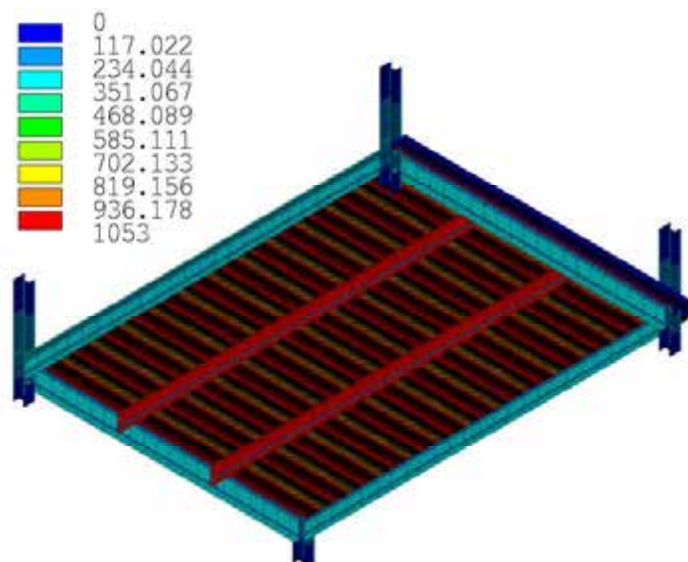


**Figure 8.5** *Temperature comparison between test and numerical calculation - composite slab*

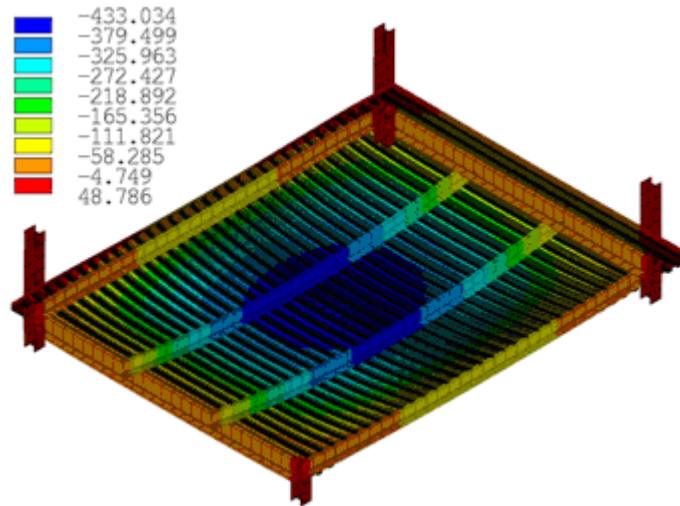
### 8.2.4 Mechanical behaviour of structural members

The structural behaviour of the floor was analysed based on the temperatures given by the heat transfer model and the structural model shown in Figure 8.1.

It can be observed easily from this model that the central part of the floor was heated much more than the boundary structural members. The simulated structural behaviour of the floor is shown in Figure 8.7, which gives the deformed shape predicted by the numerical model following 120 minutes exposure to the standard temperature-time curve.

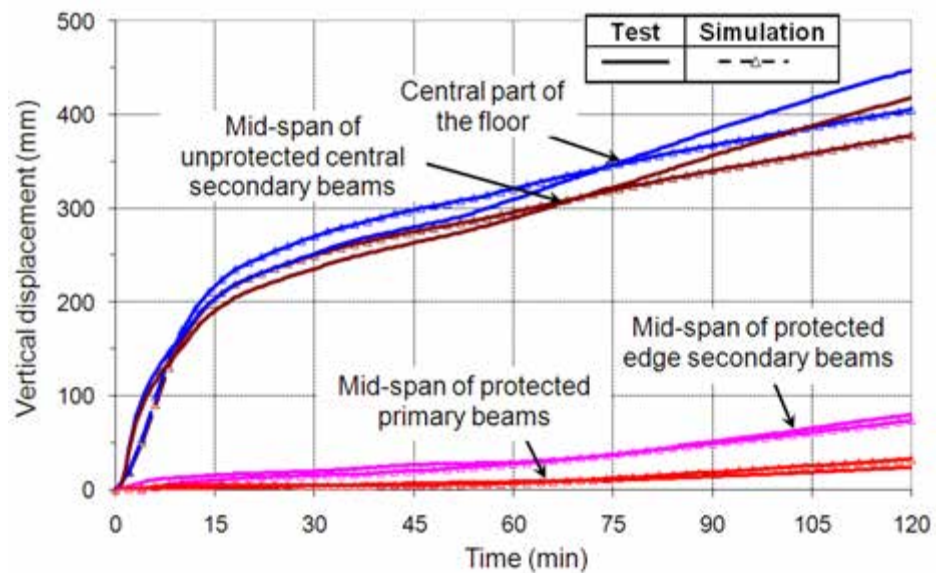


**Figure 8.6** *Global structural model and attributed temperature field at 120 minutes of ISO fire*



**Figure 8.7** Simulated deformed shape of the floor

A comparison between the vertical displacement of the floor calculated using the numerical model and the measured displacements of the test specimen is shown in Figure 8.8. It can be observed that globally the numerical modelling predicts results very close to the experimental ones. However, a slight discrepancy occurs in the deflection of the unprotected beams after 50 minutes, resulting in some divergence between the measured deflections and those predicted by the numerical analysis. This phenomenon was attributed to the loss of continuity in the reinforcing mesh during the test, which resulted in a higher value of deflection for the unprotected beams. Despite this small difference, the validity of the numerical model as well as its capacity to predict fire behaviour was demonstrated.



**Figure 8.8** Comparison of the predicted deflection of the floor recorded during the heating period of test

## 8.3 Verification of SAFIR numerical model against fire tests

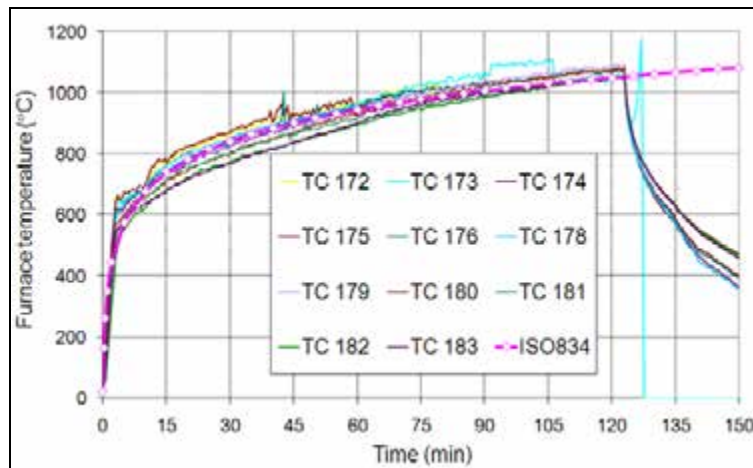
### 8.3.1 General

In order to provide a valid numerical model to simulate the fire behaviour of composite floors, numerical investigation of the full scale fire test described in Section 7 was performed using the computer software package SAFIR. The numerical model was composed of two different parts, one for heat transfer analysis and one for structural analysis.

### 8.3.2 SAFIR Vs FRACOF test

#### 8.3.2.1 Fire load

For the Fracof test, the floor was exposed to the ISO fire condition using a standard fire resistance testing furnace. The recorded temperatures in the different places of the furnace show that the ISO standard fire curve is closely followed, see Figure 8.9.

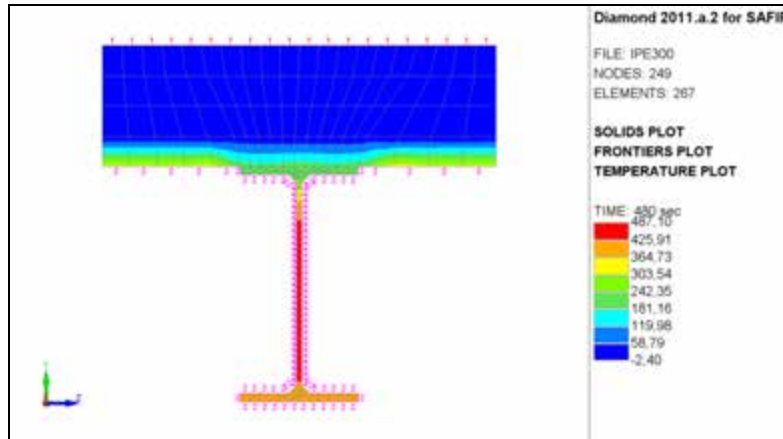


**Figure 8.9** : Comparison between measured fire curves in the compartment and the ISO-834 fire curve

#### 8.3.2.2 Thermal analyses : Numerical models and main results

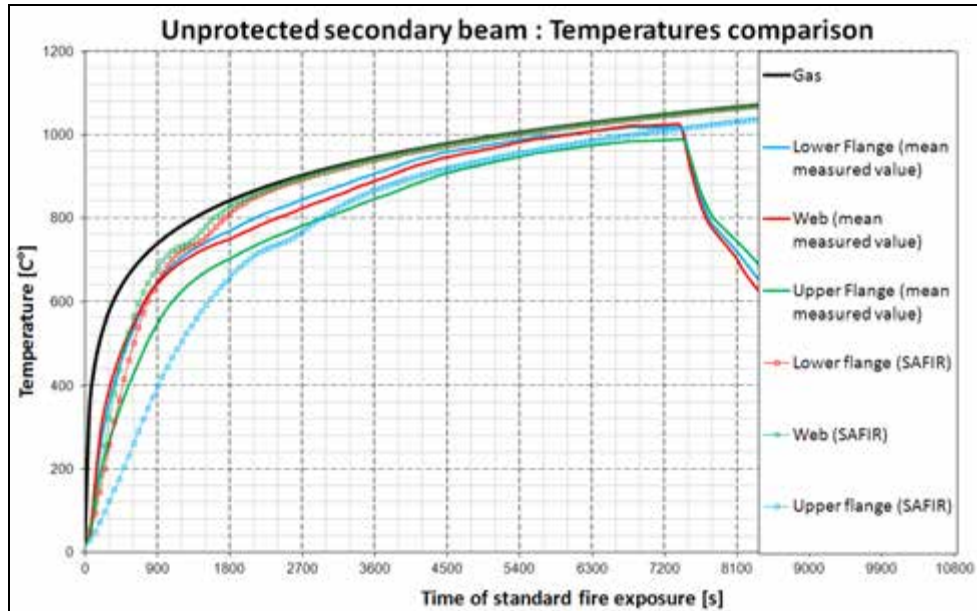
The software SAFIR has been used for the thermal analysis of the steel profiles and of the slab. For the calculation of the temperatures in the structure, the ISO-834 fire curve was applied at the boundaries of the concrete slab and of the unprotected steel profiles whereas, for the thermally protected sections, the temperatures recorded on the steel section were used (in order to eliminate all uncertainties about the thermal properties of the insulation material or about possible construction defects).

With regard to the unprotected secondary beams, the concrete slab is modeled in order to take into account its capacity of absorbing heat. This concrete above the upper flange of the steel profile is only considered for the thermal analysis and has no mechanical resistance (because this concrete will be modeled separately by the shell elements). The bottom flange, the two sides of the profiles and the bottom face of the slab are submitted to the ISO fire while the upper face of the slab remains in contact with air at 20°C during all the calculation, see Figure 8.10.



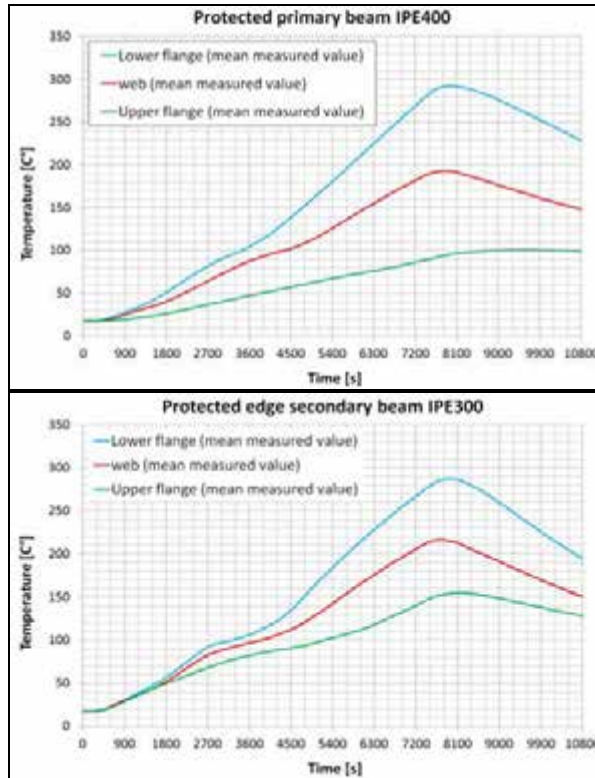
**Figure 8.10** : Fire exposure of the unprotected secondary beams

The computed results are compared with measured data in Figure 8.11 in the lower flange, in the web and in the upper flange of these profiles. The computed temperatures match well the measured temperatures.



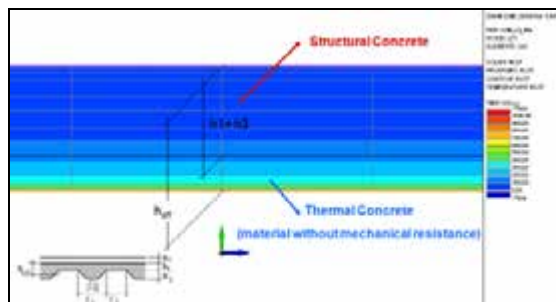
**Figure 8.11** : Comparison between the computed and measured temperatures in the unprotected secondary beams

Figure 8.12 shows the temperatures measured in the lower flange, in the web and in the upper flange of the protected profiles.



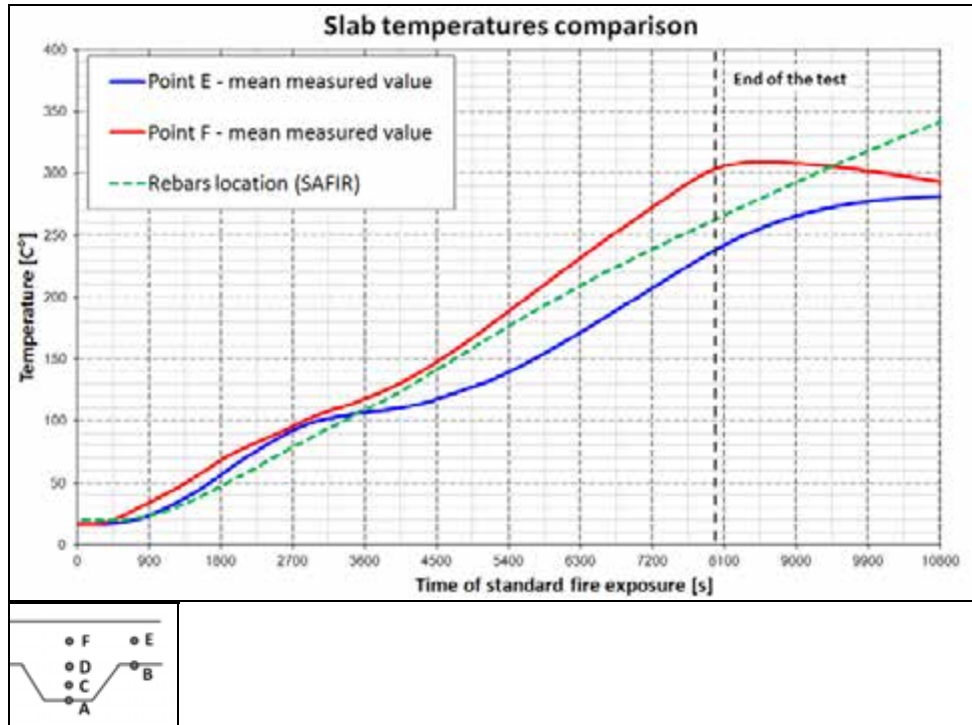
**Figure 8.12** : Measured temperatures in the protected IPE400 beam (left) and in the protected IPE300 beam (right)

For the thermal analysis in the slab, the effective thickness model for the slab as defined in Eurocode EN1994-1-2 has been used. The ribs of 58 mm and the concrete layer of 97 mm that covers the ribs are replaced by a flat slab with an effective thickness of 120 mm, see Figure 8.13. The slab is submitted to the fire on its lower face while the upper face remains in contact with air at 20°C. The height to consider for mechanical calculations is the concrete height above the steel deck.



**Figure 8.13** : Effective thickness calculation for the slab thermal analysis

In Figure 8.14a, the computed temperatures are compared with the mean measured temperatures in the slab above the rib. Point E and point F correspond to the steel rebars location, see Figure 8.14b.

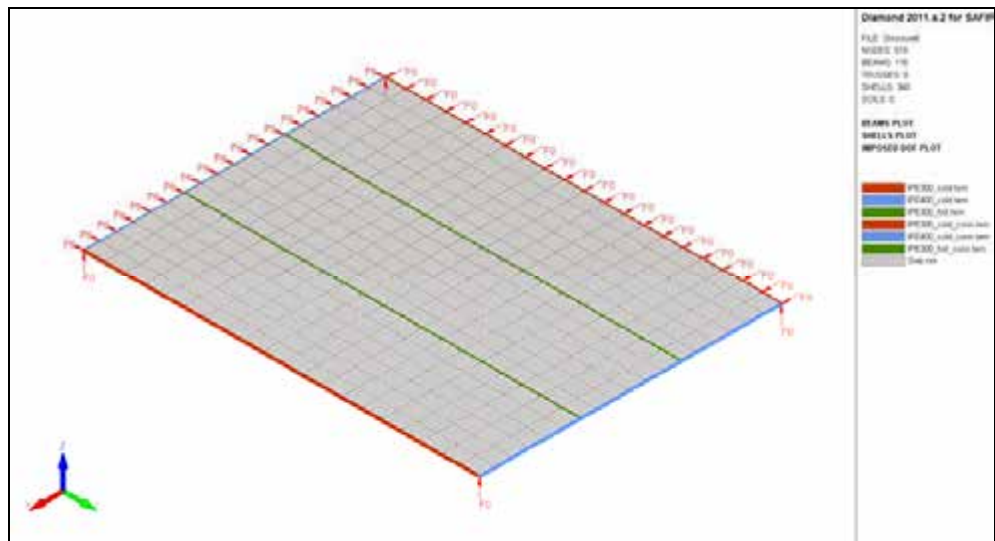


**Figure 8.14 :** a) Comparison between measured and computed temperatures with effective thickness slab (left), b) Position of the TC in the slab (right)

The temperatures in the steel rebars and in the slab are well approximated by the numerical results with the uniform thickness model.

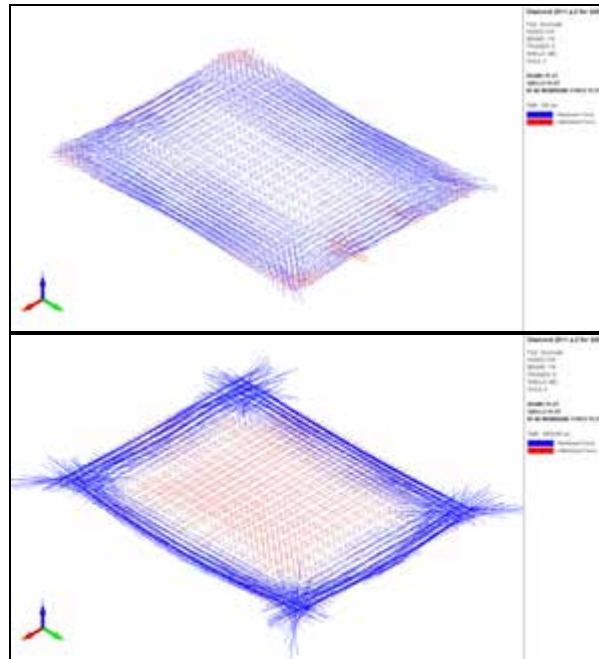
### 8.3.2.3 Structural analysis

A finite element model was built in the SAFIR software. The structure is modeled using BEAM elements for the beams and SHELL elements for the slab. The edge beams are simply supported on the columns as indicated in Figure 8.15. The slab is axially restrained on two sides in order to simulate the continuity condition of composite floor.



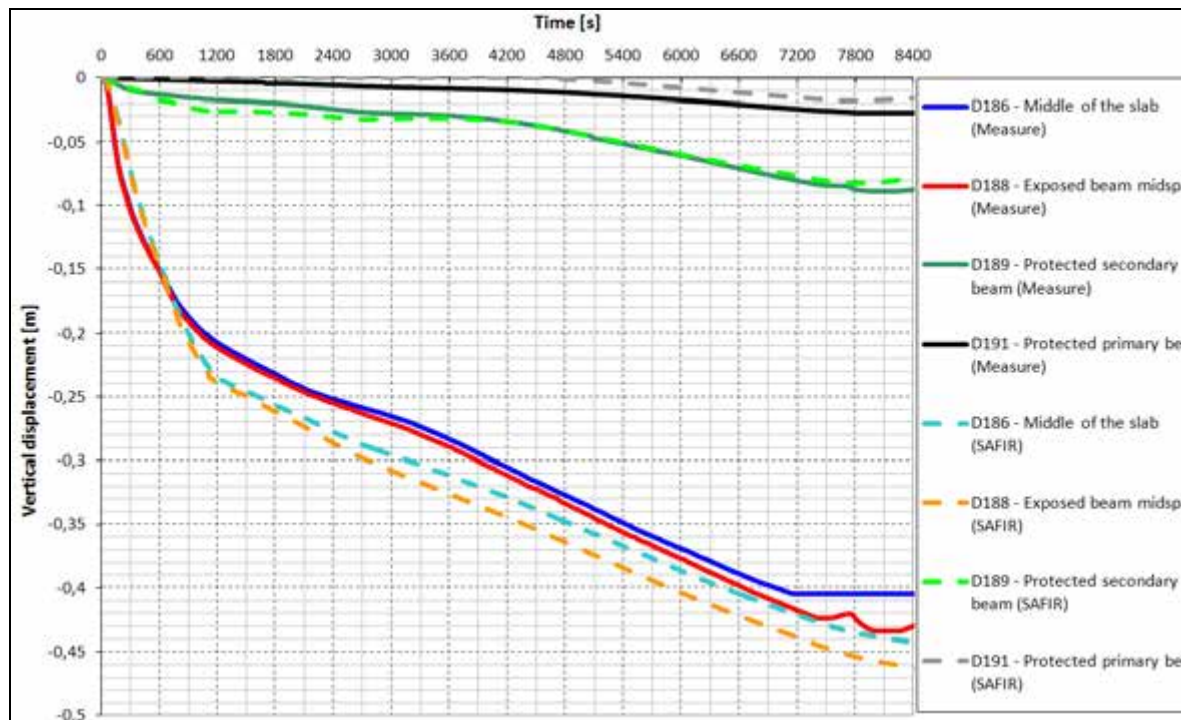
**Figure 8.15 :** Structural analysis model

The structural behavior at room temperature is a flexional mode whereas, during the fire, membrane action develops. The membrane forces for room and elevated temperatures can be observed in Figure 8.16.



**Figure 8.16** : Comparison between bending mode (left) and tensile membrane action (right): membrane forces within the slab

Finally the comparison between the measured deflections and the deflections computed with this FEM model is shown in Figure 8.17.



**Figure 8.17** : Comparison between experimental and numerical results concerning vertical displacements

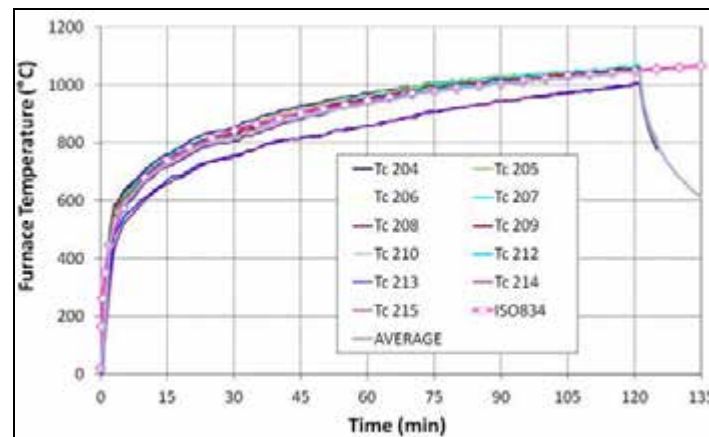


A very good correlation between the results of the FEM model and the real behaviour during the test is observed. This seems to validate the simplifications that have been introduced such as the fact that the stiffness of the columns in bending has been neglected and the fact that the ribbed slab has been modelled by an equivalent flat slab. It has also to be mentioned that the simulation of the structural behaviour has been made with measured values of the material properties.

### 8.3.3 SAFIR Vs COSSFIRE test

#### 8.3.3.1 Fire load

For the Cossfire test, the floor was exposed to the ISO fire condition using a standard fire resistance testing furnace. The recorded temperatures in the different places of the furnace show that the ISO standard fire curve is closely followed, see Figure 8.18.

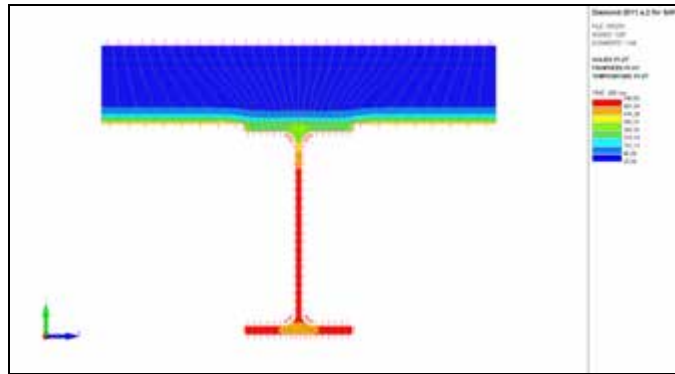


**Figure 8.18 :** Comparison between measured fire curves in the compartment and the ISO-834 fire curve

#### 8.3.3.2 Thermal analyses : Numerical models and main results

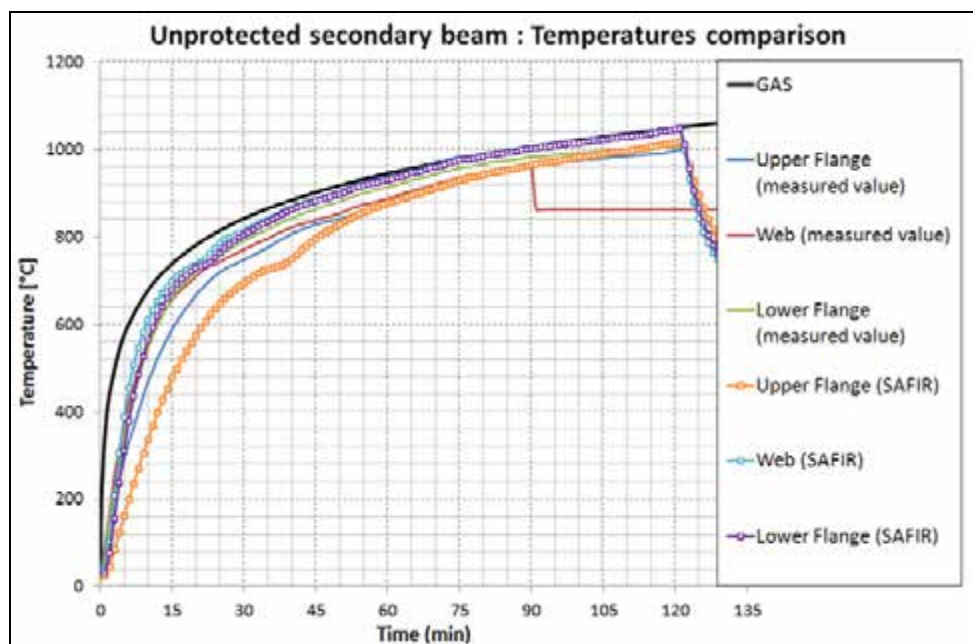
The software SAFIR has been used for the thermal analysis of the steel profiles and of the slab. For the calculation of the temperatures in the structure, the average fire curve was applied at the boundaries of the concrete slab and of the unprotected steel profiles whereas, for the thermally protected sections, the temperatures recorded on the steel section were used (in order to eliminate all uncertainties about the thermal properties of the insulation material or about possible construction defects).

With regard to the unprotected secondary beams, the concrete slab is modeled in order to take into account its capacity of absorbing heat. This concrete above the upper flange of the steel profile is only considered for the thermal analysis and has no mechanical resistance (because this concrete will be modeled separately by the shell elements). The bottom flange, the two sides of the profiles and the bottom face of the slab are submitted to the average fire while the upper face of the slab remains in contact with air at 20°C during all the calculation, see Figure 8.19.



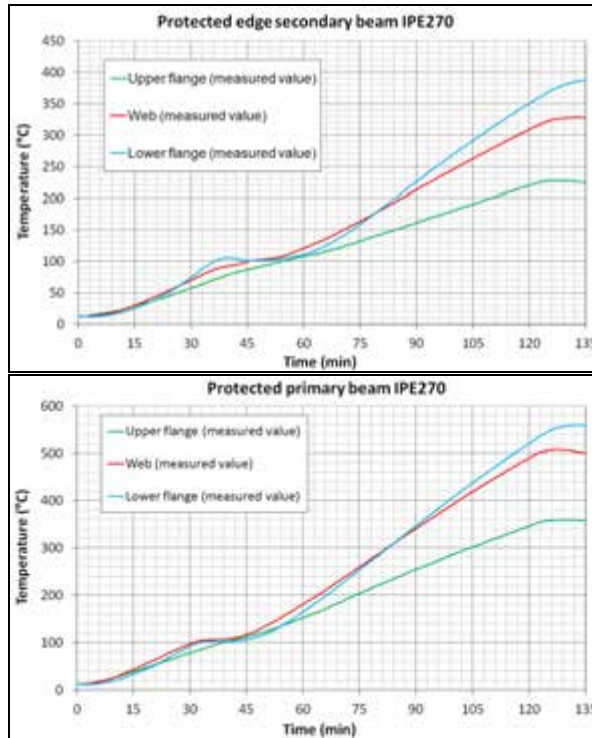
**Figure 8.19** : Fire exposure of the unprotected secondary beams

The computed results are compared with measured data in Figure 8.20 in the lower flange, in the web and in the upper flange of these profiles.



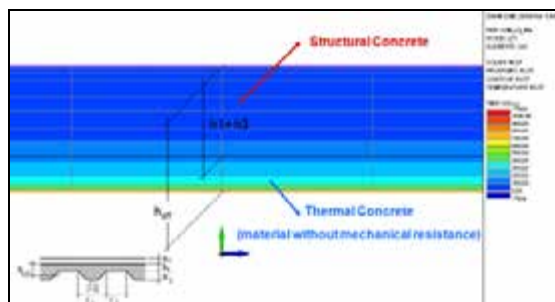
**Figure 8.20** : Comparison between the computed and measured temperatures in the unprotected secondary beams

Figure 8.21 shows the temperatures measured in the lower flange, in the web and in the upper flange of the protected profiles.



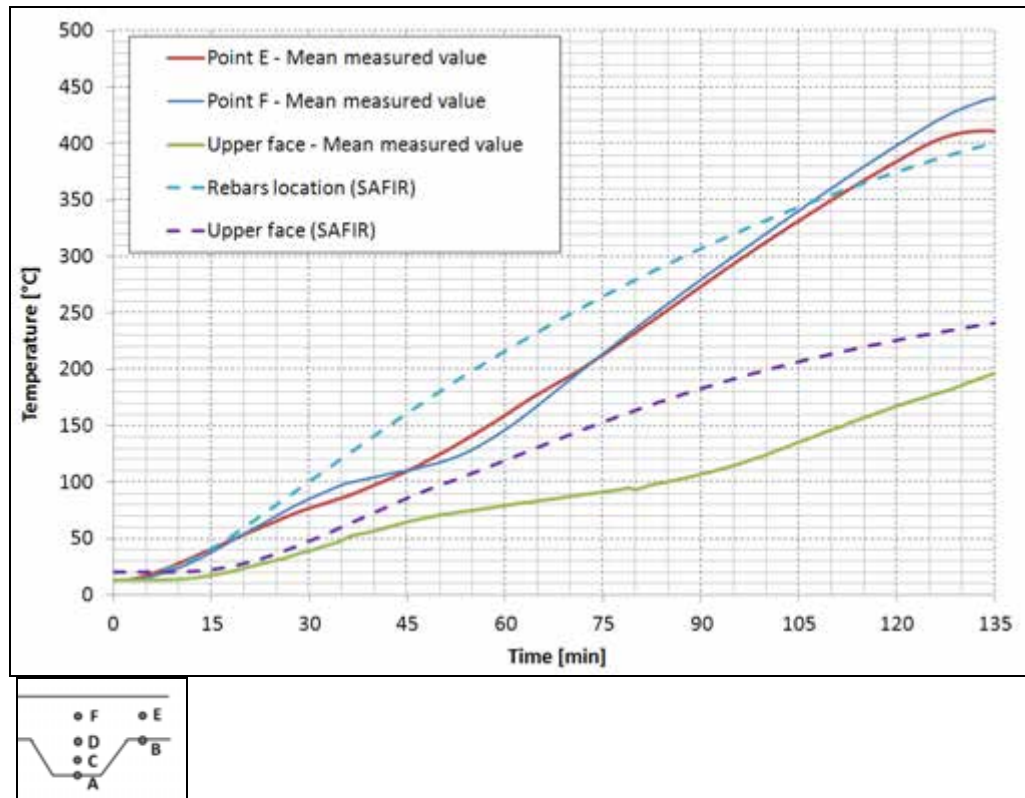
**Figure 8.21 :** Measured temperatures in the protected secondary IPE270 beam (left) and in the protected primary IPE270 beam (right)

For the thermal analysis in the slab, the effective thickness model for the slab as defined in Eurocode EN1994-1-2 has been used. The ribs of 58 mm and the concrete layer of 77 mm that covers the ribs are replaced by a flat slab with an effective thickness of 100 mm, see Figure 8.22. The slab is submitted to the average fire on its lower face while the upper face remains in contact with air at 20°C. The height to consider for mechanical calculations is the concrete height above the steel deck.



**Figure 8.22 :** Effective thickness calculation for the slab thermal analysis

In Figure 8.23a, the computed temperatures are compared with the measured temperatures in the slab above the rib. For the three considered positions above the ribs (Point E, Point F and the upper face of the slab, see Figure 8.23b, the mean measured values are given. Point E and Point F correspond to the steel rebars location.



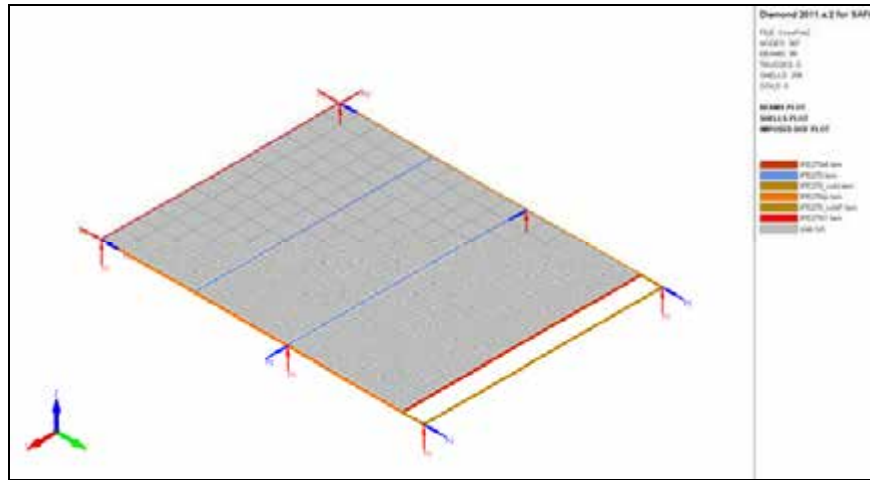
**Figure 8.23** : a) Comparison between measured temperatures and computed temperatures with effective thickness slab, b) Position of the TC in the slab

The computed temperatures match well the mean measured temperatures except at the upper face of the slab where the temperatures are slightly overestimated. As Point F and Point E correspond to the steel rebars location, the temperatures in the steel rebars are correctly approximated by the numerical results with the effective thickness model.

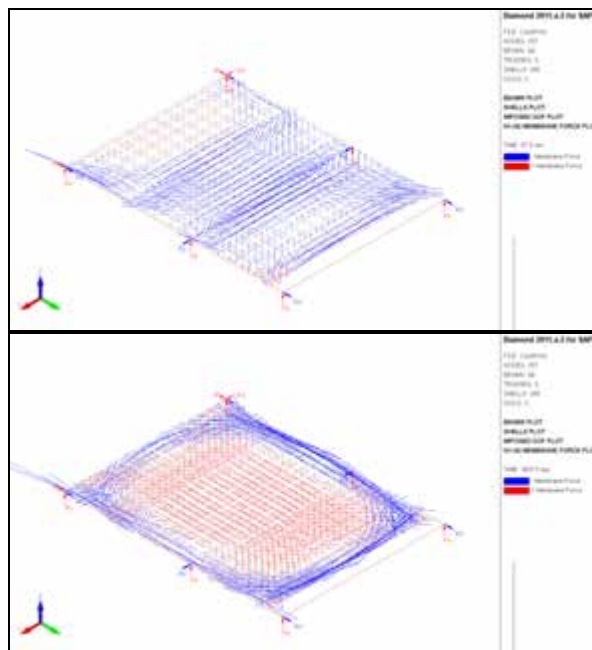
### 8.3.3.3 Structural analysis

A finite element model was built in the SAFIR software. The structure is modeled using BEAM elements for the beams and SHELL elements for the slab. The edge beams are simply supported on the columns as indicated in Figure 8.24. The slab and the beams are axially unrestrained.

The structural behavior at room temperature is a flexional mode whereas during the fire, membrane action occurs. The membrane forces for room and elevated temperatures can be observed in Figure 8.25.



**Figure 8.24** : Structural analysis model

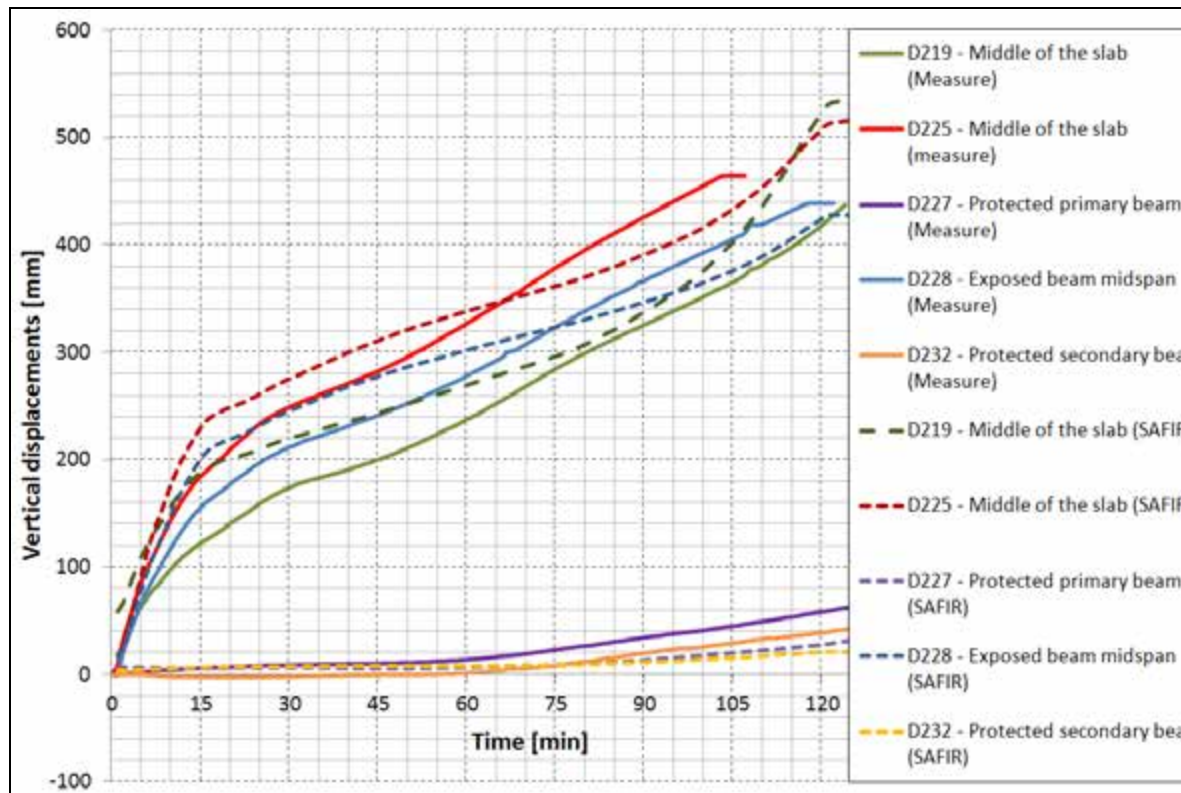


**Figure 8.25** : Comparison between bending mode (left) and tensile membrane action (right): membrane forces within the slab

Finally the comparison between the measured deflections and the deflections computed with this FEM model at different positions of the floor (see Figure 8.26) is shown in Figure 8.27.



**Figure 8.26** : Position of the transducers and of the computed deflections



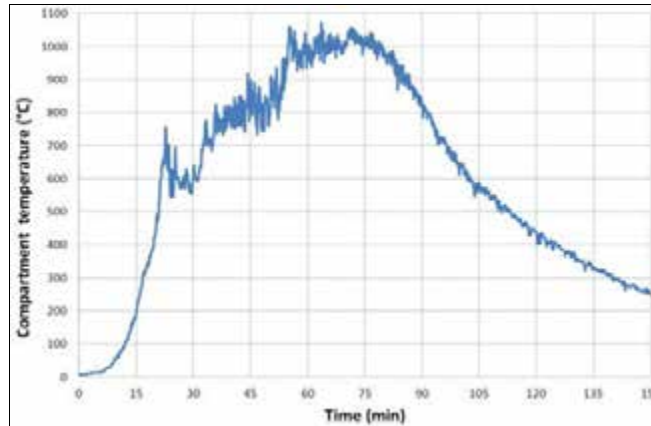
**Figure 8.27** : Comparison between experimental and numerical results concerning vertical displacements

A good correlation between the results of the FEM model and the real behaviour during the test is observed. This seems to validate the simplifications that have been introduced such as the fact that the stiffness of the columns in bending has been neglected and the fact that the ribbed slab has been modelled by an equivalent flat slab. It has also to be mentioned that the simulation of the structural behaviour has been made with the measured values of the material properties.

### 8.3.4 SAFIR Vs FICEB test

#### 8.3.4.1 Fire load

For the Ulster test, all thermal analyses were performed using the measured temperature in the middle of the compartment, see Figure 8.28, in order to focus the analyses on the ability of the software SAFIR to simulate the behavior of the floor from the real temperature curve in the compartment.



**Figure 8.28** : Measured temperature curve in the middle of the compartment

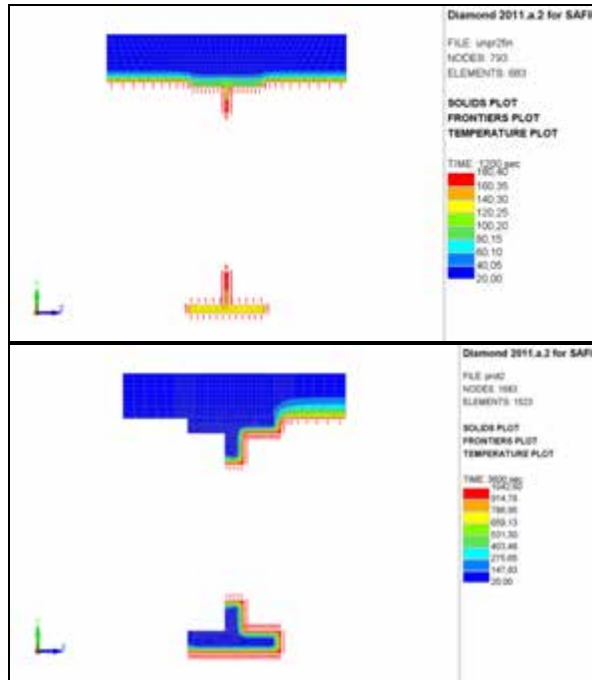
#### 8.3.4.2 Thermal analyses : Numerical models and main results

The software SAFIR has been used for the thermal analysis of the steel profiles and of the slab. The steel profiles are cellular beam profiles. As the section analyzed here thermally is then used as the section of a beam finite element in the subsequent structural analyses, a section passing through the center of a circular opening is considered, see Figure 8.29a. Indeed, the longitudinal stresses of a beam model cannot “enter” in the web posts that separate two openings.

In these thermal models of steel profiles, the concrete slab is modeled in order to take into account its capacity of absorbing heat. This concrete above the upper flange of the steel profile is only considered for the thermal analysis and has no mechanical resistance (because this concrete will be modeled separately by the shell elements). The steel profiles and the bottom face of the slab are submitted to the measured fire in the middle of the compartment while the upper face of the slab remains in contact with air at 20°C during all the calculation.

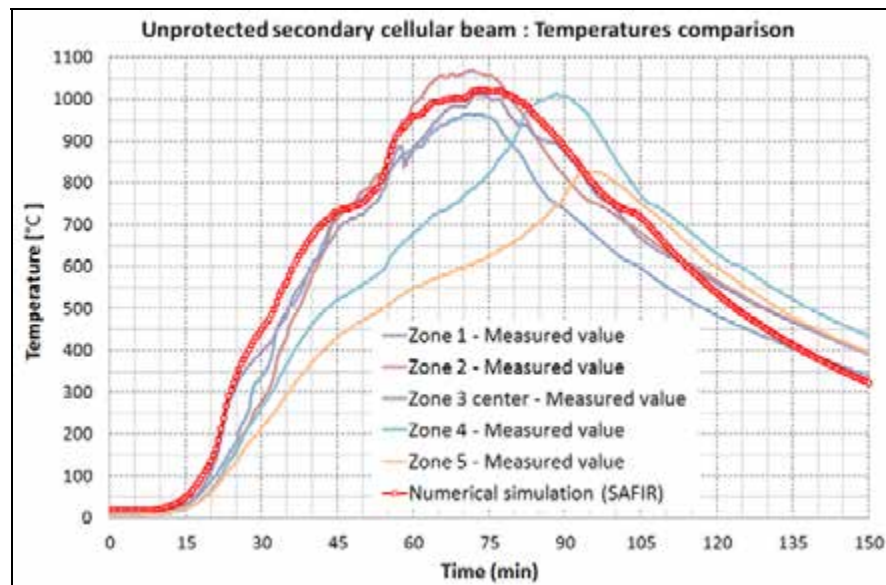
The temperatures reached in the unprotected sections are much higher than the critical temperature for such cellular beams. Indeed, when performing a structural analysis of such beams using shell elements, instabilities (mostly web post buckling or distortional buckling) can be observed for temperatures around 600°C. So, the structural model of the unprotected sections should take into account the fact that their behavior is affected by web post buckling.

An efficient way to take into account this behavior, while keeping beam elements in the structural model, is to perform the simulation using a modified steel material for the bottom flange of the unprotected beams. This modified steel material has the same mechanical properties as the steel from EN1993-1-2 under 500°C and loses irreversibly its mechanical properties between 500°C and 600°C, to take into account the instability phenomenon.



**Figure 8.29** : Fire exposure : a) of the unprotected secondary beams with the hybrid model (right) and b) of the protected beams(left)

The temperature computed in the secondary unprotected beams is compared in Figure 8.30 with the temperature measured in different longitudinal zones of this beam. The comparison seems to indicate a lower temperature toward the extremities of the beam during the test.



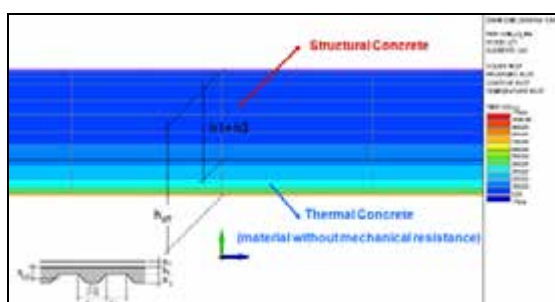
**Figure 8.30** : Comparison between the computed and measured temperatures in the unprotected secondary beams

With regard to the protected sections, the insulation material which was only considered for thermal analysis is also considered in the finite element model. The protected steel sections are affected by the fire on one side and on the bottom flange, while the other side of the profile, in front of a wall, is supposed to be an adiabatic boundary, see Figure 8.29b. The temperatures in the protected sections remained below the critical temperature for these cellular beams. So, during the



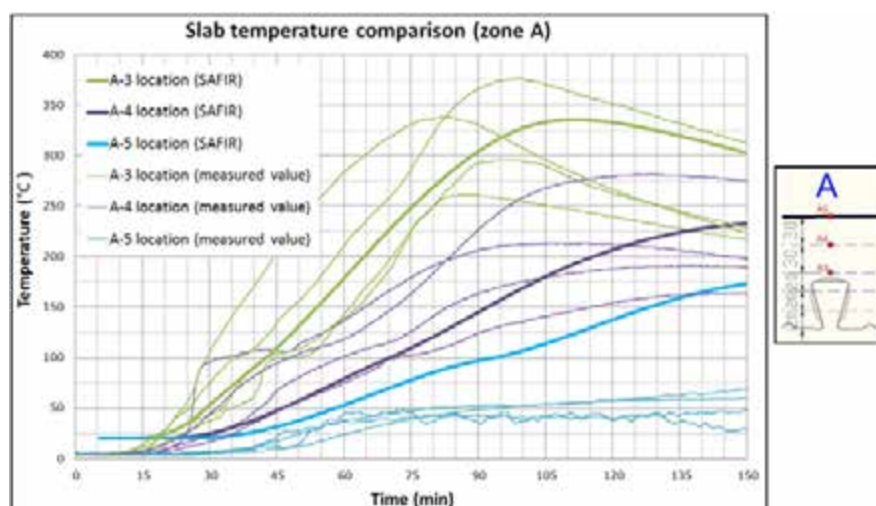
entire calculation, the standard steel material with mechanical properties as the steel from EN1993-1-2 could be considered for the bottom flange of these protected steel profiles. The fire protection of cellular beams is a key parameter that is determinant for ensuring a good membrane effect of composite floor system in case of fire.

For the thermal analysis in the slab, the effective thickness model for the slab as defined in Eurocode EN1994-1-2 has been used. The ribs of 51 mm and the concrete layer of 69 mm that covers the ribs are replaced by a flat slab with an effective thickness of 110 mm, see Figure 8.31. This effective thickness represents the height of the slab to consider for the thermal response. The slab is submitted to the fire on its lower face while the upper face remains in contact with air at 20°C. The height to consider for mechanical calculations is the concrete height above the steel deck.



**Figure 8.31** : *Effective thickness calculation for the slab thermal analysis*

In Figure 8.32a, the computed temperatures are compared with the measured temperatures in the slab above the rib. For the three considered positions above the rib (A-3, A-4 and A-5, see Figure 8.32b, four measures are given corresponding to four plan locations. The A-4 zone corresponds to the steel rebars location.



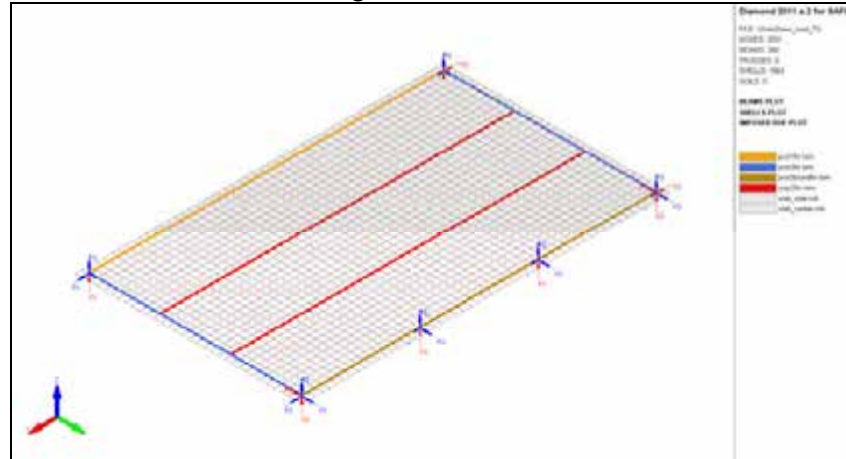
**Figure 8.32** : *Heat transfer in zones A1, A2 A3 and A4 at height A-3, A-4 and A-5 through cross section Comparison between measured and computed results with effective thickness slab model*

The computed temperatures match well the measured temperatures except at the upper face of the slab (A-5) where the temperatures are overestimated. As A-4 corresponds to the steel rebars location, the temperatures in the steel rebars are correctly approximated by the numerical results with the effective thickness model.

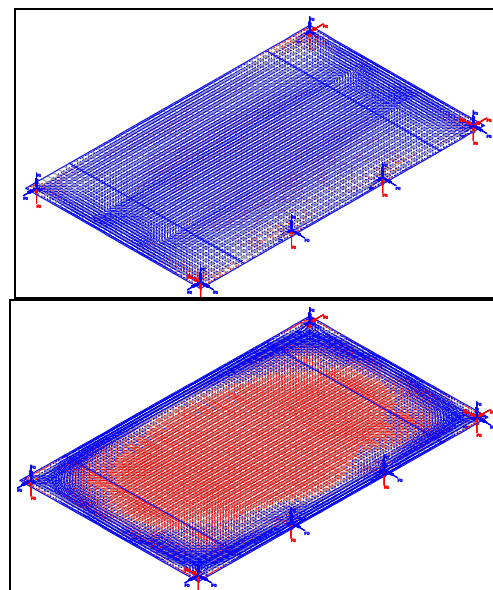
### 8.3.4.3 Structural analysis

A finite element model was built in the SAFIR software. The structure is modeled using BEAM elements for the beams and SHELL elements for the slab. The edge beams are simply supported on the columns as indicated in Figure 8.33. The slab and the beams are axially unrestrained.

The structural behavior at room temperature is a flexional mode whereas during the fire, membrane action develops. The membrane forces for room and elevated temperatures can be observed in Figure 8.34.



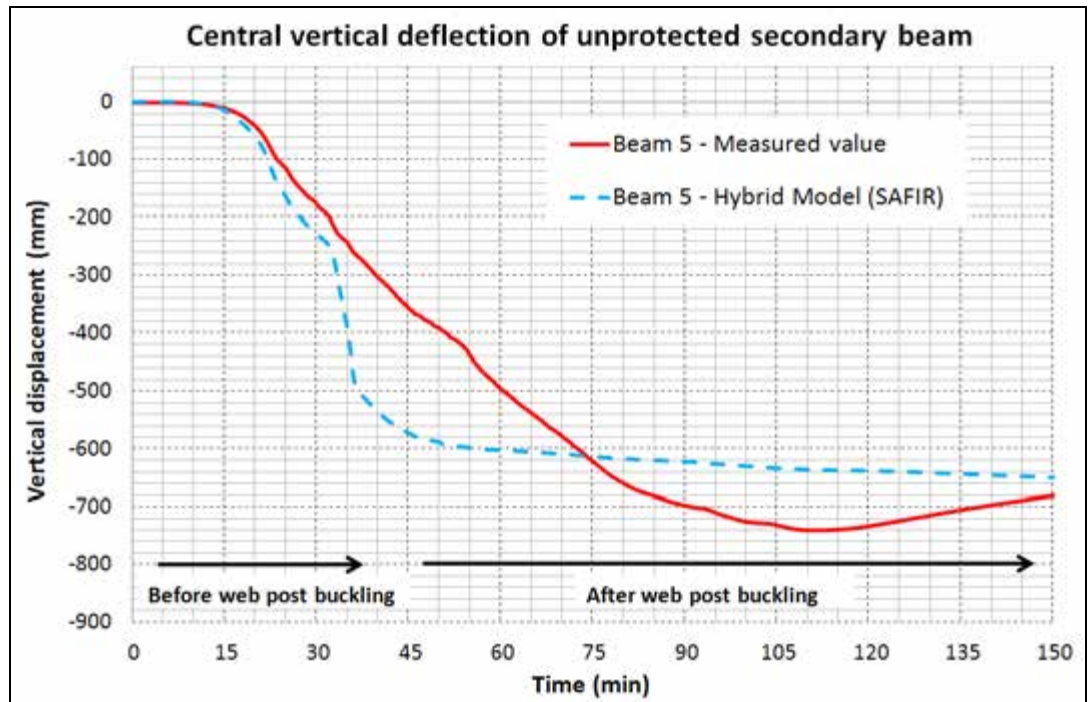
**Figure 8.33** : *Structural analysis model*



**Figure 8.34** : *Comparison between bending mode (left) and tensile membrane action (right): membrane forces within the slab*

As BEAM finite Element does not allow taking into account the web post buckling instabilities, the way to model the behaviour of the floor is to use a special material for the bottom flange of the unprotected beams. Considering this modified steel material (*STEELEC3\_WPB*) allow for a modeling of the structural behavior during the entire test with one single numerical calculation.

Finally the comparison between the measured deflections and the deflections computed with this FEM model at the middle of the unprotected secondary beams is shown in Figure 8.35.



**Figure 8.35** : Comparison between measured and computed vertical deflection at the middle of the unprotected beam with the hybrid model

After 30 minutes, the temperature of the bottom flange of the unprotected profiles overreaches 500°C. Then, performing the structural calculation with the hybrid model considering a modified steel material, the bottom flange loses quickly all mechanical properties and the deflection increases. At high temperature after the web post buckling, the hybrid model gives a good approximation of the real behavior of the slab that cannot get its stiffness back so that the deflection remains important at the end of the test.

A good correlation between the FEM model and the real behaviour of the test is observed. This seems to validate the simplifications that have been introduced such as the modelling of the instability phenomenon of the unprotected beams, the fact that the stiffness of the columns in bending has been neglected and the fact that the ribbed slab has been modelled by an equivalent flat slab. It has also to be mentioned that the simulation of the structural behaviour has been made with nominal values of the material properties.

The SAFIR structural model was capable of predicting with an acceptable level of accuracy the complex behaviour of cellular beams acting in membrane action. Using a modified steel material for the bottom flange of the unprotected cellular beams can be a simplified but efficient way for taking into account the instability phenomenon in such complex models where BEAM elements are preferable for the beams. It would also be possible to model the steel cellular beams in detail with shell elements, but such model would be too large for practical applications.

## 8.4 Parametric numerical study using standard temperature-time curve

### 8.4.1 Input data for parametric study

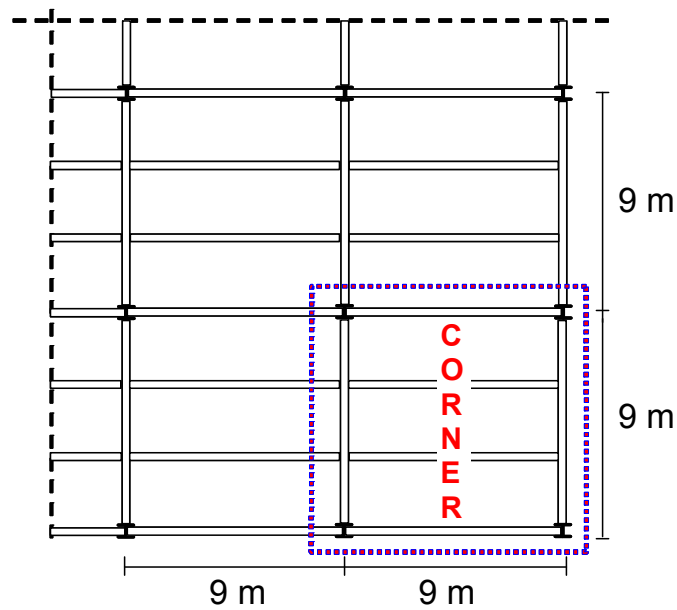
A parametric study was used to extend the investigation of the simple design method to its full application domain. However, a full parametric study would

require a great number of numerical simulations, which would necessitate a huge computation cost. Consequently the scope of the parametric study was limited to the following key parameters:

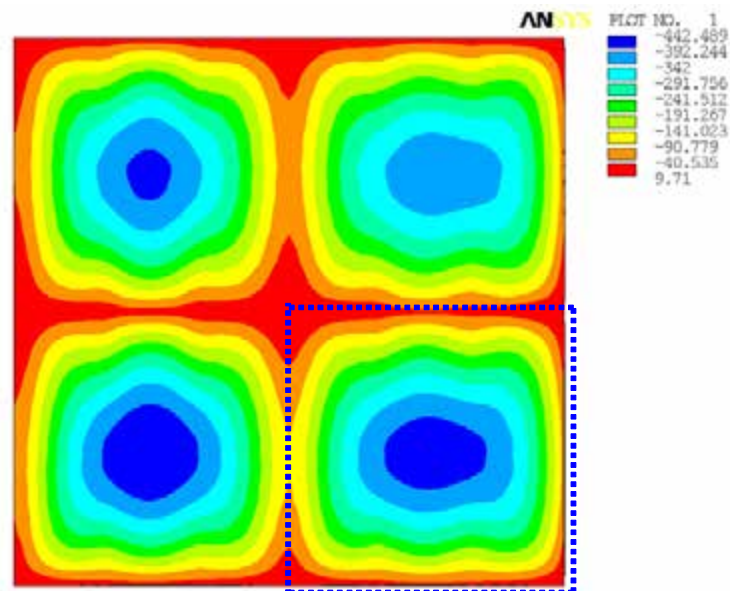
- Grid size of the floor,
- Degree of utilisation
- Fire duration

It must be pointed out that this parametric study is focused only on the behaviour of steel and concrete composite floors exposed to the standard temperature-time curve.

A preliminary numerical calculation was undertaken for a composite floor with an area of 18 m by 18 m, comprising two bays of 9 m span in each direction, (see Figure 8.36(a)). The main aim of this preliminary analysis was to determine the appropriate boundary conditions, in particular the restraint conditions of the slab to be adopted if the model is limited to one bay in the parametric study. As shown in Figure 8.36(b), the predicted deflection of the corner grid with two continuous edges is the most important among all four grids (the other three grids are with three or four continuous edges). In consequence, all numerical simulations in the parametric study simulated the restraint conditions appropriate to a corner bay with two edges laterally restrained, to simulate continuity of the slab.



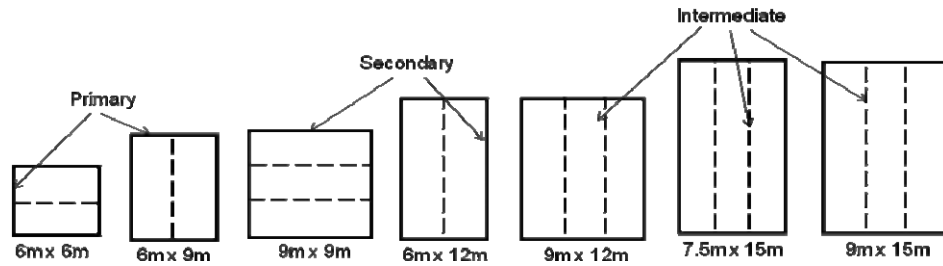
(a) Structure grid of a real building



(b) ANSYS model

**Figure 8.36** Numerical calculation of four floor grids

Seven bay sizes were investigated in the parametric study:  $6 \times 6$  m,  $6 \times 9$  m,  $6 \times 12$  m,  $9 \times 9$  m,  $9 \times 12$  m,  $9 \times 15$  m and  $7.5 \times 15$  m (Figure 8.37). All these cases were modelled with simulated continuity of the composite slab on two edges. All boundary beams were assumed to be protected but all internal secondary beams were assumed to be unprotected.



**Figure 8.37** Floors considered in the parametric numerical study

Three different intensities of variable action were considered in the study, as shown in Table 8.1. These values of variable action correspond to those commonly used in room temperature design in the French building market. Nevertheless, if different load values were used, there would be no influence on the simple design method because the applied load is only an input data given by design engineers. In the parametric study, only Case 1 and Case 3 were investigated numerically. Case 2 was considered to be covered as it is an intermediate value between Case 1 and Case 3.

**Table 8.1** Value of permanent and variable actions considered.

Case	Permanent action G	Variable action Q
1	Self weight + 1.25 kN/m <sup>2</sup>	2.5 kN/m <sup>2</sup>
2	Self weight + 1.25 kN/m <sup>2</sup>	3.5 kN/m <sup>2</sup>
3	Self weight + 1.25 kN/m <sup>2</sup>	5.0 kN/m <sup>2</sup>

Four standard fire durations, that is 30, 60, 90 and 120 minutes, were investigated. The depth of the composite slab in each case was based on the minimum depth required to fulfil the insulation criteria for these fire durations. Based on the use of a 60mm deep trapezoidal steel deck profile this resulted in composite slabs 120, 130, 140 and 150 mm deep. The geometry of the trapezoidal profile is based on the COFRAPLUS 60 product, the most commonly used deck profile on the French market. This steel deck has narrow ribs relative to other profiles, resulting in a more onerous temperature profile and lower mechanical resistance. Therefore, if the simple design method is verified with this steel decking, the conclusion could be conservatively applied to any other types of steel decking.

With the combination of all above parameters, a total of 112 numerical simulations were conducted.

Prior to the analysis of the fire behaviour of the different floor grids, preliminary designs were carried out in accordance with EN 1994-1-1<sup>(34)</sup>, to determine the size of structural members of all the composite floors. In these designs, all steel beams were considered to be connected to the composite slab with headed studs. As far as the material properties used in these designs are concerned, the quality of concrete was assumed to be C30/37 with a compressive strength of 30 MPa. The reinforcing steel mesh was steel grade B500. The steel grade of the beams was mainly S235.

An important parameter for the fire performance of composite floor designed with the simple design method is the size of reinforcing steel mesh used in the composite slab. As the parametric study was to verify the simple design method, the size of all reinforcing steel mesh was derived directly from this simple design method. In addition, the axis distance (i.e. distance between the axis of longitudinal

reinforcement and the unexposed side of concrete slab) was taken as 45 mm in all cases.

The heating of the fire protected boundary beams and columns will also influence the performance of the floor slab. In the parametric study, the thermal properties of the fire protection were modelled such that the temperature of these members at the expected fire duration was in general around 550 °C. However, if this heating was reached before the expected fire duration, the heating of the corresponding steel beam was then maintained to 550 °C for all instants following that when this heating was reached.

Details of the size of steel beams and mesh considered for each case are given in Table 8.2 to Table 8.5 The table also includes the degree of shear connection of the composite beams and the steel grade if it is different from S235. B1, B2, S and DC mean respectively primary beams, secondary beams, area of the reinforcing mesh in mm<sup>2</sup>/m and degree of shear connection of composite beams. In addition, Span 1 indicates the length of secondary beams and Span 2 that of primary beams. For each case, two simulations were conducted, one with the existence of mechanical link between slab and columns (for example, through additional reinforcing bars) and another one without this link.

**Table 8.2** Parameters selected for floors designed for 30 minutes fire resistance

R 30 Depth = 120 mm		Span1 [m]												
Span2 [m]	Load [kN/m <sup>2</sup> ]	6		9		12		15						
6	2.5+1.25	B1	IPE300 DC: 0.9	B1	IPE360 DC: 1.0	B1	IPE450 DC: 1.0							
		B2	IPE240 DC: 0.8	B2	IPE360 DC: 0.7	B2	IPE450 DC: 0.7							
		S	84	S	99	S	142							
	5.0+1.25	B1	IPE360 DC: 0.9	B1	IPE450 DC: 1.0	B1	IPE500 DC: 1.0							
		B2	IPE270 DC: 0.7	B2	IPE400 DC: 0.6	B2	IPE500 DC: 0.6							
		S	99	S	142	S	142							
	7.5	2.5+1.25										B1	IPE600 DC: 1.0	
												B2	IPE550 DC: 0.7	
												S	142	
5.0+1.25								B1	IPE600 -S355 DC: 1.0					
								B2	IPE600 DC: 0.7					
								S	142					
9	2.5+1.25	B1	IPE550 DC: 0.6	B1	IPE600 DC: 0.8	B1	IPE600 DC: 1.0							
		B2	IPE360 DC: 0.7	B2	IPE450 DC: 0.7	B2	IPE500 DC: 0.7							
		S	99	S	142	S	142							
	5.0+1.25	B1	IPE550 -S355 DC: 0.6	B1	IPE600 -S355 DC: 0.8	B1	IPE600 -S355 DC: 1.0							
		B2	IPE400 DC: 0.6	B2	IPE500 DC: 0.6	B2	IPE600 DC: 0.7							
		S	142	S	142	S	142							

**Table 8.3** Parameters selected for floors designed for 60 minutes fire resistance

R 60 Depth = 130 mm		Span1 [m]								
Span2 [m]	Load [kN/m <sup>2</sup> ]	6		9		12		15		
6	2.5+1.25	B1	IPE300	B1	IPE360	B1	IPE450			
			DC: 0.8		DC: 0.9		DC: 1.0			
		B2	IPE240	B2	IPE360	B2	IPE450			
	DC: 0.8		DC: 0.8		DC: 0.7					
	S	115	S	193	S	284				
	5.0+1.25	B1	IPE360	B1	IPE450	B1	IPE500			
DC: 0.8			DC: 0.9		DC: 1.0					
B2		IPE270	B2	IPE400	B2	IPE500				
	DC: 0.7		DC: 0.6		DC: 0.5					
S	151	S	227	S	347					
7.5	2.5+1.25						B1	IPE600		
								DC: 1.0		
							B2	IPE550		
		DC: 0.7								
	S	347								
	5.0+1.25							B1	IPE600-S355	
								DC: 1.0		
B2								IPE600		
	DC: 0.6									
S	433									
9	2.5+1.25							B1	IPE550	
									DC: 0.5	
								B1	IPE600	
		DC: 0.7								
	B2	IPE360	B2	IPE450	B2	IPE550				
		DC: 0.8		DC: 0.7		DC: 0.7				
		S		166		S	245	S	311	
	5.0+1.25								B1	IPE550-S355
										DC: 0.5
B1									IPE600-S355	
	DC: 0.7									
B2	IPE400	B2	IPE500	B2	IPE600					
	DC: 0.6		DC: 0.5		DC: 0.6					
	S		210		S	297	S	393		
							B1	IPE750 x 173		
								DC: 0.9		
							B2	IPE600		
								DC: 0.6		



**Table 8.4** Parameters selected for floors designed for 90 minutes fire resistance

R 90 Depth = 140 mm		Span1 [m]							
Span2 [m]	Load [kN/m <sup>2</sup> ]	6		9		12		15	
6	2.5+1.25	B1	IPE300	B1	IPE360	B1	IPE450		
			DC: 0.7		DC: 1.0		DC: 1.0		
		B2	IPE240	B2	IPE360	B2	IPE450		
	DC: 0.7		DC: 0.8		DC: 0.7				
	S	119	S	187	S	291			
	5.0+1.25	B1	IPE360	B1	IPE450	B1	IPE500		
DC: 0.7			DC: 1.0		DC: 1.0				
B2		IPE270	B2	IPE400	B2	IPE500			
	DC: 0.7	DC: 0.6		DC: 0.6					
S	146	S	233	S	355				
7.5	2.5+1.25							B1	IPE600
								DC: 0.9	
		B2	IPE550					DC: 0.7	
	S	393							
	5.0+1.25	B1							IPE600
									-S355
DC: 0.9									
B2	IPE600								
	DC: 0.6								
S	473								
9	2.5+1.25	B1	IPE550	B1	IPE600	B1	IPE600		
			DC: 0.5		DC: 0.6		-S355		
		DC: 0.7			DC: 0.7				
	B2	IPE360	B2	IPE450	B2	IPE550			
		DC: 0.8		DC: 0.7		DC: 0.7			
	S	177	S	252	S	340			
	5.0+1.25	B1	IPE550-	B1	IPE600	B1	IPE750		
			S355		-S355		x 173		
		DC: 0.5	DC: 0.6	DC: 0.7					
B2	IPE400	B2	IPE500	B2	IPE600				
	DC: 0.6		DC: 0.6		DC: 0.6				
S	215	S	311	S	433				

**Table 8.5** Parameters selected for floors designed for 120 minutes fire resistance

R 120 Depth = 140 mm		Span1 [m]							
Span2 [m]	Load [kN/m <sup>2</sup> ]	6		9		12		15	
6	2.5+1.25	B1	IPE300	B1	IPE360	B1	IPE450		
			DC: 0.6		DC: 1.0		DC: 1.0		
		B2	IPE240	B2	IPE360	B2	IPE450		
	DC: 0.7		DC: 0.8		DC: 0.7				
	S	132	S	204	S	318			
	5.0+1.25	B1	IPE360	B1	IPE450	B1	IPE500		
			DC: 0.6		DC: 1.0		DC: 1.0		
		B2	IPE270	B2	IPE400	B2	IPE500		
	DC: 0.7		DC: 0.6		DC: 0.6				
S	161	S	252	S	393				
7.5	2.5+1.25							B1	IPE600 DC: 0.8
								B2	IPE550 DC: 0.7
								S	417
	5.0+1.25							B1	IPE600 -S355 DC: 0.8
								B2	IPE600 DC: 0.6
								S	503
9	2.5+1.25			B1	IPE550	B1	IPE550- S355	B1	IPE600 -S355 DC: 0.7
					DC: 0.4		DC: 0.6		
		B2	IPE360	B2	IPE450	B2	IPE550 DC: 0.7		
	DC: 0.8		DC: 0.7						
	S	193	S	277	S	377			
	5.0+1.25			B1	IPE550 -S355	B1	IPE600- S355	B1	IPE750 x 173 DC: 0.7
					DC: 0.4		DC: 0.6		
		B2	IPE400	B2	IPE500	B2	IPE600 DC: 0.6		
	DC: 0.6		DC: 0.6						
S	252	S	340	S	457				

#### 8.4.2 Input data for parametric study

The results from the parametric study have been used to investigate the following two issues, which are significant to the application of the simple design method in practice.

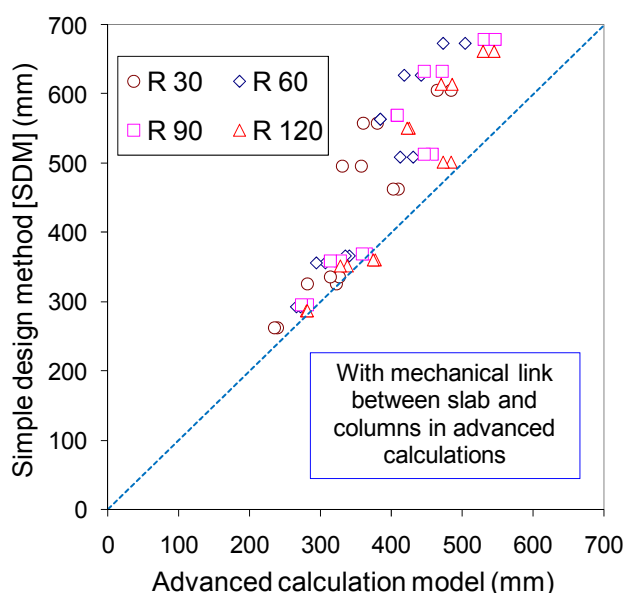
- maximum deflection of floor
- maximum mechanical elongation of reinforcing steel mesh

##### 8.4.2.1 Maximum deflection of floor

As described for the simple design method (Section 5) and demonstrated during the fire test (see Section 7), large deflection of the floor could occur before the point of structural collapse is reached. As the resistance of the slab relies on tensile membrane action of the floor slab, this large deflection is required to activate this load carrying mechanism. However, large deflections of the floor can also lead to loss of integrity performance due to concrete cracking, high strains in the reinforcement and the possible modification of loading condition if the floor becomes too sloping. Regulatory authorities are also concerned by design methods which result in deflections much larger than those experienced in traditional fire

tests, although these are not really relevant to the design method discussed in this publication. Also the simple design method assumes that the beam on the perimeter of each floor design zone remains rigid. In reality the surrounding beams deflect once subjected to fire. The parametric study therefore pays special attention to deflections in order to address these issues.

In the simple design method, a maximum allowable value of deflection has been assumed (see Section 6.2.1) to predict the ultimate load-carrying capacity of the floor. Therefore, the first step of the current investigation is to check whether this maximum allowable deflection is consistent with deflection predicted by the advanced calculation method. As a result, a comparison between deflection calculated in the numerical analysis and maximum allowable deflections according to the simple design method was carried out and the results are illustrated in Figure 8.38 (with mechanical link between slab and columns) and Figure 8.39 (without mechanical link between slab and columns). Due to the fact that the simple design method assumes the vertical restrained peripheral supports and advanced calculations takes account of flexible peripheral steel beams, the comparison between them was made with total deflection of floor under fire situation deducted of the deflection of peripheral beams.



**Figure 8.38** Comparison of the deflection predicted by the advanced calculation model with maximum allowable deflection according to the simple design method (SDM) with mechanical link between slab and columns

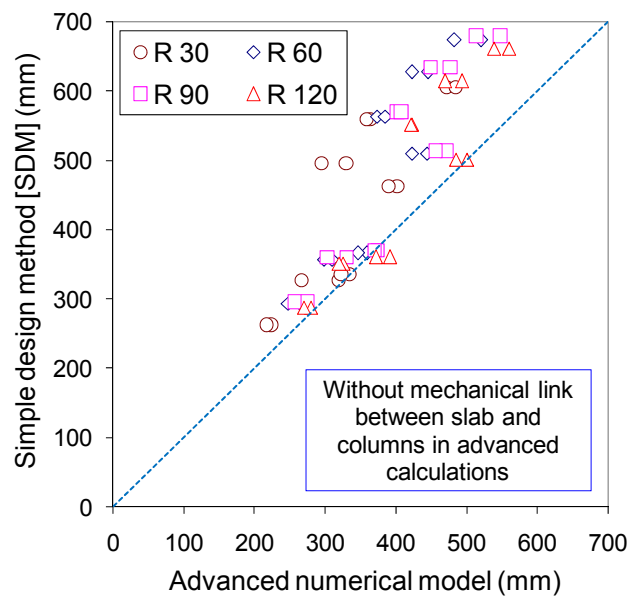
It can be found from the comparison that the maximum allowable deflection used in the simple design method is systematically greater than the maximum deflection predicted in numerical analysis. The scatter between them seems to increase as a function of floor panel size. In fact, the physical meaning of this finding is that the simple design method predicts lower load bearing capacity of the floor than the advanced calculation model under the same deflection value. From this point of view, the simple design method can be considered as conservative.

Traditionally, certain national fire regulations define the deflection value of span/30 as the failure criterion of a single structural member in bending (beams and slabs) tests under ISO fire condition<sup>(38)</sup>. In the case of composite floors comprising primary beams, secondary beams and slabs, one can propose that the total deflection limit of the floor shall be the sum of the allowable deflections of each of

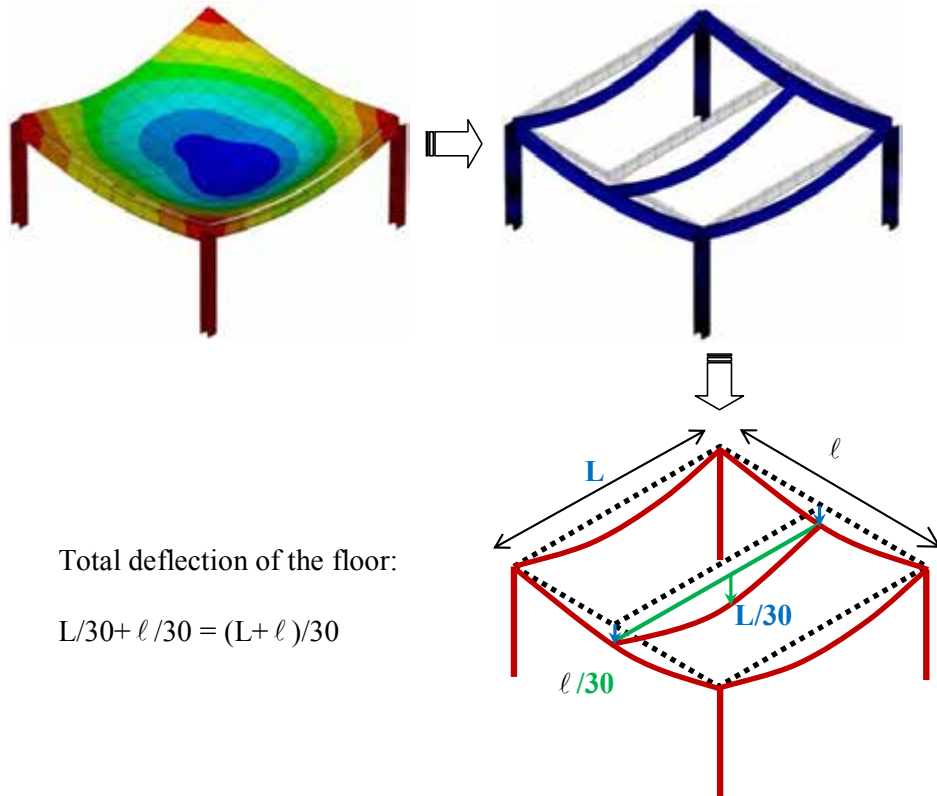
the structural members as illustrated in Figure 8.40 instead of that with each deflection considered individually because these structural members are assembled together.

Consequently, whatever the beam distribution is, the deflection limit shall be at least  $(\text{span1} + \text{span2})/30$ , where span 1 is the length of the secondary beams and span 2 is the length of the primary beams.

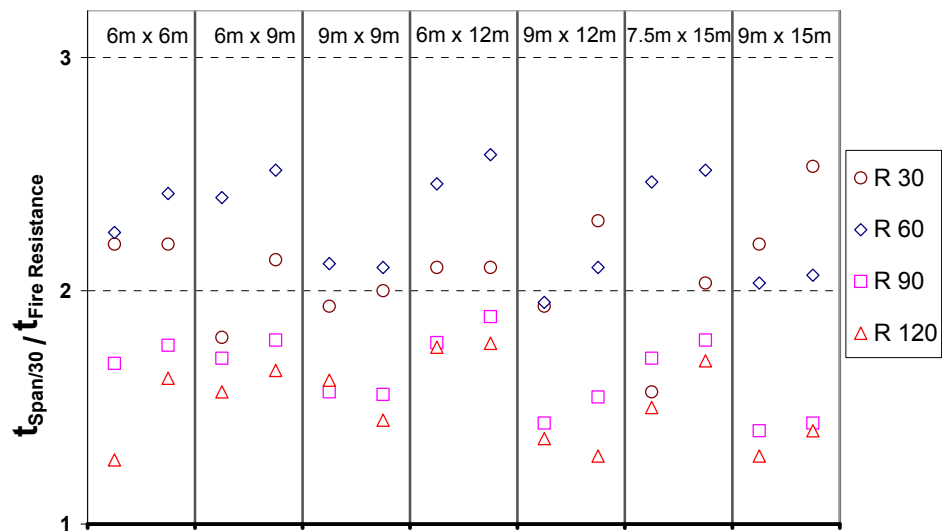
For this failure criterion, it is then interesting to check the fire rating of the floor. A comparison is illustrated in Figure 8.41, which gives the ratio between the fire duration to reach above deflection criterion according to the advanced numerical model, and the fire rating predicted by the Simple Design Method. In all cases, this ratio is greater than 1.0, which means that if the above deflection is adopted as the failure criterion, the fire rating will be greater than that given by the simple design method. Therefore, the application of the simple calculation will satisfy automatically the above deflection criterion.



**Figure 8.39** Comparison of the deflection predicted by the advanced calculation model with maximum allowable deflection according to the simple design method (SDM) without mechanical link between slab and columns



**Figure 8.40** Total deflection limit according to the criterion of span/30



**Figure 8.41** Ratio between the time when the predicted deflection reaches span/30 and the fire resistance predicted according to the simple design method

The European standard for fire resistance tests<sup>(32)</sup>, defines the following deflection limits for assessing the load bearing criterion of elements subject to bending. The load bearing failure for this type of structural element is deemed to occur if the measured deflection exceeds the limiting deflection or the limiting rate of deflection given below:

$$\text{Limiting deflection, } D = \frac{L^2}{400d} \text{ mm; and,}$$

$$\text{Limiting rate of deflection, } \frac{dD}{dt} = \frac{L^2}{9000d} \text{ mm/min}$$

where:

- $L$  is the clear span of the test specimen, in millimetres
- $d$  is the distance from the extreme fibre of the cold design compression zone to the extreme fibre of the cold design tension zone of the structural section, in millimetres.

It must be kept in mind that the criterion with respect to the rate of deflection is not applied until a deflection of span/30 has been exceeded. That is the reason why this criterion is not taken into account, since it is already included in the previous deflection criterion based on Span/30. The same principle as considered with the criterion of Span/30 can be applied to get the maximum allowable deflection limit of the floor.

#### **8.4.2.2 Elongation of the steel reinforcing mesh**

In addition to the deflection of the floor, the elongation of reinforcing steel is the second feature that is investigated in detail in this parametric study. The simple design method is based on plastic analysis for the load bearing capacity of the floor system allowing for an enhancement due to tensile membrane action. As discussed in Section 6 failure of the slab could occur due to the fracture of the mesh across the short span of the slab. Moreover, this fracture could occur equally at the edge parts of the floor where the continuity of the slab exists.

This parametric study provided the opportunity to investigate the strain in the reinforcement predicted by the advanced calculation model when the target fire resistance is reached. Knowing the elongation of the reinforcement at fracture a conclusion can then be drawn as to the margin of safety against mesh fracture provided by the simple method.

As the reinforcing steel mesh is put over the whole area of the floor, and is continuous across all beams including protected boundary beams, significant tensile strain will also occur over the protected beams and around columns.

If the elongation becomes too great, fracture of the reinforcement could occur, which may lead to loss of integrity and insulation performance of the floor before load bearing failure is reached. However, the question arises about the criterion to be applied to elongation capacity of reinforcing steel. EN 1992-1-2<sup>(35)</sup> implies that for plastic design the minimum elongation capacity at ultimate stress for reinforcing steel must be at least 5%. Therefore, this value is taken as the elongation criterion in this parametric study for reinforcing steel mesh.

The results of this parametric study related to maximum deflection of the floors obtained for all fire resistance durations and the maximum elongation of

reinforcing steel along two orthogonal directions (parallels respectively to primary and secondary beams) are summarised in Table 8.10 to Table 8.13. In these tables, SDM means simple design method and Spans means (Span 1 + Span 2). From these tables, it can be found that in all cases, the maximum allowable deflection used to evaluate the load-bearing capacity in the simple design method always exceeds the predictions of the advanced numerical model. With respect to the maximum elongation of reinforcing steel, it can be observed that the maximum values obtained with the advanced numerical model for any fire duration are always lower than 5%, which once again is very satisfactory.

**Table 8.6** *Deflection of the floor and elongation of reinforcing steel for fire duration R30 (with mechanical link between slab and columns)*

Load [kN/m <sup>2</sup> ]	Span1 L [m]	Span2 $\ell$ [m]	ANSYS [mm]		SDM [mm]	$\frac{L + \ell}{30}$ [mm]	$\frac{L^2}{400 d}$ [mm]	Elongation Span1 [%]	Elongation Span2 [%]
			Total add.	Slab					
2.5+1.25	6	6	248	239	262	400	500	2.8%	3.0%
5.0+1.25	6	6	240	235	262	400	462	2.9%	2.7%
2.5+1.25	9	6	359	322	326	500	609	2.8%	2.4%
5.0+1.25	9	6	312	282	326	500	563	3.0%	2.3%
2.5+1.26	9	9	359	331	495	600	844	3.4%	2.6%
5.0+1.25	9	9	389	358	495	600	779	3.0%	2.4%
2.5+1.25	12	6	379	326	335	600	789	3.1%	2.3%
5.0+1.25	12	6	361	314	335	600	726	3.0%	2.5%
2.5+1.25	12	9	443	381	558	700	987	3.2%	2.3%
5.0+1.25	12	9	416	361	558	700	907	3.0%	2.6%
2.5+1.25	15	7.5	480	410	462	750	1049	3.1%	3.8%
5.0+1.25	15	7.5	461	403	462	750	977	3.0%	4.0%
2.5+1.25	15	9	539	465	605	800	1234	3.2%	3.1%
5.0+1.25	15	9	578	485	605	800	1063	3.5%	4.4%

**Table 8.7** Deflection of the floor and elongation of reinforcing steel for fire duration R60 (with mechanical link between slab and columns)

Load [kN/m <sup>2</sup> ]	Span1 L [m]	Span2 $\ell$ [m]	ANSYS [mm]		SDM [mm]	$\frac{L + \ell}{30}$ [mm]	$\frac{L^2}{400d}$ [mm]	Elongation Span1 [%]	Elongation Span2 [%]
			Total add.	Slab					
2.5+1.25	6	6	288	271	293	400	486	3.6%	3.1%
5.0+1.25	6	6	280	266	293	400	450	3.7%	2.9%
2.5+1.25	9	6	348	307	356	500	597	3.5%	2.8%
5.0+1.25	9	6	334	294	356	500	552	3.4%	2.6%
2.5+1.26	9	9	434	385	563	600	827	3.9%	2.9%
5.0+1.25	9	9	429	384	563	600	764	3.6%	2.8%
2.5+1.25	12	6	409	341	366	600	776	3.3%	2.4%
5.0+1.25	12	6	397	335	366	600	714	3.1%	2.5%
2.5+1.25	12	9	527	442	627	700	970	3.7%	2.7%
5.0+1.25	12	9	499	419	627	700	893	3.4%	2.7%
2.5+1.25	15	7.5	524	431	509	750	1034	3.1%	3.7%
5.0+1.25	15	7.5	492	413	509	750	963	2.8%	3.4%
2.5+1.25	15	9	607	505	673	800	1125	3.6%	3.4%
5.0+1.25	15	9	571	474	673	800	1048	3.3%	3.1%

**Table 8.8** Deflection of the floor and elongation of reinforcing steel for fire duration R90 (with mechanical link between slab and columns)

Load [kN/m <sup>2</sup> ]	Span1 L [m]	Span2 $\ell$ [m]	ANSYS [mm]		SDM [mm]	$\frac{L + \ell}{30}$ [mm]	$\frac{L^2}{400d}$ [mm]	Elongation Span1 [%]	Elongation Span2 [%]
			Total add.	Slab					
2.5+1.25	6	6	306	282	295	400	474	2.7%	2.6%
5.0+1.25	6	6	294	274	295	400	439	2.8%	2.3%
2.5+1.25	9	6	379	328	359	500	585	2.7%	2.5%
5.0+1.25	9	6	364	314	359	500	542	2.7%	2.2%
2.5+1.26	9	9	471	408	569	600	810	3.3%	2.2%
5.0+1.25	9	9	468	409	569	600	750	3.1%	2.2%
2.5+1.25	12	6	448	365	369	600	763	2.5%	2.6%
5.0+1.25	12	6	436	360	369	600	703	2.2%	2.4%
2.5+1.25	12	9	579	472	633	700	953	3.0%	2.4%
5.0+1.25	12	9	548	447	633	700	879	2.7%	2.3%
2.5+1.25	15	7.5	579	458	513	750	1019	2.6%	3.1%
5.0+1.25	15	7.5	550	446	513	750	950	1.9%	2.9%
2.5+1.25	15	9	670	532	679	800	1109	2.6%	3.1%
5.0+1.25	15	9	668	547	679	800	1034	2.3%	2.5%



**Table 8.9** Deflection of the floor and elongation of reinforcing steel for fire duration R120 (with mechanical link between slab and columns)

Load [kN/m <sup>2</sup> ]	Span1 L [m]	Span2 $\ell$ [m]	ANSYS [mm]		SDM [mm]	$\frac{L + \ell}{30}$ [mm]	$\frac{L^2}{400 d}$ [mm]	Elongation Span1 [%]	Elongation Span2 [%]
			Total add.	Slab					
2.5+1.25	6	6	360	281	287	400	462	3.1%	2.6%
5.0+1.25	6	6	305	281	287	400	429	3.2%	2.7%
2.5+1.25	9	6	398	339	351	500	574	3.0%	2.7%
5.0+1.25	9	6	386	328	351	500	532	3.0%	2.6%
2.5+1.26	9	9	500	426	551	600	794	3.9%	2.7%
5.0+1.25	9	9	492	422	551	600	736	3.6%	2.6%
2.5+1.25	12	6	476	377	360	600	750	2.8%	3.1%
5.0+1.25	12	6	464	374	360	600	692	2.4%	3.0%
2.5+1.25	12	9	616	487	614	700	938	3.6%	2.8%
5.0+1.25	12	9	626	470	614	700	865	3.4%	2.8%
2.5+1.25	15	7.5	625	485	501	750	1004	2.6%	3.6%
5.0+1.25	15	7.5	592	473	501	750	938	2.2%	3.4%
2.5+1.25	15	9	705	545	661	800	1093	3.2%	3.3%
5.0+1.25	15	9	676	530	661	800	1020	2.7%	3.2%

The results given in these tables from the parametric investigation with the advanced calculation model ANSYS are based on the assumption that the composite slab is linked to all steel columns with additional reinforcing steel bars. Certainly, this constructional detail can reduce the deflection of the floor but in reality this is not always possible, especially for edge beams. It will be then very important to know if this constructional detail is applied what will be the impact on the global behaviour of the floor. A second series of studies was made without this constructional detail and the results are presented in the same way in tables Table 8.10 to Table 8.13. Certainly the maximum deflections are slightly higher than previously. However, they remain nearly always lower than those estimated according to different traditional criteria. Moreover, the maximum elongation of reinforcing steel mesh for all floors is lower than 5% for all given fire ratings.

**Table 8.10** Deflection of the floor and elongation of reinforcing steel for fire duration R30 (without mechanical link between slab and columns)

Load [kN/m <sup>2</sup> ]	Span1 L [m]	Span2 $\ell$ [m]	ANSYS [mm]		SDM [mm]	$\frac{L + \ell}{30}$ [mm]	$\frac{L^2}{400 d}$ [mm]	Elongation Span1 [%]	Elongation Span2 [%]
			Total add.	Slab					
2.5+1.25	6	6	305	224	262	400	500	2.8%	2.4%
5.0+1.25	6	6	285	218	262	400	462	3.0%	2.2%
2.5+1.25	9	6	363	274	326	500	609	2.9%	2.2%
5.0+1.25	9	6	330	267	326	500	563	3.0%	2.1%
2.5+1.26	9	9	406	295	495	600	844	3.2%	2.2%
5.0+1.25	9	9	394	330	495	600	779	3.1%	2.4%
2.5+1.25	12	6	415	335	335	600	789	3.4%	2.1%
5.0+1.25	12	6	392	323	335	600	726	3.0%	2.2%
2.5+1.25	12	9	464	364	558	700	987	3.3%	2.2%
5.0+1.25	12	9	442	359	558	700	907	3.0%	2.5%
2.5+1.25	15	7.5	490	402	462	750	1049	3.2%	3.0%
5.0+1.25	15	7.5	463	390	462	750	977	2.8%	3.1%
2.5+1.25	15	9	569	472	605	800	1234	3.0%	3.6%
5.0+1.25	15	9	578	485	605	800	1063	3.1%	4.0%

**Table 8.11** Deflection of the floor and elongation of reinforcing steel for fire duration R60 (without mechanical link between slab and columns)

Load [kN/m <sup>2</sup> ]	Span1 L [m]	Span2 $\ell$ [m]	ANSYS [mm]		SDM [mm]	$\frac{L + \ell}{30}$ [mm]	$\frac{L^2}{400 d}$ [mm]	Elongation Span1 [%]	Elongation Span2 [%]
			Total add.	Slab					
2.5+1.25	6	6	348	264	293	400	486	3.7%	2.6%
5.0+1.25	6	6	325	248	293	400	450	3.7%	2.6%
2.5+1.25	9	6	400	310	356	500	597	3.5%	2.5%
5.0+1.25	9	6	380	298	356	500	552	3.6%	2.5%
2.5+1.26	9	9	493	373	563	600	827	3.5%	2.5%
5.0+1.25	9	9	481	385	563	600	764	3.2%	2.5%
2.5+1.25	12	6	463	359	366	600	776	4.0%	2.6%
5.0+1.25	12	6	435	346	366	600	714	3.8%	2.8%
2.5+1.25	12	9	587	445	627	700	970	3.8%	2.6%
5.0+1.25	12	9	548	423	627	700	893	3.5%	2.8%
2.5+1.25	15	7.5	565	444	509	750	1034	3.6%	3.2%
5.0+1.25	15	7.5	520	423	509	750	963	3.3%	3.0%
2.5+1.25	15	9	660	520	673	800	1125	3.1%	3.6%
5.0+1.25	15	9	607	483	673	800	1048	2.8%	3.4%

**Table 8.12** Deflection of the floor and elongation of reinforcing steel for fire duration R90 (without mechanical link between slab and columns)

Load [kN/m <sup>2</sup> ]	Span1 L [m]	Span2 $\ell$ [m]	ANSYS [mm]		SDM [mm]	$\frac{L + \ell}{30}$ [mm]	$\frac{L^2}{400 d}$ [mm]	Elongation Span1 [%]	Elongation Span2 [%]
			Total add.	Slab					
2.5+1.25	6	6	363	275	295	400	474	4.1%	3.0%
5.0+1.25	6	6	338	257	295	400	439	4.3%	3.1%
2.5+1.25	9	6	433	331	359	500	585	2.6%	2.3%
5.0+1.25	9	6	403	303	359	500	542	3.8%	3.0%
2.5+1.26	9	9	531	402	569	600	810	3.3%	2.0%
5.0+1.25	9	9	521	408	569	600	750	2.2%	2.2%
2.5+1.25	12	6	497	375	369	600	763	2.5%	2.4%
5.0+1.25	12	6	475	370	369	600	703	3.2%	2.2%
2.5+1.25	12	9	644	477	633	700	953	3.0%	2.4%
5.0+1.25	12	9	599	450	633	700	879	2.8%	2.2%
2.5+1.25	15	7.5	624	472	513	750	1019	2.2%	3.0%
5.0+1.25	15	7.5	582	457	513	750	950	1.9%	2.8%
2.5+1.25	15	9	726	548	679	800	1109	2.6%	2.8%
5.0+1.25	15	9	670	514	679	800	1034	2.3%	2.5%

**Table 8.13** Deflection of the floor and elongation of reinforcing steel for fire duration R120 (without mechanical link between slab and columns)

Load [kN/m <sup>2</sup> ]	Span1 L [m]	Span2 $\ell$ [m]	ANSYS [mm]		SDM [mm]	$\frac{L + \ell}{30}$ [mm]	$\frac{L^2}{400 d}$ [mm]	Elongation Span1 [%]	Elongation Span2 [%]
			Total add.	Slab					
2.5+1.25	6	6	393	280	287	400	462	4.9%	3.8%
5.0+1.25	6	6	353	270	287	400	429	5.2%	3.7%
2.5+1.25	9	6	466	326	351	500	574	4.6%	4.1%
5.0+1.25	9	6	434	320	351	500	532	4.5%	3.9%
2.5+1.26	9	9	567	423	551	600	794	2.8%	2.9%
5.0+1.25	9	9	548	421	551	600	736	3.6%	4.5%
2.5+1.25	12	6	537	392	360	600	750	4.1%	2.6%
5.0+1.25	12	6	509	372	360	600	692	3.8%	2.6%
2.5+1.25	12	9	686	493	614	700	938	3.7%	2.8%
5.0+1.25	12	9	663	469	614	700	865	3.5%	2.7%
2.5+1.25	15	7.5	677	501	501	750	1004	3.2%	3.2%
5.0+1.25	15	7.5	625	485	501	750	938	2.8%	3.1%
2.5+1.25	15	9	767	560	661	800	1093	2.7%	3.5%
5.0+1.25	15	9	717	539	661	800	1020	2.8%	3.1%

## 8.5 Conclusion

The objective of the parametric study was to make a detailed investigation of the simple design method with the help of advanced calculation models validated against an ISO fire test. From the results, it can be concluded that:

- With respect to load bearing capacity, the simple design method gives conservative results compared to advanced calculation models;
- When using traditional deflection criteria based on the behaviour of single flexural structural members, the fire performance of composite flooring systems predicted with the simple design method are on the safe side;
- Concerning the elongation of reinforcing steel mesh, it remains generally below 5%, the minimum elongation requirement recommended by EN 1992-1-2 for all types of reinforcing steel;
- Mechanical links between slab and columns are not necessary. Nevertheless, this constructional detail could reduce the deflection of a composite flooring system under a fire situation.

The results derived from this parametric study show clearly that the simple design method is fully capable of predicting in a safe way the structural performance of composite steel and concrete floors subjected to an ISO fire condition, which may be taken as evidence that the design method can be used in structural fire engineering design.

## 9 REFERENCES

1. 'Fire Safe Design: A new approach to multi-storey steel framed buildings' P288, The Steel Construction Institute, 2006.
2. 'The behaviour of Multi-storey steel framed buildings in fire', A European joint research programme, British Steel Swinden Technology Centre, 1999
3. Lennon, T., 'Cardington fire tests: instrumentation locations for large compartment fire test.', Building Research Establishment Report N100/98, June 1996.
4. Lennon, T., 'Cardington fire tests: instrumentation locations for corner fire test.', Building Research Establishment Report N152/95, June 1996
5. Wainman, W. and Kirby, B., Compendium of UK standard fire test data, No.1 - Unprotected structural steel, British Steel, Swinden Technology Centre, 1987
6. Investigation of Broadgate Phase 8 Fire, SCI, Ascot, 1991.
7. Thomas, I. R., Bennetts, I. D., Dayawansa, P., Proe, D. J. and Lewins, R. R., 'Fire Tests of the 140 William Street Office Building.', BHPR/ENG/R/92/043/SG2C, BHP Research, Melbourne Australia, 1992
8. Proe, D. J. and Bennetts, I. D., 'Real Fire Tests in 380 Collins Street Office Enclosure.', BHPR/PPA/R/94/051/SG021A, BHP Research Melbourne Australia, 1994.
9. Brand Verhalten Von Stahl und Stahlverbund Konstruktionen (Fire behaviour of steel and composite construction), Verlag TUV Rheinland, 1986.
10. Johansen, K.W., 'The Ultimate strength of Reinforced Concrete Slabs.', International Association for Bridge and Structural Engineering, Final Report, Third Congress, Liege, September 1948.
11. Ockleston AJ. Load tests on a 3-storey reinforced concrete building in Johannesburg. Struct Eng 1955;33(10):304-22
12. Bailey C.G. and Moore D.B., The structural behaviour of steel frames with composite floor slabs subjected to fire: Part 1: Theory
13. Bailey C.G. and Moore D.B., The structural behaviour of steel frames with composite floor slabs subjected to fire: Part 2: Design
14. Park, R, Ultimate strength of rectangular concrete slabs under short term uniform loading with edges restrained against lateral movement. Proceedings, Institution of Civil Engineers, 28, pp125-150.
15. Wood R. H. Plastic and elastic design of slabs and plates, with particular reference to reinforced concrete floor slabs Thames and Husdon, London. 1961.
16. Taylor R. A note on a possible basis for a new method of ultimate load design of reinforced concrete slabs. Magazine of concrete research VOL 17 NO. 53 Dec 1965 pp. 183-186
17. Kemp. K.O. Yield of a square reinforced concrete slab on simple supports allowing for membrane forces. The structural Engineer Vol 45, No.7 July 1967 pp. 235-240.
18. Sawczuk A. and Winniki L. Plastic behaviour of simply supported reinforced concrete plated are moderately large deflections. Int J. Solids Structures Vol 1 1965 pp. 97 to 111.

19. Hayes B. Allowing for membrane action in the plastic analysis of rectangular reinforced concrete slabs Magazine of concrete research Vol. 20 No. 81 Dec 1968. pp 205-212.
20. Bailey C. G., White D.S. and Moore D.B. The tensile membrane action of unrestrained composite slab under fire conditions, Engineering Structures, vol. 22, no12, pp. 1583-1595
21. Bailey C. G. & Toh, W.S. 'Behaviour of concrete floor slabs at ambient and elevated temperature', Fire Safety Journal, 42, oo425-436, 2007.
22. Hayes B. and Taylor R. Load-Testing RC slabs. The Consulting Engineer. Nov. 1969. pp 46-47
23. Taylor R., Maher D.R.H. and Hayes B. Effect of arrangement of reinforcement on the behaviour of the reinforce concrete slabs. Magazine of concrete research Vol 18 No. 55. June 1966. pp 85-94
24. Moy S.S.J. Load-deflection characteristics of rectangular reinforced concrete slabs. Magazine of concrete research Vol 24 No. 81 Dec. 1972. pp 209-218.
25. Bailey, C.G., Efficient arrangement of Reinforcement for membrane behaviour of composite slabs in fire conditions, Journal of Constructional Steel Research, 59, 2003, pp931-949.
26. Bailey C.G., Membrane action of lightly reinforced concrete slabs at large displacements, Engineering Structures, 23, 2001, pp470-483.
27. Bailey, Colin G. and Toh, Wee Siang. Experimental behaviour of concrete floor slabs at ambient and elevated temperatures. SIF06
28. O'Conner MA, Kirby BR, Martin DM. Behaviour of a multi-storey composite steel framed building in fire. Struct Eng 2003;81(2):27-36.
29. Bailey CG, Lennon T, Moore DB. The behaviour of full-scale steel framed buildings subjected to compartment fires. Struct Eng 1999; 77(8):15-21.
30. Bailey CG, Membrane action of slab/beam composite floor systems in fire. Engineering Structures 26 2004:1691-1703.
31. Wang YC. Tensile membrane action in slabs and its application to the Cardington fire tests. Fire, static and dynamic tests of building structures. Proceeding of the second Cardington conference, England, 12-14 March1996: 55-67
32. EN 1992-1-2, Eurocode 2, Design of concrete structures. Part 1.2: General rules. Structural fire design, CEN
33. EN 1994-1-2, Eurocode 2, Design of composite steel and concrete structures. Part 1.2: General rules. Structural fire design, CEN
34. EN 1994-1-1, Eurocode 4 Design of composite steel and concrete structures – Part 1-1: General rules and rules for buildings, CEN
35. EN 1993-1-8, Eurocode 3 Design of steel structures – Part 1-8: Design of joints, CEN
36. EN 1992-1-1, Eurocode 2 Design of Concrete Structures – Part 1-1: General rules and rules for buildings, CEN
37. EN 1991-1-2 - Eurocode 1 " Actions on structures. General actions. " – Part 1-2: Actions on structures exposed to fire, CEN.
38. ARRETE DU 21 AVRIL 1983, Ministère de l'Intérieur Français Détermination des degrés de résistance au feu des éléments de construction.

39. EN 1363-1 - Fire resistance tests – Part 1: General requirements, CEN.(35)

**MACS\***  
**Membrane Action of Composite Structures**  
**in Case of Fire**

*Engineering Background*

Version 2012-1



## HOW TO OBTAIN EU PUBLICATIONS

### Free publications:

- one copy:  
via EU Bookshop (<http://bookshop.europa.eu>);
- more than one copy or posters/maps:  
from the European Union's representations ([http://ec.europa.eu/represent\\_en.htm](http://ec.europa.eu/represent_en.htm));  
from the delegations in non-EU countries ([http://eeas.europa.eu/delegations/index\\_en.htm](http://eeas.europa.eu/delegations/index_en.htm));  
by contacting the Europe Direct service ([http://europa.eu/eurodirect/index\\_en.htm](http://europa.eu/eurodirect/index_en.htm)) or  
calling 00 800 6 7 8 9 10 11 (freephone number from anywhere in the EU) (\*).

(\* ) The information given is free, as are most calls (though some operators, phone boxes or hotels may charge you).

### Priced publications:

- via EU Bookshop (<http://bookshop.europa.eu>).

### Priced subscriptions:

- via one of the sales agents of the Publications Office of the European Union  
([http://publications.europa.eu/others/agents/index\\_en.htm](http://publications.europa.eu/others/agents/index_en.htm)).

This project has extended recent RFCS project FICEB+ and Cossfire. Results obtained within these two projects related to membrane action are the focus of this dissemination. The first one consisted of a large-scale natural fire test on a compartment made of composite cellular beams; the second one consisted, among other tests, of one large-scale furnace test activating the membrane action with a prescriptive ISO Fire.

Both projects delivered a method, validated by a large-scale fire test, which enables the avoidance of fire protection on most of the secondary beams. This is possible due to the fact that the bearing resistance offered by the beams at room temperature is transformed into a membrane resistance provided by the reinforced concrete slab at room temperature.

The project was divided into four steps:

- Realisation of documentation and software about designing of composite floor system with unprotected secondary beams.
- Translation of the documentation and software interface.
- Training for partners involved in seminars.
- Organisation of the seminars in the different European countries.

The dissemination package consists of different documents and software which are available on the website <http://www.macsfire.eu>:

- A design guide.
- A background document.
- The Software MACS+, which is also available on <http://www.arcelormittal.com/sections>
- PowerPoint presentations.
- All the documents have been translated into nearly all the European languages.

Seminars were also organised by the different partners in 17 different countries in 16 languages.

#### *Studies and reports*